European Journal of Taxonomy 867: 1–312
https://doi.org/10.5852/ejt.2023.867.2109

ISSN 2118-9773
www.europeanjournaloftaxonomy.eu
2023 · Iniesta L.F.M. *et al.*

Research article

urn:lsid:zoobank.org:pub:8DEF295C-A8B1-4A6B-B873-B30949F64E07

A reassessment of the Neotropical genus *Pseudonannolene* Silvestri, 1895: cladistic analysis, biogeography, and taxonomic review (Spirostreptida: Pseudonannolenidae)

Luiz Felipe Moretti INIESTA [1,2,*], Rodrigo Salvador BOUZAN [1,2] &
Antonio Domingos BRESCOVIT [2,3]

[1] Pós-graduação em Zoologia, Instituto de Biociências, Universidade de São Paulo, São Paulo, Brazil.
[2] Laboratório de Coleções Zoológicas, Instituto Butantan, Avenida Vital Brasil, 1500, 05503-090, São Paulo, Brazil.

[*] Corresponding author: luiz-moretti@hotmail.com
[2] Email: rodrigobouzan@outlook.com
[3] Email: antonio.brescovit@butantan.gov.br

[1] urn:lsid:zoobank.org:author:DEEF048E-97FB-4CCD-875F-5FA6184CA8AB
[2] urn:lsid:zoobank.org:author:14A15A7F-730F-4D41-BDAC-D53514FAB85D
[3] urn:lsid:zoobank.org:author:D5B81D79-AFAE-47B1-8A6E-DAB448A24BCC

Abstract. In order to provide a reassessment of the Neotropical genus *Pseudonannolene* Silvestri, 1895, a cladistic analysis, biogeographic analysis, and taxonomic review were conducted in the present work. For the cladistic approach, 91 morphological characters were scored for 53 terminals as the ingroup and 10 as the outgroup. Three synapomorphies support the monophyly of the genus: presence of a longitudinal suture on the promentum, penial bases partially fused, and the internal branch of the gonopods surrounding the telopodite; and two homoplastic transformations: the lateral lobe of the collum densely striated and setae present up to the apical portion of the prefemoral process on the first leg-pair of males. The genus *Pseudonannolene* is recovered as sister-group of *Epinannolene* Brölemann, 1903 (Pseudonannoleninae). A total of 226 occurrence points were recorded for *Pseudonannolene*, with the majority of records from the Chacoan subregion, composed by Araucaria Forest, Atlantic, and Parana Forest provinces. The biogeographical searches using the Geographically explicit Event Model recovered two biogeographic reconstructions (cost of 79 000), with the vicariance events occurring more frequently in the deep clades, whereas sympatry and points of sympatry occurred in more inclusive clades. The first reconstruction recovered four vicariances, 13 sympatries, 4 points of sympatry, and 21 founder events, and the second reconstruction recovered four vicariances, 12–13 sympatries, 4–5 points of sympatry, and 21 founder events. The genus *Pseudonannolene* comprises 56 species, including 8 new species herein described: *P. alata* sp. nov., *P. aurea* sp. nov., *P. bucculenta* sp. nov., *P. curvata* sp. nov., *P. granulata* sp. nov., *P. insularis* sp. nov., *P. morettii* sp. nov., and *P. nicolau* sp. nov.; *P. brevis* Silvestri, 1902 and *P. rugosetta* Silvestri, 1897 are regarded as species inquirendae; a neotype of *P. alegrensis* Silvestri, 1897 is here proposed with male described for the first time. The following taxa are synonymized: *P. canastra* Gallo & Bichuette, 2020 and *P. saguassu* Iniesta & Ferreira, 2013 with *P. ambuatinga* Iniesta & Ferreira, 2013; *P. marconii* Iniesta & Ferreira, 2013 with *P. longicornis* (Porat, 1888); *P. chaimowiczi* Fontanetti, 1996, *P. gogo* Iniesta & Ferreira, 2013, *P. rosineii* Iniesta &

Ferreira, 2014, *P. taboa* Iniesta & Ferreira, 2014, and *P. longissima* Iniesta & Ferreira, 2014 with *P. microzoporus* Mauriès, 1987; *P. tricolor gracilis* Brölemann, 1902 and *P. tricolor rugosus* Schubart, 1945 with *P. tricolor* Brölemann, 1902; *P. auguralis* Silvestri, 1902 with *P. rocana* Silvestri, 1902; and *P. abbreviata* Silvestri, 1902 with *P. typica* Silvestri, 1895. *P. inops* Brölemann, 1929 is proposed here as new status from *P. bovei inops*. A dichotomous identification key is presented to facilitate the species identification.

Keywords. Chaco subregion, cave, Schubart, Juliformia, Cambalidea, distribution, new species.

Iniesta L.F.M., Bouzan R.S. & Brescovit A.D. 2023. A reassessment of the Neotropical genus *Pseudonannolene* Silvestri, 1895: cladistic analysis, biogeography, and taxonomic review (Spirostreptida: Pseudonannolenidae). *European Journal of Taxonomy* 867: 1–312. https://doi.org/10.5852/ejt.2023.867.2109

Introduction

Pseudonannolenidae Silvestri, 1895 is one of the most diverse families of the suborder Cambalidea Cook, 1895. It includes nearly 90 described species distributed in seven genera, ranging from Central America and the West Indies down to southern South America (Jeekel 2004; Enghoff *et al.* 2015; Iniesta *et al.* 2020). The family Pseudonannolenidae has been traditionally regarded as representing 'fragments of a partly transitional condition' between cambalideans [= Cambalidea] and spirostreptideans [= Spirostreptidea], due to a reduction of the posterior gonopods (present in almost all groups in Cambalidea) and the presence of some gnathochilarial features (Hoffman 1980; Jeekel 1985; Hoffman & Florez 1995; Shelley 2002; Iniesta *et al.* 2020). Currently, Pseudonannolenidae is divided into three subfamilies: Pseudonannoleninae Silvestri, 1895 (three genera), Physiostreptinae Silvestri, 1903 (three genera), and Cambalomminae Mauriès, 1977 (only *Cambalomma laevis* Loomis, 1941) (Mauriès 1977, 1987; Shelley 2002; Iniesta *et al.* 2020).

Historical background of Pseudonannolenidae

Silvestri (1895a) proposed Pseudonannolenidae early in the history of the study of cambalideans in the Neotropics. That publication provided a simplified scheme of the gnathochilarium, and included a dichotomous key separating the new family from the previously recognized families: Julidae Leach, 1814, Spirobolidae Bollman, 1893, Spirostreptidae Brandt, 1833, and Cambalidae Bollman, 1893.

The systematics of Pseudonannolenidae and its phylogenetic affinities with the other families of Spirostreptida Brandt, 1833 (Hoffman 1980; Mauriès 1987; Shelley 2002) have been strongly debated, with different hypotheses involving the suborders Cambalidea and Epinannolenidea Chamberlin, 1922. Mauriès (1980) placed Pseudonannolenidae in the so-called order Cambalida Bollman, 1893; later, he placed the family in the suborder Pseudonannolenidea Mauriès, 1983 (also in Cambalida) with Choctellidae Chamberlin & Hoffman, 1950, Iulomorphidae Verhoeff, 1924, and Physiostreptidae Silvestri, 1903 (Mauriès 1983); Mauriès (1987) recognized Pseudonannolenida Mauriès, 1983 as an order, and placed the families Iulomorphidae and Pseudonannolenidae (with the subfamilies Pseudonannoleninae and Physiostreptinae) in the suborder Pseudonannolenidea; Hoffman & Florez (1995) placed Pseudonannolenidae (including Physiostreptidae and Phallorthidae Chamberlin, 1952) in the order Spirostreptida; Hoffman (1999) placed the family in the suborder Epinannolenidea (also in Spirostreptida) (see Hoffman 1980). Jeekel (2004) placed the family in the artificial group 'Cambaloidea', which was created only to assemble all species belonging to the suborders Cambalidea and Epinannolenidea by Hoffman (1980).

The synopsis of Pseudonannolenidae, published by Mauriès (1987), was the first comprehensive taxonomic work that focused on some genera and species of the family. It included illustrations of the gonopods, the first leg-pair of males, and the penis of some species, and notes on types that had been supposedly lost or were unknown hitherto (see Taxonomic section for more details). Shelley (2002) summarized the taxonomic history of Pseudonannolenidae; Jeekel (2004) published the first tentative list of species described for the family, and Iniesta *et al.* (2020) proposed the first cladistic hypothesis, with emended diagnoses for the subfamilies Cambalomminae, Pseudonannoleninae, and Physiostreptinae.

The genus *Pseudonannolene* Silvestri, 1895

The Neotropical genus *Pseudonannolene* Silvestri, 1895, with ca 60 valid species, is the richest within Pseudonannolenidae (Hoffman 1980; Enghoff *et al.* 2015; Iniesta *et al.* 2020). The genus was proposed by Filippo Silvestri to accommodate two species: *Pseudonannolene typica* Silvestri, 1895 and *Pseudonannolene bovei* Silvestri, 1895, both collected by the Italian explorer Giacomo Bove in 1884, in the Argentine province of Misiones (Silvestri 1895a). Silvestri distinguished the monogeneric family from related taxa by the presence of a longitudinal suture on the promentum (Silvestri 1895a). Later, Silvestri (1896) designated *P. typica* Silvestri, 1895 as the type species of the genus, proposing an emended diagnosis for the family based mainly on the presence of the suture on the promentum, and the absence of posterior gonopods.

In the early 20th Century, Filippo Silvestri and Henry W. Brölemann described numerous species of *Pseudonannolene* from Argentina, Bolivia, Brazil, and Paraguay (Silvestri 1895a, 1895b, 1897b, 1902; Brölemann 1902a, 1902b, 1929). Halfway through that century, the German naturalist Otto Schubart focused part of his research on the taxonomy of the genus, describing 11 species and one subspecies. He also provided ecological information on the presence of ectoparasites, description of habitats, and agricultural importance of some species (Schubart 1944, 1945a, 1947, 1949, 1958, 1960).

Recently, there has been a growing interest in the taxonomy of *Pseudonannolene* in Brazil. The species of this group are widespread in karst regions, with occurrences of some obligatory cave-dwelling species (Iniesta & Ferreira 2013a, 2014; Gallo & Bichuette 2020). In Brazil, the identification and description of troglomorphic species (sensu troglobiont/troglobiotic species or population-race by Sket [2008]) has impacted regulations that protect certain Brazilian caves, and their surrounding areas, from mining (decree n° 6640/2008) (Karam-Gemael *et al.* 2018).

Despite recent publications on the diversity of *Pseudonannolene*, the cladistic relationships within the genus and the delimitation of some species remain poorly understood. After studying material from American and European collections, and collecting expeditions to almost all Brazilian subregions, we are now able to provide a systematic reassessment of all species of *Pseudonannolene*, including cladistic and biogeographical analyses and a taxonomic review. The aims of this study are: (i) to test the monophyly of *Pseudonannolene* in a morphology-based phylogeny; (ii) to investigate the biogeographic history of the genus using an event-based method; (iii) to present a complete taxonomic review, including redescriptions of known species, descriptions of new species, synonyms, and a dichotomous key.

Material and methods

Cladistic analysis

Group selection

The morphological cladistic analysis was performed using 91 characters (3 continuous and 88 discrete characters) and 63 terminal taxa (53 ingroup and 10 outgroup) (Supp. file 2). The list of all terminals used for the cladistic analysis is presented in Table 10. The ingroup is composed only by species of *Pseudonannolene* with males described. The outgroup is composed of terminals representing all subfamilies of Pseudonannolenidae, in addition to members of the families Choctellidae, Cambalidae, and Iulomorphidae. The species *Typhlonannolene adaptus* Chamberlin, 1923 (Pseudonannoleninae) was not included in the analysis since only female specimens are known. The terminal *Amastigogonus fossuliger* (Verhoeff, 1944) was used to root the trees based on morphological differences concerning Pseudonannolenidae (Iniesta *et al.* 2020).

Character sampling

The dataset for the analysis comprises 44 new characters here proposed and 47 previously used. Many of the characters used in this study were obtained or adapted from previous cladistic works on groups relatively close to Pseudonannolenidae, cited in the characters list: Julida Brandt, 1833 (Enghoff 1981, 1991), Spirobolida: Pachybolidae Cook, 1897 (Wesener *et al.* 2008), and Spirostreptida: Harpagophoridae Attems, 1909 (Pimvichai *et al.* 2010), as well as from descriptions of millipede genera and species (Loomis 1941; Hoffman 1965; Mauriès 1987; Korsos & Johns 2009; Mesibov 2017a, 2017b; Iniesta *et al.* 2020). Continuous characters (antennae, legs, and shape of the mentum) were coded based on their importance in previous analyses (Liu *et al.* 2017; Iniesta *et al.* 2020). For the antennae we used the length of antennomere III in relation to total length of the antenna, and for the legs we used the length of the femur in relation to the total length of the midbody leg as continuous characters. In order to remove the effects of the species size we opted for the rationalization of these characters according to their topological correspondence (see character description in Supp. file 1 for more details) (Fig. 3). The plots (Fig. 193) and the table of measured values (Tables 8–9, Supp. file 3) show all the variations obtained for the continuous characters used in the cladistic analysis. Inapplicable and unobserved characters (missing data) were scored as "–" and "?", respectively.

Analysis

The cladistic analysis was performed under the parsimony criterion, using TNT ver. 1.5 (Goloboff *et al.* 2008; Goloboff & Catalano 2016). Traditional searches were carried out heuristically with 3000 replicates by random addition sequences (RAS), followed by tree bisection-reconnection branch swapping (TBR) holding 100 trees per iteration. This procedure was repeated until the best score was hit 50 times. The random seed was set to 0. The searches of the trees were conducted under implied weights [IW] of the characters (Goloboff 1993; Goloboff *et al.* 2018) with different *k* values (1–10, 25) and equal weights [EW] in order to explore the clades variation according to the parameters tested in our analyses (Giribet 2003; Goloboff 2008; Goloboff *et al.* 2008; Grant & Kluge 2008a). Comparative analyses using frequency of clades (*commands: rfreq x [y]*) for the strict consensuses of different most-parsimonious trees under weighting regimes (IW and EW) were performed to determine topology stability. In this sense, the tree topology that shared the highest number of nodes with the other trees was considered the most stable, and thus, used for the discussion. A sensitivity plots analysis was used to indicate the frequency of clades in the preferred tree (Fig. 4). ASADO ver. 1.89 (Nixon 1999–2004) was used for character states optimizations (only discrete and non-ambiguous characters) of common synapomorphies.

In order to verify the influence of continuous characters on the results, comparisons between consensuses from a dataset with only discrete characters and one with concatenated (discrete + continuous) characters were obtained using SPR-distances (Subtree Pruning and Regrafting method) with 1000 replications and 0.100 of strength for weight moves. This procedure aimed to calculate the minimum of SPR-moves (= number of branch moves) enough to convert the tree topologies obtained from discrete characters for those of the concatenated dataset (for more details, see Goloboff *et al.* 2006; Goloboff 2008). In addition, we calculated the frequency of clades for the tree topologies with discrete and concatenated characters.

Goodman-Bremer [GBr] (Goodman *et al.* 1982; Bremer 1988, 1994; Grant & Kluge 2008b) and Bremer relative [Br] (Bremer 1994; Goloboff & Farris 2001) were used to evaluate clade support, searching for suboptimal trees with one to ten steps more than the most-parsimonious trees and retaining 2000–20 000 trees, respectively (*commands: sub 1 hold 2000; bb=tbr fillonly; unique**).

Biogeographic analysis

All the distributional data of species of *Pseudonannolene* included in the cladistic analysis were used to infer the biogeographic history of the genus using the method of Geographically explicit Event Model (GEM) (Arias 2017). This event-based method is based on the approaches of Hovenkamp (1997, 2001) using methods which explicitly incorporate the geographical information of distribution ranges (see Arias *et al.* 2011; Arias 2017). For this, the GEM does not assume predefined areas and their hierarchical relationships. The analysis was carried out using a raster grid with pixels of 1° × 1° degrees and filling of 1. The cost of the cladogenetic events associated with the nodes of the majority rule consensus tree was set to one, and to penalize large ancestral ranges a Z = 10 was used in the analysis. The search was made with the flipping algorithm applying 1000 replicates.

Taxonomic analysis

The taxonomic review is based on the study of 2404 specimens of *Pseudonannolene* housed in the following repositories indicated below.

ABAM	=	Coleção Biológica do Sul da Amazônia, Universidade Federal do Mato Grosso, Sinop, Mato Grosso, Brazil
CZUFMT	=	Coleção Zoológica da Universidade Federal do Mato Grosso, Cuiabá, Mato Grosso, Brazil
FCE	=	Faculdade de Ciências, Universidade da República, Uruguay
FMNH	=	Field Museum of Natural History, Chicago, USA
IBSP	=	Instituto Butantan, São Paulo, Brazil
ICN	=	Instituto de Ciencias Naturales de la Universidad Nacional de Colombia
INPA	=	Instituto Nacional de Pesquisas da Amazônia, Manaus, Amazonas, Brazil
ISLA	=	Invertebrados Subterrâneos de Lavras, Lavras, Minas Gerais, Brazil
ISNB	=	Institut royal des Sciences naturelles de Belgique (now IRSNB), Brussels, Belgium
MCN	=	Museu de Ciências Naturais, SEMA, Porto Alegre, Brazil
MCZ	=	Museum of Comparative Zoology, Cambridge, USA
MHNCI	=	Museu de História Natural do Capão da Imbuia, Curitiba, Paraná, Brazil
MSNG	=	Museo Civico di Storia Naturale "Giacomo Doria", Genova, Italy
MNRJ	=	Museu Nacional, Universidade Federal do Rio de Janeiro, Rio de Janeiro, Brazil
MZSP	=	Museu de Zoologia, Universidade de São Paulo, São Paulo, Brazil
NHMD	=	Zoological Museum, Natural History Museum of Denmark, Copenhagen, Denmark
UFPB	=	Coleção de Invertebrados Paulo Young, Universidade Federal da Paraíba, João Pessoa, Paraíba, Brazil
USNM	=	United States National Museum, Smithsonian Institution, Washington D.C., USA
ZMB	=	Museum für Naturkunde der Humboldt Universität zu Berlin, Berlin, Germany

Specimens were examined in 70% ethanol under a Leica MZ16A stereo microscope and Leica DM4000B microscope (Leica Camera, Wetzlar, Germany). Photographs were taken with a Leica DFC 500 digital camera mounted on a Leica MZ16A stereo microscope. Focus-stacked images were composed with Leica Application Suite ver. 2.5.0. The examined structures were clarified by 96 h in 70% lactic acid and mounted on microscope slides following Su (2016). For the Scanning Electron micrographs (SEM), the structures were cleaned ultrasonically in two cycles of 30 seconds, transferred to a 100% ethanol gradation (70%, 80%, 90%, and 100 % by 15 minutes), and left to dehydrate for ca 24 hours. These structures were then critically point dried, mounted, and coated with gold-palladium for observation. SEM images were taken using an FEI Quanta 250 (FEI Company, Hillsboro, Oregon, EUA), at the Laboratório de Biologia Celular, Instituto Butantan.

Measurements (in millimeters) of males and females were taken using the Leica Application Suite options in the Leica MZ16A. Numbers of podous and apodous rings, maximum midbody diameter, and total length were counted and measured only from complete specimens (Fig. 1). The measurements of length and diameter of podomeres follow Enghoff (1992). The coloration patterns are described based on specimens preserved in 70–80% ethanol. The descriptive notes here presented are based on the examined specimens, to supplement original description (or to describe females for the first time) and illustrate morphological features.

Since the topological terms for gonopodal views and the position of their parts have not been standardized in *Pseudonannolene* taxonomy (see Silvestri 1895a, 1897a, 1897b, 1902; Brölemann 1902a, 1929; Schubart 1944, 1945a, 1947, 1949, 1960; Mauriès 1974, 1987; Fontanetti 1996, 2000), we summarize all these different terms in the Table 1. Additionally, we used a standardized terminology for the gonopodal parts (Fig. 2), considering Koch (2015) and Iniesta *et al.* (2020). Immature males of *P. microzoporus* were analyzed regarding the ontogeny of the gonopods of *Pseudonannolene*. The abbreviations used in the taxonomic section and figures are indicated below.

Names of districts, provinces, altitude, and coordinates not included in the original labels were obtained from Google Earth (X; Y, datum WGS84). Distribution maps were made using the free software DIVA-GIS ver. 7.5.0. (Hijmans *et al.* 2001) with the locality data provided by the examined material, original descriptions, and records from literature. The biogeographical provinces (see Löwenberg-Neto 2014) were compiled following Morrone (2014). The maps of richness and records by species (Fig. 13) and the plots (Fig. 193) were obtained from packages "gplots" and "ConR ver. 1.2.2" (Dauby *et al.* 2017) in the software R ver. 3.5.0 (R Core Team 2017), respectively.

Abbreviations

amp = apicomesal process of solenomere
cx = coxa
ep = ectal process of solenomere
gcx = gonocoxa
ib = internal branch of telopodite
mp = medial process of solenomere
pn = penis
prf = prefemoral process
sa = seminal apophysis
sg = seminal groove
sh = shoulder of gonocoxa
sl = solenomere
tp = telopodite

Results

Comments on the gonopod morphology in Pseudonannolenidae

In order to clarify the issues regarding the morphology of the gonopod of species in Pseudonannolenidae (see Table 1), the following sections contain detailed comments on each gonopodal part. This discussion will serve as a guide to understand the results of the cladistic analysis, and it also serves as a template for the taxonomic descriptions that follow.

The gonopod primordia in the immatures stadia of *Pseudonannolene* correspond to a slightly differentiated plate, with rounded visible gonocoxae (***gcx***) and a constriction at about midlength, separating their distal section (Fig. 33A–C). Similar to what happens in the development of the gonopods in Spirostreptidae

Table 1. Different terminologies proposed for gonopod in *Pseudonannolene* Silvestri,1895.

	Silvestri (1895a–1902)	Brölemann (1902a–1929)	Schubart (1944–1958)	Mauriès (1974–1987)	Fontanetti (1996)
Gonocoxa	–	*Tronc des gonopodes*	*Coxa (coxito)*	*Coxite*	*Coxa*
Papillae	–	*Saillie dentiforme*	*Processos dentiformes*	–	*Dentiform processes*
Shoulder	–	*L'angle apical externe*	*Parte distal externa*	–	–
Internal branch	*Parte interna*	*Lambeau apical de la patte postérieure; Rameau secondaire (r2)*	*Telopodito*	–	*Telopodite*
Telopodite	*Parte externa*	*Lambeau apical de la patte antérieure; Rameau séminal (r1)*	*Solenomerito*	*Branche (lamelle) séminale*	*Solenomerite*
Solenomere	*Parte externa*	*Lamelles transpareates*	*Região escamosa*	*Branche (lamelle) séminale*	*Squamous portion*

(Brölemann 1920; Schubart 1945b; Krabbe 1982), the structure becomes more complex as the individual progresses from immature through, pre-adult to the adult stadium (Figs 33–34) (see also Schubart 1949: 216). In the pre-adult stadium, the gonopodal structures are already differentiated, although the apicomesal and ectal processes on the solenomere are still not fully developed (Fig. 34A–B). A single teratological case is reported for *Pseudonannolene robsoni* Iniesta & Ferreira, 2014, with the eighth and ninth leg-pairs modified into two apparently identical gonopods with seminal grooves extending from the gonocoxae to the apical region on the solenomere (Fig. 38).

Gonocoxa

It corresponds to the basal part of the gonopod, attached posteriorly to the aperture of the gonopod on the seventh body ring (Fig. 37D) by pairs of extensor and oblique muscles (Demange 1964). The gonocoxa (***gcx***) differs little in shape and size among the genera of Pseudonannolenidae. Rows of papillae are visible in the mesal portion, extending toward the telopodite (***tp***) basally (Figs 32A–C, 34A, C, 36). These projections are cuticular protrusions, apparently without any socket at their bases, and are present starting with the gonopodal primordia in the immature. They are also referred to as tubercles (in *Epinannolene* Brölemann, 1903 [Hoffman 1984]), papilliform tubercles (*Phallorthus* Chamberlin, 1952, [Hoffman & Florez 1995]), or dentiform processes (*Pseudonannolene*, Schubart 1944; Fontanetti 1996; Gallo & Bichuette 2020). The gonocoxa (***gcx***) is rounded and stout, slightly compressed longitudinally (Figs 32A–B, 34A, C, 38B), and with a small distal projection (= shoulder; ***sh***) in some species of *Pseudonannolene* (Fig. 36A).

Mesal cavity

It corresponds to a large cavity (= fossa) located mesally on the gonocoxa (***gcx***), from where the seminal groove (***sg***) emerges, extending towards the seminal apophysis (***sp***) (Figs 32, 36C). The mesal cavity of *Pseudonannolene* and *Epinannolene* have a globular projection bearing setae (Fig. 32C–F), while in the other pseudonannolenid genera these setae are arranged in a single row on the cavity and there are no globular projections.

Carl (1913a, 1913b) described for the first time the presence of a mesal cavity ("samengrube") on the gonocoxae of *Epinannolene* (Carl 1913a: 175, fig. 3) and *Holopodostreptus* Carl, 1913 (Carl 1913b: 215, fig. 4). Brölemann (1929) described the cavity ("ampoule") in *Pseudonannolene* with a globular projection (Brölemann 1929: figs 15–16, 26). Hoffman & Florez (1995) identified the cavity along the mesal region of *Phallorthus*, suggesting its possible function in the deposition of the seminal package before fecundation. Akkari & Enghoff (2012) described in detail the presence of a cavity (= fovea) for storage of spermatozoa at the base of the solenomerite on the posterior gonopod of species of *Ommatoiulus* Latzel, 1884 (Julida) (see also Verhoeff 1894; Enghoff 1995). Although this cavity is not obviously homologous with that observed in Pseudonannolenidae, in both structures the seminal groove (***sg***) extends up to the distal region of the gonopod posteriorly (Brölemann 1929: fig. 15), suggesting an analogous function for the mesal cavity and fovea. The mesal cavity is absent in the cambalidean families Cambalidae, Cambalopsidae Cook, 1895, Choctellidae, and Iulomorphidae.

Internal branch

The gonopods of Pseudonannolenidae present two well-developed distal branches (Fig. 36A): the internal and the external branch (= telopodite). The internal branch (***ib***) is located at the base of the telopodite (***tp***), bearing long setae marginally or apically (Figs 35A, C, E, 36C). Brölemann (1902a, 1929) described the internal branch (***ib***) as a secondary process, while Schubart (1944), Fontanetti (1996), and Gallo & Bichuette (2020) referred to it as the telopodite. According to the immatures of *Pseudonannolene* spp. examined by us, the branch is already noticeable in the pre-adult, and it arises from the coxal region (Figs 33C, 34A).

The internal branch (***ib***) is absent in *Holopodostreptus* and *Physiostreptus* Silvestri, 1903, while in *Phallorthus* it is reduced at the base of the stout telopodite (***tp***). In *Cambalomma* Loomis, 1941, the internal branch (***ib***) is closely adjacent to the gonocoxa (Loomis 1941: figs 4–5), and in *Epinannolene* it is well-developed and is located parallel to the telopodite (***tp***). In *Pseudonannolene* the branch is narrow and surrounds the telopodite (***tp***) basally, besides having a torsion of 180° and a distal projection in some species (Figs 69D–F, 114D–F).

Telopodite

The external branch of the gonopods is referred to here as the true telopodite (***tp***), composed of a glabrous trunk and a usually long, thin, squamous solenomere (***sl***), where the seminal apophysis (***sp***) and the opening of the seminal groove (***sg***) are located (Fig. 35). The distinction of the term telopodite (= external branch) from those used by previous authors in Pseudonannolenidae is justified by the presence of the seminal groove (***sg***) (Figs 35, 36C), used for injecting the seminal fluid from the male gonopore onto the vulvae (for more details, see Koch 2015).

The shape of the telopodite in Pseudonannolenidae tends to vary and is often used in taxonomic treatments. In *Phallorthus*, *Holopodostreptus*, and *Physiopstreptus* the telopodite (***tp***) is stout, large, and with the seminal apophysis not visible on the solenomere (***sl***). Only in *Holopodostreptus* and *Physiopstreptus*, the telopodite (***tp***) is setose and curved mesad (Carl 1913a; Mauriès 1987; Iniesta *et al.* 2020). In Cambalomminae and Pseudonannoleninae, the solenomere (***sl***) is narrow, with the seminal apophysis visible distally in most species (Loomis 1941; Hoffman 1984; Mauriès 1987). In *Epinannolene* and *Pseudonannolene* there are secondary processes, which are variable in shape and size (Figs 35, 75D–F, 110D–F, 126D–F, 141D–F).

Cladistic relationships

The heuristic searches under EW recovered 22 most parsimonious trees, with 191.40 steps, CI = 0.51, RI = 0.78, and RCI = 0.40. Under IW, values of the constant k = 4–7 recovered 27 most parsimonious trees with the same strict consensus. Searches from k = 1–3 and 8–10 recovered 15 most parsimonious trees with the same strict consensus, and k = 25 recovered 22 most parsimonious trees. All consensus trees under EW and IW are presented in the Figures 5–7, and the total fit for each k value are presented in the Table 2.

Table 2. Summary statistics from the implied weighting analysis. Abbreviations: *k* = concavity constant; T = number of topologies recovered; L = length.

	T	L	Fit
k = 1	15	197.77	55.49
k = 2	15	197.77	62.55
k = 3	15	194.64	66.57
k = 4	27	193.73	69.20
k = 5	27	193.73	71.07
k = 6	27	193.73	72.47
k = 7	27	193.73	73.56
k = 8	15	191.48	74.45
k = 9	15	191.48	75.19
k = 10	15	191.48	75.81
k = 25	22	191.40	79.69

The genus *Pseudonannolene* is recovered as monophyletic in all topologies obtained, with GBr = 0.57 and Br = 74. The genus is supported by three synapomorphies: promentum with longitudinal suture (char. 10 [1], Fig. 196D); basis of the penis not divided (char. 47 [1]; Fig. 209); internal branch surrounding the telopodite (char. 87 [1]; Figs 35, 222D), and two homoplastic transformations: lateral lobe of collum densely striated (char. 20 [1], Fig. 200B); setae of prefemoral process distributed along the entire process (char. 41 [1]; Fig. 207C). The species *P. scalaris* Brölemann, 1902 is recovered as the first lineage to diverge, followed by *P. rocana* Silvestri, 1902 and *P. alegrensis* Silvestri, 1897, respectively. Clade 11, composed of all terminals except *P. scalaris, P. rocana,* and *P. alegrensis*, is recovered by one synapomorphy: short telopodite (less than ½ gonocoxa in length) (char. 66 [1]; Fig. 214D); and one homoplastic transformation: internal branch elongated (longer or close to ½ telopodite in length) (char. 84 [1]; Fig. 220D).

The genus *Epinannolene* is recovered as sister-group of *Pseudonannolene* in Pseudonannoleninae. Two synapomorphies support the clade: a well-developed prefemoral process on the first pair of male legs (char. 36 [1]; Fig. 206D), tarsus of the second leg-pair elongated (longer than prefemur) (char. 46 [1]; Fig. 208B); and one homoplastic transformation: telopodite narrow (less than ½ gonocoxa) (char. 65 [1]; Fig. 214B), shared with *Holopodostreptus braueri* Carl, 1918. The family Pseudonannolenidae is monophyletic following the relationship (Physiostreptinae + (Cambalomminae + Pseudonannoleninae)), with five synapomorphies supporting the clade (chars. 11 [0], 32 [1], 42 [1], 50 [1], and 61 [1]) and two homoplastic transformations (chars. 28 [1] and 51 [1]).

For the following discussion we selected the consensus tree under IW and *k* = 4–7, according to the sharing of the nodes between EW and IW and the sensitivity plots analysis. The optimization of synapomorphies recovered in all resulting topologies (common synapomorphies) is shown in Figure 8, and the clade support values are shown in Figure 9. The lists of characters recovered to some clades are presented in Tables 3–7.

Biogeography

A total of 226 occurrence points were recorded for *Pseudonannolene*, with the majority of records by species and richness per grid in the Southeast region of Brazil (Fig. 13A–B). The region belongs to the Chacoan subregion (Morrone 2014), composed by Araucaria Forest, Atlantic, and Parana Forest

Table 3. List of characters recovered to support the clade *Pseudonannolene* Silvestri, 1895 from the cladistic analysis (see Fig. 4). Characters marked with an asterisk (*) are homoplastic synapomorphies.

Character	
10	Promentum, longitudinal suture: absent → present
***20**	Collum, lateral region: with few striae → densely striated
***41**	Prefemoral process, arrangement of setae: restricted to the proximal region → distributed up to the apical region
47	Penis, connection: absent → present
87	Internal Branch, position: parallel to the telopodite → enfolding the telopodite basally

Table 4. List of characters recovered to support the clade 15 and 16 from the cladistic analysis (see Fig. 4). Only discrete characters are shown. Characters marked with an asterisk (*) are homoplastic synapomorphies.

Character	**Clade 15**
***8**	Ommatidial cluster: well developed → reduced
***74**	Solenomere, apicomesal process: present → absent
	Clade 19
***73**	Seminal apophysis, position: medial → mesal
***76**	Solenomere, ectal process: absent → present

Table 5. List of characters recovered to support the clade 25 and 30 from the cladistic analysis (see Fig. 4). Only discrete characters are shown.

Character	**Clade 25**
67	Telopodite, curvature: rectilinear → strongly curved
	Clade 30
48	Penis, proximal extension: absent → present

Table 6. List of characters recovered to support the clade 36 and 38 from the cladistic analysis (see Fig. 4). Only discrete characters are shown. Characters marked with an asterisk (*) are homoplastic synapomorphies.

Character	**Clade 36**
***29**	Coxae on the first leg-pair, constriction in constriction: absent → present
	Clade 38
21	Metazonite: smooth → with granular striations
***26**	Epiproct: Apical region not exceeding the paraproct in length → Apical region exceeding the paraproct
27	Epiproct, triangular process: absent → present

Table 7. List of characters recovered to support the clade 40 and 47 from the cladistic analysis (see Fig. 4). Only discrete characters are shown. Characters marked with an asterisk (*) are homoplastic synapomorphies.

Character	Clade 40
*89	Internal branch, torsion in oral view: absent → present
	Clade 47
90	Internal branch, distal projection: absent → present

Table 8. Transformation costs for the continuous characters under equal and implied weights. Abbreviations: *k* = concavity constant; EW = equal weights; IW = implied weights.

Character	Transformation costs
1	Clade 13 (0.089–0.091 → 0.099) for EW and IW [*k* = 4–7]
2	Clade 16 (0.207 → 0.231); Clade 24 (0.231 → 0.245–0.253) for IW [*k* = 4–7] Clade 45 (0.233–0.246 → 0.285) for IW [*k* = 3–7]
3	Clade 30 (0.403 → 0.586–0.630); Clade 26 (0.403 → 0.163–0.205); Clade 50 (0.497–0.561 → 0.426); Clade 51 (0.426 → 0.422); Clade 52 (0.422 → 0.378) for EW and IW Clade 46 (0.186–0.233 → 0.267); Clade 83 (0.403 → 0.561); Clade 89 (0.442 → 0.233) for IW [*k* = 1–7] Clade 35 (0.422 → 0.497) for IW [*k* = 4–7]

provinces (Fig. 13C), with the climate ranging from humid subtropical to tropical wet and dry. The searches with GEM recovered two reconstructions with cost of 79 000, with few variations regarding different directions in the founder event and sympatry or point sympatry for some more inclusive clades (Fig. 14). The first biogeographic scenario obtained implies 4 vicariances, 13 sympatries, 4 points of sympatry, and 21 founder events (Fig. 14A), and the second scenario implies 4 vicariances, 12–13 sympatries, 4–5 points of sympatry, and 21 founder events (Fig. 14B). According to our reconstructions, the vicariance events occurred more frequently in clades closer to the root, whereas sympatry and points of sympatry occurred in more derived clades.

The first vicariance event in the cladogram was obtained in the basal node, separating *Pseudonannolene scalaris* from all other species of *Pseudonannolene*, and indicating that the first lineages to diverge within *Pseudonannolene* were distributed in the Pampas region in South America, followed by founder events towards eastern Uruguay and the Brazilian state of Rio Grande do Sul for *P. rocana* and *P. alegrensis*, respectively (Figs 14–15); a second vicariance event was recovered for *P. nicolau* sp. nov. (in the southern Amazon) + clade 12, followed by successive sympatries and founder events; the third vicariance was recovered in clade 13, with most records for the Atlantic Forest and disjunct occurrence from Xingu-Tapajós province (*P. leucomelas* Schubart, 1947 + *P. spelaea* Iniesta & Ferreira, 2013); the fourth vicariance was obtained in clade 16, composed mostly by species distributed in the Bambuí Limestone Group (a late Neoproterozoic sedimentary cover from the São Francisco craton in eastern-central Brazil) and in the coastal region of the Brazilian state of São Paulo (clades 29 + 25, respectively), and in the Cerrado biome (a tropical savanna ecoregion) from São Paulo (Fig. 14).

Table 9 (continued on next three pages). Measured values for the continuous characters (chars. 1–3) in the cladistic analysis of *Pseudonannolene* Silvestri, 1895. Abbreviations: N = number of specimens sampled; an3 = antennomere 3; anT = total length of antenna; Fm = femur of midbody leg; LeT = total length of midbody leg; GnW = gnathochilarium widht; GnL = gnathochilarium length.

Terminal			**Values**	
	N	**an^3/anT**	**Fm/LeT**	**GnW/GnL**
Cambalidae				
Cambala speobia	1	0.146	0.130	–
Choctellidae				
Choctella cumminsi	1	0.171	0.163	1.063
Choctella hubrichti	1	0.169	0.163	1.062
Pseudonannolenidae: Cambalomminae				
Cambalomma laevis	1	0.196	0.227	0.900
Pseudonannolenidae: Physiostreptinae				
Phallorthus colombianus	5	0.182–0.191	0.178–0.191	0.854
Holopodostreptus braueri	5	0.190–0.195	0.162–0.225	1.070
Pseudonannolenidae: Pseudonannoleninae				
Epinannolene paraensis	1	0.170	0.147	0.900
Epinannolene exilio	5	0.188–0.199	0.155–0.160	1.001
Epinannolene sp.	1	0.173	0.149	0.902
Pseudonannolene albiventris	5	0.194–0.204	0.167–0.189	1.057
Pseudonannolene alegrensis	5	0.196–0.228	0.149–0.233	0.769
Pseudonannolene ambuatinga	5	0.174–0.201	0.181–0.188	1.026
Pseudonannolene anapophysis	3	0.179–0.197	0.252–0.327	0.844
Pseudonannolene bovei	1	0.182	0.189	–
Pseudonannolene buhrnheimi	5	0.172–0.277	0.195–0.224	1.226
Pseudonannolene caatinga	5	0.184–0.283	0.139–0.256	0.964
Pseudonannolene centralis	1	0.188	0.199	1.014
Pseudonannolene callipyge	5	0.187–0.244	0.157–0.458	0.997
Pseudonannolene microzoporus	5	0.189–0.291	0.161–0.208	0.981
Pseudonannolene curtipes	5	0.214–0.231	0.177–0.195	0.941
Pseudonannolene erikae	5	0.202–0.280	0.196–0.220	0.841
Pseudonannolene fontanettiae	5	0.185–0.226	0.188–0.246	0.928
Pseudonannolene halophila	5	0.174–0.233	0.191–0.310	1.001
Pseudonannolene imbirensis	1	0.151	0.202	1.206
Pseudonannolene inops	5	0.195–0.215	0.182–0.233	0.891
Pseudonannolene leopoldoi	5	0.188–0.196	0.111–0.177	0.967
Pseudonannolene leucocephalus	1	0.207	0.191	0.889
Pseudonannolene leucomelas	1	0.218	0.182	–

Table 9 (continued).

Terminal	*N*	Values an³/anT	Fm/LeT	GnW/GnL
Pseudonannolenidae: Pseudonannoleninae				
Pseudonannolene longicornis	5	0.179	0.266	0.876
Pseudonannolene lundi	5	0.148–0.194	0.187–0.199	0.977
Pseudonannolene magna	1	0.195	0.206	0.953
Pseudonannolene maritima	5	0.187–0.215	0.159–0.232	0.895
Pseudonannolene mesai	5	0.194–0.227	0.187–0.221	0.844
Pseudonannolene occidentalis	5	0.181–0.202	0.174–0.189	1.040
Pseudonannolene ophiiulus	1	0.203	0.207	1.004
Pseudonannolene parvula	5	0.188–0.200	0.144–0.178	1.122
Pseudonannolene patagonica	1	0.195	0.199	1.148
Pseudonannolene paulista	5	0.175–0.226	0.176–0.198	1.071
Pseudonannolene pusilla	5	0.196–0.247	0.159–0.246	0.859
Pseudonannolene robsoni	5	0.212–0.244	0.192–0.229	0.962
Pseudonannolene rolamossa	5	0.187–0.244	0.195–0.210	0.996
Pseudonannolene sebastiana	5	0.185–0.238	0.186–0.223	1.037
Pseudonannolene segmentata	5	0.188–0.204	0.147–0.196	0.854
Pseudonannolene scalaris	1	–	0.183	–
Pseudonannolene silvestris	5	0.172–0.204	0.194–0.274	1.092
Pseudonannolene spelaea	5	0.214–0.337	0.173–0.198	0.946
Pseudonannolene strinatii	5	0.192–0.238	0.188–0.209	1.041
Pseudonannolene tocaiensis	1	0.209	0.192	1.074
Pseudonannolene tricolor	3	0.190–0.212	0.177–0.192	0.971
Pseudonannolene typica	1	0.346	0.192	1.026
Pseudonannolene urbica	5	0.191–0.204	0.153–0.220	0.962
Pseudonannolene xavieri	5	0.198	0.210	0.963
Pseudonannolene bucculenta sp. nov.	5	0.186	0.180–0.239	0.863
Pseudonannolene morettii sp. nov.	5	0.175–0.224	0.183–0.228	1.018
Pseudonannolene insularis sp. nov.	5	0.200–0.217	0.185–0.205	1.130
Pseudonannolene nicolaru sp. nov.	5	0.191–0.203	0.169–1.902	0.999
Pseudonannolene granulata sp. nov.	1	0.707	0.208	0.923
Pseudonannolene alata sp. nov.	5	0.176–0.229	0.193–0.211	0.894
Pseudonannolene curvata sp. nov.	5	0.194–0.235	0.185–0.260	1.126
Pseudonannolene aurea sp. nov.	5	0.196–0.235	0.171–0.269	1.036
T =	**224**	**0.146–0.707**	**0.111–0.458**	**0.769–1.148**

Table 10 (continued on next page). List of terminals used in the cladistic analysis of *Pseudonannolene* Silvestri, 1895. For the terminals with asterisk (*), the male characters were scored according to their descriptions since the gonopods were not found with the types.

Terminal	Data source
Outgroup	
Iulomorphidae	
Amastigogonus fossuliger	This study
Cambalidae	
Cambala speobia	This study
Choctellidae	
Choctella cumminsi	This study
Choctella hubrichti	This study
Pseudonannolenidae: Cambalomminae	
Cambalomma laevis	This study
Pseudonannolenidae: Physiostreptinae	
Phallorthus colombianus	This study
Holopodostreptus braueri	This study
Pseudonannolenidae: Pseudonannoleninae	
Epinannolene paraensis	This study
Epinannolene exilio	This study
Epinannolene sp. (Suaita, Colombia)	This study
Ingroup	
Pseudonannolene albiventris	This study
Pseudonannolene alegrensis	This study
Pseudonannolene ambuatinga	This study
Pseudonannolene anapophysis	This study
*Pseudonannolene bovei**	Silvestri (1895a) and this study
Pseudonannolene buhrnheimi	This study
Pseudonannolene caatinga	This study
Pseudonannolene caulleryi	Brölemann (1929)
Pseudonannolene centralis	This study
Pseudonannolene callipyge	This study
Pseudonannolene microzoporus	This study
Pseudonannolene curtipes	This study
Pseudonannolene erikae	This study
Pseudonannolene fontanettiae	This study
Pseudonannolene halophila	This study
Pseudonannolene imbirensis	This study
Pseudonannolene inops	This study
Pseudonannolene leopoldoi	This study
Pseudonannolene leucocephalus	This study

Table 10 (continued).

Terminal	Data source
Ingroup	
*Pseudonannolene leucomelas**	Schubart (1947) and this study
Pseudonannolene longicornis	This study
Pseudonannolene lundi	This study
Pseudonannolene magna	This study
Pseudonannolene maritima	This study
Pseudonannolene mesai	This study
Pseudonannolene occidentalis	This study
Pseudonannolene ophiiulus	This study
Pseudonannolene parvula	This study
*Pseudonannolene patagonica**	Brölemann (1902a) and this study
Pseudonannolene paulista	This study
Pseudonannolene pusilla	This study
Pseudonannolene robsoni	This study
Pseudonannolene rocana	This study
Pseudonannolene rolamossa	This study
Pseudonannolene sebastiana	This study
Pseudonannolene segmentata	This study
Pseudonannolene scalaris	This study
Pseudonannolene silvestris	This study
Pseudonannolene spelaea	This study
Pseudonannolene strinatii	This study
Pseudonannolene tocaiensis	This study
Pseudonannolene tricolor	This study
Pseudonannolene typica	This study
Pseudonannolene urbica	This study
Pseudonannolene xavieri	This study
Pseudonannolene alata sp. nov.	This study
Pseudonannolene aurea sp. nov.	This study
Pseudonannolene bucculenta sp. nov.	This study
Pseudonannolene curvata sp. nov.	This study
Pseudonannolene granulata sp. nov.	This study
Pseudonannolene insularis sp. nov.	This study
Pseudonannolene morettii sp. nov.	This study
Pseudonannolene nicolau sp. nov.	This study

Taxonomy

Class Diplopoda Gervais, 1844
Order Spirostreptida Brandt, 1833
Suborder Cambalidea Cook, 1895
Family Pseudonannolenidae Silvestri, 1895
Subfamily Pseudonannoleninae Silvestri, 1895

Genus ***Pseudonannolene*** Silvestri, 1895

Pseudonannolene Silvestri, 1895a 34: 775.

Pseudonannolene – Silvestri 1895b: 7; 1896: 170; 1897a: 651. — Cook 1895: 6. — Brölemann 1902a: 120; 1929: 7. — Carl 1913a: 174; 1914: 855. — Attems 1926: 206. — Verhoeff 1943: 269. — Jeekel 1971: 113. — Mauriès 1977: 248; 1983: 250; 1987: 170. — Hoffman 1980: 91. — Hoffman & Florez 1995: 116. — Hoffman *et al.* 1996: 14. — Golovatch *et al.* 2005: 279. — Iniesta & Ferreira 2013a: 92. — Shelley & Golovatch 2015: 7. — Hollier *et al*. 2017: 218. — Iniesta *et al.* 2020: 5.

Type species

Pseudonannolene typica Silvestri, 1895, by subsequent designation (Silvestri 1896: 170).

Etymology

From the Greek prefix 'pseudo' = 'false, not genuine', + '*nannolene*', in reference to the apparent similarity with the cambalidean genus *Nannolene* Bollman, 1887. The name is regarded as a feminine noun.

Diagnosis

A genus of Pseudonannolenidae easily diagnosed by the presence of a longitudinal suture on the promentum (Fig. 19E–F). Gonopods of *Pseudonannolene* resemble those of *Epinannolene* (Pseudonannoleninae) by the presence of rows of papillae on the mesal region of the gonocoxae and by two well-developed distal branches, but differ by the presence of a narrow internal branch enfolding the telopodite basally (Fig. 35A, C, E), vs internal branch parallel to the telopodite in *Epinannolene*. Females of *Pseudonannolene* are recognized by the vulvae connecting only distally (Fig. 39A), vs vulvae connected along their entire mesal portion in *Epinannolene*.

Redescription

Measurements. Euanamorphic species, body in adults with 50–81 body rings (1–3 apodous + telson); length 20–137.5 mm; maximum midbody diameter 1.2–6.8 mm.

Color. Variable, from depigmented (troglomorphic species) (Fig. 18B, E) to darker brown or blackish (Figs 17, 18A–D, F); most species with brownish body and metazonites with a reddish posterior band.

Head. Slightly convex, with a row of labral setae and 3+3 supralabral setae (Fig. 19A–B); scattered setae on frontal region in *P. centralis* and *P. occidentalis* (Fig. 19B). Labrum with three medial teeth (Figs 19A–B, 23A). Antennae usually elongated, slender (Figs 21–22, 163–164); bacilliform setae on antennomere V and VI (Figs 21B–E, 22B–D), and four large apical cones (Figs 21B, D, 22B, E). Ommatidial cluster well-developed; ommatidia depigmented to brownish, elliptical, arranged horizontally in 4–6 rows (Fig. 19D). Mandibular stipes usually with margin narrow; external tooth long, with 2–3 lobes; internal tooth with 4–5 lobes decreasing in size from posterior to anterior (Fig 20C–E); number of pectinate lamellae variable (Fig. 20D–E), fringes positioned basally (Fig. 20E–F). Molar plate with distal transverse groove (Fig. 20A–B, D). Epipharynx with 1+1 lateral keel and one medial keel, long fringes positioned distally; outer and inner subcylindrical palps (Fig. 24).

Gnathochilarium (Figs 19E–F, 167–176). Mentum pentagonal, males with medial depression deeply invaginated; paired projections observed in males of *P. bucculenta* sp. nov., and long setae in males of *P. morettii* sp. nov. and *P. parvula*. Promentum subtriangular, setose, with transverse suture separating it from mentum and a longitudinal suture separating promentum into two equal halves. Lamellae linguales with scattered setae surrounding central pads. Stipes slightly S-shaped, males of some species with distal region swollen (Fig. 108C); number of distal setae variable, stipital spurs absent; with proximal projections bearing setae in males of *P. granulata* sp. nov. (Figs 175A, 198B) and *P. callipyge* (Fig. 168D).

Body rings. Collum with lateral lobes broadly rounded, densely striated (Fig. 19C); in some species, the lobes are strongly curved ectad (Fig. 66A). Following body rings very faintly constricted between prozonite and metazonite (Figs 26A–B, 27A); prozonites smooth; metazonites laterally with transverse striae below ozopore (Fig. 26C), in some species metazonites are strongly granulated (Fig. 26D). Anterior sternites subrectangular; slightly curved medially (Figs 25A–B, 167–176), in some species with transverse striae. Posterior sternites elliptical (Fig. 25A–B). Spiracles positioned proximally (Fig. 25C–F). Ozopore positioned at midlength of metazonite (Figs 26A–B, E, 27A), ozadene oval (Fig. 27C). Epiproct with rounded tip (Fig. 28A, C); with subtriangular process in *P. buhrnheimi* and *P. granulata* sp. nov. (Figs 28D, 53B, 54, 153B). Paraproct with small setae on distal margin (Fig. 28); with projections bearing setae in *P. alegrensis* (Figs 44B, 202C). Hypoproct subrectangular (Fig. 28A–B). Midbody legs as long as half body diameter; without ventral pads; femur elongated. Prefemur, femur, postfemur, and tibia with long setae on mesal region (Figs 29A–D, 165–166); tarsus densely setose (Fig. 29A–D), with tarsal claw (Fig. 29E).

First leg-pair of males. Coxae elongated and setose, ranging from subtriangular (Fig. 30A) to subrectangular shape (Fig. 30B), with the base slightly arched; prefemoral process subcylindrical in most species (Fig. 30A–D), hexagonal in *P. erikae* (Fig. 30F) or absent in *P. anapophysis* Fontanetti, 1996 (Fig. 49A–B); densely setose along entire extension or up to median region; remaining podomeres with setae along the mesal region. Tarsal claw present.

Second leg-pair of males. Coxae fused basally, only distally paired (Fig. 31A); large, rounded or subrectangular-shaped; penis located at the proximal region, rounded (Fig. 31C, F); penial bases fused, extended basally in some species (Fig. 31C). Gonopore positioned distally, with short apical setae (Fig. 31C–F). Prefemur compressed dorsoventrally; remaining podomeres setose, with long setae on the mesal region (Fig. 31B); tarsal claw present.

Second leg-pair of females. Coxae fused basally; large, subrectangular-shaped (Fig. 39A); vulvar sacs large, located basally in anal view (Fig. 39B–C). Prefemur compressed dorsoventrally; remaining podomeres densely setose, with setae on the mesal region (Fig. 39C); tarsal claw present.

Gonopods (Figs 2, 32–36, 38). Gonocoxa elongated, twice as long as telopodite; with base slightly arched; antero-posteriorly flattened; with rows of papillae positioned mesally. A large cavity located mesally on gonocoxa (Fig. 32A–B); with globular projection bearing setae (Fig. 32D–F); seminal groove curved, arising medially on mesal cavity and terminating apically on the seminal apophysis. Shoulder of gonocoxa positioned apically, present in most species. Gonopods distally divided into telopodite and internal branch (Fig. 35A, C, E). Telopodite separated from gonocoxa by shallow furrow; trunk of telopodite glabrous; with rounded laterad projection in some species. Solenomere with squamous surface, rounded apically, without or with subtriangular processes: apicomesal, ectal, and medial (Figs 35, 36A–C, 217); form, length, and position of these processes are variable in most species. Seminal apophysis located at mesal, medial or ectal portion on solenomere. Internal branch located at the base of telopodite, with setae marginally or apically; the form and length of the branch is variable, in some species it is narrow (Fig. 35A), swollen apically (Fig. 35C) or with a horizontal plate (Fig. 222E). Some species with internal branch twisted 180° (Fig. 222D) and with distal projection (Fig. 222F).

Vulvae (Figs 40, 177–179). Vulvae embedded behind second leg-pair (Fig. 32A–C). Bursa subtriangular; glabrous (Fig. 32D–F). Internal valve subtriangular; connected with opposite internal valve only distally. Operculum narrow; situated laterally. External valve wide; subtriangular.

Distribution

Known only from the South American continent, ranging from French Guiana (*P. rugosetta*) down to southern Argentina (*P. patagonica* Brölemann, 1902). Despite the wide distribution of the genus throughout the Chacoan biogeographic subregion (sensu Morrone 2014) (Fig. 13), most of the species are narrowly distributed, often known only from the type locality (Figs 180–191).

Taxonomic notes

For some species described by Silvestri between the years 1895–1902 and collected by Alfredo Borelli in surrounding areas from the rivers Apa and La Plata, the type material was not found in collections where they were supposedly deposited. The same situation has been noted in other millipedes groups (for instance, Chelodesmidae Cook, 1895, Paradoxosomatidae Daday, 1889, Spirostreptidae) and centipedes (Geophilomorpha Pocock, 1895) (Jeekel 1965; Hoffman 1981, 1982; Krabbe 1982; Pena-Barbosa *et al.* 2013; Calvanese *et al.* 2019). A list of species described by Silvestri with their respective repositories was compiled by Viggiani (1973), although some species of *Pseudonannolene* were not listed by the author.

Ecological remarks

The biology of species of *Pseudonannolene* is poorly known, with some information restricted to species regarded as agricultural pests or cave-dwelling (Schubart 1942, 1944, 1945a, 1947, 1949, 1958, 1960; Bock & Lordello 1952; Lordello 1954; Freitas *et al.* 2004; Iniesta & Ferreira 2013a). The available data on the phenology of species suggest that they tend to have a predilection to warm and humid periods, varying from a subtropical climate to tropical in the Chacoan subregion (Fig. 13).

The species *P. paulista* Brölemann, 1902 and *P. tricolor* have been reported to feed on potato (*Solanum tuberosum* L.), melon (*Cucumis melo* L.), and beet (*Beta* spp. L.) (Bock & Lordello 1952; Lordello 1954). In addition to *P. ophiiulus* Schubart, 1944, these species have been also observed in second-growth forests, *Eucalyptus* spp. and *Musa* spp., and in open areas with a predominance of shrub species (Schubart 1944, 1945a). The species *P. leucomelas* has been recorded only from growing areas in northwestern Mato Grosso, Brazil (Schubart 1944), while *P. leucocephalus* Schubart, 1944, *P. silvestris* Schubart, 1944, and *P. urbica* Schubart, 1945 have been found in any area with availability of organic deposits (Schubart 1944, 1945a). The species *P. alegrensis*, *P. leucocephalus*, *P. ophiiulus*, *P. paulista*, *P. silvestris*, *P. tricolor*, and *P. urbica* are also reported in man-made and disturbed habitats such as houses, gardens, farms, and roadsides (Silvestri 1897c; Schubart 1944, 1945a, 1949; Bock & Lordello 1952).

Most species of *Pseudonannolene* are found in outcrops of limestone rocks (Trajano 1987; Trajano & Gnaspini-Netto 1991; Pinto-da-Rocha 1995; Fontanetti 1996; Trajano *et al.* 2000; Freitas *et al*. 2004; Iniesta & Ferreira 2014; Gallo & Bichuette 2019). The species *P. ambuatinga*, *P. lundi* Iniesta & Ferreira, 2015, and *P. spelaea* are restricted to caves, presenting troglomorphisms such as depigmentation and body size reduction (Iniesta & Ferreira 2013a, 2015). The troglophilic species *P. microzoporus*, *P. robsoni*, and *P. tocaiensis* Fontanetti, 1996 have been found near vegetal debris (for instance, rotten trunks and litter) or guano of *Desmodus rotundus* (Geoffroy, 1810) (Chiroptera) inside caves, while *P. robsoni*, *P. leopoldoi* Iniesta & Ferreira, 2014, and *P. callipyge* Brölemann, 1902 (Fig. 17B–C) have been commonly observed feeding on fungi and organic debris in aphotic zones and cave entrances.

Pseudonannolene albiventris Schubart, 1952
Figs 41–43, 163A, 167A, 177A, 180; Supp. file 4: Figs 218D, 219A

Pseudonannolene albiventris Schubart, 1952: 408, figs 5–8.

Pseudonannolene albiventris – Jeekel 2004: 88. — Gallo & Bichuette 2017: 4; 2020: 36.
cf. *Pseudonannolene albiventris* – Gallo & Bichuette 2017: 6, figs 4f, 5f, 9h.

Diagnosis

Males of *P. albiventris* resemble those of *P. caulleryi* Brölemann, 1929 and *P. mesai* Fontanetti, 2000 by having a large trunk of the telopodite (Fig. 42D–F), but differing by the subrectangular coxae on the first leg-pair (Fig. 42A); suboval penis (Fig. 42C); solenomere with short and rounded ectal process (Fig. 42D–F).

Etymology

Named after the Latin adjective '*albus*' = 'white', plus the masculine noun '*venter*', referring to the whitish ventral region of the body rings (Schubart 1952).

Material examined

Holotype

BRAZIL • ♂ [gonopods, gnathochilarium, first and second leg-pair on microscope slides]; São Paulo, Analândia, Fazenda Nova América; [-22.129298, -47.662635]; 665 m a.s.l.; 7 Mar. 1944; O. Schubart leg.; MZSP.

Paratypes (total: 3 ♂♂, 1 ♀, 1 immature)

BRAZIL • 1 ♂; same collection data as for holotype; MZSP 1008 • 2 ♂♂, 1 ♀, 1 immature; same collection data as for holotype; MZSP.

Other material (total: 12 ♂♂, 16 ♀♀, 23 immatures)

BRAZIL – **São Paulo** • 1 ♂, 1 ♀; same collection data as for holotype; MZSP 1007 • 1 ♂; same collection data as for holotype; MZSP 1008 • 2 ♂♂, 1 ♀, 1 ♀ immature; same collection data as for holotype; MZSP • 1 ♂; Piracicaba; [-22.735152, -47.647892]; 532 m a.s.l.; 24 Oct. 1949; F.P. Monteiro leg., MZSP • 1 ♂; same collection data as for preceding; MZSP • 1 ♀ immature, 1 ♂ immature; same collection data as for preceding; MZSP • 10 ♀♀; same collection data as for preceding; MZSP • 2 ♀♀, 8 ♀♀ immatures; Cordeirópolis, Estação Experimental de Cordeirópolis (= Centro de Citricultura Sylvio Moreira); [-22.462172, -47.399190]; 737 m a.s.l.; Feb. 1952; L.G. Lordello leg.; MZSP • 1 ♂; same collection data as for preceding; MZSP • 1 ♂; same collection data as for preceding; MZSP • 2 ♂♂, 1 ♀, 8 ♀♀ immatures; same collection data as for preceding; MZSP • 2 ♂♂, 1 ♀, 2 ♀♀ immatures; same collection data as for preceding; Dec. 1952; MZSP • 1 ♀ immature; same collection data as for preceding; Feb. 1953; MZSP • 1 ♀ immature; Campinas, Viracopos; [-22.968361, -47.153399]; 619 m a.s.l.; Feb. 1953; L.G. Lordello leg.; MZSP.

Descriptive notes

Measurements. 59–63 body rings (1–2 apodous + telson). Males: body length 35–45 mm; maximum midbody diameter 2.4–2.5 mm. Females: body length 35–45 mm; maximum midbody diameter 2.3–3.1 mm.

Color. Body color brownish; metazonites with a medial brown band and a posterior lighter band; antennae and legs light brown (Fig. 41).

Head. Antennae short (Fig. 163A), just reaching back to end of ring 4 when extended dorsally; antennomeres goblet-shaped; relative antennomere lengths 1<2<3>4=5=6>7. Mandibular cardo with ventral margin narrow. Ommatidial cluster well-developed, elliptical; ca 35 ommatidia in 5 rows.

Body rings. Collum with lateral lobes broadly rounded, with ca 4 striae, slightly curved ectad (Fig. 41A). Very faintly constriction between prozonite and metazonite; prozonites smooth; metazonites laterally with transverse striae from ca ⅓ length below ozopore. Anterior sternum subrectangular, with 8 faint transverse striae (Fig. 167A).

First leg-pair of males. Coxae (***cx***) elongated (as long as the sum of remaining podomere lengths), subrectangular, with the base arched, densely setose (Figs 42A, 43B); prefemoral process (***prf***) as long as half of prefemur, subcylindrical, densely setose up to its median region (Fig. 42B); remaining podomeres with setae along mesal region.

Second leg-pair of males. Coxa (***cx***) large and rounded; penis (***pn***) located at proximal region, suboval, extended basally (Figs 42C, 43E–F); prefemur compressed dorsoventrally; remaining podomeres setose.

Gonopods. Gonocoxa (***gcx***) elongated, almost twice as long as telopodite, with the base arched; slightly flattened antero-posteriorly (Fig. 42E–F); with rows of papillae mesally. Seminal groove (***sg***) curved; arising medially on mesal cavity and terminating apically on the seminal apophysis (***sa***). Shoulder (***sh***) rounded. Telopodite (***tp***) almost as wide as ***gcx*** (Figs 42D, 43D); solenomere (***sl***) with apicomesal process (***amp***) subtriangular, larger; ectal process (***ep***) rounded; ***sa*** located at mesal portion, slightly visible apically. Internal branch (***ib***) subtriangular, narrow, surrounding basally ***tp*** as a shield; ***ib*** with setae along its entire margin exceeding apically seminal region of ***sl*** (Fig. 42D–F).

Vulvae. As typical for the genus. Bursa subtriangular, glabrous (Fig. 177A); internal valve subtriangular; operculum narrow, curved medially; external valve wide, subtriangular.

Distribution

Known from the central-west region of the state of São Paulo, Brazil (Fig. 180); occurring in the Cerrado biome (tropical savanna ecoregion) and in second-growth forests in the region.

Pseudonannolene alegrensis Silvestri, 1897
Figs 44–45, 175E, 175B, 180; Supp. file 4: Figs 202C, 214C

Pseudonannolene alegrensis Silvestri, 1897c: 19, pl. iii fig. 28.

Pseudonannolene alegrensis – Brölemann 1909: 56. — Viggiani 1973: 366. — Jeekel 2004: 88. — Iniesta & Ferreira 2013b: 357.

Justification of neotype designation

The type material of *P. alegrensis* deposited in the Senckenberg Naturhistorische Sammlungen, Dresden, Germany (SMTD), and other types of millipedes described by Silvestri in 1897, were lost during the bombing of Dresden on October 7, 1944 (Sierwald & Reft 2004: 47). The species was described by Silvestri (1897c) based on an adult female collected in Porto Alegre, Rio Grande do Sul State, Brazil. Since no name-bearing type specimens for *P. alegrensis* exist and to secure the stability of the nomenclature, we selected topotype material from MCN to designate the neotype (for more details, see article #75.3.5 of ICZN).

Diagnosis

Males of *P. alegrensis* resemble those of *P. rocana* by having an elongated telopodite (longer than half of gonocoxa) (Fig. 45D–F), but differing by the presence of a large prefemoral process on the first leg-pair (Fig. 45A–B); subtriangular solenomere (Fig. 45D); and by having projections bearing setae on the paraproct (Supp. file 4: Fig. 202C).

Etymology

Adjective referring to the type locality of the species (Silvestri 1897c).

Material examined

Neotype (here designated)
BRAZIL • 1 ♂; Rio Grande do Sul, Porto Alegre, Lomba do Pinheiro; [-30.116949, -51.101999]; 124 m a.s.l.; 17 Jul. 2010; M. Poiret leg.; MCN 626.

Other material (total: 3 ♂♂, 6 ♀♀, 4 immatures)
BRAZIL – **Rio Grande do Sul** • 2 ♂♂, 5 ♀♀, 4 immatures; same collection data as for neotype; MCN 626 • 1 ♂, 1 ♀; Barra do Ribeiro, Fazenda Boa Vista; [-30.292875, -51.316045]; 17 m a.s.l.; 18 Dec. 2003; R. Ott leg.; MCN 521.

Descriptive notes

Measurements. 58–60 body rings (1–2 apodous + telson). Males: body length 35–42.5 mm; maximum midbody diameter 1.8–1.9 mm. Females: body length 36–41 mm; maximum midbody diameter 2–3.1 mm.

Color. Body color greyish; prozonites darker; metazonites with a medial dark grey band and a posterior lighter one; head, collum, antennae and legs lighter brown.

Head. Antennae short (Fig. 44A), just reaching back to end of ring 4 when extended dorsally; relative antennomere lengths 1<2<3>4<5≈6>7. Mandibular cardo with ventral margin swollen. Ommatidial cluster well-developed, elliptical; ca 20 ommatidia in 5 rows.

Body rings. Collum with lateral lobes broadly rounded, with ca 6 striae (Fig. 44A). Very faintly constricted between prozonite and metazonite; prozonites smooth; metazonites laterally with transverse striae below ozopore. Anterior sternum subrectangular, without transverse striae (Fig. 175E). Paraproct with rounded projections bearing setae (Fig. 44B).

First leg-pair of males. Coxae (***cx***) elongated (as long as the sum of remaining podomere lengths), subtriangular, with the base arched, densely setose (Fig. 45A); prefemoral process (***prf***) as wide as half width of prefemur, subcylindrical, densely setose up to its median region (Fig. 45B); remaining podomeres with setae along the mesal region.

Second leg-pair of males. Coxa (***cx***) large and rounded; penis (***pn***) located at proximal region, rounded, not extended basally (Fig. 45C); prefemur compressed dorsoventrally; remaining podomeres setose, with long setae mesally.

Gonopods. Gonocoxa (***gcx***) elongated, but less than twice the length of the telopodite, with the base arched; slightly flattened antero-posteriorly (Fig. 45D–F); with rows of papillae mesally. Seminal groove (***sg***) curved; arising medially on mesal cavity and terminating apically on the seminal apophysis (***sa***). Shoulder (***sh***) inconspicuous. Telopodite (***tp***) elongated, trunk stout (Fig. 45D); solenomere (***sl***) with apicomesal process (***amp***) subtriangular; ectal process absent; ***sa*** located at medial portion, visible apically. Internal branch (***ib***) subtriangular, narrow, curved ectad at midlength, surrounding the base of ***tp***; ***ib*** with setae along its entire margin not exceeding apically the seminal region of ***sl*** (Fig. 45D–F).

Vulvae. As typical for the genus. Bursa subtriangular, glabrous (Fig. 177B); internal valve subtriangular, with mesal region rounded; operculum narrow, curved medially; external valve wide, subtriangular.

Distribution

Known only from the type locality Porto Alegre, Rio Grande do Sul, Brazil (Fig. 180).

Pseudonannolene ambuatinga Iniesta & Ferreira, 2013

Figs 46–47, 165A, 167B, 177C, 180; Supp. file 4: Figs 215A, 220D, 222B

Pseudonannolene ambuatinga Iniesta & Ferreira, 2013b: 358, figs 1–6.
Pseudonannolene saguassu Iniesta & Ferreira, 2013b: 363, figs 7–10. **Syn. nov.**
Pseudonannolene canastra Gallo & Bichuette, 2020: 37, figs 3–6. **Syn. nov.**

Pseudonannolene ambuatinga – Iniesta & Ferreira 2014: 363. — Karam-Gemael *et al.* 2018: figs 2–3. — Gallo & Bichuette 2019: 42; 2020: 34.
Pseudonannolene saguassu – Gallo & Bichuette 2019: 48.

Justification of synonymy

Having studied the original descriptions, closely examined the type species of *P. ambuatinga* and *P. saguassu* and topotypes from caves in the Arcos-Pains-Doresópolis speleological unit, the species *P. saguassu* and *P. canastra* are here treated as junior synonyms of *P. ambuatinga*, according to the similarities in gonopod structure (telopodite and internal branch) and first leg-pair of males. Regarding the species *P. canastra*, the males described correspond to immatures due to the prefemoral process of first leg-pair being still incipient, short and with few and scattered setae (Gallo & Bichuette 2020: 37, fig. 3d–e), and the gonopod not fully developed, mainly the internal branch and gonocoxa (Gallo & Bichuette 2020: 37, fig. 6a–d) (see previous sections for more details on gonopod morphology and ontogeny in *Pseudonannolene*).

Diagnosis

Resembling *P. lundi* and *P. spelaea* by having head, trunk, and legs depigmented (Fig. 46). Males of *P. ambuatinga* differ from *P. lundi* by having a subtriangular solenomere (Fig. 47D) instead of a square-shaped square-shaped solenomere, and from *P. spelaea* by having seminal apophysis evident and by the number of ommatidia (ca 25) (Fig. 46A).

Etymology

A combination of words of the Brazilian Indian language Tupi-Guarani, '*ambus*' = 'millipede', and '*tinga*' = 'white', referring to the body depigmentation of the species (Iniesta & Ferreira 2013b).

Material examined

Holotypes

BRAZIL • ♂, holotype of *P. ambuatinga*; Minas Gerais, Pains, cave Loca d'Água de Baixo; [-20.369647, -45.692915]; 28 Jan. 2009; R.L. Ferreira *et al.* leg.; ISLA 2267.

BRAZIL • ♂, holotype of *P. saguassu*; Minas Gerais, Pains, cave Éden; [-20.384577, -45.666798]; 15 Mar. 2012; R. Zampaulo leg.; ISLA.

Paratypes (total: 3 ♂♂, 5 ♀♀)
BRAZIL • 1 ♂, paratype of *P. ambuatinga*; same collection data as for holotype; ISLA 2272 • 1 ♀, paratype of *P. ambuatinga*; same collection data as for holotype; ISLA 2268 • 1 ♀, paratype of *P. ambuatinga*; same collection data as for holotype; ISLA 2269 • 1 ♀, paratype of *P. ambuatinga*; same collection data

as for holotype; ISLA 2270 • 1 ♀, paratype of *P. ambuatinga*; same collection data as for holotype; ISLA 2271 • 1 ♂, paratype of *P. saguassu*; Minas Gerais, Pains, cave Éden; [-20.384577, -45.666798]; 15 Mar. 2012; R.L. Ferreira, P. Ratton and M. Souza-Silva leg.; ISLA 2273 • 1 ♂ , paratype of *P. saguassu*; same collection data as for preceding; ISLA 2275 • 1 ♀ , paratype of *P. saguassu*; same collection data as for preceding; ISLA 2274.

Other material (total: 1 ♂, 1 ♀)
BRAZIL – **Minas Gerais** • 1 ♂; Arcos, , cave Alinhamento; [-20.289079, -45.540084]; 766 m a.s.l.; 1 Jun. 2002; R.L. Ferreira *et al.* leg.; IBSP 3442 • 1 ♀; Iguatama, cave Arcaica; [-20.286839, -45.793289]; 700 m a.s.l.; 25 Jan. 2008; E.O. Machado and J.P.P. Barbosa leg.; IBSP 3315.

Descriptive notes

MEASUREMENTS. 58–60 body rings (1–2 apodous + telson). Males: body length 35–42.5 mm; maximum midbody diameter 1.8–1.9 mm. Females: body length 36–41 mm; maximum midbody diameter 2–3.1 mm.

COLOR. Living specimens depigmented. Color when stored in 70% ethanol: uniform pale brownish whitish, slightly darker posteriorly on prozonites; head, collum, antennae, and legs light brown.

HEAD. Antennae short (Fig. 46A), just reaching back to end of ring 5 when extended dorsally; relative antennomere lengths 1<2<3>4>5≈6>7. Mandibular cardo with ventral margin swollen. Ommatidial cluster well-developed, elliptical; ca 23 ommatidia in 4 rows.

BODY RINGS. Collum with lateral lobes broadly rounded, with ca 10 striae (Fig. 46A). Very faintly constricted between prozonite and metazonite; prozonites smooth; metazonites laterally with transverse striae below ozopore. Anterior sterna in midbody rings subrectangular, without transverse striae (Fig. 167B).

FIRST LEG-PAIR OF MALES. Coxae (***cx***) elongated (as long as the sum of remaining podomere lengths), subtriangular, with the base slightly arched, densely setose (Fig. 47A); prefemoral process (***prf***) as wide as half of prefemur, subcylindrical, densely setose along in its entire extension (Fig. 47B); remaining podomeres with setae along the mesal region.

SECOND LEG-PAIR OF MALES. Coxa (***cx***) large and subrectangular; penis (***pn***) located at proximal region, rounded, not extended basally (Fig. 47C); prefemur compressed dorsoventrally; remaining podomeres setose, with long setae mesally.

GONOPODS. Gonocoxa (***gcx***) elongated, but less than twice the length of the telopodite, with the base slightly arched; slightly flattened antero-posteriorly (Fig. 47D–F); with rows of papillae mesally. Seminal groove (***sg***) curved; arising medially on mesal cavity and terminating apically on the seminal apophysis (***sa***). Shoulder (***sh***) inconspicuous. Telopodite (***tp***) less than half as wide as ***gcx*** (Fig. 47D); solenomere (***sl***) with apicomesal process (***amp***) subtriangular; ectal process absent; ***sa*** located at medial portion, visible apically. Internal branch (***ib***) shovel-shaped and rounded apically, with horizontal plate; setae restricted to the apical region of ***ib*** exceeding seminal region of ***sl*** (Fig. 47D–F).

VULVAE. As typical for the genus. Bursa subtriangular, glabrous (Fig. 177C); internal valve subtriangular; operculum narrow, not curved medially; external valve wide, subtriangular.

Distribution

A troglomorphic species known only from caves in the Karst region of Pains and surrounding municipalities (Arcos-Pains-Doresópolis speleological unit), state of Minas Gerais, Brazil (Fig. 180).

This karst, which comprises the highest density of caves known for South America, harbors many other undescribed and described cave-dwelling species (Álvares & Ferreira 2002; Parizotto *et al*. 2017; Gallão & Bichuette 2018; Pellegrini *et al*. 2020).

Comments

Although the examination of the type material of the junior synonym *P. canastra* deposited at the Laboratório de Estudos Subterrâneos (LES/UFSCar) was not possible during this study, the original description and figures provided by Gallo & Bichuette (2020) are highly detailed.

Pseudonannolene anapophysis Fontanetti, 1996

Figs 48–49, 163B, 165B, 167C, 177D, 180; Supp. file 4: Figs 204E, 206A

Pseudonannolene anapophysis Fontanetti, 1996: 428, figs 1–4.

Pseudonannolene anapophysis – Iniesta & Ferreira 2013a: 92; 2013b: 366; 2013c: 79. — Gallo & Bichuette 2019: 47.
Pseudonannolene sp. "Igatu"– Gallo & Bichuette 2017: 6, figs 4f, 5f, 9h.

Diagnosis

Males of *P. anapophysis* resemble those of *P. bovei*, *P. caulleryi*, *P. inops*, and *P. xavieri* Iniesta & Ferreira, 2014 by having solenomere with subtriangular ectal process directed horizontally (Fig. 49D), but can be easily distinguished by the absence of a prefemoral process on the first leg-pair (Fig. 49A–B).

Etymology

Named after the Greek prefix '*an*-' = 'without', and '*apophysis*'. Unspecified in the original description, but likely to be related to the absence of a prefemoral process on the first leg-pair.

Material examined

Holotype
BRAZIL • ♂; Bahia, Lençóis, cave Lapão; [-12.540361, -41.402709]; Jan. 1987; F. Chaimowicz leg.; MZSP 940.

Paratypes (total: 1 ♂, 1 ♀, 1 immature)
BRAZIL • 1 ♂, 1 ♀, 1 immature; same collection data as for holotype; MZSP 940.

Other material (total: 3 ♂♂, 1 immature)
BRAZIL – **Bahia** • 1 ♂, 1 immature; Lençóis, cave Lapão de Lendres; [-12.561843, -41.389809]; 397 m a.s.l.; 3 Jan. 2010; R.L. Ferreira leg.; ISLA 20617 • 1 ♂; Lençóis, cave Lapão; [-12.540361, -41.402709]; 16 Jan. 2012; I.L.F. Magalhães leg.; IBSP 5209 • 1 ♂; same locality data as for preceding; 3 Sep. 1991; E. Trajano leg.; MZSP 1006.

Descriptive notes

Measurements. 60 body rings (1–2 apodous + telson). Males: body length 90 mm; maximum midbody diameter 5 mm.

Color. Body color greyish; collum darker; metazonites with a light posterior band; antennae and legs brownish.

Head. Antennae long (Fig. 163B), just reaching back to end of ring 6 when extended dorsally; antennomeres elongated; relative antennomere lengths 1<2<3≈4<5≈6>7. Mandibular cardo with ventral margin swollen. Ommatidial cluster well-developed, elliptical; ca 23 ommatidia in 4 rows.

Body rings. Collum with lateral lobes broadly rounded, with ca 9 striae, slightly curved ectad (Fig. 48A). Very faintly constriction between prozonite and metazonite; prozonites smooth; metazonites laterally with transverse striae. Anterior sterna in midbody rings subrectangular, without transverse striae (Fig. 167C).

First leg-pair of males. Coxae (***cx***) short (less than half of remaining podomere lengths), with the base slightly arched, densely setose, and apically projected (Fig. 49A); prefemoral process (***prf***) almost vestigial, with mesal region of prefemur whitish, covered by long setae, and ectal region more sclerotized and slightly projected apically (Fig. 49B); remaining podomeres with setae along the mesal region.

Second leg-pair of males. Coxa (***cx***) rounded; penis (***pn***) located at proximal region, rounded, not extended basally (Fig. 49C); prefemur slightly compressed dorsoventrally; remaining podomeres setose, with long setae mesally.

Gonopods. Gonocoxa (***gcx***) elongated, almost twice as long as telopodite, with the base slightly arched; flattened antero-posteriorly (Fig. 49D–F); with rows of papillae mesally. Seminal groove (***sg***) curved; arising medially on mesal cavity and terminating apically on the seminal apophysis (***sa***); protruding on squamous region of solenomere. Shoulder (***sh***) long, subtriangular. Telopodite (***tp***) as wide as half of ***gcx***, separated from ***sh*** by deep depression (Fig. 49D); solenomere (***sl***) with subtriangular apicomesal process (***amp***); ectal process (***ep***) subtriangular, elongated and perpendicular to ***amp***; ***sa*** located at mesal portion, visible apically. Internal branch (***ib***) shovel-shaped, rounded and slightly curved apically, with horizontal plate rounded; setae restricted to the apical region of ***ib***, exceeding seminal region of ***sl*** (Fig. 49D–F).

Vulvae. As typical for the genus. Bursa subtriangular, glabrous (Fig. 177D); internal valve subtriangular, with mesal region rounded; operculum narrow, constricted medially; external valve wide, subtriangular.

Distribution

Known only from the central region of the Brazilian State of Bahia (Fig. 180).

Pseudonannolene borelli Silvestri, 1895
Figs 50, 180

Pseudonannolene borelli Silvestri, 1895b: 7, fig. 12.

Pseudonannolene borelli – Silvestri 1897b: 8; 1902: 22 (description of specimens from Areguá, Central, Paraguay). — Viggiani 1973: 366. — Jeekel 2004: 88.

Diagnosis

Males of *P. borelli* slightly resemble those of *P. longicornis* and *P. tricolor* by having gonopod with subcylindrical gonocoxa, but differing by an internal branch with long setae restricted to the apical margin and the solenomere with a large trunk (Silvestri 1895b: 7, fig. 12; Fig. 50E).

Etymology

Patronym honoring the collector Dr Alfredo Borelli (Silvestri 1895b).

Material examined (total: 1 ♀)

PARAGUAY – **Central** • 1 ♀; Areguá; [-25.303669, -57.412255]; 157 m a.s.l.; 11 Oct. 1900; A. Borelli leg.; USNM 2389.

Descriptive notes

Gonopod description adapted from Silvestri (1895b: 7) to supplement original description and to introduce gonopod terminology. Non-sexual characters described as female.

Measurements. 68 body rings (1 apodous + telson). Females: body length ca 60 mm; maximum midbody diameter 3 mm.

Color. Strongly faded because of long preservation in ethanol, but apparently metazonites with a brownish posterior band; head, antennae, and legs lighter brownish.

Head. Antennae short (Fig. 50A), just reaching back to end of ring 5 when extended dorsally; relative antennomere lengths 1<2≈3≈4<5≈6>7. Mandibular cardo with ventral margin narrow. Ommatidial cluster well-developed, elliptical; ca 32 ommatidia in 5 rows.

Body rings. Collum broken. Very faintly constricted between prozonite and metazonite; prozonites smooth; metazonites laterally with transverse striae. Anterior sterna in midbody rings subrectangular, without transverse striae.

Gonopods. Gonocoxa (***gcx***) elongated, almost twice as long as telopodite, subrectangular; flattened antero-posteriorly; with rows of papillae mesally. Seminal groove (***sg***) terminating apically on the seminal apophysis (***sa***). Shoulder (***sh***) inconspicuous. Telopodite (***tp***) as wide as half of ***gcx***; solenomere (***sl***) with apicomesal process (***amp***) subtriangular; ectal process (***ep***) subtriangular, separated from ***amp*** by shallow notch; ***sa*** located at mesal portion. Internal branch (***ib***) shovel-shaped, slightly curved apically; setae restricted to the apical region of ***ib*** exceeding seminal region of ***sl*** (Fig. 50E).

Distribution

Known from Chaco in southwestern Paraguay; other records from the literature for Argentina and Bolivia (Fig. 180).

Comments

The type material described by Silvestri (1895b) was not found after consulting the Museo Regionale Scienze Naturali, Torino, Italy (MRSN). Nevertheless, a female topotype (USNM 2389) originally identified by Silvestri (but erroneously referenced as a paratype in its original label) was examined (Fig. 50A–D). Other specimens from Argentina (Santa Fé), Bolivia (Potosí and Tajira), and Paraguay (Asunción) were recorded by Silvestri (1897b, 1902).

Pseudonannolene bovei Silvestri, 1895
Figs 51–52, 165, 176, 181

Pseudonannolene bovei Silvestri, 1895a: 776, fig. 9.

Pseudonannolene bovei – Silvestri 1902: 24 (description of topotype); 1903: 23, fig. 71. — Jeekel 1965: 125; 2004: 88. — Viggiani 1973: 366. — Iniesta & Ferreira 2013c: 79.
Pseudonannolene bovei bovei [by implication] – Brölemann 1929: 16.

Diagnosis

Males of *P. bovei* resemble those of *P. anapophysis*, *P. caulleryi*, *P. inops*, and *P. xavieri* by having a triangular solenomere, with an ectal process directed horizontally (Fig. 52E), but differing by the short coxae on the first leg-pair not projected apically (Fig. 52A); and a subtriangular internal branch (Fig. 52E).

Etymology

Patronym honoring the Italian explorer Giacomo Bove (Silvestri 1895a).

Material examined

Syntypes

ARGENTINA • 1 ♂ [gonopods, second leg-pair, and gnathochilarium missing; other possible syntypes not found]; Misiones, San Ignacio, Giabibbirri; [-27.256834, -55.540414]; 30 m. a.s.l.; 1884; G. Bove leg.; MCSN.

Descriptive notes

Gonopod description adapted from Silvestri (1895a: 776) to supplement original description and to introduce gonopod terminology; remaining male sexual characters described based on examined syntype and non-sexual described as female.

Measurements. 50 body rings (1 apodous + telson). Males: body length ca 50 mm; maximum midbody diameter 3 mm.

Color. Body color faded because of long preservation in ethanol, but prozonites appearing brownish, metazonites with a brown posterior band; head, collum, antennae, and legs lighter brown.

Head. Antennae short (Fig. 51A), just reaching back to end of ring 5 when extended dorsally; relative antennomere lengths 1<2<3>4>5<6>7. Ommatidial cluster well-developed, covered partially by anterior region of collum; ca 25 ommatidia in 4 rows.

Body rings. Collum with lateral lobes broadly subrectangular, with ca 4 striae, slightly curved ectad posteriorly (Fig. 51A). Very faintly constriction between prozonite and metazonite; prozonites smooth; metazonites laterally with transverse striae below ozopore. Anterior sterna in midbody rings subrectangular, without transverse striae (Fig. 176B).

First leg-pair of males. Coxae (***cx***) short, subtriangular, with the base arched, densely setose mainly on distal region (Fig. 52A); prefemoral process (***prf***) short (less than half the length of the prefemur) and slightly constricted basally, subcylindrical, densely setose up to its median region (Fig. 52B).

Second leg-pair of males. Not examined.

Gonopods. Gonocoxa (***gcx***) elongated, almost twice as long as telopodite, subrectangular; antero-posteriorly flattened; with rows of papillae mesally. Seminal groove (***sg***) terminating apically on the seminal apophysis (***sa***). Shoulder (***sh***) rounded. Telopodite (***tp***) as wide as half of ***gcx***; solenomere (***sl***) with apicomesal process (***amp***) subtriangular; ectal process (***ep***) subtriangular, elongated and perpendicular to ***amp***. Internal branch (***ib***) subtriangular, surrounding ***tp*** basally as a shield; ***ib*** with setae along its entire margin exceeding apically the seminal region of ***sl*** (Fig. 52E).

Vulvae. Not examined.

Distribution

Known only from the type locality of Misiones, Argentina (Fig. 181).

Pseudonannolene buhrnheimi Schubart, 1960

Figs 28D, 53–55, 163D, 165E, 167D, 177E, 181; Supp. file 4: Figs 200E, 202F, 214B, 217A, 219D

Pseudonannolene buhrnheimi Schubart, 1960: 79.

Pseudonannolene buhrnheimi – Jeekel 2004: 88.

Diagnosis

Pseudonannolene buhrnheimi resembles *P. granulata* sp. nov. by having metazonites granulated (Fig. 53) and epiproct with subtriangular process (Figs 53B, 54), but differs by the absence of proximal projections on the stipes (Fig. 167D).

Etymology

Patronym honoring the collector Paulo Bührnheim (Schubart 1960).

Material examined

Holotype

BRAZIL • ♂ [gonopods and first leg-pair on microscope slides]; Rio de Janeiro, Santa Teresa; [-22.942260, -43.212212]; 16 Oct. 1960; O. Schubart, J. Schubart and P. Bührnheim leg.; MZSP.

Paratypes (total: 6 ♂♂, 3 ♀♀, 2 immatures)

BRAZIL • 6 ♂♂, 3 ♀♀, 2 immatures; same collection data as for holotype; MZSP.

Other material (total: 4 ♂♂, 7 ♀♀, 3 immatures)

BRAZIL – **Rio de Janeiro** • 1 ♂; Cachoeiras do Macacu, Reserva Ecológica Guapiassú; [-22.452806, -42.770293]; 34 m a.s.l.; 8–12 Oct. 2001; Equipe Biota leg.; IBSP 2402 • 1 ♀; same collection data as for preceding; IBSP 2406 • 1 ♀; same collection data as for preceding; IBSP 2403 • 1 ♀; same collection data as for preceding; IBSP 2397 • 1 ♀, 1 ♀ immature; same collection data as for preceding; IBSP 2404; • 1 ♂, 1 ♀; same collection data as for preceding; IBSP 2385 • 1 ♂, 1 ♀ immature; same collection data as for preceding; IBSP 2399 • 1 ♀, 1 ♂ immature; same collection data as for preceding; IBSP 2384 • 1 ♂, 1 ♀; Rio de Janeiro, Santa Teresa; [-22.942260, -43.212212]; 16 Oct. 1960; O. Schubart, J. Schubart and P. Bührnheim leg.; MZSP.

Descriptive notes

Measurements. 54–60 body rings (1–2 apodous + telson). Males: body length 55.9–69.4 mm; maximum midbody diameter 3–3.9 mm. Females: body length 67.6–76.6 mm; maximum midbody diameter 3.9–4.8 mm.

Color. Body color brownish; collum darker; prozonites greyish anteriorly; metazonites with a medial brown band and a reddish posterior band; antennae and legs lighter brown.

Head. Antennae long (Fig. 163D), just reaching back to end of ring 6 when extended dorsally; antennomeres elongated; relative antennomere lengths 1<2<3>4>5=6>7. Mandibular cardo with ventral margin narrow. Ommatidial cluster well-developed, elliptical; ca 40 ommatidia in 5 rows.

Body rings. Collum with lateral lobes rounded, with ca 9 striae, slightly curved ectad (Fig. 53A). Well demarcated constriction between prozonite and metazonite (Fig. 53B); prozonites smooth; metazonites granulated and laterally with transverse striae above ozopore. Anterior sterna in midbody rings subrectangular, without transverse striae (Fig. 167D). Epiproct with a long triangular process (Fig. 54).

First leg-pair of males. Coxae (***cx***) short (less than half of remaining podomere lengths), subtriangular, with the base arched, densely setose mainly on distal region (Fig. 55A); prefemoral process (***prf***) short (less than half of prefemur), subcylindrical, densely setose up to its median region (Fig. 55B); remaining podomeres with setae along the mesal region.

Second leg-pair of males. Coxa (***cx***) large and rounded; penis (***pn***) located at proximal region, circle-shaped (Fig. 55C); prefemur compressed dorsoventrally; remaining podomeres setose.

Gonopods. Gonocoxa (***gcx***) elongated, almost twice as long as telopodite, with the base arched; slightly flattened antero-posteriorly (Fig. 55D–F); with rows of papillae mesally. Seminal groove (***sg***) curved; arising medially on mesal cavity and terminating apically on the seminal apophysis (***sa***). Shoulder (***sh***) rounded. Telopodite (***tp***) almost as wide as ***gcx*** (Fig. 55D); solenomere (***sl***) with apicomesal process (***amp***) subtriangular, larger; ectal process (***ep***) subtriangular, separating from ***amp*** by shallow notch; ***sa*** located at mesal portion, slightly visible apically. Internal branch (***ib***) subtriangular, narrow, slightly curved ectad at midlength, surrounding base of ***tp*** as a shield; ***ib*** with setae along its entire margin exceeding apically seminal region of ***sl*** (Fig. 55D–F).

Vulvae. As typical for the genus. Bursa subtriangular, glabrous (Fig. 177E); internal valve subtriangular, with mesal region rounded; operculum narrow; external valve wide, subtriangular.

Distribution

Known from the Atlantic Forest in the southern and central regions of Rio de Janeiro State, Brazil (Fig. 181).

Pseudonannolene caatinga Iniesta & Ferreira, 2014
Figs 11, 25B, D, F, 30A–B, 32A, 36A–B, 56–57, 163E, 165F, 167E, 177F, 181;
Supp. file 4: Figs 201D, 203B, 204A, 205B, 207B, 212F, 213A, 218A, 219C

Pseudonannolene caatinga Iniesta & Ferreira, 2014: 375, figs 10, 14f.

Pseudonannolene caatinga – Gallo & Bichuette 2019: 47.

Diagnosis

Males of *P. caatinga* resemble those of *P. microzoporus*, *P. curtipes* Schubart, 1960, and *P. leopoldoi* by having gonopod with subtriangular internal branch, and solenomere with ectal and apicomesal processes (Fig. 57D–F). *Pseudonannolene caatinga* can be distinguished from those species by having a distal projection on the internal branch (Fig. 57D).

Etymology

Noun in apposition, taken from the semi-arid biome ‘Caatinga’ where the species is widely distributed (Iniesta & Ferreira 2014).

Material examined

Holotype

BRAZIL • ♂; **Bahia**, Ourolândia, cave Toca dos Ossos; [-10.858192, -41.134315]; 10 Jun. 2012; R.L. Ferreira leg.; ISLA 3627.

Paratypes (total: 5 ♂♂, 3 ♀♀)

BRAZIL • 1 ♂; same collection data as for holotype; ISLA 3628 • 1 ♂; same collection data as for holotype; ISLA 3629 • 1 ♂; same collection data as for holotype; ISLA 3630 • 1 ♂; same collection data as for holotype; ISLA 3631 • 1 ♂; same collection data as for holotype; ISLA 3634 • 1 ♀; same collection data as for holotype; ISLA 3632 • 1 ♀; same collection data as for holotype; ISLA 3633 • 1 ♀; same locality data as for holotype; 28 Jan. 2009; R.L. Ferreira leg.; ISLA 3635.

Other material (total: 28 ♂♂, 38 ♀♀, 14 immatures)

BRAZIL – **Ceará** • 1 ♂; Crato, Floresta Nacional Chapada do Araripe-Apodi; [-7.336788, -39.432647]; 941 m a.s.l.; 20–30 Jan. 2014; C. Sampaio leg.; UFPB 0086 • 1 ♂; Crato, Fonte do Xerife; [-7.230036, -39.412316]; 426 m a.s.l.; 2–3 Jun. 2000; floresta; A.B. Kury leg.; MNRJ • 1 ♂ immature; Rodovia

CE 090, Floresta IBAMA; [-3.657215, -38.689267]; 16 m a.s.l.; 18 Mar. 1999; A.B. Kury and A. Giupponi leg.; MNRJ. – **Alagoas** • 1 ♂; Murici, Estação Ecológica Murici; [-9.232525, -35.858161]; 408 m a.s.l.; 13–22 Sep. 2003; Equipe Biota leg.; IBSP 2166 • 1 ♂; same collection data as for preceding; IBSP 2166 • 1 ♂; same collection data as for preceding; IBSP 2180 • 1 ♂, 1 immature; same collection data as for preceding; IBSP 2169 • 2 ♀♀; same collection data as for preceding; IBSP 2172 • 2 ♀♀; same collection data as for preceding; IBSP 2175 • 1 ♀; same collection data as for preceding; IBSP 2173 • 1 ♀; same collection data as for preceding; IBSP 2167 • 1 ♂; same collection data as for preceding; IBSP 2178 • 1 ♂; same locality data as for preceding; 22–23 Sep. 2014; E.P. Lorenzo leg.; UFPB 0146. – **Sergipe** • 2 ♂♂, 3 ♀♀; Itabaiana, Estação Ecológica da Serra de Itabaiana (= Parque Nacional da Serra de Itabaiana); [-10.779742, -37.349371]; 343 m a.s.l.; 14–20 Sep. 1999; A.D. Brescovit leg.; IBSP 905. – **Bahia** • 1 ♀; Piatã; [-13.151128, -41.775671]; 1293m a.s.l.; 23–28 Dec. 2010; M. Teixeira Jr. leg.; IBSP 3944 • 1 ♂; Caetité, cave PF 13; [-14.066228, -42.486907]; 8–15 Dec. 2008; R. Andrade *et al.* leg. • 2 ♂♂, 1 ♀; same collection data as for preceding except for cave PF 14; IBSP 5769 • 1 ♀; same collection data as for preceding except for cave PF 04; IBSP 5770 • 2 ♀♀; same collection data as for preceding except for cave PF 22; IBSP 5776 • 3 ♂♂ immatures, 2 ♀♀ immatures; same collection data as for preceding except for cave PF 10; IBSP 5787 • 1 ♂, 5 ♀♀; same collection data as for preceding; IBSP 5788 • 2 ♀♀; same collection data as for preceding; IBSP • 1 ♂, 1 ♀; same collection data as for preceding except for cave PF 21; IBSP 5790 • 2 ♂♂, 3 ♀♀, 1 immature; same collection data as for preceding except for cave PF 10; IBSP 5791 • 2 ♀♀, 1 immature; same collection data as for preceding except for cave PF 11; IBSP 5792 • 1 immature; same collection data as for preceding except for cave PF 12; IBSP 5793 • 1 ♂; same collection data as for preceding except for cave PF 13; IBSP 5796 • 4 ♂♂, 8 ♀♀, 3 ♀♀ immatures, 1 immature; Coribe, Serra do Ramalho, cave Enfurnado [-13.645275, -44.209846]; 646 m a.s.l.; Jul. 2007; A. Perez leg.; MNRJ 30154. – **Distrito Federal** • 2 ♂♂, 3 ♀♀; Brasília, Área de Marinha; [-15.795139, -47.882086]; 1095 m a.s.l.; Oct. 1999; C. Nogueira, F. Valdujo and R. Montigello leg.; MNRJ 30149 • 1 ♂, 2 ♀♀; Brazlândia, Fazenda 33; [-15.670741, -48.200567]; 1114 m a.s.l.; 28 Dec. 2009; A. Chagas Jr., G. Segal and C. Segal leg.; MNRJ 30146.

Descriptive notes

Measurements. 55–60 body rings (1–2 apodous + telson). Males: body length 60–70.4 mm; maximum midbody diameter 3.8–4.3 mm. Females: body length 57.3–68.8 mm; maximum midbody diameter 3.5–4.5 mm.

Color. Body color brownish grey; collum darker; prozonites greyish anteriorly; metazonites with a medial brown band and a reddish posterior band; antennae and legs lighter brown.

Head. Antennae long (Fig. 163E), just reaching back to end of ring 6 when extended dorsally; antennomeres elongated; relative antennomere lengths 1<2<3>4≈5>6>7. Mandibular cardo with ventral margin narrow. Ommatidial cluster well-developed, elliptical; ca 32 ommatidia in 4 rows.

Body rings. Collum with lateral lobes rounded, with ca 9 striae, slightly curved ectad (Fig. 56A). Very faintly constricted between prozonite and metazonite; prozonites smooth; metazonites laterally with transverse striae slightly above ozopore in anterior body rings. Anterior sterna in midbody rings subrectangular, with shallow transverse striae (Fig. 167E).

First leg-pair of males. Coxae (***cx***) short (less than half of remaining podomere lengths), subtriangular, with the base arched, densely setose (Fig. 57A); prefemoral process (***prf***) as wide as half of prefemur, subcylindrical, densely setose up to its median region (Fig. 57B); remaining podomeres with setae along the mesal region.

Second leg-pair of males. Coxa (***cx***) large and rounded; penis (***pn***) located at proximal region, rounded, not extended basally (Fig. 57C); prefemur compressed dorsoventrally; remaining podomeres setose.

Gonopods. Gonocoxa (***gcx***) elongated, almost twice as long as telopodite, with the base arched; flattened antero-posteriorly (Fig. 57D–F); with rows of papillae mesally. Seminal groove (***sg***) curved; arising medially on mesal cavity and terminating apically on the seminal apophysis (***sa***). Shoulder (***sh***) rounded. Telopodite (***tp***) almost as wide as ***gcx*** (Fig. 57D); solenomere (***sl***) with apicomesal process (***amp***) subtriangular; ectal process (***ep***) subtriangular, separated from ***amp*** by deep notch; ***sa*** located at mesal portion, slightly visible apically. Internal branch (***ib***) subtriangular, narrow, curved ectad at midlength, surrounding the base of ***tp*** as a shield; with torsion of 180° in the distal portion and a rounded projection, directed ectad; ***ib*** with setae along its entire margin slightly exceeding apically seminal region of ***sl*** (Fig. 57D–F).

Vulvae. As typical for the genus. Bursa subtriangular, glabrous (Fig. 177F); internal valve subtriangular, with mesal region rounded; operculum narrow; external valve wide, subtriangular.

Distribution

The species is widely distributed in the Cerrado (tropical savanna ecoregion) of Goiás up to the southern Bahia State, in the semi-arid region of the Caatinga biome and partially some patches of Atlantic Forest in northeastern Brazil (Fig. 181).

Pseudonannolene callipyge Brölemann, 1902
Figs 17A–C, 58–60, 165G, 168D, 177G, 181

Pseudonannolene callipyge Brölemann, 1902a: 131, pl. viii, figs 154–159.

Pseudonannolene callipyge – Brölemann 1909: 57. — Jeekel 2004: 88.

Diagnosis

Males of *P. callipyge* can be easily distinguished from all congeners by having glabrous projections located proximally on the stipes of the gnathochilarium (Fig. 168D).

Etymology

Named after the Greek nouns ‘*kállos*’ = ‘beauty’, and ‘*pugḗ*’ = in reference to the pygidium, telson. Unspecified in the original description.

Material examined

Holotype

BRAZIL • ♂ [gonopods missing]; Paraná; 16 Oct. 1960; R. von Ihering leg.; MZSP 240.

Paratype (total: 1 ♀)

BRAZIL • 1 ♀; same collection data as for holotype; MZSP 240.

Other material (total: 19 ♂♂, 15 ♀♀, 4 immatures)

BRAZIL – **Paraná** • 1 ♂, 1 ♀, 2 immatures; Pinhão, Santa Clara; [-25.667400, -51.967915]; 753 m a.s.l.; 2007; IBSP 5388 • 3 ♂♂, 1 ♀; Adrianópolis, Abismo do Sumidouro Sem Nome; [-24.766670, -48.839446]; 362 m a.s.l.; 8 Dec. 2017; C.A.R. Souza and L.F.M. Iniesta leg.; IBSP 7614 • 1 ♂; same collection data as for preceding; IBSP 7615 • 1 ♂, 1 ♀, 1 immature; same collection data as for preceding; IBSP 7619 • 4 ♂♂, 1 ♀, 1 immature; cave Pássaro Preto; 362 m a.s.l.; 10 Dec. 2017; C.A.R. Souza leg.; IBSP 7616 • 1 ♂; same collection data as for preceding; IBSP 7617 • 1 ♂; same collection data as for preceding; IBSP 7618 • 1 ♀; cave Straube; 362 m a.s.l.; 9 Dec. 2017; C.A.R. Souza and L.F.M. Iniesta leg.; IBSP 7620 • 1 ♂; same collection data as for preceding; IBSP 7621 • 2 ♂♂; same collection data as for preceding; IBSP 7622 • 3 ♀♀; cave Pássaro Preto; 362 m a.s.l.; 10 Dec. 2017; L.F.M. Iniesta leg.; IBSP 7623 • 3 ♂♂; cave Straube; 362 m a.s.l.; 8 Dec. 2017; C.A.R. Souza and L.F.M. Iniesta leg.; IBSP 7624 • 2 ♀♀; same collection data as for preceding; 11 Dec. 2017; IBSP 7625 • 5 ♀♀; same collection data as for preceding; 9 Dec. 2017; IBSP 7626 • 3 ♂♂; same collection data as for preceding; IBSP 7627.

Descriptive notes

MEASUREMENTS. 58–60 body rings (1–2 apodous + telson). Males: body length 58–67 mm; maximum midbody diameter 3.8–5 mm. Females: body length 70.5–75 mm; maximum midbody diameter 5–5.2 mm.

COLOR. Body color brownish yellow; head, collum, and antennae darker; prozonites and metazonites anteriorly darker, with a posterior reddish band; legs lighter brown.

HEAD. Antennae long (Fig. 58D), just reaching back to end of ring 6 when extended dorsally; antennomeres elongated; relative antennomere lengths 1<2≈3>4=5=6>7. Mandibular cardo with ventral margin narrow. Stipes of gnathochilarium with glabrous basal projections (Fig. 168D). Ommatidial cluster well-developed, elliptical; ca 40 ommatidia in 5 rows.

BODY RINGS. Collum with lateral lobes rounded, with ca 6 deep striae, slightly curved ectad (Fig. 58A). Very faintly constricted between prozonite and metazonite; prozonites smooth; metazonites laterally with transverse striae below ozopore. Anterior sterna in midbody rings subrectangular, without transverse striae (Fig. 168D).

FIRST LEG-PAIR OF MALES. Coxae (***cx***) short (less than half of remaining podomere lengths), subtriangular, with the base arched, densely setose (Figs 59A, 60D); prefemoral process (***prf***) as wide as half of prefemur, subcylindrical, densely setose up to its median region (Fig. 59B); remaining podomeres with setae along the mesal region.

SECOND LEG-PAIR OF MALES. Coxa (***cx***) large and rounded; penis (***pn***) located at proximal region, rounded, not extended basally (Fig. 59C); prefemur compressed dorsoventrally; remaining podomeres setose.

GONOPODS. Gonocoxa (***gcx***) elongated, almost twice as long as telopodite, with the base arched; flattened antero-posteriorly (Fig. 59D–F); with rows of papillae mesally. Seminal groove (***sg***) curved; arising medially on mesal cavity and terminating apically on the seminal apophysis (***sa***). Shoulder (***sh***) rounded. Telopodite (***tp***) almost as wide as ***gcx*** (Fig. 59D); solenomere (***sl***) with apicomesal process (***amp***) rounded; ectal process (***ep***) short, subtriangular, separating from ***amp*** by notch; ***sa*** located at mesal portion, slightly visible apically. Internal branch (***ib***) subtriangular, narrow, surrounding the base of ***tp*** as a shield; with torsion of 180° in the distal portion; ***ib*** with long setae along its entire margin slightly exceeding apically seminal region of ***sl*** (Fig. 59D–F).

VULVAE. As typical for the genus. Bursa subtriangular, glabrous (Fig. 177G); internal valve subtriangular, with mesal region rounded; operculum narrow; external valve wide, subtriangular.

Distribution

Known from the Atlantic Forest in the southern and northeastern Paraná State, Brazil (Fig. 181); some records from limestone caves in the Açungui Limestone Group.

Pseudonannolene caulleryi Brölemann, 1929
Figs 61, 182

Pseudonannolene caulleryi Brölemann, 1929: 16, figs 19–26.

Pseudonannolene caulleryi – Mauriès 1987: 77 (lectotype and paralectotypes designations). — Jeekel 2004: 88.

Diagnosis

Males of *P. caulleryi* resemble those of *P. albiventris* and *P. mesai* by having a large trunk of the telopodite, but differing by an elongated gonocoxa; internal branch subtriangular; solenomere with ectal process directed horizontally (Fig. 61).

Etymology

Patronym honoring the collector Professor Caullery (Brölemann 1929).

Descriptive notes

Description adapted from Brölemann (1929: 16) to supplement original description and to introduce gonopod terminology.

MEASUREMENTS. 51–53 body rings (2–3 apodous + telson). Males: body length 34–37 mm; maximum midbody diameter 2.42–2.48 mm. Females: body length 36 mm; maximum midbody diameter 2.4 mm.

FIRST LEG-PAIR OF MALES. Coxae (***cx***) short (less than half of remaining podomere lengths), subtriangular, with the base arched, densely setose mainly on distal region; prefemoral process (***prf***) short (less than half of prefemur), subcylindrical, densely setose up to its median region.

SECOND LEG-PAIR OF MALES. Coxa (***cx***) large and rounded; penis (***pn***) located at proximal region, rounded, not extended basally; prefemur compressed dorsoventrally; remaining podomeres setose.

GONOPODS. Gonocoxa (***gcx***) elongated, almost three times longer than telopodite, subrectangular; antero-posteriorly flattened (Fig. 61A); with rows of papillae mesally. Seminal groove (***sg***) terminating apically on the seminal apophysis (***sa***). Shoulder (***sh***) subtriangular. Telopodite (***tp***) as wide as half of ***gcx***; swollen basally; solenomere (***sl***) with apicomesal process (***amp***) subtriangular; ectal process (***ep***) subtriangular, perpendicular to ***amp***; ***sa*** located at mesal portion. Internal branch (***ib***) shovel-shaped, with setae along its entire margin slightly exceeding apically seminal region of ***sl*** (Fig. 61).

Distribution

Known only from the type locality Canoinhas, Santa Catarina State, Brazil (Fig. 182).

Comments

The examination of the lectotype and paralectotypes (two males and one female) deposited at the Muséum national d'histoire naturelle, Paris, France (MNHN), was not possible during this study.

Pseudonannolene centralis Silvestri, 1902
Figs 62–63, 176D, 182

Pseudonannolene centralis Silvestri, 1902: 19.

Pseudonannolene centralis – Jeekel 2004: 88.

Diagnosis

Males of *P. centralis* resemble those of *P. typica* by having a solenomere with a short ectal process, separated from the apicomesal process by a shallow notch, and an internal branch with a distal projection (Fig. 63D). *Pseudonannolene centralis* differs from *P. typica* by an inconspicuous shoulder on the gonocoxa (Fig. 63C); a torsion of the internal branch short and starting apically (Fig. 63D); the head partially covered by scattered setae.

Etymology

Although unspecified in the original description, the species name probably refers to the central region in Paraguay where the species was found.

Material examined

Syntypes

PARAGUAY • 1 ♂; Paraguarí; [-25.621436, -57.149997]; 12 Oct. 1900; A. Borelli leg.; USNM 2033 • 1 ♀ [examined by photographs]; same collection data as for preceding; ZMB 2884.

Descriptive notes

Measurements. 62–66 body rings (1–2 apodous + telson). Males: body length ca 70 mm; maximum midbody diameter 5 mm.

Color. Body color greyish; collum darker; prozonites anteriorly greyish; metazonites with a medial brown band and a posterior lighter brown band; antennae and legs lighter brown.

Head. Antennae short (Fig. 62A), just reaching back to end of ring 5 when extended dorsally; relative antennomere lengths 1<2<3>4≈5≈6>7. Mandibular cardo with ventral margin narrow. Ommatidial cluster well-developed, elliptical; ca 30 ommatidia in 4 rows.

Body rings. Collum with lateral lobes rounded, with ca 6 striae, slightly curved ectad (Fig. 62A). Very faintly constricted between prozonite and metazonite; prozonites smooth; metazonites laterally with transverse striae below ozopore. Anterior sterna in midbody rings subrectangular, without transverse striae (Fig. 176D).

First leg-pair of males. Coxae (***cx***) short (less than half of remaining podomere lengths), subtriangular, with the base strongly arched and constricted medially, densely setose mainly on distal region (Fig. 63A); prefemoral process (***prf***) half as wide as prefemur, subcylindrical, densely setose up to its median region; remaining podomeres with setae along the mesal region.

Second leg-pair of males. Coxa (***cx***) large and rounded; penis (***pn***) located at proximal region, rounded, not extended basally (Fig. 63B); prefemur dorsoventrally compressed; remaining podomeres setose.

Gonopods. Gonocoxa (***gcx***) elongated, almost twice as long as telopodite, with the base arched; flattened antero-posteriorly (Fig. 63C); with rows of papillae mesally. Seminal groove (***sg***) curved; arising medially on mesal cavity and terminating apically on the seminal apophysis (***sa***). Shoulder (***sh***) inconspicuous. Telopodite (***tp***) almost as wide as ***gcx*** (Fig. 63D); solenomere (***sl***) with apicomesal process (***amp***) rounded; ectal process (***ep***) subtriangular, separated from ***amp*** by notch; ***sa*** located at mesal portion, slightly visible apically. Internal branch (***ib***) subtriangular, narrow, surrounding base of ***tp*** as a shield; with torsion of 180° in the distal portion and a short, rounded projection, directed ectad; ***ib*** with setae along its entire margin exceeding apically seminal region of ***sl*** (Fig. 63C–D).

Vulvae. Not examined.

Distribution

Known only from the type locality Paraguarí, Paraguay (Fig. 182).

Comments

The species was not mentioned in the list of species described by Silvestri (see Viggiani 1973).

Pseudonannolene curtipes Schubart, 1960
Figs 64–65, 165H, 168A, 182

Pseudonannolene curtipes Schubart, 1960: 78.

Pseudonannolene curtipes – Jeekel 2004: 89

Diagnosis

Males of *P. curtipes* resemble those of *P. microzoporus*, *P. caatinga*, and *P. leopoldoi* by having gonopod with subtriangular internal branch, and solenomere with ectal and apicomesal processes (Fig. 65D). *Pseudonannolene curtipes* can be distinguished from those species by having internal branch deeply notched separating from gonocoxa (Fig. 65D–F), and a circle-shaped penis (Fig. 65C).

Etymology

Named after the Latin adjective '*curtus*' = 'shortened', and the masculine noun '*pes*' = 'foot'. Unspecified in the original description, but likely to be related either with short coxae of the first leg pair of males or the size of midbody legs.

Material examined

Holotype

BRAZIL • ♂ [gonopods missing]; Goiás, Sítio d'Abadia, Fazenda Forquilha Grande; [-14.732396, -46.153622]; Feb. 1960; J. Evangelista leg.; MZSP 1001.

Paratypes (total: 2 ♂♂, 11 ♀♀)

BRAZIL • 1 ♂; same collection data as for holotype; MZSP 1027 • 1 ♂; same collection data as for preceding; MZSP 1029 • 1 ♀; same collection data as for preceding; MZSP 1022 • 1 ♀; same collection data as for preceding; MZSP 1023 • 1 ♀; same collection data as for preceding; MZSP 1024 • 1 ♀; same collection data as for preceding; MZSP 1025 • 1 ♀; same collection data as for preceding; MZSP 1026 • 1 ♀; same collection data as for preceding; MZSP 1028 • 1 ♀; same collection data as for preceding; MZSP 1030 • 1 ♀; same collection data as for preceding; MZSP 1031 • 1 ♀; same collection data as for preceding; MZSP 1032 • 1 ♀; same collection data as for preceding; MZSP 1033 • 1 ♀; same collection data as for preceding; MZSP 1034.

Descriptive notes

Measurements. 61 body rings (2 apodous + telson). Males: body length 52–55 mm; maximum midbody diameter 3–3.5 mm. Females: body length 50–55 mm; maximum midbody diameter 3.3–3.5 mm.

Color. Body color brownish grey; head, collum, antennae and legs darker brown; prozonites greyish anteriorly; metazonites with a medial brown band and a posterior reddish band.

Head. Antennae long (Fig. 64A), just reaching back to end of ring 6 when extended dorsally; antennomeres elongated; relative antennomere lengths $1<2<3>4\approx5>6>7$. Mandibular cardo with ventral margin narrow. Ommatidial cluster well-developed, elliptical; ca 35 ommatidia in 5 rows.

Body rings. Collum with lateral lobes rounded, with ca 12 striae, slightly curved ectad (Fig. 64A). Very faintly constricted between prozonite and metazonite; prozonites smooth; metazonites laterally with transverse striae slightly above ozopore in anterior body rings. Anterior sterna in midbody rings subrectangular, without transverse striae (Fig. 168A).

First leg-pair of males. Coxae (***cx***) short (less than half of remaining podomere lengths), subtriangular, with the base arched, densely setose (Fig. 65A); prefemoral process (***prf***) as wide as half of prefemur, subcylindrical, densely setose up to its median region (Fig. 65B); remaining podomeres with setae along the mesal region.

Second leg-pair of males. Coxa (***cx***) broken in paratypes, but large and rounded; penis (***pn***) located at proximal region, circle-shaped (Fig. 65C); prefemur compressed dorsoventrally; remaining podomeres setose.

Gonopods. Gonocoxa (***gcx***) elongated, almost twice as long as telopodite, with the base arched; flattened antero-posteriorly (Fig. 65D–F); with rows of papillae mesally. Seminal groove (***sg***) curved; arising medially on mesal cavity and terminating apically on the seminal apophysis (***sa***). Shoulder (***sh***) subtriangular. Telopodite (***tp***) almost as wide as ***gcx*** (Fig. 65D); solenomere (***sl***) with apicomesal process (***amp***) subtriangular; ectal process (***ep***) long, subtriangular, separated from ***amp*** by deep notch; ***sa*** located at mesal portion, slightly visible apically. Internal branch (***ib***) subtriangular, narrow, slightly curved ectad at midlength, surrounding base of ***tp*** as a shield; separated from ***gcx*** after deep constriction mesally; with torsion of 180° in the distal portion and a short, rounded projection, directed ectad; ***ib*** with setae along its entire margin slightly exceeding apically seminal region of ***sl*** (Fig. 65D–F).

Vulvae. Not examined.

Distribution

Known only from the type locality Sítio d'Abadia, Goiás State, Brazil (Fig. 182).

Pseudonannolene erikae Iniesta & Ferreira, 2014

Figs 30F, 37, 66–67, 163F, 168B, 177H, 182; Supp. file 4: Figs 192C, 197a, 214E

Pseudonannolene erikae Iniesta & Ferreira, 2014: 377, fig. 11.

Pseudonannolene erikae – Gallo & Bichuette 2019: 47.

Diagnosis

Males of *P. erikae* resemble those of *P. mesai*, *P. bucculenta* sp. nov., and *P. curvata* sp. nov. by having a mesally curving telopodite (Fig. 67D), but differing by the presence of a large and hexagonal-shaped process on the first leg-pair (Fig. 67A).

Etymology

Patronym honoring the collector Dr Erika Taylor (Iniesta & Ferreira 2014).

Material examined

Holotype

BRAZIL • ♂; Minas Gerais, Sete Lagoas, cave Rei do Mato; [-19.495666, -44.282498]; 4 Nov. 2011; R.L. Ferreira, L.F.M. Iniesta, A. Vasconcelos, P. Ratton and M. Souza-Silva leg.; ISLA 4107.

Paratypes (total: 1 ♂, 1 ♀)

BRAZIL • 1 ♂; same collection data as for holotype; ISLA 4108 • 1 ♀; same collection data as for holotype; ISLA 4109.

Other material (total: 13 ♂♂, 12 ♀♀, 2 immatures)

BRAZIL – **Minas Gerais** • 1 ♂, 5 ♀♀; Prudente de Morais, Fazenda Sapé; [-19.474888, -44.159215]; 759 m a.s.l.; 8 Dec. 2005; E.S.S. Álvares leg.; IBSP 3331 • 1 ♂; São José da Lapa; [-19.699209, -43.958311]; 732 m a.s.l.; 17–21 Dec. 2012; Bueno *et al.* leg.; IBSP 7601 • 1 ♀; same collection data as for preceding; IBSP 7602 • 2 ♂♂; same collection data as for preceding; IBSP 7603 • 1 ♀; same collection data as for preceding; IBSP 7604 • 1 ♀; same collection data as for preceding; IBSP 7605 • 1 immature; same collection data as for preceding; IBSP 7606 • 1 ♂; same collection data as for preceding; IBSP 7607 • 1 ♂, 1 ♀ immature; same collection data as for preceding; IBSP 7608 • 1 ♀; same collection data as for preceding; IBSP 7609 • 1 ♀; same collection data as for preceding; IBSP 7610 • 1 ♀; same collection data as for preceding; IBSP 7611 • 1 ♂, 1 ♀; same collection data as for preceding; IBSP 7612 • 3 ♂♂; same collection data as for preceding; IBSP 7613 • 1 ♂; Pedro Leopoldo, Campinho, cave CAMP 054; [-19.570000, -44.010291]; 826 m a.s.l.; 3–21 Nov. 2014; Equipe Spelayon leg.; IBSP 5984 • 1 ♂; cave CAMP_056; [-19.570189, -44.010147]; IBSP 5980 • 1 ♂; Matozinhos, CRH-MTZ, cave Vaca Tonta; [-19.566664, -44.078790]; 793 m a.s.l.; 4 Jan. 2018; Equipe Spelayon leg.; IBSP 7467.

Descriptive notes

Measurements. 61 body rings (2 apodous + telson). Males: body length 52–55 mm; maximum midbody diameter 3–3.5 mm. Females: body length 50–55 mm; maximum midbody diameter 3.3–3.5 mm.

Color. Body color brownish grey; head, collum, and antennae darker grey; prozonites greyish anteriorly; metazonites with a lighter posterior band; legs brownish.

Head. Antennae long (Fig. 163F), just reaching back to end of ring 6 when extended dorsally; antennomeres elongated; relative antennomere lengths 1<2<3>4>5≈6>7. Mandibular cardo with ventral margin narrow. Ommatidial cluster well-developed, elliptical; ca 32 ommatidia in 5 rows.

Body rings. Collum with lateral lobes broadly rounded, with ca 5 striae, strongly curved ectad (Fig. 66A). Very faintly constricted between prozonite and metazonite; prozonites smooth; metazonites laterally with transverse striae slightly above ozopore in anterior body rings. Anterior sterna in midbody rings subrectangular, without transverse striae (Fig. 168B).

First leg-pair of males. Coxae (***cx***) elongated (as long as the sum of remaining podomere lengths), subtriangular, with the base arched, densely setose (Fig. 67A); prefemoral process (***prf***) large, curved mesad, and projected laterally, densely setose along its entire extension (Fig. 67B); remaining podomeres with setae along the mesal region.

Second leg-pair of males. Coxa (***cx***) rounded; penis (***pn***) located at proximal region, rounded, not extended basally (Fig. 67C); prefemur slightly compressed dorsoventrally; remaining podomeres setose, with long setae mesally.

Gonopods. Gonocoxa (***gcx***) elongated, but less than twice the length of telopodite, with the base slightly arched; flattened antero-posteriorly (Fig. 67D–F); with rows of papillae mesally. Seminal groove (***sg***) curved; running mesally and terminating apically on the seminal apophysis (***sa***). Shoulder (***sh***) rounded. Telopodite (***tp***) almost as wide as ***gcx*** (Fig. 67D), strongly curved mesad; solenomere (***sl***) with apicomesal process (***amp***) subtriangular; ectal process absent; ***sa*** located at mesal portion, slightly visible apically. Internal branch (***ib***) shovel-shaped, narrow; ***ib*** with setae along its entire margin slightly exceeding apically seminal region of ***sl*** (Fig. 67D–F).

Vulvae. As typical for the genus. Bursa subtriangular, glabrous (Fig. 177H); internal valve subtriangular, with mesal region rounded; operculum narrow, curved ectad; external valve wide, subtriangular.

Distribution

The species occurs in limestone caves and surrounding forests from the south region of the Karst province of the Bambuí Group, Minas Gerais State, Brazil (Fig. 182).

Pseudonannolene fontanettiae Iniesta & Ferreira, 2014
Figs 17D, 68–69, 163G, 165I, 168C, 177I, 182; Supp. file 4: Figs 201A, 222F

Pseudonannolene fontanettiae Iniesta & Ferreira, 2014: figs 13, 14h.

Pseudonannolene fontanettiae – Gallo & Bichuette 2019: 47.

Diagnosis

Males of *P. fontanettiae* resemble those of *P. robsoni* by having the internal branch with a torsion in anal view (Fig. 69D), but differing by the torsion starting only apically; mesal margin of the internal branch straight; with a distal projection present and directed horizontally (Figs 69D, 222F).

Etymology

Patronym honoring the researcher Dr Carmen S. Fontanetti, for her important contributions to the study of Brazilian millipedes (Iniesta & Ferreira 2014).

Material examined

Holotype
BRAZIL • ♂; Minas Gerais, Tiradentes, cave Casa de Pedra; [-21.140467, -44.187566]; 992 m a.s.l.; 25 Feb. 2014; R.L. Ferreira, L.F.M. Iniesta, M. Souza-Silva, L. Ázara and M. Mendonça leg.; ISLA 5033.

Paratypes (total: 1 ♂, 1 ♀)
BRAZIL • 1 ♂; same collection data as for holotype; ISLA 5034 • 1 ♀; same collection data as for holotype; ISLA 5035.

Other material (total: 24 ♂♂, 16 ♀♀, 7 immatures)
BRAZIL – **Minas Gerais** • 1 ♀; Tiradentes, cave Casa de Pedra; [-21.140467, -44.187566]; 992 m a.s.l.; 4–7 Jan. 2011; Pellegatti leg.; IBSP 5827 • 2 ♂♂; same collection data as for preceding; IBSP 5828 • 3 ♂♂, 5 ♀♀, 3 ♂♂ immatures, 3 ♀♀ immatures; Lavras, Reserva do Boqueirão; [-21.346389, -44.990833]; 1066 m a.s.l.; 5–6 Mar. 2010; J.P.P.P. Barbosa leg.; IBSP • 4 ♂♂, 5 ♀♀; same collection data as for preceding; IBSP 3759 • 1 ♂; Sete Lagoas [-19.457188, -44.236375], cave ILCOM_07; 775 m a.s.l.; 5–14 Aug. 2013; Equipe Carste leg.; IBSP 7090 • 1 ♂; same collection data as for preceding except for cave ILCOM_15; 13–21 Mar. 2014; IBSP 7073 • 1 ♂; same collection data as for preceding except for cave ILCOM_26; 13–21 Mar. 2014; IBSP 7092 • 1 ♂; same collection data as for preceding; IBSP 7091 • 2 ♀♀; same collection data as for preceding; 2 May 2014; IBSP 7087 • 1 ♂; same collection data as for preceding except for cave ILCOM_12; 13–21 Mar 2014; IBSP 7101 • 1 ♂; same collection data as for preceding; IBSP 7102 • 1 ♂; same collection data as for preceding except for cave ILCOM_15; IBSP 7077 • 1 ♀; same collection data as for preceding; IBSP 7076 • 1 ♂, 1 ♀; same collection data as for preceding; IBSP 7075 • 1 ♂, 1 ♀, 1 immature; same collection data as for preceding except for cave ILCOM_28; IBSP 7088 • 1 ♂; same collection data as for preceding except for cave ILCOM_18; IBSP 7084 • 1 ♂; same collection data as for preceding except for cave ILCOM_19/20; IBSP 7096 • 2 ♂♂; same collection data as for preceding except for cave ILCOM_13; IBSP 7083 • 2 ♂♂; same collection data as for preceding except for cave ILCOM_11; IBSP 7080.

Descriptive notes

Measurements. 65–69 body rings (1–2 apodous + telson). Males: body length 55–76 mm; maximum midbody diameter 2.5–3 mm. Females: body length 60–81 mm; maximum midbody diameter 3–4.2 mm.

Color. Body color blackish; head, collum, and antennae darker, legs brownish; prozonites greyish anteriorly; metazonites with a medial brown band and a posterior reddish band.

Head. Antennae long (Fig. 163G), just reaching back to end of ring 6 when extended dorsally; antennomeres elongated; relative antennomere lengths 1<2<3>4>5>6>7. Mandibular cardo with ventral margin narrow. Ommatidial cluster well-developed, elliptical; ca 38 ommatidia in 5 rows.

Body rings. Collum with lateral lobes rounded, with ca 6 striae, slightly curved ectad (Fig. 68A). Very faintly constricted between prozonite and metazonite; prozonites smooth; metazonites laterally with transverse striae below ozopores. Anterior sterna in midbody rings subrectangular, without transverse striae (Fig. 168C).

First leg-pair of males. Coxae (***cx***) short (less than half of remaining podomere lengths), subtriangular, with the base arched, densely setose (Fig. 69A); prefemoral process (***prf***) as wide as half of prefemur, subcylindrical, densely setose up to its median region (Fig. 69B); remaining podomeres with setae along the mesal region.

Second leg-pair of males. Coxa (***cx***) large and rounded; penis (***pn***) located at proximal region, rounded, not extended basally (Fig. 69C); prefemur compressed dorsoventrally; remaining podomeres setose.

Gonopods. Gonocoxa (***gcx***) elongated, almost twice as long as telopodite, with the base arched; antero-posteriorly flattened (Fig. 69D–F); with rows of papillae mesally. Seminal groove (***sg***) curved; arising medially on mesal cavity and terminating apically on the seminal apophysis (***sa***). Shoulder (***sh***) long, subtriangular. Telopodite (***tp***) almost as wide as ***gcx*** (Fig. 69D), arising just before ending of ***sh***; solenomere (***sl***) with apicomesal process (***amp***) rounded; ectal process (***ep***) subtriangular, separated from ***amp*** by deep notch; ***sa*** located at mesal portion, visible apically. Internal branch (***ib***) subtriangular, narrow and with straight mesal edge, surrounding base of ***tp*** as a shield; with torsion of 180° in the distal portion, visible in anal view, and a rounded, elongated projection directed ectad; ***ib*** with setae along its entire margin exceeding apically seminal region of ***sl*** (Fig. 69D–F).

Vulvae. As typical for the genus. Bursa subtriangular, glabrous (Fig. 177I); internal valve subtriangular, with mesal region slightly rounded; operculum narrow, curved ectad; external valve wide, subtriangular.

Distribution

The species occurs in limestone caves from the south region of the Karst province of the Bambuí Limestone Group and forests in the Zona da Mata mesoregion in Minas Gerais State, Brazil (Fig. 182).

Pseudonannolene halophila Schubart, 1949
Figs 21A, 30C, 31A–E, 32E, 70–71, 163H, 165J, 168E, 177J, 183;
Supp. file 4: Figs 195C, 202A–B, 203C, 204D, 209C

Pseudonannolene halophila Schubart, 1949: 234, figs 27–30.

Pseudonannolene halophila – Fontanetti 1990: 698. — Iniesta & Ferreira 2013b: 366. — Gallo & Bichuette 2020: 36.
Pseudonannolene tricolor – Schubart 1949: 222 (misidentified females from Ilha da Queimada Grande, São Paulo, Brazil). — Jeekel 2004: 89.

Diagnosis

Males of *P. halophila* resemble those of *P. leucocephalus* by having a subtriangular solenomere (Fig. 71D), but differing by the large and subrectangular coxae on the first leg-pair (Figs 30C, 71A, 203C, 204D); suboval penis (Figs 71C, 209C); telopodite with rounded laterad projection (Fig. 71D).

Etymology

Name '*halophila*' (masculine '*halophilus*') taken from the Greek words '*háls*' = 'sea', '*salt*', plus '*phílos*' = having an attraction to something, referring to the coastal region where the species occurs (Schubart 1949).

Material examined

Holotype

BRAZIL • ♂ [gonopods, gnathochilarium, first and second leg-pair on microscope slides]; São Paulo, Arquipélago dos Alcatrazes, Ilha do Farol; [-24.099557, -45.692906]; 53 m a.s.l.; 19 Feb. 1948; A. Hoge leg.; MZSP.

Paratypes (total: 21 ♂♂, 20 ♀♀, 3 immatures)
BRAZIL – **São Paulo** • 3 ♂♂, 1 immature; same collection data as for holotype; MZSP • 8 ♂♂, 10 ♀♀; Arquipélago dos Alcatrazes [-24.099557, -45.692906], Ilha da Sapata; 50 m a.s.l.; 22 Feb. 1948; A. Hoge leg.; MZSP • 10 ♂♂, 10 ♀♀, 2 immatures; São Paulo, Arquipélago dos Alcatrazes [-24.099557, -45.692906], Ilha do Paredão; 48 m a.s.l.; 22 Feb. 1948; A. Hoge leg.; MZSP.

Other material (total: 61 ♂♂, 58 ♀♀, 22 immatures)
BRAZIL – **São Paulo** • 4 ♂♂, 2 ♀♀; Ilha dos Alcatrazes [-24.099557, -45.692906]; 53 m a.s.l.; 15 Apr. 1994; A. Eterovic leg.; IBSP 1101 • 16 ♂♂, 14 ♀♀, 7 immatures; same collection data as for preceding; 10–12 Sep. 1994; IBSP 1106 • 2 ♂♂; same collection data as for preceding; 15–17 Apr. 1994; A. Eterovic leg.; IBSP 1174 • 2 ♂♂; same collection data as for preceding; H. Luederwaldt leg.; MZSP • 1 ♂; same collection data as for preceding; 16 Feb. 1948; A. Hoge leg.; MZSP • 1 ♂, 3 ♀♀; same collection data as for preceding; 16 Feb. 1948; A. Hoge leg.; MZSP • 1 ♂; 5 ♀♀; same collection data as for preceding; 3–5 Oct. 1984; Mello leg.; MZSP • 1 ♂, 2 ♀♀; Guarujá, Ilha dos Alcatrazes; [-24.099557, -45.692906]; 53 m a.s.l.; 15 Apr. 1944; A. Eterovic leg.; IBSP • 1 ♂, 1 ♀, 1 immature; Guarujá, Ilha da Moela; [-24.050000, -46.266367]; 5 m a.s.l.; 29–31 Mar. 2009; R.P. Indicatti and F.U. Yamamoto leg.; IBSP • 3 ♂♂, 3 ♀♀, 2 ♂♂ immatures, 1 ♀ immature; same locality data as for preceding; 17–19 Jul. 2009; R.P. Indicatti and G.P. Perroni leg.; IBSP 3264 • 1 ♂; Santos, Vale do Rio Jurubatuba; [-23.876178, -46.305066]; 201 m a.s.l.; Mar.–Nov. 2007; IBSP 3163 • 1 ♀ immature; same collection data as for preceding; IBSP 3161 • 1 ♂, 1 ♂ immature; same collection data as for preceding; IBSP 3162 • 1 ♂; same collection data as for preceding; IBSP 3154 • 1 ♂; same collection data as for preceding; IBSP 3157; 1 ♀ immature; same collection data as for preceding; IBSP 3160 • 1 ♂, 1 ♀; José Menino Morro; [-23.964989, -46.355878]; 63 m a.s.l.; 2 Feb. 1960; O. Schubart leg.; MZSP • 2 ♂♂, 2 ♀♀; Praia Grande; [-24.009294, -46.412305]; 9 m a.s.l.; 18 Feb. 1940; O. Schubart leg.; MZSP • 1 ♀ immature; Jabaquara; [-23.943081, -46.339857]; 9 m a.s.l.; 12 Nov. 1955; O. Schubart leg.; MZSP • 1 ♂, 4 ♀♀; Itanhaém, Rio Branco; [-24.182030, -46.784951]; 12 m a.s.l.; 16 Jul. 1994; A. Eterovic leg.; IBSP 1091 • 1 ♂; Estação Ambiental São Camilo; 13–20 Mar. 2010; J.A. Nascimento leg.; IBSP • 1 ♂; same collection data as for preceding; IBSP 3671 • 1 ♂, 2 ♀♀; Ilha da Queimada Grande; [-24.487922, -46.674156]; 53 m a.s.l.; 13–15 Mar. 2001; C. Bertim and J.P. Guadanucci leg.; IBSP 776 • 8 ♂♂, 8 ♀♀, 1 immature; same locality data as for preceding; 28 Apr.–1 May 2003; R.P. Indicatti and C.A.R. de Souza leg.; IBSP 1336 • 1 ♀; same locality data as for preceding; 19–20 Oct. 1994; A. Eterovic leg.; IBSP 1180 • 1 ♀; same locality data as for preceding; Apr. 1993; Chammas and A. Eterovic leg.; IBSP 1151 • 1 ♀, 1 ♀ immature; same locality data as for preceding; 14–22 Apr. 1947; A. Hoge leg.; MZSP

• 2 ♂♂; Guarujá, Santo Amaro; [-23.989919, -46.252532]; 17 m a.s.l.; 19 Jan. 1961; O. Schubart Filho leg.; MZSP • 3 ♂♂, 2 ♀♀, 1 ♂ immature, 1 ♀ immature; São Vicente, Ilha Porchat; [-23.977110, -46.371616]; 9 m a.s.l.; 21–29 Jan. 1959; O. Schubart leg.; MZSP • 1 ♀; same locality data as for preceding; 24 Jan. 1961; O. Schubart leg.; MZSP • 1 ♂, 2 ♀♀ immatures; Paranapuã; [-20.105474, -50.586007]; 474 m a.s.l.; 1 Nov. 1960; O. Schubart and O. Schubart Filho leg.; MZSP • 1 ♂, 1 ♀, 2 ♀♀ immatures; same locality data as for preceding; 27 Jan. 1962; O. Schubart and O. Schubart Filho leg.; MZSP • 1 ♂, 2 ♀♀; Ponte Pênsil; [-23.974434, -46.388706]; 18 m a.s.l.; 12 Jan. 1961; O. Schubart leg.; MZSP • 1 ♂; Prainha; [-23.976751, -46.388880]; 5 m a.s.l.; 5 Feb. 1960; O. Schubart leg.; MZSP • 1 ♂; Cubatão, Mata da Copebras; [-23.847249, -46.399757]; 11 m a.s.l.; 2004; A. Nogueira leg.; IBSP 3297 • 1 ♀; same collection data as for preceding; IBSP 3296 • 1 ♀; same collection data as for preceding; IBSP 3268.

Descriptive notes

MEASUREMENTS. 49–64 body rings (1–2 apodous + telson). Males: body length 41.7–89.3 mm; maximum midbody diameter 2.7–4.1 mm. Females: body length 48.4–93 mm; maximum midbody diameter 2.5–4.9 mm.

COLOR. Body color brownish grey; head and collum darker; prozonites greyish anteriorly; metazonites with a dark medial band and a light posterior band; antennae and legs light brown.

HEAD. Antennae short (Fig. 163H), just reaching back to end of ring 5 when extended dorsally; relative antennomere lengths 1<2<3>4=5=6>7. Mandibular cardo with ventral margin narrow. Ommatidial cluster well-developed, elliptical; ca 35 ommatidia in 5 rows.

BODY RINGS. Collum with lateral lobes rounded, with ca 5 striae, slightly curved ectad (Fig. 70A). Very faintly constricted between prozonite and metazonite; prozonites smooth; metazonites laterally with transverse striae slightly above ozopore in anterior body rings. Anterior sterna in midbody rings subrectangular, with 8 transverse striae (Fig. 168E).

FIRST LEG-PAIR OF MALES. Coxae (***cx***) elongated (as long as the sum of remaining podomere lengths), subrectangular, with the base slightly arched, densely setose (Fig. 71A); prefemoral process (***prf***) as long as half of prefemur, subcylindrical, densely setose along the entire ventral region (Fig. 71B); remaining podomeres with setae along the mesal region.

SECOND LEG-PAIR OF MALES. Coxa (***cx***) elongated and rounded; penis (***pn***) located at proximal region, rounded, extended basally (Fig. 71C); prefemur compressed dorsoventrally; remaining podomeres setose.

GONOPODS. Gonocoxa (***gcx***) elongated, almost twice as long as telopodite, with the base arched; antero-posteriorly flattened (Fig. 71D–F); with rows of papillae mesally. Seminal groove (***sg***) curved; arising medially on mesal cavity and terminating apically on the seminal apophysis (***sa***). Shoulder (***sh***) inconspicuous. Telopodite (***tp***) almost as wide as ***gcx*** (Fig. 71D), with rounded laterad projection; solenomere (***sl***) with apicomesal process (***amp***) subtriangular; ectal process absent; ***sa*** located at medial portion, thickened and visible apically. Internal branch (***ib***) subtriangular, narrow, surrounding base of ***tp*** as a shield; ***ib*** with setae along its entire margin exceeding apically seminal region of ***sl*** (Fig. 71D–F).

VULVAE. As typical for the genus. Bursa subtriangular, glabrous (Fig. 177J); internal valve subtriangular, with mesal region slightly rounded; operculum narrow, curved ectad; external valve wide, subtriangular.

Distribution

The species is widely distributed in the Atlantic Forest of the Brazilian archipelago Alcatrazes and in the coastal region of São Paulo State, Brazil (Fig. 183). Importantly, some of these islands from Alcatrazes were connected to the continent by a land bridge during the recession of seawater in the Last Glacial Maximum (around 85 000–15 000 years ago) (see Martin *et al*. 1986; Fleming *et al*. 1998), and since then, populations of *P. halophila* remain supposedly isolated from each other and from the continent. As noted by Schubart (1949: 239), populations from different islands have a wide variation in body size, possibly related to intrinsic ecological factors of their habitats.

Pseudonannolene imbirensis Fontanetti, 1996
Figs 72–73, 165K, 169A, 177K, 183; Supp. file 4: Figs 209B, 216C

Pseudonannolene imbirensis Fontanetti, 1996: 430, figs 8–10.

Pseudonannolene imbirensis – Iniesta & Ferreira 2013a: 92; 2013b: 366. — Karam-Gemael *et al.* 2018: figs 2–3. — Gallo & Bichuette 2019: 43; 2020: 36.
Pseudonannolene sp. "São Bernardo II cave" – Gallo & Bichuette 2017: 7, figs 4b, 5b, 9d.
Pseudonannolene sp. "São Vicente II cave" – Gallo & Bichuette 2017: 7, figs 4c, 5c, 9e.
Pseudonannolene sp. "Terra Ronca cave" – Gallo & Bichuette 2017: 7, figs 4d, 5d, 9f.
Pseudonannolene aff. *imbirensis* – Bichuette *et al.* 2019: 24.

Diagnosis

Males of *P. imbirensis* resemble those of *P. leopoldoi* and *P. microzoporus* by having solenomere with ectal process deeply notched separating from apicomesal process (Fig. 73D–F), but differing by a head and trunk ocher (Fig. 72); short prefemoral process on the first leg-pair (Fig. 73A–B).

Etymology

Although unspecified, the name is evidently an adjective referring to the locality where the type material was found, cave São Mateus-Imbira III.

Material examined

Holotype
BRAZIL • ♂; Goiás, São Domingos, cave São Mateus-Imbira III; [-13.400307, -46.319377]; 700 m a.s.l.; Apr. 1989; Grupo Espeleológico de Geologia [GREGEO] leg.; MZSP 1035.

Paratypes (total: 3 ♀♀, 1 immature)
BRAZIL • 2 ♀♀; same collection data as for holotype; Jul. 1988; MZSP 1030 • 1 ♀, 1 ♂ immature; same collection data as for holotype; MZSP.

Other material (total: 16 ♂♂, 22 ♀♀, 6 immatures)
BRAZIL – **Goiás** • 1 ♀, 1 ♀ immature; São Domingos, cave Passa Três; [-13.612953, -46.368476]; 711 m a.s.l.; 27 Jul. 1988; MZSP • 1 ♂; 4 immatures; same collection data as for preceding; 25 Jul. 2000; M.E. Bichuette leg.; MNRJ • 3 ♂♂; same collection data as for preceding; 9 May 2001; MNRJ • 5 ♂♂, 3 ♀♀; cave São Vicente; [-13.587311, -46.358229]; 626 m a.s.l.; 2–6 Mar. 2000; A. Chagas Jr. and M.E. Bichuette leg.; MZSP • 4 ♂♂, 1 ♀, 1 ♀ immature; same collection data as for preceding; 29 Jul. 2000; MNRJ • 1 ♀; same collection data as for preceding; MNRJ • 1 ♂, 3 ♀♀; same collection data as for preceding; 11 May 2001; A. Chagas Jr. and E. Trajano leg.; MNRJ • 1 ♂, 2 ♀♀; Parque Estadual Terra Ronca, cave São Vicente; [-13.587311, -46.358229]; 626 m a.s.l.; 2–6 May 2000; A. Chagas Jr and M.E. Bichuette leg.; MZSP • 5 ♀♀; same collection data as for preceding; MZSP • 1 ♂, 2 ♀♀; cave Termas de São Vicente II; [-13.583333, -46.358229]; 617 m a.s.l.; 29 Jul. 2000; M.E. Bichuette and

A. Chagas Jr. leg.; MNRJ 30155 • 1 ♀; cave Angélica; [-13.522824, -46.382068]; 572 m a.s.l.; 1 Aug. 2000; A. Chagas Jr. leg.; MNRJ • 2 ♀♀; inside cave Angélica; [-13.522824, -46.382068]; 572 m a.s.l.; 7 May 2001; A. Chagas Jr. leg.; MNRJ • 1 ♀; cave Bezerra; [-13.547301, -46.376290]; 626 m a.s.l.; 30 Jul. 2000; A. Chagas Jr. leg.; MNRJ.

Descriptive notes

Measurements. 61–63 body rings (1–2 apodous + telson). Males: body length 55–60 mm; maximum midbody diameter 2.4–2.5 mm. Females: body length 60–65 mm; maximum midbody diameter 2.8–3 mm.

Color. Body color faded, but apparently prozonites brownish, metazonites with a brown posterior band; head, collum, antennae, and legs lighter.

Head. Antennae short (Fig. 72A), just reaching back to end of ring 5 when extended dorsally; relative antennomere lengths 1<2<3>4>5≈6>7. Mandibular cardo with ventral margin narrow. Ommatidial cluster well-developed, elliptical; ca 28 ommatidia in 5 rows.

Body rings. Collum with lateral lobes rounded, with ca 8 striae, slightly curved ectad (Fig. 72A). Very faintly constricted between prozonite and metazonite; prozonites smooth; metazonites laterally with transverse striae slightly above ozopore in anterior body rings. Anterior sterna in midbody rings subrectangular, without transverse striae (Fig. 169A).

First leg-pair of males. Coxae (***cx***) short (less than half of remaining podomere lengths), subtriangular, with the base arched, densely setose (Fig. 73A); prefemoral process (***prf***) short, less than half of prefemur, subcylindrical, densely setose up to its median region (Fig. 73B); remaining podomeres with setae along the mesal region.

Second leg-pair of males. Coxa (***cx***) large and rounded; penis (***pn***) located at proximal region, rounded, slightly flattened (Fig. 73C); prefemur compressed dorsoventrally; remaining podomeres setose.

Gonopods. Gonocoxa (***gcx***) elongated, almost twice as long as telopodite, with the base arched; antero-posteriorly flattened (Fig. 73D–F); with rows of papillae mesally. Seminal groove (***sg***) curved; arising medially on mesal cavity and terminating apically on the seminal apophysis (***sa***). Shoulder (***sh***) short, rounded. Telopodite (***tp***) almost as wide as ***gcx*** (Fig. 73D); solenomere (***sl***) with apicomesal process (***amp***) slightly subtriangular; ectal process (***ep***) short, subtriangular, separating from ***amp*** by deep notch; ***sa*** located at mesal portion, slightly visible apically. Internal branch (***ib***) subtriangular, narrow, slightly curved ectad at midlength, surrounding the base of ***tp*** as a shield; with torsion of 180° in the distal portion and a rounded projection directed ectad; ***ib*** with setae along its entire margin not exceeding apically seminal region of ***sl*** (Fig. 73D–F).

Vulvae. As typical for the genus. Bursa subtriangular, glabrous (Fig. 177K); internal valve subtriangular, with mesal region rounded; operculum narrow, slightly curved ectad; external valve wide, subtriangular.

Distribution

Known only from caves in São Domingos, Goiás State, Brazil (Fig. 183). Although no apparent restriction of *P. imbirensis* in caves may be assumed, all specimens either examined by us or recorded from the literature were collected inside caves or surrounding entrances.

Comments

Populations of *P. imbirensis* from the caves Angélica, São Bernardo II, and São Vicente II were regarded as troglobitic by Gallo & Bichuette (2017). On the other hand, in the same paper the authors regarded the population from cave Terra Ronca II as troglophilic. Excepting the pale brownish color of the species (see Fontanetti 1996), there is no morphological feature that clearly indicates troglomorphism in *P. imbirensis*, thus requiring further ecological studies and new extensive samplings to confirm its restriction to cave habitats.

Pseudonannolene inops Brölemann, 1929 stat. nov.
Figs 74–75, 163I, 165L, 169B, 177L, 183, 218B

Pseudonannolene bovei inops Brölemann, 1929: 9, figs 8–18.

Pseudonannolene bovei inops – Mauriès 1987: 177 (lectotype and paralectotypes designations). — Jeekel 2004: 88.

Diagnosis

Males of *P. inops* resemble those of *P. anapophysis*, *P. bovei,* and *P. xavieri* by having a solenomere with an elongated ectal process directed horizontally (Figs 75D–F, 218B), but differing by having a S-shaped internal branch swollen apically (Fig. 75D).

Etymology

Named after the Latin adjective '*inops*' = 'weak', 'helpless', 'lacking'. Unspecified in the original description.

Material examined (total: 17 ♂♂, 7 ♀♀, 1 immature)

BRAZIL – **Rio Grande do Sul** • 1 ♂; Maquiné, Fepagro; [-29.65, -50.2]; 22 m a.s.l.; Jan. 2002; Equipe Biota leg.; IBSP 2505 • 1 ♂, 1 immature; same collection data as for preceding; IBSP 2542 • 3 ♂♂; same collection data as for preceding; IBSP 2550 • 7 ♂♂, 5 ♀♀; same collection data as for preceding; IBSP 2488 • 1 ♀; same collection data as for preceding; IBSP 2544 • 2 ♂♂; same collection data as for preceding; IBSP 2559 • 3 ♂♂, 1 ♀; same collection data as for preceding; IBSP 2533.

Descriptive notes

MEASUREMENTS. 61–62 body rings (1 apodous + telson). Males: body length 55 mm; maximum midbody diameter 2.5 mm. Females: body length 55–60 mm; maximum midbody diameter 3–3.5 mm.

COLOR. Body color brownish grey; head, collum, antennae and legs darker; prozonites greyish anteriorly; metazonites with a brown medial band and a lighter posterior band.

HEAD. Antennae long (Fig. 163I), just reaching back to end of ring 6 when extended dorsally; antennomeres elongated; relative antennomere lengths 1<2<3>4≈5≈6>7. Mandibular cardo with ventral margin swollen. Ommatidial cluster well-developed, covered partially by anterior region of collum, elliptical; ca 25 ommatidia in 4 rows.

BODY RINGS. Collum with lateral lobes broadly rounded, with ca 6 striae, slightly curved ectad (Fig. 74A). Very faintly constricted between prozonite and metazonite; prozonites smooth; metazonites laterally with transverse striae below ozopore. Anterior sterna in midbody rings subrectangular, without transverse striae (Fig. 169B).

FIRST LEG-PAIR OF MALES. Coxae (***cx***) short (less than half of remaining podomere lengths), subtriangular, with the base arched and slightly expanded, densely setose (Fig. 75A); prefemoral process (***prf***) as long as half of prefemur, subcylindrical, densely setose along the entire ventral region (Fig. 75B); remaining podomeres with setae along the mesal region.

SECOND LEG-PAIR OF MALES. Coxa (***cx***) large and subrectangular; penis (***pn***) located at proximal region, rounded, not extended basally (Fig. 75C); prefemur compressed dorsoventrally; remaining podomeres setose.

GONOPODS. Gonocoxa (***gcx***) elongated, almost twice as long as telopodite, with the base slightly arched; antero-posteriorly flattened (Fig. 75D–F); with rows of papillae mesally. Seminal groove (***sg***) curved; arising medially on mesal cavity and terminating apically on the seminal apophysis (***sa***); thickened basally and protruded on squamous region of ***sl*** (Fig. 75E). Shoulder (***sh***) inconspicuous. Telopodite (***tp***) as wide as half of ***gcx*** (Fig. 75D); solenomere (***sl***) with apicomesal process (***amp***) short; ectal process (***ep***) subtriangular, elongated and perpendicular to ***amp***; ***sa*** located at mesal portion, visible apically. Internal branch (***ib***) swollen, curved apically, S-shaped, and enfolding ***sl*** in anal view; ***ib*** with setae along its entire margin not exceeding apically seminal region of ***sl*** (Fig. 75D–F).

VULVAE. As typical for the genus. Bursa subtriangular, glabrous (Fig. 177L); internal valve subtriangular, with mesal region rounded; operculum large, curved ectad; external valve wide, subtriangular.

Distribution

The species occurs in the Atlantic Forest from Rio Grande do Sul up to Santa Catarina State, Brazil (Fig. 183).

Comments

Although the examination of the lectotype and paralectotypes (two males and two females) deposited at the Muséum national d'histoire naturelle, Paris, France (MNHN), was not possible during this study, the original description and drawings provided by Brölemann (1929) are highly detailed.

Pseudonannolene leopoldoi Iniesta & Ferreira, 2014
Figs 76–77, 163J, 165M, 169C, 183

Pseudonannolene leopoldoi Iniesta & Ferreira, 2014: 365, figs 3–4, 14b.

Pseudonannolene leopoldoi – Gallo & Bichuette 2019: 47.

Diagnosis

Males of *P. leopoldoi* resemble those of *P. imbirensis* and *P. microzoporus* by having a solenomere with the ectal process deeply notched separating it from the apicomesal process (Fig. 77D), but differing of *P. imbirensis* by having the head light brown, collum, antennae, and legs darker brown (Fig. 76), and of *P. microzoporus* by having the internal branch not curved ectad (Fig. 77D–F).

Etymology

Patronym honoring the Brazilian biospeleologist Dr Leopoldo Bernardi (Iniesta & Ferreira 2014).

Material examined

Holotype

BRAZIL • ♂; Minas Gerais, São João da Lagoa, cave Zú; [-16.843178, -44.263017]; 25 Sep. 2013; R.L. Ferreira, L.F.M. Iniesta, M. Souza-Silva, L. Ázara and M. Mendonça leg.; ISLA 4123.

Paratypes (total: 3 ♂♂, 2 ♀♀)

BRAZIL – **Minas Gerais** • 1 ♂; same collection data as for preceding; ISLA 4124 • 1 ♂; same collection data as for preceding; ISLA 4125 • 1 ♂; same collection data as for preceding; ISLA 4126 • 1 ♀; same collection data as for preceding; ISLA 4127 • 1 ♀; same collection data as for preceding; ISLA 4128.

Other material (total: 2 ♂♂, 1 immature)
BRAZIL – **Minas Gerais** • 1 ♂; Montes Claros, cave OCM02; [-16.733518, -43.858071]; 53 m a.s.l.; 19 Aug. 2016; A. Koken leg.; IBSP 7890 • 1 ♂; same collection data as for preceding except for cave OCM61B; [-16.733518, -43.858071]; 19 Aug. 2016; A. Koken leg.; IBSP 7892 • 1 immature; same collection data as for preceding except for cave OCML28; [-16.733518, -43.858071]; 21 Aug. 2016; A. Koken leg.; IBSP 7891.

Descriptive notes

MEASUREMENTS. 61–64 body rings (1–2 apodous + telson). Males: body length 50–52 mm; maximum midbody diameter 2.8–3 mm. Females: body length 55 mm; maximum midbody diameter 3.3 mm.

COLOR. Body color brownish; head light brown; collum, antennae, and legs darker brown; prozonites and metazonites dark brownish anteriorly, with a lighter posterior band.

HEAD. Antennae short (Fig. 163J), just reaching back to end of ring 5 when extended dorsally; relative antennomere lengths 1<2<3>4≈5<6>7. Mandibular cardo with ventral margin narrow. Ommatidial cluster well-developed, elliptical; ca 30 ommatidia in 5 rows.

BODY RINGS. Collum with lateral lobes rounded, with ca 9 shallow striae, slightly curved ectad (Fig. 76A). Very faint constriction between prozonites and metazonites; prozonites smooth; metazonites laterally with transverse striae below ozopore. Anterior sterna in midbody rings subrectangular, without transverse striae (Fig. 169C).

FIRST LEG-PAIR OF MALES. Coxae (***cx***) short (less than half of remaining podomere lengths), subtriangular, with the base arched, densely setose (Fig. 77A); prefemoral process (***prf***) as wide as half of prefemur, subcylindrical, densely setose up to its median region (Fig. 77B); remaining podomeres with setae along the mesal region.

SECOND LEG-PAIR OF MALES. Coxa (***cx***) large and rounded; penis (***pn***) located at proximal region, rounded, not extended basally (Fig. 77C); prefemur compressed dorsoventrally; remaining podomeres setose.

GONOPODS. Gonocoxa (***gcx***) elongated, almost twice as long as telopodite, with the base arched; antero-posteriorly flattened (Fig. 77D–F); with rows of papillae mesally. Seminal groove (***sg***) curved; arising medially on mesal cavity and terminating apically on the seminal apophysis (***sa***). Shoulder (***sh***) rounded. Telopodite (***tp***) almost as wide as ***gcx***, with well-demarcated separation in relation to ***sh*** (Fig. 77D); solenomere (***sl***) with apicomesal process (***amp***) slightly subtriangular; ectal process (***ep***) short, subtriangular, separating from ***amp*** by deep notch; ***sa*** located at mesal portion, slightly visible apically. Internal branch (***ib***) subtriangular, narrow, surrounding base of ***tp*** as a shield; with torsion of 180° in the distal portion but without projection; setae starting at midlength of ***ib*** not exceeding seminal region of ***sl*** (Fig. 77D–F).

VULVAE. As typical for the genus. Bursa subtriangular, glabrous; internal valve subtriangular, with mesal region rounded; operculum narrow; external valve wide, subtriangular.

Distribution

The species occurs in limestone caves and surrounding forests from the Bambuí Group in the northern and central region of Minas Gerais State, Brazil (Fig. 183).

Pseudonannolene leucocephalus Schubart, 1944
Figs 78–80, 169D, 177M, 183; Supp. file 4: Fig. 204B

Pseudonannolene leucocephalus Schubart, 1944: 413, figs 75–76.

Pseudonannolene leucocephalus – Schubart 1952: 418. — Iniesta & Ferreira 2013b: 366. — Gallo & Bichuette 2019: 47; 2020: 36.
Pseudonannolene leucocephala – Jeekel 2004: 89.

Diagnosis

Males of *P. leucocephalus* slightly resemble those of *P. halophila* by having the solenomere subtriangular (Figs 79D, 80D), but differing by having short coxae on the first leg-pair with a constriction at about midlength (Figs 79A, 80B); the prefemoral process wide (Fig. 79B); internal branch with a horizontal plate (Fig. 79D).

Etymology

Name 'leucocephalus' (feminine 'leucocephala') taken from the Greek words '*lefkó*' = 'white', plus '*kephalos*' = 'head', referring to the whitish coloration of the head and antennae of the species (Schubart 1944).

Material examined

Holotype

BRAZIL • ♂ [gonopods, gnathochilarium, first and second leg-pair on microscope slides]; São Paulo, Mogi Guaçu, Cachoeira de Cima; [-22.223841, -47.049620]; 610 m a.s.l.; 12 Oct. 1941; J. Gaspar and O. Schubart leg.; MZSP 1101.

Paratypes (total: 4 ♂♂, 5 ♀♀, 3 immatures)
BRAZIL • 4 ♂♂, 5 ♀♀, 3 immatures; same collection data as for holotype; MZSP.

Other material (total: 14 ♂♂, 22 ♀♀, 14 immatures)
BRAZIL – **São Paulo** • 1 ♀; Mogi Mirim, Usina Mogi-Guaçu; [-22.432213, -46.950871]; 623 m a.s.l.; 12 Oct. 1941; J. Gaspar leg.; MZSP 1054 • 2 ♂♂, 1 ♀; same collection data as for preceding; MZSP 1060 • 4 ♂♂, 1 ♀; same collection data as for preceding; MZSP; • 1 ♂; Descalvado, Escaramuça; [-21.916757, -47.620295]; 685 m a.s.l; 4 Mar. 1941; O. Schubart leg.; MZSP • 1 ♂; same locality data as for preceding; 4 Mar. 1941; MZSP • 2 ♂♂, 9 ♀♀, 2 ♂♂ immatures, 8 ♀♀ immatures, 1 immature; same locality data as for preceding; 6 Jan. 1940; MZSP • 1 ♀; São José do Rio Preto, Fazenda Itália; [-20.816500, -49.376402]; 506 m a.s.l.; 25 Oct. 1945; F.P. Mello leg.; MZSP • 1 ♂, 2 immatures; Cachoeira de Cima, Rio Mogi Guaçu; [-21.087289, -48.180398]; 498 m a.s.l.; 15 Jan. 1947; O. Schubart leg.; MZSP • 2 ♂♂, 7 ♀♀, 1 ♀ immature; Leme, Fazenda Graminha; [-22.183853, -47.384995]; 624 m a.s.l.; 10 Dec. 1948; O. Schubart leg.; MZSP • 2 ♂♂, 2 ♀♀; Porto Ferreira, Mata do Procópio; [-21.842360, -47.471538]; 565 m a.s.l.; 7 Mar. 1944; N. dos Santos leg. MZSP.

Descriptive notes

MEASUREMENTS. 58–63 body rings (2–3 apodous + telson). Males: body length 25–35 mm; maximum midbody diameter 1.4–1.8 mm. Females: body length 28–38 mm; maximum midbody diameter 1.6–2.1 mm.

COLOR. Body color faded, but apparently prozonites brownish, metazonites with a brown posterior band; head, antennae, and legs lighter; collum brown.

HEAD. Antennae short, just reaching back to end of ring 5 when extended dorsally; relative antennomere lengths 1<2≈3>4≈5<6>7. Mandibular cardo with ventral margin narrow. Ommatidial cluster well-developed, covered partially by anterior region of collum, elliptical; ca 20 ommatidia in 4 rows.

BODY RINGS. Collum with lateral lobes broadly subrectangular, with ca 6 striae (Fig. 78A). Very faintly constricted between prozonite and metazonite; prozonites smooth; metazonites laterally with transverse striae from ca ⅓ length below ozopore. Anterior sterna in midbody rings subrectangular, without transverse striae (Fig. 169D).

First leg-pair of males. Coxae (***cx***) short (less than half of remaining podomere lengths), subtriangular, with the base arched, slightly expanded, and constricted medially, densely setose (Figs 79A, 80B, 204B); prefemoral process (***prf***) as long as half length of prefemur, subcylindrical, densely setose along the entire ventral region, central groove deep (Fig. 79B); remaining podomeres with setae along the mesal region.

Second leg-pair of males. Coxa (***cx***) subrectangular; penis (***pn***) located at proximal region, rounded, not extended basally (Fig. 79C); prefemur compressed dorsoventrally; remaining podomeres setose.

Gonopods. Gonocoxa (***gcx***) elongated, almost twice as long as telopodite, with the base arched; slightly flattened antero-posteriorly (Figs 79D–F, 80C); with rows of papillae mesally. Seminal groove (***sg***) curved; arising medially on mesal cavity and terminating apically on the seminal apophysis (***sa***). Shoulder (***sh***) inconspicuous. Telopodite (***tp***) almost as wide as ***gcx*** (Figs 79D, 80D), with rounded laterad projection; solenomere (***sl***) with apicomesal process (***amp***) short, subtriangular; ectal process absent; ***sa*** located at medial portion, slightly visible apically. Internal branch (***ib***) shovel-shaped, apically enfolding ***sl***, with horizontal plate; setae restricted to the apical region of ***ib*** exceeding seminal region of ***sl*** (Figs 79D–F, 80D).

Vulvae. As typical for the genus. Bursa subtriangular, glabrous (Fig. 177M); internal valve subtriangular, with its sides having the same length; operculum large, curved ectad; external valve narrow, in oral view, subtriangular.

Distribution

Known from the central-west region of São Paulo State, Brazil (Fig. 183); occurring in the Cerrado biome (tropical savanna ecoregion) and in second-growth forests in the region.

Pseudonannolene leucomelas Schubart, 1947
Figs 12, 81–82, 165N, 184

Pseudonannolene leucomelas Schubart, 1947: 32, figs 32–34.

Pseudonannolene leucomelas – Schubart 1958: 240. — Jeekel 2004: 89. — Golovatch *et al.* 2005: 279. — Gallo & Bichuette 2020: 36.

Diagnosis

Adults resemble those of *P. spelaea* by the reduced number of ommatidia (less than 15 ommatidia) (Fig. 81A), but differing by having solenomere with evident and elongated seminal apophysis; internal branch with long setae restricted to the apical margin (Fig. 82D).

Etymology

Name 'leucomelas' taken from the Greek words '*lefkó*' = 'white', plus '*mélās*' = 'black', referring to the pattern of coloration of the body rings of the species (Schubart 1947).

Material examined

Holotype

BRAZIL • ♂ [fragmented in two different vials and in microscope slide; gonopod, first and second leg-pair missing]; Mato Grosso, Barra do Tapirapé [= Santa Terezinha]; [-10.501639, -50.731877]; Dec.

1939; A.L. Carvalho leg.; MNRJ 11828 [some body rings], MNRJ 11826 [head and remaining body rings], MZSP [body ring on microscope slide].

Paratypes (total: 3 ♀♀, 2 immatures)
BRAZIL • 1 ♀; same collection data as for holotype; MZSP • 2 ♀♀, 2 immatures; same collection data as for holotype; MNRJ 11829.

Descriptive notes

Gonopod description adapted from Schubart (1947: 32) to supplement original description and to introduce gonopod terminology; remaining male sexual characters described based on examined syntype and non-sexual characters described only for female.

Measurements. 62–65 body rings (2–3 apodous + telson). Males: fragmented, body length ca 25 mm; maximum midbody diameter 1.5 mm. Females: fragmented, body length 27–30 mm; maximum midbody diameter 1.6 mm.

Color. Body color faded, but apparently prozonites dark brown, metazonites with a lighter posterior band; head, collum, antennae, and legs dark brownish.

Head. Antennae short (Fig. 81A), just reaching back to end of ring 5 when extended dorsally; relative antennomere lengths $1<2<3>4<5\approx6>7$. Mandibular cardo with ventral margin narrow. Ommatidial cluster reduced and almost entirely covered by collum; ca 15 ommatidia in 3 rows.

Body rings. Collum with lateral lobes broadly subrectangular, with ca 5 thickened striae, slightly curved mesad (Fig. 81A). Very faintly constricted between prozonite and metazonite; prozonites smooth; metazonites laterally with transverse striae below ozopore. Anterior sterna in midbody rings subrectangular, without transverse striae (Fig. 82C).

First leg-pair of males. Coxae (***cx***) short (less than half of remaining podomere lengths), subtriangular, with the base arched, densely setose; prefemoral process (***prf***) as wide as half of prefemur, subcylindrical, densely setose up to its median region; remaining podomeres with setae along the mesal region.

Second leg-pair of males. Coxa (***cx***) large and rounded; penis (***pn***) located at proximal region, rounded, not extended basally; prefemur compressed dorsoventrally; remaining podomeres setose.

Gonopods. Gonocoxa (***gcx***) elongated, medially expanded and thinning towards apex; slightly flattened antero-posteriorly; with rows of papillae mesally. Seminal groove (***sg***) protruded on squamous region of ***sl***, terminating apically on the seminal apophysis (***sa***). Shoulder absent. Telopodite (***tp***) less wide than half of ***gcx***; solenomere (***sl***) with ***sa*** thickened, visible apically; ectal process absent; ***sa*** located at medial portion, visible apically. Internal branch (***ib***) shovel-shaped, with horizontal plate; setae restricted to the apical region of ***ib*** exceeding seminal region of ***sl*** (Fig. 82D).

Vulvae. As typical for the genus. Bursa subtriangular, glabrous; internal valve subtriangular; operculum narrow, curved medially; external valve wide, subtriangular.

Distribution

Known only from the type locality Santa Terezinha (formerly Barra do Tapirapé), Mato Grosso, Brazil (Fig. 184). The indigenous region of "Barra do Tapirapé" is restricted to the marginal forests in the Araguaia River, with typical Amazonian fauna and flora interspersed by patches of Cerrado (tropical savannah).

Pseudonannolene longicornis (Porat, 1888)
Figs 83–84, 163K, 165O, 169E, 177N, 184

Alloporus longicornis Porat, 1888: 256.
Pseudonannolene marconii Iniesta & Ferreira, 2014: 371, figs 8, 14d. **Syn. nov.**

Pseudonannolene longicornis – Brölemann 1909: 57 (transference *Alloporus longicornis* Porat, 1888 in pars); 1919: 275. — Mauriès 1987: 170, figs 1–3 (neotype designation). — Jeekel 2004: 89. — Iniesta & Ferreira 2013a: 92; 2014: 361.
Pseudonannolene marconii – Gallo & Bichuette 2019: 47.
Pseudonannolene ? *silvestris* – Mauriès 1987: 180, figs 20–22 (misidentified males from Fazenda Cachoeira, Vassouras, Rio de Janeiro, Brazil).

Justification of synonymy

Through the examination of the type material of both species, as well as additional specimens from the type localities, we concluded that the male morphology of both nominal species agree completely when considering the gonopods and first and second leg-pairs. Slight differences in the forms of the gonocoxae and solenomere are treated as intraspecific variation. Therefore, *P. marconii* is proposed here as a junior synonym of *P. longicornis*.

Diagnosis

Males of *P. longicornis* resemble those of *P. tricolor* by having gonocoxa largely subcylindrical with large shoulder (Fig. 84D–F), but differing by an enlargement of the solenomere base, and a subtriangular internal branch that is not excavated at midlength, when viewed anally (Fig. 84D–E).

Etymology

Named after the Latin adjective '*longus*' = 'long', and the noun '*cornus*'. Unspecified in the original description, but likely to be related to the frontal projection on the head of the species.

Material examined

Holotype

BRAZIL • ♂, holotype of *P. marconii*; Bahia, Pau Brasil, Pedra Suspensa cave; [-15.568625, -39.686560]; 180 m a.s.l.; 21 Jan. 2005; R.L. Ferreira *et al.* leg.; ISLA 4106.

Other material (total: 16 ♂♂, 2 ♀♀)

BRAZIL – **Bahia** • 1 ♂; Pau Brasil, Córrego Verde cave; [-15.466728, -39.674896]; 183 m a.s.l.; 21 Jan. 2005; R.L. Ferreira *et al.* leg.; ISLA 15678. – **Espírito Santo** • 5 ♂♂, 2 ♀♀; Aracruz, Parque Natural Municipal do Aricanga; [-19.830269, -40.328487]; 37 m a.s.l.; 22–27 Apr. 2010; IBSP 3734 • 1 ♂; REFMU do Morro do Aricanga; [-19.822498, -40.334524]; 122 m a.s.l.; 14–16 Oct. 2005; A. Giupponi, V. Orrico, M. Milleri, R. Rodrigues and T. Souza leg. MNRJ • 1 ♂; Linhares; [-19.395994, -40.065472]; 33 m a.s.l.; 23 Oct. 1944; O. Schubart leg.; MZSP • 6 ♂♂; Mata Alta; Apr. 1993; MNRJ 30155. – **Rio de Janeiro** • 1 ♂; Nova Iguaçu, Reserva Ecológica Tinguá; [-22.565598, -43.410073]; 392 m a.s.l.; Feb. 2002; E.F. Ramos leg.; IBSP 1921 • 1 ♂; Vassouras, Fazenda da Cachoeira; [-22.458059, -43.615817]; 680 m a.s.l.; 30 Apr. 1994; Boving-Petersen leg.; NHMD.

Descriptive notes

Measurements. 54–60 body rings (1–2 apodous + telson). Males: body length 58–82 mm; maximum midbody diameter 4.7–5 mm. Females: body length 35–45 mm; maximum midbody diameter 5.3 mm.

Color. Body color brownish grey; head and collum darker; prozonites greyish anteriorly; metazonites with a light posterior band; antennae and legs lighter.

Head. Antennae long (Fig. 163K), just reaching back to end of ring 6 when extended dorsally; antennomeres elongated; relative antennomere lengths $1<2<3>4\approx5>6>7$. Mandibular cardo with ventral margin narrow. Ommatidial cluster well-developed, elliptical; ca 40 ommatidia in 5 rows. Frontal region with rounded projection.

Body rings. Collum with lateral lobes rounded, with 10 striae, curved ectad (Fig. 83A). Very faint constriction between prozonites and metazonites; prozonites smooth; metazonites laterally with transverse striae slightly above ozopore in anterior body rings. Anterior sterna in midbody rings subrectangular, with shallow transverse striae (Fig. 169E).

First leg-pair of males. Coxae (***cx***) short (less than half of remaining podomere lengths), subtriangular, with the base strongly arched and expanded, densely setose (Fig. 84A); prefemoral process (***prf***) twice as long as prefemur, subcylindrical, apically narrow and slightly curved ectad, densely setose up to its median region (Fig. 84B); remaining podomeres with setae along the mesal region.

Second leg-pair of males. Coxa (***cx***) large and rounded; penis (***pn***) located at proximal region, rounded, not extended basally (Fig. 84C); prefemur compressed dorsoventrally; remaining podomeres setose.

Gonopods. Gonocoxa (***gcx***) elongated, largely subcylindrical, with the base arched; antero-posteriorly flattened (Fig. 84D–F); with rows of papillae mesally. Seminal groove (***sg***) curved; arising medially on mesal cavity and terminating apically on the seminal apophysis (***sa***). Shoulder (***sh***) large, rounded. Telopodite (***tp***) almost as wide as ***gcx*** (Fig. 84D); solenomere (***sl***) enlarged basally, with apicomesal process (***amp***) subtriangular, short; ectal process (***ep***) subtriangular, separating from ***amp*** by shallow notch; ***sa*** located at mesal portion, slightly visible apically. Internal branch (***ib***) subtriangular, narrow and foliaceous; setae starting at midlength of ***ib*** slightly exceeding seminal region of ***sl*** (Fig. 84D–F).

Vulvae. As typical for the genus. Bursa subtriangular, glabrous (Fig. 177N); internal valve subtriangular, with mesal region rounded; operculum narrow, curved ectad; external valve wide, subtriangular.

Distribution

The species is distributed in the coastal region of the Atlantic Forest from Rio de Janeiro up to the southern Bahia State, Brazil (Fig. 184).

Comments

The descriptive notes are based on topotypes of the species, since the examination of the neotype deposited at the Muséum national d'histoire naturelle, Paris, France (MNHN), was not possible during this study.

Pseudonannolene lundi Iniesta & Ferreira, 2015
Figs 85–86, 165P, 170A, 177O, 184; Supp. file 4: Fig. 212B

Pseudonannolene lundi Iniesta & Ferreira, 2015: 124, figs 1–3.

Pseudonannolene lundi – Deharveng & Bedos 2018: fig. 7.4d. — Gallo & Bichuette 2019: 42; 2020: 34.

Diagnosis

Resembling *P. ambuatinga* and *P. spelaea* by having head, trunk, and legs depigmented (Fig. 85). Males of *P. lundi* differ from *P. ambuatinga* by square-shaped solenomere (Fig. 86D), and from *P. spelaea* by having an evident seminal apophysis and a greater number of ommatidia (ca 25) (Fig. 85A).

Etymology

Patronym honoring the Danish naturalist Peter Wilhelm Lund, who is considered the founder of speleology as a science in Brazil. The name also refers to the caving Brazilian group “Espeleo Grupo Peter Lund”, for their contributions to our knowledge of the caves of the region where the species occurs (Iniesta & Ferreira 2015).

Material examined

Holotype

BRAZIL • ♂; Minas Gerais, Luislândia, Lapa Sem Fim cave; [-16.233458, -44.585626]; 17 Apr. 2014; R.L. Ferreira, L.F.M. Iniesta, L. Rabello and M. Souza-Silva leg.; ISLA 8684.

Paratypes (total: 2 ♂♂, 3 ♀♀)

BRAZIL • 1 ♂; same collection data as for holotype; ISLA 8685 • 1 ♂; same collection data as for holotype; ISLA 8686 • 1 ♀; same collection data as for holotype; ISLA 8687 • 1 ♀; same collection data as for holotype; ISLA 8688 • 1 ♀; same collection data as for holotype; ISLA 8689.

Descriptive notes

Measurements. 62–68 body rings (1–2 apodous + telson). Males: body length 49.5 mm; maximum midbody diameter 2.7–2.8 mm. Females: body length 61.9 mm; maximum midbody diameter 2.8–3 mm.

Color. Living specimens depigmented. Color when stored in 70% ethanol: uniform pale brownish white, faint dark shadows posteriorly on prozonites; head, collum, antennae, and legs brownish.

Head. Antennae long (Fig. 85A), just reaching back to end of ring 6 when extended dorsally; antennomeres elongated; relative antennomere lengths $1<2<3>4>5\approx6>7$. Mandibular cardo with ventral margin swollen. Ommatidial cluster well-developed, elliptical; ca 30 ommatidia in 5 rows.

Body rings. Collum with lateral lobes rounded, with ca 10 striae, slightly curved ectad (Fig. 85A). Very faint constriction between prozonites and metazonites; prozonites smooth; metazonites laterally with transverse striae below ozopore. Anterior sterna in midbody rings subrectangular, with shallow transverse striae (Fig. 170A).

First leg-pair of males. Coxae (***cx***) elongated (as long as the sum of remaining podomere lengths), subtriangular, with the base slightly arched and expanded, densely setose (Fig. 86A); prefemoral process (***prf***) as wide as half of prefemur, subcylindrical, densely setose along its entire extension (Fig. 86B); remaining podomeres with setae along the mesal region.

Second leg-pair of males. Coxa (***cx***) large and subrectangular; penis (***pn***) located at proximal region, large and rounded, not extended basally (Fig. 86C); prefemur compressed dorsoventrally; remaining podomeres setose.

Gonopods. Gonocoxa (***gcx***) rounded, basally expanded and progressively less wide, with the base arched; flattened antero-posteriorly (Figs 86D–F, 212B); with rows of papillae mesally. Seminal groove (***sg***) curved; arising medially on mesal cavity and terminating apically on the seminal apophysis (***sa***). Shoulder absent. Telopodite (***tp***) almost as wide as ***gcx*** (Fig. 86D); solenomere (***sl***) with apicomesal process (***amp***) short, rounded; ectal process (***ep***) rounded, separated from ***amp*** by shallow notch; ***sa*** located at mesal portion, slightly visible apically. Internal branch (***ib***) shovel-shaped and rounded apically, with horizontal plate; setae restricted to the apical region of ***ib*** exceeding seminal region of ***sl*** (Fig. 86D–F).

Vulvae. As typical for the genus. Bursa subtriangular, glabrous (Fig. 177O); internal valve subtriangular, strongly inclined towards the mesal region; operculum narrow, constricted medially; external valve wide, subtriangular.

Distribution

A troglomorphic species known only from the type locality Lapa Sem Fim cave, Luislândia, state of Minas Gerais, Brazil (Fig. 184). The Lapa Sem Fim cave corresponds to the largest cave in the Brazilian state, with at least 15 km of an intricate system of conduits and only two known entrances located in the extremities of the only intermittent drainage.

Pseudonannolene magna Udulutsch & Pietrobon, 2003
Figs 87–88, 163L, 165Q, 170B, 178A, 184; Supp. file 4: Fig. 206D

Pseudonannolene magna Udulutsch & Pietrobon in Fontanetti *et al.,* 2003: 66, figs 1–9.

Diagnosis

Males of *P. magna* are similar to most species of the genus by having a subtriangular solenomere (Fig. 88D–F), but differing by a mesally situated seminal apophysis (Fig. 88D) and a long, densely setose prefemoral process on the first leg-pair (Fig. 88A).

Etymology

Named after the Latin adjective '*magna*' = 'large', 'huge'. Unspecified in the original description, but likely to be related to the body size of the species.

Material examined

Holotype
BRAZIL • ♂ [fragmented]; São Paulo, Valinhos, Serra dos Cocais; [-23.024107, -46.894115]; Mar. 2000; F.B. Britto leg.; MZSP 941.

Paratypes (total: 3 ♂♂, 4 ♀♀)
BRAZIL • 3 ♂♂, 4 ♀♀; same collection data as for holotype; MZSP 941.

Other material (total: 2 ♂♂, 7 ♀♀, 8 immatures)
BRAZIL – **São Paulo** • 2 ♂♂, 7 ♀♀, 1 ♀ immature, 7 immatures; Valinhos, Serra dos Cocais; [-23.023664, -46.893820]; 807 m a.s.l.; Mar. 2001; Pietrobon leg.; MZSP.

Descriptive notes

Measurements. 60–62 body rings (1 apodous + telson). Males: body length 84 mm; maximum midbody diameter 4 mm. Females: body length 86 mm; maximum midbody diameter 4 mm.

Color. Body color greyish; head, collum, antennae, and legs darker; prozonites greyish anteriorly; metazonites with a reddish posterior band.

Head. Antennae long (Fig. 163L), just reaching back to the end of ring 6 when extended dorsally; antennomeres elongated; relative antennomere lengths 1<2<3>4>5<6>7. Mandibular cardo with narrow ventral margin. Ommatidial cluster well-developed, elliptical; ca 30 ommatidia in 5 rows.

Body rings. Collum with lateral lobes rounded, with ca 7 striae, curved mesad (Fig. 87A). Very faint constriction between prozonites and metazonites; prozonites smooth; metazonites laterally with transverse striae above ozopores. Anterior sterna in midbody rings subrectangular, with shallow transverse striae (Fig. 170B).

First leg-pair of males. Coxae (***cx***) short, subtriangular, with the base arched, densely setose, mainly on distal region (Fig. 88A); prefemoral process (***prf***) elongated and as wide as half of prefemur, subcylindrical, slightly curved ectad, densely setose up to its median region (Figs 88B, 206D).

Second leg-pair of males. Coxa (***cx***) large and subrectangular; penis (***pn***) located at proximal region, rounded, not extended basally (Fig. 88C); prefemur compressed dorsoventrally; remaining podomeres setose.

Gonopods. Gonocoxa (***gcx***) elongated, rectangular-shaped, with the base slightly arched; flattened antero-posteriorly (Fig. 88D–F); with rows of papillae mesally. Seminal groove (***sg***) slightly curved; arising medially on mesal cavity and terminating apically on the seminal apophysis (***sa***). Shoulder (***sh***) subtriangular. Telopodite (***tp***) less wide than half of ***gcx*** (Fig. 88D); solenomere (***sl***) with apicomesal process (***amp***) subtriangular; ectal process absent; ***sa*** located at mesal portion, visible apically. Internal branch (***ib***) subtriangular, surrounding base of ***tp*** as a shield; ***ib*** with setae along its entire margin exceeding apically seminal region of ***sl*** (Fig. 88D–F).

Vulvae. As typical for the genus. Bursa subtriangular, glabrous (Fig. 178A); internal valve subtriangular, with mesal region rounded; operculum narrow, slightly curved ectad, constricted medially; external valve wide, subtriangular.

Distribution

Known only from the type locality Serra dos Cocais, Valinhos, state of São Paulo, Brazil (Fig. 184).

Pseudonannolene maritima Schubart, 1949

Figs 10, 30E, 32B, D, 35C–D, 89–91, 163M, 165R, 170C, 178B, 184; Supp. file 4: Figs 207C, 211B

Pseudonannolene maritima Schubart, 1949: 214, figs 12–17, 26.

Pseudonannolene maritima – Jeekel 2004: 89. — Gallo & Bichuette 2020: 36.

Diagnosis

Males of *P. maritima* resemble those of *P. halophila*, *P. sebastianus* Brölemann, 1902, *P. patagonica* Brölemann, 1902, and *P. insularis* sp. nov. by having large and subrectangular coxae on the first leg-pair (Figs 30E, 90A, 91B) and suboval penis (Figs 90C, 91E–F), but differing by having the internal branch rounded; horizontal plate large, apically swollen when viewed anally (Figs 32B, 35C, 90D).

Etymology

Adjective referring to the geographical distribution of the species, occurring in islands of the Brazilian state of São Paulo (Schubart 1949).

Material examined

Holotype

BRAZIL • ♂ [antennae, gonopod, gnathochilarium, first and second leg-pair on microscope slides]; São Paulo, Peruíbe, Ilha da Queimada Pequena; [-24.489198, -46.674305]; 100 m a.s.l.; 30 Sep. 1947; Expedição A. Hoge leg.; MZSP.

Paratypes (total: 13 ♂♂, 24 ♀♀, 12 immatures)
BRAZIL – **São Paulo** • 1 ♂, 13 ♀♀, 6 immatures; same collection data as for holotype; MZSP; • 2 ♂♂, 1 ♀, 6 immatures; Peruíbe, Ilha da Queimada Grande; [-24.487922, -46.674156]; 14–22 Apr. 1947; Expedição A. Hoge leg.; MZSP • 10 ♂♂, 10 ♀♀; Ilha Grande; [-24.098785, -45.693242]; Luederwaldt and Fonseca leg.; MZSP.

Other material (total: 17 ♂♂, 36 ♀♀, 6 immatures)
BRAZIL – **São Paulo** • 5 ♂♂ immatures; Itanhaém, Ilha da Queimada Grande; [-24.487922, -46.674156]; 103 m a.s.l.; 1–2 Apr. 2003; R. Martins and R. Bertani leg.; IBSP 1530 • 1 ♀; same locality data as for preceding; 2003; IBSP 1213 • 2 ♂♂, 4 ♀♀, 1 immature; same locality data as for preceding; IBSP 1176 • 1 ♀; same locality data as for preceding; 29 Apr.–1 May 2003; R.P. Indicatti leg.; IBSP 2829 • 1 ♂, 13 ♀♀; Ilha dos Alcatrazes; [-24.098785, -45.693242]; 60 m a.s.l.; 4–6 Jul. 1998; M.E. Calleffo leg.; IBSP 658 • 7 ♂♂, 4 ♀♀; same locality data as for preceding; 15–17 May 1994; A. Eterovic leg.; IBSP 1102 • 1 ♂, 2 ♀♀; same locality data as for preceding; 26 Aug. 2005; Equipe Herpetologia IBSP leg.; IBSP 3932 • 1 ♂, 3 ♀♀; same locality data as for preceding; 10–12 Jun. 1994; A. Eterovic leg.; IBSP 7898 • 4 ♂♂, 7 ♀♀; same locality data as for preceding; 16 Feb. 1948; A. Hoge leg.; MZSP • 1 ♂, 1 ♀; Peruíbe, Estação Ecológica Juréia/Itatins; [-24.380787, -47.078906]; 16 m a.s.l.; Dec. 1998; A.D. Brescovit leg.; IBSP 979.

Descriptive notes

Measurements. 70–81 body rings (1–2 apodous + telson). Males: body length 70–102 mm; maximum midbody diameter 3.7–5.9 mm. Females: body length 60–80 mm; maximum midbody diameter 3.8–4.8 mm.

Color. Body color greyish; head and collum darker; prozonites greyish anteriorly; metazonites with a dark medial band and a light posterior band; antennae and legs light brown.

Head. Antennae short (Fig. 163M), just reaching back to end of ring 5 when extended dorsally; relative antennomere lengths $1<2<3>4>5\approx6>7$. Mandibular cardo with ventral margin swollen. Ommatidial cluster well-developed, elliptical; ca 40 ommatidia in 5 rows.

Body rings. Collum with lateral lobes rounded, with ca 8 thickened striae, curved ectad anteriorly (Fig. 89A). Very faint constriction between prozonites and metazonites; prozonites smooth; metazonites laterally with transverse striae below ozopores. Anterior sterna in midbody rings subrectangular, with shallow transverse striae (Fig. 170C).

First leg-pair of males. Coxae (***cx***) elongated (as long as the sum of remaining podomere lengths), subrectangular, with the base arched, densely setose (Figs 30E, 90A, 91B); prefemoral process (***prf***) as wide as half of prefemur, subcylindrical, densely setose along the entire ventral region (Fig. 90B); remaining podomeres with setae along the mesal region.

Second leg-pair of males. Coxa (***cx***) elongated and subrectangular; penis (***pn***) located at proximal region, rounded, slightly extended basally (Fig. 90C, 91E–F); prefemur dorsoventrally compressed; remaining podomeres setose.

Gonopods. Gonocoxa (***gcx***) elongated, almost twice as long as telopodite, with the base slightly arched; flattened antero-posteriorly (Fig. 91C, 90D–F); with rows of papillae mesally. Seminal groove (***sg***) curved; protruded on squamous region of ***sl***, arising medially on mesal cavity and terminating apically on the seminal apophysis (***sa***). Shoulder (***sh***) inconspicuous. Telopodite (***tp***) less than half as wide as ***gcx*** (Figs 32B, 35C–D, 91D, 90D); solenomere (***sl***) with apicomesal process (***amp***) subtriangular; ectal process absent; ***sa*** located at mesal portion, thickened apically. Internal branch (***ib***) shovel-shaped and rounded apically, with horizontal plate; setae restricted to the apical region of ***ib*** not exceeding seminal region of ***sl*** (Fig. 91C, 90D–F).

VULVAE. As typical for the genus. Bursa subtriangular, glabrous (Fig. 178B); internal valve subtriangular, with mesal region rounded; operculum narrow; external valve wide, subtriangular.

Distribution

The species is widely distributed in the Atlantic Forest of the Brazilian archipelago Alcatrazes and in the coastal region of São Paulo State, Brazil (Fig. 184).

Pseudonannolene meridionalis Silvestri, 1902
Figs 92, 185

Pseudonannolene meridionalis Silvestri, 1902: 22.

Pseudonannolene cf. *meridionalis* – Mauriès 1987: 173 (description of male topotype).
Pseudonannolene meridionalis – Jeekel 2004: 89. — Gallo & Bichuette 2020: 36.

Diagnosis

Males of *P. meridionalis* resemble those of *P. centralis* and *P. typica* by having a short ectal process on the solenomere, separated from the apicomesal process by a shallow notch. *Pseudonannolene meridionalis* differs by having gonocoxa enlarged basally, and internal branch without torsion (Fig. 92C–D).

Etymology

Although unspecified, the name is probably referring to the geographical distribution of the species in southern South America.

Material examined (total: 2 ♂♂, 10 ♀♀, 1 immature)

ARGENTINA – **Buenos Aires** • 1 ♂, 10 ♀♀, 1 immature; Buenos Aires; [-34.638212, -58.470722]; 25 m a.s.l.; 5 Jun. 1947; Exp. Galathea leg.; NHMD.

URUGUAY – **Colonia** • 1 ♂; Barra del Rosario; [-34.455863, -57.824967]; 26 m a.s.l.; 12 Jun. 1960; L.C. de Zolessi leg.; FCE 219.

Descriptive notes

MEASUREMENTS. 57–58 body rings (2 apodous + telson). Males: body length 45 mm; maximum midbody diameter 2.5 mm. Females: body length 45–48 mm; maximum midbody diameter 2.5 mm.

COLOR. Body color faded, but apparently prozonites brownish, metazonites with a posterior brown band; head, collum, antennae, and legs lighter brown.

HEAD. Antennae short, just reaching back to end of ring 5 when extended dorsally; relative antennomere lengths 1<2<3>4≈5≈6>7. Mandibular cardo with ventral margin narrow. Ommatidial cluster well-developed, elliptical; ca 26 ommatidia in 5 rows.

BODY RINGS. Collum with lateral lobes rounded, with ca 7 shallow striae, slightly curved ectad. Very faintly constricted between prozonite and metazonite; prozonites smooth; metazonites laterally with transverse striae below ozopore. Anterior sterna in midbody rings subrectangular, without transverse striae.

First leg-pair of males. Coxae (***cx***) short, subtriangular, with the base arched, densely setose mainly on distal region (Fig. 92A); prefemoral process (***prf***) short (less than half of prefemur), subcylindrical, densely setose up to its median region.

Second leg-pair of males. Coxa (***cx***) subrectangular; penis (***pn***) located at proximal region, rounded, not extended basally (Fig. 92B); prefemur compressed dorsoventrally; remaining podomeres setose.

Gonopods. Gonocoxa (***gcx***) subtriangular, basally expanded and progressively less wide, with the base arched; antero-posteriorly flattened (Fig. 92C–D); with rows of papillae mesally. Seminal groove (***sg***) curved; arising medially on mesal cavity and terminating apically on the seminal apophysis (***sa***). Shoulder (***sh***) short, rounded. Telopodite (***tp***) almost as wide as ***gcx*** (Fig. 92C–D); solenomere (***sl***) with apicomesal process (***amp***) short, slightly rounded; ectal process (***ep***) short, subtriangular, separating from ***amp*** by shallow notch; ***sa*** located at mesal portion, slightly visible apically. Internal branch (***ib***) subtriangular, narrow, surrounding only basally ***tp*** as a shield; without torsion; ***ib*** with short setae along its entire margin slightly exceeding apically seminal region of ***sl***.

Vulvae. Not examined.

Distribution

The species occurs in the grasslands of the Río de la Plata basin, from the eastern region of Argentina up to the southern Uruguay (Fig. 185).

Comments

The type material described by Silvestri (1902) from Tandil, Argentina, was not found. Nevertheless, topotypes deposited at the NHMD and FCE were examined (Fig. 92), including those described by Mauriès (1987: 173).

Pseudonannolene mesai Fontanetti, 2000
Figs 11, 93–94, 163N, 166A, 170D, 178C, 185

Pseudonannolene mesai Fontanetti, 2000: 188, figs 1–7.

Pseudonannolene mesai – Iniesta & Ferreira 2013b: 366; 2013c: 78.

Diagnosis

Males of *P. mesai* resemble those of *P. curvata* sp. nov., *P. erikae*, and *P. bucculenta* sp. nov. by having a mesally curving telopodite, but differing from those species by a larger trunk of the telopodite, projected laterad (Fig. 94D).

Etymology

Patronym honoring the collector A. Mesa (Fontanetti 2000).

Material examined

Holotype

BRAZIL • ♂; São Paulo, Salesópolis, Estação Biológica de Boracéia; [-23.633126, -45.882183]; 943 m a.s.l.; Apr. 1984; C.S. Fontanetti leg.; MZSP.

Paratypes (total: 1 ♂, 1 ♀, 1 immature)

BRAZIL – **São Paulo** • 1 ♂, 1 ♀, 1 ♂ immature; same collection data as for holotype; Nov. 1990; A. Mesa and J.A. Diniz-Filho leg.; MZSP.

Other material (total: 2 ♂♂, 7 ♀♀, 8 immatures)
BRAZIL – **São Paulo** • 1 ♂; Salesópolis, Estação Biológica de Boracéia; [-23.633126, -45.882183]; 943 m a.s.l.; May 2001; Equipe Biota leg.; IBSP • 1 ♀ immature; same collection data as for preceding; IBSP 1890 • 1 ♂; same collection data as for preceding; IBSP 816 • 2 ♀♀; Cotia, Reserva Florestal do Morro Grande; [-23.603506, -46.919463]; 798 m a.s.l.; 13–30 Jun. 2002; Equipe Biota leg.; IBSP 2041 • 1 ♂; same collection data as for preceding; IBSP 2039 • 1 ♀; same collection data as for preceding; IBSP 2042.

Descriptive notes

Measurements. 54–60 body rings (1–2 apodous + telson). Males: body length 60.8–61.8 mm; maximum midbody diameter 3.1–3.6 mm. Females: body length 71.6–81.4 mm; maximum midbody diameter 4.6–4.8 mm.

Color. Body color brownish grey; head, collum, antennae and legs brownish darker; prozonites anteriorly greyish; metazonites with a medial brown band and a posterior lighter.

Head. Antennae long (Fig. 163N), just reaching back to end of ring 6 when extended dorsally; antennomeres elongated; relative antennomere lengths 1<2<3>4>5≈6>7. Mandibular cardo with ventral margin narrow. Ommatidial cluster well-developed, elliptical; ca 33 ommatidia in 5 rows.

Body rings. Collum with lateral lobes rounded, with ca 9 striae, slightly curved ectad (Fig. 93A). Very faintly constricted between prozonite and metazonite; prozonites smooth; metazonites laterally with transverse striae below ozopore. Anterior sterna in midbody rings subrectangular, with 7 transverse striae (Fig. 170D).

First leg-pair of males. Coxae (***cx***) short (less than half of remaining podomere lengths), subtriangular, with the base arched, densely setose mainly on distal region (Fig. 94A); prefemoral process (***prf***) as wide as half of prefemur, subcylindrical, densely setose up to its median region (Fig. 94B); remaining podomeres with setae along the mesal region.

Second leg-pair of males. Coxa (***cx***) large and rounded; penis (***pn***) located at proximal region, rounded, not extended basally (Fig. 94C); prefemur compressed dorsoventrally; remaining podomeres setose.

Gonopods. Gonocoxa (***gcx***) rounded and elongated, almost twice as long as telopodite, with the base arched; antero-posteriorly slightly flattened (Fig. 94D–F); with rows of papillae mesally. Seminal groove (***sg***) curved; arising medially on mesal cavity and terminating apically on the seminal apophysis (***sa***). Shoulder (***sh***) inconspicous. Telopodite (***tp***) large, strongly curved mesad, projected laterad (Fig. 94D); solenomere (***sl***) with small squamous region; apicomesal process (***amp***) subtriangular; ectal process absent; ***sa*** located at mesal portion, slightly visible apically. Internal branch (***ib***) short and narrow, subtriangular, surrounding basally ***tp*** as a shield; ***ib*** with setae along its entire margin exceeding apically seminal region of ***sl*** (Fig. 94D–F).

Vulvae. As typical for the genus. Bursa subtriangular, glabrous (Fig. 178C); internal valve subtriangular, with mesal region rounded; operculum narrow; external valve wide, subtriangular.

Distribution

The species occurs in the Atlantic Forest from the coastal region of São Paulo State, Brazil (Fig. 185).

Pseudonannolene microzoporus Mauriès, 1987
Figs 19E–F, 29A, 30B, 33–34, 35A–B, 36C–D, 39A–B, D, 95–97, 163O, 166B, 170E, 178D, 185;
Supp. file 4: Figs 194D, 210B, 211C

Pseudonannolene microzoporus Mauriès, 1987: 180, figs 23–25.
Pseudonannolene chaimowiczi Fontanetti, 1996: 428, figs 5–7. **Syn. nov.**
Pseudonannolene gogo Iniesta & Ferreira, 2013c: 75, figs 1a–c. **Syn. nov.**
Pseudonannolene longissima Iniesta & Ferreira, 2014: 313, figs 13–14. **Syn. nov.**
Pseudonannolene taboa Iniesta & Ferreira, 2014: 363, fig. 2. **Syn. nov.**
Pseudonannolene rosineii Iniesta & Ferreira, 2014: 370, fig. 7. **Syn. nov.**

Pseudonannolene microzoporus – Jeekel 2004: 89. — Iniesta & Ferreira 2013a: 92. — Gallo & Bichuette 2019: 47; 2020: 37.
Pseudonannolene chaimowiczi – Iniesta & Ferreira 2013a: 92; 2013b: 366; 2013c: 79. — Gallo & Bichuette 2019: 43; 2020: 36.
Pseudonannolene gogo – Karam-Gemael *et al.* 2018: figs 2–3. — Gallo & Bichuette 2019: 47.
Pseudonannolene longissima – Gallo & Bichuette 2019: 47.
Pseudonannolene taboa – Gallo & Bichuette 2019: 48; 2020: 43.
Pseudonannolene rosineii – Gallo & Bichuette 2019: 48.

Justification of synonymy

The ontogeny of the gonopods of *Pseudonannolene* is gradual, with morphological changes not abrupt during the development (see gonopod ontogeny in *Pseudonannolene* in the previous sections). *Pseudonannolene microzoporus* was described based on a male immature, considering the number of ommatidia (Fig. 97A), apodous body rings (Fig. 97B), and first leg-pair not fully developed (Mauriès 1987: figs 23–25). The remaining species are described based on adult males, although with a slight difference in the form of the internal branch and solenomere. Through the examination of the type material of all these nominal species and extensive samplings from localities where the species have been recorded, we conclude that they are junior subjective synonyms of *P. microzoporus*, and their morphological differences just intraspecific variations since the populations are widely distributed across a huge Karst area (Fig. 185).

Diagnosis

Males of *P. microzoporus* resemble those of *P. imbirensis* and *P. leopoldoi* by having a solenomere with an ectal process deeply notched separating it from the apicomesal process (Figs 35A–B, 96D, 211C); but differing of *P. imbirensis* by the having body color brownish grey, head, collum, and antennae darker (Fig. 95A), and differing of *P. leopoldoi* by having the internal branch curved ectad at midlength (Fig. 96D–F).

Etymology

Referring to the small size of the ozopores of the types (Mauriès 1987).

Material examined

Holotypes

BRAZIL • ♂ [immature], holotype of *P. microzoporus*; Minas Gerais, Lagoa Santa, Lapa Vermelha cave; [-19.609759, -44.003778]; Reinhardt leg.; NHMD 00101549.

BRAZIL • ♂, holotype of *P. chaimowiczi*; Minas Gerais, Lagoa Santa, Helictites cave; [-19.628840, -43.901935]; May 1987; F. Chaimowicz leg.; MZSP 939.

BRAZIL • ♂, holotype of *P. gogo*; Minas Gerais, Mariana; [-20.365015, -43.414773]; 13 May 2011; T. Pellegrini leg.; ISLA 4000.

BRAZIL • ♂, holotype of *P. longissima*; Minas Gerais, Sete Lagoas, Rei do Mato cave; [-19.495677, -44.282477]; Jan. 2001; R.L. Ferreira leg.; ISLA 4110.

BRAZIL • ♂, holotype of *P. taboa*; Minas Gerais, Sete Lagoas, Taboa cave; [-19.495666, -44.282498]; 15 Mar. 2005; R.L. Ferreira leg.; ISLA 4129.

BRAZIL • ♂, holotype of *P. rosineii*; Minas Gerais, Pains, Paranoá cave; [-20.369647, -45.669438]; 27 Jan. 2009; R. Zampaulo leg.; ISLA 4094.

Paratypes (total: 5 ♂♂, 8 ♀♀, 2 immatures)
BRAZIL • 1 ♀, 1 ♂ immature, 1 ♀ immature, paratypes of *P. microzoporus*; same collection data as for holotype; NHMD.

BRAZIL • 1 ♂, 2 ♀♀, paratypes of *P. chaimowiczi*; same collection data as for holotype; Mar. 1986; MZSP.

BRAZIL • 1 ♂, paratype of *P. gogo*; same collection data as for holotype; ISLA 4001 • 1 ♀, paratype of *P. gogo*; same collection data as for holotype; ISLA 4002 • 1 ♀, paratype of *P. gogo*; same collection data as for holotype; ISLA 4003.

BRAZIL • 1 ♂, paratype of *P. taboa*; same collection data as for holotype; ISLA 4130 • 1 ♂, paratype of *P. taboa*; same collection data as for holotype; ISLA 4131 • 1 ♀, paratype of *P. taboa*; same collection data as for holotype; ISLA 4132 • 1 ♀, paratype of *P. taboa*; same collection data as for holotype; ISLA 4133 • 1 ♀, paratype of *P. taboa*; same collection data as for holotype; ISLA 4134.

BRAZIL • 1 ♂, paratype of *P. rosineii*; Minas Gerais, Pains, Ninfeta III cave; [-20.369647, -45.669438]; 25 Jan. 2009; R. Zampaulo leg.; ISLA 4095 • 1 ♀, paratype of *P. rosineii*; same collection data as for preceding; ISLA 4121.

Other material (total: 117 ♂♂, 85 ♀♀, 12 immatures)
BRAZIL – **Bahia** • 4 ♂♂, 10 ♀♀, 4 immatures; Santana, Gruta do Padre cave; [-12.980311, -44.051343]; 543 m a.s.l.; 11 Jul. 2014; R.L. Ferreira, Souza-Silva and T.G. Pellegrini leg.; ISLA 20624 • 3 ♀♀; same locality data as for preceding; L.S. Silva leg.; IBSP 7637 • 2 ♂♂; same collection data as for preceding; IBSP 7636 • 1 ♂; same collection data as for preceding; IBSP 7638. – **Minas Gerais** • 1 ♀; Mocambeiro, MOC 01 cave; [-19.535426, -44.026975]; 4–15 Apr. 2011; F.P. Franco *et al.* leg.; IBSP 5717 • 1 ♀; IBSP 5718; same collection data as for preceding • 1 ♀; same collection data as for preceding except for MOC 03 cave; IBSP 5742 • 2 ♂♂; same collection data as for preceding except for MOC 04 cave; IBSP 5743 • 1 ♀; same collection data as for preceding except for MOC 100 cave; IBSP 5752 • 1 ♀; same collection data as for preceding except for MOC 101 cave; IBSP 5698 • 3 ♂♂; same collection data as for preceding; IBSP 5716 • 1 ♀; same collection data as for preceding except for MOC 105 cave; IBSP 5695 • 1 ♂, 1 ♀; same collection data as for preceding; IBSP 5700 • 1 ♂; same collection data as for preceding; IBSP 5701 • 1 ♀; same collection data as for preceding; IBSP 5702 • 1 ♀; same collection data as for preceding; IBSP 5703 • 1 ♂; same collection data as for preceding except for MOC 113 cave; IBSP 5715 • 1 ♂; same collection data as for preceding; IBSP 5738 • 1 ♂; same collection data as for preceding except for MOC 117 cave; IBSP 5637 • 2 ♀♀; same collection data as for preceding except for MOC 118 cave; IBSP 5706 • 1 immature; same collection data as for preceding except for MOC 120 cave; IBSP 5741 • 1 ♂, 1 ♀; same collection data as for preceding except for MOC 124 cave; IBSP 5640 • 2 ♂♂; same collection data as for preceding except for MOC 126 cave; IBSP 5739 • 1 ♂; same collection data as for

preceding except for MOC 13 cave; IBSP 5730 • 1 immature; same collection data as for preceding; IBSP 5731 • 1 ♂; same collection data as for preceding except for MOC 131 cave; IBSP 5719 • 1 ♀; same collection data as for preceding; IBSP 5720 • 1 ♀; same collection data as for preceding except for MOC 132 cave; IBSP 5735 • 1 ♂, 1 ♀; same collection data as for preceding except for MOC 134 cave; IBSP 5725 • 1 ♀; IBSP 5726 • 1 ♂, 1 ♀; same collection data as for preceding except for MOC 135 cave; IBSP 5707 • 1 ♂, 1 ♀; same collection data as for preceding; IBSP 5708 • 1 ♀; same collection data as for preceding; IBSP 5709 • 1 ♂; same collection data as for preceding except for MOC 137 cave; IBSP 5714 • 1 ♂; same collection data as for preceding except for MOC 20 cave; IBSP 5745 • 1 ♂, 1 ♀; same collection data as for preceding except for MOC 38 cave; IBSP 5727 • 1 ♂, 1 ♀; same collection data as for preceding; IBSP 5728 • 2 ♂♂, 1 ♀; same collection data as for preceding except for MOC 45 cave; IBSP 5747 • 1 ♂; same collection data as for preceding except for MOC 47 cave; IBSP 5723 • 1 ♂; same collection data as for preceding; IBSP 5724 • 1 ♂; same collection data as for preceding except for MOC 47 cave; IBSP 5723 • 1 ♂; same collection data as for preceding; IBSP 5724 • 2 ♀♀; same collection data as for preceding except for MOC 50 cave; IBSP 5696 • 2 ♂♂; same collection data as for preceding; IBSP 5699 • 1 ♂; same collection data as for preceding; IBSP 5703 • 1 ♂; same collection data as for preceding; IBSP 5704 • 1 ♀; same collection data as for preceding except for MOC 53 cave; IBSP 5705 • 1 ♀; same collection data as for preceding; IBSP 5744 • 2 ♀♀; same collection data as for preceding except for MOC 61 cave; IBSP 5694 • 1 ♂; same collection data as for preceding; IBSP 5721 • 1 ♀; same collection data as for preceding; IBSP 5722 • 1 ♀; same collection data as for preceding except for MOC 63 cave; IBSP 5749 • 1 ♂; same collection data as for preceding except for MOC 05 cave; 8–18 Feb. 2011; IBSP 5677 • 1 ♂; same collection data as for preceding; IBSP 5678 • 1 ♂; same collection data as for preceding except for MOC 10 cave; IBSP 5679 • 1 ♂; same collection data as for preceding except for MOC 113 cave; IBSP 5691 • 1 ♂; same collection data as for preceding except for MOC 14 cave; IBSP 5682 • 1 ♂; same collection data as for preceding; IBSP 5683 • 1 ♀; same collection data as for preceding except for MOC 15 cave; IBSP 5661 • 1 ♂; same collection data as for preceding; IBSP 5662 • 1 ♂, 1 ♀; same collection data as for preceding except for MOC 16 cave; IBSP 5685 • 1 ♂; same collection data as for preceding; IBSP 5686 • 1 ♀; same collection data as for preceding; IBSP 5687 • 1 ♂; same collection data as for preceding except for MOC 17 cave; IBSP 5653 • 1 ♂; same collection data as for preceding except for MOC 18 cave; IBSP 5655 • 1 ♂; same collection data as for preceding; IBSP 5656 • 1 ♀; same collection data as for preceding except for MOC 19 cave; IBSP 5659 • 1 ♂; same collection data as for preceding except for MOC 22 cave; IBSP 5692 • 1 ♂, 1 ♀; same collection data as for preceding except for MOC 24 cave; IBSP 5680 • 1 ♂; same collection data as for preceding; IBSP 5681 • 1 ♂; same collection data as for preceding except for MOC 25 cave; IBSP 5684 • 1 ♂; same collection data as for preceding except for MOC 29 cave; IBSP 5674 • 1 ♂; same collection data as for preceding except for MOC 30 cave; IBSP 5648 • 1 ♂; same collection data as for preceding; IBSP 5650 • 1 ♂; same collection data as for preceding except for MOC 32 cave; IBSP 5648 • 1 ♂; same collection data as for preceding except for MOC 67 cave; IBSP 5675 • 1 ♀; same collection data as for preceding; IBSP 5676 • 1 ♂; same collection data as for preceding except for MOC 68 cave; IBSP 5690 • 2 ♂♂; same collection data as for preceding except for MOC 70 cave; IBSP 5665 • 1 ♂; same collection data as for preceding; IBSP 5666 • 1 ♀; same collection data as for preceding; IBSP 5667 • 1 ♂; same collection data as for preceding; IBSP 5668 • 1 ♂; same collection data as for preceding; IBSP 5670 • 1 ♀; same collection data as for preceding; IBSP 5671 • 1 ♂; same collection data as for preceding; IBSP 5672 • 1 ♀; same collection data as for preceding except for MOC 84 cave; IBSP 5689 • 1 ♂; same collection data as for preceding except for MOC 94 cave; IBSP 5688 • 1 ♀; same collection data as for preceding except for MOC 96 cave; IBSP 5693 • 1 ♂; same collection data as for preceding except for MOC 28 cave; 8–23 Nov. 2011; IBSP 5627 • 1 ♀; same collection data as for preceding; IBSP 5628 • 1 ♂; same collection data as for preceding except for MOC 05 cave; IBSP 5625 • 1 ♂; same collection data as for preceding; IBSP 5626 • 1 ♂; same collection data as for preceding except for MOC 70 cave; 28 Jun.–1 Jul. 2011; IBSP 5669 • 1 ♀; same collection data as for preceding except for MOC 16 cave; IBSP 5644 • 1 ♂; same collection data as for preceding except for MOC 28 cave; IBSP 5663 • 1 ♂; same collection data as for preceding; IBSP 5664 • 1 ♂; same collection data as for preceding except for MOC 29 cave; IBSP 5673 • 1 ♀; same collection data as for preceding except for MOC 30 cave; IBSP 5645 • 1 ♀; same collection data as for preceding except for MOC 32 cave; IBSP 5646 • 1 ♀; same collection data as for preceding; IBSP 5647 • 1 ♂; same collection data as for preceding except for MOC 17 cave; IBSP 5651 • 1 ♀; same collection data as for preceding; IBSP 5652 • 1 ♂; same collection data as for preceding; IBSP 5654 • 1 ♂; same collection data as for preceding except for MOC 19 cave; IBSP 5657 • 1 ♀; same collection data as for preceding; IBSP 5658 • 1 ♂; same collection data as for preceding except for MOC 117 cave; 1–8 Mar. 2011; IBSP 5634 • 1 ♀; same collection data as for preceding except for MOC 124 cave; IBSP 5630 • 1 ♂; same collection data as for preceding except for MOC 13 cave; IBSP 5632 • 1 ♂; same collection data as for preceding except for MOC 45 cave; IBSP 5635 • 1 ♂; same collection data as for preceding except for MOC 50 cave; IBSP 5631 • 1 ♂; same collection data as for preceding except for MOC 53 cave; IBSP 5637 • 1 ♂; same collection data as for preceding except for MOC 61 cave; IBSP 5633 • 1 ♂; same collection data as for preceding except for MOC 63 cave; IBSP 5636 • 1 ♂, 3 ♀♀, 1 ♀ immature; Lagoa Santa, Grilão cave; [-19.535426, -44.026975]; 774 m a.s.l.; 7 Oct. 2012; T.G. Pellegrini leg.; ISLA 20619 • 1 ♂, 1 ♀, 1 ♀ immature; Lagoa Santa, Helictites cave; [-19.560285, -43.960153]; 745 m a.s.l.; 11 Oct. 2011; R. Ferreira leg.; ISLA 20611 • 1 ♂, 1 ♀; Lagoa Santa, Túneis cave; [-19.560699, -43.960511]; 744 m a.s.l.; 10 Oct. 2011; R. Ferreira leg.; ISLA 20621 • 1 ♀; same locality data as for preceding; Mar. 2000; É.S.S. Álvares leg.; IBSP 1368 • 1 ♀ immature; Matozinhos, Piriás cave; [-19.523028, -44.039009]; 692 m a.s.l.; 28 Jul. 2000; IBSP 3430 • 1 ♂ immature; same locality data as for preceding; 27 Jan. 2000; IBSP 3435 • 1 ♂; Sete Lagoas, Taboa cave; [-19.474917, -44.328137]; 761 m a.s.l.; 15 Jan. 2000; R.L. Ferreira *et al.* leg.; IBSP 2913 • 1 ♂; 1 ♂; same locality data as for preceding; 19 Jan. 2001; IBSP 3431 • 1 ♀; same collection data as for preceding; IBSP 3432 • 1 ♀ immature; Sete Lagoas, Mata Grande III cave; [-19.457380, -44.241670]; 778 m a.s.l.; 16 Nov. 2016; F. Bondezan leg.; IBSP 5426 • 1 ♂; Prudente de Morais; [-19.474888, -44.159215], 759 m a.s.l.; 23 Jan. 2003; IBSP 3427 • 1 ♂; Jaboticatubas, PARNA Serra do Cipó; [-19.349275, -43.619430]; 805 m a.s.l.; 7–14 Sep. 2003; Equipe Biota leg.; IBSP 1742 • 1 ♀; same collection data as for preceding; IBSP 1734 • 1 ♂, 1 ♀; same collection data as for preceding; IBSP 1752 • 1 ♂; same collection data as for preceding; IBSP 1755 • 1 ♀; same collection data as for preceding; IBSP 1746 • 2 ♂♂, 1 ♂ immature, 1 ♀; same collection data as for preceding; IBSP 1723 • 1 ♀; same collection data as for preceding; IBSP 1751 • 1 ♂; Cordisburgo, Morena cave; [-19.169167, -44.331667]; 846 m a.s.l.; 12 Oct. 2007; Equipe Disciplina leg.; IBSP 3554 • 1 ♀; same locality data as for preceding; 12 Oct. 2017; D. Polotow leg.; IBSP 3547 • 1 ♀; same locality data as for preceding; Oct. 2007; Equipe Disciplina leg.; IBSP 3544 • 5 ♂♂, 4 ♀♀; Pains, 13 Mineração Supercal I cave; [-20.373525, -45.661813]; 692 m a.s.l.; Apr. 2008; E.O. Machado and J.P.P.P. Barbosa leg.; IBSP 3497 • 2 ♂♂, 2 ♀♀; same collection data as for preceding except for 10 Mineração Supercal I cave; IBSP 3496 • 2 ♂♂; same collection data as for preceding except for 15.16 Mineração Supercal III cave; IBSP 3500 • 4 ♂♂, 1 ♀; same collection data as for preceding except for 11 Mineração Supercal I cave; IBSP 3502 • 1 ♂; Pains, Ninfeta III cave; [-20.338284, -45.615531]; 724 m a.s.l.; 25 Jan. 2009; R. Zampaulo leg.; ISLA • 1 ♂; Paranoá cave; [-20.365455, -45.669428]; 686 m a.s.l.; 27 Jan. 2009; R. Zampaulo leg.; ISLA • 1 ♂, 3 ♀♀; Mariana; [-20.365880, -43.415007]; 698 m a.s.l; 13 May 2011; T.G. Pellegrini leg.; ISLA.

Descriptive notes

Measurements. 60–64 body rings (1–2 apodous + telson). Males: body length 95.8–100.7 mm; maximum midbody diameter 3.8–5.8 mm. Females: body length 93–137.5 mm; maximum midbody diameter 4.4–6.1 mm.

Color. Body color brownish grey; head, collum, and antennae darker; prozonites anteriorly greyish; metazonites with a posterior band lighter; legs brownish.

HEAD. Antennae long (Fig. 163O), just reaching back to end of ring 6 when extended dorsally; antennomeres elongated; relative antennomere lengths 1<2<3>4≈5≈6>7. Mandibular cardo with ventral margin narrow. Ommatidial cluster well-developed, elliptical; ca 26 ommatidia in 4 rows.

BODY RINGS. Collum with lateral lobes rounded, with ca 9 striae, slightly curved ectad (Fig. 95A). Very faintly constricted between prozonite and metazonite; prozonites smooth; metazonites laterally with transverse striae up to ozopore in anterior body rings. Anterior sterna in midbody rings subrectangular, without transverse striae (Fig. 170E).

FIRST LEG-PAIR OF MALES. Coxae (***cx***) short (less than half of remaining podomere lengths), subtriangular, with the base arched and expanded, densely setose (Figs 30B, 96A); prefemoral process (***prf***) about as wide as half of prefemur, subcylindrical, densely setose up to its median region (Fig. 96B); remaining podomeres with setae along the mesal region.

SECOND LEG-PAIR OF MALES. Coxa (***cx***) large and rounded; penis (***pn***) located at proximal region, rounded, not extended basally (Fig. 96C); prefemur compressed dorsoventrally; remaining podomeres setose.

GONOPODS. Gonocoxa (***gcx***) elongated, almost twice as long as telopodite, with the base arched; antero-posteriorly flattened (Figs 96D–F, 211C); with rows of papillae mesally. Seminal groove (***sg***) curved; arising medially on mesal cavity and terminating apically on the seminal apophysis (***sa***). Shoulder (***sh***) rounded. Telopodite (***tp***) almost as wide as ***gcx*** (Fig. 96D); solenomere (***sl***) with apicomesal process (***amp***) subtriangular; ectal process (***ep***) subtriangular, separating from ***amp*** by deep notch; ***sa*** located at mesal portion, slightly visible apically. Internal branch (***ib***) subtriangular, narrow, slightly curved ectad at midlength, surrounding basally ***tp*** as a shield; with torsion of 180° in the distal portion but without projection; ***ib*** with setae along its entire margin slightly exceeding apically seminal region of ***sl*** (Figs 96D–F, 211C).

VULVAE. As typical for the genus. Bursa subtriangular, glabrous (Figs 39D, 178D, 210B); internal valve subtriangular, with mesal region slightly rounded; operculum narrow (Fig. 39D); external valve wide, subtriangular (Fig. 39A).

Distribution

The species is widely distributed in caves and surrounding forests from the Karst province of the Bambuí Group and from iron ore formations in the Minas Gerais State, Brazil (Fig. 185). The species is also associated to partially anthropized karst areas in Minas Gerais.

Pseudonannolene occidentalis Schubart, 1958

Figs 19B, 98–100, 164D, 171A, 178E, 185; Supp. file 4: Figs 194B, 199D, 208C, 212A, 216E, 222E

Pseudonannolene occidentalis Schubart, 1958: 214, figs 12–13.

Pseudoannolene [sic!] *occidentalis* – Krabbe 1982: 71.
Pseudonannolene occidentalis – Jeekel 2004: 89. — Golovatch *et al.* 2005: 279.

Diagnosis

Males of *P. occidentalis* differ from all congeners by having the frontal region of the head densely setose, overlapping the supralabral and labral setae (Fig. 19B); mandibular cardo finely granular, with swollen ventral margin (Figs 171A, 199D); solenomere with seminal apophysis located ectally (Fig. 99D).

Etymology

Adjective referring to the geographical distribution of the species in western Brazil (Schubart 1958).

Material examined

Holotype

BRAZIL • ♂ [gonopods, first and second leg-pair on microscope slides]; Mato Grosso do Sul, Salobra; [-20.187516, -56.547016]; 112 m a.s.l.; 22 Jan. 1955; L. Travassos leg.; MZSP.

Paratypes (total: 2 ♀♀)

BRAZIL • 2 ♀♀; same collection data as for holotype; MZSP.

Other material (total: 9 ♂♂, 7 ♀♀, 4 immatures)

BRAZIL – **Mato Grosso** • 2 ♂♂; Chapada dos Guimarães, close to Aldeia Velha; [-15.464565, -55.760228]; 823 m a.s.l.; 6 Mar. 2014; A. Chagas-Jr and M. Karam-Gemael leg.; CZUFMT 808 • 2 ♂♂, 1 ♀, 4 immatures; Chapada Aventura; [-15.464283, -55.759722]; 820 m a.s.l.; 7 Nov. 2015; A. Chagas-Jr *et al.* leg.; CZUFMT 818 • 1 ♂, 4 ♀♀; same locality data as for preceding; 28 Aug. 2014; A. Chagas-Jr leg.; CZUFMT 823. – **Mato Grosso do Sul** • 1 ♂; Salobra; [-20.189192, -56.547513]; 112 m a.s.l.; 19 Jan. 1941; F. Lane leg.; MZSP. – **São Paulo** • 3 ♂♂, 1 ♀; Jundiaí, Serra do Japi; [-23.226630, -46.924751]; 871 m a.s.l.; 6–10 Aug. 2001; Equipe Biota leg.; IBSP 1998 • 1 ♀; Jundiaí, Reserva Natural Municipal da Serra do Japi; [-23.236337, -46.943607]; 1069 m a.s.l.; Mar. 2007; A.D. Brescovit leg.; IBSP 3100.

Descriptive notes

Measurements. 70–73 body rings (2 apodous + telson). Males: body length 70–80 mm; maximum midbody diameter 4.4–5 mm. Females: body length 70 mm; maximum midbody diameter 4.8 mm.

Color. Body color brownish yellow; head, collum, and antennae darker; prozonites and metazonites anteriorly darker, with a posterior band reddish; legs brownish.

Head. Antennae short (Fig. 164D), just reaching back to end of ring 5 when extended dorsally; relative antennomere lengths 1≈2≈3>4=5=6>7. Frontal setae overlapping supralabral and labral ones (Fig. 19B). Mandibular cardo with ventral margin swollen (Figs 171A, 199D). Ommatidial cluster well-developed, elliptical; ca 25 ommatidia in 4 rows.

Body rings. Collum with lateral lobes rounded, with ca 7 striae, slightly curved ectad (Fig. 98A). Very faintly constricted between prozonite and metazonite; prozonites smooth; metazonites laterally with transverse striae up to ozopore in anterior body rings. Anterior sterna in midbody rings subrectangular, without transverse striae (Fig. 171A).

First leg-pair of males. Coxae (***cx***) elongated (as long as the sum of remaining podomere lengths), subrectangular, with the base arched, densely setose (Figs 99A, 100B); prefemoral process (***prf***) elongated and as wide as half of prefemur, subcylindrical, densely setose along the entire ventral region (Fig. 99B); remaining podomeres with setae along the mesal region.

Second leg-pair of males. Coxa (***cx***) large and subrectangular; penis (***pn***) located at proximal region, rounded, not extended basally (Figs 99C, 100E–F, 208C); prefemur compressed dorsoventrally; remaining podomeres setose.

Gonopods. Gonocoxa (***gcx***) subtriangular, basally expanded and progressively less wide, with the base slightly arched; antero-posteriorly strongly flattened, longitudinal thickened ridge with rows of papillae mesally (Figs 99D–F, 100C–D). Seminal groove (***sg***) curved; arising medially on mesal cavity and terminating apically on the seminal apophysis (***sa***). Shoulder absent. Telopodite (***tp***) arising from ***gcx*** by short, compressed trunk (Figs 99D, 100D); solenomere (***sl***) with apicomesal process (***amp***) short; ectal process (***ep***) short, subtriangular, separating from ***amp*** by shallow notch; ***sa*** located at ectal portion, elongated and thickened apically. Internal branch (***ib***) shovel-shaped and rounded apically, with horizontal plate; setae restricted to the apical region of ***ib*** exceeding seminal region of ***sl*** (Figs 99D–F, 100C–D).

VULVAE. As typical for the genus. Bursa subtriangular, glabrous (Fig. 178E); internal valve subtriangular; operculum large, slightly expanded apically; external valve wide, subtriangular.

Distribution

Known from the west region of São Paulo up to the states of Mato Grosso do Sul and Mato Grosso, Brazil (Fig. 185); the distribution range of *P. occidentalis* partially covers the biomes Atlantic Forest, Cerrado, and Pantanal.

Pseudonannolene ophiiulus Schubart, 1944
Figs 101–102, 166C, 171B, 178F, 185; Supp. file 4: Fig. 210D

Pseudonannolene ophiiulus Schubart, 1944: 410, figs 72–74.

Pseudonannolene ophiiulus – Schubart 1945a: 295; 1952: 418. — Jeekel 2004: 90. — Iniesta & Ferreira 2013b: 366. — Gallo & Bichuette 2020: 36.
Pseudoannolene ophiulus [sic!] – Fontanetti 1990: 698.

Diagnosis

Males of *P. ophiiulus* resemble those of *P. strinatii* Mauriès, 1974 and *P. tocaiensis* by having an internal branch shovel-shaped with horizontal plate (Fig. 102D), but differing by a large prefemoral process (Fig. 102B); solenomere rounded, with seminal apophysis thickened and visible apically (Fig. 102D).

Etymology

Name 'ophiiulus' is derived from the Greek words '*óphis*' = 'snake', plus the suffix '-ulus'. Although unspecified in the original description, the species name evidently refers to the popular Brazilian reference that millipedes resemble snakes (suborder Serpentes).

Material examined

Holotype
BRAZIL • ♂ [gonopods, gnathochilarium, first and second leg-pair on microscope slides]; São Paulo, Pirassununga, Cachoeira; [-22.002342, -47.429793]; 630 m a.s.l.; 17 Feb. 1942; J. Gaspar leg.; MZSP.

Other material (total: 23 ♂♂, 23 ♀♀, 43 immatures)
BRAZIL – **São Paulo** • 1 ♀; Amparo; [-22.708627, -46.772544]; 703 m a.s.l.; Apr. 1943; F. Lane leg.; MZSP • 1 ♀; same collection data as for preceding; MZSP • 2 ♂♂; Analândia; [-22.131017, -47.663024]; 657 m a.s.l.; 7 Mar. 1944; O. Schubart leg.; MZSP • 2 ♂♂, 6 ♀♀, 1 ♂ immature; Fazenda Landgraf; 7 Mar. 1944; O. Schubart leg.; MZSP • 1 ♀; Nova Odessa; [-22.785705, -47.294204]; 657 m a.s.l.; Apr. 1951; O. Schubart leg.; MZSP • 1 ♂, 1 ♀, 1 ♀ immature; Pirassununga, Emas; [-22.001668, -47.427853]; 631 m a.s.l.; 10 Mar. 1948; O. Schubart leg.; inside hole of *Dasypus novemcinctus* Linnaeus, 1758 (ca 180 cm); MZSP • 2 ♀♀ immatures; same locality data as for preceding; 12 Mar. 1948; O. Schubart leg.; MZSP • 3 ♂♂, 2 ♀♀, 2 ♂♂ immatures, 2 ♀♀ immatures; same locality data as for preceding; 7 Jul. 1945; O. Schubart leg.; MZSP • 2 ♀♀; same locality data as for preceding; 13 Jan. 1955; Guimarães leg.; MZSP • 1 ♀, 1 ♀ immature; same locality data as for preceding; 22 May

1940; O. Schubart leg.; MZSP • 1 ♂; same locality data as for preceding; 3 Apr. 1940; O. Schubart leg.; MZSP • 1 ♂ immature; Estação Experimental de Pirassununga; 30 Apr. 1940; O. Schubart leg.; MZSP • 1 ♂; same locality data as for preceding; 21 Aug. 1945; O. Schubart leg.; MZSP • 1 ♀, 2 ♀♀ immatures; same locality data as for preceding; 24 May 1940; O. Schubart leg.; MZSP • 1 ♀; same locality data as for preceding; 31 Jan. 1940; O. Schubart leg.; MZSP • 1 ♀ immature; Baguassú; 10 Jan. 1939; O. Schubart leg.; MZSP • 1 ♀; Fazenda Pedra Branca; 30 Mar. 1944; J. Gaspar leg.; MZSP • 14 ♀♀ immatures; Cachoeira; 17 Feb. 1942; J. Gaspar leg.; MZSP • 5 ♂♂, 1 ♀ immature; same collection data as for preceding; MZSP • 3 ♂♂; same collection data as for preceding; MZSP 1061 • 1 ♀; Cachoeira de Emas; [-22.001668, -47.427853]; 631 m a.s.l.; 20 Jan. 1953; J.P. de Lima leg.; MZSP • 2 ♂♂ immatures, 8 ♀♀ immatures; same collection data as for preceding; MZSP • 1 ♂; Porto Ferreira, Fazenda Santa Maria do Sul; [-21.842440, -47.471357]; 567 m a.s.l.; 1 Aug. 1940; O. Schubart leg.; MZSP • 1 ♂♂ immature; same locality data as for preceding; Aug. 1940; O. Schubart leg.; MZSP • 2 ♀♀ immatures; Rio Claro; [-22.415956, -47.565350]; 614 m a.s.l.; 16 Nov. 1941; O. Schubart leg.; MZSP • 1 ♀ immature; same locality data as for preceding; 8 Jan. 1942; O. Schubart leg.; MZSP 1062 • 1 ♀, 1 ♀ immature; Fazenda São José; 29 Sep. 1941; O. Schubart leg.; MZSP • 1 ♂, 3 ♀♀; Bairro São Benedito; [-22.41916, -47.565652]; 677 m a.s.l.; 17 Nov. 1984; E. Giannoti leg.; MZSP • 1 ♂; São Carlos; [-22.010944, -47.890554]; 870 m a.s.l.; 20 Mar. 1944; O. Schubart leg.; MZSP.

Descriptive notes

Measurements. 59–63 body rings (2–3 apodous + telson). Males: body length 35–45 mm; maximum midbody diameter 2.4–2.5 mm. Females: body length 35–45 mm; maximum midbody diameter 2.3–3.1 mm.

Color. Body color faded, but apparently prozonites brownish, metazonites with a posterior brown band; head, antennae, and legs lighter; collum brown brownish.

Head. Antennae short (Fig. 101A), just reaching back to end of ring 5 when extended dorsally; relative antennomere lengths 1<2<3>4=5=6>7. Mandibular cardo with ventral margin swollen. Ommatidial cluster well-developed, elliptical; ca 25 ommatidia in 5 rows.

Body rings. Collum with lateral lobes broadly rounded, with ca 7 striae, slightly curved ectad (Fig. 101A). Very faintly constricted between prozonite and metazonite; prozonites smooth; metazonites laterally with transverse striae below ozopore. Anterior sterna in midbody rings subrectangular, without transverse striae (Fig. 171B).

First leg-pair of males. Coxae (***cx***) elongated (as long as the sum of remaining podomere lengths), subtriangular, with the base slightly arched and expanded, densely setose (Fig. 102A); prefemoral process (***prf***) as wide as half of prefemur, subcylindrical, densely setose along in its entire extension (Fig. 102B); remaining podomeres with setae along the mesal region.

Second leg-pair of males. Coxa (***cx***) large and subrectangular; penis (***pn***) located at proximal region, rounded, not extended basally (Fig. 102C); prefemur compressed dorsoventrally; remaining podomeres setose.

Gonopods. Gonocoxa (***gcx***) subtriangular, basally expanded and progressively less wide, with the base slightly arched; antero-posteriorly strongly flattened, longitudinal thickened ridge with rows of papillae mesally (Fig. 102D–F). Seminal groove (***sg***) curved; arising medially on mesal cavity and terminating apically on the seminal apophysis (***sa***). Shoulder absent. Telopodite (***tp***) almost as wide as ***gcx*** (Fig. 102D); solenomere (***sl***) with apicomesal process (***amp***) short; ectal process (***ep***) short, rounded, separating from ***amp*** by shallow notch; ***sa*** located at mesal portion, thickened apically. Internal branch (***ib***) shovel-shaped, with horizontal plate; setae restricted to the apical region of ***ib*** exceeding seminal region of ***sl*** (Fig. 102D–F).

Vulvae. As typical for the genus. Bursa subtriangular, glabrous (Figs 178F, 210D); internal valve subtriangular, with its sides having the same length; operculum slightly expanded apically; external valve large in oral view, subtriangular.

Distribution

Known from the central region of São Paulo State, Brazil (Fig. 185); occurring in the Cerrado biome (tropical savanna ecoregion) and in second-growth forests in the region.

Pseudonannolene parvula Silvestri, 1902
Figs 103–105, 164E, 166D, 171C, 178G, 186

Pseudonannolene parvula Silvestri, 1902: 24.

Pseudonannolene parvula – Brölemann 1909: 85. — Viggiani 1973: 367. — Jeekel 2004: 90. — Iniesta & Ferreira 2013a: 92; 2013c: 79.

Diagnosis

Males of *P. parvula* slightly resemble those of *P. spelaea* by having the solenomere rounded apically and with seminal apophysis located mesally (Fig. 104D–F), but differing by the absence of a squamous membrane on the seminal apophysis (Fig. 104D); and by the presence of spiniform setae in the proximal region of the mentum and stipes (Fig. 171C).

Etymology

Named after the Latin adjective '*parvus*' = 'few', 'small', plus the suffix '-ulus' (feminine '-ula'). Unspecified in the original description.

Material examined

Syntypes

PARAGUAY • 2 ♀♀; Alto Paraná, Bella Vista; [-25.528108, -54.583762]; 8 Jul. 1900; A. Borelli leg.; USNM 2020 • 1 ♂ [fragmented], 2 ♀♀ [examined by photographs]; same collection data as for preceding; ZMB 2888.

Other material (total: 6 ♂♂, 18 ♀♀, 11 immatures)

BRAZIL – **Paraná** • 1 ♀; Foz do Iguaçu, Parque Nacional do Iguaçu; [-25.500435, -54.583352]; 195 m a.s.l.; 3–12 Mar. 2002; Equipe Biota leg.; IBSP 1488 • 1 ♀; same collection data as for preceding; IBSP 1504 • 1 ♀ immature; same collection data as for preceding; IBSP 1463 • 2 ♀♀; same collection data as for preceding; IBSP 1437 • 1 ♀; same collection data as for preceding; IBSP 1451 • 2 ♀♀; same collection data as for preceding; IBSP 1462 • 1 ♀; same collection data as for preceding; IBSP 1443 • 1 ♀; same collection data as for preceding; IBSP 1482 • 1 ♂; same collection data as for preceding; IBSP 1474 • 1 ♂, 1 ♀; same collection data as for preceding; IBSP 1486 • 1 ♀; same collection data as for preceding; IBSP 1962 • 1 ♀; same collection data as for preceding; IBSP 1967 • 1 ♀; same collection data as for preceding; IBSP 1961 • 1 ♀; same collection data as for preceding; IBSP 1954 • 1 ♀; same collection data as for preceding; IBSP 1952 • 1 ♀; same collection data as for preceding; IBSP 1956 • 1 ♀ immature; same collection data as for preceding; IBSP 1963 • 1 ♀ immature; same collection data as for preceding; IBSP 1960 • 1 ♀ immature; same collection data as for preceding; IBSP 1958 • 1 ♀ immature; same collection data as for preceding; IBSP 1955 • 1 ♀ immature; same collection data as for preceding; IBSP 1957 • 1 ♀ immature; same collection data as for preceding; IBSP 1959 • 1 ♀

immature; same collection data as for preceding; IBSP 1966 • 1 ♀; same collection data as for preceding; IBSP 1953 • 2 ♂♂, 1 ♀; same locality data as for preceding; 28–31 Jul. 2016; V. Calvanese leg.; IBSP 7629 • 2 ♂♂; same collection data as for preceding; IBSP 7630 • 3 immatures; same collection data as for preceding; IBSP 7628.

Descriptive notes

MEASUREMENTS. 58–61 body rings (1–2 apodous + telson). Males: body length 51.9–55.4 mm; maximum midbody diameter 3.4–4.9 mm. Females: body length 56–57.9 mm; maximum midbody diameter 4–4.1 mm.

COLOR. Body color brownish grey; collum darker; prozonites anteriorly greyish; metazonites with a medial brown band and a posterior lighter one; head, antennae, and legs lighter brown.

HEAD. Antennae short (Fig. 164E), just reaching back to end of ring 5 when extended dorsally; relative antennomere lengths 1<2<3>4>5=6>7. Mandibular cardo with ventral margin narrow. Mentum and stipes of gnathochilarium with scattered spiniform setae (Fig. 171C). Ommatidial cluster well-developed, elliptical; ca 30 ommatidia in 5 rows.

BODY RINGS. Collum with lateral lobes rounded, with ca 6 shallow striae, slightly curved ectad (Fig. 103A). Very faintly constricted between prozonite and metazonite; prozonites smooth; metazonites laterally with transverse striae up to ozopore in anterior body rings. Anterior sterna in midbody rings subrectangular, without transverse striae (Fig. 171C).

FIRST LEG-PAIR OF MALES. Coxae (***cx***) short (less than half of remaining podomere lengths), subtriangular, with the base arched and strongly expanded, densely setose (Fig. 104A); prefemoral process (***prf***) as wide as half of prefemur, subcylindrical, curved ectad, densely setose up to its median region (Fig. 104B); remaining podomeres with setae along the mesal region.

SECOND LEG-PAIR OF MALES. Coxa (***cx***) large and rounded; penis (***pn***) located at proximal region, rounded, not extended basally (Fig. 104C); prefemur compressed dorsoventrally; remaining podomeres setose.

GONOPODS. Gonocoxa (***gcx***) elongated, almost twice as long as telopodite, with the base slightly arched; antero-posteriorly flattened (Fig. 104D–F); with rows of papillae mesally. Seminal groove (***sg***) curved; arising medially on mesal cavity and terminating apically on the seminal apophysis (***sa***). Shoulder absent. Telopodite (***tp***) almost as wide as ***gcx*** (Fig. 104D); solenomere (***sl***) with apicomesal process (***amp***) rounded; ectal process (***ep***) short, nearly not distinguished from ***amp*** by inconspicuous notch; ***sa*** located at mesal portion, slightly visible apically. Internal branch (***ib***) subtriangular, narrow, surrounding basally ***tp*** as a shield; setae starting at midlength of ***ib*** exceeding seminal region of ***sl*** (Fig. 104D–F).

VULVAE. As typical for the genus. Bursa subtriangular, glabrous (Fig. 178G); internal valve subtriangular, with mesal region rounded; operculum narrow, curved ectad; external valve wide, subtriangular.

Distribution

Known from the region of Iguaçu Falls and surrounding forests on the border of the Argentine province of Misiones, Paraguayan department of Alto Paraná, and the Brazilian state of Paraná (Fig. 186).

Comments

Male syntypes from Alto dell'Iguazú and Puerto Bertoni described by Silvestri (1902) were not found. Nevertheless, syntypes from Bella Vista (Fig. 105C) and topotypes from Foz do Iguaçu were examined (Fig. 105D).

Pseudonannolene patagonica Brölemann, 1902
Figs 106–108, 164F, 166E, 186

Pseudonannolene patagonica Brölemann, 1902a: 135, pl. vii figs 160–165.

Pseudonannolene patagonica – Jeekel 2004: 90.

Diagnosis

Males of *P. patagonica* resemble those of *P. halophila*, *P. maritima*, *P. sebastianus*, and *P. insularis* sp. nov. by having large and subrectangular coxae on the first leg-pair (Fig. 107A) and a suboval penis (Fig. 107C–D), but differing by having the stipes of gnathochilarium swollen distally (Fig. 108C).

Etymology

Although unspecified, the name is evidently an adjective referring to the locality where the type material was found, Carmen de Patagones.

Material examined

Holotype

ARGENTINA • ♂ [gonopods missing]; Buenos Aires, Carmen de Patagones; [-40.783233, -62.982821]; R. von Ihering leg.; MZSP 242.

Descriptive notes

Gonopod description adapted from Brölemann (1902a: 135) to supplement original description and to introduce gonopod terminology; remaining male sexual characters described based on examined holotype.

Measurements. 60 body rings (2 apodous + telson). Males: fragmented, body length ca 47 mm; maximum midbody diameter 2.6 mm.

Color. Body color faded, but apparently prozonites brownish, metazonites with a posterior brown band; head, collum, and legs lighter brown.

Head. Antennae long (Fig. 164F), just reaching back to end of ring 6 when extended dorsally; antennomeres elongated; relative antennomere lengths 1<2<3>4=5=6>7. Mandibular cardo with ventral margin narrow. Ommatidial cluster well-developed, elliptical; ca 45 ommatidia in 6 rows.

Body rings. Collum with lateral lobes broadly rounded, with ca 12 striae (Fig. 106A). Very faintly constricted between prozonite and metazonite; prozonites smooth; metazonites laterally with transverse striae below ozopore. Anterior sterna in midbody rings subrectangular, without transverse striae.

First leg-pair of males. Coxae (***cx***) elongated (as long as the sum of remaining podomere lengths), subrectangular, with the base arched, densely setose (Fig. 107A); prefemoral process (***prf***) thinner than half the prefemur, subcylindrical, densely setose up to its median region (Fig. 107B); remaining podomeres with setae along the mesal region.

Second leg-pair of males. Coxa (***cx***) large and rounded; penis (***pn***) located at proximal region, rounded, extended basally (Fig. 107C); prefemur compressed dorsoventrally; remaining podomeres setose.

Gonopods. Gonocoxa (***gcx***) subtriangular, short (Fig. 108D); with rows of papillae mesally. Seminal groove (***sg***) not visible on mesal cavity. Shoulder (***sh***) rounded. Telopodite (***tp***) large, but not as wide as ***gcx***; solenomere (***sl***) with apicomesal process (***amp***) rounded; ectal process absent; ***sa*** located at mesal portion, slightly visible apically. Internal branch (***ib***) short, subtriangular, with horizontal plate; setae apparently starting at midlength of ***ib*** exceeding seminal region of ***sl*** (Fig. 108D).

Distribution

Known only from the type locality Carmen de Patagones, Buenos Aires, Argentina (Fig. 186).

Pseudonannolene paulista Brölemann, 1902
Figs 25A, C, E, 32C, 109–110, 164G, 166F, 171D, 178I, 186;
Supp. file 4: Figs 199B, 201B, 212D, 213B, 218E

Pseudonannolene paulista Brölemann, 1902a: 129, pl. vi figs 142–147.

Pseudonannolene paulista – Jeekel 2004: 90. — Iniesta & Ferreira 2013a: 92. — Gallo & Bichuette 2020: 36.

Diagnosis

Males of *P. paulista* slightly resemble those of *P. aurea* sp. nov. by having a solenomere with a spiniform ectal process deeply notched separating it from the apicomesal process (Fig. 110D), but differing by an internal branch shovel-shaped with horizontal plate (Fig. 110D–F).

Etymology

Although unspecified, the name is evidently related to the demonym “paulista”, in reference to the inhabitants of the Brazilian state of São Paulo, where the species occurs.

Material examined

Paralectotypes (total: 1 ♂, 1 ♀)
BRAZIL • 1 ♂, 1 ♀; São Paulo, Cerqueira César; [-23.067354, -49.157619]; Dec. 1896; R. von Ihering leg.; MZSP.

Other material (total: 20 ♂♂, 37 ♀♀, 1 immature)
BRAZIL – **São Paulo** • 1 ♀; Assis, Estação Ecológica de Assis; [-22.661071, -50.419104]; 576 m a.s.l.; 25–30 Nov. 2002; Equipe Biota leg.; IBSP 7896 • 2 ♀♀; same collection data as for preceding; IBSP 2972 • 1 ♂, 1 ♀; same collection data as for preceding; IBSP 7894 • 2 ♂♂; same collection data as for preceding; 20 Oct. 2002; Equipe Biota leg.; IBSP 2982 • 1 ♂; Angatuba, Estação Ecológica de Angatuba; [-23.415855, -48.360834]; 761 m a.s.l.; 11–16 Nov. 2002; Equipe Biota leg.; IBSP 1908 • 2 ♀♀; same collection data as for preceding; IBSP 1915 • 1 ♀; same collection data as for preceding; IBSP 1912 • 1 ♂, 1 ♀; Piracicaba, Escola Superior de Agricultura Luiz de Queiroz (ESALQ-USP); [-22.711635, -47.627783]; 548 m a.s.l.; 11–31 Mar. 1994; A. Eterovic leg.; IBSP 1261 • 1 ♂, 1 ♀; same collection data as for preceding; IBSP 1261 • 1 ♂, 15 ♀♀, 1 immature; Anhembi, Fazenda Barreiro Rico; [-22.788342, -48.131224]; 469 m a.s.l.; C. Fontanetti leg.; MZSP • 11 ♂♂, 11 ♀♀; same collection data as for preceding; Dec. 1896; A. Mesa leg.; MZSP • 1 ♂, 2 ♀♀; Teodoro Sampaio, Parque Estadual Morro do Diabo; [-22.524723, -52.298448]; 367 m a.s.l.; 24–31 Mar. 2003; Equipe Biota leg.; IBSP 2409 • 1 ♂; same collection data as for preceding; IBSP 2424.

Descriptive notes

Measurements. 55–71 body rings (1–2 apodous + telson). Males: body length 67.9–79.4 mm; maximum midbody diameter 3.2–3.6 mm. Females: body length 76.4–87 mm; maximum midbody diameter 4.1–4.9 mm.

Color. Body color brownish yellow; head, collum, and antennae darker; prozonites and metazonites anteriorly darker, with a posterior band lighter; legs brownish.

Head. Antennae short (Fig. 164G), just reaching back to end of ring 5 when extended dorsally; relative antennomere lengths 1<2≈3>4=5≈6>7. Mandibular cardo with ventral margin swollen. Ommatidial cluster well-developed, elliptical; ca 40 ommatidia in 5 rows.

Body rings. Collum with lateral lobes broadly rounded, with ca 6 striae (Fig. 109A). Very faintly constricted between prozonite and metazonite; prozonites smooth; metazonites laterally with transverse striae below ozopore. Anterior sterna in midbody rings subrectangular, without transverse striae (Fig. 171D).

First leg-pair of males. Coxae (***cx***) elongated (as long as the sum of remaining podomere lengths), subtriangular, with the base slightly arched and expanded, densely setose (Fig. 110A); prefemoral process (***prf***) as wide as half of prefemur, subcylindrical, densely setose along in its entire extension (Fig. 110B); remaining podomeres with setae along the mesal region.

Second leg-pair of males. Coxa (***cx***) large and subrectangular; penis (***pn***) located at proximal region, rounded, not extended basally (Fig. 110C); prefemur compressed dorsoventrally; remaining podomeres setose.

Gonopods. Gonocoxa (***gcx***) elongated, almost twice as long as telopodite, with the base arched; antero-posteriorly flattened (Figs 110D–F, 212D, 213B); with rows of papillae mesally. Seminal groove (***sg***) curved; arising medially on mesal cavity and terminating apically on the seminal apophysis (***sa***). Shoulder absent. Telopodite (***tp***) almost as wide as ***gcx*** (Figs 110D, 218E); solenomere (***sl***) with apicomesal process (***amp***) subtriangular; ectal process (***ep***) spiniform, elongated, separating from ***amp*** by deep notch; ***sa*** located at mesal portion, curved mesad, elongated. Internal branch (***ib***) shovel-shaped, with horizontal plate; long setae restricted to the apical region of ***ib*** exceeding seminal region of ***sl*** (Figs 110D–F, 213B).

Vulvae. As typical for the genus. Bursa subtriangular, glabrous (Fig. 178I); internal valve subtriangular, with mesal region rounded; operculum narrow, S-shaped; external valve wide, subtriangular.

Distribution

Known from the central-west region of São Paulo State, Brazil (Fig. 186); occurring in the Cerrado biome (tropical savanna ecoregion) and in second-growth forests in the region.

Comments

The lectotype from Cerqueira César and the paralectotypes (two females) from Batista Botelho, deposited at the Muséum national d'histoire naturelle, Paris, France (MNHN), were not examined during this study.

Pseudonannolene pusilla Silvestri, 1895
Figs 111–112, 176A, 178H, 186

Pseudonannolene pusilla Silvestri, 1895b: 7, fig. 13.

Pseudonannolene pusilla – Silvestri 1902: 23. — Schubart 1958: 240. — Viggiani 1973: 367. — Jeekel 2004: 90. — Golovatch *et al.* 2005: 279. — Iniesta & Ferreira 2013a: 92; 2013c: 79.

Diagnosis

Males of *P. pusilla* resemble those of *P. morettii* sp. nov. by having short coxae on the first leg-pair with a constriction at about midlength (Fig. 112A), but differing by the absence of long scattered setae on the mentum and stipes (Fig. 176A); solenomere short and subtriangular (Fig. 112D).

Etymology

Named after the Latin adjective '*pusillus*' (feminine '*pusilla*') = 'very little', 'tiny'. Unspecified in the original description.

Material examined (total: 5 ♂♂, 2 ♀♀, 3 immatures)

BRAZIL – **Mato Grosso** • 2 ♂♂; Pindaíba, Barra das Garças; [-15.881182, -52.238738]; 337 m a.s.l.; 19–31 Jan. 1998; M.E.V. Callefo leg.; IBSP 13390 • 3 ♂♂, 2 ♀♀, 3 immatures; same collection data as for preceding; IBSP 13391.

Descriptive notes

Measurements. 55–57 body rings (1 apodous + telson). Males: body length 39.7 mm; maximum midbody diameter 2.4 mm. Females: body length 43.1–44 mm; maximum midbody diameter 3.7–4 mm.

Color. Body color brownish grey; head and collum darker; prozonites anteriorly greyish; metazonites with a posterior band lighter; antennae and legs brownish.

Head. Antennae long (Fig. 111A), just reaching back to end of ring 6 when extended dorsally; antennomeres elongated; relative antennomere lengths 1<2<3>4=5≈6>7. Mandibular cardo with ventral margin narrow. Ommatidial cluster well-developed, elliptical; ca 40 ommatidia in 5 rows.

Body rings. Collum with lateral lobes rounded, with ca 12 striae, strongly curved ectad (Fig. 111A). Very faintly constricted between prozonite and metazonite; prozonites smooth; metazonites laterally with transverse striae above ozopore in anterior body rings. Anterior sterna in midbody rings subrectangular, without transverse striae (Fig. 176A).

First leg-pair of males. Coxae (***cx***) short (less than half of remaining podomere lengths), subtriangular, with the base strongly arched and constricted medially, sparsely setose (Fig. 112A); prefemoral process (***prf***) less than half of prefemur, subcylindrical, densely setose up to its median region (Fig. 112B); remaining podomeres with setae along the mesal region.

Second leg-pair of males. Coxa (***cx***) rounded; penis (***pn***) located at proximal region, rounded, not extended basally (Fig. 112C); prefemur compressed dorsoventrally; remaining podomeres setose.

Gonopods. Gonocoxa (***gcx***) elongated, twice longer than telopodite, with the base arched; antero-posteriorly flattened (Fig. 112D–F); with rows of papillae mesally. Seminal groove (***sg***) curved; arising medially on mesal cavity and terminating apically on the seminal apophysis (***sa***). Shoulder (***sh***) inconspicuous. Telopodite (***tp***) almost as wide as ***gcx*** (Fig. 112D); solenomere (***sl***) with small squamous region; apicomesal process (***amp***) subtriangular; ectal process absent; ***sa*** located at mesal portion, slightly visible apically in oral view (Fig. 112F). Internal branch (***ib***) subtriangular, narrow and foliaceous, surrounding basally ***tp*** as a shield; ***ib*** with setae along its entire margin nearly not exceeding apically seminal region of ***sl*** (Fig. 112D–F).

Vulvae. As typical for the genus. Bursa subtriangular, glabrous (Fig. 178H); internal valve subtriangular, with its sides having the same length; operculum slightly curved ectad; external valve large, subtriangular.

Distribution

Known from Cerrado biome in the west region of Mato Grosso State, Brazil; other records from the literature for the Brazilian states of Mato Grosso do Sul and Goiás, and region of the Chaco in Argentina and Paraguay (Fig. 186).

Comments

The type material was described by Silvestri (1895b) and supposedly deposited at the Museo Regionale Scienze Naturali, Torino, Italy (MRSN) (Viggiani 1973: 367), but was not found. Nevertheless, near-topotypes from Mato Grosso were examined (Fig. 186). Other specimens from Brazil (Goiás, Mato Grosso, and Mato Grosso do Sul) and Paraguay (Asunción) were recorded by Silvestri (1902).

Pseudonannolene robsoni Iniesta & Ferreira, 2014
Figs 19A, C–D, 20, 21B–E, 23–24, 26A, C, 28A–C, 29B–C, 38, 39C, 39E–F, 113–114, 164H, 166G, 171E, 178J, 186; Supp. file 4: Figs 194A, 195B, 196D, 197D, 199A, 200B–C, 218C, 222D

Pseudonannolene robsoni Iniesta & Ferreira, 2014: 367, figs 5–6, 14c.

Pseudonannolene robsoni – Gallo & Bichuette 2019: 47.

Diagnosis

Males of *P. robsoni* resemble those of *P. fontanettiae* by having the internal branch with a torsion, in anal view (Fig. 114D), but differing by the torsion starting at midlength, and enlarged apically (Figs 114D–F, 222D); with distal projection present and directed diagonally upwards (Figs 114D, 218C).

Etymology

Patronym honoring the Brazilian biospeleologist Robson Zampaulo (Iniesta & Ferreira 2014).

Material examined

Holotype
BRAZIL • ♂; Minas Gerais, Pains, Água Limpa cave; [-20.452013, -45.65294]; 28 May 2009; R. Zampaulo leg.; ISLA 4080.

Paratypes (total: 3 ♂♂)
BRAZIL – **Minas Gerais** • 1 ♂; Pains, Bicho Desconhecido cave; [-20.405566, -45.590194]; 4 Apr. 2009; R. Zampaulo leg.; ISLA 4083 • 1 ♂; Pains, Loca dos Negros cave; [-20.435462, -45.659638]; 21 Mar. 2009; R. Zampaulo leg.; ISLA 4084 • 1 ♂; Pains, Duas Bocas cave; [-20.347712, -45.612605]; 1 Apri. 2009; R. Zampaulo leg.; ISLA 4085.

Other material (total: 75 ♂♂, 78 ♀♀, 7 immatures)
BRAZIL – **Minas Gerais** • 1 ♂; Pains, Zé da Fazenda cave; [-20.369647, -45.669438]; 691 m a.s.l.; 9 Mar. 2009; R. Zampaulo leg.; ISLA 4079 • 2 ♂; same data as for preceding except for Cerâmicas cave; 28 May 2009; ISLA 4081 • 1 ♂; Fumaça III cave; [-20.319627, -45.814827]; ISLA 4082 • 1 ♂; same collection data as for preceding; 28 May 2009; ISLA 4082 • 1 ♂; Tio Rafa III cave; [-20.413392, -45.665192]; 735 m a.s.l.; 24 Jan. 2009; R. Zampaulo leg.; ISLA 4086 • 1 ♂; Ninfeta de Baixo cave; [-20.338226, -45.615253]; 725 m a.s.l.; 25 Jan. 2009; R. Zampaulo leg.; ISLA 4087 • 1 ♂; Cinderela cave; [-20.445910, -45.606112]; 837 m a.s.l.; 18 Sep. 2009; R. Zampaulo leg.; ISLA 4089 • 2 ♂♂; Macacos 01 cave; [-20.407618, -45.672563]; 738 m a.s.l.; 29 Mar. 2013; M.P. Oliveira leg.; ISLA • 1 ♂, 5 ♀♀; 02 Mineração Supercal II cave; Apr. 2008; E.O. Machado and J.P.P.P. Barbosa leg.; IBSP 3498 • 8 ♂♂, 6 ♀♀; same collection data as for preceding; IBSP 3525 • 1 ♂; same collection data as for preceding;

IBSP 3501 • 9 ♂♂, 4 ♀♀; same data as for preceding except for 05 Mineração Solo Fértil cave; IBSP 3530 • 5 ♂♂, 7 ♀♀, 2 immatures; same collection data as for preceding; IBSP 3526 • 1 ♂, 1 ♀ immature; same data as for preceding except for 10 Mineração Supercal I cave; IBSP 3506 • 1 ♂, 2 ♀♀; same data as for preceding except for 11 Mineração Supercal I cave; IBSP 3513 • 1 ♂; same data as for preceding except for 13 Mineração Supercal I cave; IBSP 3519 • 3 ♂♂, 2 ♀♀; same data as for preceding except for 14 Mineração Supercal I cave; IBSP 3499 • 3 ♀♀; same collection data as for preceding; IBSP 3505 • 1 ♂; same collection data as for preceding; IBSP 3495 • 1 ♀; same collection data as for preceding; IBSP 3507 • 1 ♀; same data as for preceding except for 15.16 Mineração Supercal I cave; IBSP 3504 • 1 ♀; Três Idas cave; [-20.395293, -45.583257]; 831 m a.s.l.; Jul. 2008; E.O. Machado and J.P.P.P. Barbosa leg.; IBSP 3543 • 1 ♀; same collection data as for preceding; IBSP 3539 • 1 ♀; same collection data as for preceding; IBSP 3537 • 1 ♀; same collection data as for preceding; IBSP 3540 • 1 ♂; Alecrim II cave; [-20.286680, -45.793531]; 698 m a.s.l.; 22–25 Jan. 2008; E.O. Machado and J.P.P.P. Barbosa leg.; IBSP 3308 • 1 ♂, 1 ♀; same collection data as for preceding; IBSP 3310 • 1 ♂, 1 ♀; same collection data as for preceding; IBSP 3329 • 1 ♀; same collection data as for preceding; IBSP 3325 • 1 ♀; same collection data as for preceding; IBSP 3327 • 1 ♂; same collection data as for preceding; IBSP 3328 • 1 ♂; Arcaica cave; [-20.286846, -45.793296]; 700 m a.s.l.; 21 Jan. 2008; E.O. Machado and J.P.P.P. Barbosa leg.; IBSP 3316 • 1 ♀; Canudos cave; [-20.374367, -45.603485]; 794 m a.s.l.; 10 Oct. 2010; E.O. Machado and J.P.P.P. Barbosa leg.; IBSP 3438 • 1 ♀; Catedral cave; 24 Jan. 2008; E.O. Machado and J.P.P.P. Barbosa leg.; IBSP 3320 • 1 ♀; same collection data as for preceding; IBSP 3321 • 1 ♀; Entalhadeira cave; [-20.400391, -45.583857]; 828 m a.s.l.; Jul. 2008; E.O. Machado and J.P.P.P. Barbosa leg.; IBSP 3541 • 1 ♀; Alto Boqueirão cave; [-20.350962, -45.570567]; 872 m a.s.l.; 29 Nov. 1999; R.L. Ferreira *et al.* leg.; IBSP 3599 • 1 ♀; Bicho Que Foi cave; 3 Oct. 2003; IBSP 3433 • 1 ♀; Bode cave; 13 Oct. 2000; R.L. Ferreira and M. Souza-Silva leg.; IBSP 3588 • 1 ♀; Davi cave; [-20.338470, -45.779095]; 699 m a.s.l.; 10 Oct. 2000; R.L. Ferreira and M. Souza-Silva leg.; IBSP 3589 • 1 ♀; Massambará cave; [-20.328400, -45.809900]; 674 m a.s.l.; 12 Oct. 2000; R.L. Ferreira and M. Souza-Silva leg.; IBSP 3591 • 1 ♀; Peixe cave; 11 Oct. 2000; R.L. Ferreira and M. Souza-Silva leg.; IBSP 3612 • 1 ♀; Ronco cave; [-20.432907, -45.611615]; 785 m a.s.l.; 28 Nov. 1999; R.L. Ferreira and M. Souza-Silva leg.; IBSP 3607 • 1 ♂; Teto Plano cave; [-20.402395, -45.578811]; 863 m a.s.l.; 1 Jun. 2003; IBSP 3440 • 1 ♀; Vento cave; [-20.354472, -45.770592]; 699 m a.s.l.; 12 Oct. 2000; R.L. Ferreira and M. Souza-Silva leg.; IBSP 3586 • 1 ♀; Loca d'água cave; [-20.423987, -45.691977]; 820 m a.s.l.; 2 Sep. 1999; R.L. Ferreira and M. Souza-Silva leg.; IBSP 3606 • 1 ♀; PTO04 cave; 5 Apr. 2003; IBSP 3437 • 1 ♂; Sem Fim cave; [-20.285179, -45.791732]; 704 m a.s.l.; 24 Jan. 2008; E.O. Machado and J.P.P.P. Barbosa leg. IBSP 3318 • 3 ♂♂, 5 ♀♀; same collection data as for preceding; IBSP 3317 • 1 ♀; Simone do Davi cave; 6 Nov. 2000; R.L. Ferreira and M. Souza-Silva leg.; IBSP 3615 • 1 ♂; SPA_006 cave; 6 Feb. 2004; N.T. Pimental and T.F. Ferreira leg.; IBSP 3841 • 1 ♀; SPA_010 cave; 6 Feb. 2004; F.O. Borges and M. Barcelos leg.; IBSP 3850 • 1 ♀; SPA_011 cave; 6 Feb. 2004; M.T.M. Souza leg.; IBSP 3845 • 1 ♀; SPA_012/13 cave; 23 Jan. 2004; F.O. Borges and M. Barcelos leg.; IBSP 3835 • 1 ♂; SPA_014 cave; 4 Feb. 2004; F.O. Borges and M. Barcelos leg.; IBSP 3843 • 1 ♀; SPA_015 cave; 27 Jul. 2003; F.O. Borges leg.; IBSP 3844 • 1 ♀; SPA_023 cave; 4 Feb. 2004; IBSP 3849 • 1 ♀; SPA_034 cave; IBSP 3838 • 1 ♂; SPA_036 cave; 22 Aug. 2003; IBSP 3847 • 1 ♀; SPA_043 cave; 22 Aug. 2003; IBSP 3851 • 1 ♀; SF_1568 cave; 21 Jul. 2015; F. Bondezan leg.; IBSP 5946 • 1 ♂; S1_Am_007 cave; 12 Feb. 2014; E.L. Borges and M. Barcelos leg.; IBSP 6011 • 1 ♀; 644_SF cave; 14 Dec. 2015; F. Bondezan leg.; IBSP 5952 • 1 ♂; TVS_353 cave; 21–30 Aug. 2014; Soares *et al.* leg.; IBSP 6014 • 1 ♀; SF_1671 cave; 15 Dec. 2015; F. Bondezan leg.; IBSP 5951 • 1 ♀; SF_1687 cave; 15 Dec. 2015; F. Bondezan leg.; IBSP 5949 • 1 ♀; S2_AM_028 cave; 18 Feb. 2014; F. Bondezan leg.; IBSP 5951 • 1 ♂; S2_AM_028 cave; 18 Feb. 2014; M.T.M. Souza leg.; IBSP 6007 • 1 ♂; SF_1662 cave; 23 Nov. 2015; F. Bondezan leg.; IBSP 5947 • 1 ♂; Lagoa da Prata; [-20.024458, -45.540700]; 666 m a.s.l.; 25 May 2003; IBSP 3434 • 1 ♀; Pains; [-20.373442, -45.661809]; 694 m a.s.l.; 10 Dec. 2001; IBSP 3436 • 1 ♂; same locality data as for preceding; 15 Jan. 2014; M. Barcelos and N.T. Pimentel leg.; IBSP 5966 • 1 ♂; Campo Belo; [-23.623135, -46.672269]; 765 m a.s.l.; 25 Mar. 2012; T. Portella leg.; ISLA • 1 ♂; Pains, Zé da

Fazenda II cave; [-20.369635, -45.669427]; 692 m a.s.l.; 9 Mar. 2009; R. Zampaulo leg.; ISLA • 1 ♂; Água Limpa III cave; 28 May 2009; R. Zampaulo leg.; ISLA • 1 ♂; Duas Bocas cave; [-20.285634, -45.796845]; 707 m a.s.l.; 1 Apr. 2009; R. Zampaulo leg.; ISLA • 1 ♂ immature; Capoeirão cave; 22 Jan. 2009; R. Zampaulo leg.; ISLA • 1 ♂; Lenticular cave; [-20.377211, -45.596513]; 792 m a.s.l.; 31 Mar. 2009; R. Zampaulo leg.; ISLA • 1 ♂; Cerâmicas cave; 3 Apr. 2009; R. Zampaulo leg.; ISLA • 1 ♂; Fumaça cave; 12 Feb. 2009; R. Zampaulo leg.; ISLA • 1 ♂ immature; Dolina dos Angicos cave; [-20.418300, -45.678800]; 790 m a.s.l.; 2009; R. Zampaulo leg.; ISLA • 1 ♂; Doresópolis, Ninfeta de Baixo cave; [-20.338226, -45.615253]; 723 m a.s.l.; 2009; R. Zampaulo leg.; ISLA • 1 ♂; Córrego Fundo; [-20.450349, -45.554866]; 853 m a.s.l.; Aug. 2014; Santos *et al.* leg.; IBSP 5602 • 1 ♂; same collection data as for preceding; IBSP 5604 • 1 ♂, 1 immature; same collection data as for preceding; IBSP 5603 • 1 ♂; same collection data as for preceding; IBSP 5600 • 1 ♀, 1 immature; same collection data as for preceding; IBSP 5605 • 1 ♂; same collection data as for preceding; IBSP 5601 • 1 ♂; same collection data as for preceding; IBSP 5606 • 1 ♂; same collection data as for preceding; IBSP 5599.

Descriptive notes

Measurements. 60–78 body rings (1–3 apodous + telson). Males: body length 65.3–120 mm; maximum midbody diameter 3.8–6.6 mm. Females: body length 70–122 mm; maximum midbody diameter 5–6.8 mm.

Color. Body color brownish grey; head and collum darker; prozonites anteriorly greyish; metazonites with a medial brown band and a posterior lighter one; antennae and legs brownish.

Head. Antennae long (Figs 21, 113A, 164H), just reaching back to end of ring 6 when extended dorsally; antennomeres elongated; relative antennomere lengths $1<2<3>4\approx5<6>7$. Mandibular cardo with ventral margin narrow. Ommatidial cluster well-developed, elliptical; ca 30 ommatidia in 5 rows.

Body rings. Collum with lateral lobes rounded, with ca 7 striae, curved ectad (Fig. 19C–D). Very faintly constricted between prozonite and metazonite; prozonites smooth; metazonites laterally with transverse striae above ozopore in anterior body rings. Anterior sterna in midbody rings subrectangular, without transverse striae (Figs 26C, 171E).

First leg-pair of males. Coxae (***cx***) short (less than half of remaining podomere lengths), subtriangular, with the base strongly arched, densely setose (Fig. 114A); prefemoral process (***prf***) as wide as half of prefemur, subcylindrical, curved ectad, densely setose up to its median region (Fig. 114B); remaining podomeres with setae along the mesal region.

Second leg-pair of males. Coxa (***cx***) large and rounded; penis (***pn***) located at proximal region, rounded, not extended basally (Fig. 114C); prefemur compressed dorsoventrally; remaining podomeres setose.

Gonopods. Gonocoxa (***gcx***) elongated, twice longer than telopodite, with the base arched; antero-posteriorly flattened (Fig. 114D–F); with rows of papillae mesally. Seminal groove (***sg***) curved; arising medially on mesal cavity and terminating apically on the seminal apophysis (***sa***). Shoulder (***sh***) short, subtriangular. Telopodite (***tp***) almost as wide as ***gcx*** (Figs 114D, 218C, 222D), arising just before ending of ***sh***; solenomere (***sl***) with apicomesal process (***amp***) rounded; ectal process (***ep***) subtriangular, separating from ***amp*** by deep notch; ***sa*** located at mesal portion, visible apically. Internal branch (***ib***) subtriangular, narrow, surrounding basally ***tp*** as a shield; with torsion of 180° starting at midlength, enlarged apically and clearly visible in anal view, with elongated projection directed diagonally upwards; ***ib*** with setae along its entire margin exceeding apically seminal region of ***sl*** (Fig. 114D–F).

Vulvae. As typical for the genus. Bursa subtriangular, glabrous (Figs 39E–F, 178J); internal valve subtriangular, with mesal region rounded; operculum narrow, slightly curved ectad; external valve short in oral view, subtriangular.

Distribution

The species is widely distributed in the Karst region of Pains and surrounding counties (Arcos-Pains-Doresópolis speleological unit), Minas Gerais State, Brazil (Fig. 186).

Pseudonannolene rocana Silvestri, 1902
Figs 115–116, 187

Pseudonannolene rocana Silvestri, 1902: 21.
Pseudonannolene auguralis Silvestri, 1902: 21. **Syn. nov.**

Pseudonannolene rocana – Jeekel 2004: 90. — Iniesta & Ferreira 2013a: 92; 2013b: 366.
Pseudonannolene auguralis – Jeekel 2004: 88. — Iniesta & Ferreira 2013a: 92; 2013b: 366.

? *Pseudonannolene rocana* – Mauriès 1987: 175, figs 11–13 (description of specimens from Montevideo, Uruguay, Apr. 1947, Reinhardt leg.).

Justification of synonymy

Both nominal species present complete agreement when considering the morphology of the gonopod, mainly the stout and elongated telopodite, short squamous region of solenomere, and seminal apopohysis in medial portion.

Diagnosis

Males of *P. rocana* resemble those of *P. alegrensis* by having an elongated telopodite (longer than half of gonocoxa), but differing by having solenomere short (Fig. 116C–D); rounded coxae of the first leg-pair (Fig. 116A); and by the absence of projections bearing setae on the paraproct (Fig. 115B).

Etymology

Although unspecified, the name is probably referring to the locality where the type material was found, Rocha, southeastern Uruguay.

Material examined (total: 8 ♂♂, 21 ♀♀)

URUGUAY – **Montevideo** • 6 ♀♀; [-34.901076, -56.164503]; 38 m a.s.l.; Apr. 1947; Reinhardt leg.; NHMD • 8 ♂♂, 15 ♀♀; same locality data as for preceding; Exp. Galathea leg.; NHMD.

Descriptive notes

Measurements. 50–60 body rings (1–2 apodous + telson). Males: body length 20–28 mm; maximum midbody diameter 1.2–1.7 mm. Females: body length 22–34 mm; maximum midbody diameter 1.3–1.8 mm.

Color. Body color faded, but apparently, prozonites brownish, metazonites with a posterior band lighter; head, collum, antennae, and legs lighter.

Head. Antennae short (Fig. 115A), just reaching back to end of ring 5 when extended dorsally; relative antennomere lengths $1<2=3=4<5<6>7$. Mandibular cardo with ventral margin narrow. Ommatidial cluster well-developed, elliptical; ca 23 ommatidia in 4 rows.

BODY RINGS. Collum with lateral lobes rounded, with ca 6 shallow striae (Fig. 115A). Very faintly constricted between prozonite and metazonite; prozonites smooth; metazonites laterally with transverse striae from ca ⅓ length below ozopore. Anterior sterna in midbody rings subrectangular, without transverse striae.

FIRST LEG-PAIR OF MALES. Coxae (***cx***) elongated (as long as the sum of remaining podomere lengths), laterally rounded and with the base arched, densely setose (Fig. 116A); prefemoral process (***prf***) as wide as half of prefemur, subcylindrical, densely setose up to its median region; remaining podomeres with setae along the mesal region.

SECOND LEG-PAIR OF MALES. Coxa (***cx***) rounded; penis (***pn***) located at proximal region, rounded, not extended basally (Fig. 116B); prefemur compressed dorsoventrally; remaining podomeres setose.

GONOPODS. Gonocoxa (***gcx***) subcylindrical, expanded medially, with the base slightly arched; antero-posteriorly flattened (Fig. 116C–D); with rows of papillae mesally. Seminal groove (***sg***) curved; protruded basally on trunk of telopodite, terminating apically on the seminal apophysis (***sa***). Shoulder absent. Telopodite (***tp***) stout, longer than half of ***gcx***, slightly curved mesad; solenomere (***sl***) with small squamous region, but expanded laterad; apicomesal process (***amp***) short; ectal process absent; ***sa*** located at medial portion, slightly visible apically. Internal branch (***ib***) short, shovel-shaped, nearly not covering ***tp*** basally in anal view; long setae restricted to the apical region of ***ib*** (Fig. 116C–D).

VULVAE. As typical for the genus. Bursa subtriangular, glabrous; internal valve subtriangular, with mesal region rounded; operculum narrow; external valve wide, subtriangular.

Distribution

Known only from southern and southeastern Uruguay (Fig. 187).

Comments

Type material of *P. rocana* and *P. auguralis* described by Silvestri (1902) was not found after consulting the museums where the species were supposedly deposited (see Mauriès 1987). Additionally, Viggiani (1973) did not list either species according to material described by Silvestri. Nevertheless, topotypes described by Mauriès (1987) and deposited at the NHMD were examined (Fig. 115).

Pseudonannolene rolamossa Iniesta & Ferreira, 2013
Figs 30D, 117–118, 164I, 166H, 172A, 178K, 187; Supp. file 4: Figs 217C, 219B

Pseudonannolene rolamossa Iniesta & Ferreira, 2013c: 77, figs 2a–c.

Pseudonannolene rolamossa – Gallo & Bichuette 2019: 48.

Diagnosis

Males of *P. rolamossa* differ from those of all other species of the genus by having a solenomere with a subtriangular and elongated ectal process exceeding in length the rounded apicomesal process (Fig. 118D).

Etymology

Noun in apposition, taken from the State Park "Parque Estadual do Rola Moça" where the species was found (Iniesta & Ferreira 2013c).

Material examined

Holotype

BRAZIL • ♂; Minas Gerais, Nova Lima, Rola Moça I cave; [-20.020857, -43.812518]; 22 Mar. 2012; R.L. Ferreira and M. Souza-Silva leg.; ISLA 4004.

Paratypes (total: 1 ♀)
BRAZIL • 1 ♀; same collection data as for holotype; ISLA 4005.

Other material (total: 7 ♂♂, 2 ♀♀, 4 immatures)
BRAZIL – **Minas Gerais** • 1 ♂; Brumadinho, Serrinha 02 cave; [-20.151476, -44.201095]; 784 m a.s.l.; M.P. Oliveira leg.; ISLA 15054 • 1 ♂; PBR_18 cave; 15–20 Mar. 2010; R. Bessi *et al.* leg.; IBSP 5903 • 1 ♂, 2 immatures; Nova Lima, TUTA-14 cave; [-19.993344, -43.849412]; 763 m a.s.l.; M.P. Oliveira leg.; ISLA 15038 • 1 ♂; Rio Acima, ABOB_0028 cave; [-20.087775, -43.790650]; 743 m a.s.l.; 13 Jun. 2019; Equipe Spelayon leg.; IBSP 7766 • 1 immature; same collection data as for preceding; IBSP 7767 • 2 immatures; same collection data as for preceding; IBSP 7769 • 1 ♂; same collection data as for preceding; IBSP 7772 • 1 ♂, 2 ♀♀; same collection data as for preceding; IBSP 7773 • 1 ♂; Mariana, GS_25 cave; [-20.365015, -43.414773]; 780 m a.s.l.; 16 Jan.–11 Feb. 2011; Bessi *et al.* leg.; ISLA 6594.

Descriptive notes

Measurements. 60–62 body rings (1–2 apodous + telson). Males: body length 56 mm; maximum midbody diameter 4 mm. Females: body length 58 mm; maximum midbody diameter 4.1 mm.

Color. Body color brownish grey; head, antennae, collum, and legs darker; prozonites anteriorly greyish; metazonites with a medial darker band and a posterior lighter one.

Head. Antennae long (Fig. 164I), just reaching back to end of ring 6 when extended dorsally; antennomeres elongated; relative antennomere lengths 1<2<3>4>5≈6>7. Mandibular cardo with ventral margin narrow. Ommatidial cluster well-developed, elliptical; ca 38 ommatidia in 6 rows.

Body rings. Collum with lateral lobes rounded, with ca 10 striae, strongly curved ectad (Fig. 117A). Very faintly constricted between prozonite and metazonite; prozonites smooth; metazonites laterally with transverse striae above ozopore in anterior body rings. Anterior sterna in midbody rings subrectangular, without transverse striae (Fig. 172A).

First leg-pair of males. Coxae (***cx***) short (less than half of remaining podomere lengths), subtriangular, with the base arched and expanded, densely setose (Fig. 118A); prefemoral process (***prf***) about as wide as half of prefemur, subcylindrical, densely setose up to its median region (Fig. 118B); remaining podomeres with setae along the mesal region.

Second leg-pair of males. Coxa (***cx***) large and rounded; penis (***pn***) located at proximal region, rounded, not extended basally (Fig. 118C); prefemur compressed dorsoventrally; remaining podomeres setose.

Gonopods. Gonocoxa (***gcx***) elongated, twice longer than telopodite, with the base slightly arched; antero-posteriorly flattened (Fig. 118D–F); with rows of papillae mesally. Seminal groove (***sg***) curved; arising medially on mesal cavity and terminating apically on the seminal apophysis (***sa***). Shoulder (***sh***) long, subtriangular. Telopodite (***tp***) almost as wide as ***gcx*** (Figs 118D, 217C, 219B); solenomere (***sl***) with apicomesal process (***amp***) short, rounded; ectal process (***ep***) subtriangular, elongated, exceeding in length the ***amp***; ***sa*** located at mesal portion, nearly not visible apically. Internal branch (***ib***) subtriangular, narrow, surrounding basally ***tp*** as a shield; with torsion of 180° in the distal portion but without projection; ***ib*** with setae along its entire margin slightly exceeding apically seminal region of ***sl*** (Fig. 118D–F).

Vulvae. As typical for the genus. Bursa subtriangular, glabrous (Fig. 178K); internal valve subtriangular; operculum narrow; external valve wide, subtriangular.

Distribution

The species is widely distributed in iron ore caves and surrounding forests in the central region of Minas Gerais State, Brazil (Fig. 187).

Pseudonannolene scalaris Brölemann, 1902
Figs 119–120, 187; Supp. file 4: Fig. 223A

Pseudonannolene scalaris Brölemann, 1902a: 133, pl. vi–vii figs 148–153.

Pseudonannolene scalaris – Brölemann 1904: pl. ii fig. 3. — Jeekel 2004: 90.

Diagnosis

Males of *P. scalaris* differ from those of all other species of the genus by having internal branch contiguous to gonocoxa, without a notch separating both structures (Fig. 119B–D); internal branch longer than half of gonocoxa; seminal apophysis located medially (Fig. 119D).

Etymology

Although unspecified, the name is probably related to the Latin '*scalaris*' = 'pertaining to' or 'resembling a flight of stairs' or 'of a ladder'.

Material examined

Holotype

ARGENTINA • ♂ [head and first leg-pair missing]; Buenos Aires, Buenos Aires; [-34.638212, -58.470722]; 25 m a.s.l.; R. von Ihering leg.; MZSP 232.

Other material (total: 1 ♂, 1 immature)

ARGENTINA – **Buenos Aires** • 1 ♂ [on microscope slide]; Buenos Aires, Tandil; [-34.638212, -58.470722]; 25 m a.s.l.; Aug. 1952; MZSP • 1 ♂ immature [on microscope slide]; Balcarce; [-37.846741, -58.255617]; 123 m a.s.l.; Aug. 1952; MZSP.

Descriptive notes

Anterior region of holotype missing, descriptive notes of anterior body rings, first and second leg-pairs of males adapted from Brölemann (1902a: 133) and from topotype to supplement original description.

MEASUREMENTS. 61 body rings (2 apodous + telson). Males: body length ca 50 mm (without head); maximum midbody diameter 2.6 mm.

COLOR. Body color faded, but apparently prozonites brownish, metazonites with a posterior band brown; legs lighter brown.

BODY RINGS. Very faintly constricted between prozonite and metazonite; prozonites smooth; metazonites laterally with transverse striae below ozopore in posterior body rings. Anterior sterna in midbody rings subrectangular, without transverse striae.

FIRST LEG-PAIR OF MALES. Coxae (***cx***) short (less than half of remaining podomere lengths), subtriangular, with the base arched, densely setose mainly on distal region (Fig. 120D); prefemoral process (***prf***) as wide as half of prefemur, subcylindrical; remaining podomeres with setae along the mesal region.

SECOND LEG-PAIR OF MALES. Coxa (***cx***) large and rounded; penis (***pn***) located at proximal region, rounded, not extended basally (Fig. 120C); prefemur compressed dorsoventrally; remaining podomeres setose.

Gonopods. Gonocoxa (***gcx***) as long as the telopodite, square-shaped and abruptly constricted towards apical region, with the base slightly arched (Fig. 119B–D); scattered rows of papillae mesally. Seminal groove (***sg***) arising medially on mesal cavity, curved ectad at midlength of ***tp*** and terminating apically on the seminal apophysis (***sa***). Shoulder absent. Telopodite (***tp***) elongated (Figs 119D, 120E–F); solenomere (***sl***) with small squamous region; apicomesal process (***amp***) subtriangular, mesal; ectal process absent; ***sa*** located at medial portion, visible apically. Internal branch (***ib***) elongated and positioned parallel to the ***tp***; contiguous to ***gcx***, without a notch separating both structures; long setae restricted to the apical region of ***ib*** exceeding seminal region of ***sl*** (Figs 119D, 120F).

Distribution

Known only from Buenos Aires, Argentina (Fig. 187).

Pseudonannolene sebastianus Brölemann, 1902
Figs 31F, 121–122, 172B, 178L, 187; Supp. file 4: Fig. 201C

Pseudonannolene longicornis var. *sebastianus* Brölemann, 1902a: 126, pl. vi figs 128–133.

Pseudonannolene longicornis var. *sebastianus* – Brölemann 1909: 57.
Pseudonannolene sebastiana – Verhoeff 1943: 269, figs 23–27 (misidentified specimens from Viçosa, Minas Gerais, Brazil). — Jeekel 2004: 91.
Pseudonannolene sebastianus – Mauriès 1987: 173, figs 6–8 (lectotype and paralectotype designations). — Gallo & Bichuette 2020: 36.

Diagnosis

Males of *P. sebastianus* resemble those of *P. halophila*, *P. maritima*, *P. patagonica*, and *P. insularis* by having large and subrectangular coxae on the first leg-pair (Fig. 122A) and a suboval penis (Fig. 122C), but differing by having the solenomere rounded, seminal apophysis located medially (Fig. 122D), and internal branch without horizontal plate (Fig. 122D–F).

Etymology

Although unspecified, the name is evidently an adjective referring to the locality where the type material was found, Ilhabela (formerly Ilha de São Sebastião).

Material examined

Paralectotypes (total: 2 ♂♂, 2 ♀♀, 1 immature)
BRAZIL • 2 ♂♂, 2 ♀♀, 1 ♀ immature; São Paulo, Ilhabela (formerly Ilha de São Sebastião); [-23.812818, -45.362573]; 1 m a.s.l.; Sep. 1896; MZSP.

Other material (total: 18 ♂♂, 26 ♀♀, 62 immatures)
BRAZIL – **São Paulo** • 9 ♂♂, 5 ♀♀, 1 ♀ immature; Ilhabela; [-23.818664, -45.368161]; 1 m a.s.l.; Aug. 1950; H. Urban leg.; IBSP 7902 • 1 ♂; same collection data as for preceding; IBSP 7905 • 1 ♂; same locality data as for preceding; 9–15 Oct. 2001; Equipe Biota leg.; IBSP 1389 • 1 ♀; same collection data as for preceding; IBSP 7890 • 1 ♀; same collection data as for preceding; IBSP 1393 • 2 ♀♀, 1 immature; same collection data as for preceding; IBSP 1386 • 1 ♂; same collection data as for preceding; IBSP 1390 • 1 ♂; same collection data as for preceding; IBSP 1396 • 1 ♀ immature; same collection data as for preceding; IBSP 7789 • 1 ♀, 1 ♀ immature; same collection data as for preceding; IBSP 1391 • 1 ♀; same collection data as for preceding; IBSP 1392 • 1 ♀; same collection data as for preceding; IBSP 7891 • 1 ♂; Ubatuba, Fazenda Angelim; [-23.433713, -45.083857]; 5 m a.s.l.; Dec. 2003; IBSP 3651 • 1 ♂, 6 ♀♀, 4 immatures; Ilha de Dentro; 19 Jun. 1994; C.F. Vieira and A. Eterovic leg.; IBSP 1110 • 2 ♀♀, 4 ♂♂ immatures, 10 ♀♀ immatures; Ilha da Pesca; 2–10 Sep. 1994; C.F. Vieira and A.

Eterovic leg.; IBSP 1117 • 2 ♂♂ immatures, 1 ♀ immature; Ilha Anchieta; [-23.550426, -45.066637]; 162 m a.s.l.; 23–30 Jul. 2001; Equipe Biota leg.; IBSP 1424 • 4 ♂♂ immatures, 3 ♀♀ immatures; same collection data as for preceding; IBSP 1435 • 2 ♂♂ immatures, 5 ♀♀ immatures; same collection data as for preceding; IBSP 7904 • 1 ♀, 4 ♀♀ immatures; same collection data as for preceding; IBSP 1404 • 1 ♂ immature; same collection data as for preceding; IBSP 1416 • 1 ♀, 1♀ immature; same collection data as for preceding; IBSP 1420 • 1 ♂ immature; same collection data as for preceding; IBSP 1425 • 1 ♀ immature; same collection data as for preceding; IBSP 1421 • 1 ♂ immature; same collection data as for preceding; IBSP 1411 • 1 ♂ immature; same collection data as for preceding; IBSP 1406 • 1 ♂ immature; same collection data as for preceding; IBSP 1419 • 1 ♀ immature; same collection data as for preceding; IBSP 1428 • 1 ♂ immature, 1 ♀ immature; same collection data as for preceding; IBSP 1415 • 1 ♂ immature; same collection data as for preceding; IBSP 7903 • 1 ♀, 2 ♀♀ immatures; same collection data as for preceding; IBSP 1432 • 1 ♂ immature; same collection data as for preceding; IBSP 1427 • 1 ♂ immature, 1 ♀ immature; same collection data as for preceding; IBSP 1403 • 3 ♂♂ immatures; same collection data as for preceding; IBSP 1405 • 2 ♂♂, 2 ♀♀; Santos; [-23.967882, -46.328886]; 6 m a.s.l.; Sep. 1896; MZSP • 1 ♀; Cubatão; [-23.894019, -46.424589]; 6 m a.s.l.; 1990; MZSP • 1 ♂; São Paulo, Belém; [-23.547131, -46.591176]; 750 m a.s.l.; 1990; MZSP.

Descriptive notes

Measurements. 55–58 body rings (1 apodous + telson). Males: body length 49.5–63.5 mm; maximum midbody diameter 3–3.3 mm. Females: body length 59–90 mm; maximum midbody diameter 3.4–4.8 mm.

Color. Body color brownish grey; head and collum darker; antennae greyish; prozonites anteriorly greyish; metazonites with a medial darker band and a posterior brownish; legs brownish.

Head. Antennae short (Fig. 121A), just reaching back to end of ring 5 when extended dorsally; relative antennomere lengths 1<2≈3>4>5≈6>7. Mandibular cardo with ventral margin narrow. Ommatidial cluster well-developed, elliptical; ca 35 ommatidia in 5 rows.

Body rings. Collum with lateral lobes broadly rounded, with ca 9 deep striae (Fig. 121A). Very faintly constricted between prozonite and metazonite; prozonites smooth; metazonites laterally with transverse striae above ozopore in anterior body rings. Anterior sterna in midbody rings subrectangular, with 8–9 transverse striae (Fig. 172B).

First leg-pair of males. Coxae (***cx***) elongated (as long as the sum of remaining podomere lengths), subrectangular, with the base arched, densely setose (Fig. 122A); prefemoral process (***prf***) elongated and as wide as half of prefemur, subcylindrical, densely setose along the entire ventral region (Fig. 122B); remaining podomeres with setae along the mesal region.

Second leg-pair of males. Coxa (***cx***) as long as the sum of remaining podomere lengths, rounded; penis (***pn***) located at proximal region, rounded, extended basally (Fig. 122C); prefemur compressed dorsoventrally; remaining podomeres setose.

Gonopods. Gonocoxa (***gcx***) elongated, almost twice as long as telopodite, with the base arched; antero-posteriorly flattened (Fig. 122D–F); with rows of papillae mesally. Seminal groove (***sg***) curved; arising medially on mesal cavity and terminating apically on the seminal apophysis (***sa***). Shoulder (***sh***) rounded. Telopodite (***tp***) almost as wide as ***gcx*** (Fig. 122D), with short laterad projection; solenomere (***sl***) rounded, with apicomesal process (***amp***) subtriangular; ectal process absent; ***sa*** located at medial portion, visible apically. Internal branch (***ib***) subtriangular, narrow, surrounding basally ***tp*** as a shield; ***ib*** with setae along its entire margin nearly exceeding apically seminal region of ***sl*** (Fig. 122D–F).

Vulvae. As typical for the genus. Bursa subtriangular, glabrous (Fig. 178L); internal valve subtriangular, with mesal region rounded; operculum narrow, slightly curved ectad; external valve wide, subtriangular.

Distribution

The species is widely distributed in the Atlantic Forest of the coastal region of São Paulo State, Brazil, including some continental islands (Fig. 187).

Comments

The lectotype and paralectotypes (two males) from Ilha de São Sebastião deposited at the Muséum national d'histoire naturelle, Paris, France (MNHN), were not examined during this study.

Pseudonannolene segmentata Silvestri, 1895
Figs 123–124, 172C, 178M, 188

Pseudonannolene segmentata Silvestri, 1895b: 7.

Pseudonannolene segmentata – Silvestri 1902: 19 (description of female topotype). — Viggiani 1973: 367. — Jeekel 2004: 91. — Iniesta & Ferreira 2013a: 92; 2013b: 366.

Diagnosis

Males of *P. segmentata* slightly resemble those of *P. bucculenta* sp. nov. and *P. morettii* sp. nov. by having the internal branch narrow, foliaceus (Fig. 124D–F), but differing by the short prefemoral process on the first leg-pair (Fig. 124A); solenomere with ectal process subtriangular, separated from the apicomesal process by a shallow notch (Fig. 124D).

Etymology

Named after the Latin adjective '*segmentatus*' = 'adorned with borders or patches'. Unspecified in the original description.

Material examined (total: 9 ♂♂, 6 ♀♀, 9 immatures)

BRAZIL – **Mato Grosso do Sul** • 1 ♂, 1 ♀ immature; Bonito, Pitangueira; [-21.136212, -56.485720]; 297 m a.s.l.; Oct. 2002; C.A. Rheims leg.; IBSP 1929 • 1 ♂, 1 immature; same locality data as for preceding; V.C. Onofre leg.; IBSP 1928 • 1 ♂, 1 ♀, 2 ♀♀ immatures; same collection data as for preceding; IBSP 1931 • 1 ♂, 1 ♀; same collection data as for preceding; I. Cizauskas leg.; IBSP 1930 • 1 ♀; Bonito; [-21.128974, -56.481720]; 294 m a.s.l.; 14–23 Oct. 2002; Equipe Biota leg.; IBSP 2592 • 1 ♀; same collection data as for preceding; IBSP 2599 • 1 ♀ immature; same collection data as for preceding; IBSP 2601 • 1 ♂; same collection data as for preceding; IBSP 2605 • 1 ♀; same collection data as for preceding; IBSP 2583 • 1 ♀; same collection data as for preceding; IBSP 2603 • 1 ♂; same collection data as for preceding; IBSP 2602 • 2 ♂♂, 2 ♀♀ immatures; same collection data as for preceding; IBSP 2609 • 1 ♂, 2 ♀♀ immatures; same collection data as for preceding; 16 Jul. 1992; E. Trajano and P. Gnaspini leg; MZSP.

Descriptive notes

Measurements. 55–62 body rings (1–2 apodous + telson). Males: body length 45.6–52.5 mm; maximum midbody diameter 2.8–4.1 mm. Females: body length 37.4–42.5 mm; maximum midbody diameter 2.7–3.1 mm.

Color. Body color reddish brown; head, antennae, and collum little darker; prozonites anteriorly greyish; metazonites with a medial brown band and a posterior lighter; legs yellowish brown.

HEAD. Antennae short (Fig. 123A), just reaching back to end of ring 5 when extended dorsally; relative antennomere lengths 1<2≈3>4>5≈6>7. Mandibular cardo with ventral margin narrow. Ommatidial cluster well-developed, elliptical; ca 25 ommatidia in 5 rows.

BODY RINGS. Collum with lateral lobes broadly rounded, with ca 8 striae, curved ectad (Fig. 123A). Very faintly constricted between prozonite and metazonite; prozonites smooth; metazonites laterally with transverse striae below ozopore. Anterior sterna in midbody rings subrectangular, without transverse striae (Fig. 172C).

FIRST LEG-PAIR OF MALES. Coxae (***cx***) short (less than half of remaining podomere lengths), subtriangular, densely setose (Fig. 124A); prefemoral process (***prf***) about as wide as half of prefemur, subcylindrical, densely setose up to its median region (Fig. 124B); remaining podomeres with setae along the mesal region.

SECOND LEG-PAIR OF MALES. Coxa (***cx***) large and rounded; penis (***pn***) located at proximal region, rounded, not extended basally (Fig. 124C); prefemur compressed dorsoventrally; remaining podomeres setose.

GONOPODS. Gonocoxa (***gcx***) elongated, almost twice as long as telopodite, with the base slightly arched; antero-posteriorly flattened (Fig. 124D–F); with rows of papillae mesally. Seminal groove (***sg***) curved; arising medially on mesal cavity and terminating apically on the seminal apophysis (***sa***). Shoulder (***sh***) subtriangular. Telopodite (***tp***) as wide as half of ***gcx*** (Fig. 124D); solenomere (***sl***) with apicomesal process (***amp***) short, rounded; ectal process (***ep***) subtriangular, perpendicular to ***amp***; ***sa*** located at mesal portion, visible apically. Internal branch (***ib***) narrow, foliaceus; almost not surrounding basally ***tp***; ***ib*** with setae along its entire margin exceeding apically seminal region of ***sl*** (Fig. 124D–F).

VULVAE. As typical for the genus. Bursa subtriangular, glabrous (Fig. 178M); internal valve subtriangular, with mesal region rounded; operculum slightly curved ectad, expanded apically; external valve wide, subtriangular.

Distribution

Known from the Cerrado biome (tropical savanna ecoregion) on the border of the Brazilian state of Mato Grosso do Sul and the Paraguayan department of Concepción (Fig. 188).

Comments

The type material described by Silvestri (1895b) was not found after consulting the Museo Regionale Scienze Naturali, Torino, Italy (MRSN). Nevertheless, topotypes from surrounding areas in the Apa River were examined (Fig. 188). Other specimens from Apa River in Paraguay were also recorded by Silvestri (1902).

Pseudonannolene silvestris Schubart, 1944
Figs 125–126, 164J, 166J, 172D, 178N, 188

Pseudonannolene silvestris Schubart, 1944: 419, figs 79–81.

Pseudonannolene silvestris – Schubart 1952: 419. — Souza *et al.* 2012: 47. — Gallo & Bichuette 2020: 36.

Diagnosis

Males of *P. silvestris* slightly resemble those of *P. fontanettiae*, *P. robsoni*, and *P. typica* by having the internal branch with a slight torsion in anal view (Fig. 126D–F), but differing by having triangular coxae on the first leg-pair (Fig. 126A); solenomere with short apicomesal process and short subtriangular ectal process (Fig. 126D).

Etymology

Although unspecified, the name is probably related to either a patronym honoring the Italian naturalist Filippo Silvestri or to the Latin adjective '*silvestris*' = 'pertaining to a forest', 'living in wild area'.

Material examined

Holotype

BRAZIL • ♂ [gonopods and first leg-pair on microscope slides]; São Paulo, Descalvado, Escaramuça; [-21.930038, -47.600826]; 687 m a.s.l.; 6 Mar. 1941; O. Schubart leg.; MZSP.

Paratypes (total: 4 ♂♂, 5 ♀♀, 1 immature)

BRAZIL • 4 ♂♂, 5 ♀♀, 1 immature; same collection data as for holotype; MZSP.

Other material (total: 22 ♂♂, 15 ♀♀, 21 immatures)

BRAZIL – **São Paulo** • 1 ♂; Iporanga, Parque Estadual Turístico do Alto Ribeira (PETAR); [-24.485866, -48.646697]; 570 m a.s.l.; 8–15 Nov. 2001; Equipe Biota leg.; IBSP 2271 • 1 ♂; same collection data as for preceding; IBSP 2273 • 1 ♂, 1 ♂ immature; same collection data as for preceding; IBSP 2230 • 2 ♂♂, 1 immature; same collection data as for preceding; IBSP 2234 • 5 ♂♂, 1 ♀ immature; same collection data as for preceding; IBSP 2262 • 1 ♀; same collection data as for preceding; IBSP 2278 • 3 ♂♂, 1 ♀, 1 ♂ immature, 1 immature; same collection data as for preceding; IBSP 2261 • 1 ♂; same collection data as for preceding; IBSP 2267 • 1 ♀; same collection data as for preceding; IBSP 2282 • 1 ♀; same collection data as for preceding; IBSP 2284 • 1 ♀; same collection data as for preceding; IBSP 2283 • 1 ♂ immature; same collection data as for preceding; IBSP 2245 • 2 ♂♂ immatures; same collection data as for preceding; IBSP 2237 • 1 ♂ immature; same collection data as for preceding; IBSP 2238 • 1 ♂, 1 ♂ immature, 1 immature; same collection data as for preceding; IBSP 2272 • 1 ♂ immature, 1 immature; same collection data as for preceding; IBSP 2241 • 1 ♂ immature; same collection data as for preceding; IBSP 2244 • 1 immature; same collection data as for preceding; IBSP 2258 • 1 immature; same collection data as for preceding; IBSP 2252 • 1 immature; same collection data as for preceding; IBSP 2291 • 1 ♀, 1 immature; same collection data as for preceding; IBSP 2265 • 1 immature; same collection data as for preceding; IBSP 2227 • 1 ♀; same collection data as for preceding; IBSP 2289 • 1 immature; same collection data as for preceding; IBSP 2248 • 1 immature; same collection data as for preceding; IBSP 2242 • 2 ♀♀; Analândia, São Sebastião; [-22.129316, -47.662849]; 663 m a.s.l.; 28 Dec. 1951; O. Schubart leg.; MZSP • 7 ♂♂, 6 ♀♀; Descalvado, Escaramuça; 687 m a.s.l.; 6 Mar. 1941; O. Schubart leg.; MZSP.

Descriptive notes

MEASUREMENTS. 58–61 body rings (1–2 apodous + telson). Males: body length 62.5–76.4 mm; maximum midbody diameter 3.8–4.4 mm. Females: body length 73–74 mm; maximum midbody diameter 4–4.4 mm.

COLOR. Body color brownish grey; head, antennae, and collum darker; prozonites anteriorly greyish; metazonites with a medial darker band and a posterior lighter one; legs brownish.

HEAD. Antennae short (Fig. 164J), just reaching back to end of ring 5 when extended dorsally; relative antennomere lengths 1<2<3>4=5=6>7. Mandibular cardo with ventral margin narrow. Ommatidial cluster well-developed, elliptical; ca 35 ommatidia in 5 rows.

Body rings. Collum with lateral lobes rounded, with ca 6 striae, slightly curved ectad anteriorly (Fig. 125A). Very faintly constricted between prozonite and metazonite; prozonites smooth; metazonites laterally with transverse striae up to ozopore in anterior body rings. Anterior sterna in midbody rings subrectangular, without transverse striae (Fig. 172D).

First leg-pair of males. Coxae (***cx***) short (less than half of remaining podomere lengths), subtriangular, densely setose (Fig. 126A); prefemoral process (***prf***) about as wide as half of prefemur, subcylindrical, curved ectad, densely setose up to its median region (Fig. 126B); remaining podomeres with setae along the mesal region.

Second leg-pair of males. Coxa (***cx***) large and rounded; penis (***pn***) located at proximal region, rounded, not extended basally (Fig. 126C); prefemur compressed dorsoventrally; remaining podomeres setose.

Gonopods. Gonocoxa (***gcx***) elongated, almost twice as long as telopodite, with the base slightly arched; antero-posteriorly flattened (Fig. 126D–F); with rows of papillae mesally. Seminal groove (***sg***) curved; arising medially on mesal cavity and terminating apically on the seminal apophysis (***sa***). Shoulder (***sh***) short, rounded. Telopodite (***tp***) almost as wide as ***gcx*** (Fig. 126D); solenomere (***sl***) with apicomesal process (***amp***) short, rounded; ectal process (***ep***) short, slightly subtriangular, separating from ***amp*** by shallow notch; ***sa*** located at mesal portion, not visible apically. Internal branch (***ib***) short and narrow, subtriangular, surrounding basally ***tp*** as a shield; slightly twisted in the distal portion and with short projection; ***ib*** with setae along its entire margin slightly exceeding apically seminal region of ***sl*** (Fig. 126D–F).

Vulvae. As typical for the genus. Bursa subtriangular, glabrous (Fig. 178N); internal valve subtriangular; operculum narrow; external valve wide, subtriangular.

Distribution

Known from the central region and southern São Paulo State, Brazil (Fig. 188). Intriguingly, *P. silvestris* is well distributed in forests of the region of Alto Ribeira (PETAR), but it has not ever been recorded inside caves, while the species *P. strinatii* has been recorded only in caves (or in rocky outcrops) of the same region, suggesting a possible environmental and geographical partitioning for both species.

Pseudonannolene spelaea Iniesta & Ferreira, 2013
Figs 18E, 22, 32F, 35E–F, 127–128, 166K, 172E, 178O, 188; Supp. file 4: Figs 195D, 219E

Pseudonannolene spelaea Iniesta & Ferreira, 2013a: 85, figs 2–6.

Pseudonannolene spelaea – Iniesta & Ferreira 2013b: 366; 2013c: 78; 2014: 364. — Enghoff & Reboleira 2017: 131, fig. 1d. — Karam-Gemael *et al.* 2018: figs 2–3. — Gallo & Bichuette 2020: 34.

Diagnosis

Resembling *P. ambuatinga* and *P. lundi* by having head, trunk, and legs depigmented (Figs 18E, 127), and *P. leucomelas* by the reduced number of ommatidia (adults with less than 15 ommatidia) (Fig. 127A). Males of *P. spelaea* differ from the latter by having solenomere rounded, with seminal apophysis covered by squamous membrane (Figs 35E–F, 128D–F), and from adults of *P. ambuatinga* and *P. lundi* by the number of ommatidia.

Etymology

Name given as reference to the Latin word '*spelaea*' = 'cave', referring to the restriction of the species in caves (Iniesta & Ferreira 2013a).

Material examined

Holotype

BRAZIL • ♂; Pará, Parauapebas, GEM-1770 cave; [-6.13239, -50.136453]; 21 Oct. 2010; M.P. Oliveira leg.; ISLA 3797.

Paratypes (total: 1 ♂, 2 ♀♀)

BRAZIL – **Pará** • 1 ♂; Parauapebas, GEM-1744 cave; [-6.125219, -50.131775]; 20 Sep. 2010; M.P. Oliveira leg.; ISLA 3796 • 1 ♀; Parauapebas, GEM-1712 cave; [-6.142353, -50.133647]; 30 Oct. 2010; M.P. Oliveira leg.; ISLA 3794 • 1 ♀; same collection data as for preceding; ISLA 3795.

Other material (total: 26 ♂♂, 20 ♀♀, 4 immatures)

BRAZIL – **Pará** • 1 ♂; Canaã dos Carajás, GEM_1427 cave; [-6.316577, -49.99301]; 270 m a.s.l.; 29 Aug.–27 Sep. 2012; Pellegatti leg.; IBSP 5923 • 1 ♂; S11D_01 cave; [-6.398743, -50.357217]; 28 Oct. 2016; M.P. Oliveira *et al.* leg.; IBSP 7631 • 1 ♀; S11C_153 cave; [-6.367796, -50.389552]; 25 Oct. 2016; M.P. Oliveira *et al.* leg.; IBSP 7632 • 1 ♂; same locality data as for preceding; 15 Mar. 2016; Biospeleo leg.; IBSP 4898 • 2 ♀♀; same collection data as for preceding; IBSP 4899 • 1 immature; S11C_0046 cave; [-6.401051, -50.379098]; 19 Apr. 2016; Biospeleo leg.; IBSP 4746 • 1 immature; S11C_0002 cave; [-6.382172, -50.380279]; 16 Apr. 2016; Biospeleo leg.; IBSP 4685 • 1 ♀; same collection data as for preceding; IBSP • 1 ♂; Parauapebas, FLONA Carajás, N1_37 cave; [-6.030922, -50.27478]; 28 Sep.–3 Oct. 2007; R. Andrade leg.; IBSP 7328 • 1 ♂; same collection data as for preceding; IBSP 7328 • 1 ♂; N4E_14 cave; [-6.038547, -50.160737]; 20 Apr.–4 May 2010; R. Andrade leg.; IBSP 6222 • 1 ♂, 2 ♀♀; N4E_22 cave; [-6.034235, -50.168171]; 20 Oct.–1 Nov. 2006; R. Andrade leg.; IBSP 6071 • 1 ♂; same locality data as for preceding; 7–12 Oct. 2008; R. Andrade leg.; IBSP 7337 • 1 ♀; N4E_10 cave; [-6.039316, -50.161025]; 7–12 Oct. 2008; R. Andrade leg.; IBSP 7329 • 2 ♂♂; N3_024 cave; [-6.041148, -50.218744]; 2–23 Aug. 2013; R. Andrade leg.; IBSP 7364 • 1 ♀, 1 immature; N4E_61 cave; [-6.03948, -50.167921]; 7–12 Oct. 2008; R. Andrade leg.; IBSP 7330 • 1 ♂, 1 ♀; N4E_14 cave; [-6.038547, -50.160737]; 20 Apr.–4 May 2010; R. Andrade leg.; IBSP 6254 • 1 ♂; N1_08 cave; [-6.039257, -50.270721]; 28 Sep.–3 Oct. 2007; R. Andrade leg.; IBSP 7334 • 2 ♂♂, 2 ♀♀, 1 immature; N4E_61 cave; [-6.03948, -50.167921]; 24–30 Jul. 2009; R. Andrade leg.; IBSP 6258 • 1 ♂, 1 ♀; N1_04 cave; [-6.040225, -50.270456]; 28 Sep.–3 Oct. 2007; R. Andrade leg.; IBSP 7327 • 3 ♀♀; N1_08 cave; [-6.039257, -50.270721]; R. Andrade leg.; IBSP 7333 • 3 ♂♂, 1 ♀; N4E_14 cave; [-6.038547, -50.160737]; 7–12 Oct. 2008; R. Andrade leg.; IBSP 7335 • 3 ♂♂, 1 ♀; same collection data as for preceding; IBSP 7336 • 1 ♂, 1 ♀; N4E_61 cave; [-6.03948, -50.167921]; 7–12 Oct. 2008; R. Andrade leg.; IBSP 7332 • 1 ♀; N5W_01 cave; [-6.07974, -50.133343]; 4–7 Dec. 2013; Guarda *et al.* leg.; IBSP 7336 • 2 ♂♂; same data as for preceding except for N5W_03 cave; [-6.081198, -50.134398]; IBSP 7367 • 1 ♂; N3_024 cave; [-6.041148, -50.218744]; IBSP 7363 • 1 ♂; same collection data as for preceding; IBSP 7362 • 1 ♀; N5W_03 cave; [-6.081198, -50.134398]; IBSP 7356.

Descriptive notes

Measurements. 60–65 body rings (1 apodous + telson). Males: body length 41.6–42 mm; maximum midbody diameter 1.6–1.8 mm. Females: body length 34.8–35 mm; maximum midbody diameter 1.7–1.8 mm.

Color. Living specimens depigmented. Color when stored in 70% ethanol: uniform brownish, faint dark shadows posteriorly on prozonites; metazonites little lighter.

Head. Antennae short (Fig. 22), just reaching back to end of ring 5 when extended dorsally; relative antennomere lengths 1<2<3>4<5≈6>7. Mandibular cardo with ventral margin narrow. Ommatidial cluster reduced and almost entirely covered by collum; ca 12 ommatidia in 3 rows loosely grouped (Fig. 127A).

Body rings. Collum with lateral lobes broadly subrectangular, with ca 6 thickened striae, curved mesad (Fig. 127A). Very faintly constricted between prozonite and metazonite; prozonites smooth; metazonites laterally with transverse striae below ozopore. Anterior sterna in midbody rings subrectangular, without transverse striae (Fig. 172E).

First leg-pair of males. Coxae (***cx***) short (less than half of remaining podomere lengths), subtriangular, with the base slightly arched, densely setose (Fig. 128A); prefemoral process (***prf***) as wide as half of prefemur, subcylindrical, densely setose along in its entire extension (Fig. 128B); remaining podomeres with setae along the mesal region.

Second leg-pair of males. Coxa (***cx***) large and rounded; penis (***pn***) located at proximal region, large and rounded, not extended basally (Fig. 128C); prefemur compressed dorsoventrally; remaining podomeres setose.

Gonopods. Gonocoxa (***gcx***) elongated, almost twice as long as telopodite, antero-posteriorly flattened (Fig. 128D–F); with rows of papillae mesally (Fig. 32F). Seminal groove (***sg***) almost imperceptible in oral view, terminating apically on the seminal apophysis (***sa***) (Figs 35E–F, 128D–F, 219E). Shoulder absent. Telopodite (***tp***) almost as wide as ***gcx*** (Fig. 128D–F); solenomere (***sl***) rounded, with ***sa*** covered by a secondary squamous membrane (Figs 35E–F, 128D, 219E), not protruded apically; ectal process absent. Internal branch (***ib***) short, subtriangular; short setae restricted to the apical region of ***ib*** not exceeding seminal region of ***sl*** (Figs 35E–F, 128D–F, 219E).

Vulvae. As typical for the genus. Bursa subtriangular, glabrous (Fig. 178O); internal valve subtriangular, with its sides having the same length; operculum subrectangular, as wide as half of internal valve; external valve short in oral view, subtriangular.

Distribution

A troglomorphic species known only from iron ore caves in the Carajás region, Pará State, Brazil (Fig. 188), an outstanding region for environmental and economic activities in Brazil due to its extensive iron ore reserves. These caves are small, with their sizes varying around 30 meters to 200 meters, connected to a huge network of small channels (= canaliculi, typically found in the Canga formation), which considerably increases the habitats for cave-dwelling species. The Carajás region is also the shelter of several troglobitic and troglophilic species such as spiders, beetles, centipedes, crickets, and other invertebrates (Pinto-da-Rocha 1995; Ázara & Ferreira 2014; Parizotto *et al*. 2017; Chagas-Jr & Bichuette 2018; Rodrigues *et al*. 2018; Bouzan *et al.* 2019a; Oliveira *et al.* 2019; Junta *et al*. 2020).

Pseudonannolene strinatii Mauriès, 1974

Figs 29D–E, 129–130, 164K, 166L, 173A, 179A, 188; Supp. file 4: Figs 192A–B, 211D

Pseudonannolene strinatii Mauriès, 1974: 546, figs 1–2.

Pseudonannolene strinatii – Mauriès & Geoffroy 2000: 155. — Campos & Fontanetti 2004: 53. — Iniesta & Ferreira 2013a: 92; 2013b: 357; 2013c: 79; 2014: 361. — Gallo & Bichuette 2019: 43; 2020: 43.

Diagnosis

Males of *P. strinatii* resemble those of *P. ophiiulus* and *P. tocaiensis* by having an internal branch shovel-shaped and with a horizontal plate (Fig. 130D), but differing by having the head and collum depigmented (Fig. 129A); solenomere with short ectal process, separated from the apicomesal process by a shallow notch (Fig. 130D–F).

Etymology

Patronym honoring the biospeleologist and collector of the type material Pierri Strinati (Mauriès 1974).

Material examined (total: 12 ♂♂, 25 ♀♀, 5 immatures)

BRAZIL – **São Paulo** • 1 ♀; Iporanga, Parque Estadual Turístico do Alto Ribeira (PETAR); [-24.485866, -48.646697]; 570 m a.s.l.; Jul. 1992; A. Eterovic leg.; IBSP 1257 • 1 ♂; same collection data as for preceding; IBSP 7633 • 2 ♀♀; same collection data as for preceding; IBSP 7634 • 1 ♀; same collection data as for preceding; IBSP 7635 • 1 ♂, 1 ♀; Iporanga, Parque Estadual Turístico do Alto Ribeira (PETAR), Areias cave; [-24.583809, -48.700458]; 497 m a.s.l.; 7 Apr. 2012; R.L. Ferreira *et al.* leg.; ISLA 20615 • 3 ♀♀; same collection data as for preceding; ISLA 20622 • 1 ♂, 4 ♀♀; same locality data as for preceding; 1–18 Jul. 1991; R. Pinto-da-Rocha leg.; MZSP • 3 ♂♂, 3 ♀♀; Ressurgência das Areias; [-24.583809, -48.700458]; 497 m a.s.l.; Apr. 1985; MZSP • 3 ♀♀; Jeremias cave; [-24.637976, -48.701058]; 456 m a.s.l.; R. Enfurnado leg.; MZSP • 2 ♀♀; same locality data as for preceding; 18 Aug. 1991; R. Pinto-da-Rocha leg.; MZSP • 3 ♂♂, 1 ♀ immature; Casa de Pedra; [-24.245425, -48.452803]; 895 m a.s.l.; MZSP • 1 ♀ immature; Toca do Tigre; [-24.666864, -49.054852]; 574 m a.s.l.; 9 Mar. 1991; R. Pinto-da-Rocha leg.; MZSP. – **Paraná** • 1 ♀; Rio Branco do Sul, Joca cave; [-25.194050, -49.314003]; 950 m a.s.l.; 18 Aug. 1989; R. Pinto-da-Rocha leg.; MZSP • 1 ♀; Itacolombo cave; 28 Apr. 1990; R. Pinto-da-Rocha leg.; MZSP • 1 ♂, 1 ♀ immature, 1 immature; Lancinha cave; 19 Aug. 1989; MZSP • 1 ♂, 1 ♀; Bom Sucesso cave; 3 Apr. 1991; R. Pinto-da-Rocha leg.; MZSP • 1 ♂, 2 ♀, 1 ♀ immature; Cerro Azul, Rocha cave; [-24.893123, -49.243774]; 640 m a.s.l.; 2 Apr. 1991; MZSP.

Descriptive notes

Measurements. 68–72 body rings (1–2 apodous + telson). Males: body length 60–90 mm; maximum midbody diameter 3.1–4 mm. Females: body length 78–95 mm; maximum midbody diameter 3.5–4.1 mm.

Color. Body color greyish; head, antennae, collum, and legs whitish; prozonites anteriorly darker; metazonites with a medial darker band and a posterior whitish.

Head. Antennae long (Fig. 164K), just reaching back to end of ring 6 when extended dorsally; antennomeres elongated; relative antennomere lengths 1<2<3>4>5≈6>7. Mandibular cardo with ventral margin swollen. Ommatidial cluster well-developed, elliptical; ca 23 ommatidia in 4 rows.

Body rings. Collum with lateral lobes rounded, with ca 13 shallow striae, slightly curved ectad (Fig. 129A). Very faintly constricted between prozonite and metazonite; prozonites smooth; metazonites laterally with transverse striae up to ozopore in anterior body rings. Anterior sterna in midbody rings subrectangular, without transverse striae (Fig. 173A).

First leg-pair of males. Coxae (***cx***) short (less than half of remaining podomere lengths), subtriangular, with the base arched and expanded, densely setose (Fig. 130A); prefemoral process (***prf***) as wide as half of prefemur, subcylindrical, densely setose along the entire ventral region (Fig. 130B); remaining podomeres with setae along the mesal region.

Second leg-pair of males. Coxa (***cx***) subrectangular; penis (***pn***) located at proximal region, rounded, not extended basally (Fig. 130C); prefemur compressed dorsoventrally; remaining podomeres setose.

Gonopods. Gonocoxa (***gcx***) subtriangular, basally expanded and progressively less wide (Fig. 130D–F), with the base not arched; antero-posteriorly strongly flattened, longitudinal thickened ridge with rows of papillae mesally. Seminal groove (***sg***) curved; arising medially on mesal cavity and terminating apically on the seminal apophysis (***sa***). Shoulder absent. Telopodite (***tp***) almost as wide as ***gcx*** (Fig. 130D); solenomere (***sl***) with apicomesal process (***amp***) short, rounded; ectal process (***ep***) short, subtriangular, separating from ***amp*** by shallow notch; ***sa*** located at mesal portion, not visible apically. Internal branch (***ib***) shovel-shaped and rounded apically, with horizontal plate; setae restricted to the apical region of ***ib*** exceeding seminal region of ***sl*** (Fig. 130D–F).

VULVAE. As typical for the genus. Bursa subtriangular, glabrous (Fig. 179A); internal valve subtriangular; operculum expanded apically, curved ectad; external valve subtriangular, as wide as half of internal valve in oral view.

Distribution

Known only from the Karst region of Alto Ribeira on the border of the Brazilian states of São Paulo and Paraná (Fig. 188). Although no restriction of *P. strinatii* to caves or rocky outcrops may be assumed, the species has not ever been recorded free-living in the forests of the region.

Comments

The lectotype and the paralectotypes (one male, two females, and two immatures) from Areias Cave, Iporanga, deposited at the Muséum national d'histoire naturelle, Paris, France (MNHN), were not examined during this study. Nevertheless, topotypes from caves in Iporanga were examined (Fig. 188).

Pseudonannolene sulcatula Silvestri, 1895
Figs 131, 176F, 188

Pseudonannolene sulcatula Silvestri, 1895b: 7, fig. 14.

Pseudonannolene sulcatula – Viggiani 1973: 367. — Jeekel 2004: 91.

Diagnosis

Males of *P. sulcatula* resemble those of *P. ophiiulus*, *P. strinatii*, and *P. tocaiensis* by having a gonopod with a subtriangular gonocoxa; the internal branch being shovel-shaped, but differing by the absence of a horizontal plate in the internal branch (Silvestri 1895b: 8, fig. 14; Fig. 131C).

Etymology

Unspecified in the original description and not related to any morphological structure of the species.

Material examined (total: 1 ♀)

ARGENTINA – **Salta** • 1 ♀; Rosário de la Frontera; [-25.800215, -64.967830]; 200 m a.s.l.; 11 Apr. 1979; Misión Científica Danesa leg.; NHMD.

Descriptive notes

Gonopod description adapted from Silvestri (1895b: 7) to supplement original description and to introduce gonopod terminology; non-sexual characters described based on examined topotype.

MEASUREMENTS. 73 body rings (1 apodous + telson). Males: body length ca 85 mm; maximum midbody diameter 3.5 mm.

COLOR. Body color greyish; prozonites anteriorly greyish; metazonites with a medial greyish band and a posterior whitish; legs lighter brown.

HEAD. Antennae short, just reaching back to end of ring 5 when extended dorsally; relative antennomere lengths 1<2≈3>4=5≈6>7. Mandibular cardo with ventral margin narrow. Ommatidial cluster well-developed, elliptical; ca 30 ommatidia in 5 rows.

Body rings. Collum with lateral lobes rounded, with ca 7 shallow striae. Very faintly constricted between prozonite and metazonite; prozonites smooth; metazonites laterally with transverse striae below ozopore. Anterior sterna in midbody rings subrectangular, without transverse striae (Fig. 176F).

Gonopods. Gonocoxa (***gcx***) subtriangular, progressively less wide (Fig. 131C), with the base not arched; antero-posteriorly flattened; with rows of papillae mesally. Seminal groove (***sg***) not visible. Shoulder absent. Telopodite (***tp***) almost as wide as ***gcx***; solenomere (***sl***) with apicomesal process (***amp***) short, subtriangular; ectal process (***ep***) inconspicuous, apparently separated from ***amp*** by shallow notch; ***sa*** not not visible apically. Internal branch (***ib***) shovel-shaped, narrow; almost not surrounding basally ***tp***; setae restricted to the apical region of ***ib*** exceeding seminal region of ***sl*** (Fig. 131C).

Vulvae. As typical for the genus. Bursa subtriangular, glabrous; internal valve subtriangular; operculum narrow; external valve wide, subtriangular.

Distribution

Known only from northern Argentina (Fig. 188).

Comments

The type material described by Silvestri (1895b) and supposedly deposited at the Museo Regionale Scienze Naturali, Torino, Italy (MRSN) (Viggiani 1973: 367), was not found. Nevertheless, a topotype from northern Argentina was examined (Fig. 188).

Pseudonannolene tocaiensis Fontanetti, 1996
Figs 132–133, 166M, 173B, 179B, 189

Pseudonannolene tocaiensis Fontanetti, 1996: 419, figs 1–3.

Pseudonannolene tocaiensis – Freitas *et al.* 2004: 38. — Souza *et al.* 2012: 47. — Iniesta & Ferreira 2013b: 357; 2013c: 78. — Karam-Gemael *et al.* 2018: figs 2–3. — Gallo & Bichuette 2019: 43; 2020: 36.

Diagnosis

Males of *P. tocaiensis* resemble those of *P. ophiiulus*, *P. strinatii*, and *P. sulcatula* by having an internal branch shovel-shaped (see Figs 130D, 133D), but differing by having the first leg-pair with subrectangular coxae, prefemoral process larger than half of prefemur (Fig. 133B); solenomere with rounded ectal process (Fig. 133D–F).

Etymology

Although unspecified, the name is evidently an adjective referring to the locality where the type material was found, Toca Cave.

Material examined

Holotype

BRAZIL • ♂ [fragmented, gonopods missing]; São Paulo, Itirapina, Fazenda da Toca, Toca cave; [-22.272463, -47.776046]; 776 m a.s.l.; 27 Aug. 1985; C.S. Fontanetti, A. Mesa and F.A.G. Mello leg.; MZSP 942.

Paratypes (total: 6 ♂♂, 1 ♀)

BRAZIL • 6 ♂♂, 1 ♀ [all fragmented]; same collection data as for holotype; MZSP 942.

Other material (total: 3 ♂♂, 2 ♀♀, 2 immatures)
BRAZIL – **São Paulo** • 3 ♂♂, 1 ♀, 1 ♂ immature, 1 ♀ immature; Itirapina, Fazenda da Toca, Toca cave; [-22.2531, -47.8228]; 776 m a.s.l.; 24 Feb. 1989; A. Mesa leg.; MZSP • 1 ♀; Estação Ecológica Itirapina; [-22.249596, -47.825980]; 764 m a.s.l.; 30 Apr.–5 May 2001; Equipe Biota leg.; IBSP 1935.

Descriptive notes

MEASUREMENTS. 60 body rings (1 apodous + telson). Males: body length ca 50 mm; maximum midbody diameter 2 mm.

COLOR. Body color faded, but apparently uniform pale brownish; metazonites with a posterior band brown; head, collum, antennae, and legs brownish.

HEAD. Antennae short, just reaching back to end of ring 5 when extended dorsally; relative antennomere lengths 1<2<3>4>5≈6>7. Mandibular cardo with ventral margin narrow. Ommatidial cluster well-developed, elliptical; ca 28 ommatidia in 5 rows.

BODY RINGS. Collum with lateral lobes rounded, with ca 9 shallow striae (Fig. 132A). Very faintly constricted between prozonite and metazonite; prozonites smooth; metazonites laterally with transverse striae from ca ⅓ length below ozopore. Anterior sterna in midbody rings subrectangular, without transverse striae (Fig. 173B).

FIRST LEG-PAIR OF MALES. Coxae (***cx***) short (less than half of remaining podomere lengths), subrectangular, with the base arched and expanded, densely setose (Fig. 133A); prefemoral process (***prf***) as wide as half of prefemur, subcylindrical, densely setose along the entire ventral region (Fig. 133B); remaining podomeres with setae along the mesal region.

SECOND LEG-PAIR OF MALES. Coxa (***cx***) subrectangular; penis (***pn***) located at proximal region, rounded, not extended basally (Fig. 133C); prefemur compressed dorsoventrally; remaining podomeres setose.

GONOPODS. Gonocoxa (***gcx***) subtriangular, basally expanded and progressively less wide, with the base arched; antero-posteriorly flattened; with rows of papillae mesally (Fig. 133D–F). Seminal groove (***sg***) straight up to ending of ***gcx***, arising medially on mesal cavity, curved ectad in ***tp*** and terminating apically on the seminal apophysis (***sa***). Shoulder absent. Telopodite (***tp***) almost as wide as ***gcx*** (Fig. 133D); solenomere (***sl***) with apicomesal process (***amp***) short, slightly subtriangular; ectal process (***ep***) short, rounded, separating from ***amp*** by shallow notch; ***sa*** located at mesal portion, not visible apically. Internal branch (***ib***) shovel-shaped and rounded apically, with horizontal plate; setae restricted to the apical region of ***ib*** exceeding seminal region of ***sl*** (Fig. 133D–F).

VULVAE. As typical for the genus. Bursa subtriangular, glabrous (Fig. 179B); internal valve subtriangular; operculum narrow, curved ectad; external valve wide, subtriangular.

Distribution

Known only from the type locality Fazenda da Toca, Itirapina, São Paulo State, Brazil (Fig. 189).

Pseudonannolene tricolor Brölemann, 1902
Figs 1, 134–135, 164L, 166N, 173C, 179C, 189; Supp. file 4: Figs 211E, 221B

Pseudonannolene tricolor Brölemann, 1902a: 122, pl. vi figs 134–141.
Pseudonannolene tricolor var. *gracilis* Brölemann, 1902a: 125. **Syn. nov.**
Pseudonannolene tricolor var. *rugosus* Schubart, 1945a: 313. **Syn. nov.**

Pseudonannolene tricolor – Brölemann 1909: 58. — Schubart 1944: 416, figs 77–78; 1945a: 294; 1952: 419. — Lordello 1954: 73. — Mauriès 1987: 177, figs 14–16 (lectotype and paralectotypes designations). — Fontanetti 1990: 698. — Penteado & Hebling-Beraldo 1991: 232. — Jeekel 2004: 91. — Miyoshi *et al.* 2005: 183. — Gallo & Bichuette 2019: 48; 2020: 36.
Pseudonannolene tricolor tricolor [by implication] – Brölemann 1902a: 125.
Pseudonannolene tricolor var. *gracilis* – Brölemann 1909: 58. — Jeekel 2004: 92.
Pseudonannolene tricolor var. *rugosa* – Jeekel 2004: 92.

Justification of synonymy

Pseudonannolene tricolor rugosus and *P. tricolor gracilis* were described considering only the body color variation and number of transverse striae on metazonites. Through the examination of the type material, as well as the accurate exam of additional specimens, we conclude that there is no morphological difference to justify the separation of these taxa. Therefore, both subspecies are considered junior synonyms of *P. tricolor*.

Diagnosis

Males of *P. tricolor* resemble those of *P. longicornis* by having the gonocoxa largely subcylindrical and a large shoulder (Fig. 135D–F), but differing by a shovel-shaped internal branch, slightly curved ectad at midlength, in anal view (Fig. 135D).

Etymology

Although unspecified, the name is evidently referring to the pattern of coloration of the body rings of living specimens: black, white and red.

Material examined

Holotypes

BRAZIL • 1 ♀, holotype of *P. tricolor* var. *gracilis*; São Paulo, Piquete; [-22.601629, -45.176698]; 642 m a.s.l.; Jan. 1897; R. von Ihering leg.; MZSP.

BRAZIL • 1 ♂, holotype of *P. tricolor* var. *rugosus*; São Paulo, Monte Alegre do Sul, Fazenda Santa Maria; [-22.689959, -46.682377]; 779 m a.s.l.; 27 Feb. 1942; F. Lane leg.; MZSP.

Paratypes (total: 1 ♀)

BRAZIL • 1 ♀, paratype of *P. tricolor* var. *rugosus*; São Paulo, Monte Alegre do Sul, Fazenda Santa Maria; [-22.689959, -46.682377]; 779 m a.s.l.; 27 Feb. 1942; F. Lane leg.; MZSP.

Paralectotypes (total: 1 ♂, 1 ♀)

BRAZIL • 1 ♂, 1 ♀, paralectotypes of *P. tricolor*; São Paulo, Santo André, Alto da Serra (= Paranapiacaba); [-23.777531, -46.299860]; Jan. 1897; Diego leg.; MZSP.

Other material (total: 49 ♂♂, 65 ♀♀, 36 immatures)

BRAZIL – **Tocantins** • 1 ♂, 1 ♀; Miracema do Tocantins/Lajeado, U.H.E Luiz Eduardo de Magalhães; [-9.754609, -48.380952]; 264 m a.s.l.; 2 Nov. 2001; IBSP 2031. – **Minas Gerais** • 1 ♂; Poços de Caldas; [-21.797214, -46.559999]; 1216 m a.s.l.; IBSP 7885 • 3 ♂♂, 2 ♀♀; Monte Verde; [-22.865145, -46.039188]; 1550 m a.s.l.; 21 Feb. 2018; B. Challupe leg.; IBSP 7880. – **São Paulo** • 11 ♂♂, 4 ♀♀, 3 immatures; Barra Bonita, Hotel Estância Barra Bonita; [-22.515267, -48.532787]; 485 m a.s.l.; 21–27 Nov. 2001; M.E. Calleffo leg.; IBSP 964 • 1 ♀; same collection data as for preceding; IBSP 7882 • 1 ♀; same collection data as for preceding; IBSP 7883 • 1 ♂; Jaú, Independência; [-23.680577, -46.598126]; 766 m a.s.l.; 21 Dec. 2011; A.M. Giroti leg.; IBSP 7881 • 1 ♂, 1 ♀; Franco da Rocha; [-23.323672, -46.729425]; 785 m a.s.l.; 30 Jan. 2002; A. Cazdorroa leg.; IBSP 954 • 1 ♂; same collection data as for preceding; IBSP 7884 • 3 ♀♀; Amparo, Fazenda São Bento; [-22.708067, -46.772670]; 713 m a.s.l.; 8 Mar. 1943; F. Lane leg.; MZSP • 1 ♂; Sítio de Oliveira Pinto; 21 Dec. 1949; O. Schubart leg.; MZSP • 1 ♀ immature; Monte Alegre do Sul; [-22.690558, -46.682531]; 779 m a.s.l.; 1 Nov. 1943; O. Schubart leg.; MZSP • 2 ♀♀; Analândia; [-22.129316, -47.662849]; 663 m a.s.l.; 7 Mar. 1944; O. Schubart leg.; MZSP • 1 ♀; Anhembi, Barraco Rico; [-22.788342, -48.131224]; 469 m a.s.l; 10 Dec. 1956; Travassos leg.; MZSP • 1 ♂, 1 ♀; same locality data as for preceding; Feb. 1990; C. Fontanetti leg.; MZSP • 1 ♀ immature; Araraquara, mata Mogi-Guaçu; [-21.784967, -48.178945], 685 m a.s.l.; 28 Aug. 1944; O. Schubart leg.; MZSP • 3 ♂♂, 7 ♀♀; Corumbatá, Cerrado biome – FAPESP; [-22.222984, -47.623304]; 586 m a.s.l.; 1 Nov. 1985; O.A. Mesa leg.; MZSP • 2 ♂♂; Leme, Fazenda Graminha; [-22.182038, -47.384897]; 621 m a.s.l.; 10 Dec. 1948; O. Schubart leg.; MZSP • 1 ♂, 1 ♀; Lindóia; [-22.523300, -46.650246]; 703 m a.s.l.; 2 Feb. 1947; J. Schubart leg.; MZSP • 1 ♀ immature; Mogi Guaçu; [-22.370451, -46.943508]; 602 m a.s.l.; 31 Jul. 1944; O. Schubart leg.; MZSP • 1 ♀, 1 ♂ immature, 1 ♀ immature; Monte Alegre do Sul, Fazenda Ponte Alta; [-22.690149, -46.682657]; 767 m a.s.l.; 20 Jan. 1947; O. Schubart leg.; MZSP • 1 ♀; same locality data as for preceding; Dec. 1949; J. Schubart leg.; MZSP • 3 ♂♂, 1 ♀; same locality data as for preceding; 21 Jan. 1947; J. Schubart leg.; MZSP • 1 ♀; same locality data as for preceding; 21 Jan. 1947; D. Gaspar leg.; MZSP • 2 ♀♀; same locality data as for preceding; 25 Oct. 1948; O. Schubart leg.; MZSP • 2 ♂♂, 2 ♀♀, 1 ♂ immature, 1 ♀ immature; same locality data as for preceding; 26 Oct. 1948; O. Schubart leg.; MZSP • 1 ♂; same locality data as for preceding; 30 Oct. 1943; O. Schubart leg.; MZSP • 2 ♀♀; same collection data as for preceding; MZSP • 3 ♀♀ immatures; same collection data as for preceding; 31 Oct. 1943; MZSP • 2 ♀♀; same collection data as for preceding; 25 Oct. 1948; MZSP • 1 ♀; Piracicaba, Escola Superior de Agronômia Luiz Queiroz – ESALQ; [-22.715040, -47.629727]; 555 m a.s.l.; Nov. 1952; L.G. Lordello leg.; MZSP • 1 ♂; Piracicaba; [-22.734558, -47.647966]; 533 m a.s.l.; 7 Nov. 1985; L. Gignoretti leg.; MZSP • 1 ♂, 2 ♀♀, 1 immature; Pirassununga, Baguassú; [-21.996797, -47.426165]; 633 m a.s.l.; 27 Dec. 1938; O. Schubart leg.; MZSP • 1 ♀, 1 ♀ immature; Cachoeira; 5 Dec. 1939; O. Schubart leg.; MZSP • 1 ♂; same locality data as for preceding; 8 Jan. 1939; O. Schubart leg.; MZSP • 1 ♂, 2 ♀♀, 1 ♀ immature, 3 immatures; same locality data as for preceding; 16–20 Dec. 1938; O. Schubart leg.; MZSP • 1 ♀; same locality data as for preceding; 16–21 Nov. 1942; O. Schubart leg.; MZSP • 1 ♂, 1 ♀ immature; same locality data as for preceding; 25 Dec. 1938; O. Schubart leg.; MZSP • 1 ♀; Cupinzeiro; Sep. 1943; O. Schubart leg.; MZSP • 1 ♂ immature; Emas; 1 Dec. 1940; O. Schubart leg.; MZSP • 1 ♀; same locality data as for preceding; 28 Jan. 1940; O. Schubart leg.; MZSP • 1 ♂ immature, 1 ♀ immature; Fazenda Campo Alegre; 24 Feb. 1945; O. Schubart leg.; MZSP • 2 ♂♂; Fazenda Pedra Branca; 15 Feb. 1942; J. Gaspar leg.; MZSP • 1 ♀; Laranja Azeda; 5 Jan. 1939; O. Schubart leg.; MZSP • 1 ♀, 1 ♀ immature, 1 immature; 28 Nov. 1940; O. Schubart leg.; MZSP • 1 ♂; Jaguarí-Mirim River; 16 Mar. 1945; N. dos Santos leg.; MZSP • 1 ♀; same locality data as for preceding; 1940; A. Boggi leg.; MZSP • 3 ♀♀, 1 ♀ immature; same locality data as for preceding; 4 Feb. 1941; O. Schubart leg.; MZSP • 1 ♀; same locality data as for preceding; 4 Oct. 1941; H. Rosa leg.; MZSP • 1 ♀ immature; same locality data as for preceding; 11 Jan. 1939; O. Schubart leg.; MZSP • 1 ♀ immature; same locality data as for preceding; 11 Nov. 1947; O. Schubart leg.; MZSP • 2 ♂♂, 1 ♀; 13 Jan. 1940; O. Schubart leg.; MZSP • 1 ♀, 1 ♂ immature, 2 ♀♀ immatures, 3 immatures; same locality data as for preceding; 14–17 Feb. 1940; O. Schubart leg.; MZSP • 1 ♀; same locality data as for preceding; 22 Nov. 1942; H. Rosa leg.; MZSP • 1 immature; same locality data as for preceding; 25 May 1940; O. Schubart leg.; MZSP • 1 ♀; same locality data as for preceding; 29 Dec. 1938; O. Schubart leg.; MZSP • 1 ♀; same locality data as for preceding; Jan. 1941; Aguirre leg.; MZSP • 1 ♂, 2 ♀♀; same locality data as for preceding; Oct. 1920; Aguirre leg.; MZSP • 1 ♂, 3 ♀♀; Pitangueiras; [-21.011223, -48.217526]; 520 m a.s.l.; 24 Oct. 1943; F. Lane leg.; MZSP • 1 ♀; Santa Rita do Passa Quatro; [-21.707953, -47.479092]; 761 m a.s.l.; 24 Nov. 1949; O. Schubart leg.; MZSP • 1 ♂; Amparo, Fazenda São Bento; [-22.707856, -46.774107]; 760 m a.s.l.; 18 Dec. 1942; B. Soares leg.; MZSP • 1 ♀; Piquete; [-22.612999, -45.179019]; 642 m a.s.l.; Jan. 1897; MZSP • 1 ♂, 1 ♀ immature; Águas da Prata, Obelisque; [-21.947598, -46.718978]; 830 m a.s.l.; 31 Oct. 1952; O. Schubart leg.; MZSP.

Descriptive notes

Measurements. 55–61 body rings (1–2 apodous + telson). Males: body length 79.3–81.9 mm; maximum midbody diameter 4.8–4.9 mm. Females: body length 68–81 mm; maximum midbody diameter 4.8–5 mm.

Color. Body color brownish; head, collum, and antennae darker; prozonites anteriorly greyish; metazonites with a posterior band reddish; legs lighter brown.

Head. Antennae short (Fig. 164L), just reaching back to end of ring 5 when extended dorsally; relative antennomere lengths $1<2<3>4>5=6>7$. Mandibular cardo with ventral margin narrow. Ommatidial cluster well-developed, elliptical; ca 35 ommatidia in 5 rows.

Body rings. Collum with lateral lobes rounded, with 8 striae, curved ectad (Fig. 134A). Very faintly constricted between prozonite and metazonite; prozonites smooth; metazonites laterally with transverse striae slightly above ozopore in anterior body rings. Anterior sterna in midbody rings subrectangular, with shallow transverse striae (Fig. 173C).

First leg-pair of males. Coxae (***cx***) short (less than half of remaining podomere lengths), subtriangular, with the base strongly arched and expanded, densely setose (Fig. 135A); prefemoral process (***prf***) as long as prefemur, subcylindrical, apically narrow, densely setose up to its median region (Fig. 135B); remaining podomeres with setae along the mesal region.

Second leg-pair of males. Coxa (***cx***) large and rounded; penis (***pn***) located at proximal region, rounded, not extended basally (Fig. 135C); prefemur compressed dorsoventrally; remaining podomeres setose.

Gonopods. Gonocoxa (***gcx***) elongated, largely subcylindrical, with the base arched; antero-posteriorly flattened (Figs 135D–F, 211E); with rows of papillae mesally. Seminal groove (***sg***) curved; arising medially on mesal cavity and terminating apically on the seminal apophysis (***sa***). Shoulder (***sh***) large, rounded. Telopodite (***tp***) almost as wide as ***gcx*** (Fig. 135D); solenomere (***sl***) with apicomesal process (***amp***) subtriangular, short; ectal process (***ep***) subtriangular, separating from ***amp*** by shallow notch; ***sa*** located at mesal portion, slightly visible apically. Internal branch (***ib***) shovel-shaped, narrow and foliaceous; slightly curved ectad at midlength; setae of ***ib*** exceeding seminal region of ***sl*** (Figs 135D–F, 211B).

Vulvae. As typical for the genus. Bursa subtriangular, glabrous (Fig. 179C); internal valve subtriangular, with mesal region clearly rounded; operculum curved ectad; external valve wide, subtriangular.

Distribution

The species is widely distributed in the São Paulo State, and intriguingly with a disjunct population from the Araguaia-Tocantins basin (ca 1500 km from São Paulo) (Fig. 189).

Comments

The lectotype of *P. tricolor* from Paranapiacaba deposited at the Muséum national d’histoire naturelle, Paris, France (MNHN), was not examined during this study.

Pseudonannolene typica Silvestri, 1895

Figs 136–139, 164M, 166O, 173D, 179D, 189; Supp. file 4: Figs 214D, 220B, 222F

Pseudonannolene typica Silvestri, 1895a: 775.
Pseudonannolene abbreviata Silvestri, 1902: 20. **Syn. nov.**

Pseudonannolene typica – Silvestri 1896: 170; 1903: 74, fig. 119. — Brölemann 1909: 85. — Viggiani 1973: 367. — Jeekel 2004: 92. — Iniesta & Ferreira 2013c: 79.
Ppseudonannolene [sic!] *typica* – Silvestri 1902: 18 (description of male from Puerto Piray, Argentina, 1884, NHMD; examined).
Pseudonannolene abbreviata – Jeekel 2004: 87. — Iniesta & Ferreira 2013c: 79.

Justification of synonymy

Based on the examination of the type material of *P. abbreviata* (USNM 2031 and ZMB 2887) and the original description, the sexual and somatic characters are in complete agreement with those described for *P. typica*. Therefore, *P. abbreviata* is herein proposed as a junior synonym of *P. typica.*

Diagnosis

Males of *P. typica* resemble those of *P. centralis* by having a solenomere with short ectal process, separated from apicomesal process by a shallow notch; internal branch with distal projection (Figs 137D, 220B). *Pseudonannolene typica* differs by an evident shoulder on gonocoxa (Fig. 137D–F); head without frontal setae (Fig. 136A).

Etymology

Name 'typica' is derived from the Latin word '*typus*', plus the suffix '-icus' = belonging to. Although unspecified in the original description, the species name is probably an allusion to the name-bearing type of the genus.

Material examined

Syntypes
ARGENTINA • 1 ♂, 2 ♀♀, syntypes of *P. typica*; Misiones, Candelaria; [-27.462447, -55.744566]; 53 m a.s.l.; 1884; G. Bove leg.; MCSN.

BRAZIL • 1 ♀, syntype of *P. typica*; Paraná; G. Bove leg.; USNM.

URUGUAY • 1 ♀, syntype of *P. abbreviata*; Maldonado, Estación La Sierra; [-34.747175, -55.404774]; 30 m a.s.l.; 27 May 1899; F. Silvestri leg.; USNM 2031 • 1 ♀, syntype of *P. abbreviata*; same collection data as for preceding; ZMB 2887.

Other material (total: 2 ♂♂, 5 ♀♀)
ARGENTINA – **Misiones** • 1 ♂, 5 ♀♀; Candelaria; [-27.462447, -55.744566]; 53 m a.s.l.; 1884; G. Bove leg.; MCSN • 1 ♂; Puerto Piray; [-26.468823, -54.715889]; 50 m a.s.l.; 1884; NHMD.

Descriptive notes

Measurements. 60–65 body rings (2–3 apodous + telson). Males: body length 55 mm; maximum midbody diameter 3.3–4 mm. Females: body length 53–66 mm; maximum midbody diameter 3.6–4.3 mm.

Color. Body color brownish grey; head, collum, antennae darker; prozonites anteriorly greyish; metazonites with a medial darker band and a posterior reddish; legs brownish.

Head. Antennae short (Fig. 164M), just reaching back to end of ring 5 when extended dorsally; relative antennomere lengths 1<2<3>4=5=6>7. Mandibular cardo with ventral margin narrow. Ommatidial cluster well-developed, elliptical; ca 35 ommatidia in 5 rows.

Body rings. Collum with lateral lobes rounded, with 9 striae, slightly curved ectad (Fig. 136A). Very faintly constricted between prozonite and metazonite; prozonites smooth; metazonites laterally with transverse striae slightly above ozopore in anterior body rings. Anterior sterna in midbody rings subrectangular, with shallow transverse striae (Fig. 173D).

First leg-pair of males. Coxae (***cx***) short (less than half of remaining podomere lengths), subtriangular, with the base arched and slightly expanded, densely setose (Fig. 137A); prefemoral process (***prf***) about as wide as half of prefemur, subcylindrical, curved ectad, densely setose up to its median region (Fig. 137B); remaining podomeres with setae along the mesal region.

Second leg-pair of males. Coxa (***cx***) large and rounded; penis (***pn***) located at proximal region, rounded, not extended basally (Fig. 137C); prefemur compressed dorsoventrally; remaining podomeres setose.

Gonopods. Gonocoxa (***gcx***) elongated, almost twice as long as telopodite, with the base arched; antero-posteriorly flattened (Figs 137D–F, 214D); with rows of papillae mesally. Seminal groove (***sg***) curved; arising medially on mesal cavity and terminating apically on the seminal apophysis (***sa***). Shoulder (***sh***) subtriangular. Telopodite (***tp***) almost as wide as ***gcx*** (Figs 137D, 220B); solenomere (***sl***) with apicomesal process (***amp***) slightly subtriangular; ectal process (***ep***) short, subtriangular, separating from ***amp*** by shallow notch; ***sa*** located at mesal portion, slightly visible apically. Internal branch (***ib***) subtriangular, narrow, surrounding basally ***tp*** as a shield; with a short torsion of 180° starting at midlength, with projection directed diagonally upwards; ***ib*** with setae along its entire margin exceeding apically seminal region of ***sl*** (Figs 137D–F, 214D).

Vulvae. As typical for the genus. Bursa subtriangular, glabrous (Fig. 179D); internal valve subtriangular, slightly compressed medially; operculum large, curved ectad; external valve wide, subtriangular.

Distribution
Known from the border of northeastern Argentina with southern Paraguay (Fig. 189).

Pseudonannolene urbica Schubart, 1945
Figs 18A, 140–142, 164O, 166P, 173E, 189; Supp. file 4: Fig. 223B

Pseudonannolene urbica Schubart, 1945a: 313, figs 13–14.

Pseudonannolene urbica – Jeekel 2004: 92. — Gallo & Bichuette 2020: 36.

Diagnosis
Males of *P. urbica* differ from all congeners by having the telopodite and internal branch short (less than ⅓ of gonocoxa in length) (Fig. 141D–F); solenomere short and trianguliform; apicomesal process located medially (Figs 141D, 223B).

Etymology
Although unspecified, the name is evidently related to the Latin adjective '*urbicus*' (feminine '*urbica*') = 'related to city', referring to the occurrence of the species in urban areas.

Material examined
Holotype
BRAZIL • ♂ [gonopods, gnathochilarium, first and second leg-pair on microscope slides]; São Paulo, São Paulo, Jardim do Museu de Zoologia [MZSP], Ipiranga; [-23.585105, -46.600998]; 790 m a.s.l.; 3 Mar. 1943; F. Lane leg.; MZSP.

Paratypes (total: 1 ♂, 1 immature)
BRAZIL • 1 ♂, 1 ♂ immature; same collection data as for holotype; MZSP.

Other material (total: 9 ♂♂, 4 ♀♀, 1 immature)
BRAZIL – **São Paulo** • 1 ♀; São Paulo, Parque dos Príncipes; [-23.572951, -46.772286]; 794 m a.s.l.; 14 Mar. 2003; IBSP 7887 • 1 ♂; São Paulo; [-23.550439, -46.633317]; 769 m a.s.l.; IBSP 2007 • 1 ♂, 1 ♀; same collection data as for preceding; IBSP 2008 • 1 ♂; campus USP, Mata do Cuaso; [-23.561075, -46.724394]; 730 m a.s.l.; 12–19 Dec. 1999; D.F. Candiani leg.; IBSP 1249 • 1 ♂; Mata da Previdência; [-23.571120, -46.709728]; 732 m a.s.l.; 22 Feb. 2001; F.S. Cunha leg.; IBSP 716 • 1 ♂; Bairro Ipiranga; [-23.530503, -46.666090]; 744 m a.s.l.; 31 Jan. 1944; O. Schubart leg.; MZSP • 1 ♀; Bairro Morumbi; [-23.598485, -46.720072]; 746 m a.s.l.; 6 Dec. 1948; E. Marcus leg.; MZSP • 3 ♂♂, 1 ♀; Eldorado; [-23.709807, -46.627225]; 785 m a.s.l.; 1 Nov. 1947; E. Marcus leg.; MZSP • 1 ♂ immature; Mogi das Cruzes, Jundiapeba, Parque São Martinho; [-23.614280, -46.236089]; 814 m a.s.l.; 6–7 Jan. 2017; R.S. Bouzan leg.; IBSP 7886 • 1 ♂; Amparo, Fazenda São Bento; [-22.708011, -46.772597]; 687 m a.s.l.; 8 Mar. 1943; F. Lane leg.; MZSP.

Descriptive notes

Measurements. 50–53 body rings (1–2 apodous + telson). Males: body length 47.6–50.2 mm; maximum midbody diameter 2.5–2.7 mm. Females: body length 52–53 mm; maximum midbody diameter 2.8–3 mm.

Color. Body color brownish grey; head, collum, antennae darker; prozonites anteriorly greyish; metazonites with a posterior band lighter; legs brownish.

Head. Antennae short (Fig. 164O), just reaching back to end of ring 5 when extended dorsally; relative antennomere lengths 1<2<3>4>5≈6>7. Mandibular cardo with ventral margin narrow. Ommatidial cluster well-developed, elliptical; ca 41 ommatidia in 6 rows.

Body rings. Collum with lateral lobes rounded, with ca 9 striae, slightly curved ectad (Fig. 140A). Very faintly constricted between prozonite and metazonite; prozonites smooth; metazonites laterally with transverse striae below ozopore. Anterior sterna in midbody rings subrectangular, without transverse striae (Fig. 173E).

First leg-pair of males. Coxae (***cx***) short (less than half of remaining podomere lengths), subtriangular, with the base arched, densely setose (Fig. 141A); prefemoral process (***prf***) about as wide as half of prefemur, subcylindrical, curved ectad, densely setose up to its median region (Fig. 141B); remaining podomeres with setae along the mesal region.

Second leg-pair of males. Coxa (***cx***) rounded; penis (***pn***) located at proximal region, rounded, not extended basally (Fig. 141C); prefemur compressed dorsoventrally; remaining podomeres setose.

Gonopods. Gonocoxa (***gcx***) rounded, with the base arched; antero-posteriorly flattened (Fig. 141D–F); with rows of papillae mesally. Seminal groove (***sg***) curved; arising medially on mesal cavity and terminating apically on the seminal apophysis (***sa***). Shoulder (***sh***) rounded. Telopodite (***tp***) shorter than ⅓ of ***gcx*** (Fig. 141D); solenomere (***sl***) with short squamous region; apicomesal process (***amp***) subtriangular, located medially, with ***sa*** also at medial portion and visible apically; ectal process absent. Internal branch (***ib***) short, subtriangular, surrounding basally ***tp*** as a shield; ***ib*** with setae along its entire margin, but only with the apical setae exceeding seminal region of ***sl*** (Figs 141D–F, 223B).

Vulvae. As typical for the genus. Bursa subtriangular, glabrous; internal valve subtriangular; operculum large, curved ectad; external valve wide, subtriangular.

Distribution

The species has been recorded only in the metropolitan region of the Brazilian city of São Paulo and surrounding area (Fig. 189).

Pseudonannolene xavieri Iniesta & Ferreira, 2014
Figs 143–144, 166Q, 174A, 179E, 189

Pseudonannolene xavieri Iniesta & Ferreira, 2014: 373, figs 9, 14f.

Pseudonannolene xavieri – Gallo & Bichuette 2019: 48.

Diagnosis

Males of *P. xavieri* resemble those of *P. anapophysis*, *P. bovei,* and *P. inops* by having solenomere with elongated ectal process directed horizontally (Fig. 144D), but differing by having the telopodite larger than half of gonocoxa in width; subtriangular internal branch (Fig. 144D–F).

Etymology

Patronym honoring the Brazilian biospeleologist Xavier Prous (Iniesta & Ferreira 2014).

Material examined

Holotype

BRAZIL • ♂; Bahia, Iraquara, Fumaça cave; [-12.33169, -41.59664]; 723 m a.s.l.; 7 Jan. 2001; R.L. Ferreira *et al.* leg.; ISLA 4105.

Other material (total: 1 ♂, 2 ♀♀)

BRAZIL – **Bahia** • 2 ♀♀; same collection data as for holotype; 2014; ISLA 20618 • 1 ♂; Lapa Doce; 11 Nov. 2002; A. Giupponi and R. Baptista leg.; MNRJ 30148.

Descriptive notes

MEASUREMENTS. 60–61 body rings (1 apodous + telson). Males: body length 44 mm; maximum midbody diameter 3.3 mm. Females: body length 46 mm; maximum midbody diameter 3.4 mm.

COLOR. Body color brownish grey; head, collum, antennae little darker; prozonites anteriorly greyish; metazonites with a posterior band lighter; legs brownish.

HEAD. Antennae short (Fig. 143A), just reaching back to end of ring 5 when extended dorsally; antennomeres elongated; relative antennomere lengths 1<2<3>4>5<6>7. Mandibular cardo with ventral margin narrow. Ommatidial cluster well-developed, elliptical; ca 26 ommatidia in 5 rows.

BODY RINGS. Collum with lateral lobes rounded, with ca 4 shallow striae (Fig. 143A). Very faintly constricted between prozonite and metazonite; prozonites smooth; metazonites laterally with transverse striae slightly above ozopore in anterior body rings. Anterior sterna in midbody rings subrectangular, with 7 transverse striae (Fig. 174A).

FIRST LEG-PAIR OF MALES. Coxae (***cx***) short (less than half of remaining podomere lengths), subtriangular, with the base arched and slightly expanded, densely setose (Fig. 144A); prefemoral process (***prf***) about as wide as half of prefemur, subcylindrical, densely setose up to its median region (Fig. 144B); remaining podomeres with setae along the mesal region.

SECOND LEG-PAIR OF MALES. Coxa (***cx***) large and rounded; penis (***pn***) located at proximal region, circle-shaped (Fig. 144C); prefemur compressed dorsoventrally; remaining podomeres setose.

GONOPODS. Gonocoxa (***gcx***) elongated, subrectangular, with the base slightly arched; antero-posteriorly flattened (Fig. 144D–F); with rows of papillae mesally. Seminal groove (***sg***) curved; arising medially on mesal cavity and terminating apically on the seminal apophysis (***sa***). Shoulder (***sh***) subtriangular. Telopodite (***tp***) as wide as half of ***gcx*** (Fig. 144D); solenomere (***sl***) with apicomesal process (***amp***) short; ectal process (***ep***) subtriangular, elongated and perpendicular to ***amp***; ***sa*** located at mesal portion, elongated, visible apically. Internal branch (***ib***) subtriangular, narrow, surrounding basally ***tp*** as a shield; ***ib*** with setae along its entire margin exceeding apically seminal region of ***sl*** (Fig. 144D–F).

Vulvae. As typical for the genus. Bursa subtriangular, glabrous (Fig. 179E); internal valve subtriangular; operculum slightly curved ectad; external valve subtriangular.

Distribution

Known only from Iraquara, Bahia State, Brazil (Fig. 189).

Pseudonannolene alata sp. nov.

urn:lsid:zoobank.org:act:C18F0776-3DA0-4571-91C9-0584F601B97F

Figs 145–146, 163C, 165C, 175B, 179K, 190; Supp. file 4: Fig. 215B

Diagnosis

Males of *P. alata* sp. nov. can be distinguished from those of all other species of *Pseudonannolene* by having a large, rounded projection on the telopodite (Fig. 146D).

Etymology

The species epithet is derived from the Latin adjective ‘*alata*’ = ‘winged’, in reference to the ectal projection on the telopodite.

Material examined

Holotype

BRAZIL • ♂; Santa Catarina, Florianópolis, Ilha do Arvoredo; [-27.281906, -48.366245]; 130 m a.s.l.; 15 May 2018; R.S. Bouzan leg.; IBSP 7874.

Paratype (total: 1 ♀)

BRAZIL • 1 ♀; same collection data as for holotype; IBSP 7875.

Referred non-type material (total: 5 ♂♂, 12 ♀♀; 5 immatures)

BRAZIL – **Santa Catarina** • 6 ♀♀, 5 immatures; Florianópolis, Ilha do Arvoredo; [-27.281094, -48.366610]; 130 m a.s.l.; 15 May 2018; R.S. Bouzan leg.; IBSP 7876 • 4 ♀♀; same collection data as for preceding; IBSP 7877 • 2 ♀♀; same collection data as for preceding; IBSP 7878 • 5 ♂♂; same collection data as for preceding; IBSP 7879.

Description

Measurements. 53–55 body rings (1–2 apodous + telson). Males: body length 43.8–64.8 mm; maximum midbody diameter 3.2–4.5 mm. Females: body length 56.5–72.2 mm; maximum midbody diameter 4–5.4 mm.

Color. Body color brownish grey; head and collum darker; prozonites anteriorly greyish; metazonites with a medial band darker and a posterior reddish; antennae and legs reddish.

Head. Antennae short (Fig. 163C), just reaching back to end of ring 5 when extended dorsally; relative antennomere lengths $1<2<3>4\approx5\approx6>7$. Mandibular cardo with ventral margin narrow. Ommatidial cluster well-developed, elliptical; ca 40 ommatidia in 6 rows.

Body rings. Collum with lateral lobes rounded, with ca 6 deep striae, strongly curved ectad (Fig. 145A). Very faintly constricted between prozonite and metazonite; prozonites smooth; metazonites laterally with transverse striae below ozopore. Anterior sterna in midbody rings subrectangular, without transverse striae (Fig. 175B).

First leg-pair of males. Coxae (***cx***) elongated (as long as the sum of remaining podomere lengths), subtriangular, with the base slightly arched and expanded, densely setose mainly on distal region (Fig. 146A); prefemoral process (***prf***) as wide as half of prefemur, subcylindrical, densely setose along in its entire extension (Fig. 146B); remaining podomeres with setae along the mesal region.

Second leg-pair of males. Coxa (***cx***) large and subrectangular; penis (***pn***) located at proximal region, rounded, not extended basally (Fig. 146C); prefemur compressed dorsoventrally; remaining podomeres setose.

Gonopods. Gonocoxa (***gcx***) elongated, almost twice as long as telopodite, with the base slightly arched; antero-posteriorly flattened (Fig. 146D–F); with rows of papillae mesally. Seminal groove (***sg***) curved; arising medially on mesal cavity and terminating apically on the seminal apophysis (***sa***). Shoulder (***sh***) inconspicuous. Telopodite (***tp***) almost as wide as ***gcx*** (Figs 146D, 215B), with large and rounded laterad projection; solenomere (***sl***) expanded laterad, rounded, with apicomesal process (***amp***) subtriangular; ectal process absent; ***sa*** located at mesal portion, visible apically. Internal branch (***ib***) subtriangular, narrow, surrounding basally ***tp*** as a shield; ***ib*** with setae along its entire margin nearly exceeding apically seminal region of ***sl*** (Fig. 146D–F).

Vulvae. As typical for the genus. Bursa subtriangular, glabrous (Fig. 179K); internal valve subtriangular, mesally rounded; operculum narrow, curved ectad, slightly compressed basally; external valve subtriangular.

Distribution

Known only from the type locality Ilha do Arvoredo, Florianópolis, Santa Catarina State, Brazil (Fig. 190).

Pseudonannolene aurea sp. nov.
urn:lsid:zoobank.org:act:0458352D-56B7-4A58-A71A-7E502759CA27
Figs 147–148, 175D, 179M, 190

Diagnosis

Males of *P. aurea* sp. nov. slightly resemble those of *P. paulista* by having a solenomere with a spiniform ectal process deeply notched separating from apicomesal process (Fig. 148D), but differing by an internal branch subtriangular with distal projection (Fig. 148D–F).

Etymology

The species epithet is derived from the Latin adjective '*aurum*' = 'golden'; in reference to the type locality Dianópolis, which is historically known for the gold mining activities in the region.

Material examined

Holotype

BRAZIL • ♂; Tocantins, Dianópolis, Mojadores cave; [-11.624226, -46.820593]; 672 m a.s.l.; 4–9 Dec. 2017; F. Pellegatti leg.; IBSP 5858.

Paratypes (total: 1 ♂, 3 ♀♀)
BRAZIL – **Tocantins** • 1 ♂, 2 ♀♀; Dianópolis, Areia cave; [-11.624226, -46.820593]; 670 m a.s.l.; 21–29 May 2008; F. Pellegatti leg.; IBSP 5854 • 1 ♀; same collection data as for holotype; 4–12 Mar. 2008; IBSP 5856.

Referred non-type material (total: 3 ♂♂, 7 ♀♀; 16 immatures)
BRAZIL – **Tocantins** • 2 ♀♀, 4 immatures; Dianópolis, Vozinha cave; [-11.624226, -46.820593]; 672 m a.s.l.; 21–29 May 2008; F. Pellegatti leg.; IBSP 5859 • 3 ♂♂, 2 ♀♀, 7 immatures; Onça cave; 4–12 Mar. 2008; F. Pellegatti leg.; IBSP 5840 • 5 immatures; same locality data as for preceding; 4–9 Dec. 2007; F. Pellegatti leg.; IBSP 5843 • 1 ♀; Coluna cave; 21–29 May 2008; F. Pellegatti leg.; IBSP 5836 • 2 ♀♀; Vertebra cave; 21–29 May 2009; F. Pellegatti leg.; IBSP 5837.

Description

Measurements. 58–63 body rings (1–2 apodous + telson). Males: body length 63.1 mm; maximum midbody diameter 3.6–3.8 mm. Females: body length 61.4–67.8 mm; maximum midbody diameter 3.7–4.1 mm.

Color. Body color brownish red; head, antennae, collum, and legs brownish; prozonites anteriorly greyish; metazonites with a medial band brown and a posterior lighter.

Head. Antennae short, just reaching back to end of ring 5 when extended dorsally; relative antennomere lengths 1<2<3>4≈5≈6>7. Mandibular cardo with ventral margin narrow. Ommatidial cluster well-developed, elliptical; ca 35 ommatidia in 5 rows.

Body rings. Collum with lateral lobes rounded, with ca 10 striae, slightly curved ectad (Fig. 147A). Very faintly constricted between prozonite and metazonite; prozonites smooth; metazonites laterally with transverse striae slightly above ozopore in anterior body rings. Anterior sterna in midbody rings subrectangular, without transverse striae (Fig. 175D).

First leg-pair of males. Coxae (*cx*) short (less than half of remaining podomere lengths), subtriangular, with the base arched and strongly expanded, densely setose (Fig. 148A); prefemoral process (***prf***) as long as prefemur, subcylindrical, densely setose up to its median region (Fig. 148B); remaining podomeres with setae along the mesal region.

Second leg-pair of males. Coxa (***cx***) large and rounded; penis (***pn***) located at proximal region, rounded, not extended basally (Fig. 148C); prefemur compressed dorsoventrally; remaining podomeres setose.

Gonopods. Gonocoxa (***gcx***) elongated, almost twice as long as telopodite, with the base arched; antero-posteriorly flattened (Fig. 148D–F); with rows of papillae mesally. Seminal groove (***sg***) curved; arising medially on mesal cavity and terminating apically on the seminal apophysis (***sa***). Shoulder (***sh***) subtriangular. Telopodite (***tp***) almost as wide as ***gcx***, with deep depression separating from ***sh*** (Fig. 148D); solenomere (***sl***) with apicomesal process (***amp***) subtriangular; ectal process (***ep***) spiniform, elongated, separating from ***amp*** by deep notch; ***sa*** located at mesal portion, slightly visible apically. Internal branch (***ib***) subtriangular, narrow, surrounding basally ***tp*** as a shield; with torsion of 180° in the distal portion and projection directed diagonally upwards; ***ib*** with setae along its entire margin exceeding apically seminal region of ***sl*** (Fig. 148D–F).

Vulvae. As typical for the genus. Bursa subtriangular, glabrous (Fig. 179M); internal valve subtriangular, slightly rounded mesally; operculum narrow, curved ectad; external valve subtriangular.

Distribution

Known only from caves and surrounding forests in Dianópolis, Tocantins State, Brazil (Fig. 190).

Pseudonannolene bucculenta sp. nov.

urn:lsid:zoobank.org:act:5CFFCC61-1C8A-4DE7-BF92-46C53D80A6FC
Figs 149–150, 164C, 174B, 179F, 190; Supp. file 4: Fig. 197E

Diagnosis

Males of *P. bucculenta* sp. nov. resemble those of *P. erikae*, *P. mesai*, and *P. curvata* sp. nov. by having a mesally curving telopodite (Fig. 150D), but differing clearly by a narrow and elongated prefemoral process of the first leg-pair (Fig. 150B) and by the presence of paired projections in the proximal region of the mentum on the gnathochilarium (Figs 174B, 197E).

Etymology

The species epithet is derived from the Latin adjective '*bucculentus*' = 'having fat cheek'; referring to the thickened projections on the mentum.

Material examined

Holotype

BRAZIL • ♂; Minas Gerais, Nova Lima, RPPN Samuel de Paula; [-20.001055, -43.871088]; 975 m a.s.l.; Oct. 2006; J.P.P. Pena-Barbosa leg.; IBSP 3352.

Paratypes (total: 3 ♂♂, 1 ♀)

BRAZIL • 3 ♂♂; same collection data as for holotype; IBSP 3358 • 1 ♀; same collection data as for holotype; IBSP 3396.

Referred non-type material (total: 57 ♂♂, 40 ♀♀; 19 immatures)

BRAZIL – **Minas Gerais** • 1 ♂; Belo Horizonte, Campus Pampulha, UFMG; [-19.868399, -43.959965]; 830 m a.s.l.; 6 Jan. 2006; L. Bernardi leg.; IBSP 2905 • 1 ♂, 2 ♀♀; same collection data as for holotype; IBSP 3350 • 2 ♂♂, 2 ♀♀; same collection data as for holotype; IBSP 3359 • 1 ♂; same collection data as for holotype; IBSP 3361 • 3 ♂♂, 2 ♀♀, 2 ♂♂ immatures, 1 ♀ immature; same collection data as for holotype; IBSP 3344 • 3 ♂♂, 3 ♀♀, 3 ♂♂ immatures, 5 immatures; same collection data as for holotype; IBSP 3348 • 1 ♂; same collection data as for holotype; IBSP 3353 • 8 ♂♂, 3 ♀♀; same collection data as for holotype; IBSP 3410 • 1 ♂, 2 ♀♀, 2 immatures; same collection data as for holotype; IBSP 3407 • 1 ♂, 2 immatures; same collection data as for holotype; IBSP 3403 • 2 ♂♂, 3 ♀♀, 1 ♂ immature; same collection data as for holotype; IBSP 3415 • 3 ♂♂, 2 ♀♀; same collection data as for holotype; IBSP 3426 • 3 ♂♂, 2 ♀♀; same collection data as for holotype; IBSP 3426 • 1 ♂, 1 ♀; same collection data as for holotype; IBSP 3408 • 2 ♂♂; same collection data as for holotype; IBSP 3406 • 3 ♂♂, 2 ♀♀; same collection data as for holotype; IBSP 3413 • 5 ♂♂, 2 ♀♀; same collection data as for holotype; IBSP 3416 • 2 ♂♂, 4 ♀♀; same collection data as for holotype; IBSP 3412 • 2 ♂♂, 1 immature; same collection data as for holotype; IBSP 3321 • 6 ♂♂, 1 ♀; same collection data as for holotype; IBSP 3417 • 1 ♂, 1 ♀; same collection data as for holotype; IBSP 3404 • 2 ♀♀; same collection data as for holotype; IBSP 3411 • 1 ♂, 1 ♀; same collection data as for holotype; IBSP 3424 • 1 ♂ immature, 1 ♀ immature; same collection data as for holotype; IBSP 3420 • 1 ♂, 2 ♀♀; same collection data as for holotype; IBSP 3402 • 1 ♂, 1 ♀; same collection data as for holotype; IBSP 3422 • 2 ♂♂, 2 ♀♀; same collection data as for holotype; IBSP 3423.

Description

Measurements. 51–53 body rings (1–2 apodous + telson). Males: body length 40.2–45.5 mm; maximum midbody diameter 2.2–2.59 mm. Females: body length 38.2–40.2 mm; maximum midbody diameter 2.4–2.6 mm.

Color. Body color brownish grey; head and collum darker; prozonites anteriorly greyish; metazonites with a medial band darker and a posterior reddish; antennae and legs lighter brown.

Head. Antennae short (Fig. 164C), just reaching back to end of ring 5 when extended dorsally; relative antennomere lengths 1<2<3>4=5=6>7. Mandibular cardo with ventral margin narrow. Mentum of gnathochilarium with thickened basal projections (Figs 174B, 197E). Ommatidial cluster well-developed, elliptical; ca 25 ommatidia in 4 rows.

Body rings. Collum with lateral lobes rounded, with ca 9 shallow striae (Fig. 149A). Very faintly constricted between prozonite and metazonite; prozonites smooth; metazonites laterally with transverse striae above ozopore in anterior body rings. Anterior sterna in midbody rings subrectangular, without transverse striae (Fig. 174B).

First leg-pair of males. Coxae (***cx***) short (less than half of remaining podomere lengths), subtriangular, with the base strongly arched, densely setose (Fig. 150A); prefemoral process (***prf***) narrow and as longer as prefemur, subcylindrical, densely setose up to its median region (Fig. 150B); remaining podomeres with setae along the mesal region.

Second leg-pair of males. Coxa (***cx***) large and rounded; penis (***pn***) located at proximal region, rounded, not extended basally (Fig. 150C); prefemur compressed dorsoventrally; remaining podomeres setose.

Gonopods. Gonocoxa (***gcx***) elongated, but less than twice telopodite, with the base arched; antero-posteriorly flattened (Fig. 150D–F); with rows of papillae mesally. Seminal groove (***sg***) curved mesad; running mesally and terminating apically on the seminal apophysis (***sa***). Shoulder (***sh***) short, slightly subtriangular. Telopodite (***tp***) almost as wide as ***gcx*** (Fig. 150D), strongly curved mesad; solenomere (***sl***) with apicomesal process (***amp***) subtriangular; ectal process absent; ***sa*** located at mesal portion, not protruded apically. Internal branch (***ib***) narrow, foliaceus; with basal constriction in relation to ***gcx***; ***ib*** with setae along its entire margin slightly exceeding apically seminal region of ***sl*** (Fig. 150D–F).

Vulvae. As typical for the genus. Bursa subtriangular, glabrous (Fig. 179F); internal valve subtriangular, with mesal region clearly rounded; operculum narrow, rounded apically; external valve wide, subtriangular.

Distribution

Known only from forests in the central region of Minas Gerais State, Brazil (Fig. 190).

Pseudonannolene curvata sp. nov.

urn:lsid:zoobank.org:act:789F5690-028D-4681-9025-41E7D902A7E6

Figs 151–152, 175C, 179L, 190

Diagnosis

Males of *P. curvata* sp. nov. resemble those of *P. mesai*, *P. erikae*, and *P. bucculenta* sp. nov. by having mesally curving telopodite (Fig. 152D). *Pseudonannolene curvata* differs from *P. erikae* and *P. bucculenta* by having the prefemoral process digitiform and larger than half of the prefemur (Fig. 152B), and from *P. mesai* by a narrow trunk of telopodite (Fig. 152D–F).

Etymology

The species epithet is derived from the Latin adjective '*curvatus*' = 'curved, bent'; in reference to the curved telopodites.

Material examined

Holotype

BRAZIL • ♂; Rio Grande do Sul, Santana do Livramento, APA Cerrito; [-30.877251, -55.538789]; 208 a.s.l.; 10 Dec. 2012; R. Ott leg.; MCN.

Paratypes (total: 2 ♂♂, 2 ♀♀)

BRAZIL • 2 ♂♂; same collection data as for holotype; MCN • 2 ♀♀; same collection data as for holotype; MCN.

Referred non-type material (total: 13 ♂♂, 8 ♀♀; 3 immatures)

BRAZIL – **Rio Grande do Sul** • 6 ♂♂, 2 ♀♀, 3 immatures; Santana do Livramento, APA Cerrito; [-30.877251, -55.538789]; 208 m a.s.l.; 10 Dec. 2012; R. Ott leg.; MCN • 4 ♀♀; same collection data as for preceding; IBSP 7877 • 2 ♀♀; same collection data as for preceding; IBSP 7878 • 5 ♂♂; same collection data as for preceding; IBSP 7879.

URUGUAY – **Salto** • 1 ♂; Arapey River; [-31.147443, -56.882060]; 98 m a.s.l.; 20 Dec. 1954; FCE 433. – **Tacuarembó** • 1 ♂; Laureles, Puntas de Arroio, Rincón de la Vasoura; [-31.362767, -55.882940]; 147 m a.s.l.; 20 Jan. 1960; FCE 343.

Description

Measurements. 51–56 body rings (1–2 apodous + telson). Males: body length 33.4–40.6 mm; maximum midbody diameter 2.3–2.4 mm. Females: body length 45.4–49.9 mm; maximum midbody diameter 3.1–3.5 mm.

Color. Body color greenish grey; head and antennae darker, and collum little lighter; prozonites anteriorly greyish; metazonites with a medial band brown and a posterior whitish; legs brownish.

Head. Antennae short (Fig. 151A), just reaching back to end of ring 5 when extended dorsally; relative antennomere lengths <2<3>4≈5≈6>7. Mandibular cardo with ventral margin swollen. Ommatidial cluster well-developed, elliptical; ca 25 ommatidia in 4 rows.

Body rings. Collum with lateral lobes rounded, with ca 6 striae (Fig. 151A). Very faintly constricted between prozonite and metazonite; prozonites smooth; metazonites laterally with transverse striae below ozopore. Anterior sterna in midbody rings subrectangular, without transverse striae (Fig. 175C).

First leg-pair of males. Coxae (***cx***) short (less than half of remaining podomere lengths), subtriangular, with the base arched and expanded, densely setose (Fig. 152A); prefemoral process (***prf***) as wide as half of prefemur, subcylindrical, densely setose along the entire ventral region (Fig. 152B); remaining podomeres with setae along the mesal region.

Second leg-pair of males. Coxa (***cx***) as long as the sum of remaining podomere lengths, rounded; penis (***pn***) located at proximal region, rounded, slightly constricted basally (Fig. 152C); prefemur compressed dorsoventrally; remaining podomeres setose.

Gonopods. Gonocoxa (***gcx***) elongated, almost twice as long as telopodite, with the base slightly arched; antero-posteriorly flattened (Fig. 152D–F); with rows of papillae mesally. Seminal groove (***sg***) curved mesad; running mesally and terminating apically on the seminal apophysis (***sa***). Shoulder (***sh***) elongated, subtriangular. Telopodite (***tp***) almost as wide as ***gcx*** (Fig. 152D), strongly curved mesad; solenomere (***sl***) with apicomesal process (***amp***) rounded; ectal process absent; ***sa*** located at mesal portion, protruded apically. Internal branch (***ib***) shovel-shaped and rounded apically; setae restricted to the apical region of ***ib*** not exceeding seminal region of ***sl*** (Fig. 152D–F).

Vulvae. As typical for the genus. Bursa subtriangular, glabrous (Fig. 179L); internal valve subtriangular; operculum narrow, curved ectad; external valve subtriangular.

Distribution

Known from the border of the Brazilian state of Rio Grande do Sul, northern Uruguay, and Argentina (Fig. 190).

Pseudonannolene granulata sp. nov.
urn:lsid:zoobank.org:act:6AE0ABDC-08C5-47E4-A941-A3DE4234297C
Figs 18C–D, 26B, D–E, 27, 153–154, 175A, 179J, 190; Suppl. file 4: Figs 198B, 200D, 202E

Diagnosis

Pseudonannolene granulata sp. nov. resembles *P. buhrnheimi* by having metazonites granulated (Figs 26B, D, 27, 153, 200D) and epiproct with triangular process (Figs 153B, 202E). Males of *P. granulata* differ by having stipes of gnathochilarium with proximal projections bearing setae (Figs 175A, 198B).

Etymology

The species epithet is derived from the Latin adjective '*granulatus*'; in reference to the granular striations on metazonite of the species.

Material examined

Holotype

BRAZIL • ♂; Rio de Janeiro, Cambuci, Balneário Santa Inês; [-21.541444, -41.931761]; 29 Dec. 2017; L. Ázara, M. Medrano and A.B. Kury leg.; MNRJ.

Paratypes (total: 4 ♂♂, 2 ♀♀, 3 immatures)

BRAZIL • 1 ♀; same collection data as for holotype; MNRJ • 4 ♂♂, 1 ♀, 3 immatures; same collection data as for holotype; MNRJ.

Description

Measurements. 53–55 body rings (1–2 apodous + telson). Males: body length 43.8–64.7 mm; maximum midbody diameter 3.2–4.5 mm. Females: body length 56.5–72.2 mm; maximum midbody diameter 4–5.4 mm.

Color. Body color brownish; head, antennae, and collum darker; prozonites anteriorly greyish; metazonites with a medial band darker and a posterior reddish; legs brownish.

Head. Antennae short, just reaching back to end of ring 5 when extended dorsally; relative antennomere lengths 1<2<3>4>5=6>7. Mandibular cardo with ventral margin narrow. Stipes of gnathochilarium with basal projections bearing setae. Ommatidial cluster well-developed, elliptical; ca 40 ommatidia in 5 rows.

Body rings. Collum with lateral lobes broadly rounded, with ca 6 deep striae, strongly curved ectad (Fig. 153A). Well demarcated constriction between prozonite and metazonite (Figs 26B, 27A, 153, 200D); prozonites smooth; metazonites densely granulated and laterally with transverse striae above ozopore (Figs 26B, 27A, 200D). Anterior sterna in midbody rings subrectangular, without transverse striae (Fig. 175A). Epiproct with a long triangular process (Figs 153B, 202E).

First leg-pair of males. Coxae (***cx***) short (less than half of remaining podomere lengths), subtriangular, with the base arched, densely setose (Fig. 154A); prefemoral process (***prf***) short (less than half of prefemur), subcylindrical, with long setae up to its median region (Fig. 154B); remaining podomeres with setae along the mesal region.

Second leg-pair of males. Coxa (***cx***) large and rounded; penis (***pn***) located at proximal region, rounded, not extended basally (Fig. 154C); prefemur compressed dorsoventrally; remaining podomeres setose.

Gonopods. Gonocoxa (***gcx***) elongated, almost twice as long as telopodite, with the base arched; antero-posteriorly slightly flattened (Fig. 154D–F); with rows of papillae mesally. Seminal groove (***sg***) curved; arising medially on mesal cavity and terminating apically on the seminal apophysis (***sa***); protruded on squamous region of ***sl*** (Fig. 154D). Shoulder (***sh***) long, subtriangular. Telopodite (***tp***) almost as wide as ***gcx***, with deep depression separating from ***sh*** and laterad projection (Fig. 154D); solenomere (***sl***) thin, with apicomesal process (***amp***) subtriangular; ectal process (***ep***) short, subtriangular, separating from ***amp*** by shallow notch; ***sa*** located at mesal portion, slightly curved ectad, visible apically. Internal branch (***ib***) subtriangular, narrow, surrounding basally ***tp*** as a shield; ***ib*** with setae along its entire margin exceeding apically seminal region of ***sl*** (Fig. 154D–F).

Vulvae. As typical for the genus. Bursa square-shaped, glabrous (Fig. 179J); internal and external valvae square-shaped, not acuminated apically; operculum narrow, slightly curved ectad.

Distribution

Known only from the type locality Cambuci, Rio de Janeiro State, Brazil (Fig. 190).

Pseudonannolene insularis sp. nov.

urn:lsid:zoobank.org:act:E22AC8BA-3062-470B-8A34-E2D0B3FF5A6D

Figs 155–156, 164N, 166R, 174D, 179H, 191

Diagnosis

Males of *P. insularis* sp. nov. resemble those of *P. halophila*, *P. maritima*, *P. patagonica*, and *P. sebastianus* by having large and subrectangular coxae on the first leg-pair (Fig. 156A) and suboval penis (Fig. 156C), but differing by having the internal branch with horizontal plate; solenomere with apicomesal process and seminal apophysis elongated (Fig. 156D).

Etymology

The species epithet is derived from the Latin adjective '*insularis*'; in reference to the insular distribution of the species.

Material examined

Holotype

BRAZIL • ♂; São Paulo, Ubatuba, Ilha Prumirim; [-23.385245, -44.944144]; 75 m a.s.l.; 2–10 Sep. 1994; C.F. Vieira and A. Eterovic leg.; IBSP 7888.

Paratypes (total: 1 ♂, 2 ♀♀)

BRAZIL • 1 ♂; same collection data as for holotype; IBSP 7889 • 2 ♀♀; same collection data as for holotype; IBSP 1231.

Referred non-type material (total: 3 ♂♂, 9 ♀♀; 1 immature)

BRAZIL – **São Paulo** • 2 ♀♀; Ubatuba, Ilha Prumirim; [-23.385075, -44.944205]; 75 m a.s.l.; 2–10 Sep. 1994; C.F. Viera and A. Eterovic leg.; IBSP 1231 • 1 ♂, 3 ♀♀; same collection data as for preceding; IBSP 1233 • 2 ♂♂, 4 ♀♀, 1 ♀ immature; same collection data as for preceding; IBSP 1116.

Description

MEASUREMENTS. 62–66 body rings (1 apodous + telson). Males: body length 71.8 mm; maximum midbody diameter 4.9 mm. Females: body length 70.4–79.5 mm; maximum midbody diameter 3.9–5.4 mm.

COLOR. Body color brownish grey; head, antennae, and collum darker; prozonites anteriorly greyish; metazonites with a medial band darker and a posterior lighter; legs brownish.

HEAD. Antennae short (Fig. 164N), just reaching back to end of ring 5 when extended dorsally; relative antennomere lengths 1<2<3>4≈5≈6>7. Mandibular cardo with ventral margin swollen. Ommatidial cluster well-developed, elliptical; ca 30 ommatidia in 4 rows.

BODY RINGS. Collum with lateral lobes rounded, with ca 10 striae, curved ectad posteriorly (Fig. 155A). Very faintly constricted between prozonite and metazonite; prozonites smooth; metazonites laterally with transverse striae up to ozopore in anterior body rings. Anterior sterna in midbody rings subrectangular, without transverse striae (Fig. 174D).

FIRST LEG-PAIR OF MALES. Coxae (***cx***) elongated (as long as the sum of remaining podomere lengths), subrectangular, with the base slightly arched, sparsely setose (Fig. 156A); prefemoral process (***prf***) as long as half of prefemur, subcylindrical, densely setose along the entire ventral region (Fig. 156B); remaining podomeres with setae along the mesal region.

SECOND LEG-PAIR OF MALES. Coxa (***cx***) as long as the sum of remaining podomere lengths, subrectangular; penis (***pn***) located at proximal region, rounded, extended basally (Fig. 156C); prefemur compressed dorsoventrally; remaining podomeres setose.

GONOPODS. Gonocoxa (***gcx***) elongated, almost twice as long as telopodite, expanded medially, with the base not arched; antero-posteriorly strongly flattened (Fig. 156D–F); with rows of papillae mesally. Seminal groove (***sg***) curved; slightly protruded on squamous region of ***sl***, arising medially on mesal cavity and terminating apically on the seminal apophysis (***sa***). Shoulder (***sh***) inconspicuous. Telopodite (***tp***) almost as wide as ***gcx*** (Fig. 156D); solenomere (***sl***) with squamous region expanded laterally and folded apically; apicomesal process (***amp***) elongated, subtriangular; ectal process absent; ***sa*** located at mesal portion, elongated, thickened apically on squamous region. Internal branch (***ib***) shovel-shaped and rounded apically, with large horizontal plate, rounded; setae restricted to the apical region of ***ib*** exceeding seminal region of ***sl*** (Fig. 156D–F).

VULVAE. As typical for the genus. Bursa subtriangular, glabrous (Fig. 179H); internal valve subtriangular, slightly rounded; operculum narrow; external valve subtriangular, covering operculum basally.

Distribution

Known only from the type locality Ilha Prumirim, Ubatuba, São Paulo State, Brazil (Fig. 191).

Pseudonannolene morettii sp. nov.
urn:lsid:zoobank.org:act:C1C691B6-E5F5-4538-A235-0D33B7EFF734
Figs 157–158, 164A, 174C, 179G, 191; Supp. file 4: Figs 197F, 199C

Diagnosis

Males of *P. morettii* sp. nov. resemble those of *P. pusilla* by having short coxae on the first leg-pair with constriction at about midlength (Fig. 158A), but differing by having mentum and stipes of gnathochilarium with long scattered setae (Figs 174C, 197F, 199C); solenomere with seminal apophysis located medially (Fig. 158D).

Etymology

Species named after the beloved grandfather of the first author, Roberto Moretti (1933–2019). Noun in the genitive case.

Material examined

Holotype

BRAZIL • ♂; São Paulo, Mogi das Cruzes, Parque Municipal da Serra do Itapety; [-23.493336, -46.196382]; 881 m a.s.l.; 13–19 Oct. 2003; Equipe Biota leg.; IBSP 2481.

Paratypes (total: 2 ♂♂, 1 ♀)

BRAZIL • 2 ♂♂; same collection data as for holotype; IBSP 2484 • 1 ♀; same collection data as for holotype; IBSP 2486.

Referred non-type material (total: 15 ♂♂, 36 ♀♀; 20 immatures)

BRAZIL – **São Paulo** • 1 ♀, 1 ♂ immature, 1 ♀ immature; same collection data as for holotype; IBSP 2471 • 1 ♀; same collection data as for holotype; IBSP 2464 • 1 ♂, 1 ♀; same collection data as for holotype; IBSP 2461 • 1 ♂ immature; same collection data as for holotype; IBSP 2458 • 1 ♂; same collection data as for holotype; IBSP 2459 • 1 ♂; same collection data as for holotype; IBSP 2485 • 1 ♂; same collection data as for holotype; IBSP 2480 • 1 ♀, 1 ♀ immature; same collection data as for holotype; IBSP 2469 • 1 ♀; same collection data as for holotype; IBSP 2468 • 3 ♀♀, 3 ♂♂ immatures, 3 ♀♀ immatures; same collection data as for holotype; IBSP 2467 • 1 ♀, 1 ♂ immature; same collection data as for holotype; IBSP 2465 • 1 ♀, 1 ♀ immature; same collection data as for holotype; IBSP 2474 • 1 ♀; same collection data as for holotype; IBSP 2457 • 1 ♀; same collection data as for holotype; IBSP 2475 • 1 ♀ immature; same collection data as for holotype; IBSP 2477 • 1 ♀ immature, 1 ♀ immature; same collection data as for holotype; IBSP 2462 • 1 ♀; same collection data as for holotype; IBSP 2473 • 1 ♂; same collection data as for holotype; IBSP 2466 • 1 ♂; same collection data as for holotype; IBSP 2472 • 2 ♂♂; same collection data as for holotype; IBSP 2482 • 1 ♂; same collection data as for holotype; IBSP 2460 • 1 ♀ immature; same collection data as for holotype; IBSP 2479 • 1 ♂, 1 ♀; same collection data as for holotype; IBSP 2476 • 1 ♂ immature; same collection data as for holotype; IBSP 2478 • 1 ♀; same collection data as for holotype; IBSP 2483 • 3 ♂♂, 6 ♀♀; Jundiaí, Parque Municipal da Serra do Japí; [-23.226630, -46.924751]; 871 m a.s.l.; 12–14 Oct. 2017; A.D. Brescovit leg.; IBSP 7893 • 3 ♀♀; same collection data as for preceding; IBSP 7895 • 1 ♂ immature; same collection data as for preceding; IBSP 7894 • 1 ♀; São Paulo, Parque Estadual do Jaraguá; [-23.459535, -46.755378]; 783 m a.s.l.; 14–19 Oct. 2002; Equipe Biota leg.; IBSP 3180 • 1 ♂, 1 immature; same collection data as for preceding; IBSP 2368 • 2 ♀♀; same collection data as for preceding; IBSP 2367 • 1 ♀; same collection data as for preceding; IBSP 2379 • 1 ♀; same collection data as for preceding; IBSP 2372 • 1 ♀; same collection data as for preceding; IBSP 2358 • 1 ♀; same collection data as for preceding; IBSP 2374 • 1 ♂, 1 ♀, 1 immature; same collection data as for preceding; IBSP 2359 • 1 ♀; same collection data as for preceding; IBSP 2360.

Description

Measurements. 55–58 body rings (1–2 apodous + telson). Males: body length 45.4–67.9 mm; maximum midbody diameter 2.8–3.8 mm. Females: body length 45.3–68 mm; maximum midbody diameter 2.8–5 mm.

Color. Body color brownish grey; head and collum darker; prozonites anteriorly greyish; metazonites with a medial band darker and a posterior lighter; antennae and legs brownish.

Head. Antennae short (Fig. 164A), just reaching back to end of ring 5 when extended dorsally; relative antennomere lengths 1<2<3>4=5=6>7. Mandibular cardo with ventral margin narrow. Mentum and stipes of gnathochilarium with scattered long setae (Figs 174C, 197F, 199C). Ommatidial cluster well-developed, elliptical; ca 35 ommatidia in 5 rows.

Body rings. Collum with lateral lobes rounded, with ca 7 shallow striae, curved ectad posteriorly (Fig. 157A). Very faintly constricted between prozonite and metazonite; prozonites smooth; metazonites laterally with transverse striae up to ozopore in anterior body rings. Anterior sterna in midbody rings subrectangular, without transverse striae (Fig. 174C).

First leg-pair of males. Coxae (***cx***) short (less than half of remaining podomere lengths), subtriangular, with the base strongly arched and constricted medially, sparsely setose (Fig. 158A); prefemoral process (***prf***) less than half of prefemur, subcylindrical, curved ectad, densely setose up to its median region (Fig. 158B); remaining podomeres with setae along the mesal region.

Second leg-pair of males. Coxa (***cx***) large and rounded; penis (***pn***) located at proximal region, rounded, not extended basally (Fig. 158C); prefemur compressed dorsoventrally; remaining podomeres setose.

Gonopods. Gonocoxa (***gcx***) longer than twice telopodite, with the base arched; antero-posteriorly strongly flattened (Fig. 158D–F); with rows of papillae mesally. Seminal groove (***sg***) curved; arising medially on mesal cavity and terminating apically on the seminal apophysis (***sa***). Shoulder (***sh***) large, rounded. Telopodite (***tp***) almost as wide as ***gcx*** (Fig. 158D); solenomere (***sl***) with short squamous region; apicomesal process (***amp***) elongated, subtriangular; ectal process absent; ***sa*** located at medial portion, not visible apically. Internal branch (***ib***) narrow and foliaceus; ***ib*** with setae along its entire margin, but only with the apical setae exceeding seminal region of ***sl*** (Fig. 158D–F).

Vulvae. As typical for the genus. Bursa subtriangular, glabrous (Fig. 179G); internal valve subtriangular, slightly rounded; operculum narrow; external valve subtriangular.

Distribution

Known only from the mountain range of Serra do Itapety, a partially preserved area with patches of Atlantic Forest in São Paulo State, Brazil (Fig. 191).

Pseudonannolene nicolau sp. nov.

urn:lsid:zoobank.org:act:69C209DC-C284-46AB-BF9D-8F71D4795DAD

Figs 159–160, 164B, 174E, 179I, 191; Supp. file 4: Figs 216D, 217B, 221C

Diagnosis

Males of *P. nicolau* sp. nov. can be distinguished from those of all other species of *Pseudonannolene* by having apicomesal, medial, and ectal processes on the solenomere (Fig. 160D).

Etymology

The species epithet is a noun in apposition derived from the type locality Fazenda São Nicolau, Cotriguaçu, Mato Grosso, an important area of reforestation and environmental education in the Amazon rainforest.

Material examined

Holotype

BRAZIL • ♂; Mato Grosso, Cotriguaçu, Fazenda São Nicolau; [-9.902508, -58.568103]; 370 m a.s.l.; 9 Dec. 2009; D. Rodrigues leg.; ABAM.

Paratypes (total: 1 ♂, 4 ♀♀, 1 immature)

BRAZIL • 1 ♂, 2 ♀♀, 1 immature; same locality data as for holotype; 8 Dec. 2009; D.A. Batistella leg.; ABAM • 2 ♀♀; same locality data as for holotype; 14 Dec. 2009; L.D. Battirola leg.; ABAM 76.

Referred non-type material (total: 26 ♂♂, 32 ♀♀; 3 immatures)
BRAZIL – **Mato Grosso** • 1 ♂, 2 ♀♀, 1 immature; Cotriguaçu, Fazenda São Nicolau; [-9.902508, -58.568103]; 370 m a.s.l.; 8 Dec. 2009; D.A. Battistela leg.; ABAM 0146 • 1 ♀; same locality data as for preceding; 14 Dec. 2009; L.D. Battirola leg.; ABAM 0147 • 2 ♀♀; same locality data as for preceding; ABAM 0153 • 1 ♀; same locality data as for preceding; 9 Dec. 2009; D. Rodrigues leg.; ABAM 0155 • 4 ♂♂, 2 ♀♀; same locality data as for preceding; 12 Nov. 2010; R.E. Vicente leg.; ABAM 0160 • 1 ♂, 1 ♀; same locality data as for preceding; 13 Nov. 2010; R.E. Vicente leg.; ABAM 0161 • 2 ♂♂, 2 ♀♀, 2 immatures; same locality data as for preceding; 3 Nov. 2016; R.E. Vicente leg.; ABAM 0173 • 15 ♂♂, 17 ♀♀; same locality data as for preceding; 2 Nov. 2014; M. Karam-Gemael leg.; CZUFMT 815 • 3 ♂♂, 4 ♀♀; Aripuanã; [-10.306043, -59.658975]; 214 m a.s.l.; 15 Dec. 2003; C. Strussmann leg.; CZUFMT 831.

Description

Measurements. 55–61 body rings (1 apodous + telson). Males: body length 65–71.5 mm; maximum midbody diameter 3.1–4.5 mm. Females: body length 68.4–78.5 mm; maximum midbody diameter 3.9–5.5 mm.

Color. Body color brownish grey; head, antennae, and collum darker; prozonites anteriorly greyish; metazonites with a medial band darker and a posterior lighter; legs brownish.

Head. Antennae short (Fig. 164B), just reaching back to end of ring 5 when extended dorsally; antennomeres elongated; relative antennomere lengths 1<2≈3>4>5≈6>7. Mandibular cardo with ventral margin swollen. Ommatidial cluster well-developed, elliptical; ca 20 ommatidia in 4 rows.

Body rings. Collum with lateral lobes rounded, with ca 12 shallow striae, slightly curved ectad posteriorly (Fig. 159A). Very faintly constricted between prozonite and metazonite; prozonites smooth; metazonites laterally with transverse striae up to ozopore in anterior body rings. Anterior sterna in midbody rings subrectangular, without transverse striae (Fig. 174E).

First leg-pair of males. Coxae (***cx***) elongated (as long as the sum of remaining podomere lengths), subrectangular, with the base arched and expanded, densely setose (Fig. 160A); prefemoral process (***prf***) as long as half of prefemur, subcylindrical, densely setose along the entire ventral region (Fig. 160B); remaining podomeres with setae along the mesal region.

Second leg-pair of males. Coxa (***cx***) large and rounded; penis (***pn***) located at proximal region, rounded, not extended basally (Fig. 160C); prefemur compressed dorsoventrally; remaining podomeres setose.

Gonopods. Gonocoxa (***gcx***) rounded, basally expanded and progressively less wide, with the base arched; antero-posteriorly flattened (Fig. 160D–F); with rows of papillae mesally. Seminal groove (***sg***) curved; arising medially on mesal cavity and terminating apically on the seminal apophysis (***sa***). Shoulder absent. Telopodite (***tp***) almost as wide as ***gcx*** (Figs 160D, 216D, 217B); solenomere (***sl***) with apicomesal process (***amp***) short, subtriangular; medial process (***mp***) present, subtriangular; ectal process (***ep***) elongated, projected ectad; ***sa*** located at medial portion on ***mp***, elongated, visible apically. Internal branch (***ib***) swollen and rounded apically, with large horizontal plate covering entirely trunk of ***tp*** in anal view; setae restricted to the apical region of ***ib*** not exceeding seminal region of ***sl*** (Fig. 160D–F).

Vulvae. As typical for the genus. Bursa clearly subtriangular, glabrous (Fig. 179I); internal valve subtriangular, acuminated apically; operculum narrow, slightly curved ectad; external valve subtriangular, covering operculum basally.

Distribution

Known only from the type locality Fazenda São Nicolau, Cotriguaçu, Mato Grosso State, Brazil (Fig. 191), an important region of international efforts for reforestation in the Amazonian region (see Rodrigues *et al*. 2011, 2019).

Species inquirendae

Because crucial aspects for proper identification such as morphology of the gonopod, first and second leg-pair of males were not described or sufficiently documented in the original descriptions and types poorly preserved, the following species are considered species inquirendae:

Pseudonannolene brevis Silvestri, 1902
Figs 161, 176C, 181

Pseudonannolene brevis Silvestri, 1902: 20.

Pseudonannolene brevis – Brölemann 1909: 86. — Jeekel 2004: 88. — Iniesta & Ferreira 2013c: 79.

Material examined

Syntypes
BRAZIL • 1 ♀; Mato Grosso do Sul, Corumbá, Urucum; [-19.200684, -57.599997]; 20 Oct. 1900; A. Borelli leg.; USNM 2021.

Distribution

Known from the Brazilian state Paraná (without exact location); another record from the literature for Corumbá, Mato Grosso State (Fig. 181).

Comments

According to Sierwald & Reft (2004), the type material of some species described by Silvestri is deposited in American and European museums. In subsequent works, not one reference was made for *Pseudonannolene brevis* or in which museum its types were supposedly deposited (see Viggiani 1973). The male syntypes of *P. brevis* described by (Silvestri 1902) were not found, but through consultations and visits made to some museums one female syntype was found and examined (USNM 2021; see article #73, ICZN) (Fig. 161). The original description of *P. brevis* does not provide illustrations or diagnostic features for the species. Nonetheless, the species clearly belongs to *Pseudonannolene* by having the longitudinal suture on promentum (Fig. 176C).

Pseudonannolene rugosetta Silvestri, 1897
Figs 162, 166I, 176E, 187

Pseudonannolene rugosetta Silvestri, 1897d: 355, fig. 37.

Pseudonannolene rugosetta – Viggiani 1973: 367. — Mauriès 1987: 175, figs 9–10 (redescription of female holotype; longitudinal suture on promentum is omitted in the fig. 9). — Jeekel 2004: 90. — Iniesta & Ferreira 2013a: 92; 2013c: 79.

Material examined

Holotype
FRENCH GUIANA • ♀ [fragmented]; Cayenne; [4.936964, -52.312784]; ISNB.

Distribution

Known only from the type locality Cayenne, French Guiana (Fig. 187).

Comments

Pseudonannolene rugosetta was described by Silvestri (1897d) based on an adult female apparently collected in French Guiana. Mauriès (1987) examined this holotype, confirming its generic position but questioning the doubtful location from the northernmost region of the Amazon basin. To date, this is the northernmost record of the genus, with the closer occurrence only by the troglobitic species *P. spelaea* from Pará State, Brazil. The female holotype of *P. rugosetta* is not sufficiently distinguished from all congeners (Fig. 162). Nonetheless, the species clearly belongs to *Pseudonannolene* by having the longitudinal suture on promentum (Fig. 176E).

Identification key to species of Pseudonannolene

1. Head, trunk, and legs pigmented (non-troglomorphic species) (Fig. 17) 4
– Head, trunk, and legs depigmented (troglomorphic species) (Fig. 18E) 2

2. Solenomere not rounded, without a squamous membrane covering seminal apophysis (Figs 47D, 86D) 3
– Solenomere rounded, with a squamous membrane covering seminal apophysis (Fig. 128D–F) .... ***P. spelaea*** Iniesta & Ferreira, 2013

3. Solenomere square-shaped (Fig. 86D) .... ***P. lundi*** Iniesta & Ferreira, 2015
– Solenomere subtriangular (Fig. 47D) .... ***P. ambuatinga*** Iniesta & Ferreira, 2013

4. Telopodite straight, not curved mesally (Figs 35, 36A, C) 8
– Telopodite strongly curved mesally (Figs 67D, 94D, 150D, 152D) 5

5. First leg-pair of males with subcylindrical prefemoral process (Figs 94B, 150B, 152B) 6
– First leg-pair of males with large and hexagonal-shaped prefemoral process (Fig. 67B) .... ***P. erikae*** Iniesta & Ferreira, 2014

6. Trunk of telopodite not laterad projected (Figs 150D, 152D) 7
– Trunk of telopodite larger and laterad projected (Fig. 94D) ....***P. mesai*** Fontanetti, 2000

7. Gnathochilarium with paired projections in the proximal region of the mentum (Figs 174B, 197E in Supp. file 4) ....***P. bucculenta*** sp. nov.
– Gnathochilarium without paired projections in the mentum (Fig. 175C) ....***P. curvata*** sp. nov.

8. Solenomere without ectal process (Fig. 35C, E) or with ectal process, but not directed horizontally (Fig. 35A) 13
– Solenomere with ectal process directed horizontally (Figs 49D–F, 52E, 61, 75D–F, 144D–F) 9

9. First leg-pair of males with prefemoral process (Figs 52A–B, 75A–B, 144A–B) 10
– First leg-pair of males without prefemoral process (Fig. 49A–B) ...***P. anapophysis*** Fontanetti, 1996

10. Internal branch subtriangular or shovel-shaped, not curved apically (Figs 52E, 61, 144D–F) 11
– Internal branch S-shaped, swollen, and curved apically (Fig. 75D–F) .....***P. inops*** Brölemann, 1929

11. Telopodite as wide as half of gonocoxa in width (Figs 52E, 61) 12
– Telopodite larger than half of gonocoxa in width (Fig. 144D–F) ....***P. xavieri*** Iniesta & Ferreira, 2014

12. Telopodite not swollen basally (Fig. 52E) ....***P. bovei*** Silvestri, 1895
– Telopodite swollen basally (Fig. 61) .... ***P. caulleryi*** Brölemann, 1929

13. Telopodite short, less than half of gonocoxa 16
– Telopodite elongated, longer than half of gonocoxa (Figs 45D–F, 116C–D, 119B–D) 14

14. Internal branch short and enfolding the telopodite basally (Figs 45D, 116C–D) 15
– Internal branch elongated and positioned parallel to the telopodite (Fig. 119D) ....
....***P. scalaris*** Brölemann, 1902

15. Solenomere short and projected laterally (Fig. 116C–D) ....***P. rocana*** Silvestri, 1902
– Solenomere subtriangular, not projected laterally (Fig. 45D–F) ....***P. alegrensis*** Silvestri, 1897

16. Penis rounded, not extended basally (Figs 47C, 49C, 55C) 22
– Penis suboval, extended basally (Figs 31C, 42C, 71C, 90C, 107D, 122C, 156C) 17

17. Internal branch subtriangular, narrow (Figs 42D, 71D, 108C, 122C) 19
– Internal branch shovel-shaped, rounded apically (Fig. 90D, 156D) 18

18. Solenomere with squamous region not expanded laterally, seminal apophysis thickened apically (Fig. 90D) ....***P. maritima*** Schubart, 1949
– Solenomere with squamous region expanded laterally, folded apically, seminal apophysis not thickened apically (Fig. 156D) ....***P. insularis*** sp. nov.

19. Solenomere without ectal process (Figs 71D, 108D, 122D) 20
– Solenomere with rounded ectal process (Fig. 42D) ....***P. albiventris*** Schubart, 1952

20. Gonocoxa elongated, almost twice as long as telopodite (Figs 71E–F, 122E–F) 21
– Gonocoxa short, subtriangular (Fig. 108D) ....***P. patagonica*** Brölemann, 1902

21. Solenomere rounded (Fig. 122D) ....***P. sebastianus*** Brölemann, 1902
– Solenomere subtriangular, not rounded apically (Fig. 71D) ....***P. halophila*** Schubart, 1949

22. Head only with supralabral and labral setae (Supp. file 4: Fig. 194A) 24
– Frontal region of the head densely setose, overlapping the supralabral and labral setae (Supp. file 4: Fig. 194B) 23

23. Solenomere with seminal apophysis located mesally (Fig. 63D) ....***P. centralis*** Silvestri, 1902
– Solenomere with seminal apophysis located ectally (Fig. 99D) ....***P. occidentalis*** Schubart, 1958

24. Gnathochilarium of males without long setae scattered on the mentum and stipes (Supp. file 4: Fig. 199A–B) 26
– Gnathochilarium of males with long setae scattered on the mentum and stipes (Supp. file 4: Fig. 197F) 25

25. Coxae of the first leg-pair of males with a constriction at about midlength (Fig. 158A–B) ....
.... ***P. morettii*** sp. nov.
– Coxae of the first leg-pair of males without a constriction (Fig. 104A–B) ....
....***P. parvula*** Silvestri, 1902

26. Body rings with metazonites smooth, not granulated (Fig. 26A) 28
– Body rings with metazonites granulated (Fig. 26B) 27

27. Gnathochilarium of males without proximal projections bearing setae on the stipes (Fig. 167D) ....***P. buhrnheimi*** Schubart, 1960
– Gnathochilarium of males with proximal projections bearing setae on the stipes (Supp. file 4: Figs 175A, 198B) ....***P. granulata*** sp. nov.

28. Solenomere without medial process (Fig. 36A–C) 29
– Solenomere with medial process (Fig. 160D–F) ....***P. nicolau*** sp. nov.

29. Telopodite without a large projection (Fig. 36A–C) 30
– Telopodite with a large and rounded projection (Fig. 146D) ....***P. alata*** sp. nov.

30. Adults with more than 15 ommatidia (Fig.19D) 31
– Adults with less than 15 ommatidia (Fig. 81A) ....***P. leucomelas*** Schubart, 1947

31. Gonocoxae not largely subcylindrical, without a large shoulder (Fig. 36A) 33
– Gonocoxae largely subcylindrical, with a large shoulder (Figs 84E–F, 135E–F) 32

32. Internal branch shovel-shaped, slightly curved ectad at midlength in anal view (Fig. 135D) ....***P. tricolor*** Brölemann, 1902
– Internal branch subtriangular, not excavated at midlength in anal view (Fig. 84D–E) ....***P. longicornis*** (Porat, 1888)

33. Gnathochilarium of males without glabrous projections on the stipes (Fig. 19E) 34
– Gnathochilarium of males with glabrous projections located proximally on the stipes (Fig. 168D) . ...***P. callipyge*** Brölemann, 1902

34. Internal branch without torsion of 180° in anal view 36
– Internal branch with torsion of 180° in anal view 35

35. Torsion of the internal branch starting only apically, with distal projection directed horizontally (Fig. 69D) ....***P. fontanettiae*** Iniesta & Ferreira, 2014
– Torsion of the internal branch starting at midlength, enlarged apically, with distal projection directed diagonally upwards (Fig. 114D) ....***P. robsoni*** Iniesta & Ferreira, 2014

36. Solenomere with ectal process (Fig. 35A) 40
– Solenomere without ectal process (Fig. 35C, E) 37

37. Telopodite and internal branch elongated (Figs 79D, 88D, 112D) 38
– Telopodite and internal branch short, less than ⅓ of gonocoxa in length) (Fig. 141D–F) ....***P. urbica*** Schubart, 1945

38. Coxae of the first leg-pair of males with constriction at about midlength (Figs 79A, 112A) 39
– Coxae of the first leg-pair of males without constriction at about midlength (Fig. 88A) ....***P. magna*** Udulutsch & Pietrobon, 2003

39. First leg-pair of males with prefemoral process wide, about half the width of prefemur (Fig. 79B) . ...***P. leucocephalus*** Schubart, 1944
– First leg-pair of males with prefemoral process short, less than half of prefemur (Fig. 112B) ....***P. pusilla*** Silvestri, 1895

40. Solenomere with ectal process subtriangular (Figs 35A, 36A–C) 42
– Solenomere with ectal process spiniform (Figs 110D, 148D) 41

41. Internal branch shovel-shaped, with horizontal plate (Fig. 110D–F) ....***P. paulista*** Brölemann, 1902
– Internal branch subtriangular, without horizontal plate (Fig. 148D–F) ....***P. aurea*** sp. nov.

42. Internal branch subtriangular (Fig. 35A) 47
– Internal branch shovel-shaped (Figs 50E, 102D, 130D, 131C, 133D) 43

43. Solenomere with ectal process rounded (Figs 102D, 133D) or inconspicuous (Fig. 131C) 45
– Solenomere with ectal process subtriangular (Figs 50E, 130D) 44

44. Gonocoxae subrectangular (Fig. 50E) ....***P. borelli*** Silvestri, 1895
– Gonocoxae subtriangular, basally expanded and progressively less wide (Fig. 130D–F) ....***P. strinatii*** Mauriès, 1974

45. Internal branch with a horizontal plate basally (Figs 102D, 133D) 46
– Internal branch without a horizontal plate basally (Fig. 131D) ....***P. sulcatula*** Silvestri, 1895

46. Solenomere with seminal apophysis long, thickened apically (Fig. 102D, F) ....***P. ophiiulus*** Schubart, 1944
– Solenomere with seminal apophysis short, not thickened apically (Fig. 133D, F) ....***P. tocaiensis*** Fontanetti, 1996

47. Solenomere with ectal process short or as long as apicomesal process (Figs 35A, 36A–C) 48
– Solenomere with ectal process exceeding in length the rounded apicomesal process (Fig. 118D) .... ***P. rolamossa*** Iniesta & Ferreira, 2013

48. Solenomere with apicomesal and ectal processes visible apically (Figs 35A, 36A–C) 49
– Solenomere with apicomesal and ectal processes short, almost not visible apically (Fig. 126D) ....***P. silvestris*** Schubart, 1944

49. Internal branch without a rounded projection directed ectad (Figs 77F, 92D, 96F, 124F) 53
– Internal branch with a rounded projection directed ectad (Figs 57F, 65F, 73F, 137D–F) 50

50. Body color brownish grey (Figs 56, 64, 136) 51
– Body with head and trunk light ocher color (Fig. 72) ....***P. imbirensis*** Fontanetti, 1996

51. Penis rounded, subelliptical (Figs 57C, 137C) 52
– Penis circle-shaped (Fig. 65C) ....***P. curtipes*** Schubart, 1960

52. Internal branch with a short torsion apically (Fig. 137D) .... ***P. typica*** Silvestri, 1895
– Internal branch without a torsion apically (Fig. 57D) ....***P. caatinga*** Iniesta & Ferreira, 2014

53. Internal branch narrow, but not foliaceus (Figs 77F, 92D, 96F) 54
– Internal branch foliaceus (Fig. 124F) ....***P. segmentata*** Silvestri, 1895

54. Internal branch not curved ectad (Fig. 77F, 92D) 55
– Internal branch curved ectad (Fig. 96F) ....***P. microzoporus*** Mauriès, 1987

55. Gonocoxae subrectangular (Fig. 77E–F) ....***P. leopoldoi*** Iniesta & Ferreira, 2014
– Gonocoxae subtriangular, basally expanded and progressively less wide (Fig. 92C–D) ....***P. meridionalis*** Silvestri, 1902

Discussion

Cladistic relationships of Pseudonannolenidae

Although the focus of our analysis was testing the monophyly of *Pseudonannolene*, the topologies recovered by us corroborates the family relationships suggested by Jeekel (1985), Mauriès (1987) and Hoffman & Flórez (1995). The clade Cambalomminae + Pseudonannoleninae (*Pseudonannolene* + *Epinannolene*) is recovered in all topologies based mainly on male characters, for instance the antero-posteriorly flattened gonocoxa, solenomere thinner than telopodite, and apicomesal process of telopodite visible apically. The internal branch of the gonopod appears in our analysis as homoplastic in *Phallorthus* (Physiostreptinae) and Cambalomminae + Pseudonannoleninae, suggesting either a single origin at the basal split of Pseudonannolenidae and a reversion in the remaining genera of Physiostreptinae, or independent origins in *Phallorthus* and Cambalomminae + Pseudonannoleninae.

Since Silvestri (1895a) proposed Pseudonannolenidae, the internal classification of the family has in part relied on the morphology of the gnathochilarium (see Hoffman 1980; Jeekel 1985). The topology (Physiostreptinae + (Cambalomminae + Pseudonannoleninae)) is strongly supported by the morphological variation in the promentum and mentum (Fig. 10). The clade *Holopodostreptus braueri* + *Phallorthus colombianus* (Physiostreptinae) is recovered based on the loss of the promentum, which is here regarded as a putative synapomorphy, as observed in some members of Cambalopsidae (for instance, *Chonecambala crassicauda* Mauriès & Enghoff, 1990) and convergent in Spirostreptidea Brandt, 1833 (Hoffman 1980; Krabbe 1982; Enghoff *et al.* 2015). The monotypic subfamily Cambalomminae is characterized by promentum fused to the mentum, which has also been observed in some species of Cambalidae (e.g., *Leiodere* Loomis, 1938) and Cambalopsidae (e.g., *Trachyjulus* Peters, 1864), while in Pseudonannoleninae (*Pseudonannolene* + *Epinannolene*) the promentum is present with a transverse suture separating it from the mentum. In *Pseudonannolene*, the presence of a longitudinal suture separating the promentum into two equal halves is recovered as a single non-sexual synapomorphy (Figs 8, 10).

Taxonomy and monophyly of *Pseudonannolene*

Part of the problem with the taxonomy of Cambalidea is due to some characteristics of the anterior (eighth leg-pair) and posterior (ninth leg-pair) gonopods. In Pseudonannolenidae, the posterior gonopods are reduced to tiny vestiges and are useless for species identifications (Hoffman 1980; Jeekel 1985; Hoffman & Florez 1995; Enghoff *et al.* 2015; Iniesta *et al.* 2020). The first illustrations of anterior gonopods in Pseudonannolenidae were published for *Pseudonannolene bovei* and *P. typica* by Silvestri (1895a: figs 8–9). Subsequently, Brölemann (1929) complemented the description of the gonopods of some members of *Pseudonannolene*, illustrating structures hitherto insufficiently explored, such as the papillae and the gonocoxal mesal cavities. Although these authors have differentiated the gonopods among the Pseudonannolenidae genera, the correspondences assumed for the gonopodal parts are based solely on topological correspondences, since the homology of these structures was only ascertained recently, in a morphology-based phylogeny conducted by Iniesta *et al*. (2020).

Many characters used in our analysis are in the gonopods (40 out of a total of 91 characters), with important synapomorphies in the telopodite and internal branch. Therefore, most clades recovered from our data are supported by male characters (Fig. 8). Schubart (1949, 1960) suggested that the presence of processes on the solenomere and the proportion of the telopodite in relation to the gonocoxa are relevant to resolve the relationships among some groups of species. As far as can be seen from the available material, three processes are observed on the solenomere: apicomesal, ectal, and medial (Figs 35–36, 217). The apicomesal process is present in all terminals of the clade Cambalomminae + Pseudonannoleninae, except the clade *P. spelaea* + *P. leucomelas*, in which the process has been secondarily lost (char. 74:1). The ectal process arises independently at least four times in *Pseudonannolene*, being recovered in the clades 19 and 37 and in the terminals *P. albiventris* and *P. nicolau* sp. nov. (Fig. 11) (char. 76:1). In *P. nicolau* the medial process is recovered as autapomorphic with the seminal apophysis displaced medially (Fig. 217B) (char. 75:1).

In the first leg-pair, the character states corresponding to the podomeres and prefemoral process are highly homoplastic, with several independent origins and reversions within *Pseudonannolene*. Most *Pseudonannolene* species can be artificially grouped based on the shape of the coxae (see Brölemann 1902a; Schubart 1949, 1952). The subrectangular shape (char. 28:2) appears independently in *P. occidentalis* and in clade 28; the subtriangular shape (char. 28:1) is observed in *Holopodostreptus braueri* + *Phallorthus colombianus*, *Cambalomma laevis*, and in most species of *Pseudonannolene*, while the semicircular shape (char. 28:0) occurs in *Epinannolene* and in *P. anapophysis* (Fig. 203). The presence of a prefemoral process (char. 36:1), suggested by Fontanetti (2002) as an important diagnostic character of the genus, is recovered as a synapomorphy of Choctellidae + Pseudonannolenidae and reversed in *P. anapophysis* (Fig. 206A).

Regarding the penis, Enghoff (1981, 1991, 1996) highlighted the cladistic importance of the structure in putative groups within Julida. Wesener *et al.* (2008) and Iniesta *et al.* (2020) tested the information content of the penial characters of Pachybolini (Spirobolida, Pachybolidae) and Pseudonannolenidae, respectively. Although the morphology of the penis is poorly known for most *Pseudonannolene* species (see Brölemann 1929; Schubart 1949, 1952), our results suggest that the partial fusion of the penial bases (char. 47:1) is synapomorphic for *Pseudonannolene* (Fig. 31C, F), while the presence of a basal extension (char. 48:1) is synapomorphic for clade 30, which is composed of species that are mostly distributed on the coasts of Argentina and Brazil.

A reduction in the number of ommatidia is a convergent trait in obligatory cave-dwelling species that have exclusively subterranean populations (Shear 1969, 1973a, 1973b; Culver & Shear 2012; Liu *et al.* 2017; Deharveng & Bedos 2018; Enghoff & Reboleira 2020). For instance, the central-American species *Orthoporus kiemi* Loomis, 1962 and the Moroccan species *Odontostreptus fadriquei* Enghoff & Reboleira, 2020 (Spirostreptidae) were characterized according to their reduced number of ommatidia (Loomis 1962; Krabbe 1982; Enghoff & Reboleira 2020). The shape of the ommatidial cluster has also been used in the systematics of Spirostreptida (see Jeekel 1963). It is elliptical to subtriangular (in Spirostreptidae, for instance) or in a single row with 4–8 ommatidia (in Cambalidae).

Although some authors have argued in favor of inclusion of homoplastic characters (convergent apomorphic characters states that correspond to adaptations to the cave environment, for instance) in cladistics analyses (Marques & Gnaspini 2001), Desutter-Grandcolas *et al*. (2003) recommend the evaluation directly in the outcome of analysis including these characters instead of excluding those associated with troglomorphism (specialized morphological trait in obligatory cave-dwelling species). In our analysis, the reduction in the number of ommatidia is homoplastic for the clade *P. leucomelas* + *P. spelaea* and for the outgroup *Cambala speobia* (in blue, Fig. 12). Although *P. spelaea* and *C. speobia* are cave-dwelling, *P. leucomelas* occurs in agricultural areas, suggesting that the loss of ommatidia is not a direct result of their subterranean habit. Therefore, this character state cannot be entirely regarded as a troglomorphism in species of *Pseudonannolene*.

The use of body measurements and proportions has been widely accepted in morphology-based analyses for some millipede taxa (Bueno-Villegas *et al.* 2008; Wesener *et al.* 2008; Wesener & VandenSpiegel 2009; Pimvichai *et al.* 2010; Pena-Barbosa *et al.* 2013; Liu *et al.* 2017; Bouzan *et al.* 2019b, 2021; Rodrigues *et al.* 2019). Additionally, characters of the antennae, midbody legs, and gnathochilarium have been important to ascertain relationships within Spirostreptida (Hoffman *et al.* 1996, 2002; Iniesta *et al.* 2020). In our analysis, some of the internal clades of *Pseudonannolene* were only resolved when continuous characters were added. According to Koch *et al.* (2014), the implementation of continuous characters in phylogenetic analyses, such as those suggested by Goloboff *et al.* (2006) and Goloboff & Catalano (2010, 2016), recovers more inclusive clades with better resolution. The consensus of our analysis using only discrete characters is congruent with the consensus obtained using the concatenated dataset (discrete + continuous), with an SPR-distance value of 0.9696 (0 = maximum incongruity; 1 = identical topologies using only discrete characters or discrete + continuous characters) and a great number of shared clades, suggesting that these continuous characters are informative (Fig. 9).

In our study, new characters from the gnathochilarium are described for males of *Pseudonannolene*. In *P. bucculenta* sp. nov. the mentum has proximal projections bearing setae (in purple, Fig. 197E). This condition is apparently analogous to the condition observed in some species of *Coromus* Gervais, 1847 (Polydesmida: Oxydesmidae) (Hoffman 1990), for instance. *Pseudonannolene morettii* sp. nov. and *P. parvula* have long and spiniform setae on the mentum and stipes (in yellow, Fig. 197F), whereas *P. granulata* sp. nov. and *P. callipyge* have proximal and rounded projections bearing setae on the stipes (Fig. 198B). These two character states seem to have arisen independently in both species.

Patterns of distribution and biogeography

According to the biogeographical hypothesis postulated by Jeekel (1985), Pseudonannolenidae originated in southern South America. Subsequently, there were migration events toward northern South America, Central America, and the West Indies. All those regions are biodiversity hotspots of the family harboring at least 6 of 7 known genera (Jeekel 2004; Iniesta *et al.* 2020). The distribution pattern of *Pseudonannolene* also suggests that the first lineages to diverge within genus were distributed in the southern South America, with the first vicariant event obtained in the basal nodes (Fig. 14A–B).

The biogeographic history of *Pseudonannolene* is complex with multiple dispersal and founder events. Even though the event-based method used to infer the biogeographic history of the genus is not time-calibrated, some important points have been brought forth: *P. scalaris*, *P. rocana*, and *P. alegrensis* are the first taxa to branch out in our topologies and are restricted to the southern portion of the Chacoan subregion, specifically the Pampas and Platina Plain (Fig. 15). These species present plesiomorphic gonopodal features according to our cladistic results, such as elongated telopodites compared to the gonocoxae and a short squamous region of the solenomere. It is likely that the current diversity of the genus and its distribution pattern in the Chacoan subregion can be explained by assuming vicariance events in the first nodes of the recovered topology and founder events in most of the more inclusive clades (Fig. 14A–B). Surprisingly, the second founder event recovered in our analysis resulted in the dichotomy between *P. alegrensis* (the most northern species among those with elongated telopodites) and the strongly supported clade 11 (Fig. 15).

The distributional partitioning of the Pseudonannoleninae genera has been widely discussed (Mauriès 1974, 1987; Hoffman 1984; Iniesta *et al.* 2020), with *Epinannolene* widespread across the Amazon River basin and *Pseudonannolene* occurring in the southern regions of the basin. The distribution of clade 15 is remarkable within *Pseudonannolene* with occurrences points in the Xingu-Tapajós Province. This clade is composed of species with highly restricted distributions, which are endemic to the Amazon region: *P. leucomelas* has been recorded only from marginal forests in the Araguaia River, while the troglomorphic species *P. spelaea* is restricted to the iron ore caves in the Carajás region. One of the unique records of *Pseudonannolene* in the north region of the basin is *P. spelaea* (Fig. 16A) (the other record is for *P. rugosetta* in French Guiana), indicating that the restricted distribution of this species is related to presumed relics of an ancient distributional pattern or lineage of clade 15. Additionally, this relictual distribution in the Amazon region may be support the hypothesis of refuges created by climatic oscillation during the Pleistocene, which promoted allopatric speciation.

Most of the current distribution patterns of the clades that compose *Pseudonannolene* and their supposed ancestral distributions can be explained by the existence of a mosaic of mountain ranges in the biogeographical provinces of the Araucaria, Atlantic, and Parana Forests (Fig. 16B–F). Clade 38, composed of species with granulated metazonites and an epiproct with a subtriangular process, is geographically limited by the Serra Mantiqueira and Serra do Mar in the southern portion, and by the Serra do Caparaó in the northern portion (Fig. 16B). In the case of clade 25, which is supported by one synapomorphy, a strongly curved telopodite, the Serra Geral seems to act as a geographic barrier for the first terminal that diverges within this clade, *P. curvata* sp. nov. The remaining species, *P. mesai*, *P. erikae*, and *P. bucculenta* sp. nov., are partially limited by Serra da Cantareira and Serra da Mantiqueira in the northern region (Fig. 16E).

One of the remarkable distribution patterns within *Pseudonannolene* is that of clade 29. The clade is restricted to but widely distributed within the islands of the Atlantic Forest and in the coastal region of southeastern Brazil. Except for *P. albiventris*, which occurs in the interior region of the state of São Paulo up to Serra de São Pedro, the remaining species are geographically isolated by the large mountain ranges of Serra da Paranapiacaba and Serra da Bocaina, and mainly by the Serra do Mar (Fig. 16D). According to multiple biogeographic approaches, the region of Serra do Mar has been important in determining patterns of distribution of vertebrates and invertebrates in the Atlantic Forest (Silva *et al.* 2004; Pinto-da-Rocha *et al.* 2005; Yamaguti *et al.* 2009; Bornschein *et al.* 2016; Barcia *et al.* 2020; Barbo *et al.* 2021; Batista *et al.* 2021), suggesting that the mountain range could be acting as a diversification route rather than a barrier to the species of *Pseudonannolene*. The occurrence of *P. halophila*, *P. sebastianus*, and *P. maritima* in the Alcatrazes archipelago and adjacent islands also suggests that their populations have been somewhat isolated from each other and from the continent since the last land bridge formed during the Last Glacial Maximum (around 85 000–15 000 years ago) (see Martin *et al.* 1986; Fleming *et al.* 1998). A similar scenario can be inferred to for *P. alata* sp. nov. and *P. insularis* sp. nov., which are restricted to islands in the southeastern Brazil (Fig. 16D).

Despite our efforts, this study is only a first step towards a more comprehensive understanding of the Neotropical genus *Pseudonannolene*. Here, we provide a systematic reassessment of the genus, with cladistic and biogeographical analyses and a taxonomic review. The genus is now composed of 56 species, most of which occur in the Chacoan subregion. The cladistic analysis confirms that *Pseudonannolene* is monophyletic, supported by the presence of a longitudinal suture on the promentum as an exclusive synapomorphy, and that the genus is recovered as sister-group of *Epinannolene* (Pseudonannoleninae), based on male synapomorphies. The biogeographical reconstructions showed that vicariance events occurred more frequently in the deep clades of *Pseudonannolene*, with the earliest species recovered in our topologies restricted to the southern portion of the Chacoan subregion, as the Pampas and Platina Plain. Further studies, especially if including molecular markers, and concatenated with morphological approaches, are still needed to better resolve the phylogeny of the genus.

Acknowledgments

We are most grateful to all curators and curatorial assistants from the institutions named in the methods section for their hospitality during the visits and for lending the specimens examined. Special thanks to Adriano B. Kury and Carla Barros (MNRJ), Amazonas Chagas-Jr (UFMT), Leandro D. Battirola (UFMT), Ricardo Pinto-da-Rocha (MZSP), and Rodrigo L. Ferreira (ISLA) for lending a bulk of specimens continuously analyzed by us during this project. Dione Seripierri (MZSP Library service) and A. Chagas-Jr kindly helped us to clarify some ambiguities in distributional data of some species. Numerous colleagues kindly made literature available to us for years even before the start of this study: Drs Henrik Enghoff (NHMD), Petra Sierwald (FMNH), Sergei I. Golovatch (Institute of Problems for Ecology and Evolution, RAS, Russia), and William Shear (Hampden-Sydney College, Hampden-Sydney, USA). Thanks to Ross Thomas and Sionei Bonatto for the language review; to Silvio S. Nihei

(USP), Ricardo Ott (FZB-RS), and L.D. Battirola for their suggestions; to A.B. Kury, Marcus P. Oliveira and Cláudio A.R. Souza for sending us photos of specimens; to Beatriz Mauricio from the Laboratory de Biologia Celular, Instituto Butantan, for providing access to the scanning microscope; to the Willi Hennig Society for allowing the use of the software TNT. We are most obliged to the anonymous reviewers and to Sergei I. Golovatch, Henrik Enghoff, and Nesrine Akkari (Naturhistorisches Museum Wien, Austria) for their valuable comments and corrections, which helped us to improve the manuscript. A special thanks to Pepe Fernández for all attention with our manuscript. We are in debt with all colleagues who contributed in various ways with our study. This work was supported by the São Paulo Research Foundation (FAPESP) grant to L.F.M. Iniesta (number 2016/24248-0) and by the Research Internships Abroad (BEPE/ FAPESP, number 2018/25864-1). R.S. Bouzan was supported by grant 2018/00103-8 (FAPESP), and A.D. Brescovit by the grant CNPq (303903/20019-8). This study was financed in part by the Coordenação de Aperfeiçoamento de Pessoal de Nível Superior–Brasil (CAPES–Finance Code 001).

Fig. 1. *Pseudonannolene tricolor* Brölemann, 1902 (IBSP 2031) in lateral view.

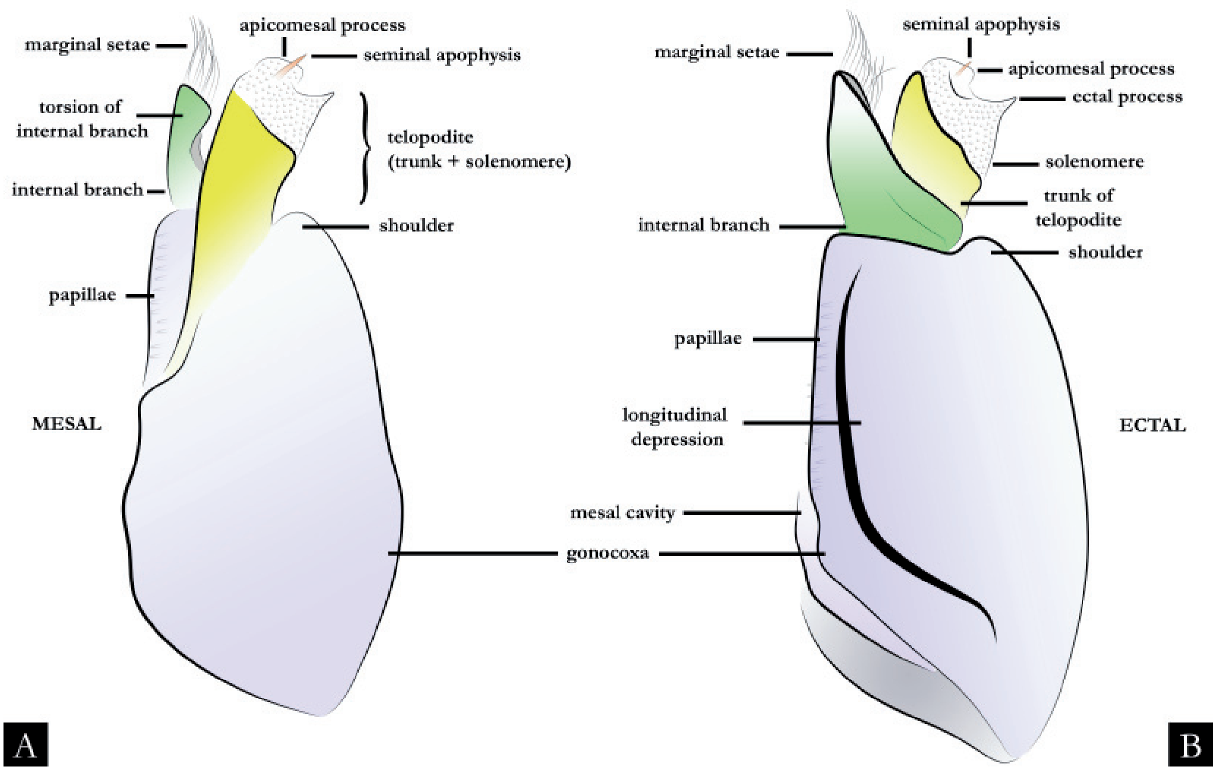

Fig. 2. Schematic drawing of the gonopods of *Pseudonannolene* Silvestre, 1895. **A**. Right gonopod in oral view. **B**. Left gonopod in anal view.

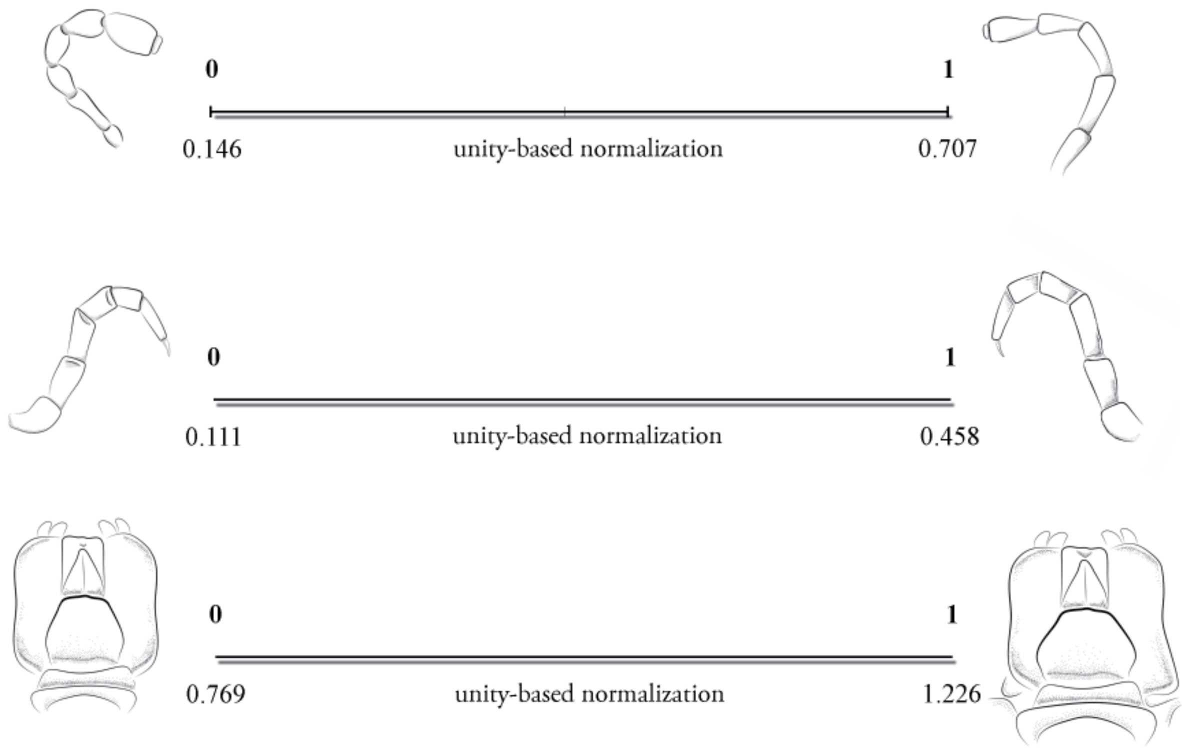

Fig. 3. Transformation of the continuous characters of antennae, midleg pairs, and shape of mentum (chars. 1–3) by unity-based normalization (0–1).

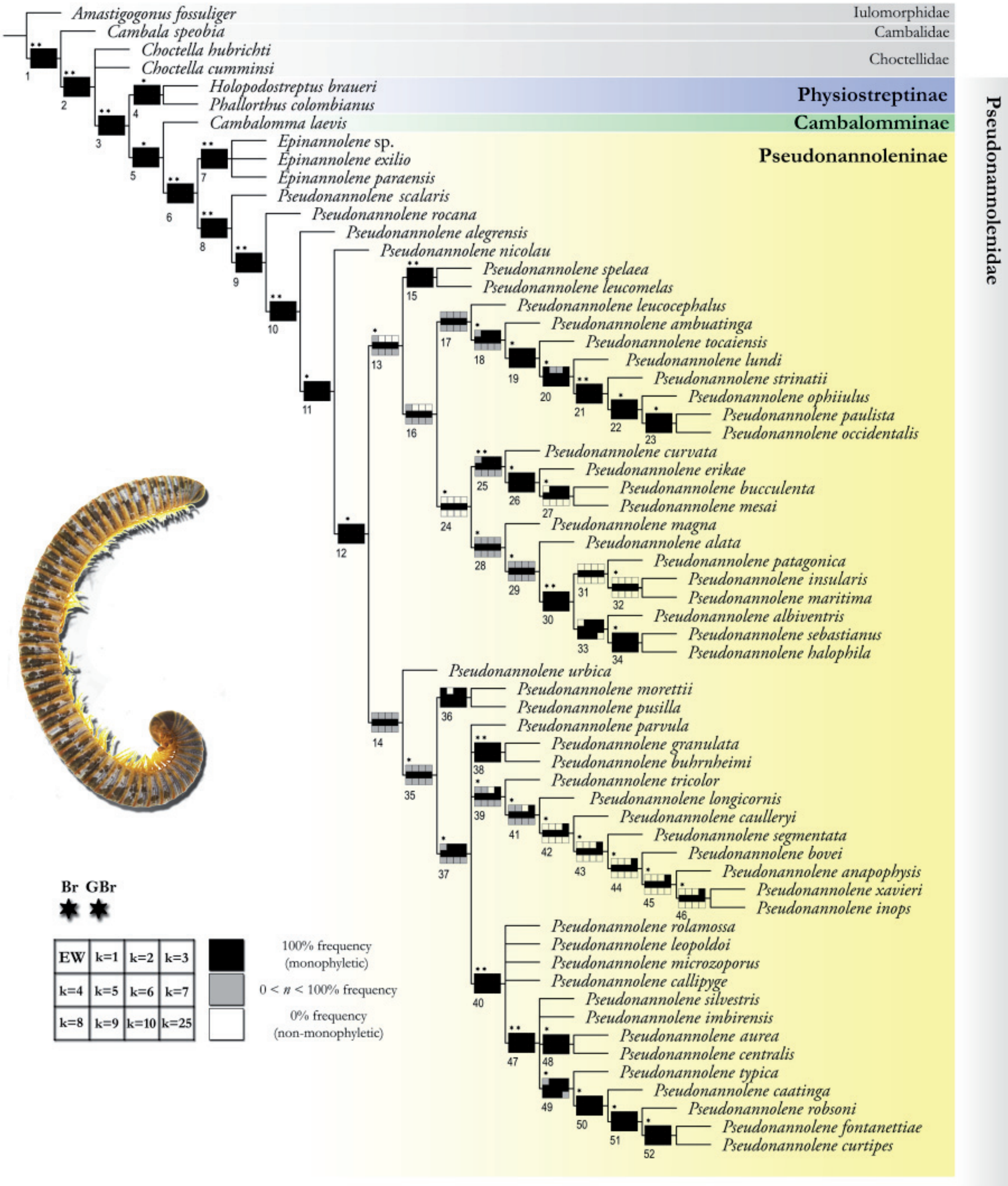

Fig. 4. Strict consensus of 27 equally parsimonious trees under implied weighting ($k = 4–7$). Clades with the sensitivity to different k values are represented by the frequency on the Navajo–rugs. Clades with asterisk have values of Bremer relative [Br] above 50 and Goodman-Bremer [GBr] of 0.1.

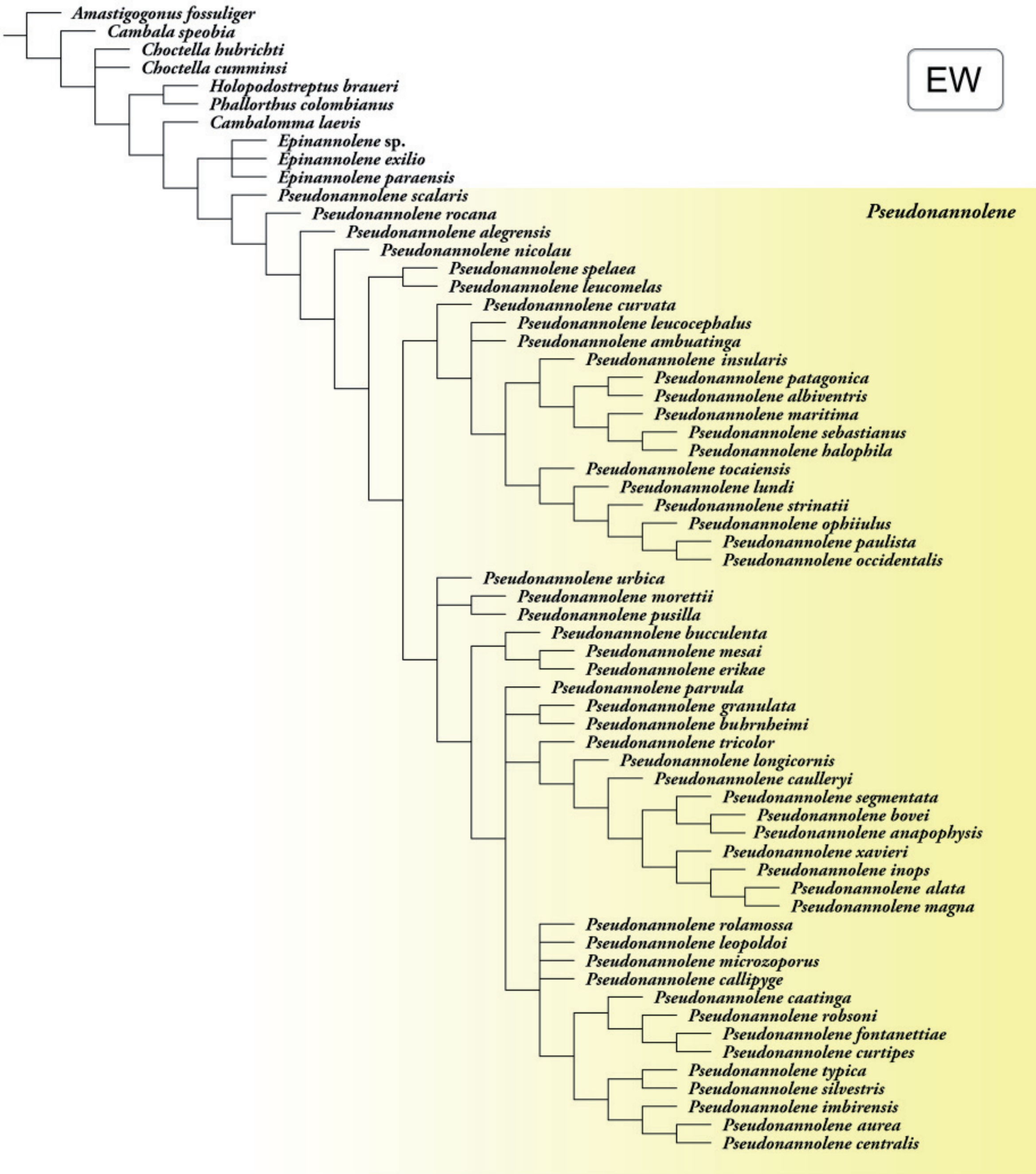

Fig. 5. Strict consensus of 22 equally parsimonious trees with equal weights.

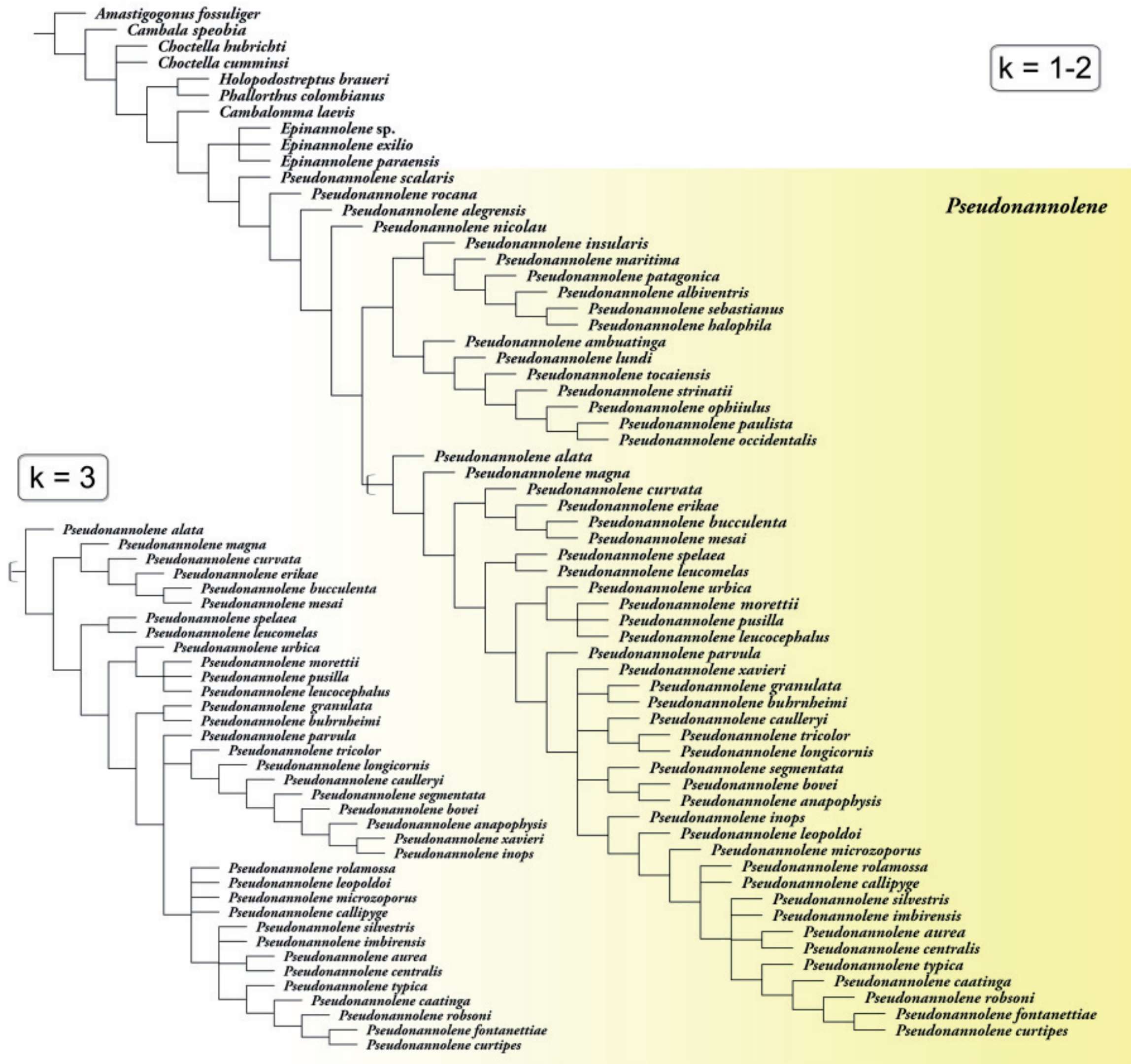

Fig. 6. Strict consensus of equally parsimonious trees under implied weighting (*k* = 1–2 and 3).

Fig. 7. Strict consensus of equally parsimonious trees under implied weighting (*k* = 8–10 and 25).

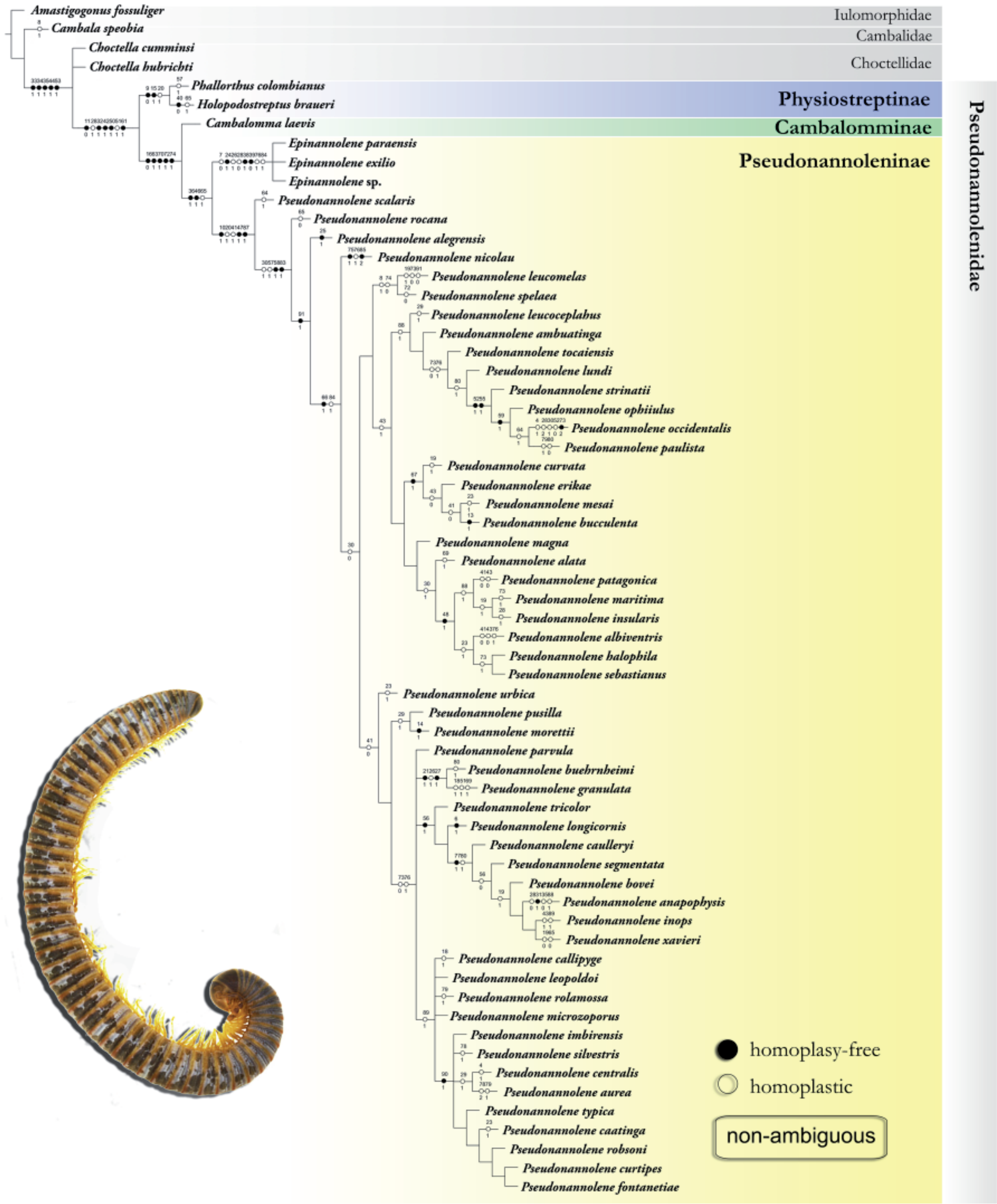

Fig. 8. Strict consensus with optimization of the synapomorphies recovered in all resulting topologies under implied weighting (k = 4–7). Only discrete characters are represented.

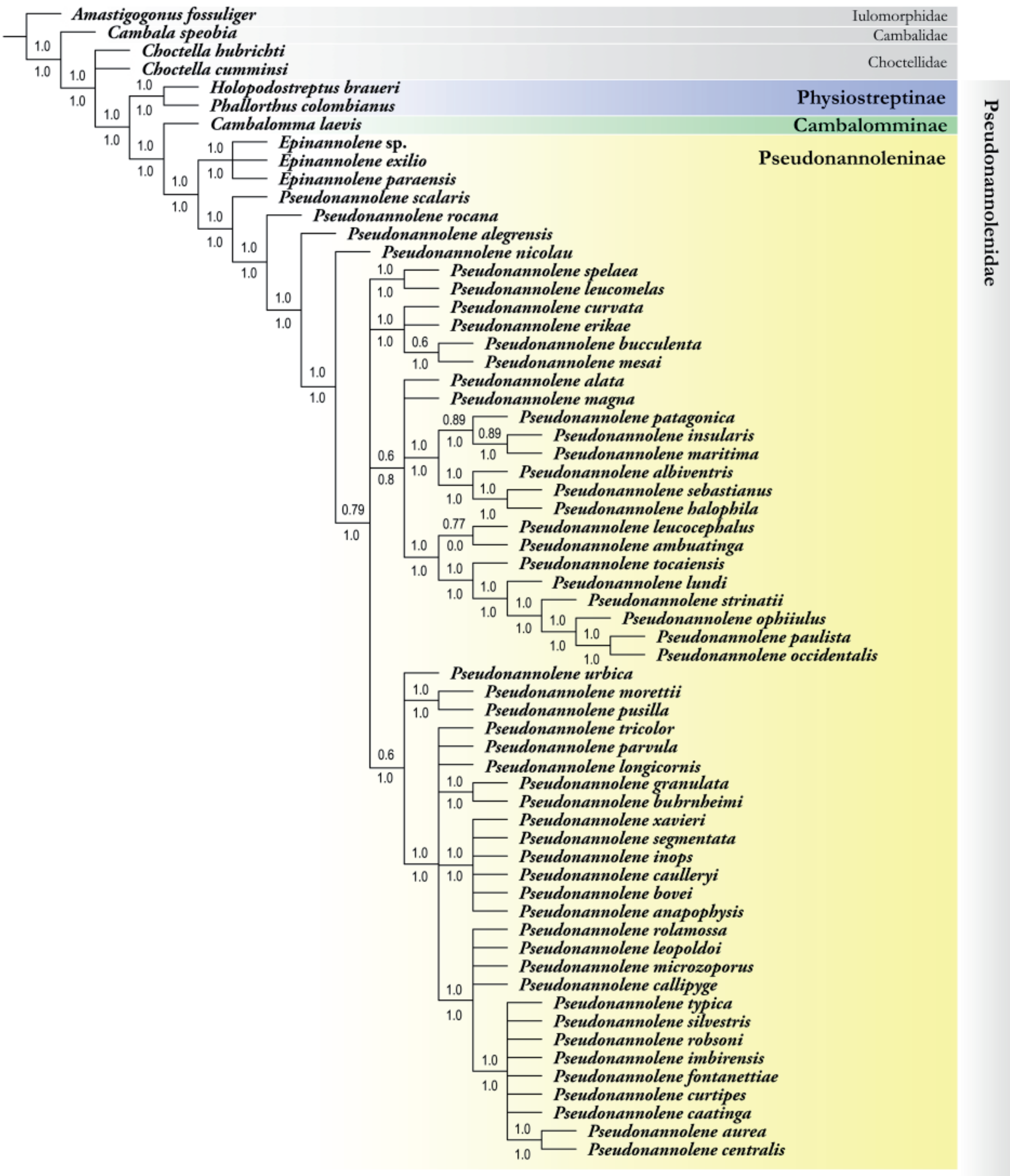

Fig. 9. Majority rule consensus of equally parsimonious trees under implied weighting (k = 4–7) and recovered only by discrete characters. The values indicated above each clade refer to the frequency of the clade on the majority rule consensus, and the values below refer to the frequency of clades in comparative analysis.

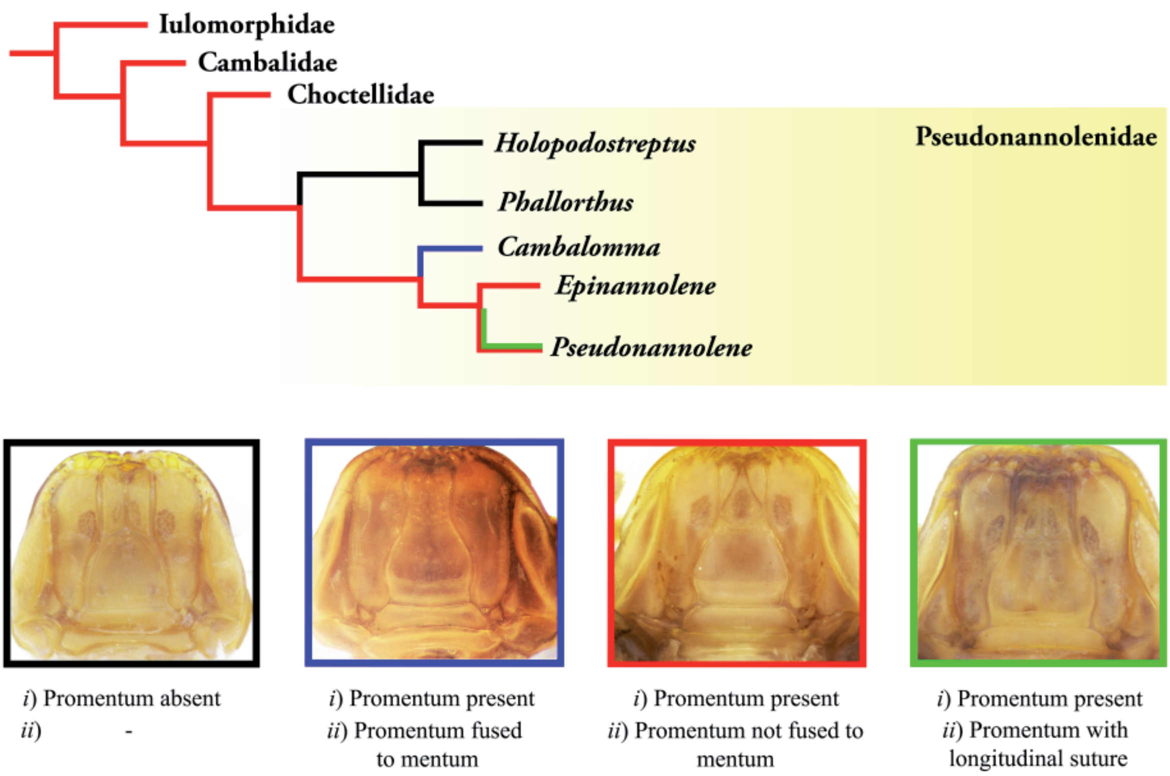

Fig. 10. Morphology of gnathochilarium based on the tree topology summarized under implied weighting (k = 4–7). Images of gnathochilarium: black = *Holopodostreptus braueri* Carl, 1918 (MNRJ); blue = *Cambalomma laevis* Loomis, 1941 (MCZ); red = *Epinannolene* sp. (ICN); green = *Pseudonannolene maritima* Schubart, 1949 (IBSP 1176).

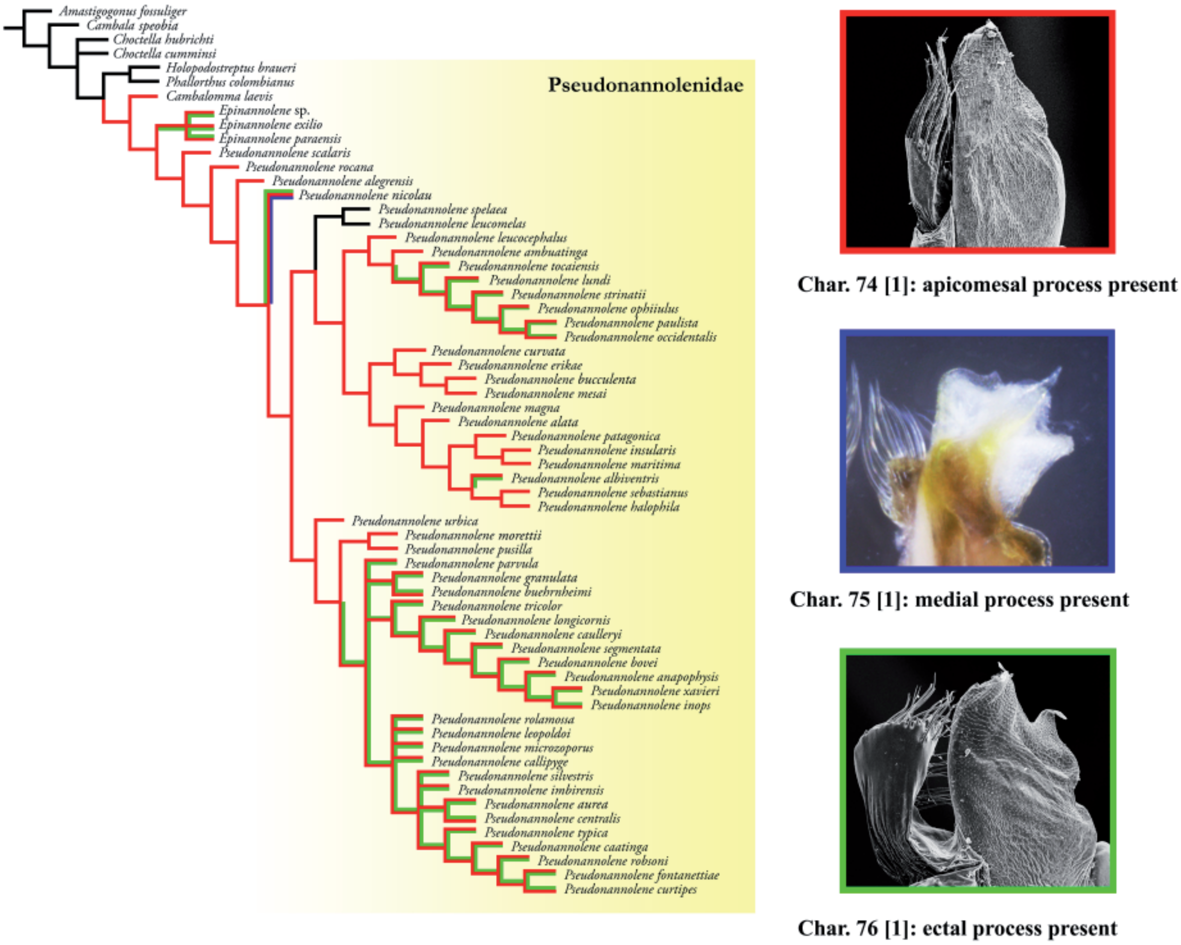

Fig. 11. Evolution of the processes on solenomere. Mapping on the strict consensus of 27 equally parsimonious trees under implied weighting (k = 4–7). Images of solenomere: red = *Pseudonannolene mesai* Fontanetti, 2000 (IBSP 816); blue = *P. nicolau* sp. nov.; green = *P. caatinga* Iniesta & Ferreira, 2014 (IBSP 2166).

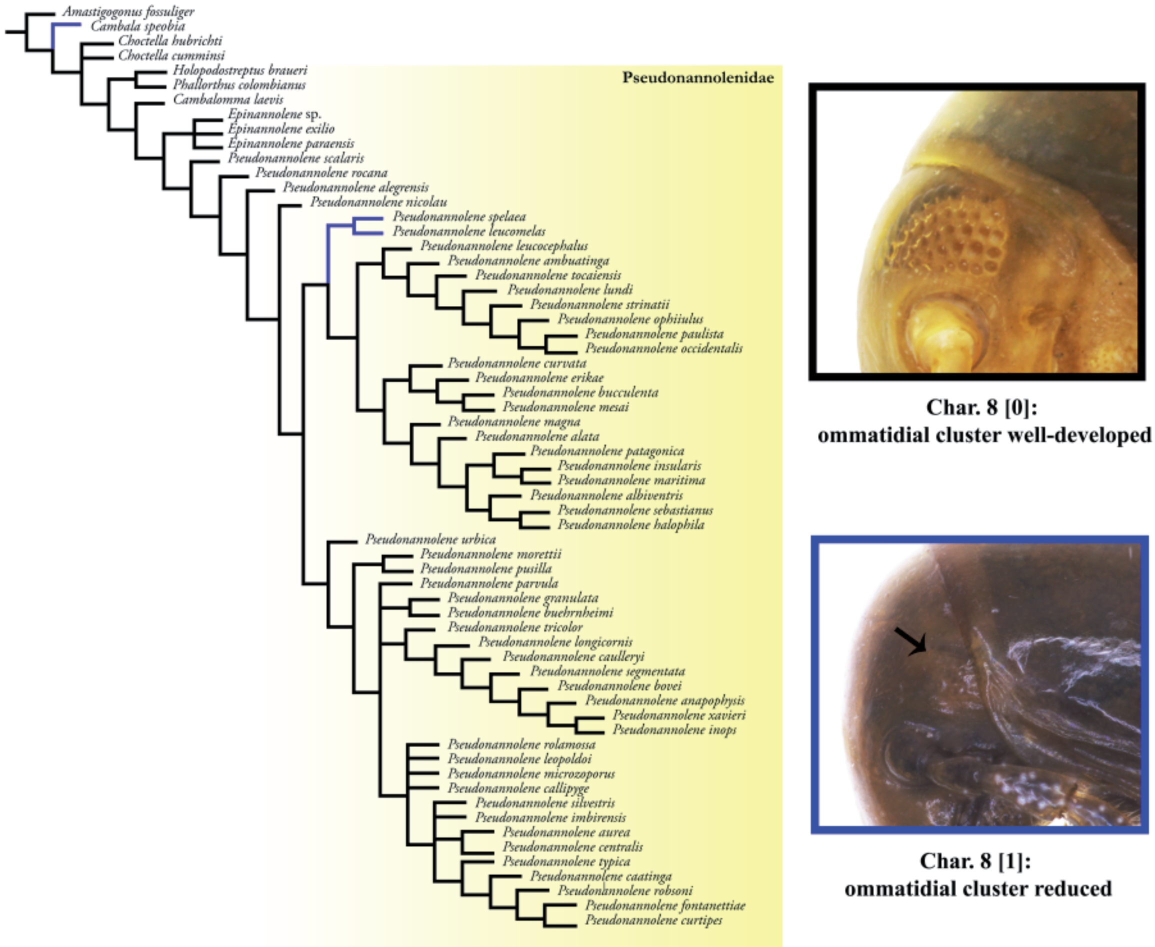

Fig. 12. Evolution of ommatidial cluster. Mapping on the strict consensus of 27 equally parsimonious trees under implied weighting (k = 4–7). Images of ommatidial cluster: black = *Pseudonannolene buhrnheimi* Schubart, 1960 (IBSP 2397); blue = *P. leucomelas* Schubart, 1947 (MNRJ 11829).

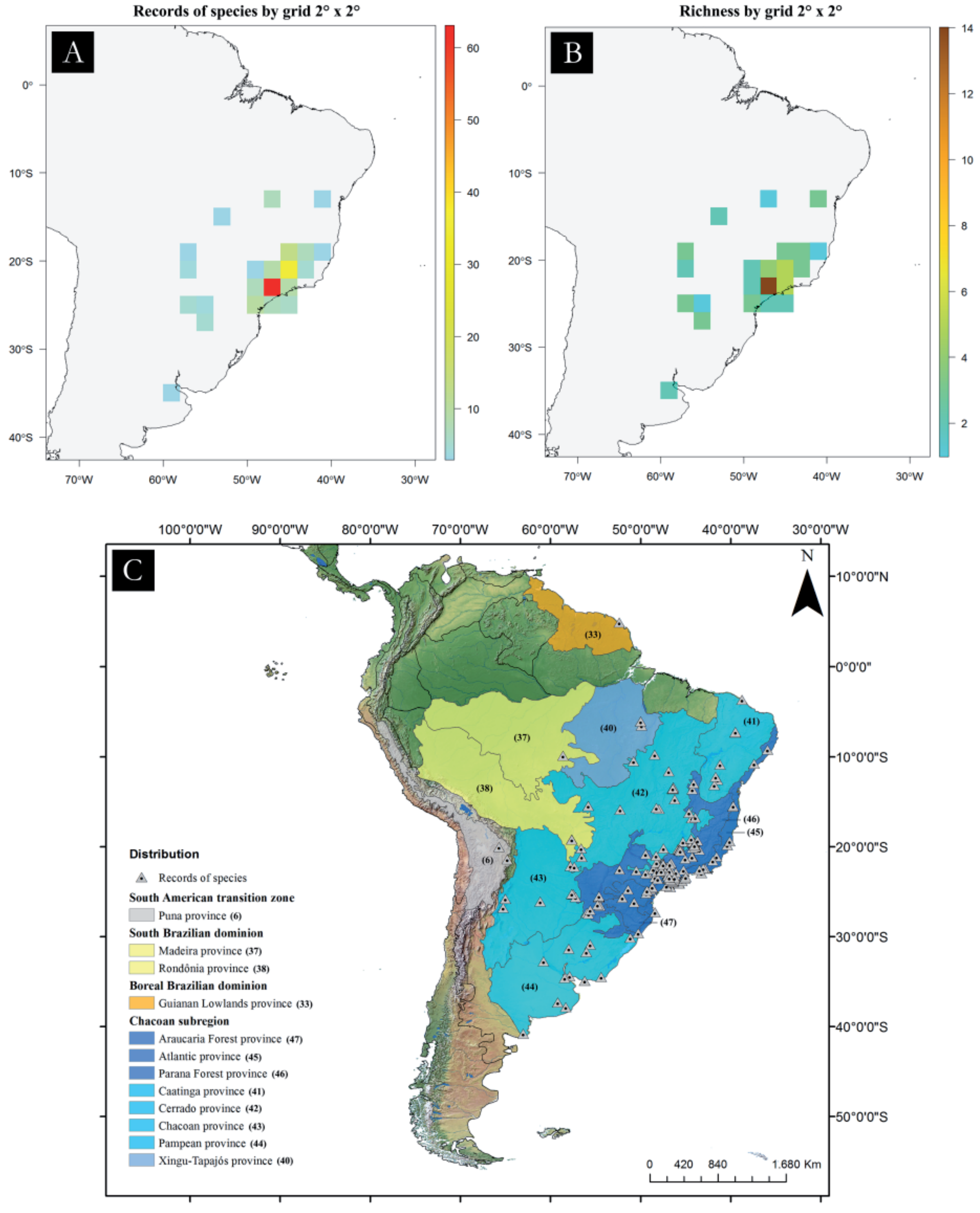

Fig. 13. Distribution maps of *Pseudonannolene* Silvestri, 1895. **A**. Records of species by grid 2° × 2°. **B**. Richness by grid 2° × 2°. **C**. Distribution of the genus in South America. The colored areas represent the biogeographical division of the Neotropical region (Morrone 2014; Löwenberg-Neto 2014). Grids containing only one record of a single species are omitted in the maps A and B.

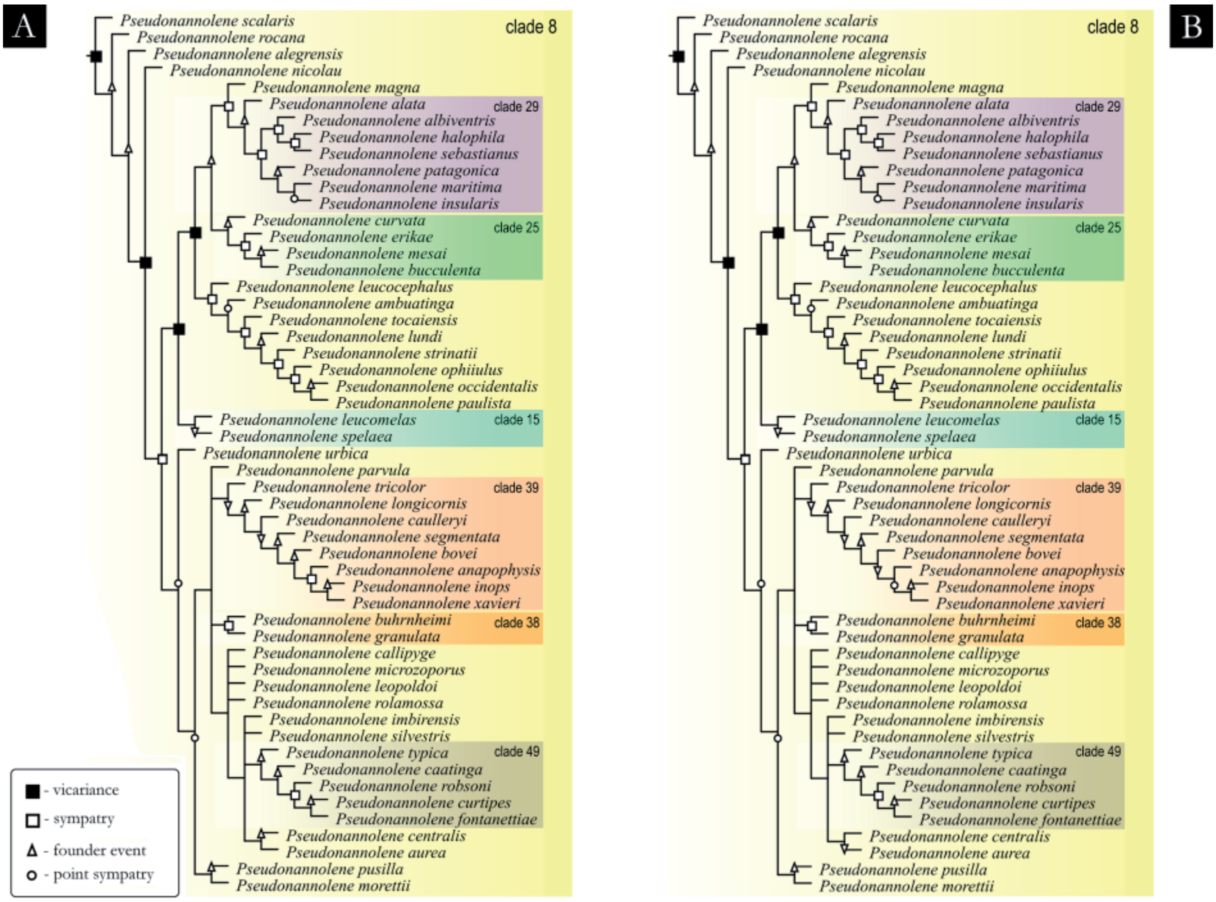

Fig. 14. The equally parsimonious optimal reconstructions of the biogeographic history inferred for *Pseudonannolene* Silvestri, 1895 using GEM. The reconstructions A and B were based on the majority rule consensus tree. The symbols refer to the cladogenetic events recovered: *white triangle* = founder event; *white squares* = sympatry, *black square* = vicariance; *white circle* = point sympatry.

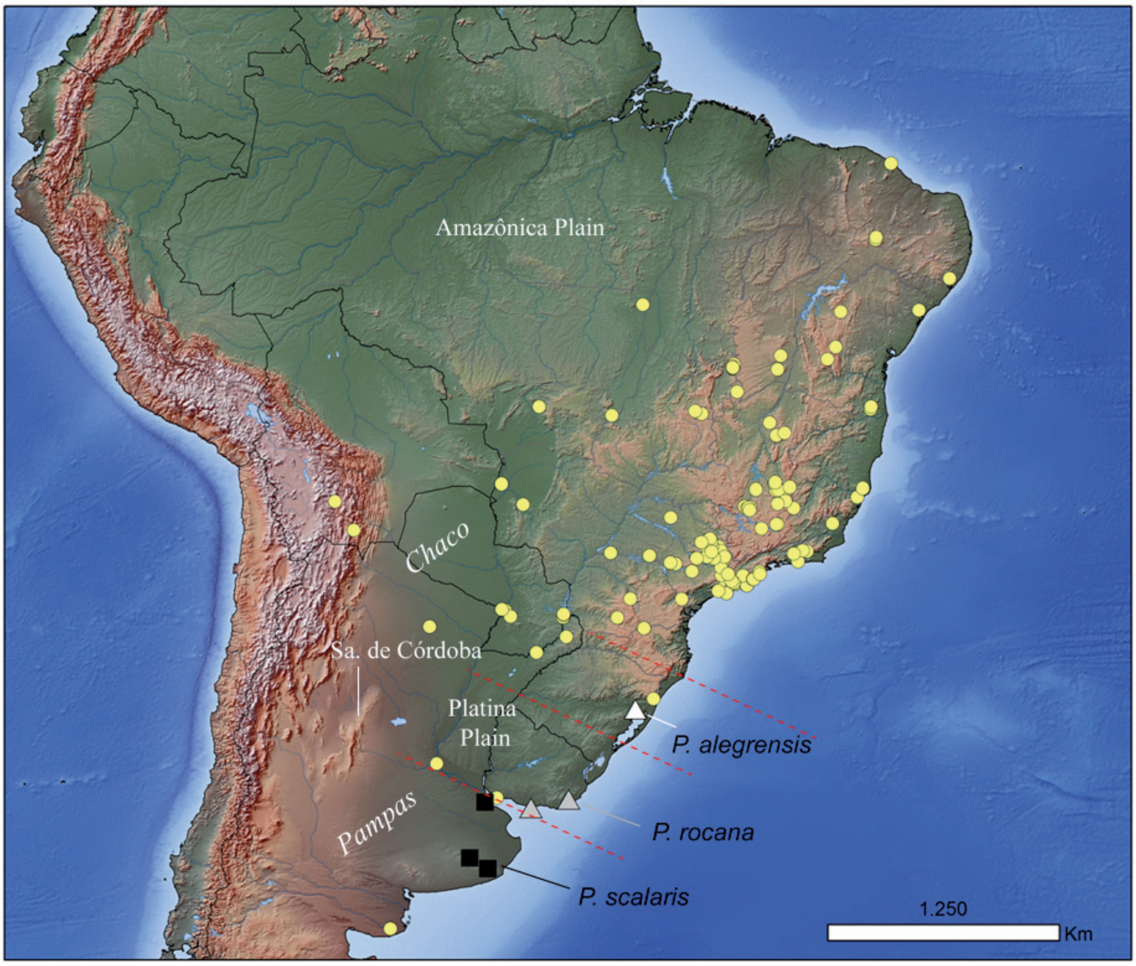

Fig. 15. Biogeographic history of the genus *Pseudonannolene* Silvestri, 1895. The symbols refer to the distribution data of *P. scalaris* Brölemann, 1902 (black squares), *P. rocana* Silvestri, 1902 (grey triangles), *P. alegrensis* Silvestri, 1897 (white triangle), and remaining species (yellow circles).

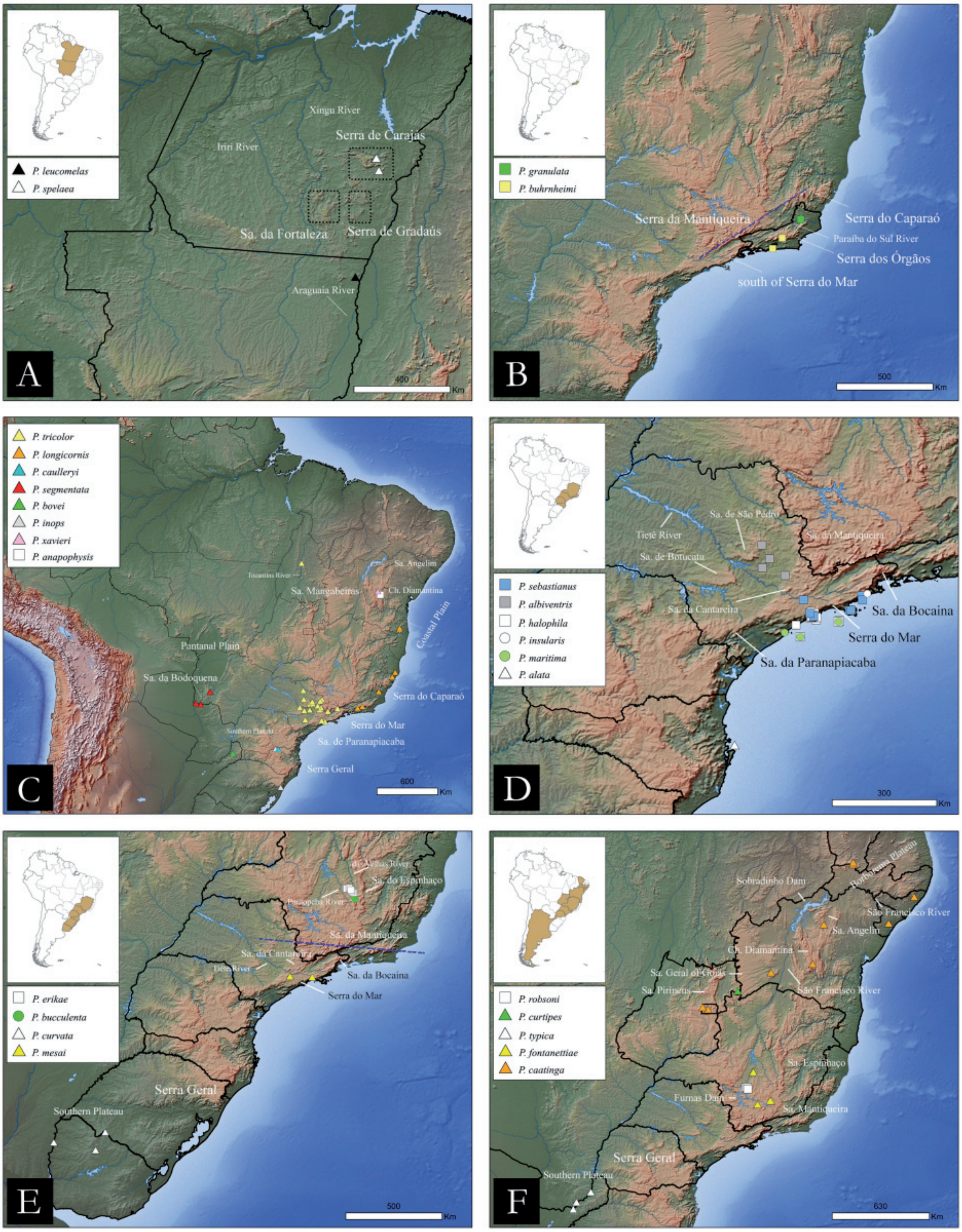

Fig. 16. Biogeographic history of the clades recovered in the analysis. **A**. Clade 15 (the stippled rectangles refer to the delimitation of the mountain ranges Fortaleza, Gradaús, and Carajás). **B**. Clade 38. **C**. Clade 39. **D**. Clade 29 (record of *Pseudonannolene patagonica* Brölemann, 1902 in Argentina is omitted). **E**. Clade 25. **F**. Clade 49.

Fig. 17. Living specimens. **A–C**. *Pseudonannolene callipyge* Brölemann, 1902, from Adrianópolis, PR, Brazil. **D**. *P. fontanettiae* Iniesta & Ferreira, 2014, from Lavras, MG, Brazil. **E**. *Pseudonannolene* spp. from Piquete, SP, Brazil. **F**. *Pseudonannolene* spp. from Lassance, MG, Brazil. Photos (A–F) by L.F.M. Iniesta.

Fig. 18. Living specimens. **A**. *Pseudonannolene urbica* Schubart, 1945, from Mogi das Cruzes, SP, Brazil. **B**. *Pseudonannolene* spp. (troglophilic and troglomorphic species) from Lassance, MG, Brazil. **C–D**. *P. granulata* sp. nov., from Cambuci, RJ, Brazil. **E**. *P. spelaea* Iniesta & Ferreira, 2013, from Carajás, PA, Brazil. **F**. *Pseudonannolene* spp., from Adrianópolis, PR, Brazil. Photos (A–B) by L.F.M. Iniesta; (C–D) courtesy of A.B. Kury, (E) courtesy of M.P. Oliveira, and (F) courtesy of C.A.R. Souza.

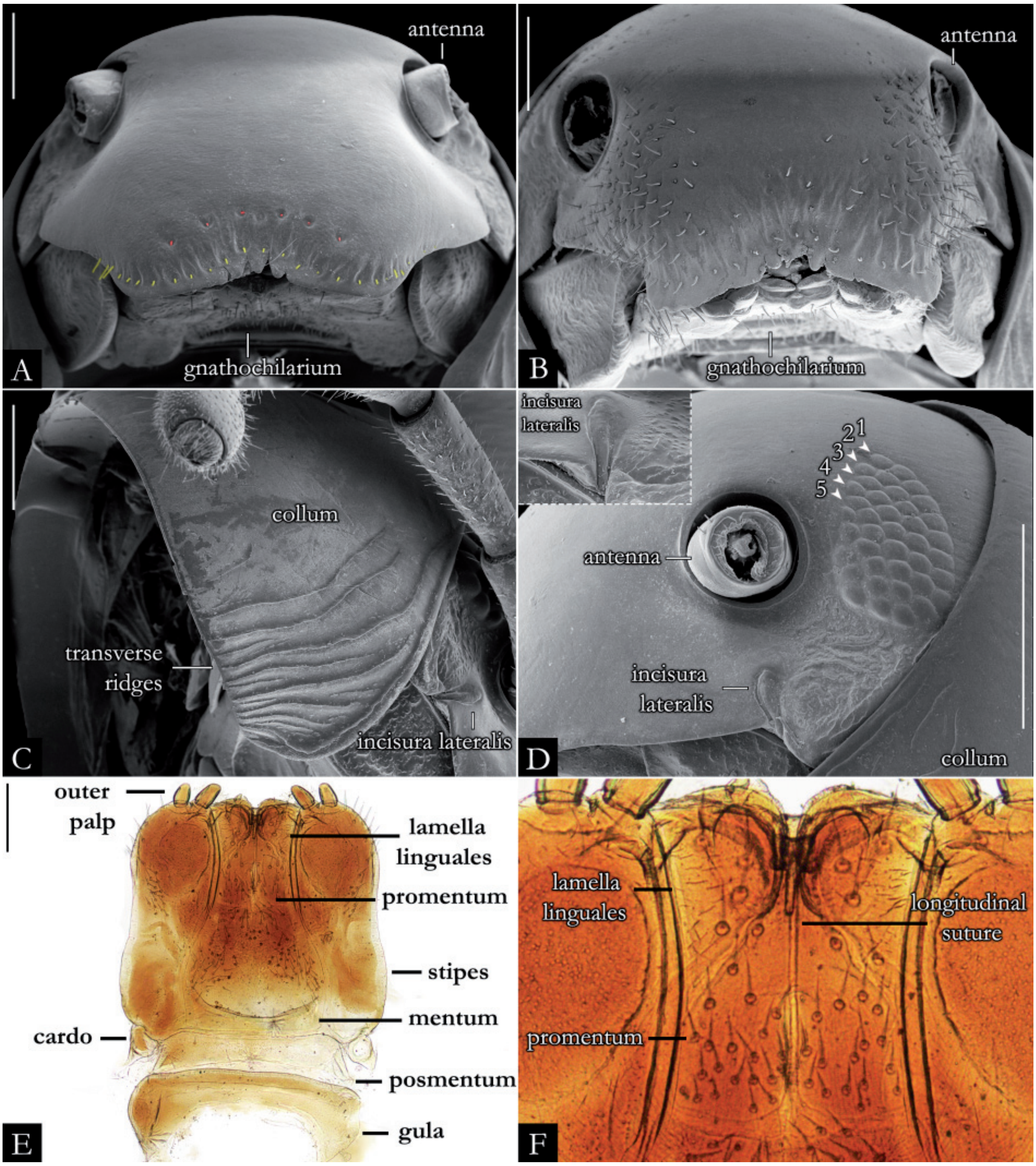

Fig. 19. SEM and microscope images. **A**. Head of *Pseudonannolene robsoni* Iniesta & Ferreira, 2014 (IBSP 3526), in frontal view. **B**. Head of *P. occidentalis* Schubart, 1958 (IBSP 1998), in frontal view. **C**. Collum of *P. robsoni* (IBSP 3506), in lateral view. **D**. Head of *P. robsoni* (IBSP 3526), in lateral view. **E**. Gnathochilarium of *P. microzoporus* Mauriès, 1987 (IBSP 3497). **F**. Detail of gnathochilarium of *P. microzoporus* (IBSP 3497). Scale bars: A–B = 500 µm; C, F, = 200 µm; D = 1 mm; E = 100 µm.

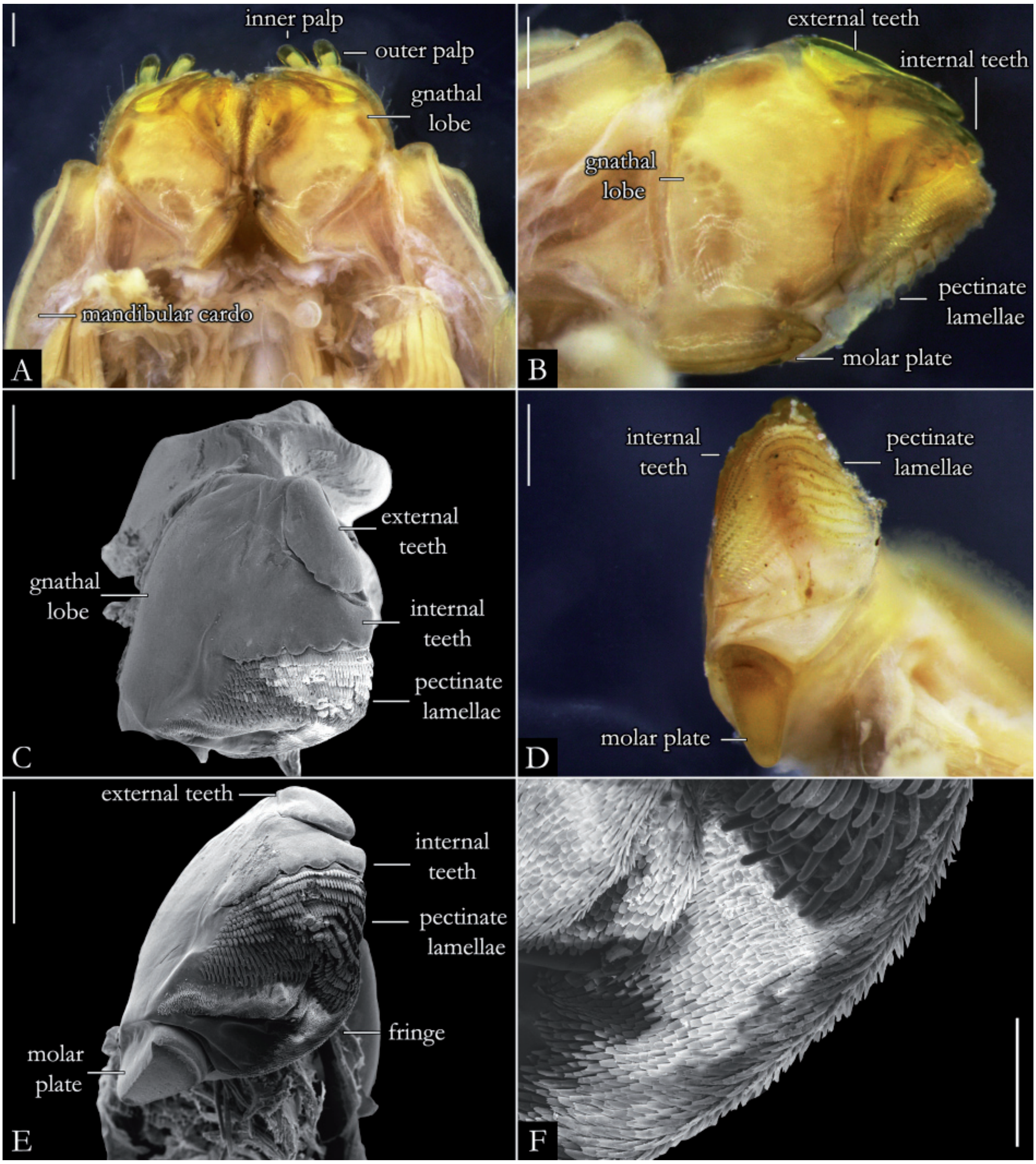

Fig. 20. SEM and stereoscopic images of mandibles. **A**. Ventral view, *Pseudonannolene robsoni* Iniesta & Ferreira, 2014 (IBSP 3526). **B**. Right mandible, *P. robsoni* (IBSP 3526). **C**. Oral view of right mandible, *P. robsoni* (IBSP 3505). **D**. Mesal view of right mandible, *P. robsoni* (IBSP 3526). **E**. Mesal view of right mandible, *P. robsoni* (IBSP 3505). **F**. Detail of pectinate lamellae of right mandible, *P. robsoni* (IBSP 3505). Scale bars: A, C, F = 200 µm; B = 300 µm; D = 500 µm; E = 250 µm.

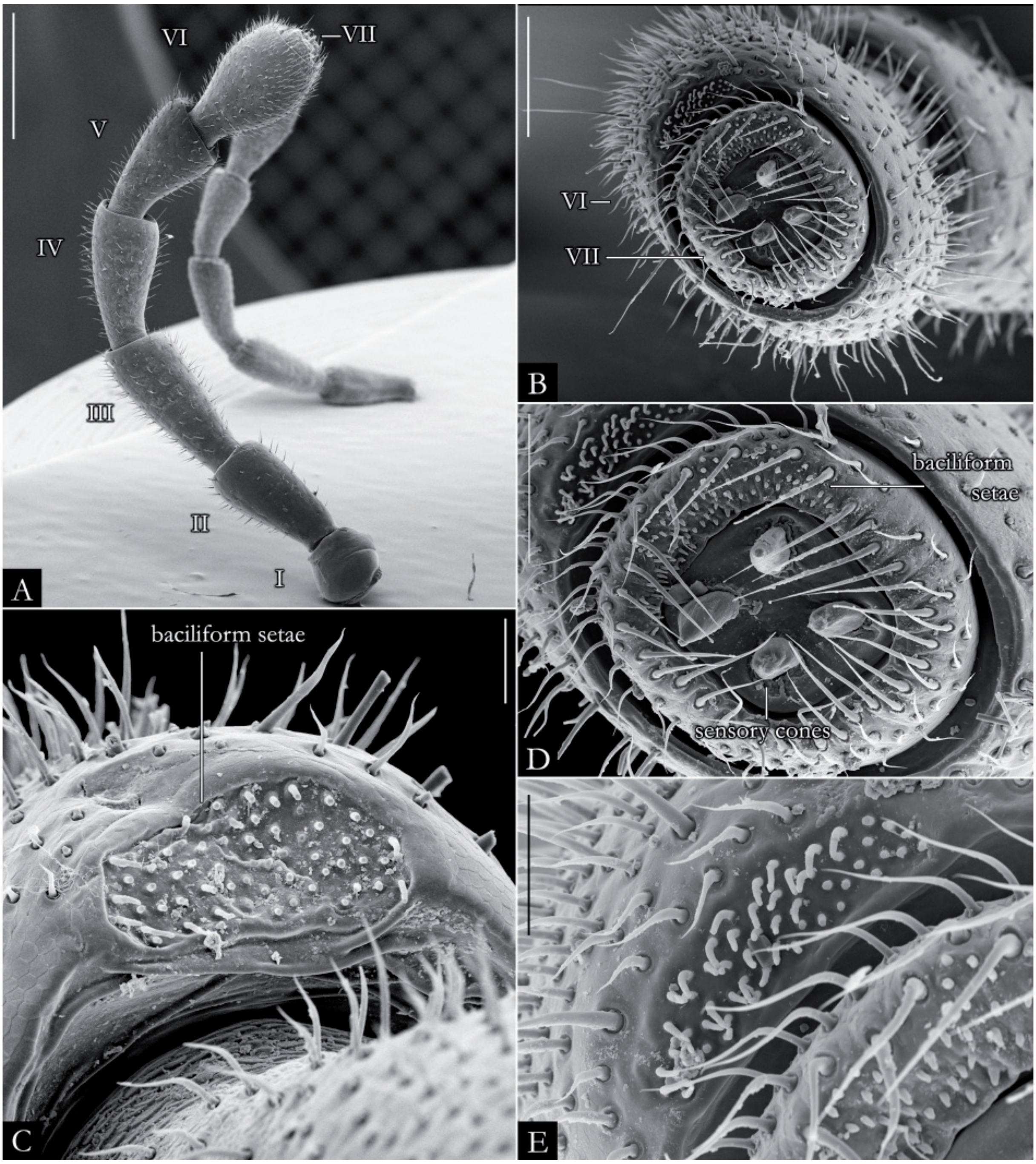

Fig. 21. SEM images of antennae. **A**. Antenna of female of *Pseudonannolene halophila* Schubart, 1949 (IBSP 1101). **B**. Apical view of antenna of female of *P. robsoni* Iniesta & Ferreira, 2014 (IBSP 3506). **C**. Detail of antennomere V of male of *P. robsoni* (IBSP 3526). **D**. Detail in apical view of antennomere VII of female of *P. robsoni* (IBSP 3506). **E**. Detail of antennomere VI of female of *P. robsoni* (IBSP 3506). Scale bars: A = 1 mm; B = 0.15 mm; C, E = 0.05 mm; D = 0.1 mm.

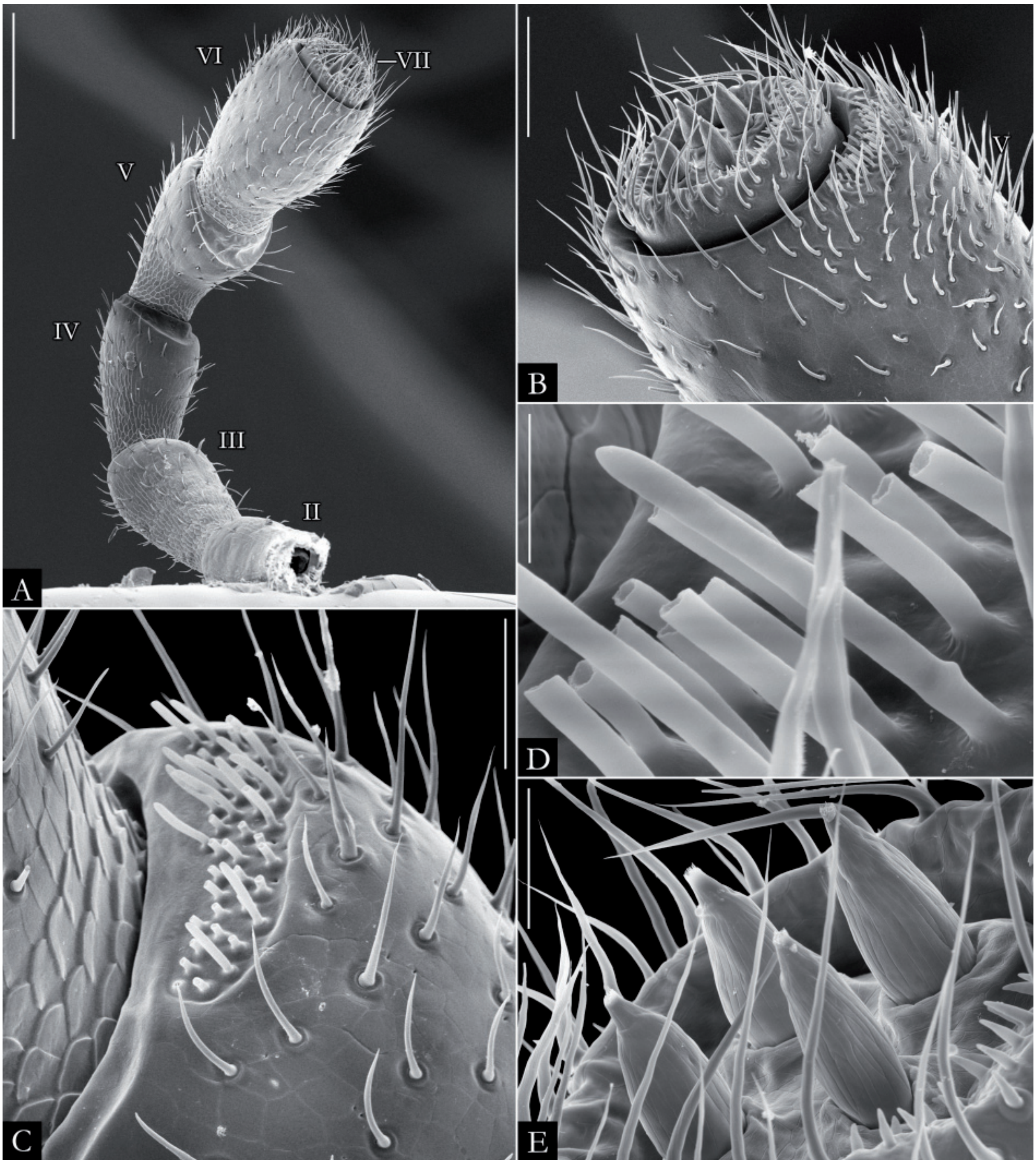

Fig. 22. SEM images of the antenna of Pseudonannolene spelaea Iniesta & Ferreira, 2013 (IBSP 6071). A. Antenna, in mesal view. B. Lateral view of antenna. C. Detail of antennomere V. D. Detail of the baciliform setae on antennomere V. E. Detail of sensory cones. Scale bars: A = 0.25 mm; B = 0.1 mm; C, E = 0.05 mm; D = 0.01 mm.

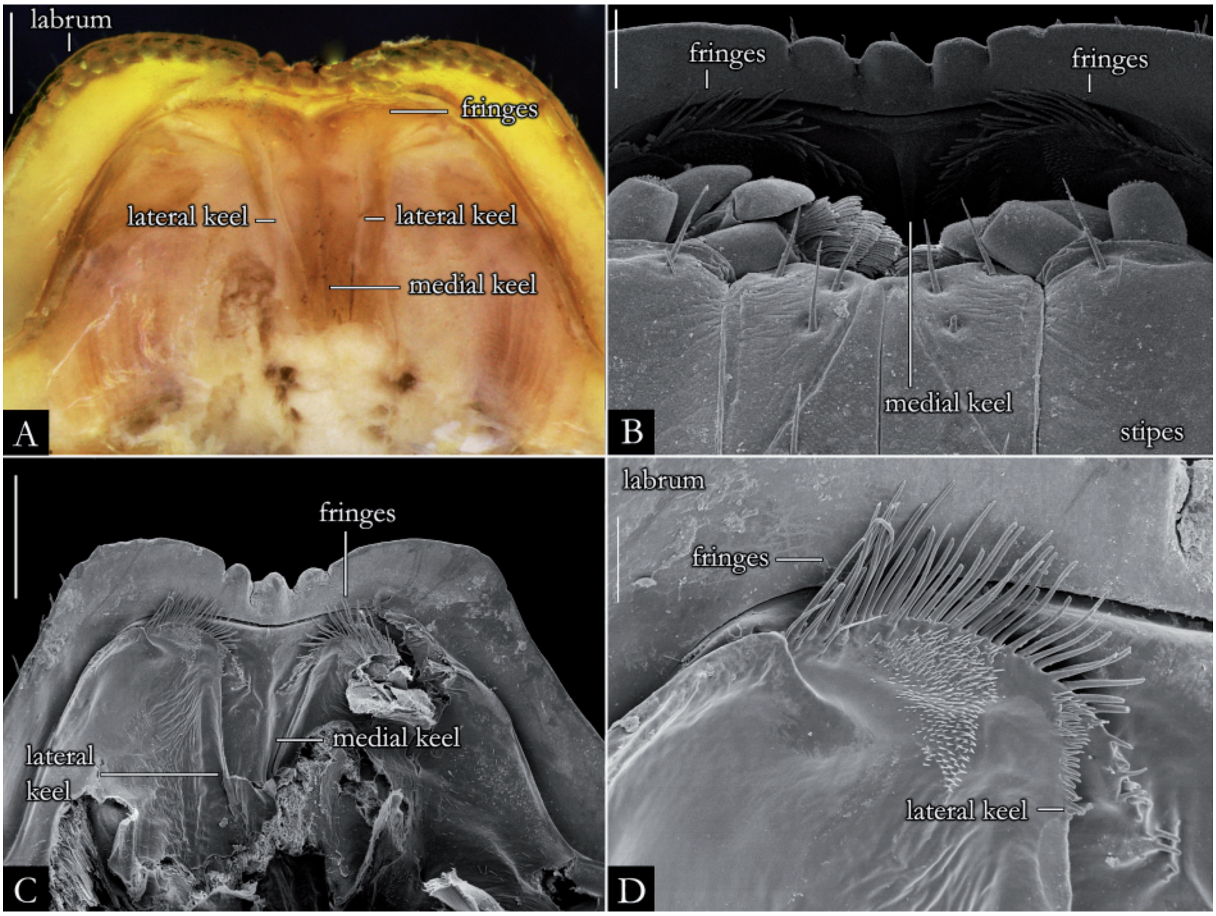

Fig. 23. SEM and stereoscopic images of epipharynx *Pseudonannolene robsoni* Iniesta & Ferreira, 2014. **A**. Ventral view (IBSP 3526). **B**. Ventral view (IBSP 3506). **C–D**. Ventral view (IBSP 3504). Scale bars: A, C = 0.5 mm; B = 0.2 mm; D = 1 mm.

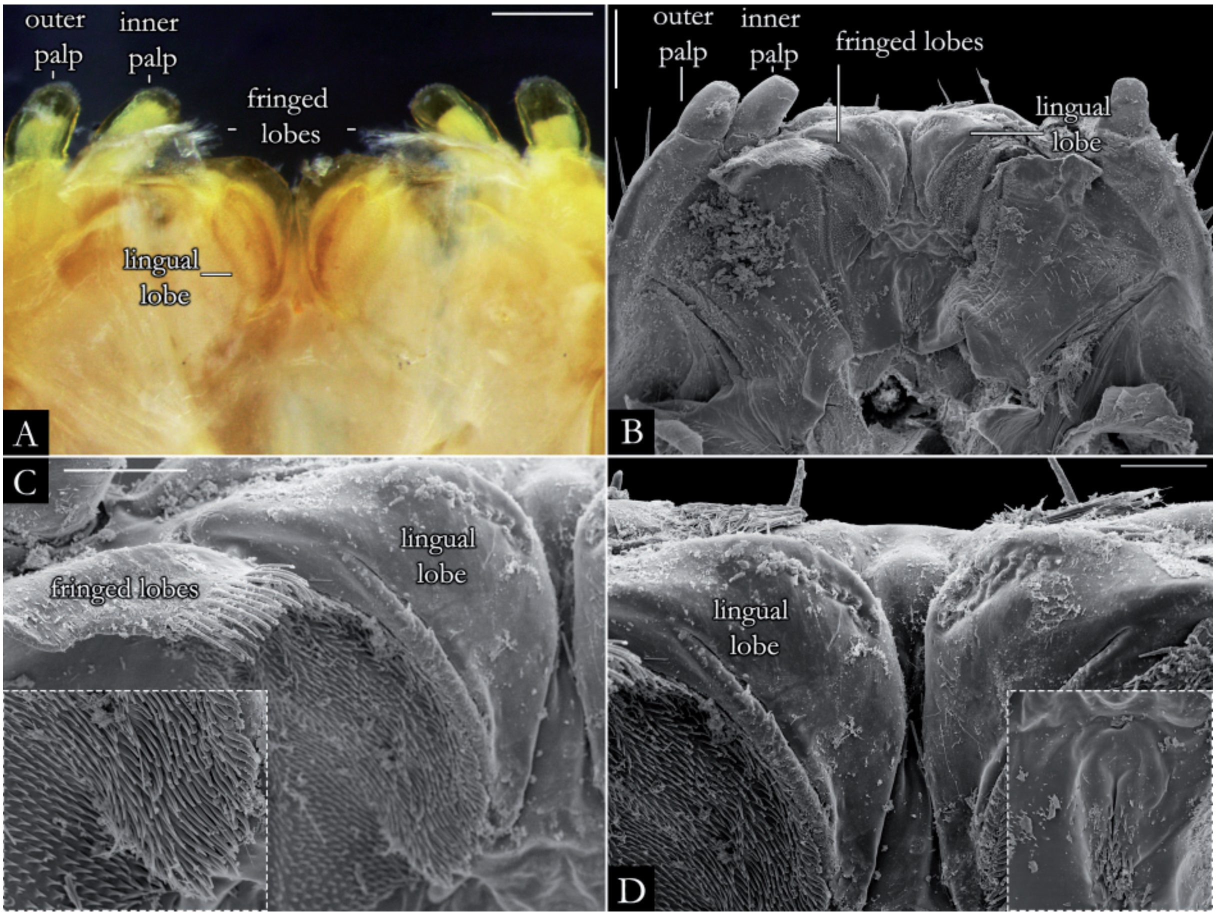

Fig. 24. SEM and stereoscopic images of hypopharynx *Pseudonannolene robsoni* Iniesta & Ferreira, 2014. **A**. Ventral view (IBSP 3526). **B–D**. Ventral view (IBSP 3504). Scale bars: A = 1 mm; B = 0.2 mm; C–D = 0.1 mm.

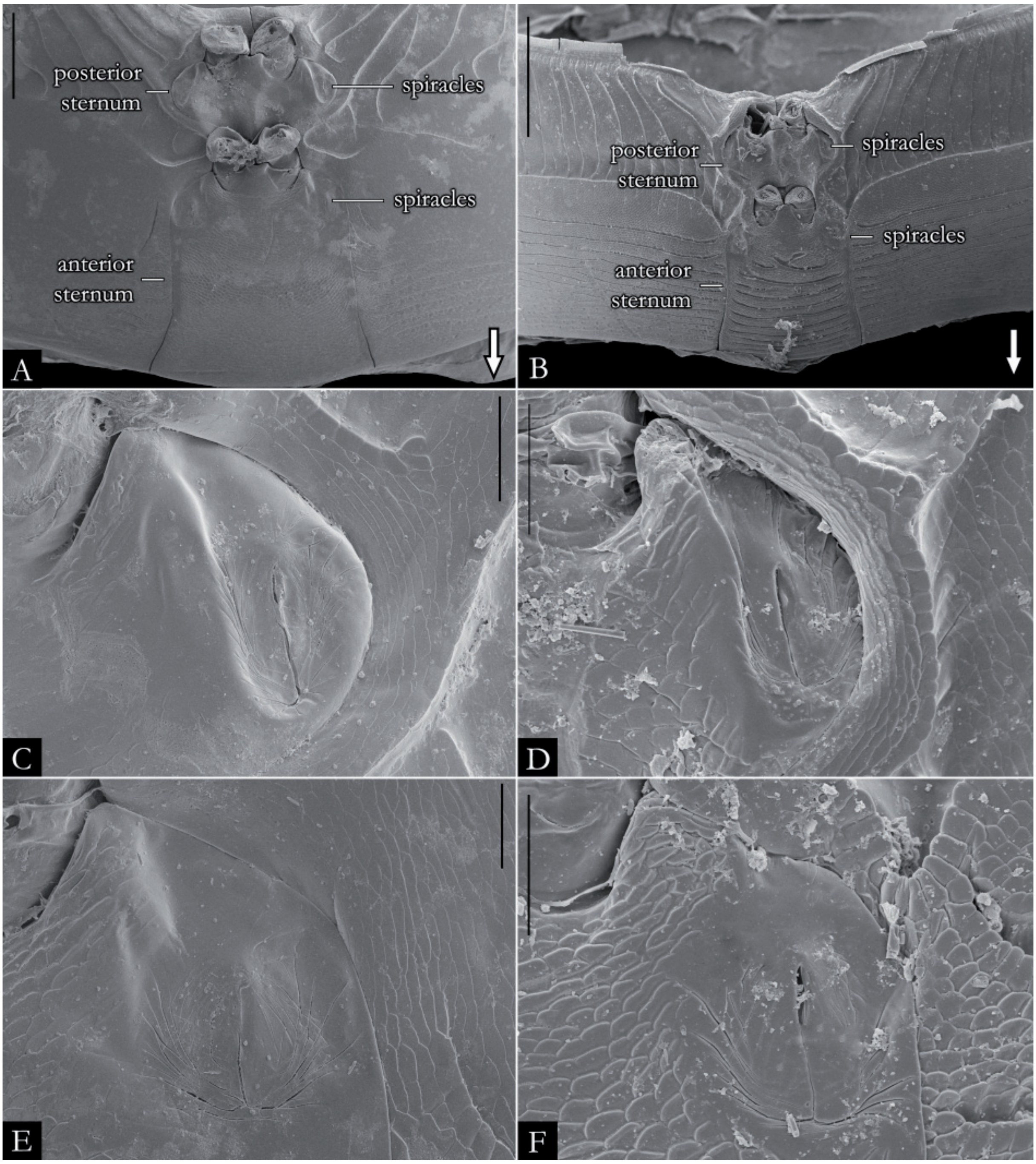

Fig. 25. SEM images of sternum. **A**. *Pseudonannolene paulista* Brölemann, 1902 (IBSP 1908). **B**. *P. caatinga* Iniesta & Ferreira, 2014 (IBSP 2180). **C**. Spiracle on the posterior sternum of *P. paulista* (IBSP 1908). **D**. Spiracle on the posterior sternum of *P. caatinga* (IBSP 2180). **E**. Spiracle on the anterior sternum of *P. paulista* (IBSP 1908). **F**. Spiracle on the anterior sternum of *P. caatinga* (IBSP 2180). Scale bars: A = 0.25 mm; B = 0.5 mm; C, E = 0.05 mm; D = 0.1 mm; F = 0.2 mm.

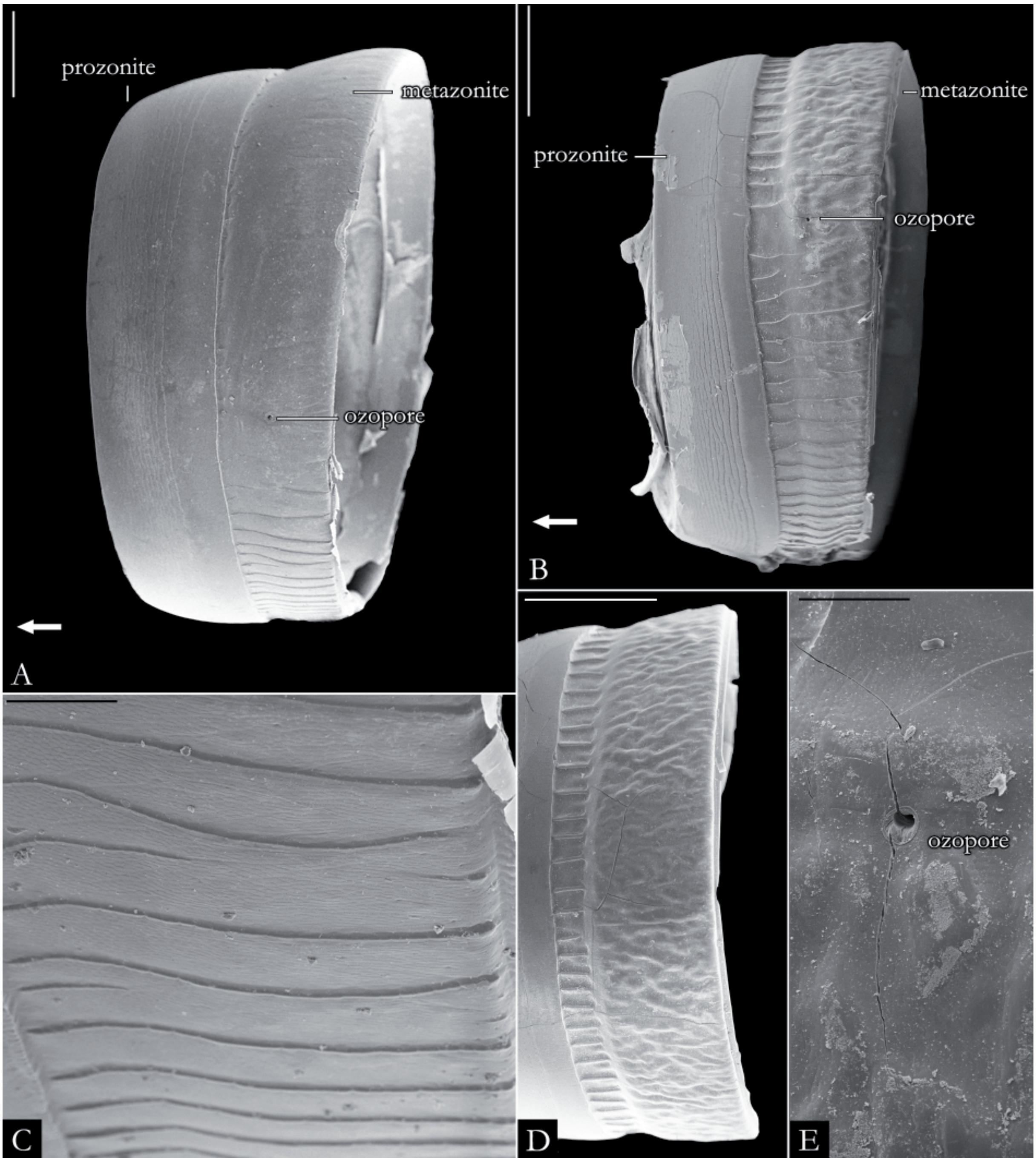

Fig. 26. SEM images of midbody rings. **A**. *Pseudonannolene robsoni* Iniesta & Ferreira, 2014 (IBSP 3506). **B**. *P. granulata* sp. nov. (MNRJ). **C**. Detail of the transverse striae of *P. robsoni* (IBSP 3506). **D**. Midbody ring in dorsal view of *P. granulata* sp. nov. (MNRJ). **E**. Ozospore of *P. granulata* sp. nov. (MNRJ). Scale bars: A–B, D = 1 mm; C = 0.1 mm; E = 0.02 mm.

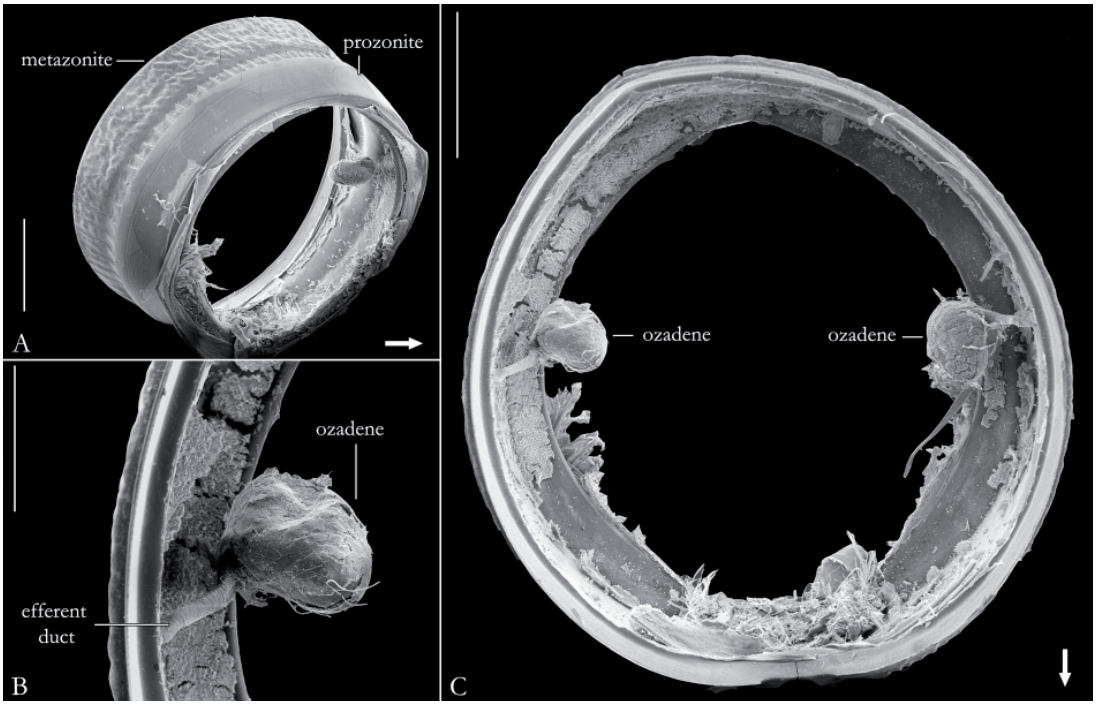

Fig. 27. SEM images of midbody rings of *Pseudonannolene granulata* sp. nov. (MNRJ). **A**. Lateral view. **B**. Detail of the ozadene. **C**. Midbody ring in transversal view. Scale bars: A, C = 1 mm; B = 0.5 mm.

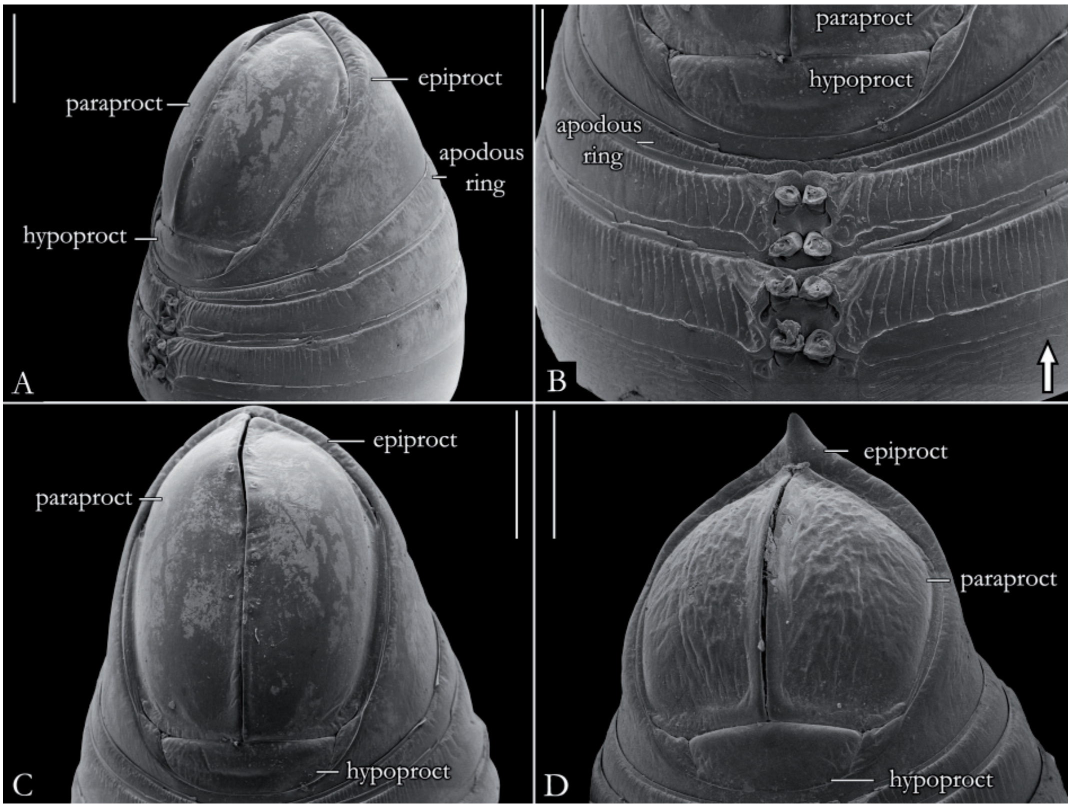

Fig. 28. SEM images of posterior rings. **A–C**. *Pseudonannolene robsoni* Iniesta & Ferreira, 2014 (IBSP 3506). **D**. *P. buhrnheimi* Schubart, 1960 (IBSP 2397). Scale bars: A, C–D = 1 mm; B = 0.5 mm.

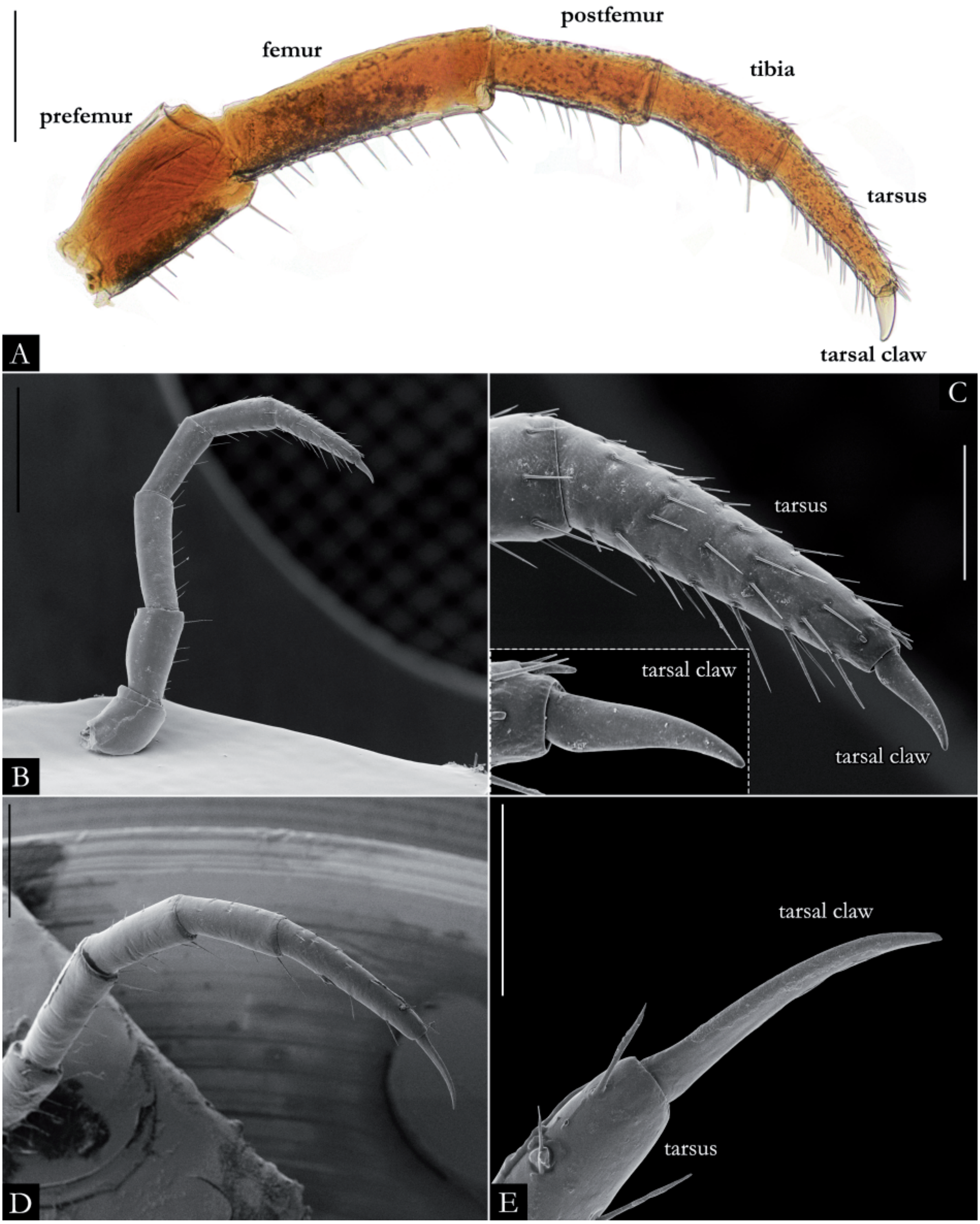

Fig. 29. Microscope and SEM images of midbody legs. **A**. *Pseudonannolene microzoporus* Mauriès, 1987 (IBSP 3497). **B–C**. *P. robsoni* Iniesta & Ferreira, 2014 (IBSP 3526). **D–E**. *P. strinatii* Mauriès, 1974 (IBSP 7633). Scale bars: A, D = 0.5 mm; B = 1 mm; C = 0.3 mm; E = 0.2 mm.

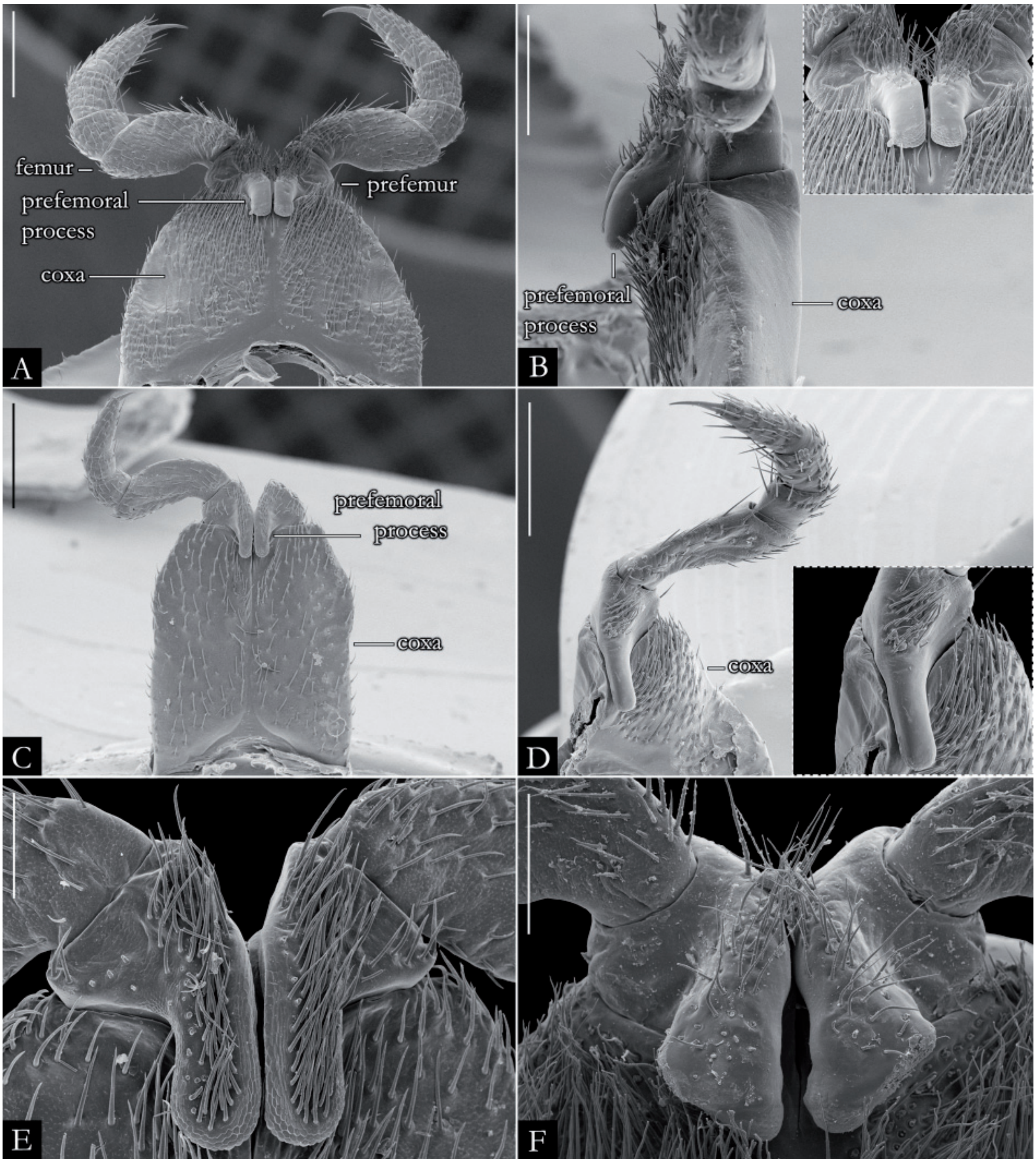

Fig. 30. SEM images of first leg-pair of males. **A**. *Pseudonannolene caatinga* Iniesta & Ferreira, 2014 (IBSP 2180). **B**. *P. microzoporus* Mauriès, 1987 (IBSP 3526), detail of prefemoral process of *P. caatinga* (IBSP 2180). **C**. *P. halophila* (IBSP 1091). **D**. *P. rolamossa* Iniesta & Ferreira, 2013 (IBSP 7772). **E**. *P. maritima* Schubart, 1949 (IBSP 979). **F**. *P. erikae* Iniesta & Ferreira, 2014 (IBSP 7607). Scale bars: A, C–D = 0.5 mm; B = 0.3 mm; E = 0.2 mm; F = 0.3 mm.

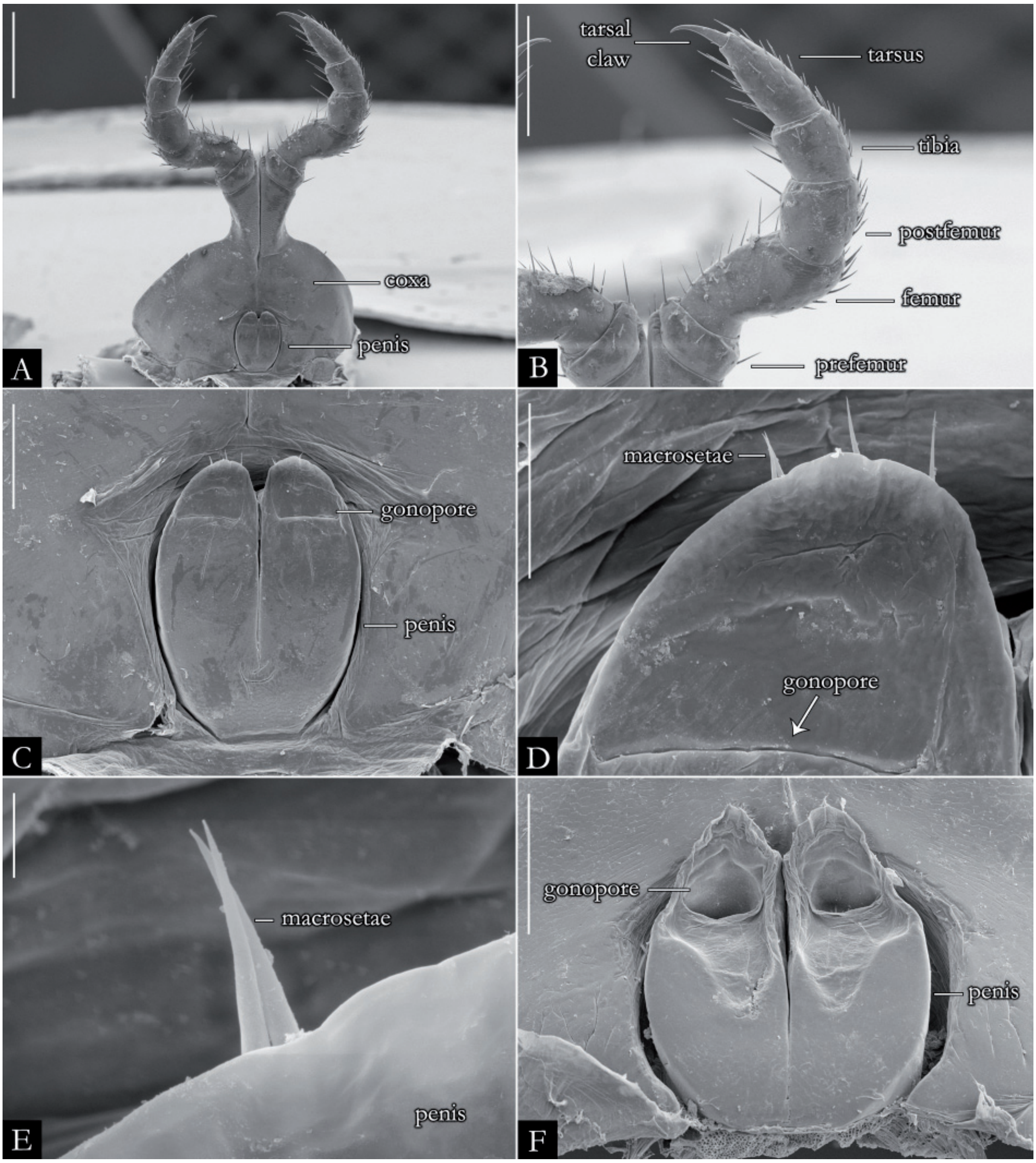

Fig. 31. SEM images of second leg-pair of males. **A–E**. *Pseudonannolene halophila* Schubart, 1949 (IBSP). **F**. *P. sebastianus* Brölemann, 1902 (IBSP). Scale bars: A–B = 0.5 mm; C, F = 0.2 mm; D = 0.05 mm; E = 0.005 mm.

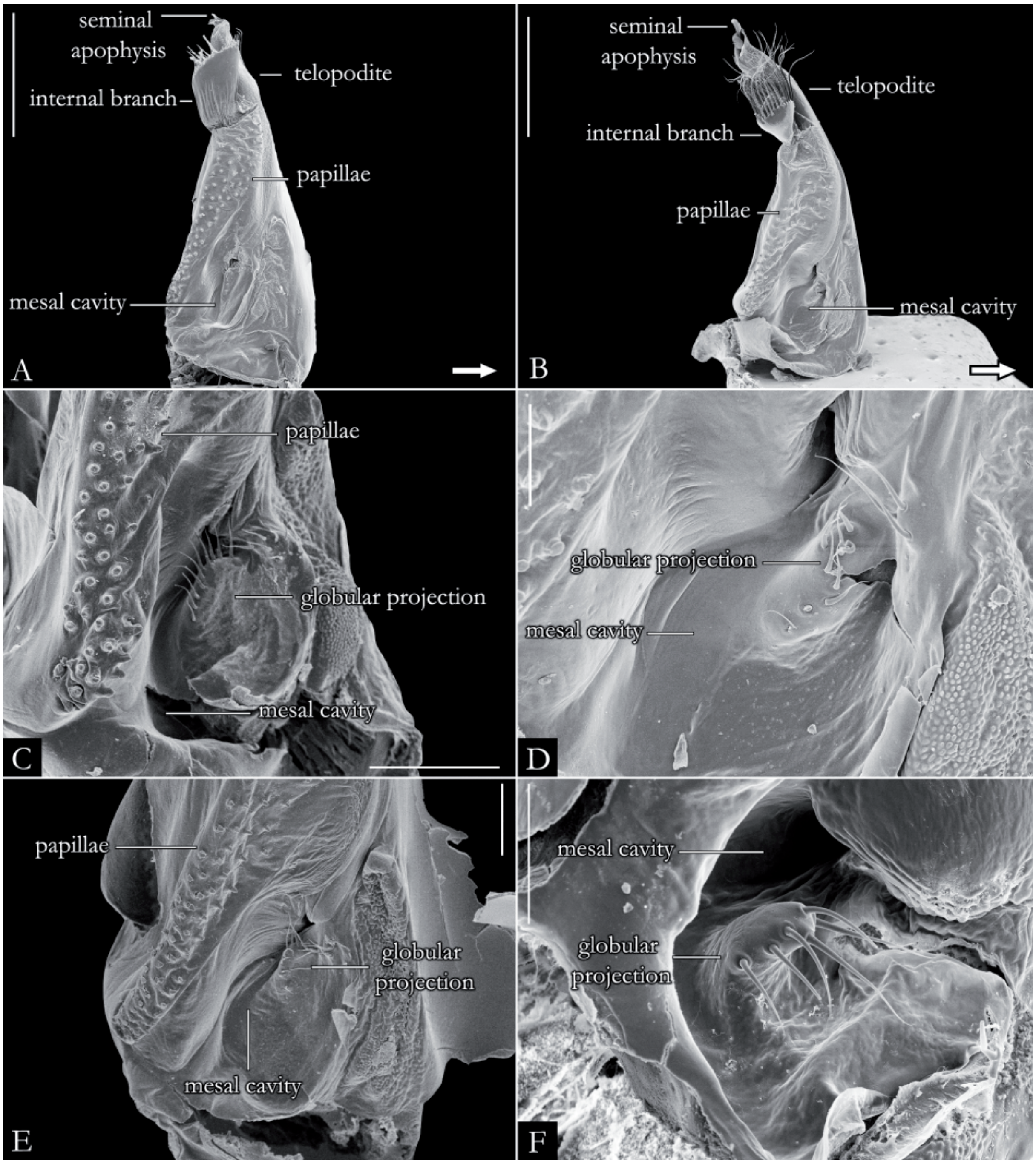

Fig. 32. SEM images of right gonopods in mesal view. **A**. *Pseudonannolene caatinga* Iniesta & Ferreira, 2014 (IBSP 2166). **B**. *P. maritima* Schubart, 1949 (IBSP 979). **C**. Detail of mesal cavity, *P. paulista* Brölemann, 1902 (IBSP 1908). **D**. Detail of mesal cavity, *P. maritima* (IBSP 979). **E**. Detail of mesal cavity, *P. halophila* Schubart, 1949 (IBSP 1091). **F**. Detail of mesal cavity, *P. spelaea* Iniesta & Ferreira, 2013 (IBSP 6071). Scale bars: A–B = 0.5 mm; C, F = 0.2 mm; D–E = 0.1 mm.

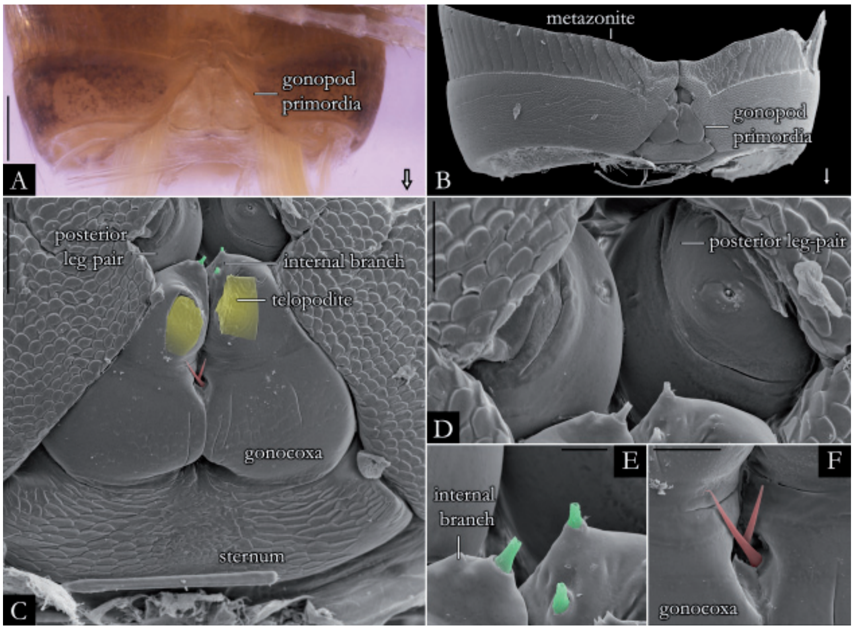

Fig. 33. Ontogeny of the gonopods in *Pseudonannolene microzoporus* Mauriès, 1987 (IBSP). **A–B**. Seventh body ring with the gonopod primordia in early stadium, ventral view. **C**. Gonopod primordia in intermediate stadium, ventral view. Telopodite highlighted in yellow. **D**. Detail of posterior leg-pair modified. **E**. Setae (highlighted in green) on internal branch of the gonopod primordia. **F**. Macroseta (highlighted in red) on gonocoxa of the gonopod primordia. Scale bars: A–B = 0.5 mm; C = 0.2 mm; D = 0.04 mm; E = 0.01 mm; F = 0.02 mm.

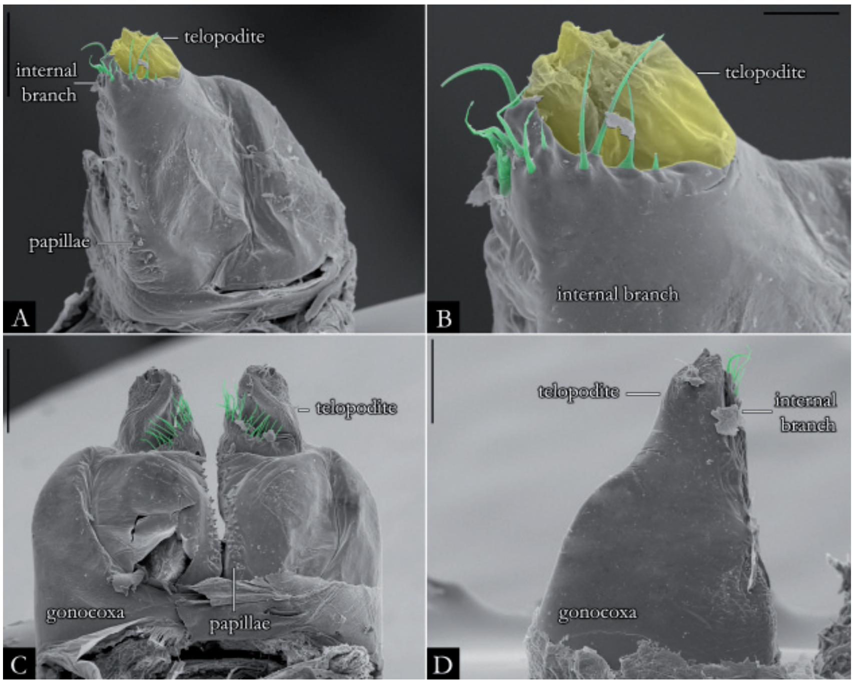

Fig. 34. Gonopod primordia in final stadia in *Pseudonannolene microzoporus* Mauriès, 1987 (IBSP). **A–B**. Left gonopod, in anal view. Setae on internal branch and telopodite highlighted in green and yellow, respectively. **C**. Gonopods, in anal view. **D**. Left gonopod, in oral view. Scale bars: A = 0.1 mm; B = 0.02 mm; C = 0.2 mm; D = 0.1 mm.

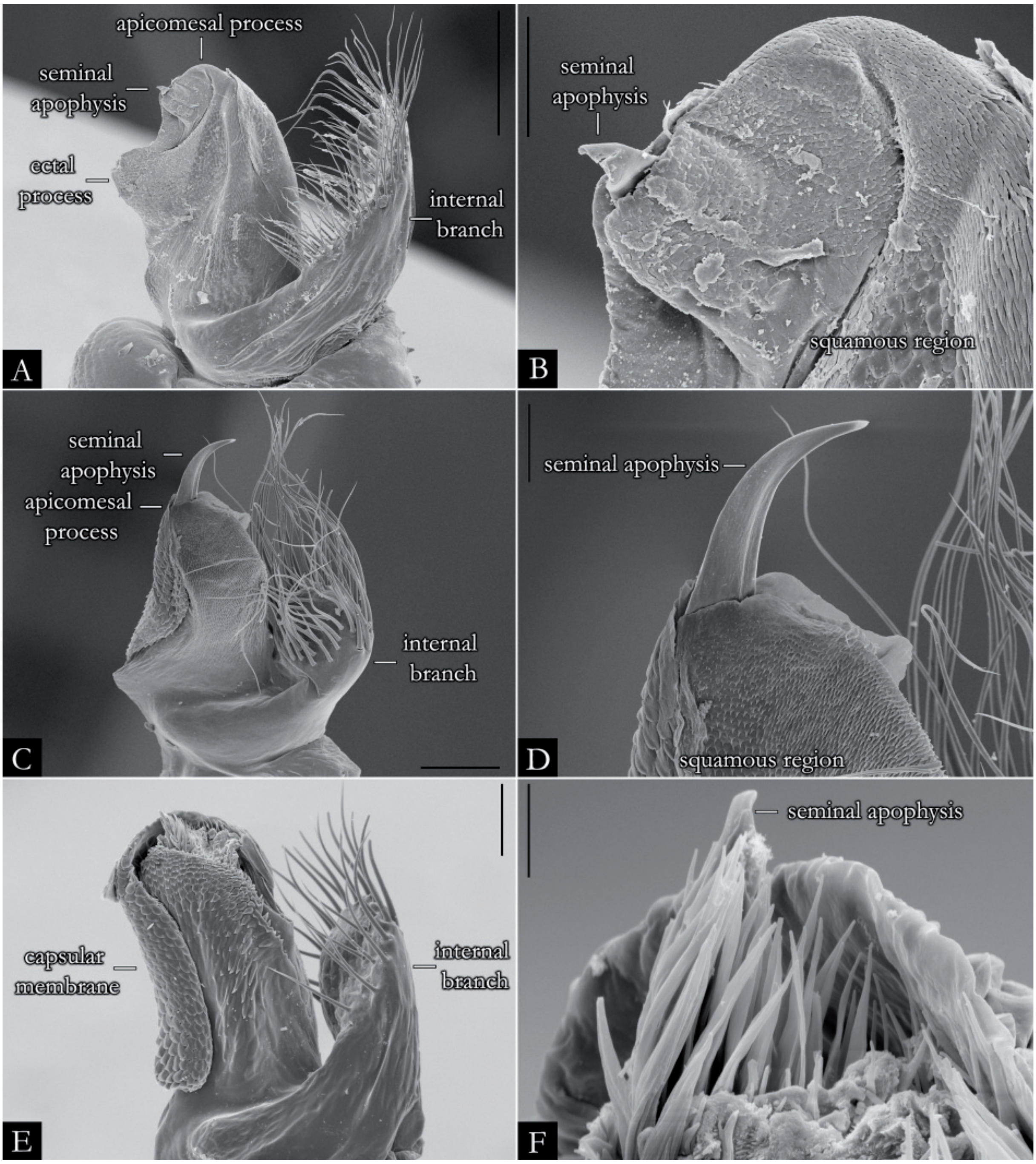

Fig. 35. SEM images of telopodite of right gonopod, in anal view. **A**. *Pseudonannolene microzoporus* Mauriès, 1987 (IBSP 5733). **B**. Detail of apical region, *P. microzoporus* (IBSP 5733). **C**. *P. maritima* Schubart, 1949 (IBSP 979). **D**. Detail of apical region, *P. maritima* (IBSP 979). **E**. *P. spelaea* Iniesta & Ferreira, 2013 (IBSP 6071). **F**. Detail of apical region, *P. spelaea* (IBSP 6071). Scale bars: A = 0.3 mm; B, E = 0.05 mm; C–D = 0.1 mm; F = 0.2 mm.

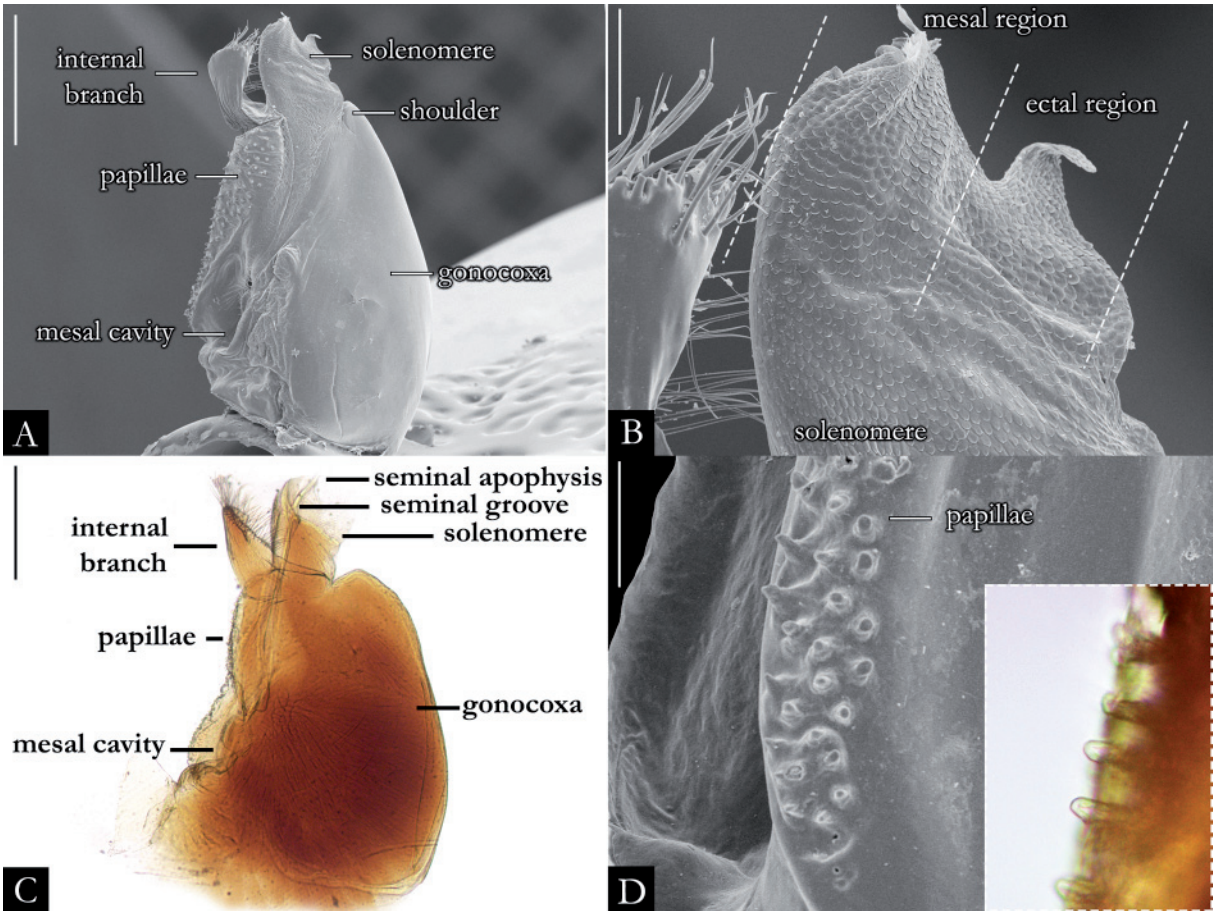

Fig. 36. Microscope and SEM images of right gonopod. **A**. *Pseudonannolene caatinga* Iniesta & Ferreira, 2014 (IBSP 2166). **B**. Telopodite, *P. caatinga* (IBSP 2166). **C**. *P. microzoporus* Mauriès, 1987 (IBSP 3497). **D**. Gonocoxa, *P. microzoporus* (IBSP 5733). Detail of the papillae. Scale bars: A, C = 0.5 mm; B, D = 0.1 mm.

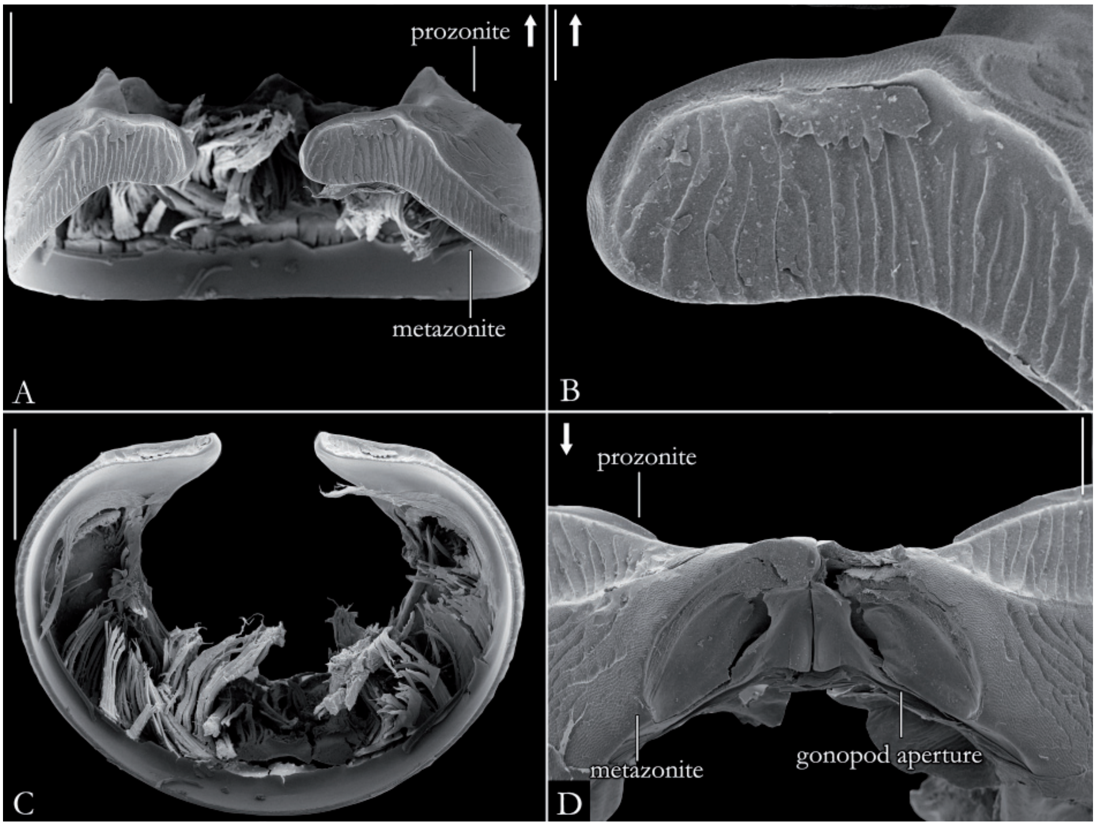

Fig. 37. SEM images of anterior body rings of males of *Pseudonannolene erikae* Iniesta & Ferreira, 2014 (IBSP 7607). **A–B**. Ventral view. **C**. Transversal view. **D**. Detail of seventh body ring with gonopod aperture. Scale bars: A, C–D = 1 mm; B = 0.2 mm.

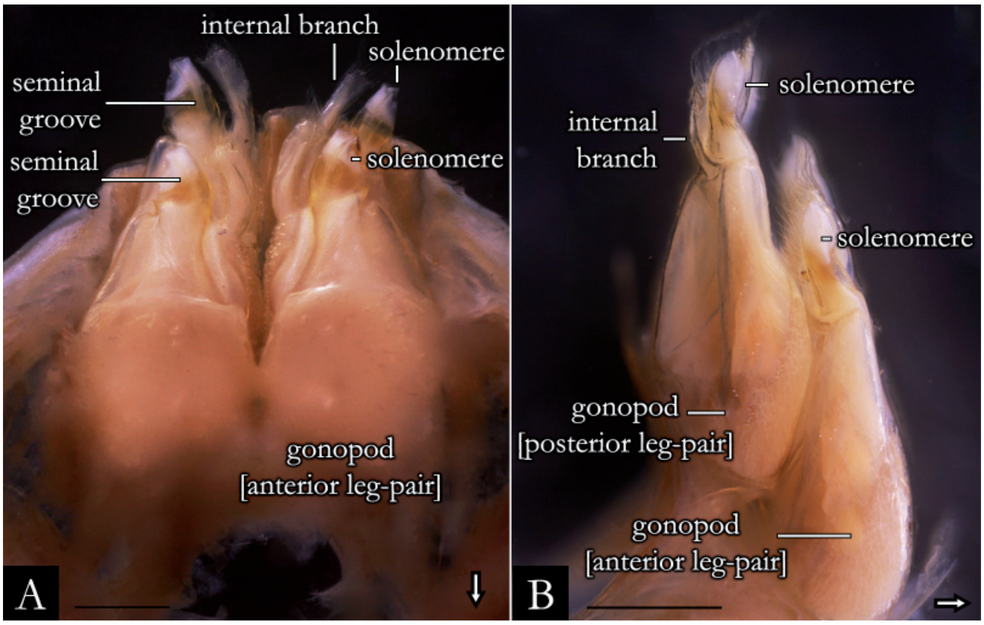

Fig. 38. Duplicate gonopods of *Pseudonannolene robsoni* Iniesta & Ferreira, 2014 (ISLA). **A**. Oral view. **B**. Ectal view. Scale bars = 0.5 mm.

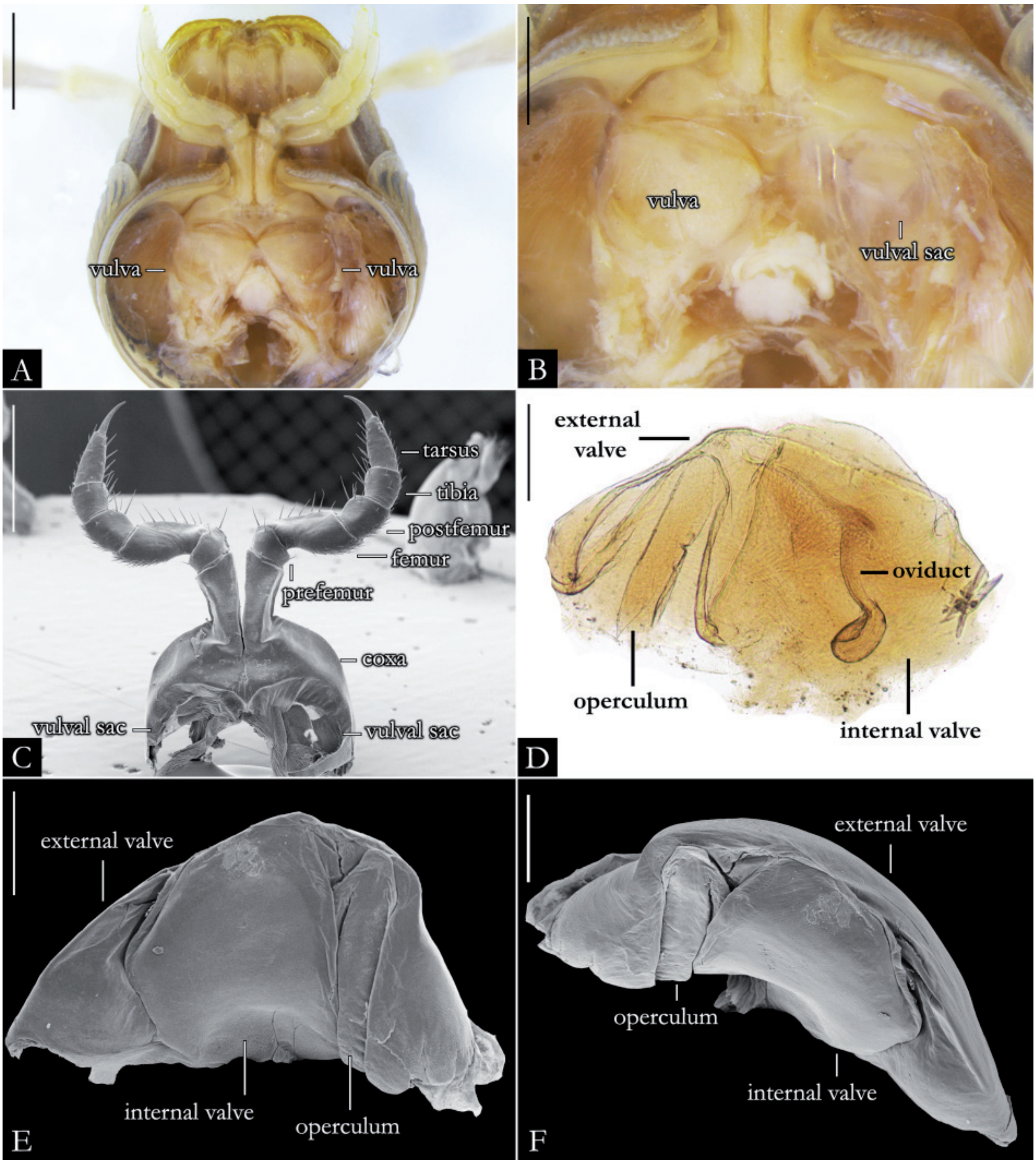

Fig. 39. SEM and stereoscopic images of sexual structures of females. **A**. Anterior rings in anal view, *Pseudonannolene microzoporus* Mauriès, 1987 (IBSP 3497). **B**. Detail of second leg-pair of *P. microzoporus* (IBSP 3497). **C**. Second leg-pair of *P. robsoni* Iniesta & Ferreira, 2014 (IBSP 3504). **D**. Left vulva of *P. microzoporus* (IBSP 3497). **E–F**. Right vulva of *P. robsoni* (IBSP 3504). Scale bars: A, C = 1 mm; B, D = 0.5 mm; E = 0.25 mm; F = 0.2 mm.

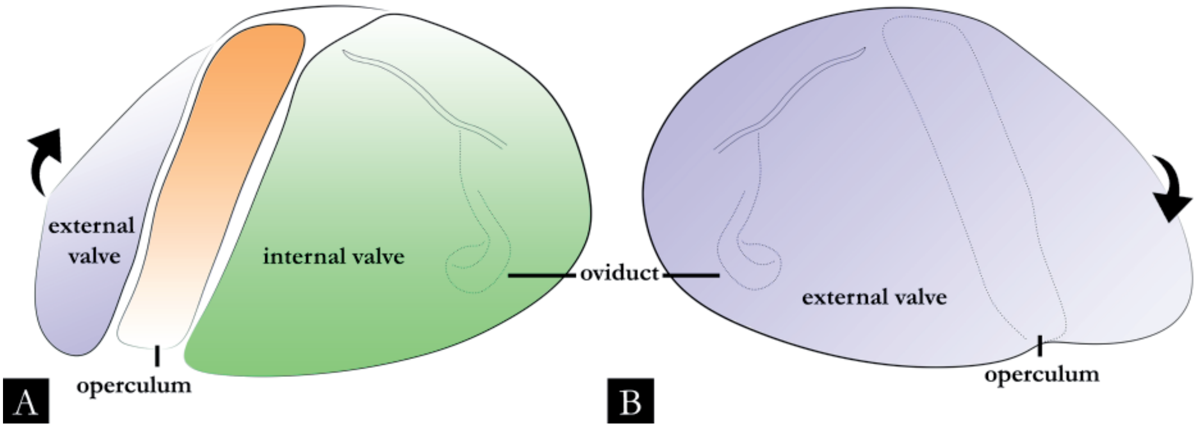

Fig. 40. Schematic drawing of left vulva of species of *Pseudonannolene* Silvestri, 1895. **A**. Anal view. **B**. Oral view.

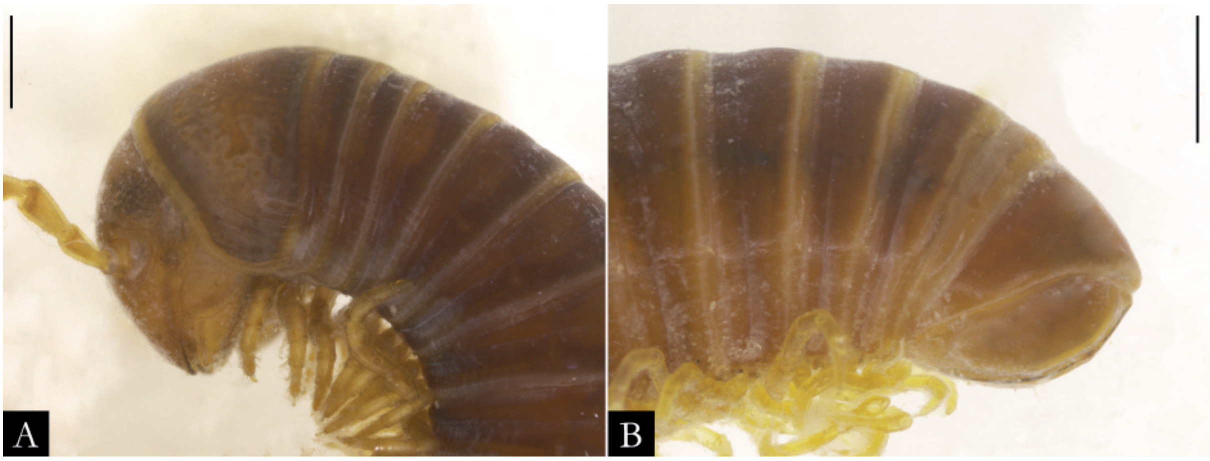

Fig. 41. *Pseudonannolene albiventris* Schubart, 1952, ♂ (MZSP 1007), in lateral view. **A**. Anterior region. **B**. Posterior region. Scale bars: A = 0.1 mm; B = 1 mm.

Fig. 42. *Pseudonannolene albiventris* Schubart, 1952, ♂ (MZSP 1007). **A**. First leg-pair. **B**. Detail of prefemur. **C**. Second leg-pair. **D**. Detail of telopodites, in anal view. **E**. Gonopods, in anal view. **F**. Gonopods, in oral view. Abbreviations: see Material and methods. Scale bars: A, C = 0.5 mm; B, D–F = 0.2 mm.

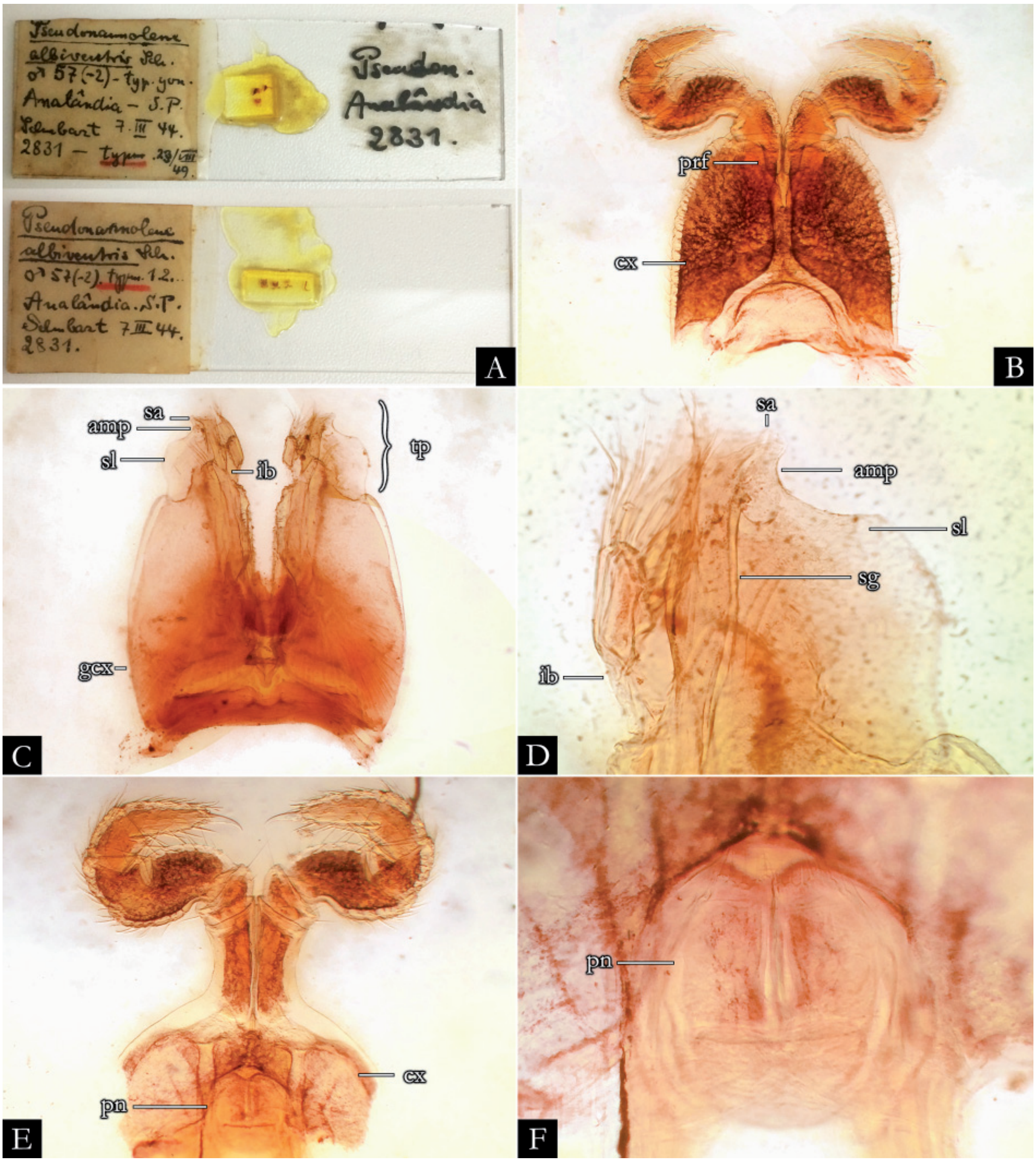

Fig. 43. *Pseudonannolene albiventris* Schubart, 1952, ♂ (MZSP). **A**. Sexual structures and gnathochilarium of type material mounted on microscope slide. **B**. First leg-pair. **C**. Gonopods, in oral view. **D**. Detail of telopodites, in oral view. **E**. Second leg-pair. **F**. Detail of penis. Abbreviations: see Material and methods. Images not to scale.

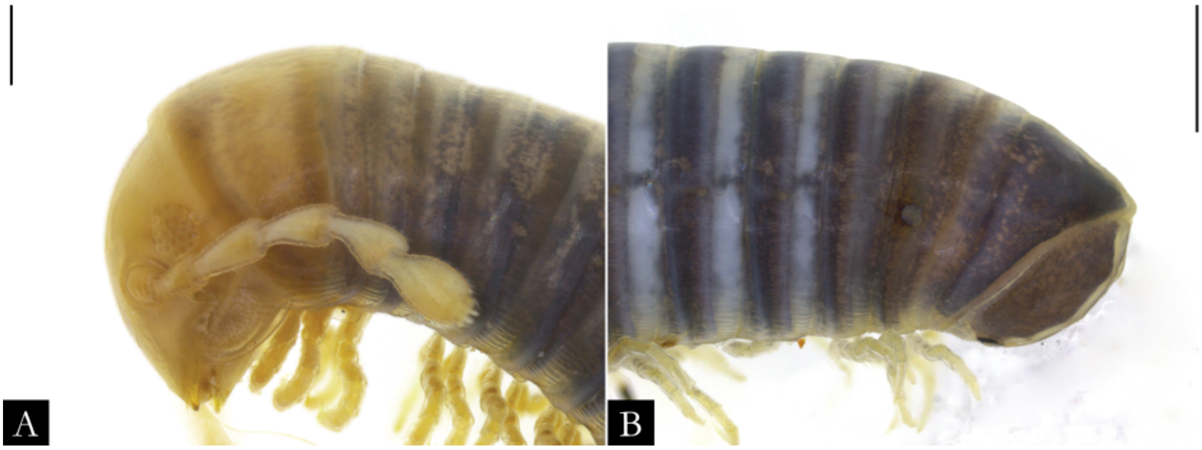

Fig. 44. *Pseudonannolene alegrensis* Silvestri, 1897 (MCN 626), in lateral view. **A**. Anterior region. **B**. Posterior region. Scale bars: A = 0.5 mm; B = 1 mm.

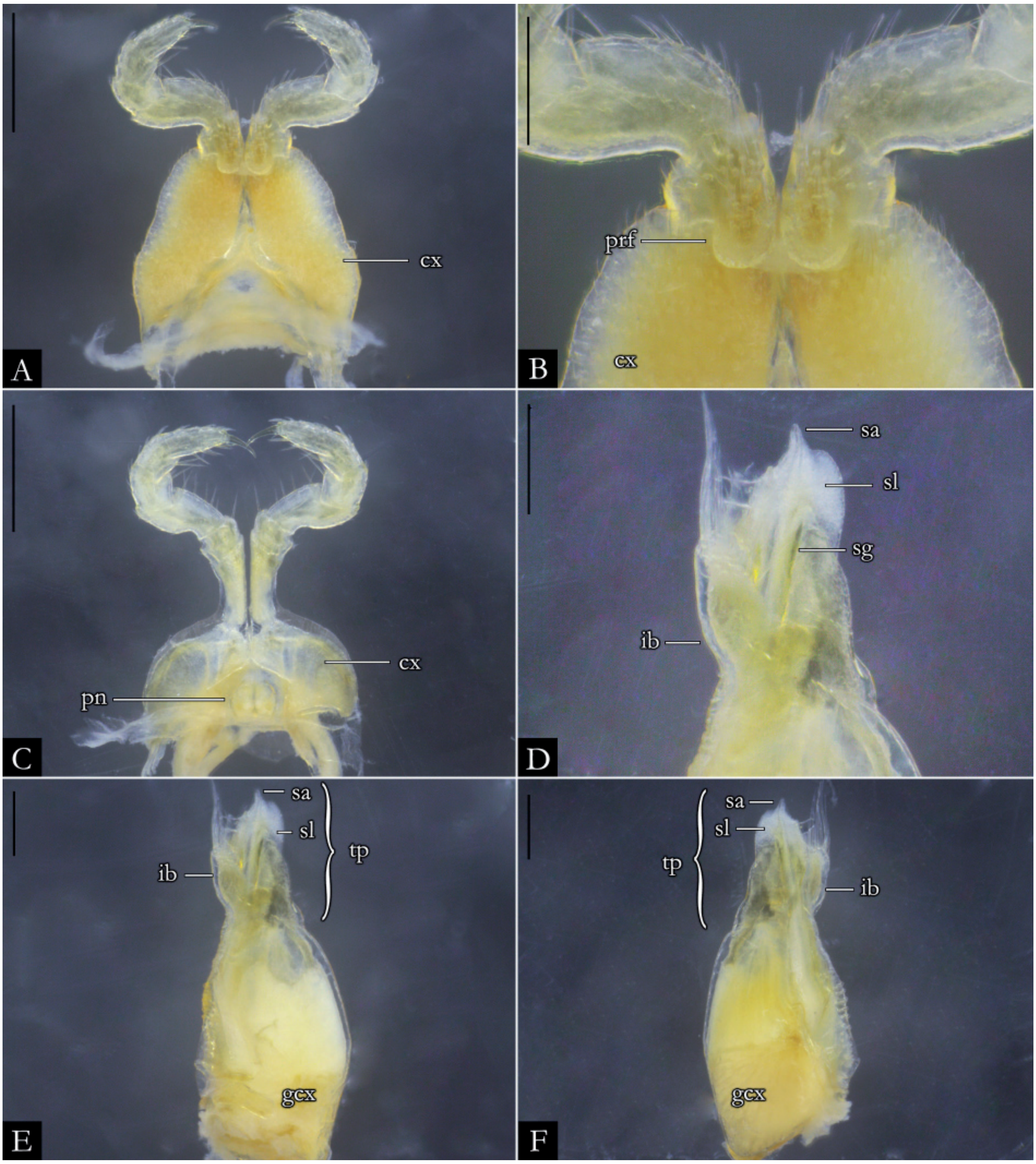

Fig. 45. *Pseudonannolene alegrensis* Silvestri, 1897, neotype, ♂ (MCN 626). **A**. First leg-pair. **B**. Detail of prefemur. **C**. Second leg-pair. **D**. Detail of telopodite, in anal view. **E**. Left gonopod, in anal view. **F**. Left gonopod, in oral view. Abbreviations: see Material and methods. Scale bars: A, C = 0.5 mm; B, D–F = 0.2 mm.

Fig. 46. *Pseudonannolene ambuatinga* Iniesta & Ferreira, 2013, paratype, ♀ (ISLA 2274), in lateral view. **A**. Anterior region. **B**. Posterior region. Scale bars: A = 0.5 mm; B = 1 mm.

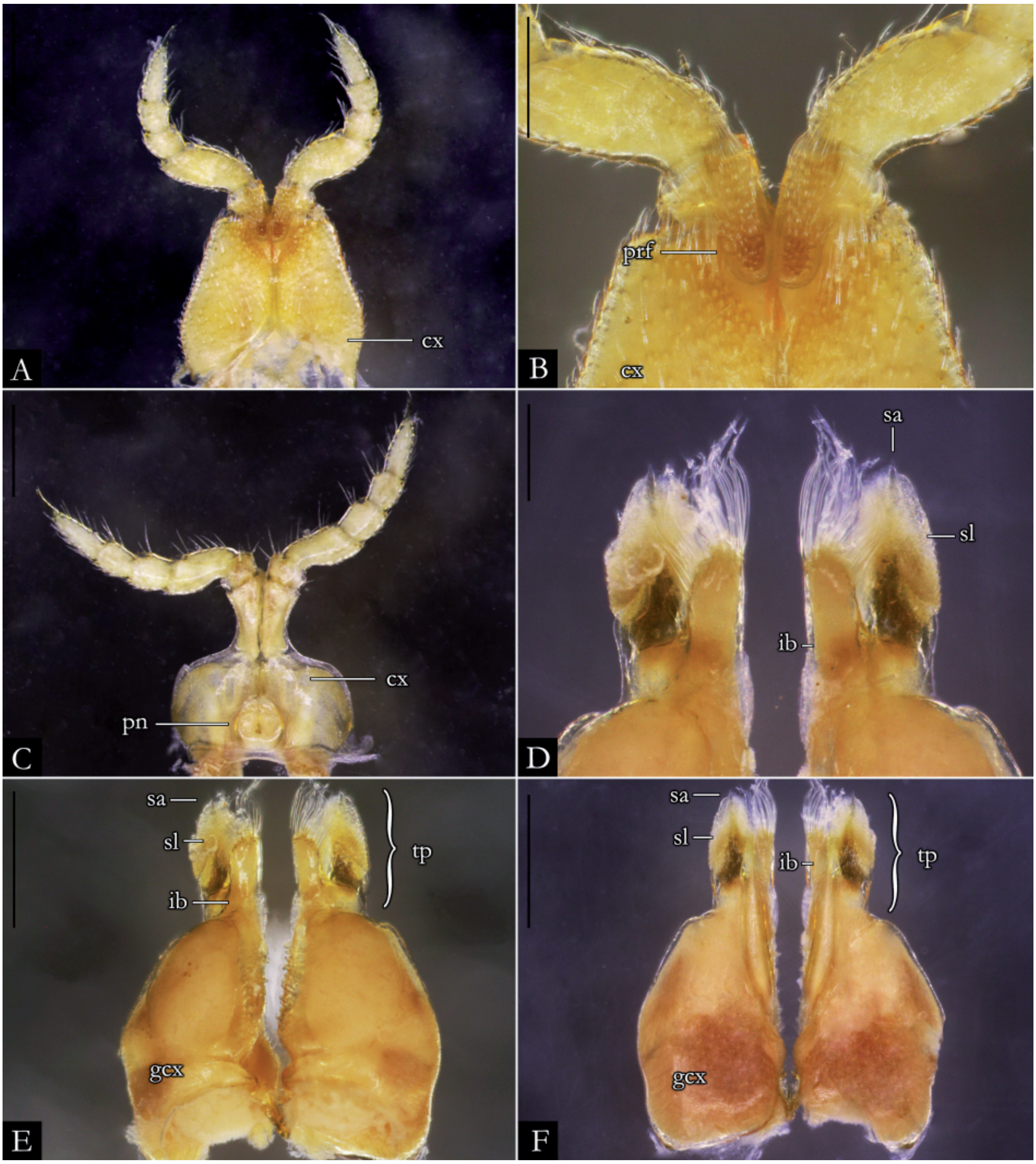

Fig. 47. *Pseudonannolene ambuatinga* Iniesta & Ferreira, 2013, ♂ (IBSP 3442). **A**. First leg-pair. **B**. Detail of prefemur. **C**. Second leg-pair. **D**. Detail of telopodites, in anal view. **E**. Gonopods, in anal view. **F**. Gonopods, in oral view. Abbreviations: see Material and methods. Scale bars: A, C, E–F = 0.5 mm; B, D = 0.2 mm.

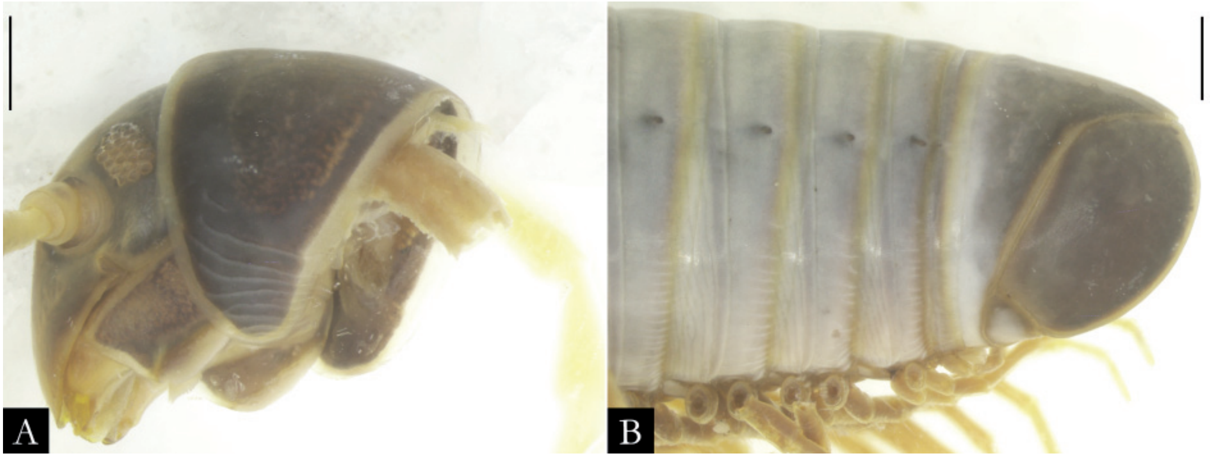

Fig. 48. *Pseudonannolene anapophysis* Fontanetti, 1996, ♂ (IBSP 5209), in lateral view. **A**. Anterior region. **B**. Posterior region. Scale bars = 1 mm.

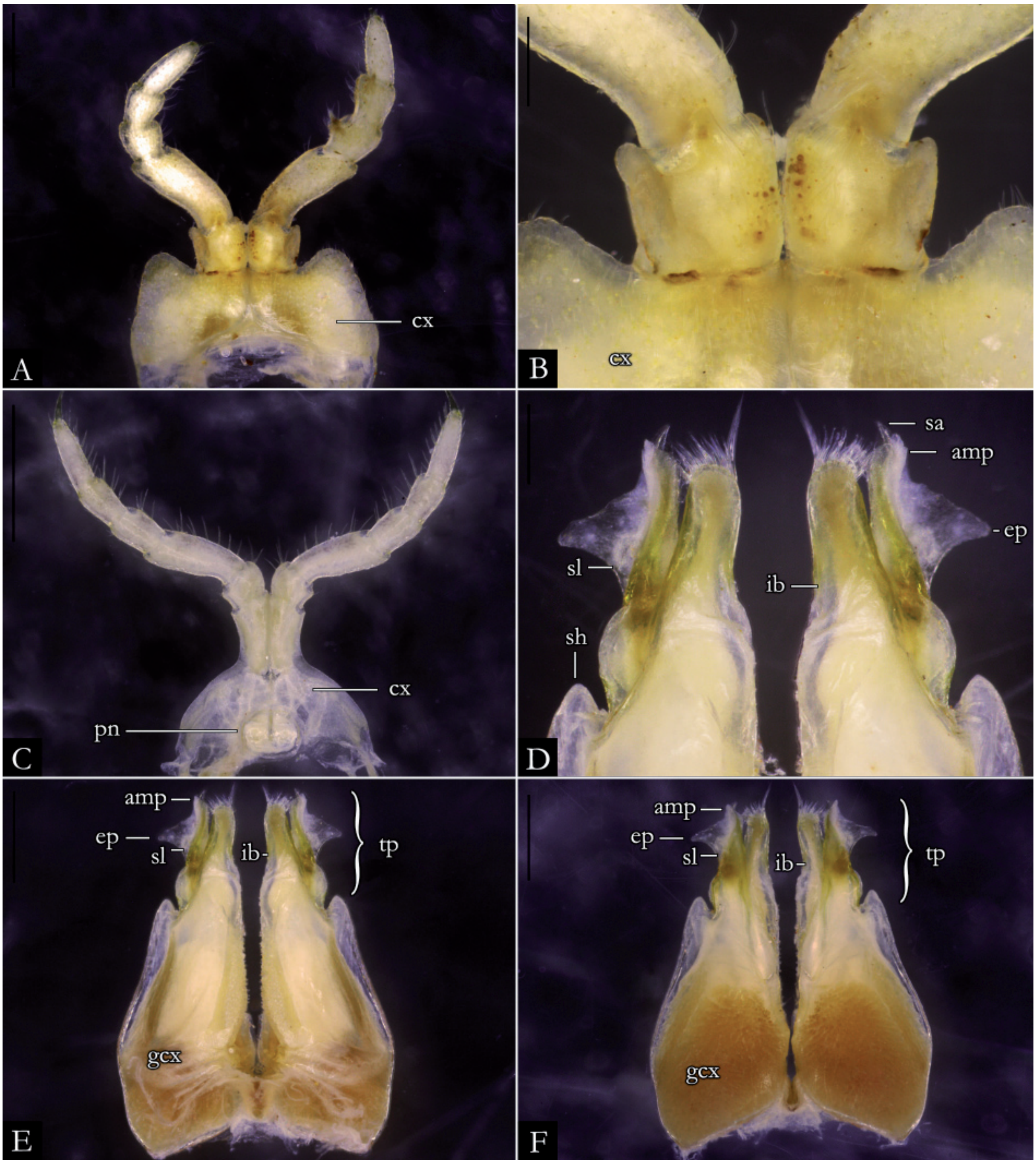

Fig. 49. *Pseudonannolene anapophysis* Fontanetti, 1996, ♂ (IBSP 5209). **A**. First leg-pair. **B**. Detail of prefemur. **C**. Second leg-pair. **D**. Detail of telopodites, in anal view. **E**. Gonopods, in anal view. **F**. Gonopods, in oral view. Abbreviations: see Material and methods. Scale bars: A, E–F = 0.5 mm; B, D = 0.2 mm; C = 1 mm.

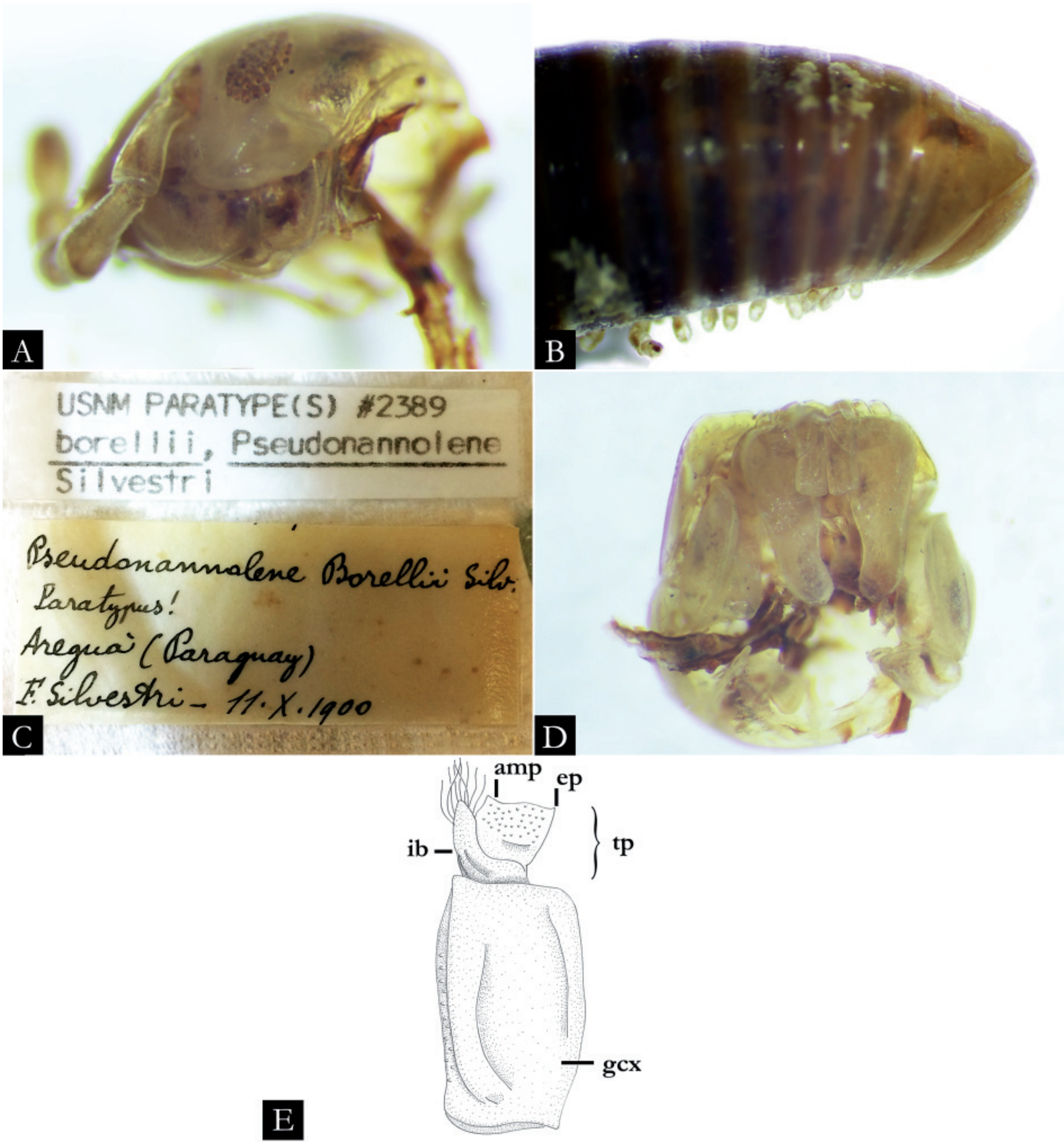

Fig. 50. *Pseudonannolene borelli* Silvestri, 1895, topotype, ♀ (USNM 2389). **A**. Head in lateral view. **B**. Posterior region. **C**. Original label of topotype (erroneously labeled as paratype by F. Silvestri). **D**. Gnathochilarium in ventral view. **E**. Schematic drawing of left gonopod in anal view (modified from Silvestri 1895b: fig. 12). Abbreviations: see Material and methods. Images not to scale.

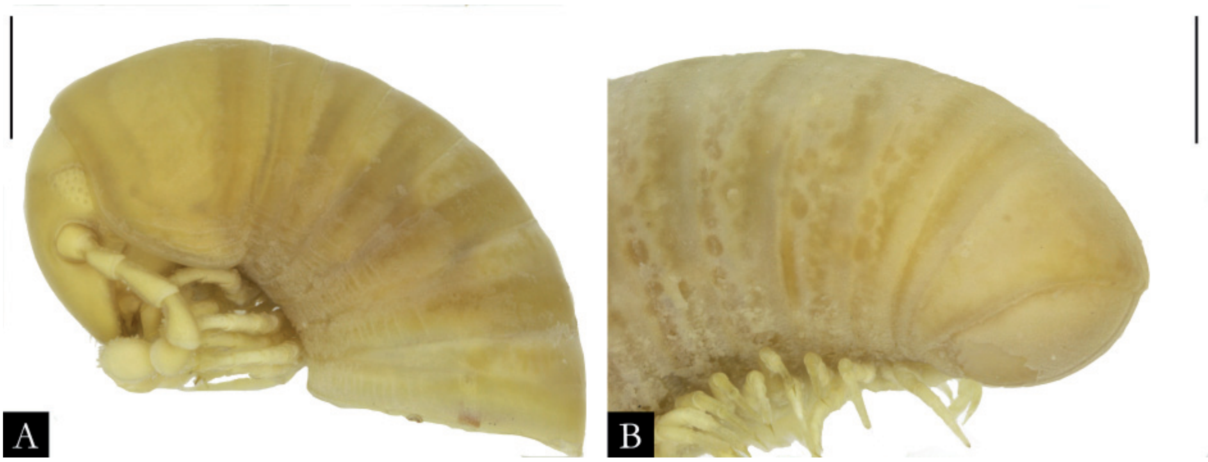

Fig. 51. *Pseudonannolene bovei* Silvestri, 1895, syntype, ♂ (MCSN), in lateral view. **A**. Anterior region. **B**. Posterior region. Scale bars = 1 mm.

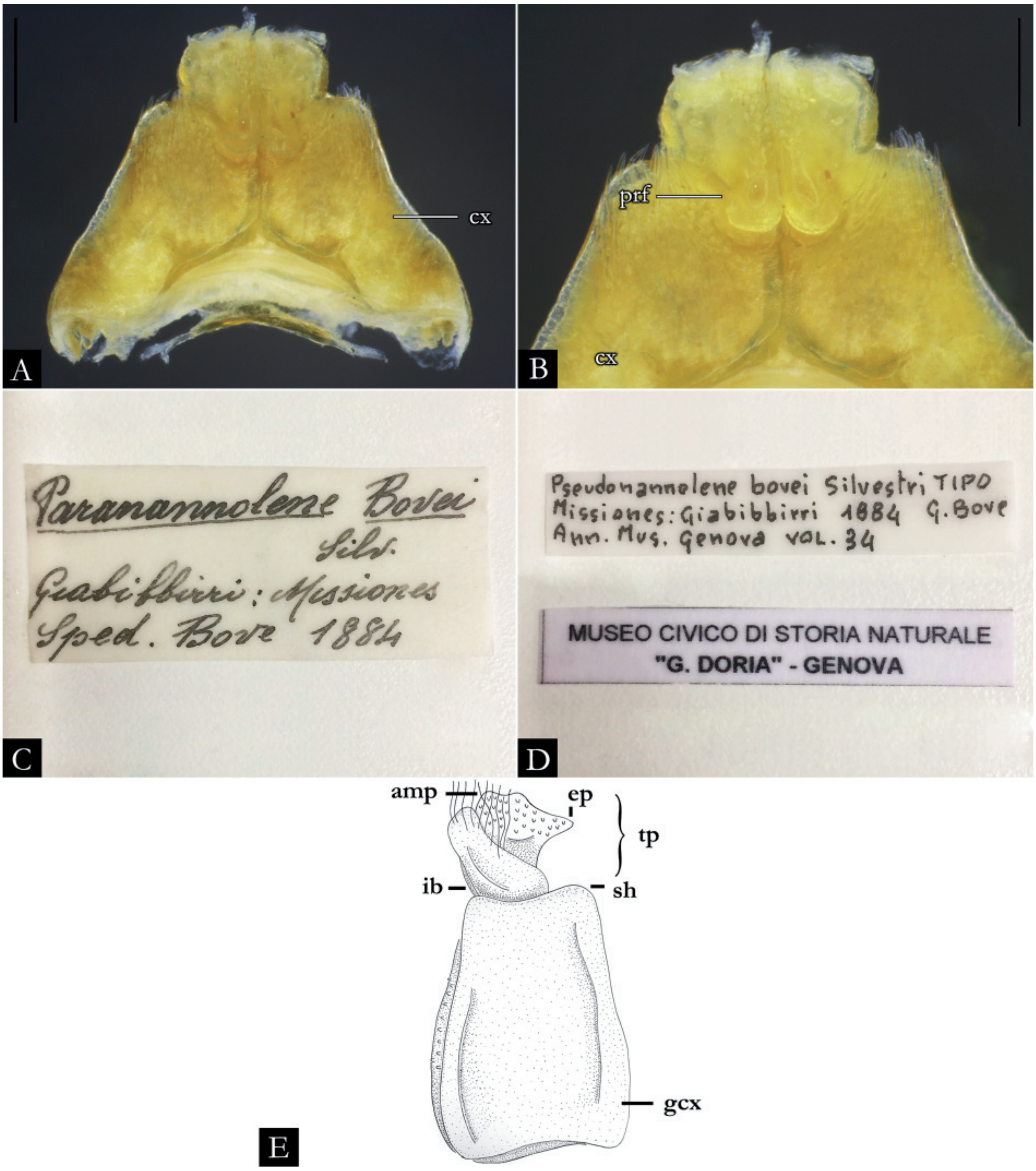

Fig. 52. *Pseudonannolene bovei* Silvestri, 1895, syntype, ♂ (MCSN). **A**. First leg-pair. **B**. Detail of prefemur. **C–D**. Original label of type material. **E**. Schematic drawing of left gonopod in anal view (modified from Silvestri 1895a: fig. 9). Abbreviations: see Material and methods. Scale bars = 0.2 mm.

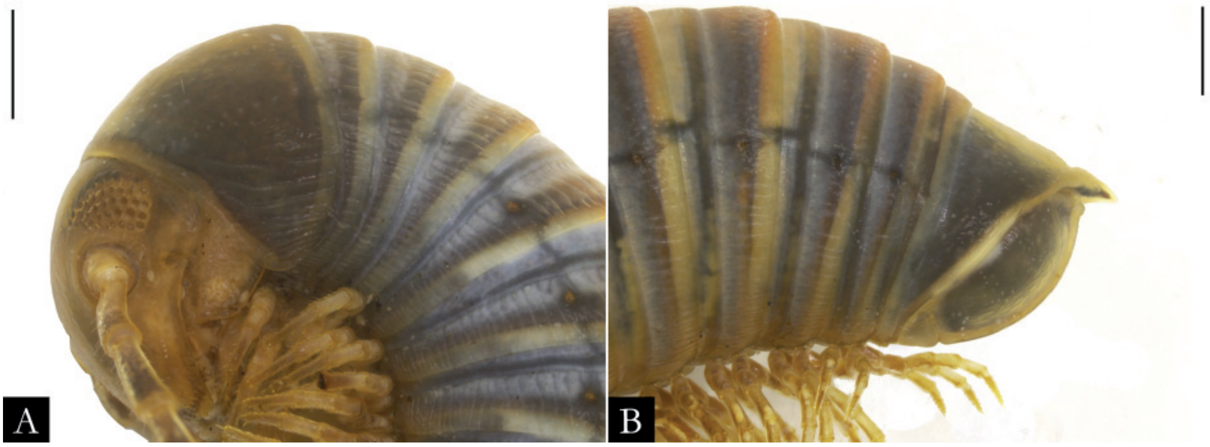

Fig. 53. *Pseudonannolene buhrnheimi* Schubart, 1960, ♀ (IBSP 2397), in lateral view. **A**. Anterior region. **B**. Posterior region. Scale bars = 1 mm.

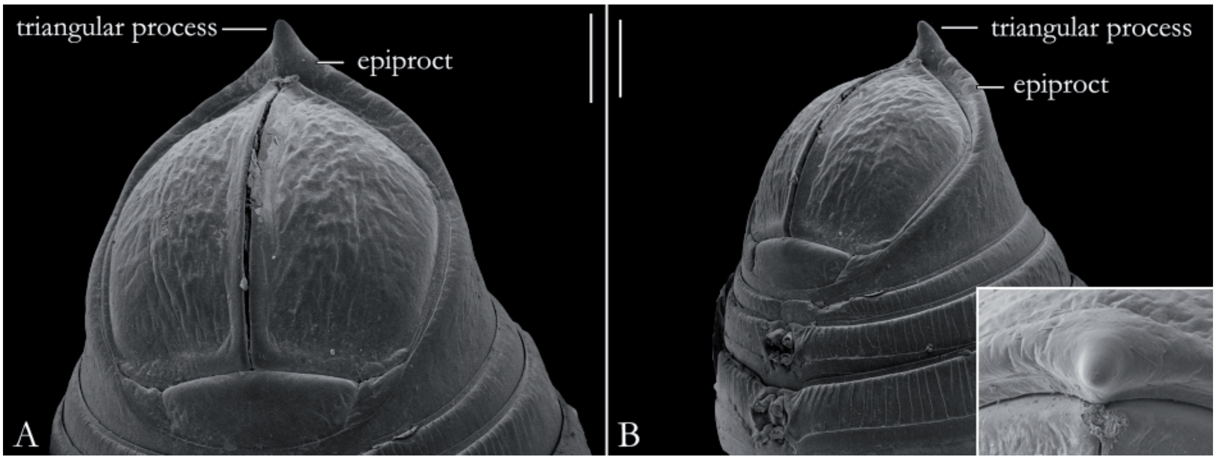

Fig. 54. *Pseudonannolene buhrnheimi* Schubart, 1960, ♀ (IBSP 2397), posterior region. **A**. Ventral view. **B**. Lateral view. Detail of epiproct with triangular process. Scale bars = 0.25 mm.

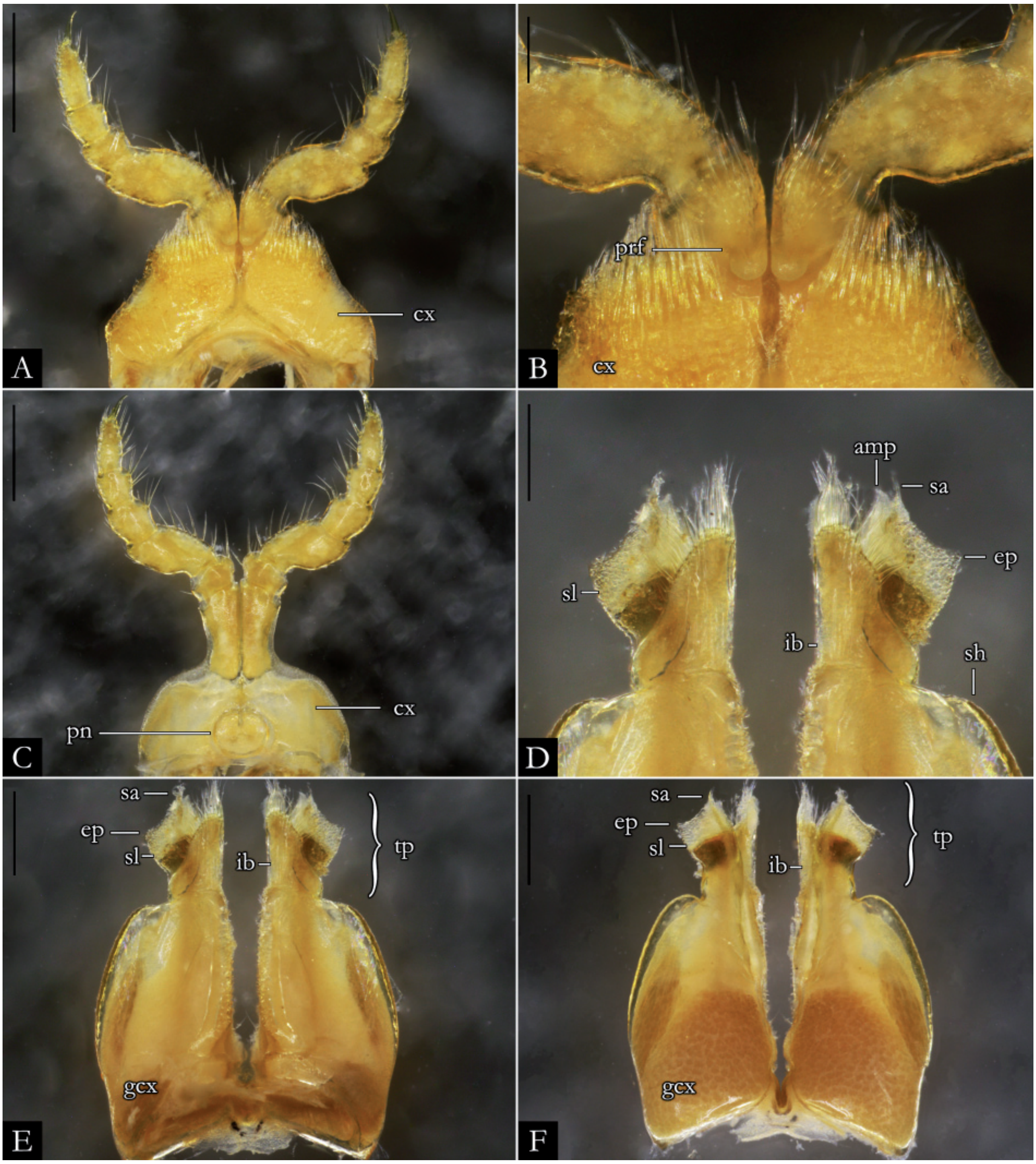

Fig. 55. *Pseudonannolene buhrnheimi* Schubart, 1960, ♂ (IBSP 2399). **A**. First leg-pair. **B**. Detail of prefemur. **C**. Second leg-pair. **D**. Detail of telopodites, in anal view. **E**. Gonopods, in anal view. **F**. Gonopods, in oral view. Abbreviations: see Material and methods. Scale bars: A, C = 0.5 mm; B, D–F = 0.2 mm.

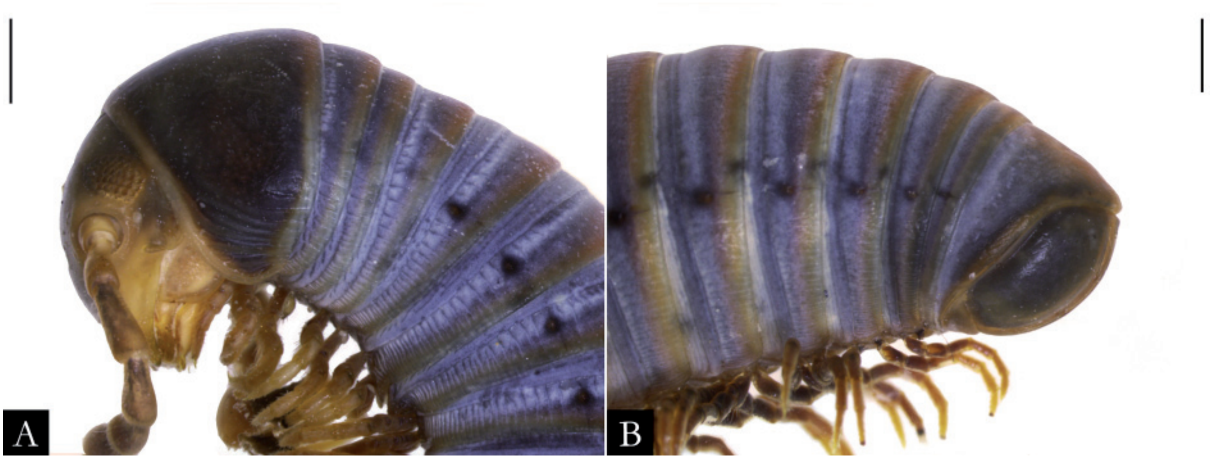

Fig. 56. *Pseudonannolene caatinga* Iniesta & Ferreira, 2014, ♂ (IBSP 2178), in lateral view. **A**. Anterior region. **B**. Posterior region. Scale bars = 1 mm.

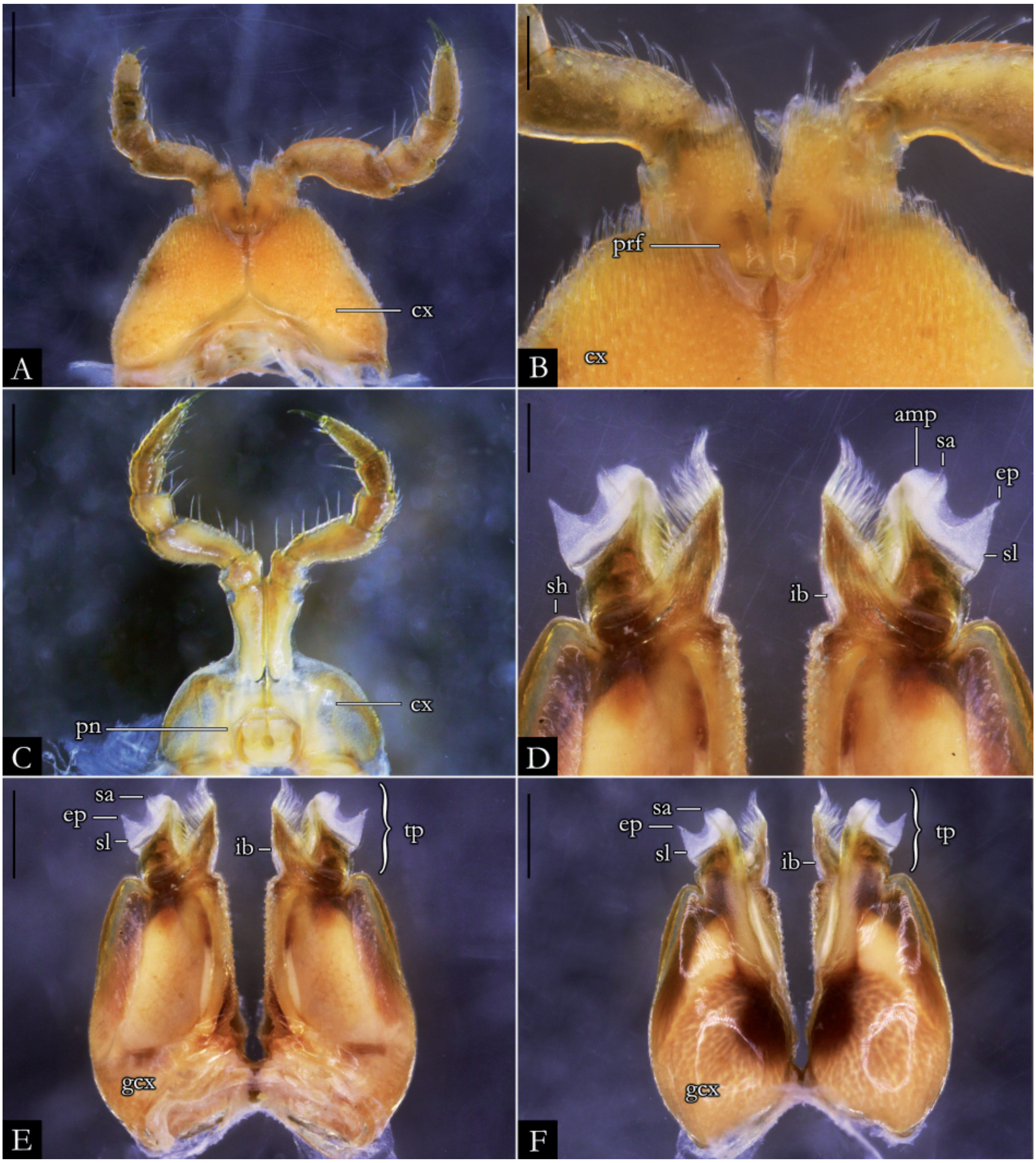

Fig. 57. *Pseudonannolene caatinga* Iniesta & Ferreira, 2014, ♂ (IBSP 2166). **A**. First leg-pair. **B**. Detail of prefemur. **C**. Second leg-pair. **D**. Detail of telopodites, in anal view. **E**. Gonopods, in anal view. **F**. Gonopods, in oral view. Abbreviations: see Material and methods. Scale bars: A, C = 0.5 mm; B, D–F = 0.2 mm.

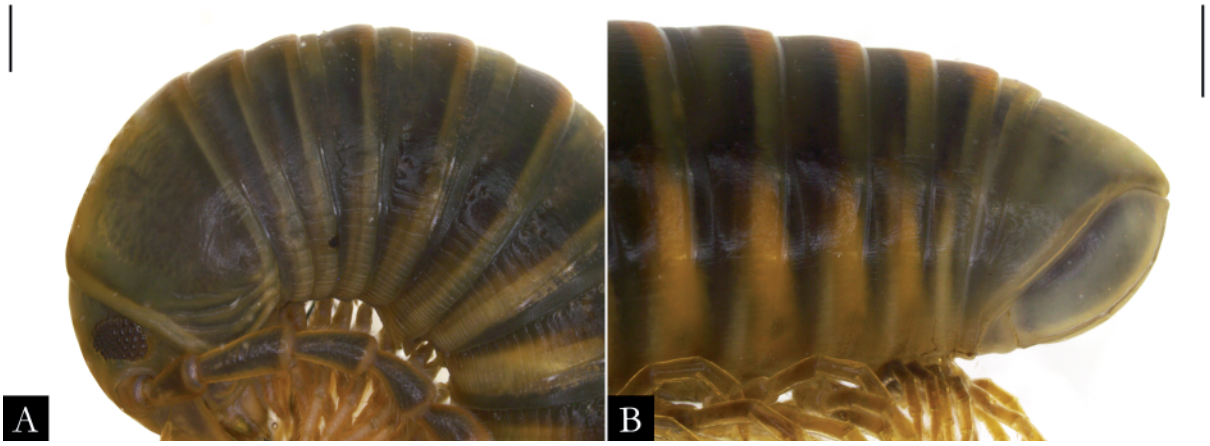

Fig. 58. *Pseudonannolene callipyge* Brölemann, 1902, ♂ (IBSP 7619), in lateral view. **A**. Anterior region. **B**. Posterior region. Scale bars = 1 mm.

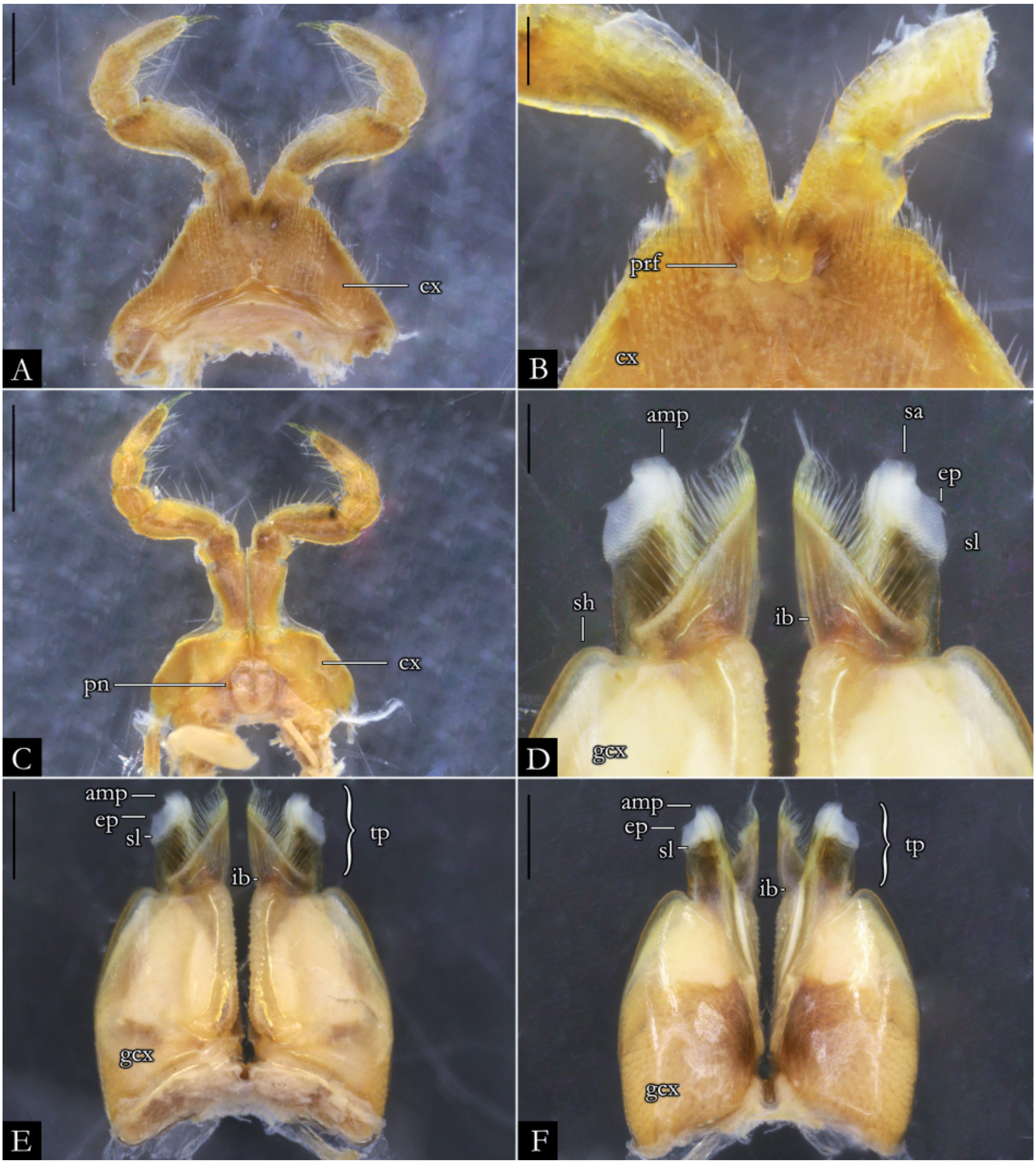

Fig. 59. *Pseudonannolene callipyge* Brölemann, 1902, ♂ (IBSP 7615). **A**. First leg-pair. **B**. Detail of prefemur. **C**. Second leg-pair. **D**. Detail of telopodites, in anal view. **E**. Gonopods, in anal view. **F**. Gonopods, in oral view. Abbreviations: see Material and methods. Scale bars: A, E–F = 0.5 mm; B, D = 0.2 mm; C = 1 mm.

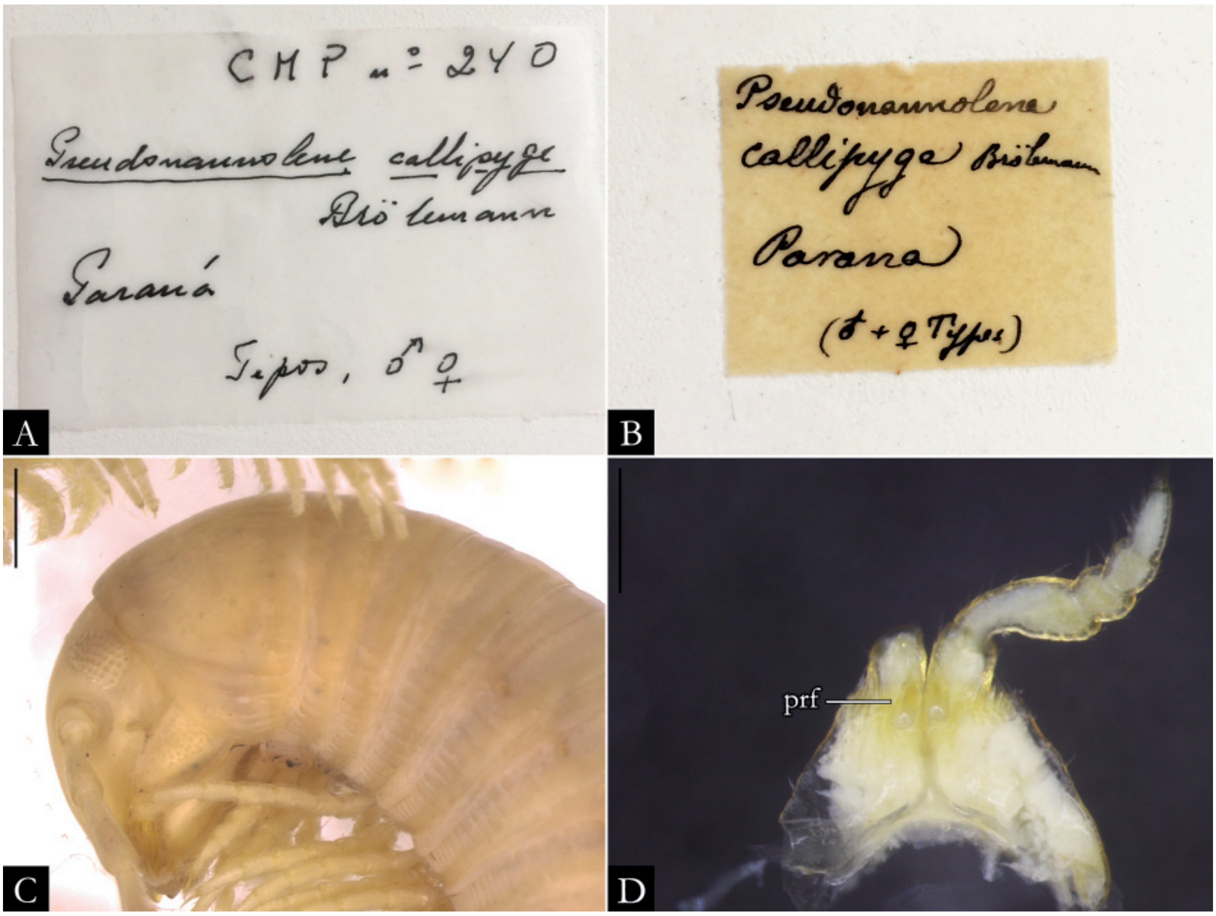

Fig. 60. *Pseudonannolene callipyge* Brölemann, 1902, ♂ (MZSP). **A–B**. Original label of type material. **C**. Anterior region. **D**. First leg-pair. Abbreviation: see Material and methods. Scale bars: C = 1 mm; D = 0.5 mm.

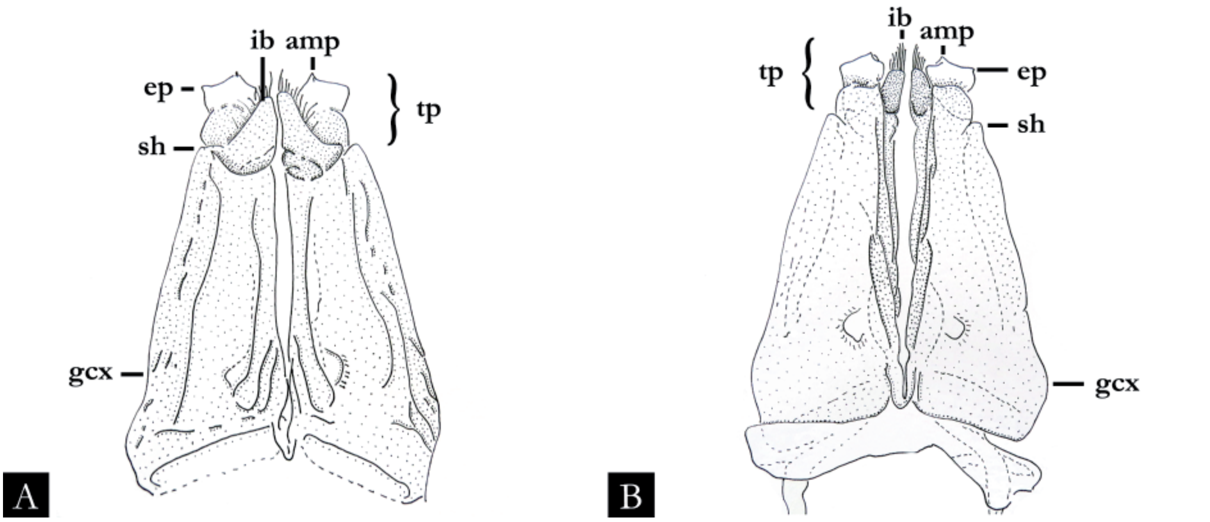

Fig. 61. Schematic drawings of gonopods of *Pseudonannolene caulleryi* Brölemann, 1929 (modified from Brölemann 1929: figs 24–25). **A**. Oral view. **B**. Anal view. Abbreviations: see Material and methods. Images not to scale.

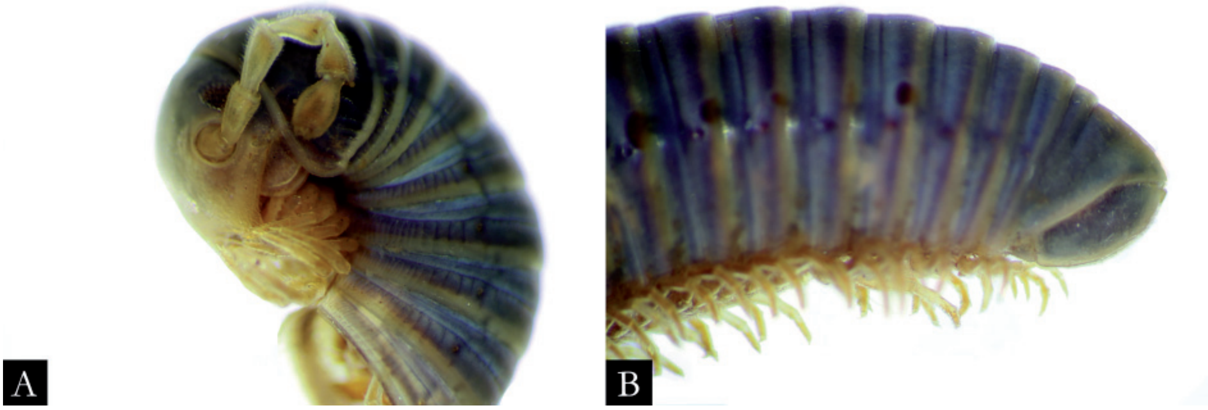

Fig. 62. *Pseudonannolene centralis* Silvestri, 1902, syntype, ♂ (USNM 2033), in lateral view. **A**. Anterior region. **B**. Posterior region. Images not to scale.

Fig. 63. *Pseudonannolene centralis* Silvestri, 1902, syntype, ♂ (USNM 2033). **A**. First leg-pair. **B**. Second leg-pair. **C**. Gonopods, in anal view. **D**. Detail of telopodites, in anal view. **E**. Original label of type material. **F**. Body of female syntype, in lateral view (ZMB 2884). Abbreviations: see Material and methods. Images not to scale.

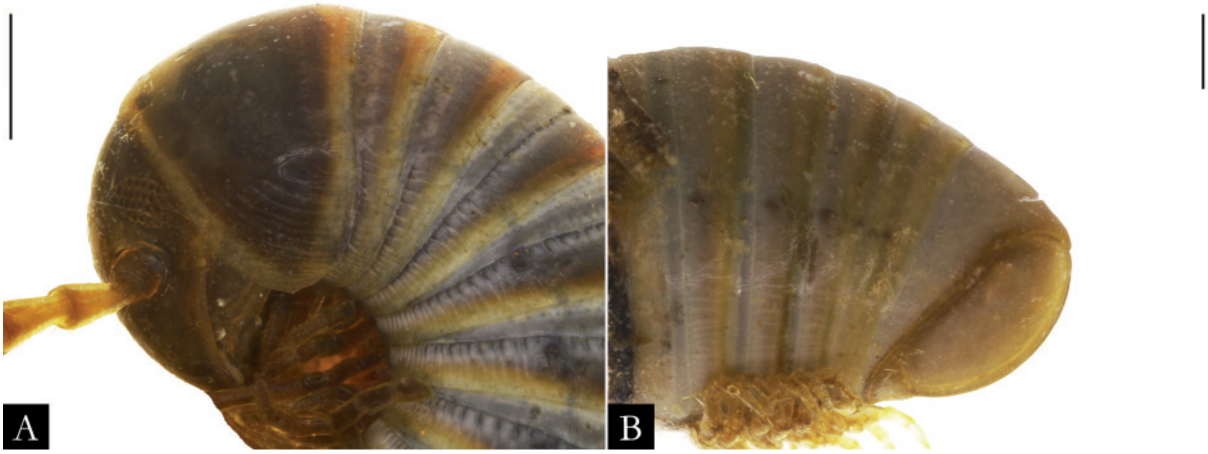

Fig. 64. *Pseudonannolene curtipes* Schubart, 1960, paratype. ♀ (MZSP 1022), in lateral view. **A**. Anterior region. **B**. Posterior region. Scale bars = 1 mm.

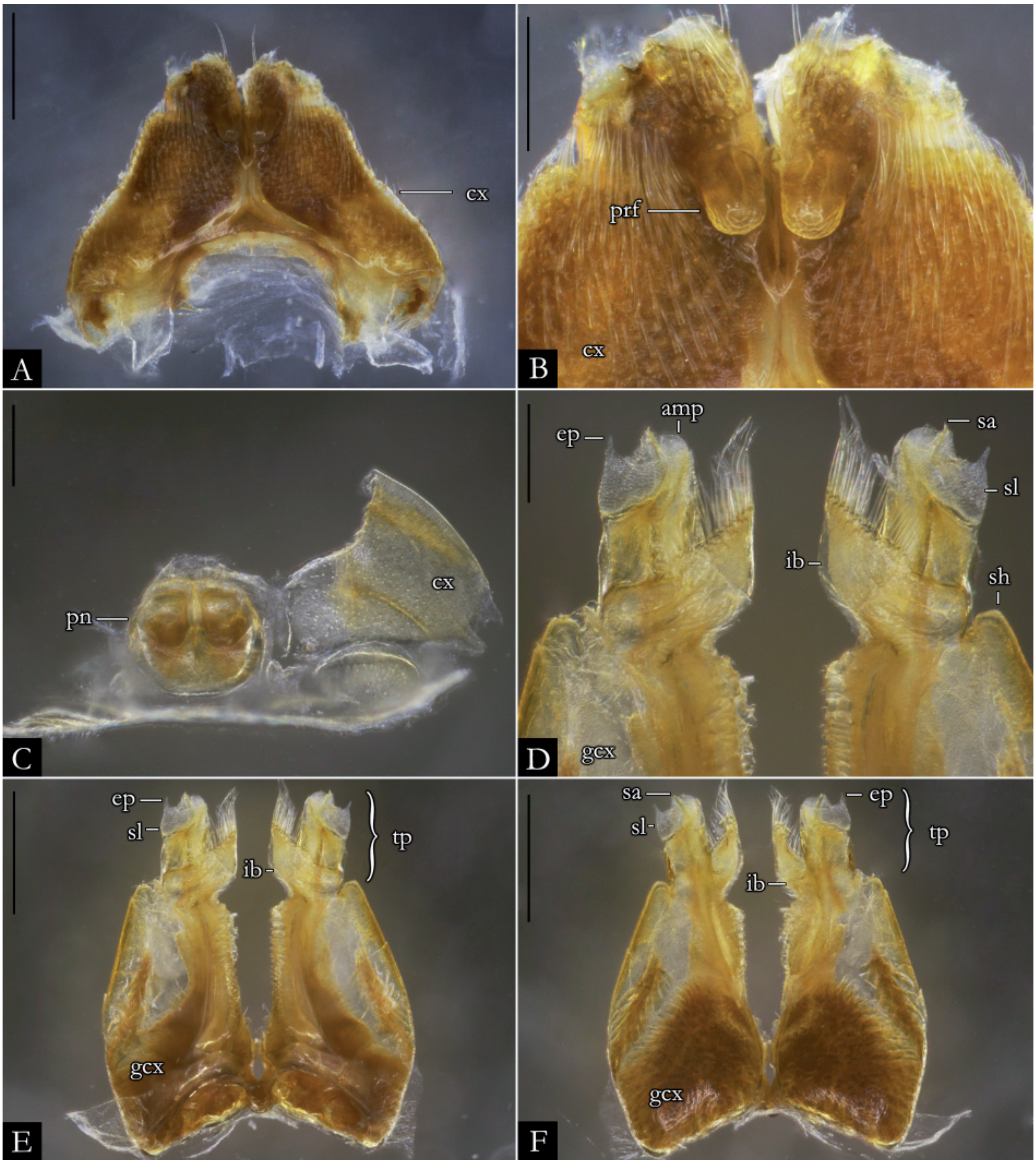

Fig. 65. *Pseudonannolene curtipes* Schubart, 1960, paratype. ♂ (MZSP 1027). **A**. First leg-pair. **B**. Detail of prefemur. **C**. Second leg-pair. **D**. Detail of telopodites, in anal view. **E**. Gonopods, in anal view. **F**. Gonopods, in oral view. Abbreviations: see Material and methods. Scale bars: A, E–F = 0.5 mm; B–D = 0.2 mm.

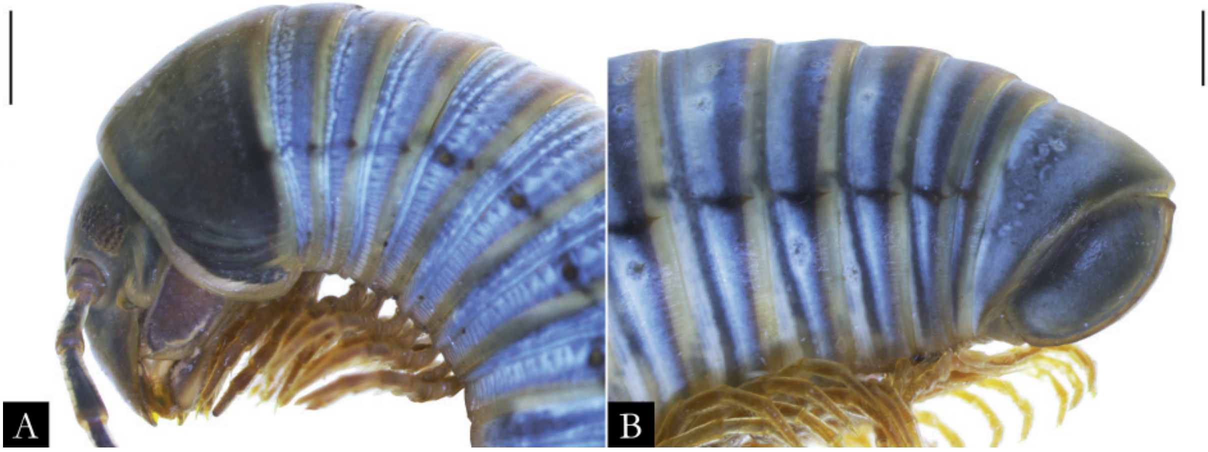

Fig. 66. *Pseudonannolene erikae* Iniesta & Ferreira, 2014, ♀ (IBSP 3331), in lateral view. **A**. Anterior region. **B**. Posterior region. Scale bars = 1 mm.

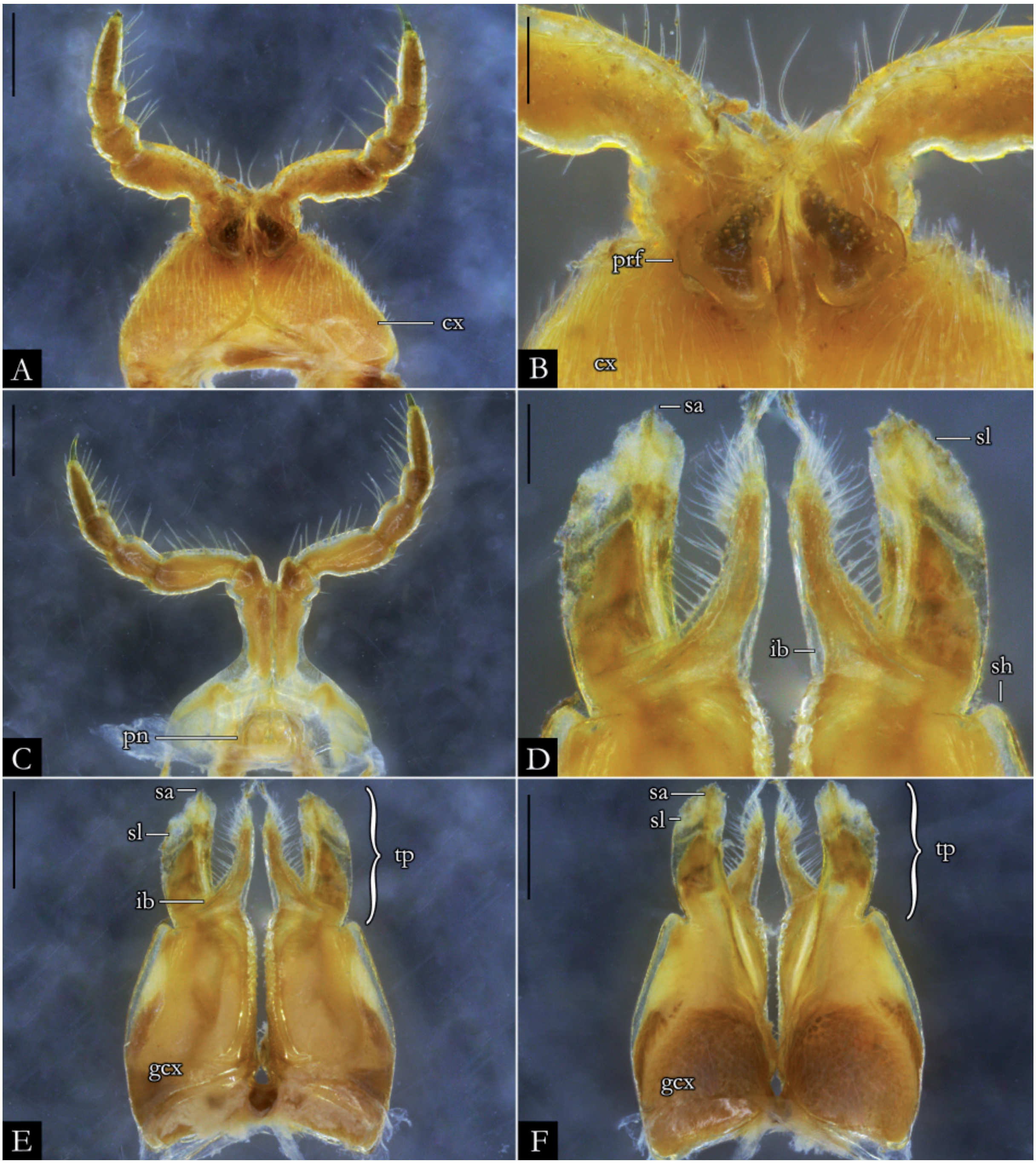

Fig. 67. *Pseudonannolene erikae* Iniesta & Ferreira, 2014, ♂ (IBSP 3331). **A**. First leg-pair. **B**. Detail of prefemur. **C**. Second leg-pair. **D**. Detail of telopodites, in anal view. **E**. Gonopods, in anal view. **F**. Gonopods, in oral view. Abbreviations: see Material and methods. Scale bars: A, E–F = 0.5 mm; B–D = 0.2 mm.

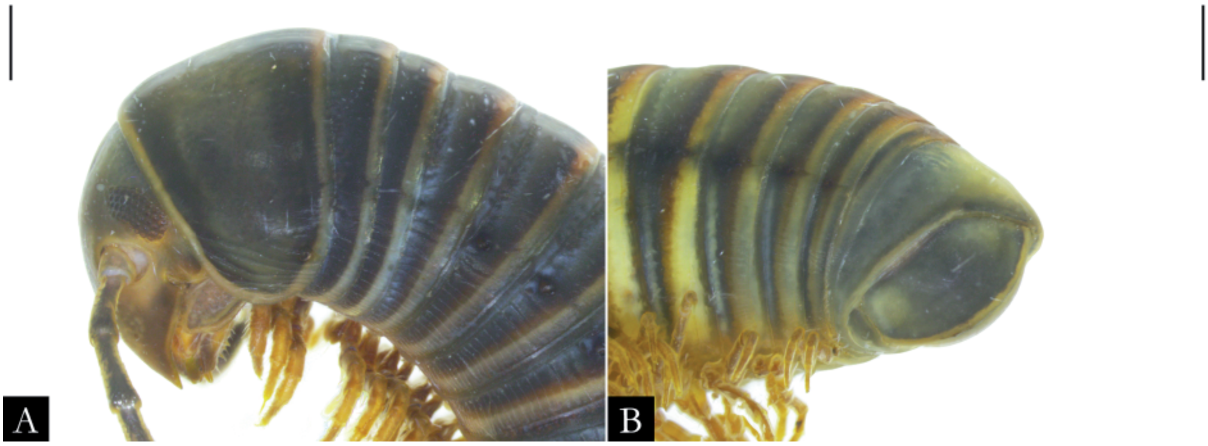

Fig. 68. *Pseudonannolene fontanettiae* Iniesta & Ferreira, 2014, ♀ (IBSP 3759), in lateral view. **A**. Anterior region. **B**. Posterior region. Scale bars = 1 mm.

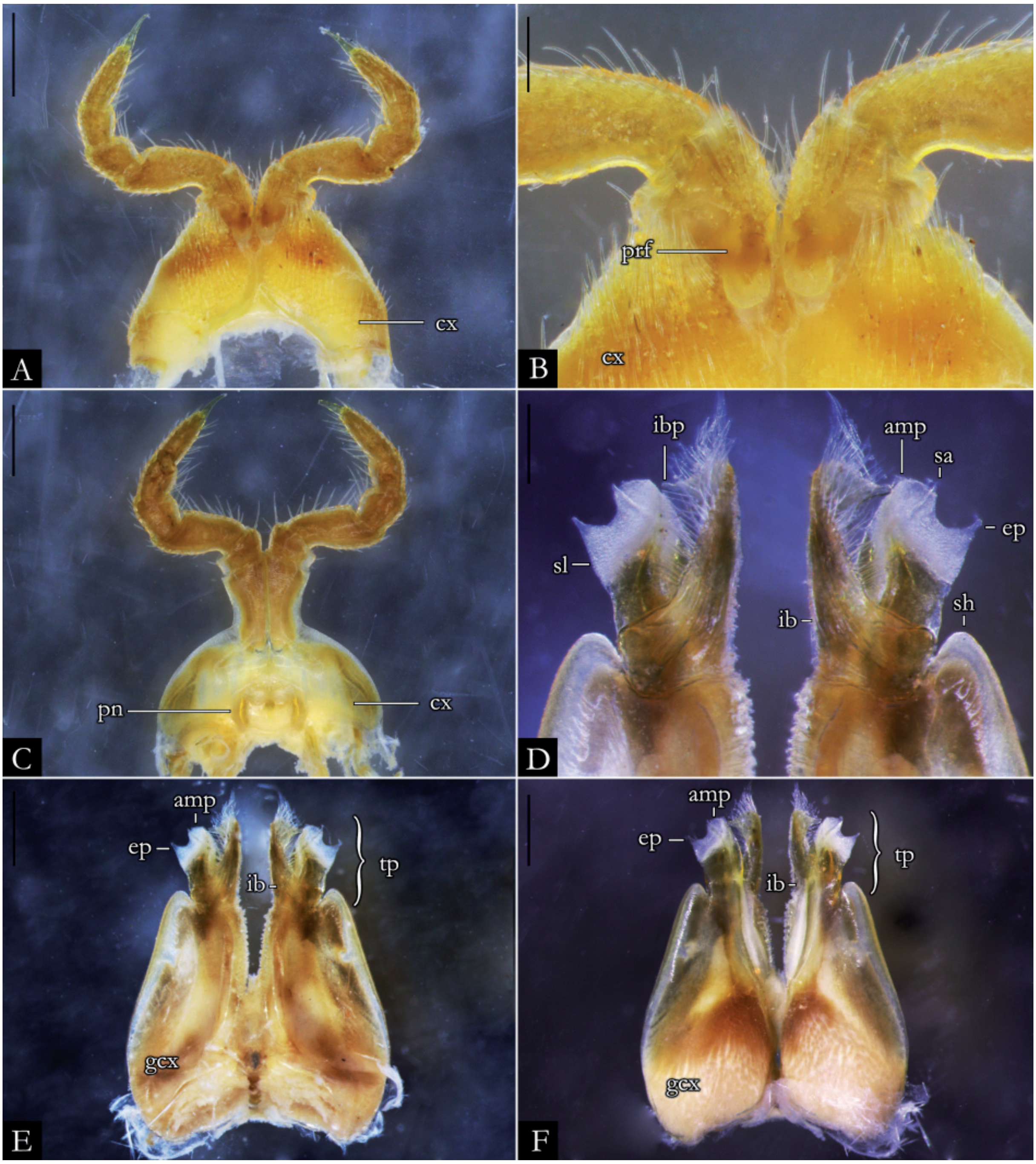

Fig. 69. *Pseudonannolene fontanettiae* Iniesta & Ferreira, 2014, ♂ (IBSP 3760). **A**. First leg-pair. **B**. Detail of prefemur. **C**. Second leg-pair. **D**. Detail of telopodites, in anal view. **E**. Gonopods, in anal view. **F**. Gonopods, in oral view. Abbreviations: see Material and methods. Scale bars: A, E–F = 0.5 mm; B–D = 0.2 mm.

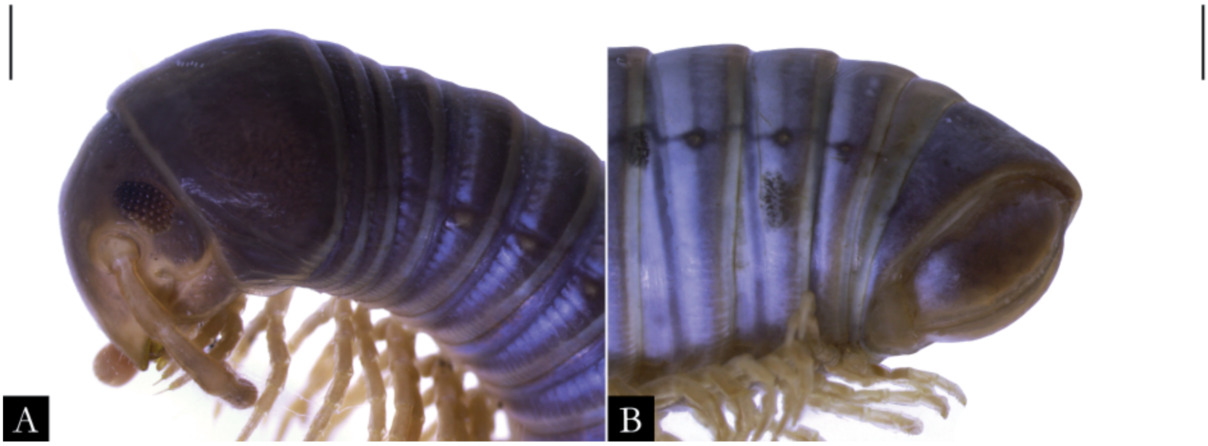

Fig. 70. *Pseudonannolene halophila* Schubart, 1949, ♀ (IBSP 1101), in lateral view. **A**. Anterior region. **B**. Posterior region. Scale bars = 0.5 mm.

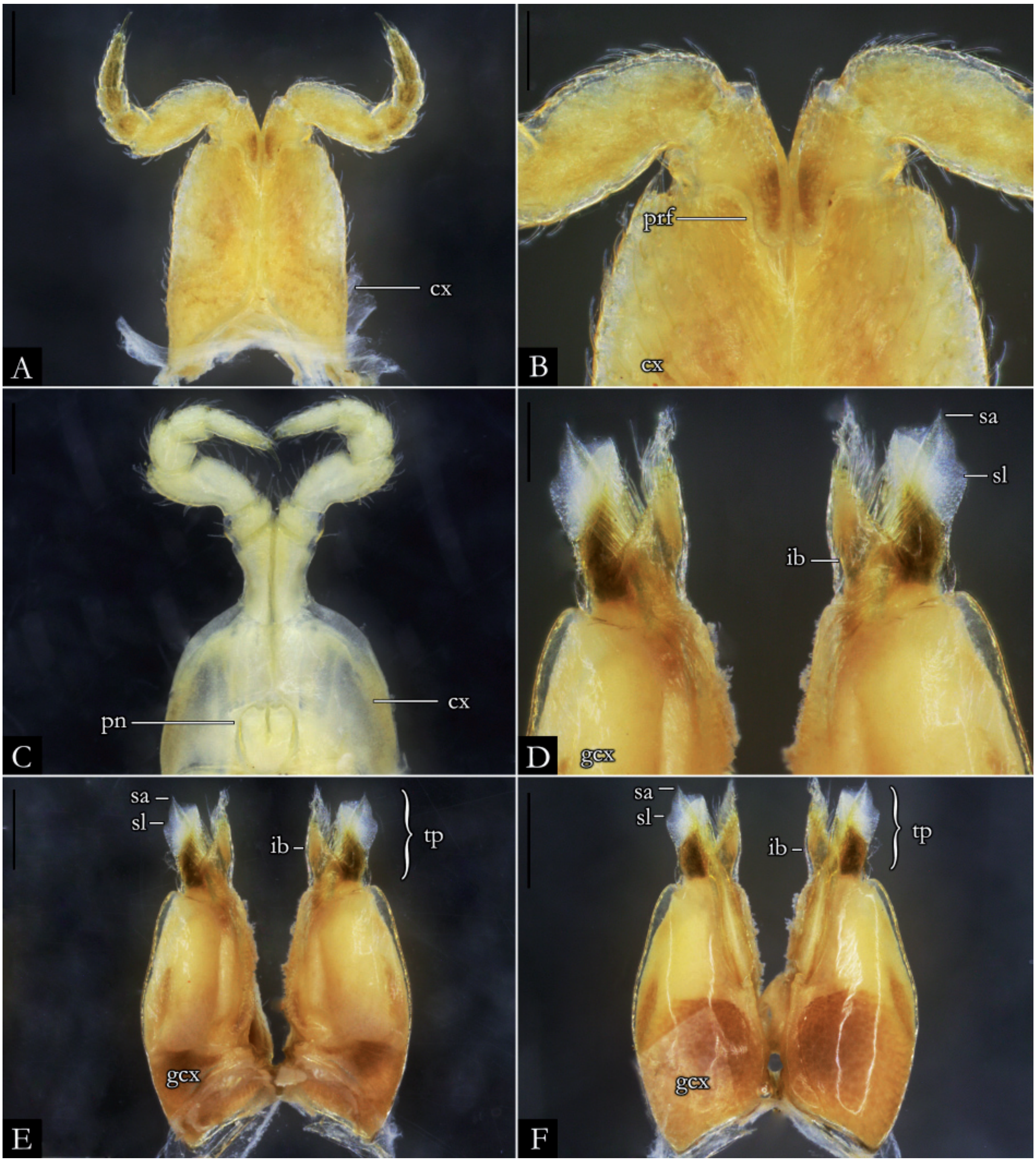

Fig. 71. *Pseudonannolene halophila* Schubart, 1949, ♂ (IBSP 3671). **A**. First leg-pair. **B**. Detail of prefemur. **C**. Second leg-pair. **D**. Detail of telopodites, in anal view. **E**. Gonopods, in anal view. **F**. Gonopods, in oral view. Abbreviations: see Material and methods. Scale bars: A, E–F = 0.5 mm; B–D = 0.2 mm.

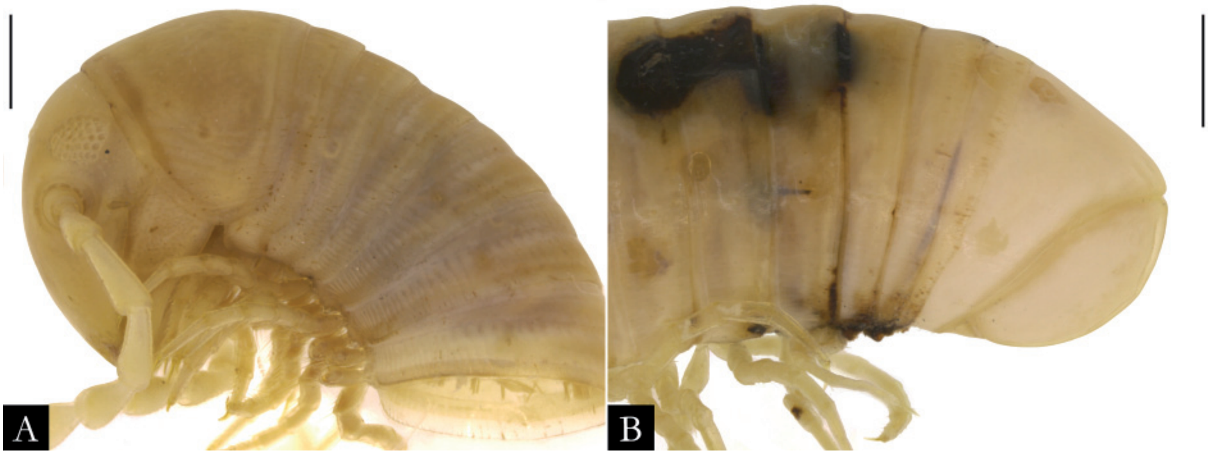

Fig. 72. *Pseudonannolene imbirensis* Fontanetti, 1996, paratype, ♀ (MZSP 1030), in lateral view. **A**. Anterior region. **B**. Posterior region. Scale bars = 1 mm.

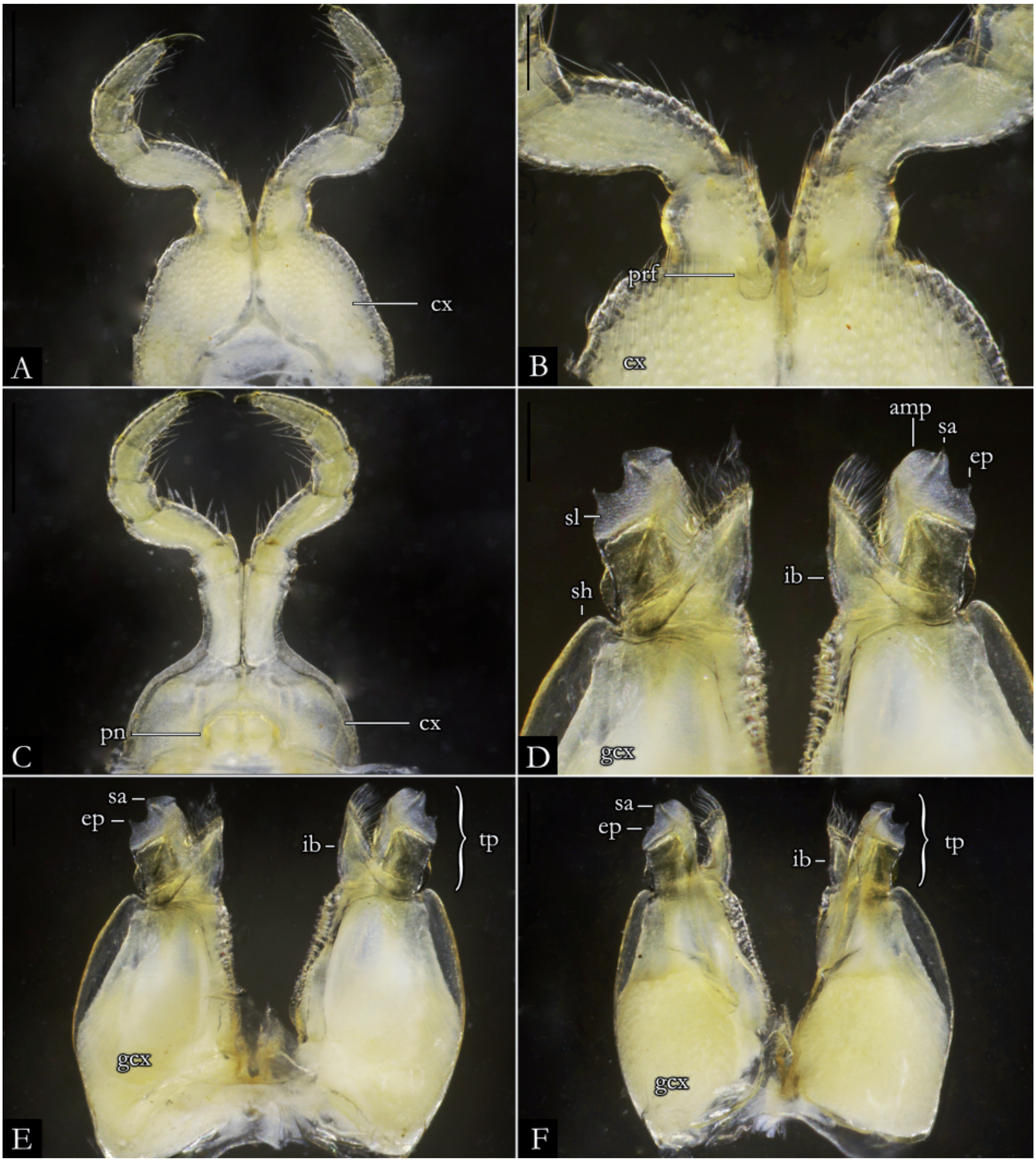

Fig. 73. *Pseudonannolene imbirensis* Fontanetti, 1996, holotype, ♂ (MZSP 1035). **A**. First leg-pair. **B**. Detail of prefemur. **C**. Second leg-pair. **D**. Detail of telopodites, in anal view. **E**. Gonopods, in anal view. **F**. Gonopods, in oral view. Abbreviations: see Material and methods. Scale bars: A, E–F = 0.5 mm; B–D = 0.2 mm.

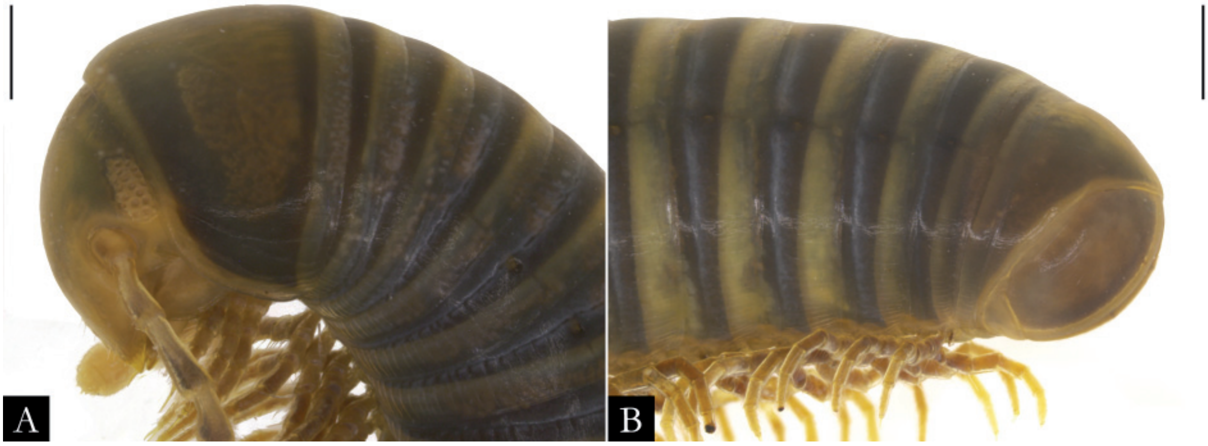

Fig. 74. *Pseudonannolene inops* Brölemann, 1929, ♂ (IBSP 2559), in lateral view. **A**. Anterior region. **B**. Posterior region. Scale bars = 1 mm.

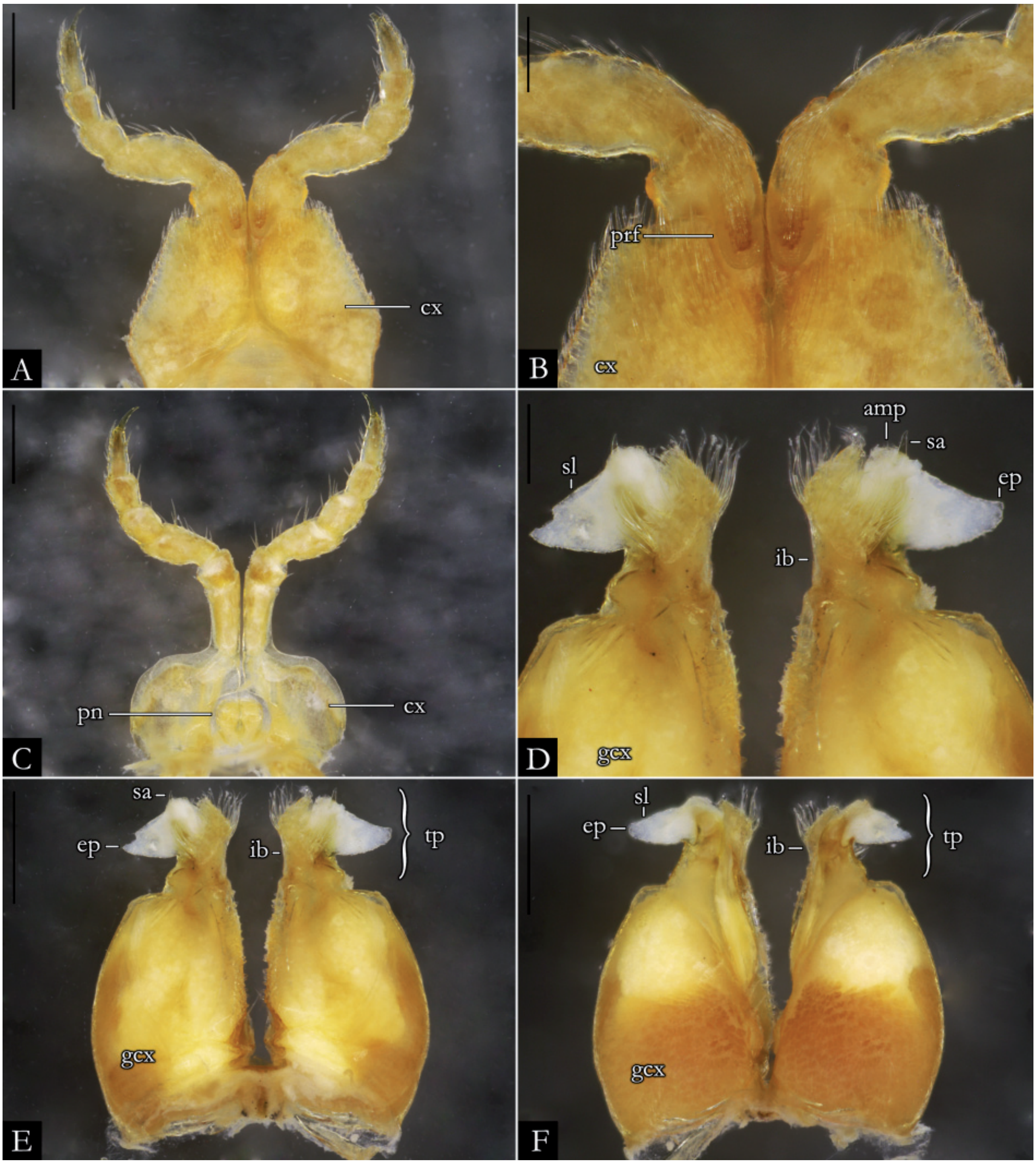

Fig. 75. *Pseudonannolene inops* Brölemann, 1929, ♂ (IBSP 2559). **A**. First leg-pair. **B**. Detail of prefemur. **C**. Second leg-pair. **D**. Detail of telopodites, in anal view. **E**. Gonopods, in anal view. **F**. Gonopods, in oral view. Abbreviations: see Material and methods. Scale bars: A, E–F = 0.5 mm; B–D = 0.2 mm.

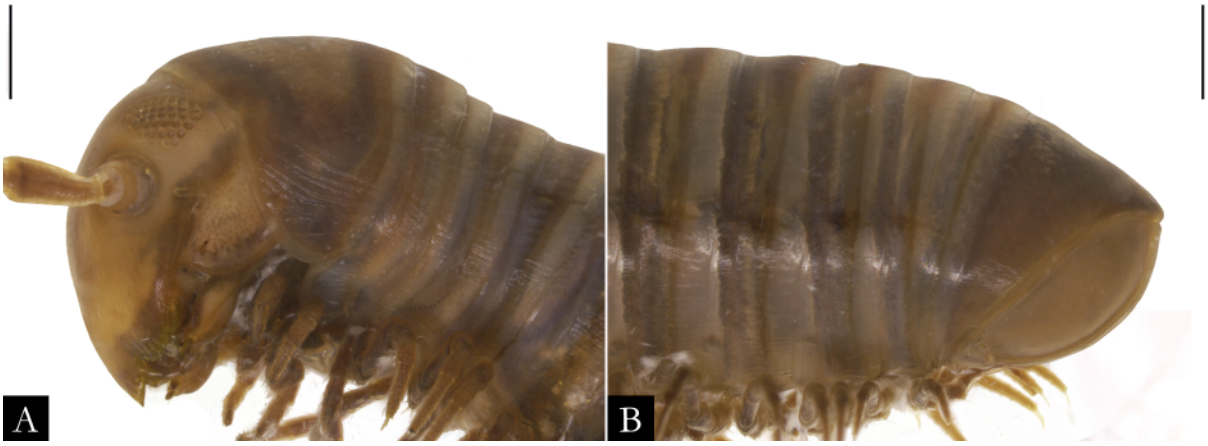

Fig. 76. *Pseudonannolene leopoldoi* Iniesta & Ferreira, 2014, paratype, ♂ (ISLA 4127), in lateral view. **A**. Anterior region. **B**. Posterior region. Scale bars = 1 mm.

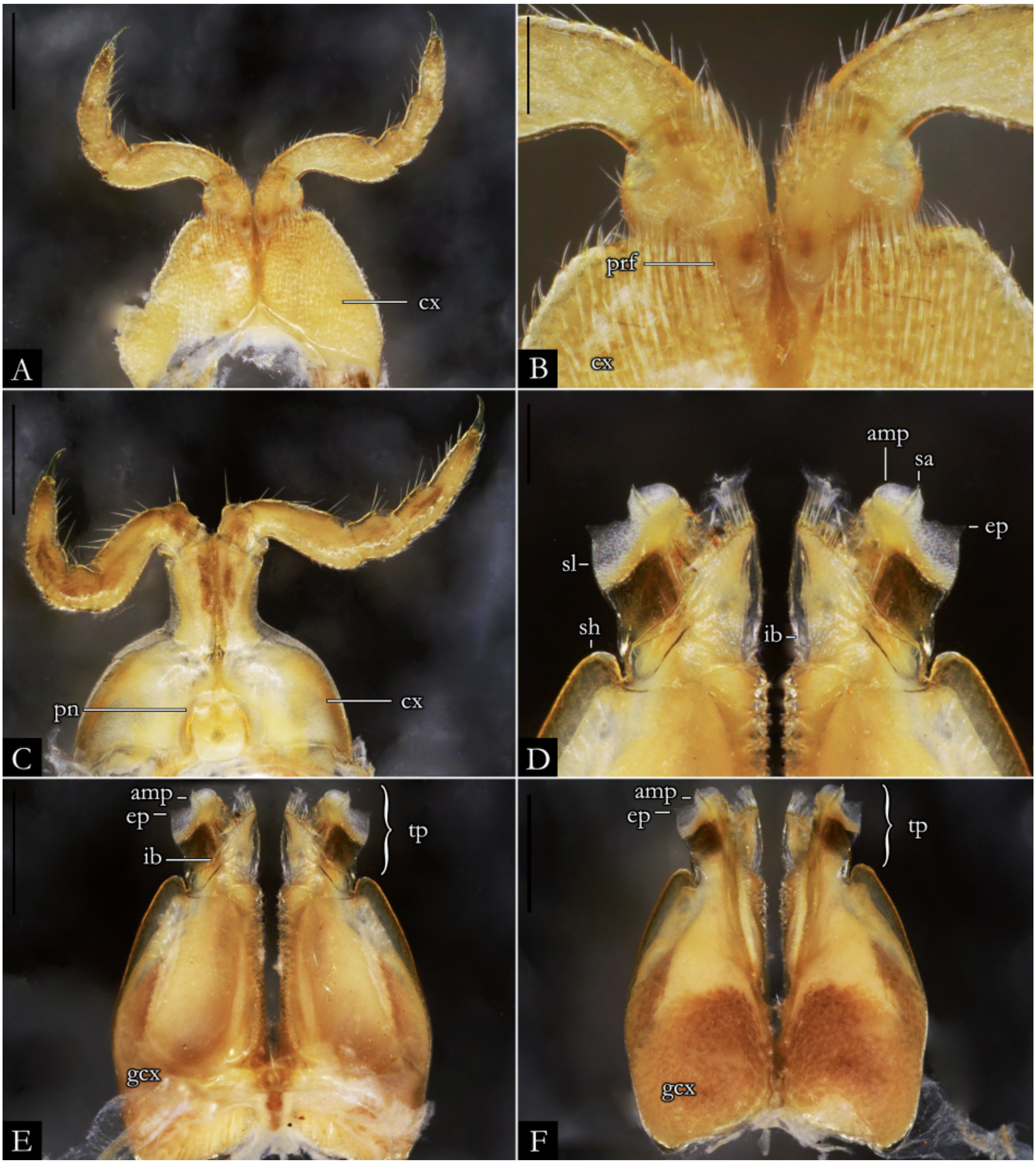

Fig. 77. *Pseudonannolene leopoldoi* Iniesta & Ferreira, 2014, paratype, ♂ (ISLA 4125). **A**. First leg-pair. **B**. Detail of prefemur. **C**. Second leg-pair. **D**. Detail of telopodites, in anal view. **E**. Gonopods, in anal view. **F**. Gonopods, in oral view. Abbreviations: see Material and methods. Scale bars: A, E–F = 0.5 mm; B–D = 0.2 mm.

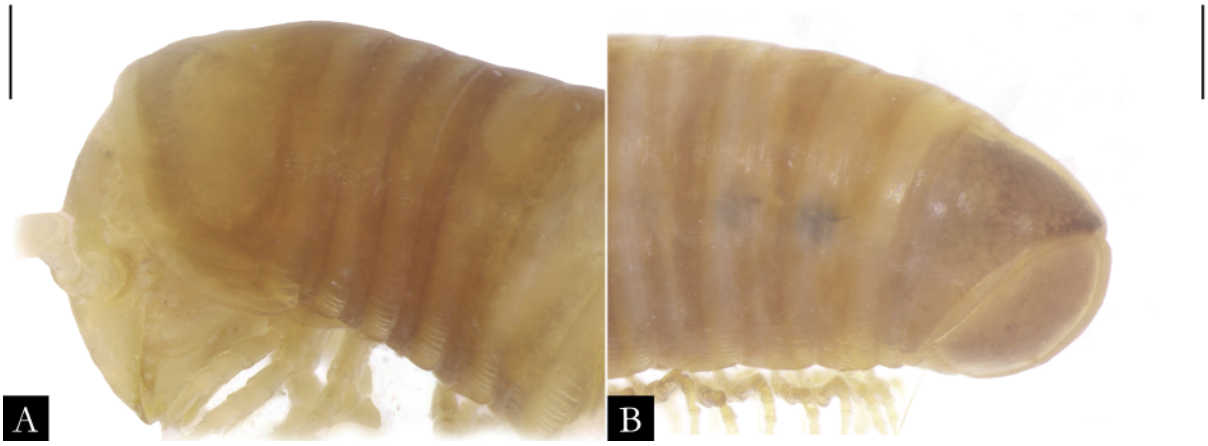

Fig. 78. *Pseudonannolene leucocephalus* Schubart, 1944, ♂ (MZSP 1060), in lateral view. **A**. Anterior region. **B**. Posterior region. Scale bars = 0.5 mm.

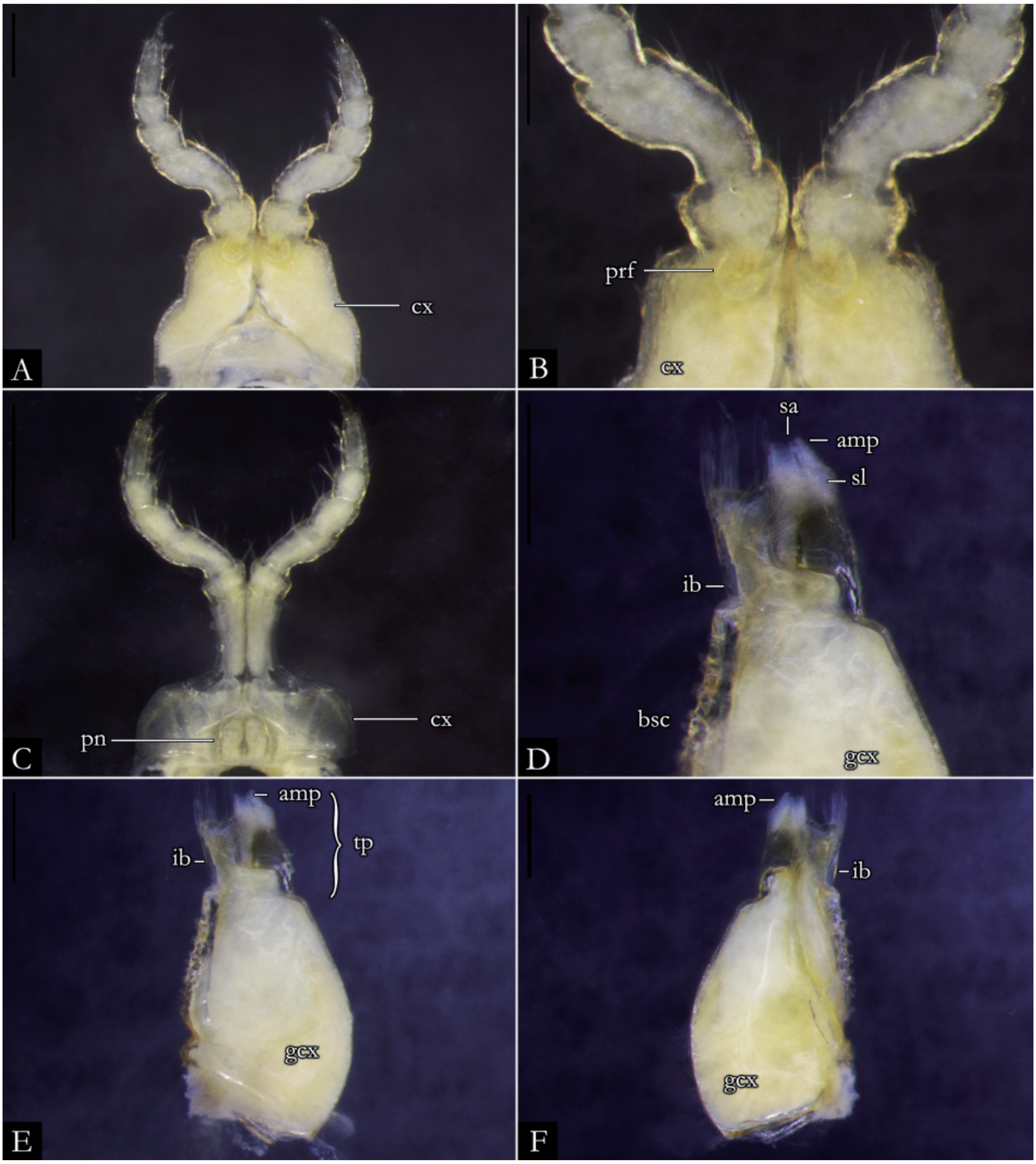

Fig. 79. *Pseudonannolene leucocephalus* Schubart, 1944, ♂ (MZSP 1060). **A**. First leg-pair. **B**. Detail of prefemur. **C**. Second leg-pair. **D**. Detail of telopodite, in anal view. **E**. Left gonopod, in anal view. **F**. Left gonopod, in oral view. Abbreviations: see Material and methods. Scale bars = 0.2 mm.

Fig. 80. *Pseudonannolene leucocephalus* Schubart, 1944, ♂ (MZSP). **A**. Sexual structures and gnathochilarium of type material mounted on microscope slide. **B**. First leg-pair. **C**. Gonopods, in oral view. **D**. Detail of telopodites, in oral view. **E–F**. Original labels of type material. Abbreviations: see Material and methods. Images not to scale.

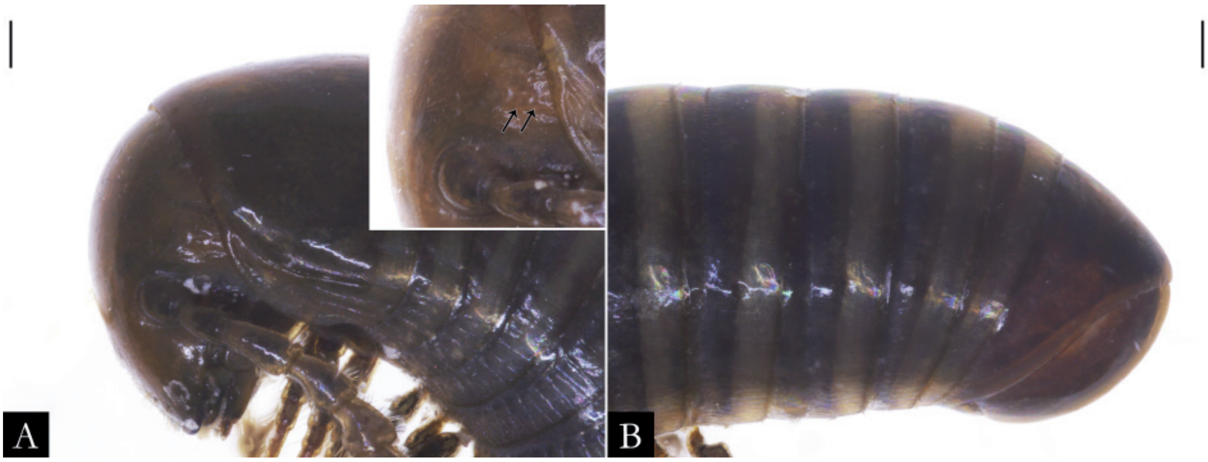

Fig. 81. *Pseudonannolene leucomelas* Schubart, 1947, paratype, ♀ (MNRJ 11829), in lateral view. **A**. Anterior region (arrows indicating the ommatidial cluster). **B**. Posterior region. Scale bars = 0.2 mm.

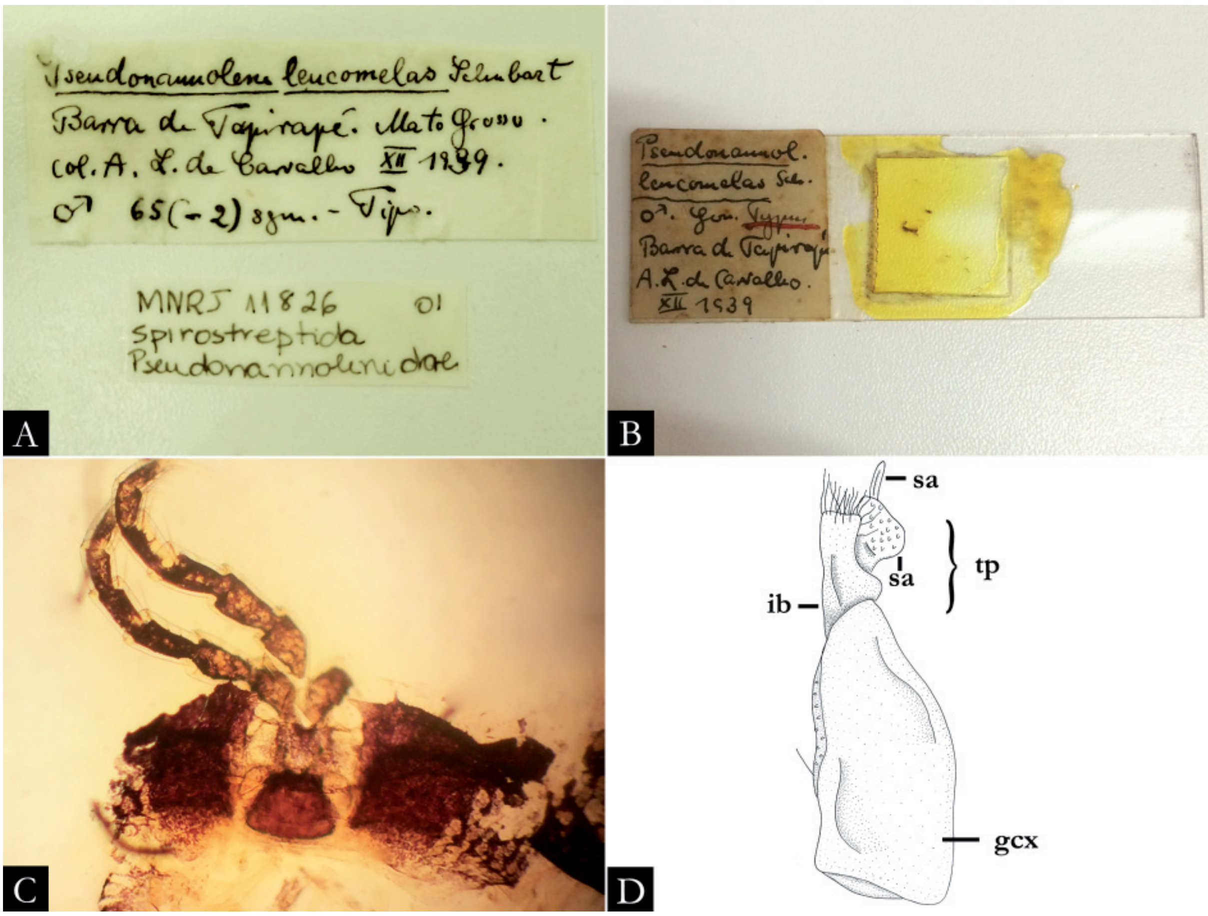

Fig. 82. *Pseudonannolene leucomelas* Schubart, 1947*,* males. **A**. Original labels of type material (MNRJ 11826). **B–C**. Midbody ring of holotype (MZSP), in ventral view, mounted on microscope slide. **D**. Schematic drawing of left gonopod in anal view (modified from Schubart 1947: figs 33–34). Abbreviations: see Material and methods. Images not to scale.

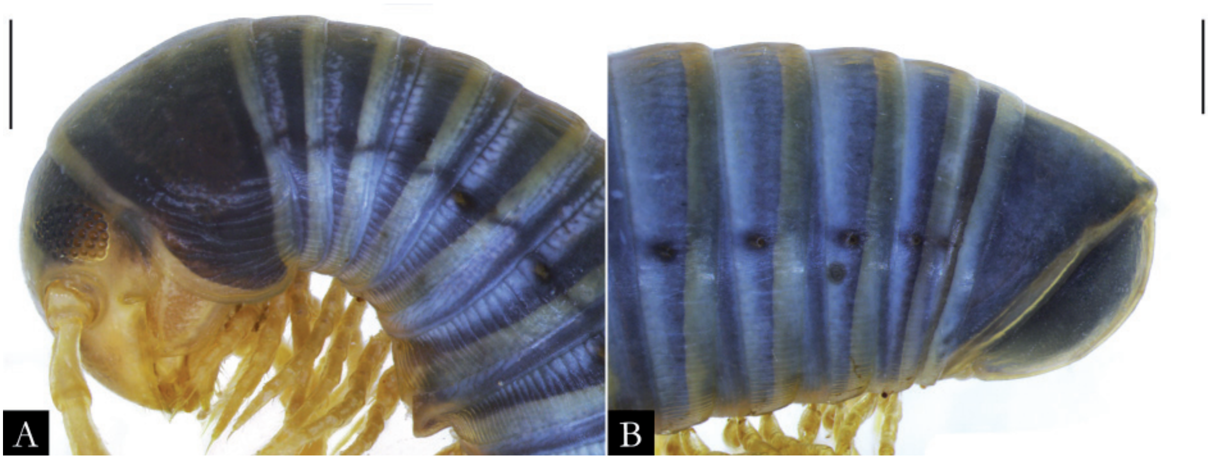

Fig. 83. *Pseudonannolene longicornis* (Porat, 1888), ♂ (IBSP 3734), in lateral view. **A**. Anterior region. **B**. Posterior region. Scale bars = 1 mm.

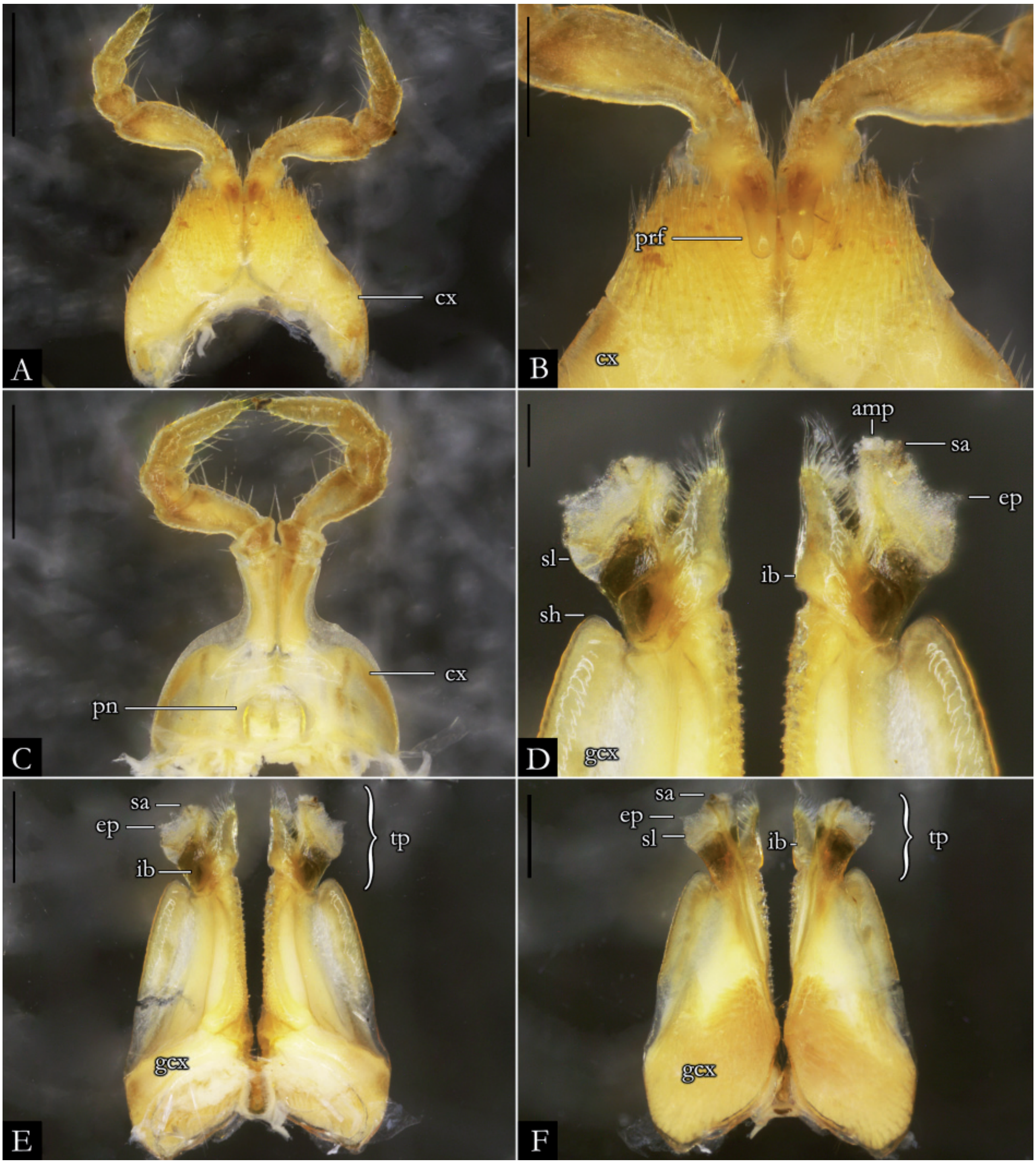

Fig. 84. *Pseudonannolene longicornis* (Porat, 1888), ♂ (IBSP 3734). **A**. First leg-pair. **B**. Detail of prefemur. **C**. Second leg-pair. **D**. Detail of telopodites, in anal view. **E**. Gonopods, in anal view. **F**. Gonopods, in oral view. Abbreviations: see Material and methods. Scale bars: A, E–F = 0.5 mm; B–D = 0.2 mm.

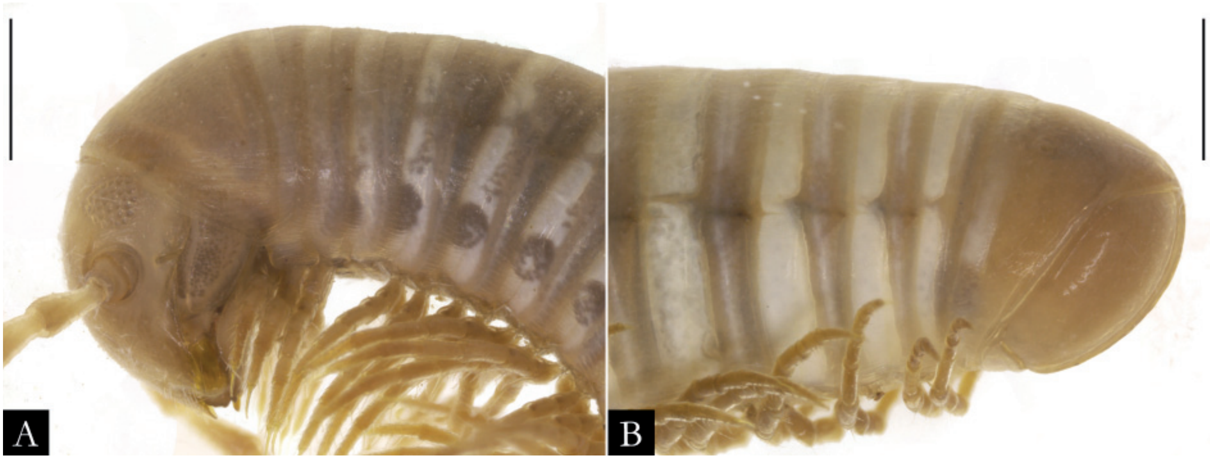

Fig. 85. *Pseudonannolene lundi* Iniesta & Ferreira, 2015, holotype, ♂ (ISLA 8684), in lateral view. **A**. Anterior region. **B**. Posterior region. Scale bars = 1 mm.

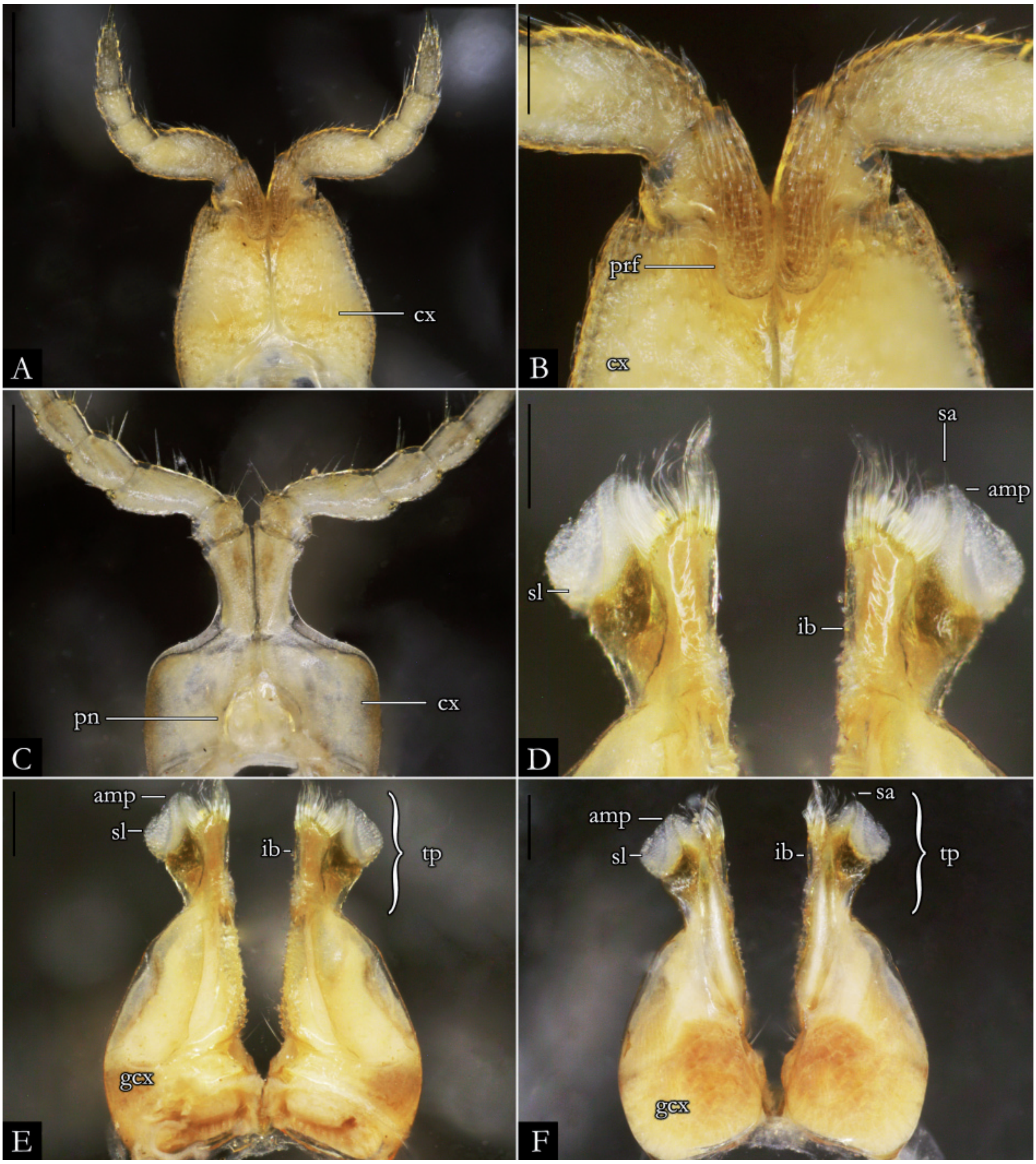

Fig. 86. *Pseudonannolene lundi* Iniesta & Ferreira, 2015, paratype, ♂ (ISLA 8685). **A**. First leg-pair. **B**. Detail of prefemur. **C**. Second leg-pair. **D**. Detail of telopodites, in anal view. **E**. Gonopods, in anal view. **F**. Gonopods, in oral view. Abbreviations: see Material and methods. Scale bars: A, C, E–F = 0.5 mm; B, D = 0.2 mm.

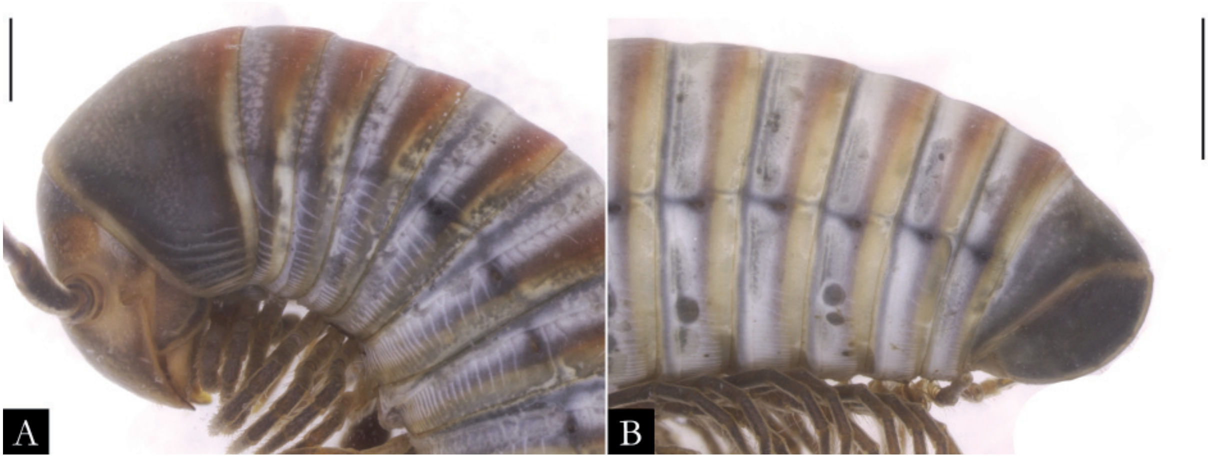

Fig. 87. *Pseudonannolene magna* Udulutsch & Pietrobon, 2003, paratype, ♂ (MZSP 941), in lateral view. **A**. Anterior region. **B**. Posterior region. Scale bars = 1 mm.

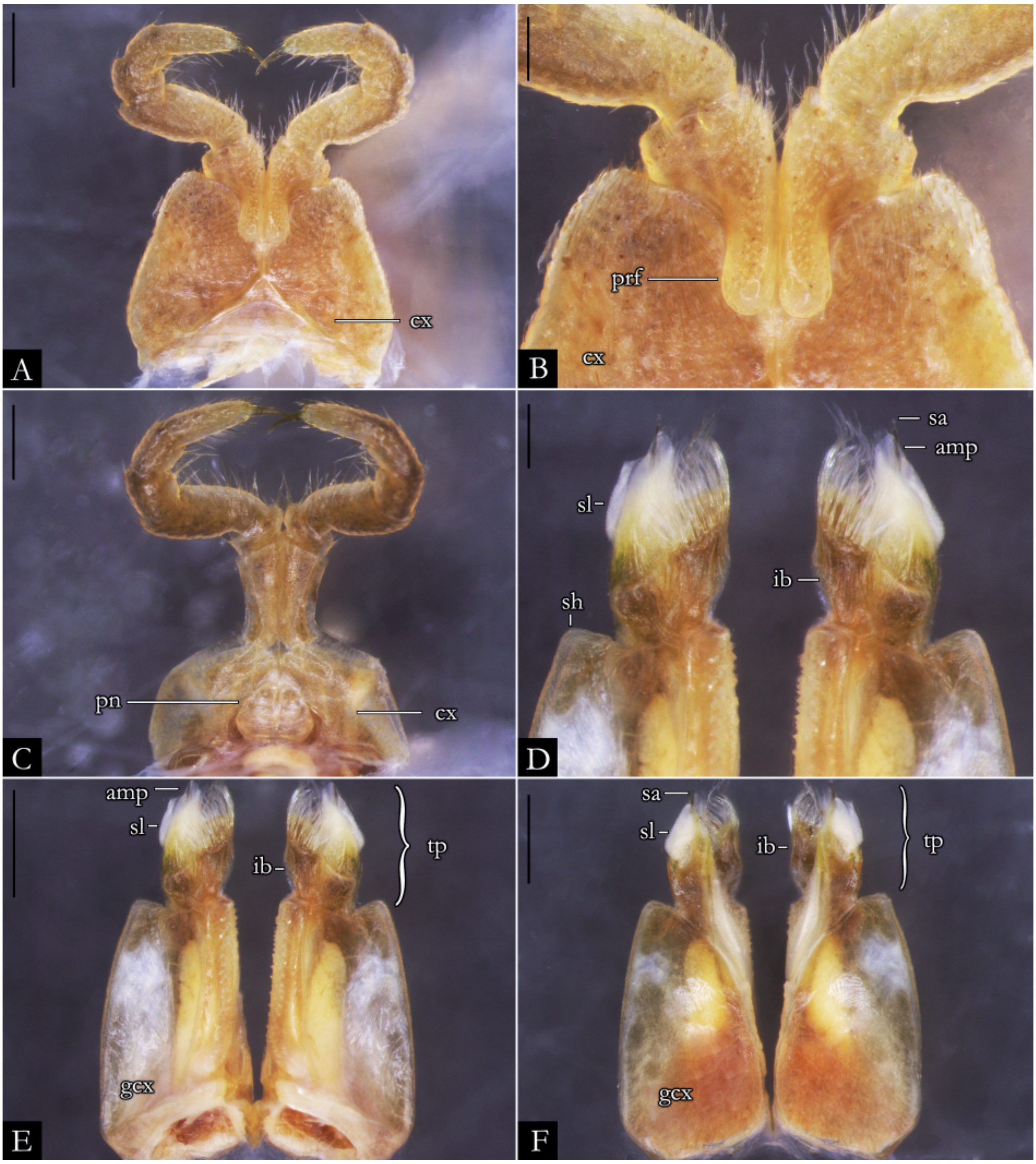

Fig. 88. *Pseudonannolene magna* Udulutsch & Pietrobon, 2003, paratype, ♂ (MZSP 941). **A**. First leg-pair. **B**. Detail of prefemur. **C**. Second leg-pair. **D**. Detail of telopodites, in anal view. **E**. Gonopods, in anal view. **F**. Gonopods, in oral view. Abbreviations: see Material and methods. Scale bars: A, C, E–F = 0.5 mm; B, D = 0.2 mm.

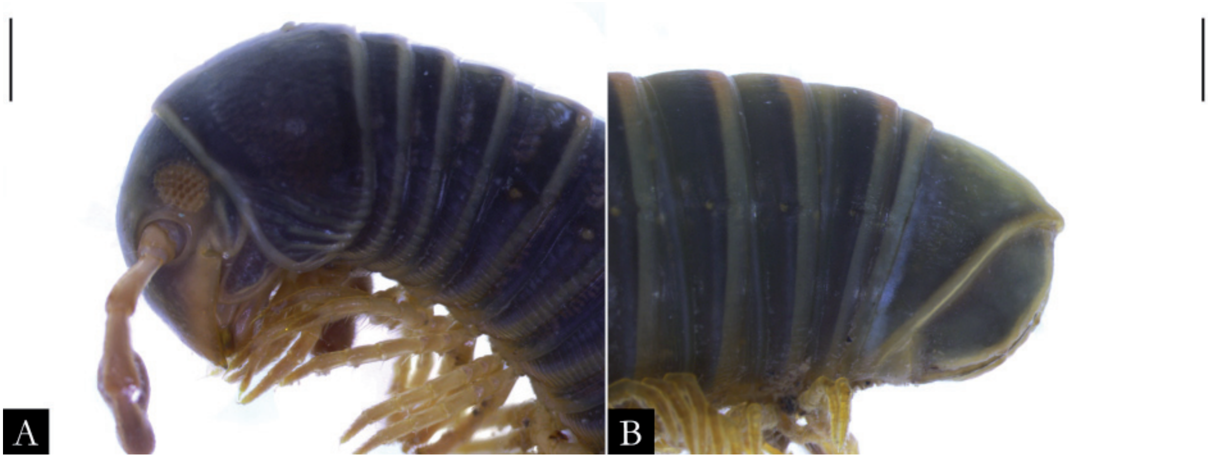

Fig. 89. *Pseudonannolene maritima* Schubart, 1949, ♀ (IBSP 658), in lateral view. **A**. Anterior region. **B**. Posterior region. Scale bars = 1 mm.

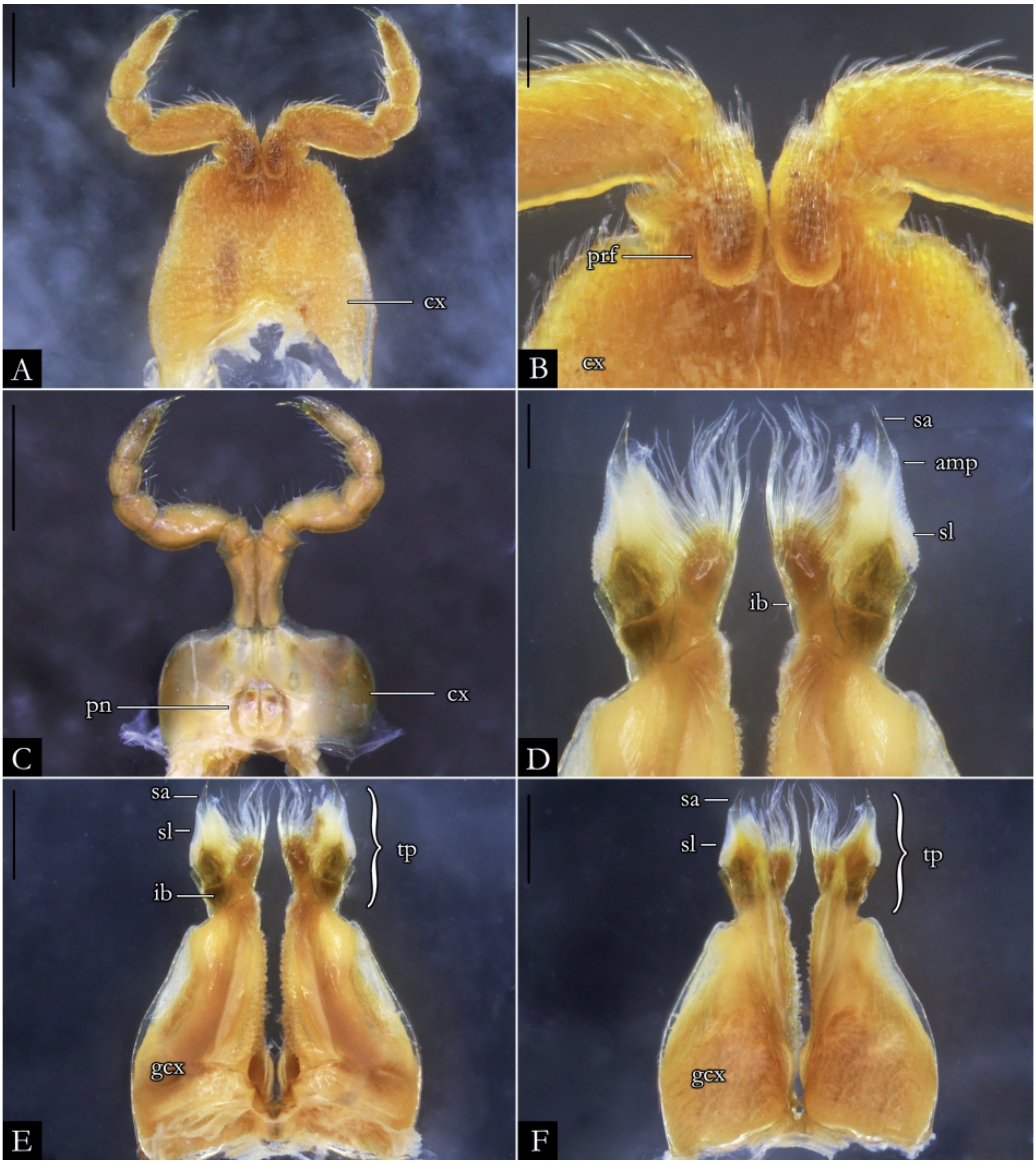

Fig. 90. *Pseudonannolene maritima* Schubart, 1949, ♂ (IBSP 658). **A**. First leg-pair. **B**. Detail of prefemur. **C**. Second leg-pair. **D**. Detail of telopodites, in anal view. **E**. Gonopods, in anal view. **F**. Gonopods, in oral view. Abbreviations: see Material and methods. Scale bars: A, C, E–F = 0.5 mm; B, D = 0.2 mm.

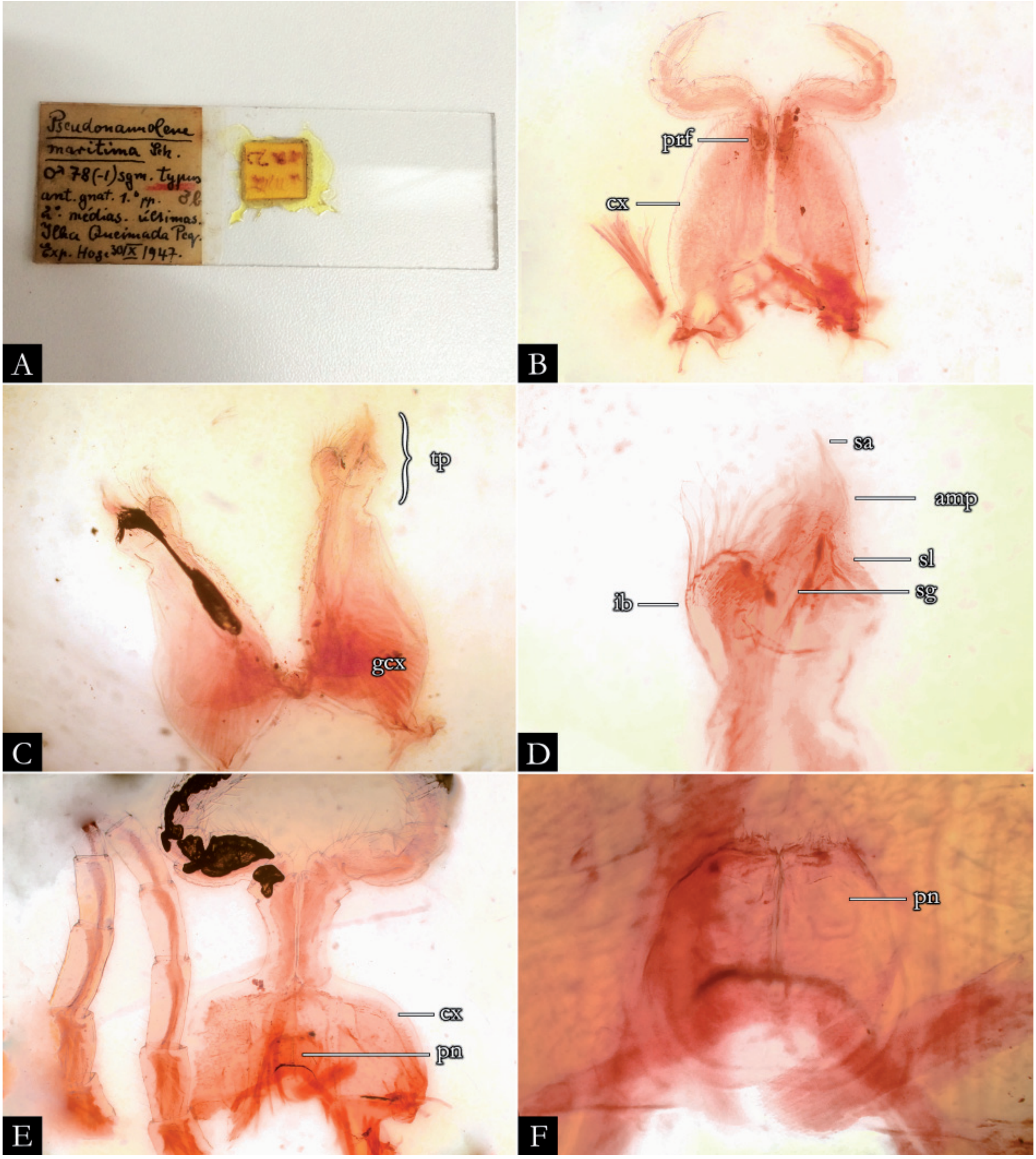

Fig. 91. *Pseudonannolene maritima* Schubart, 1949, holotype, ♂ (MZSP). **A**. Sexual structures, antennae, and gnathochilarium of type material mounted on microscope slide. **B**. First leg-pair. **C**. Gonopods, in oral view. **D**. Detail of telopodites, in oral view. **E**. Second leg-pair. **F**. Detail of penis. Abbreviations: see Material and methods. Images not to scale.

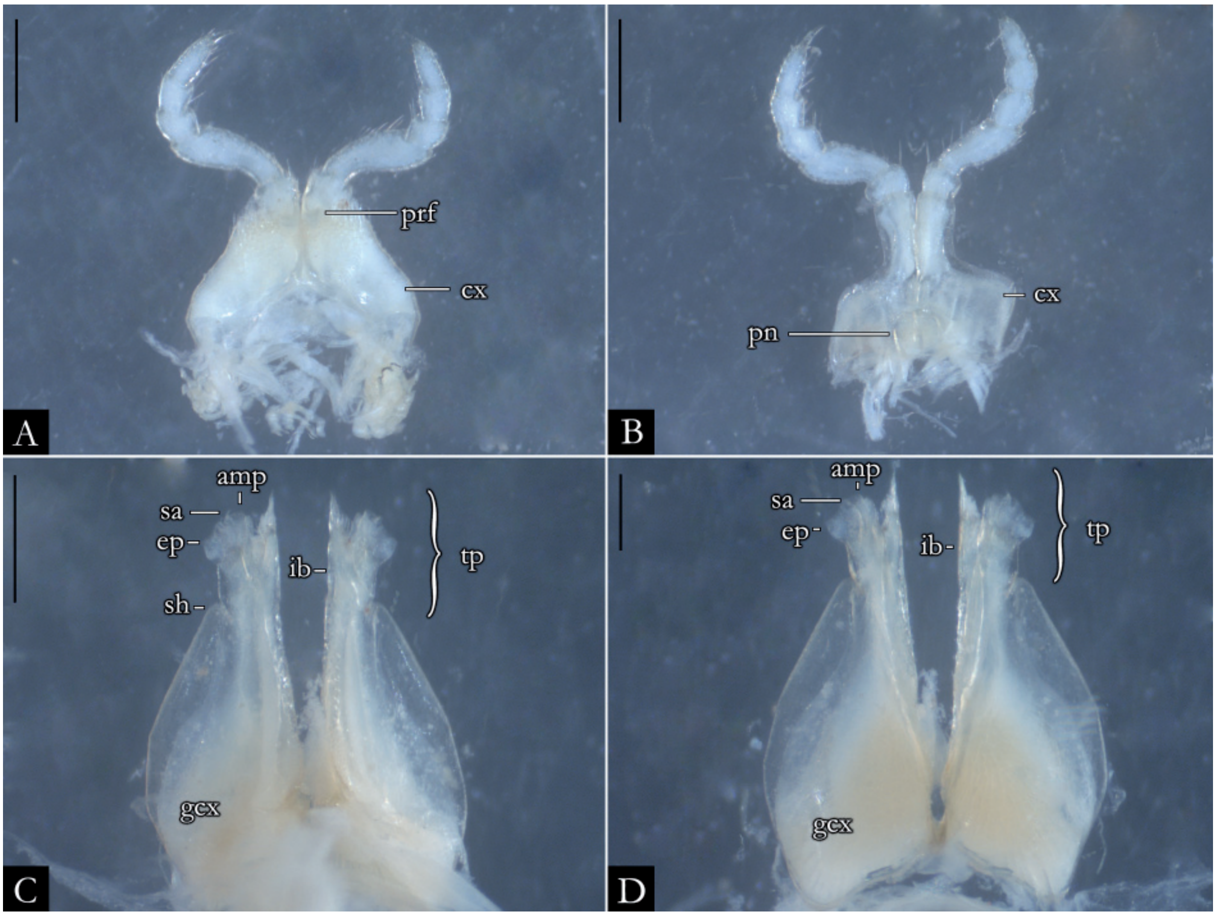

Fig. 92. *Pseudonannolene meridionalis* Silvestri, 1902, ♂ (NHMD). **A**. First leg-pair. **B**. Second leg-pair. **C**. Gonopods, in oral view. **D**. Gonopods, in anal view. Abbreviations: see Material and methods. Scale bars: A–B = 0.5 mm; C = 0.25 mm; D = 0.15 mm.

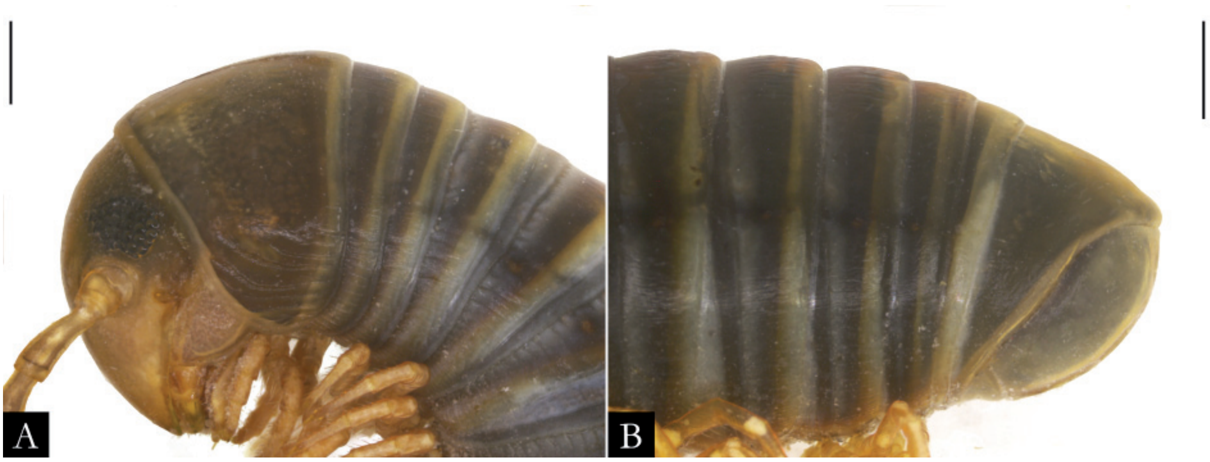

Fig. 93. *Pseudonannolene mesai* Fontanetti, 2000, ♀ (IBSP 2041), in lateral view. **A**. Anterior region. **B**. Posterior region. Scale bars = 1 mm.

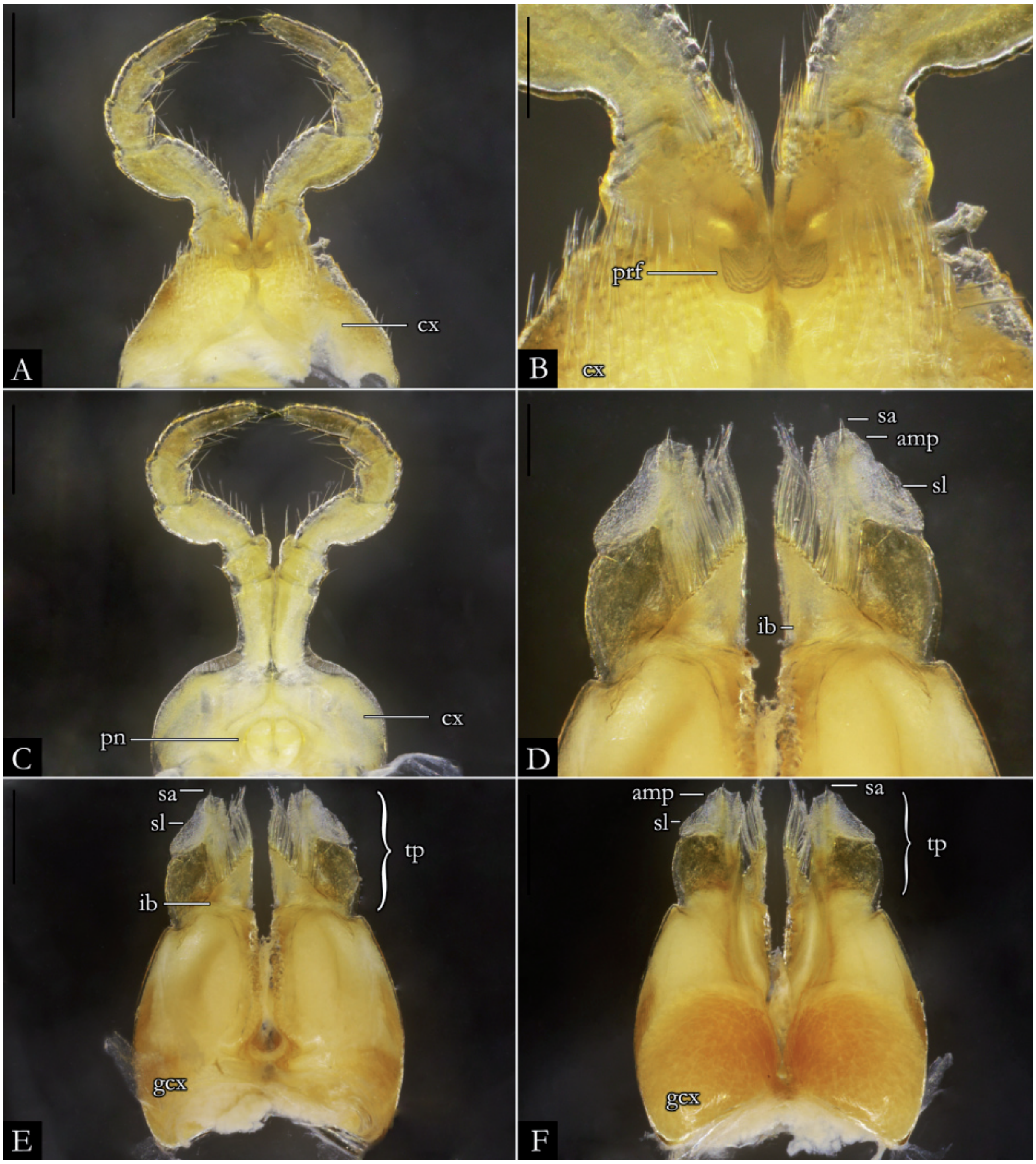

Fig. 94. *Pseudonannolene mesai* Fontanetti, 2000, ♂ (IBSP 1888). **A**. First leg-pair. **B**. Detail of prefemur. **C**. Second leg-pair. **D**. Detail of telopodites, in anal view. **E**. Gonopods, in anal view. **F**. Gonopods, in oral view. Abbreviations: see Material and methods. Scale bars: A, C, E–F = 0.5 mm; B, D = 0.2 mm.

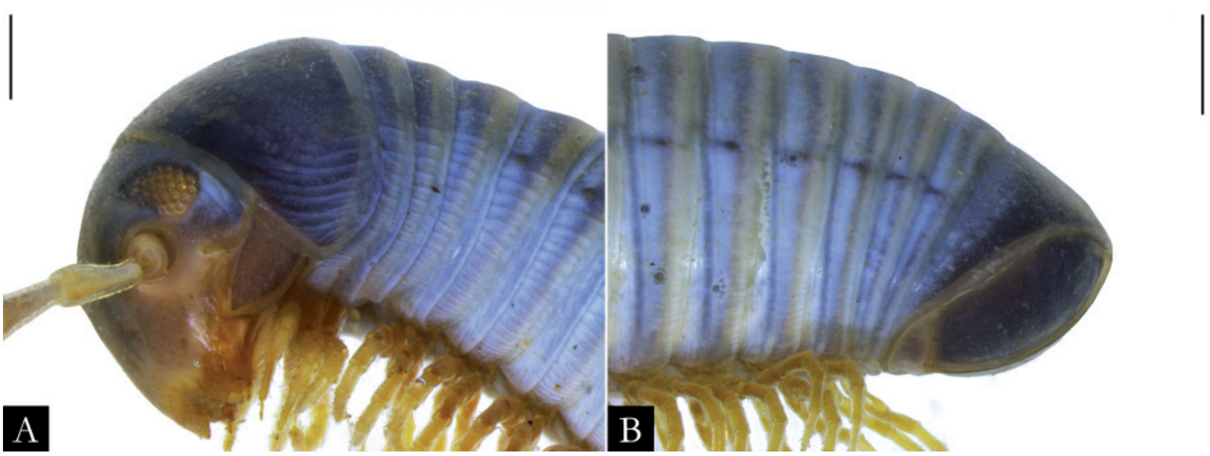

Fig. 95. *Pseudonannolene microzoporus* Mauriès, 1987, ♀ (IBSP 1368), in lateral view. **A**. Anterior region. **B**. Posterior region. Scale bars = 1 mm.

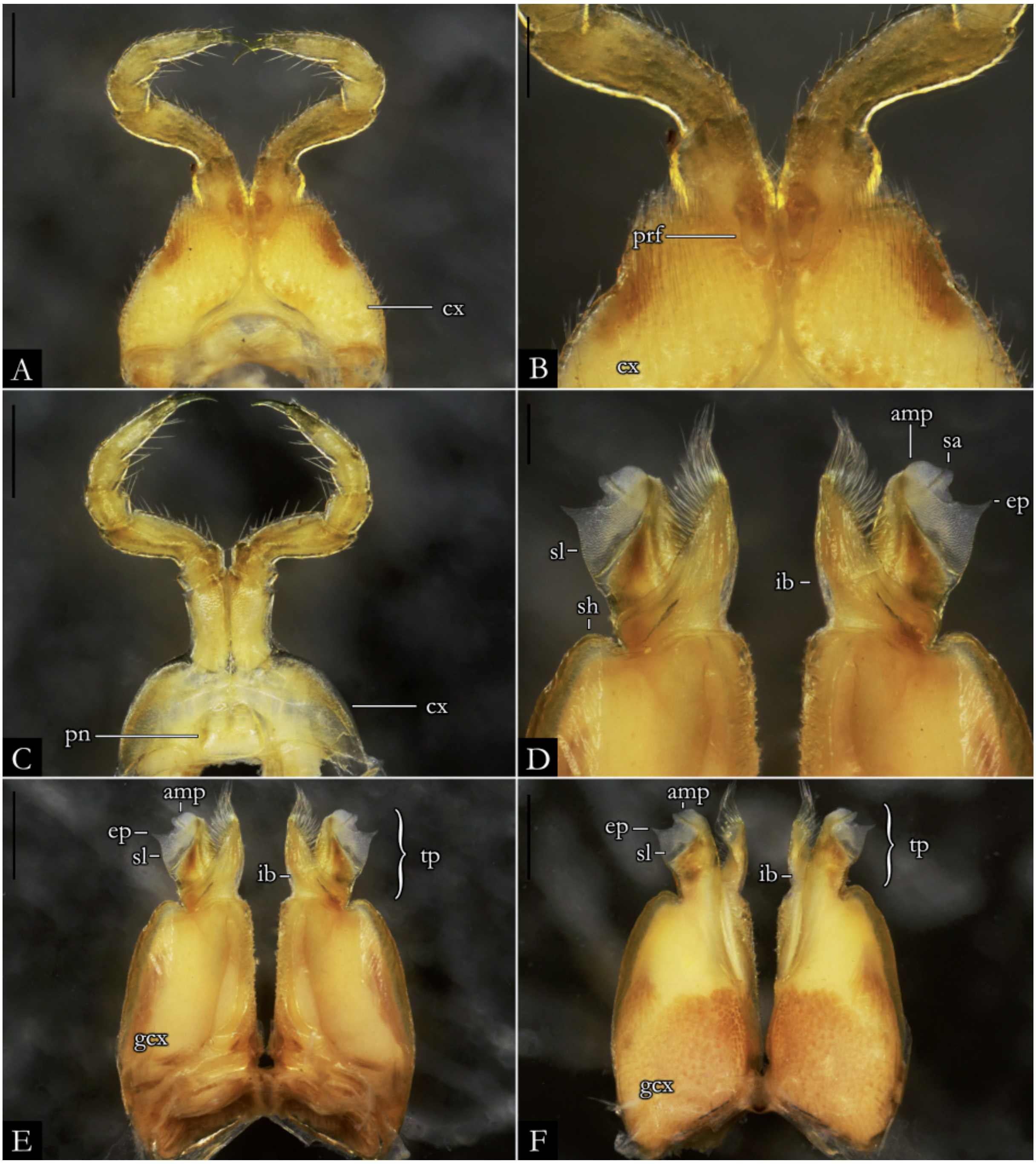

Fig. 96. *Pseudonannolene microzoporus* Mauriès, 1987, ♂ (IBSP 3427). **A**. First leg-pair. **B**. Detail of prefemur. **C**. Second leg-pair. **D**. Detail of telopodites, in anal view. **E**. Gonopods, in anal view. **F**. Gonopods, in oral view. Abbreviations: see Material and methods. Scale bars: A, C, E–F = 0.5 mm; B, D = 0.2 mm.

Fig. 97. *Pseudonannolene microzoporus* Mauriès, 1987, holotype, ♂ (NHMD), in lateral view. **A**. Anterior region. **B**. Posterior region. **C**. Original label of type material. Scale bars = 0.5 mm.

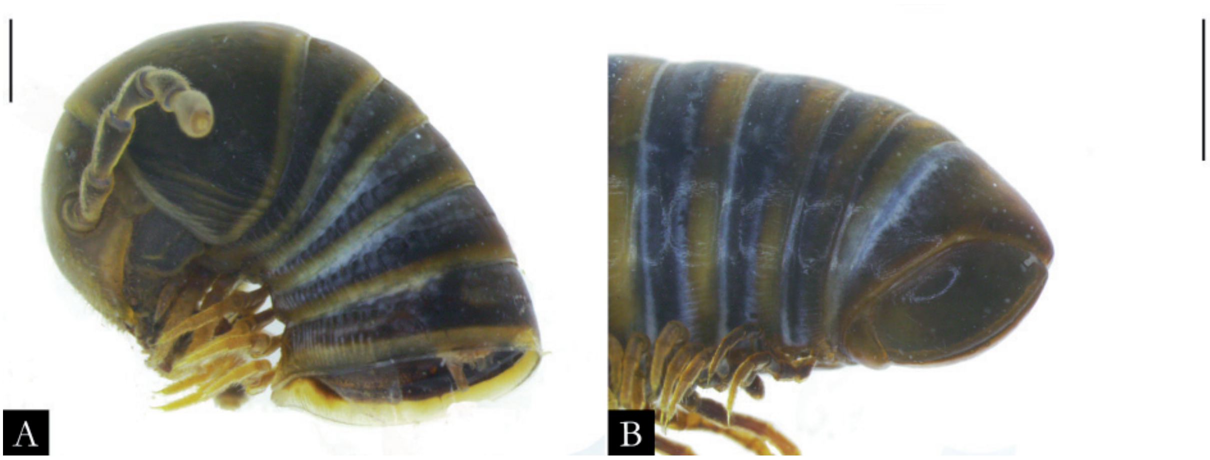

Fig. 98. *Pseudonannolene occidentalis* Schubart, 1958, ♂ (IBSP 1998), in lateral view. **A**. Anterior region. **B**. Posterior region. Scale bars = 1 mm.

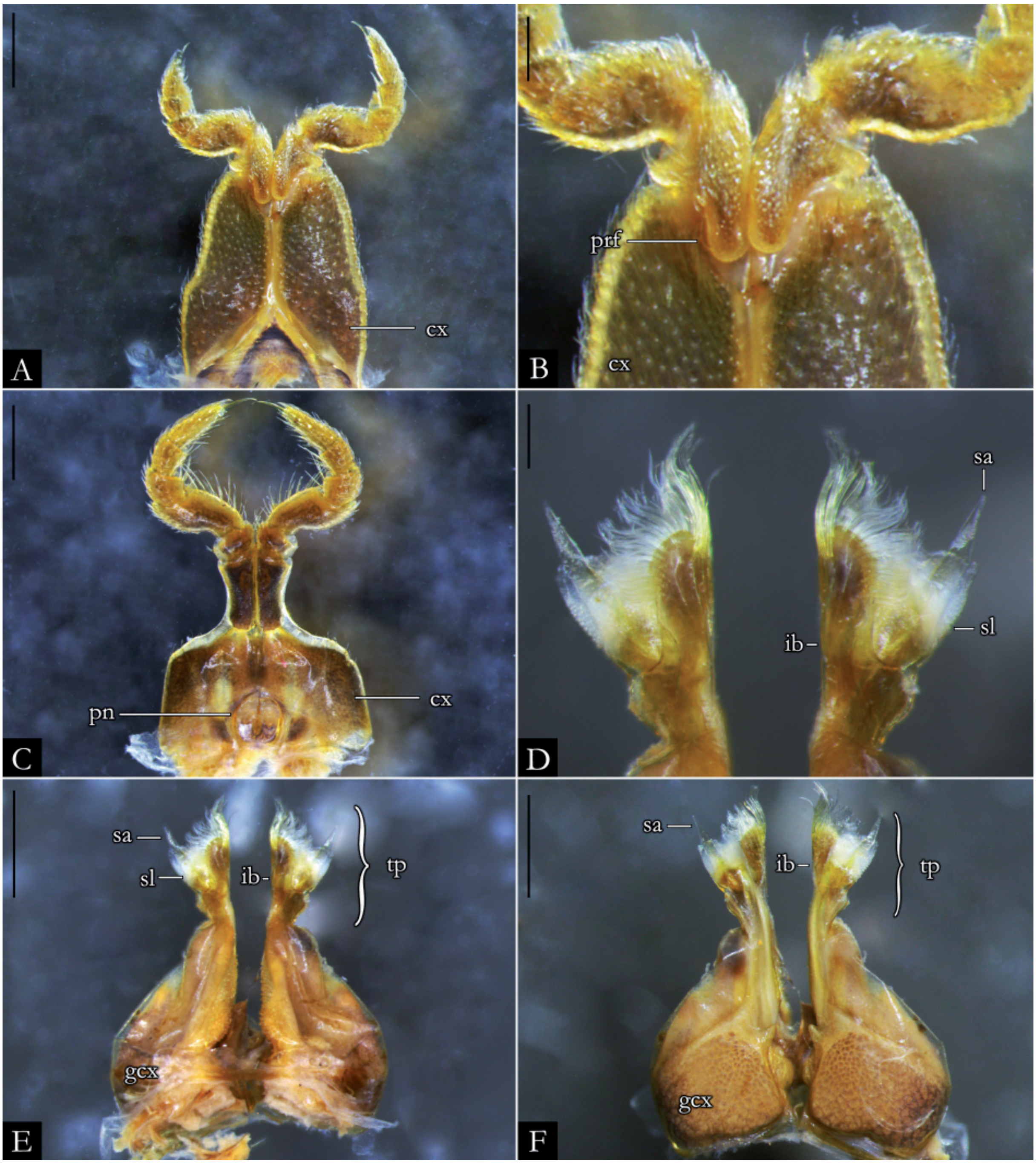

Fig. 99. *Pseudonannolene occidentalis* Schubart, 1958, ♂ (IBSP 1998). **A**. First leg-pair. **B**. Detail of prefemur. **C**. Second leg-pair. **D**. Detail of telopodites, in anal view. **E**. Gonopods, in anal view. **F**. Gonopods, in oral view. Abbreviations: see Material and methods. Scale bars: A, C, E–F = 0.5 mm; B, D = 0.2 mm.

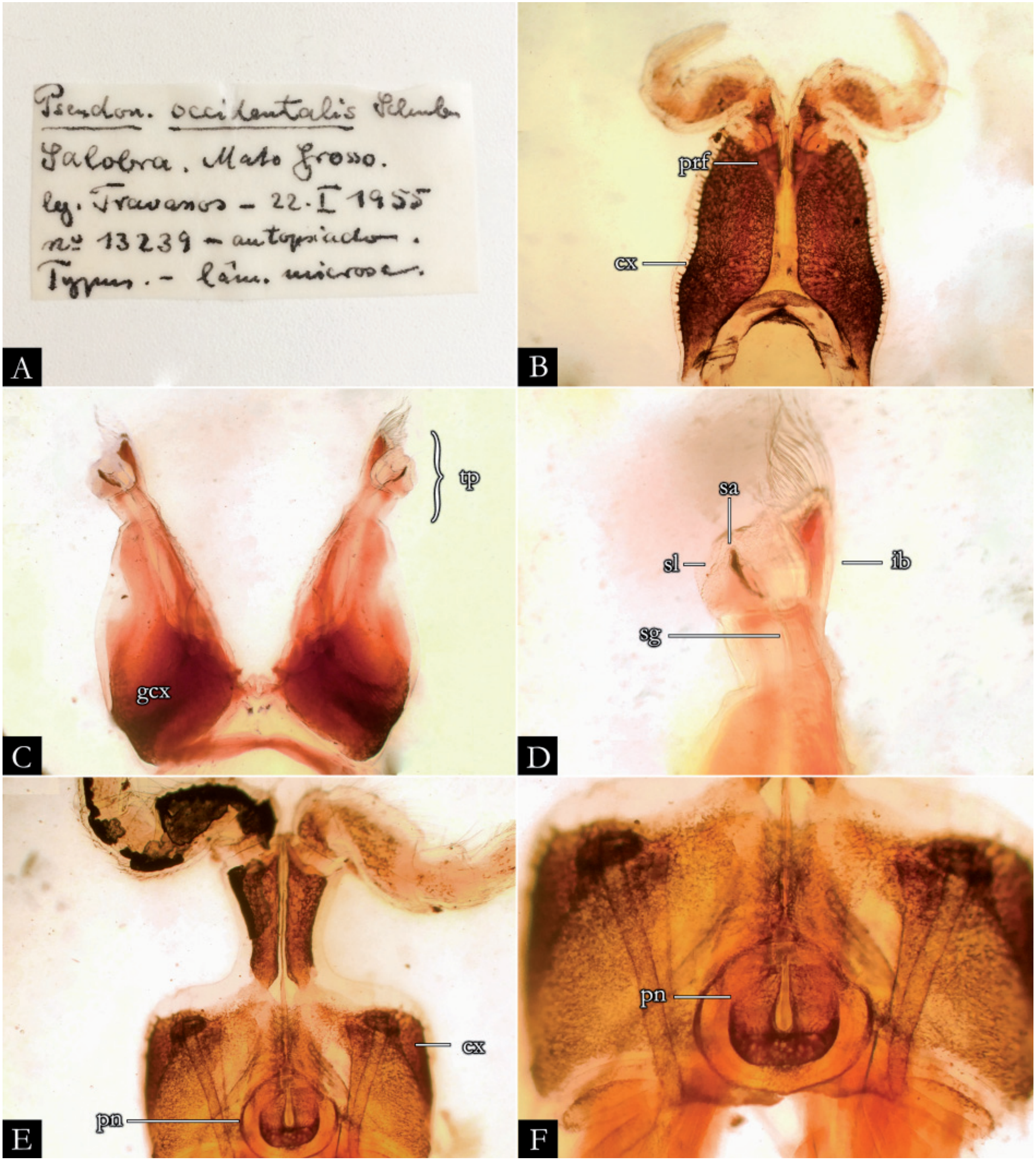

Fig. 100. *Pseudonannolene occidentalis* Schubart, 1958, holotype, ♂ (MZSP). **A**. Original label of type material mounted on microscope slide. **B**. First leg-pair. **C**. Gonopods, in oral view. **D**. Detail of telopodites, in oral view. **E**. Second leg-pair. **F**. Detail of penis. Abbreviations: see Material and methods. Images not to scale.

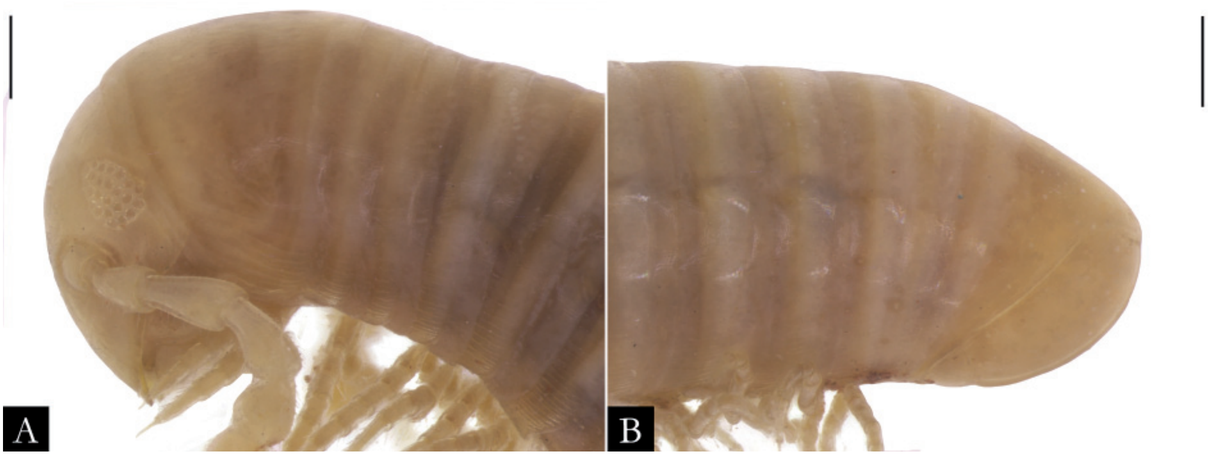

Fig. 101. *Pseudonannolene ophiiulus* Schubart, 1944, ♂ (MZSP 1061), in lateral view. **A**. Anterior region. **B**. Posterior region. Scale bars = 0.5 mm.

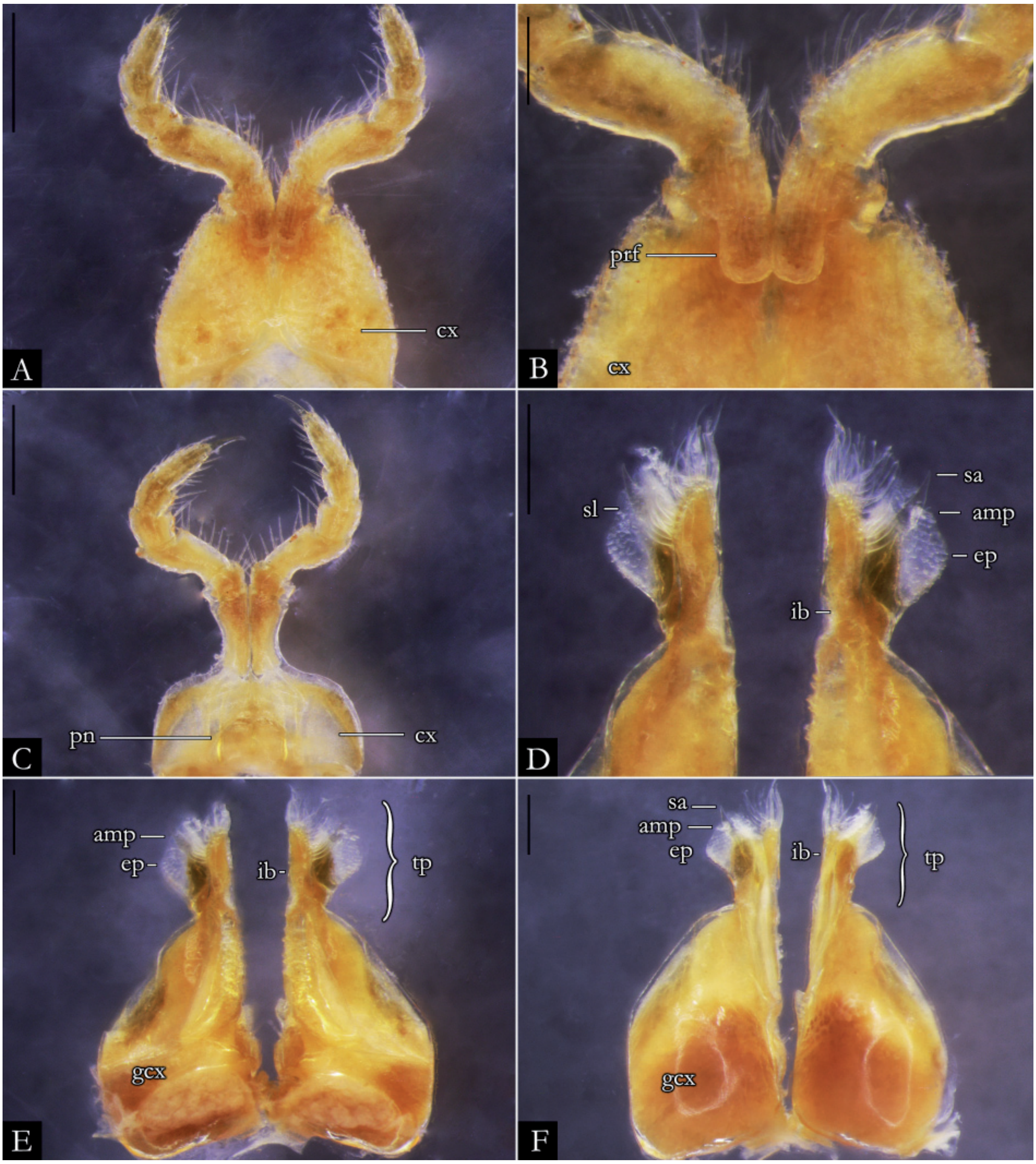

Fig. 102. *Pseudonannolene ophiiulus* Schubart, 1944, ♂ (MZSP 1061). **A**. First leg-pair. **B**. Detail of prefemur. **C**. Second leg-pair. **D**. Detail of telopodites, in anal view. **E**. Gonopods, in anal view. **F**. Gonopods, in oral view. Abbreviations: see Material and methods. Scale bars: A, C, E–F = 0.5 mm; B, D = 0.2 mm.

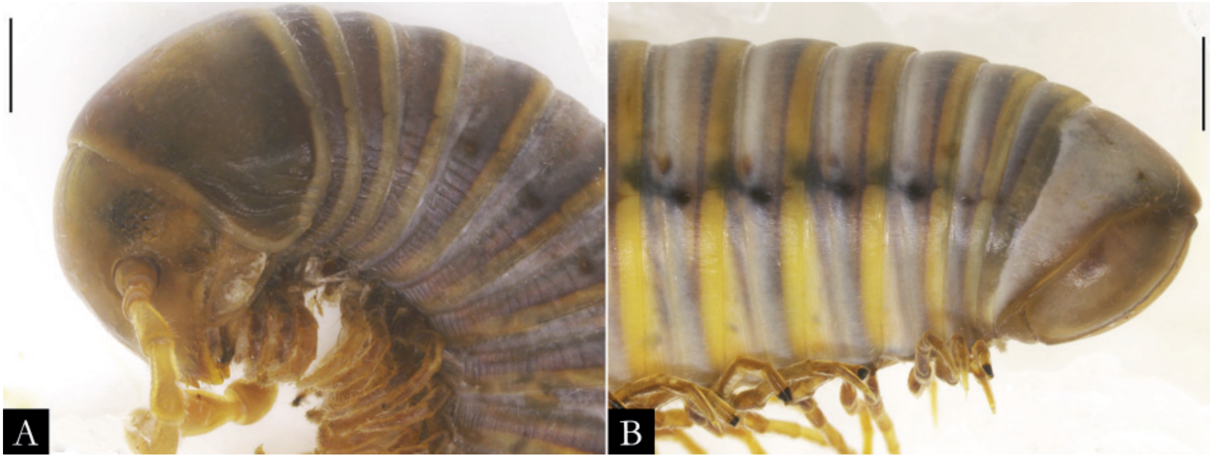

Fig. 103. *Pseudonannolene parvula* Silvestri, 1902, ♂ (IBSP 7630), in lateral view. **A**. Anterior region. **B**. Posterior region. Scale bars = 0.5 mm.

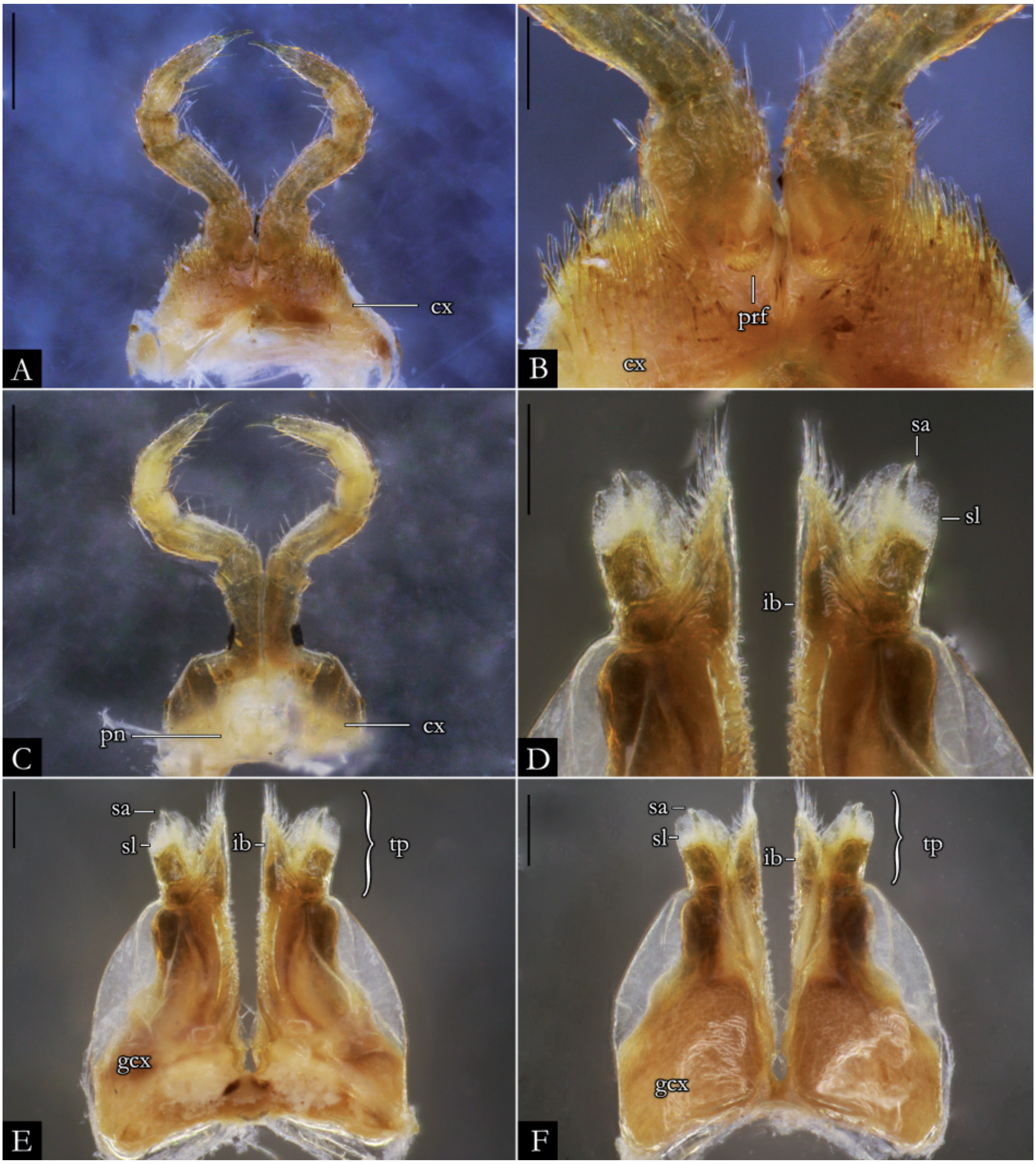

Fig. 104. *Pseudonannolene parvula* Silvestri, 1902, ♂ (IBSP 7630). **A**. First leg-pair. **B**. Detail of prefemur. **C**. Second leg-pair. **D**. Detail of telopodites, in anal view. **E**. Gonopods, in anal view. **F**. Gonopods, in oral view. Abbreviations: see Material and methods. Scale bars: A, C, E–F = 0.5 mm; B, D = 0.2 mm.

Fig. 105. *Pseudonannolene parvula* Silvestri, 1902, ♀ syntype (USNM 2020). **A**. Anterior region. **B**. Posterior region. **C**. Original label of type material. **D**. Body of syntypes (ZMB 2888), in lateral view. Images not to scale.

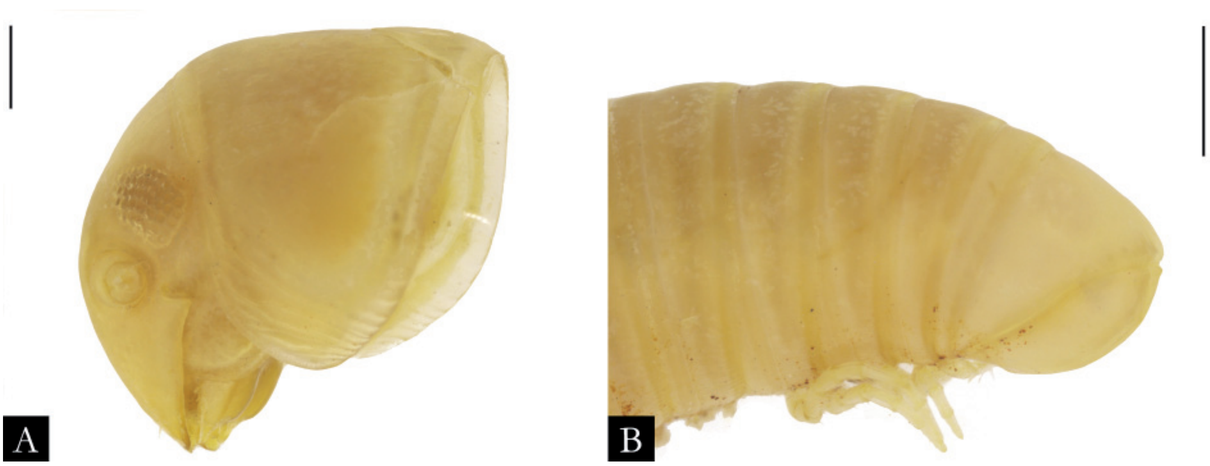

Fig. 106. *Pseudonannolene patagonica* Brölemann, 1902, holotype, ♂ (MZSP 0242), in lateral view. **A**. Anterior region. **B**. Posterior region. Scale bars = 0.5 mm.

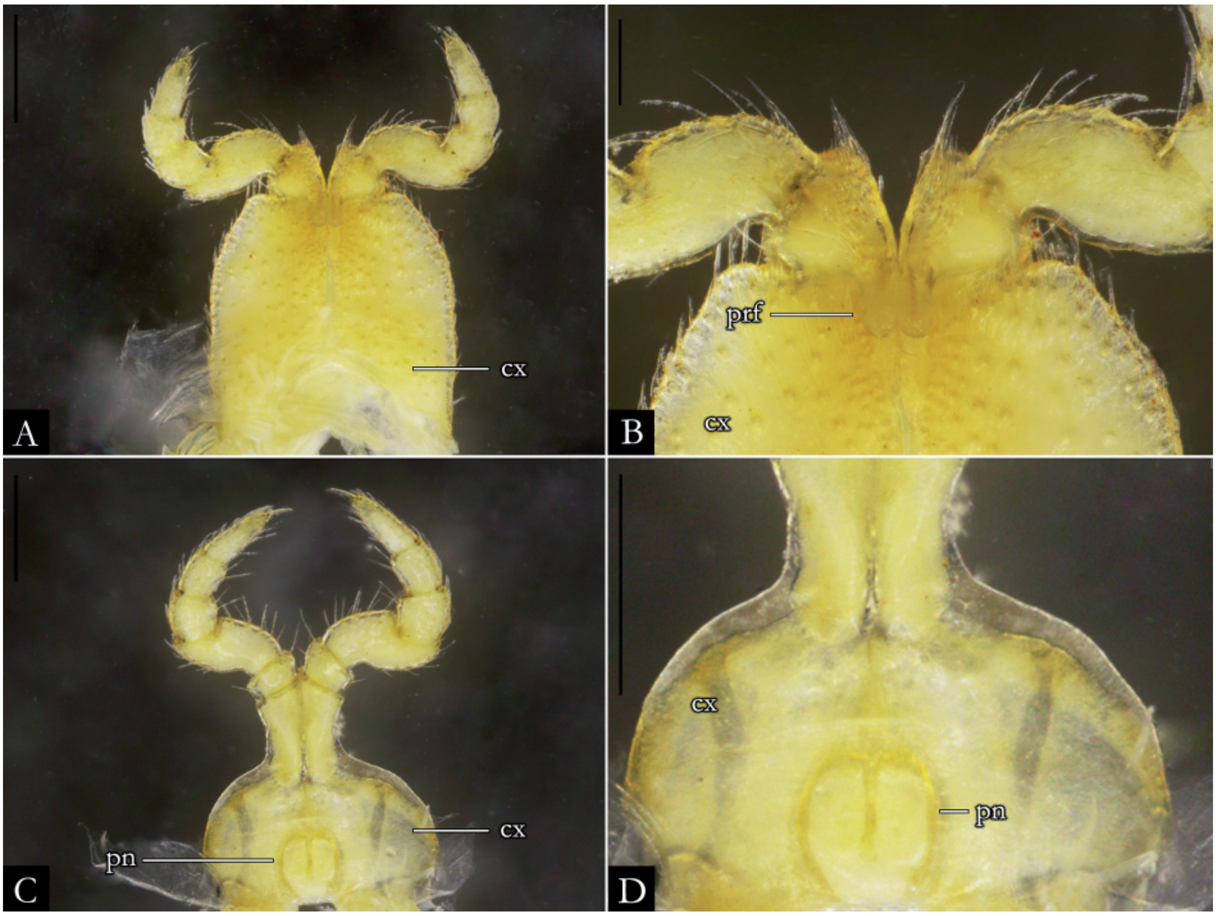

Fig. 107. *Pseudonannolene patagonica* Brölemann, 1902, holotype, ♂ (MZSP 0242). **A**. First leg-pair. **B**. Detail of prefemur. **C**. Second leg-pair. **D**. Detail of penis. Abbreviations: see Material and methods. Scale bars: A, C = 0.5 mm; B, D = 0.2 mm.

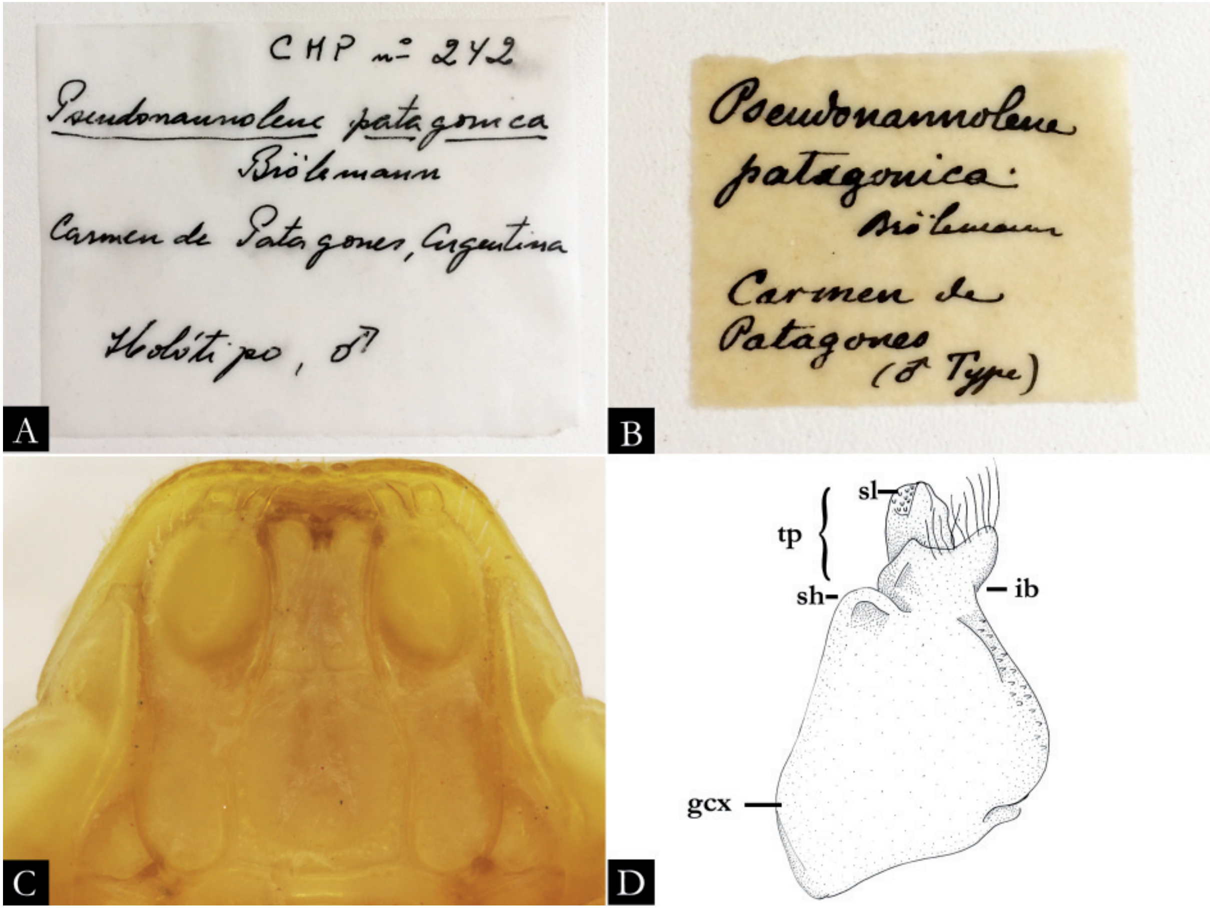

Fig. 108. *Pseudonannolene patagonica* Brölemann, 1902, holotype, ♂ (MZSP 0242). **A–B**. Original label of type material. **C**. Gnathochilarium in ventral view. **D**. Schematic drawing of right gonopod in anal view (modified from Brölemann 1902a: fig. 164). Abbreviations: see Material and methods. Images not to scale.

Fig. 109. *Pseudonannolene paulista* Brölemann, 1902, ♀ (IBSP 1915), in lateral view. **A**. Anterior region. **B**. Posterior region. Scale bars = 1 mm.

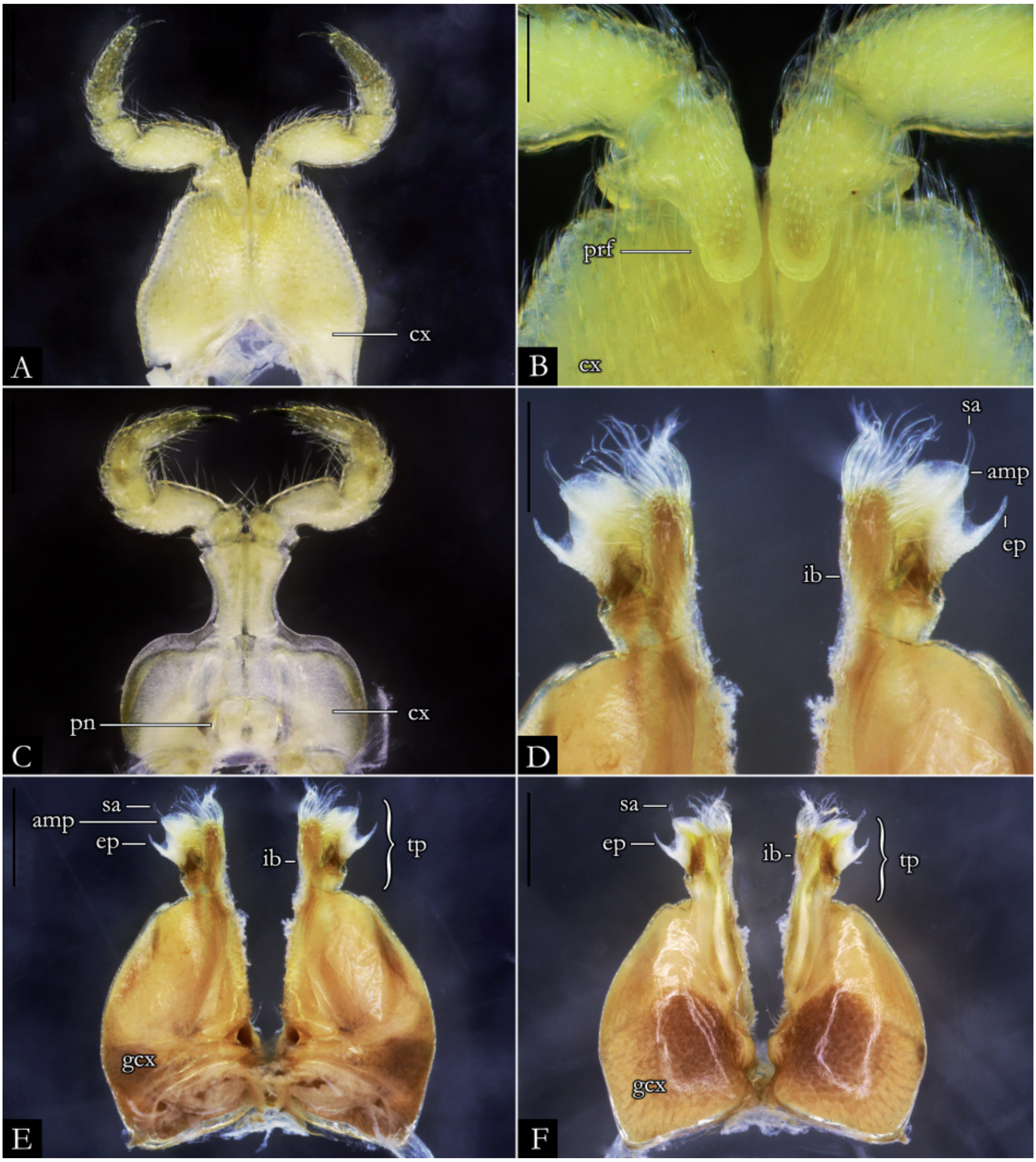

Fig. 110. *Pseudonannolene paulista* Brölemann, 1902, ♂ (IBSP 1908). **A**. First leg-pair. **B**. Detail of prefemur. **C**. Second leg-pair. **D**. Detail of telopodites, in anal view. **E**. Gonopods, in anal view. **F**. Gonopods, in oral view. Abbreviations: see Material and methods. Scale bars: A, C, E–F = 0.5 mm; B, D = 0.2 mm.

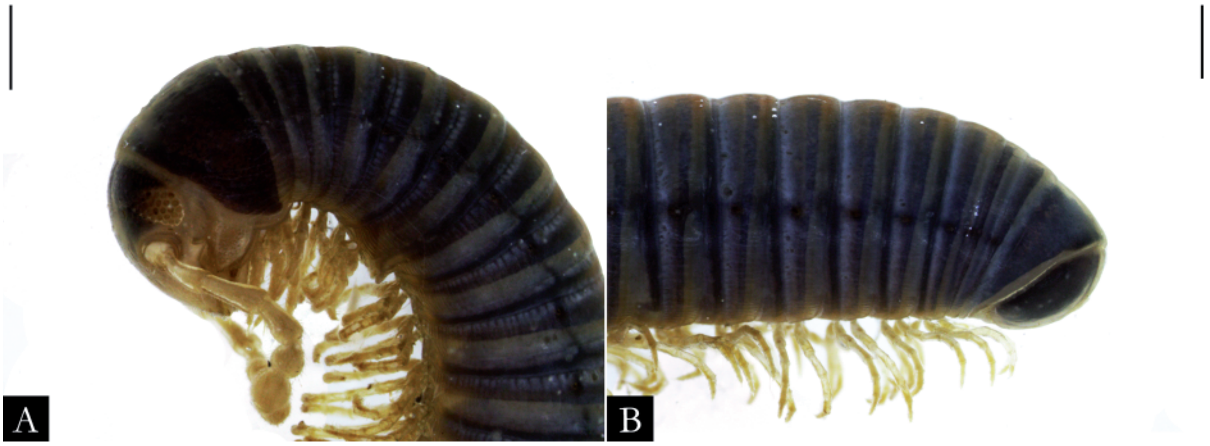

Fig. 111. *Pseudonannolene pusilla* Silvestri, 1895, ♂ (IBSP 13390), in lateral view. **A**. Anterior region. **B**. Posterior region. Scale bars = 0.5 mm.

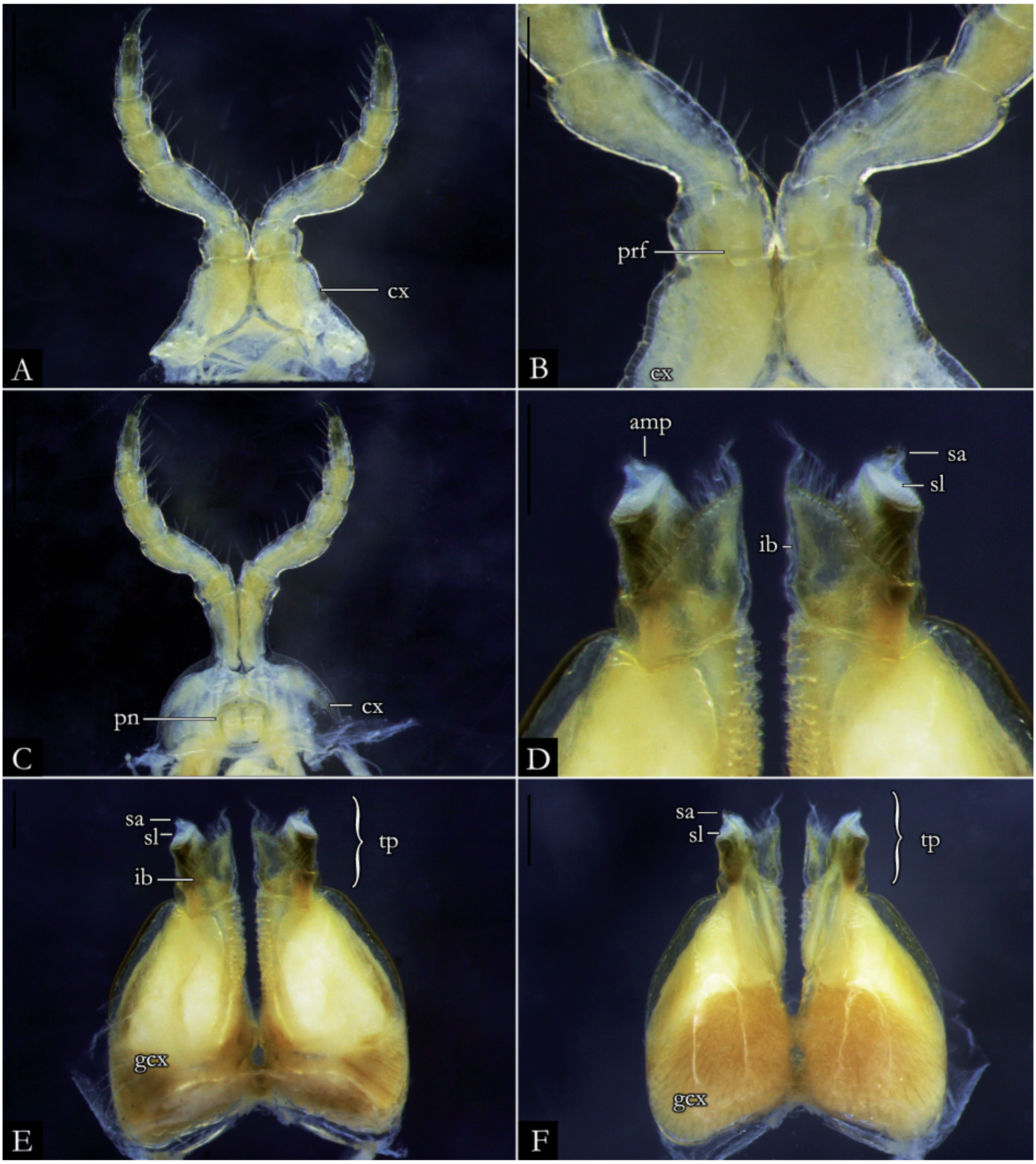

Fig. 112. *Pseudonannolene pusilla* Silvestri, 1895, ♂ (IBSP 13390). **A**. First leg-pair. **B**. Detail of prefemur. **C**. Second leg-pair. **D**. Detail of telopodites, in anal view. **E**. Gonopods, in anal view. **F**. Gonopods, in oral view. Abbreviations: see Material and methods. Scale bars: A, C, E–F = 0.5 mm; B, D = 0.2 mm.

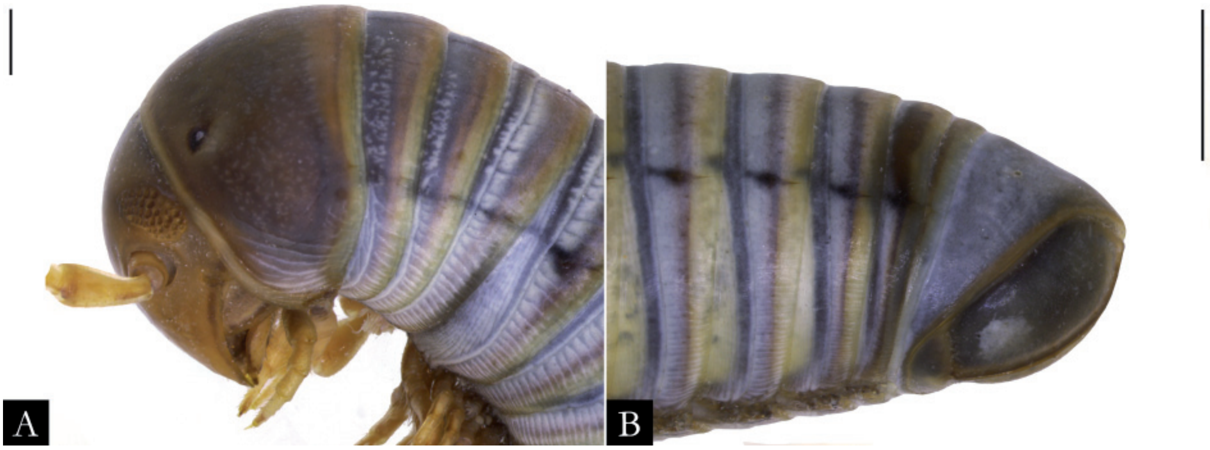

Fig. 113. *Pseudonannolene robsoni* Iniesta & Ferreira, 2014, ♂ (IBSP 3441), in lateral view. **A**. Anterior region. **B**. Posterior region. Scale bars = 0.5 mm.

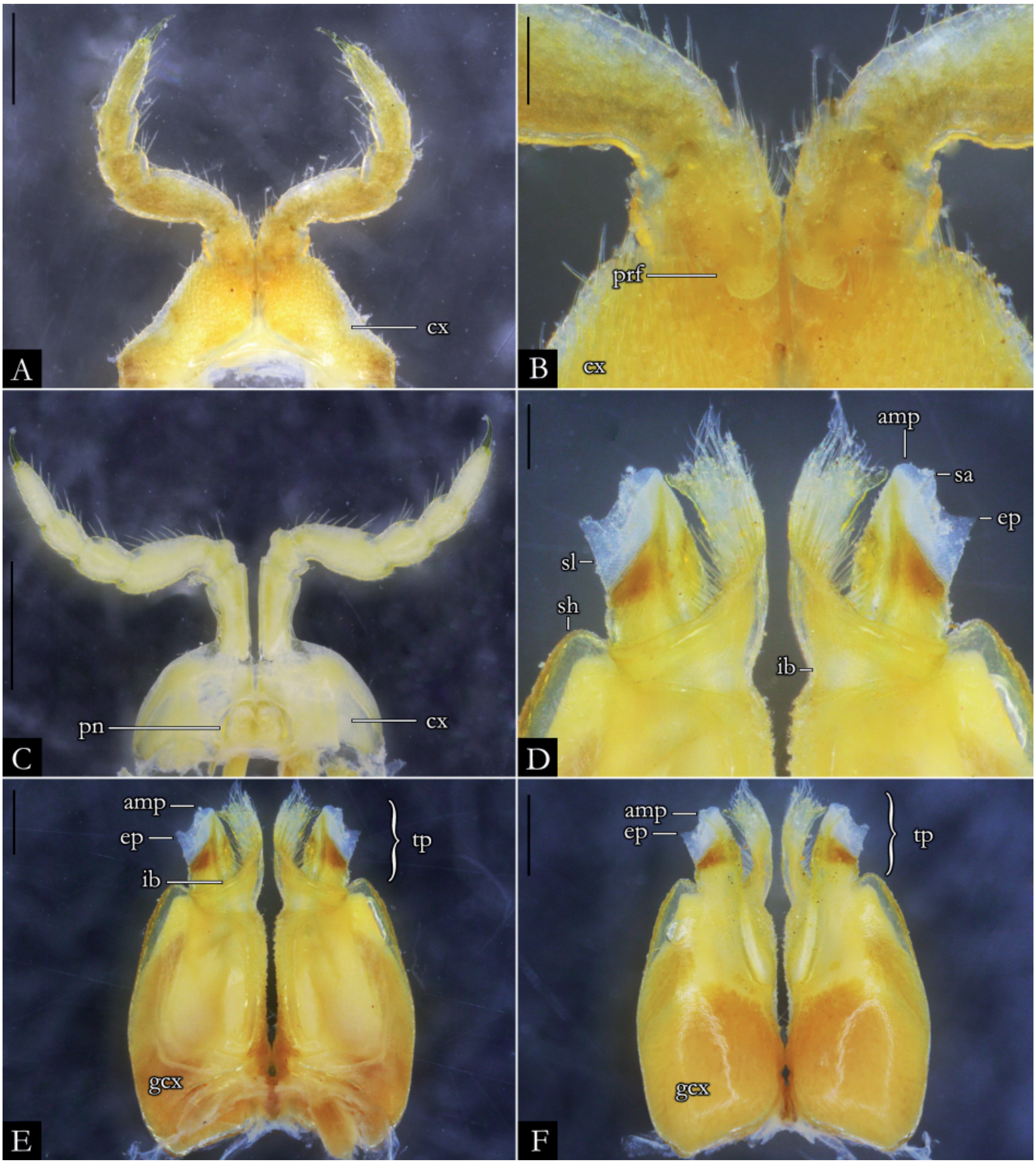

Fig. 114. *Pseudonannolene robsoni* Iniesta & Ferreira, 2014, ♂ (IBSP 3441). **A**. First leg-pair. **B**. Detail of prefemur. **C**. Second leg-pair. **D**. Detail of telopodites, in anal view. **E**. Gonopods, in anal view. **F**. Gonopods, in oral view. Abbreviations: see Material and methods. Scale bars: A, C, E–F = 0.5 mm; B, D = 0.2 mm.

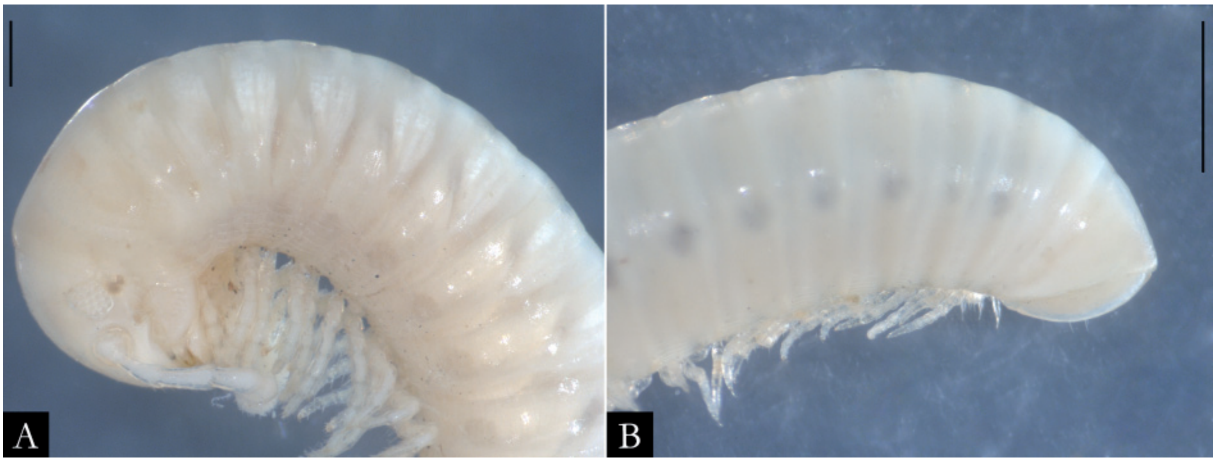

Fig. 115. *Pseudonannolene rocana* Silvestri, 1902, ♂ (NHMD), in lateral view. **A**. Anterior region. **B**. Posterior region. Scale bars = 1 mm.

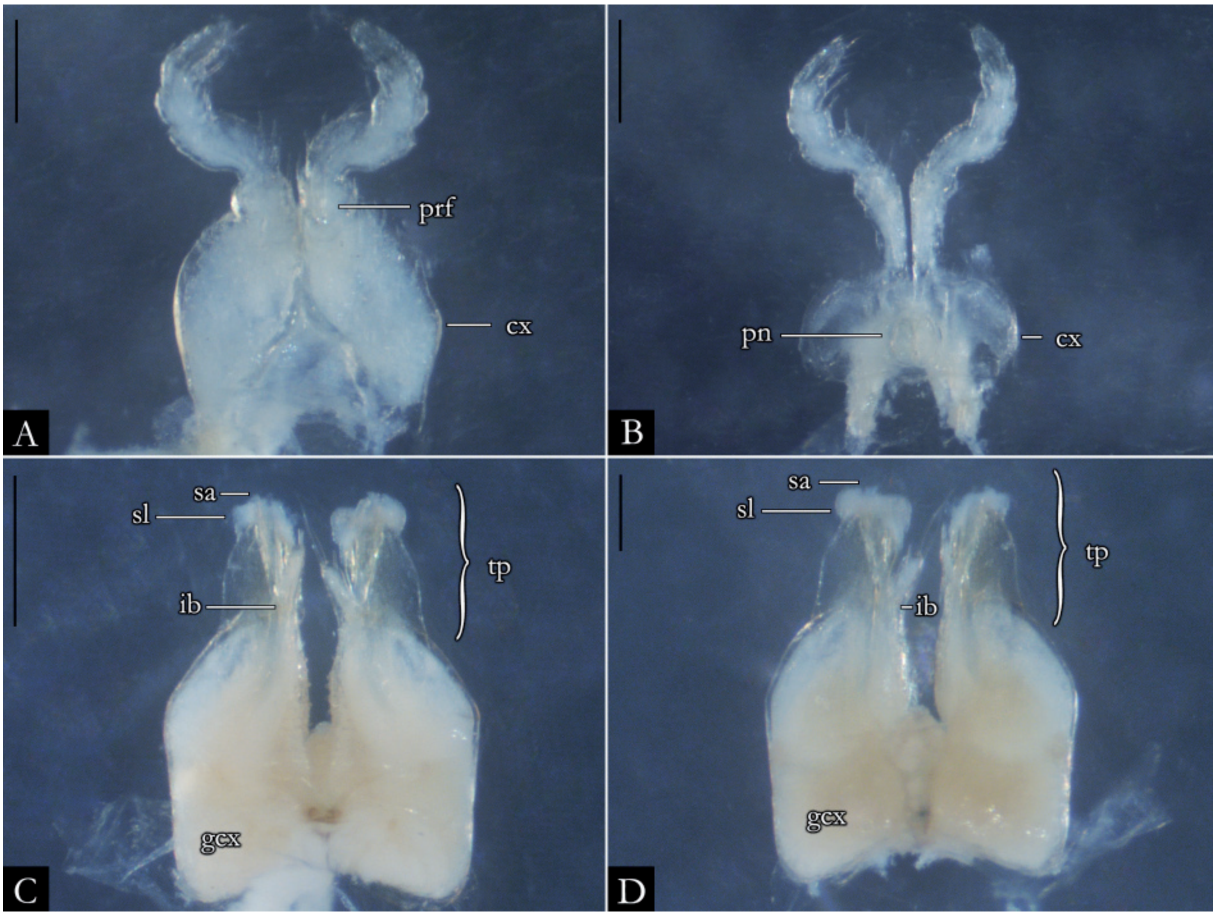

Fig. 116. *Pseudonannolene rocana* Silvestri, 1902, ♂ (NHMD). **A**. First leg-pair. **B**. Second leg-pair. **C**. Gonopods, in anal view. **D**. Gonopods, in oral view. Abbreviations: see Material and methods. Scale bars = 0.5 mm.

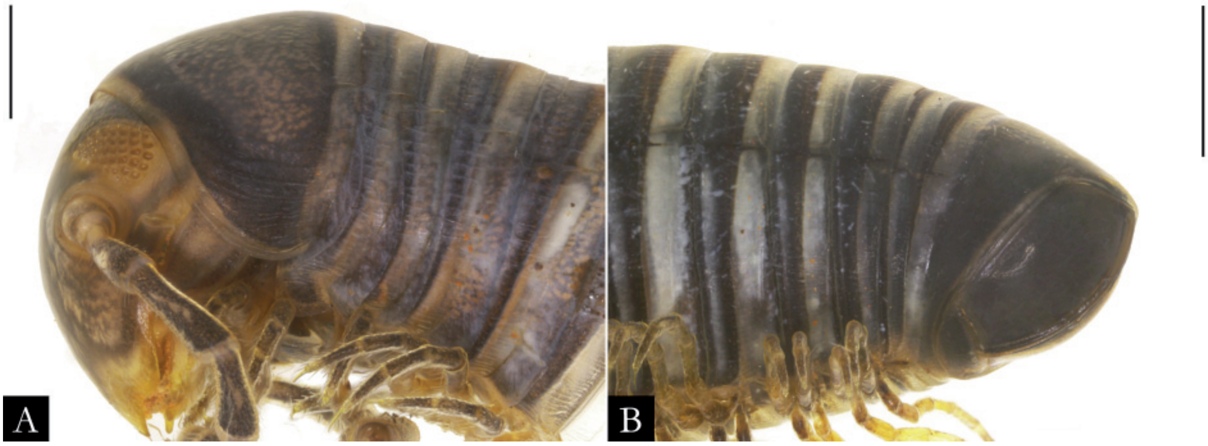

Fig. 117. *Pseudonannolene rolamossa* Iniesta & Ferreira, 2013, ♂ (ISLA 15054), in lateral view. **A**. Anterior region. **B**. Posterior region. Scale bars = 1 mm.

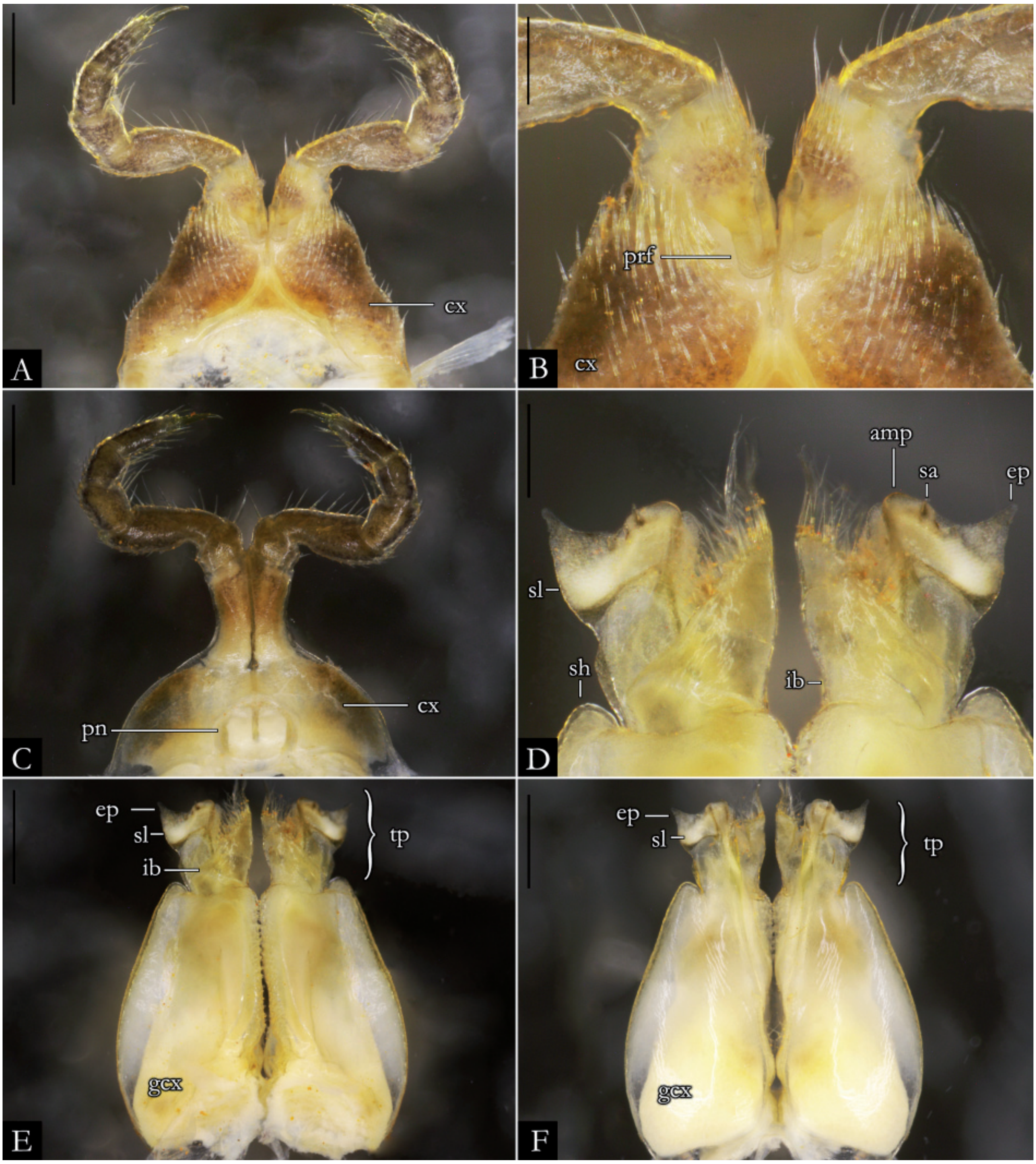

Fig. 118. *Pseudonannolene rolamossa* Iniesta & Ferreira, 2013, ♂ (ISLA 15054). **A**. First leg-pair. **B**. Detail of prefemur. **C**. Second leg-pair. **D**. Detail of telopodites, in anal view. **E**. Gonopods, in anal view. **F**. Gonopods, in oral view. Abbreviations: see Material and methods. Scale bars: A, C, E–F = 0.5 mm; B, D = 0.2 mm.

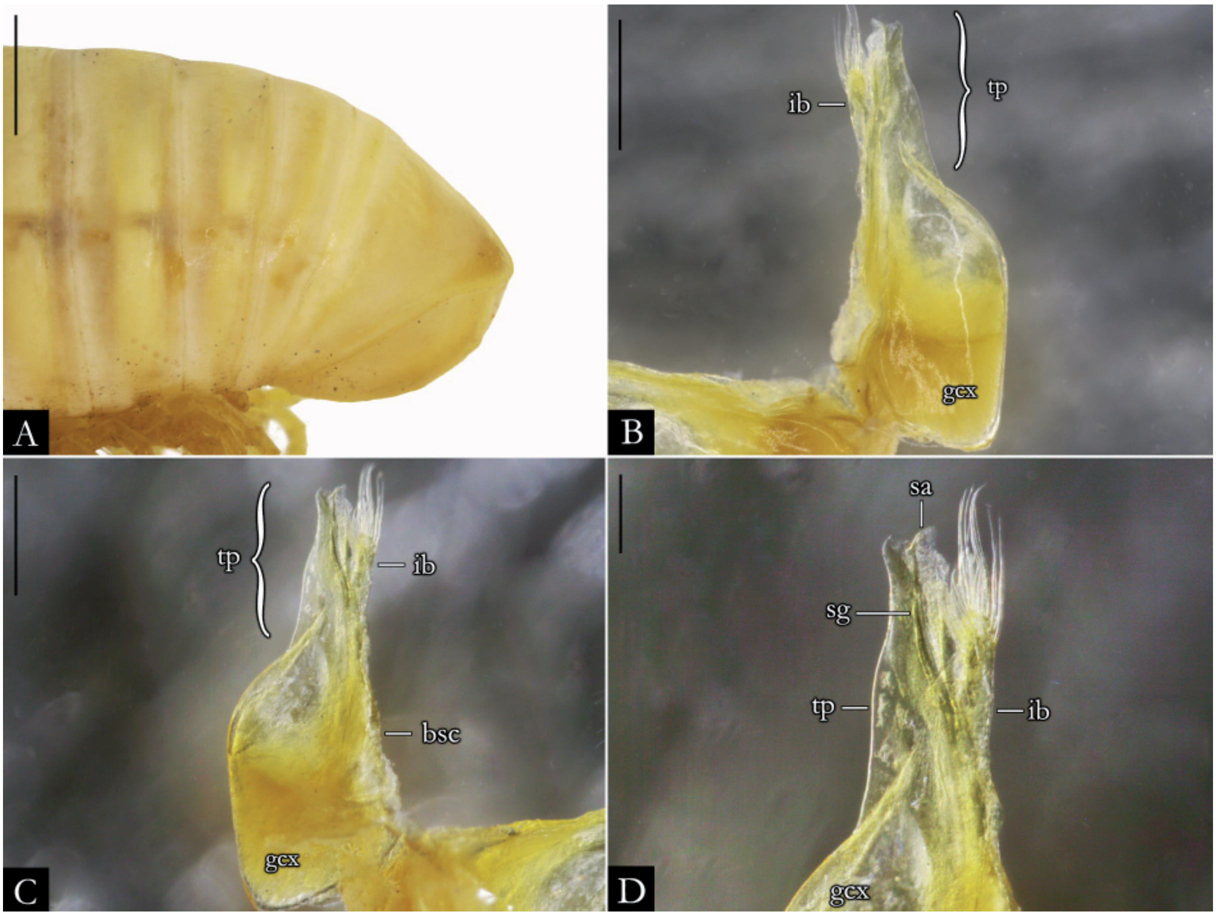

Fig. 119. *Pseudonannolene scalaris* Brölemann, 1902, holotype, ♂ (MZSP 232). **A**. Posterior region. **B**. Right gonopod, in oral view. **C**. Right gonopod, in anal view. **D**. Detail of telopodites, in anal view. Abbreviations: see Material and methods. Scale bars: A = 1 mm; B–C = 0.5 mm; D = 0.2 mm.

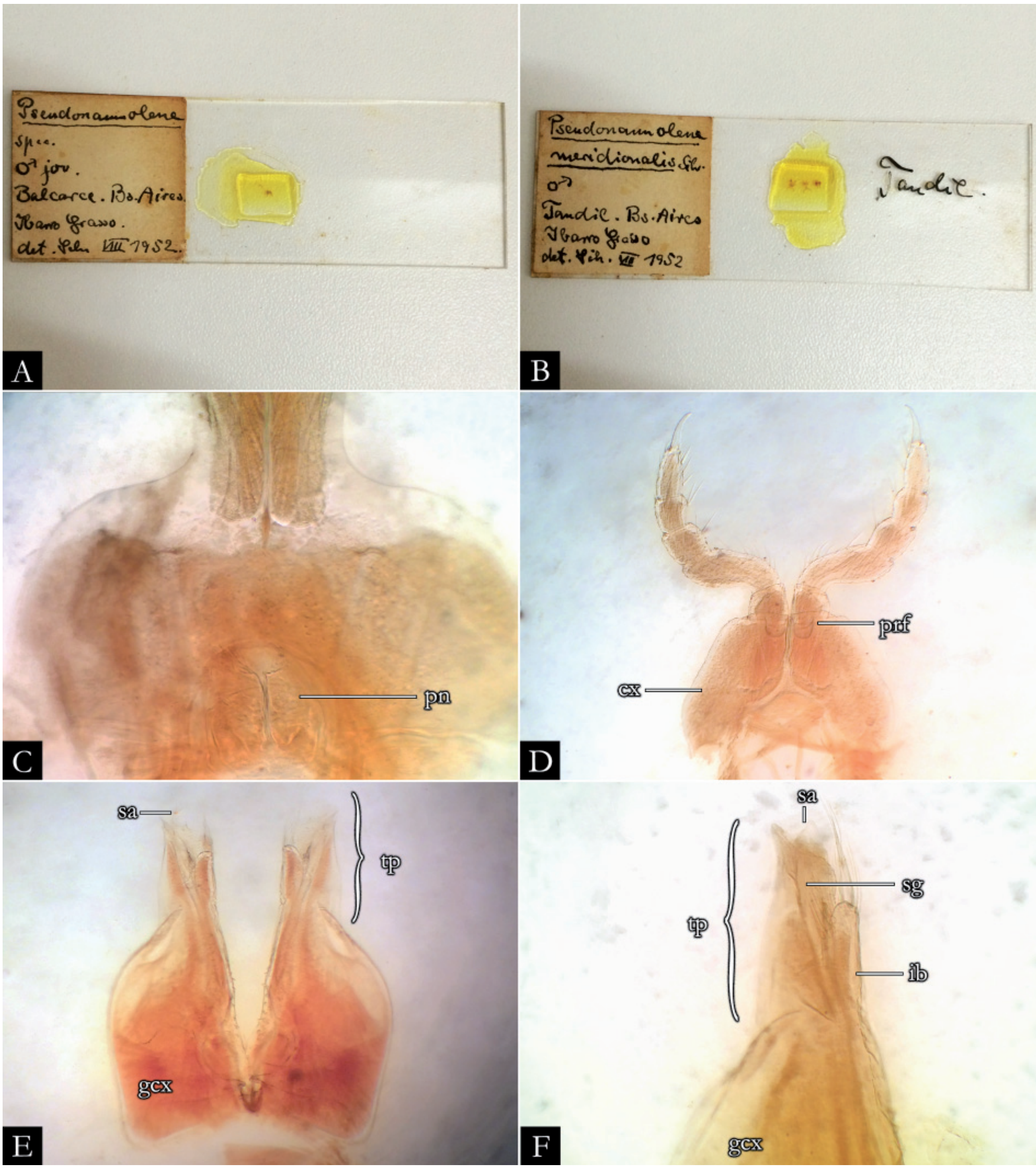

Fig. 120. *Pseudonannolene scalaris* Brölemann, 1902, ♂ (MZSP). **A**. Gonopods of immature ♂ mounted on microscope slide. **B**. Sexual structures of ♂ adult mounted on microscope slide. **C**. Detail of penis. **D**. Second leg-pair. **E**. Gonopods, in anal view. **F**. Detail of telopodites, in anal view. Abbreviations: see Material and methods. Images not to scale.

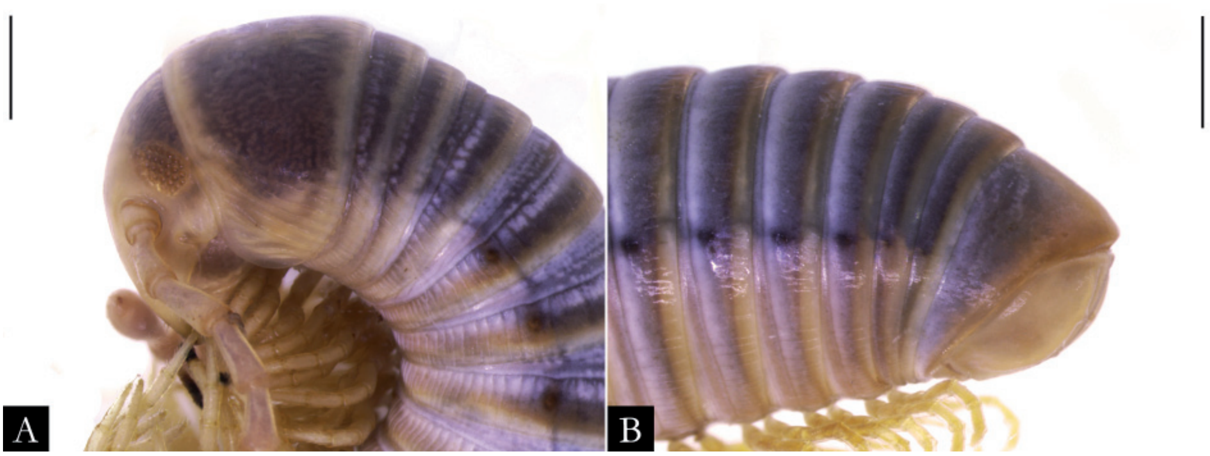

Fig. 121. *Pseudonannolene sebastianus* Brölemann, 1902, ♀ (IBSP 1110), in lateral view. **A**. Anterior region. **B**. Posterior region. Scale bars = 0.5 mm.

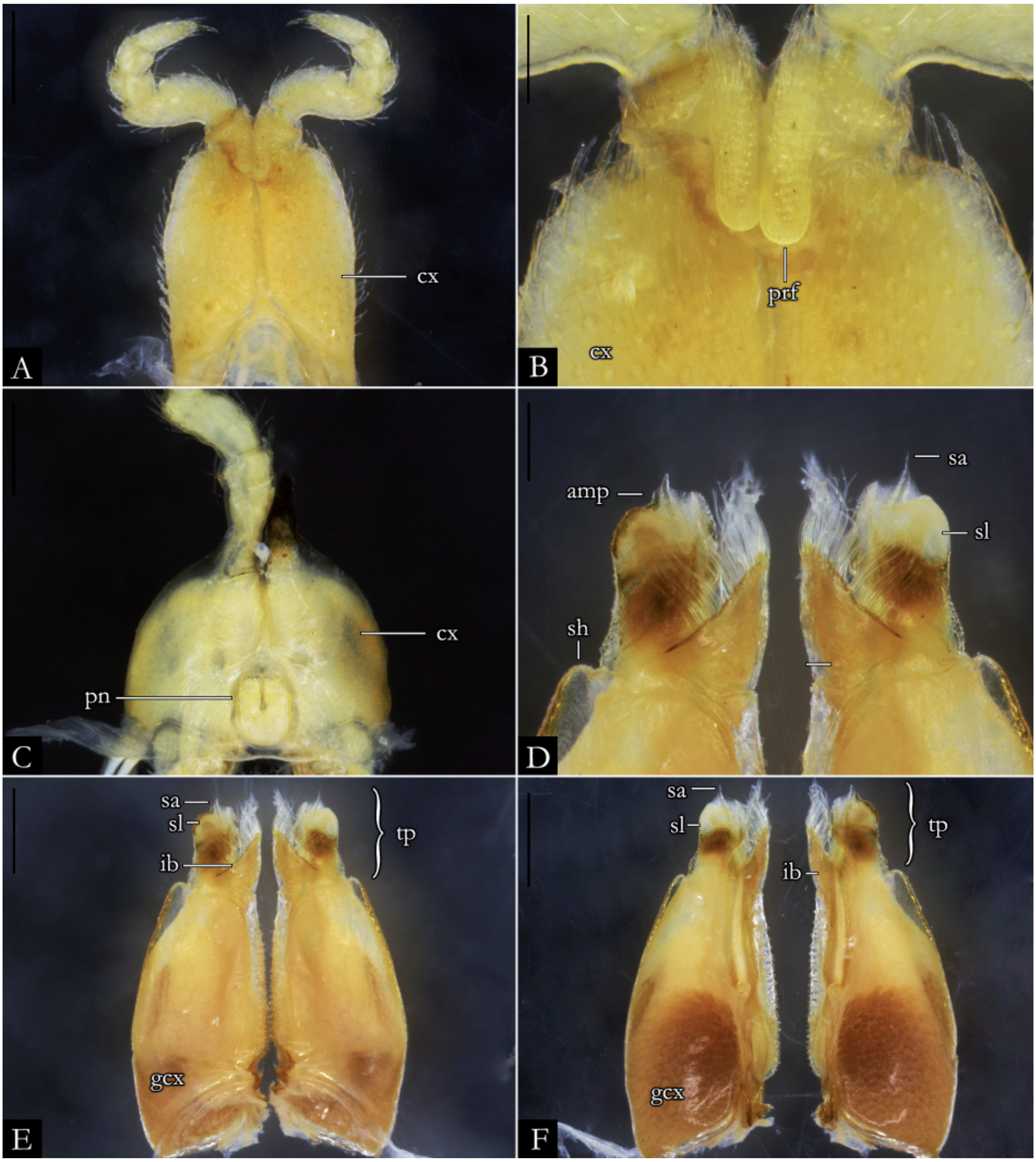

Fig. 122. *Pseudonannolene sebastianus* Brölemann, 1902, ♂ (IBSP 1390). **A**. First leg-pair. **B**. Detail of prefemur. **C**. Second leg-pair. **D**. Detail of telopodites, in anal view. **E**. Gonopods, in anal view. **F**. Gonopods, in oral view. Abbreviations: see Material and methods. Scale bars: A, C, E–F = 0.5 mm; B, D = 0.2 mm.

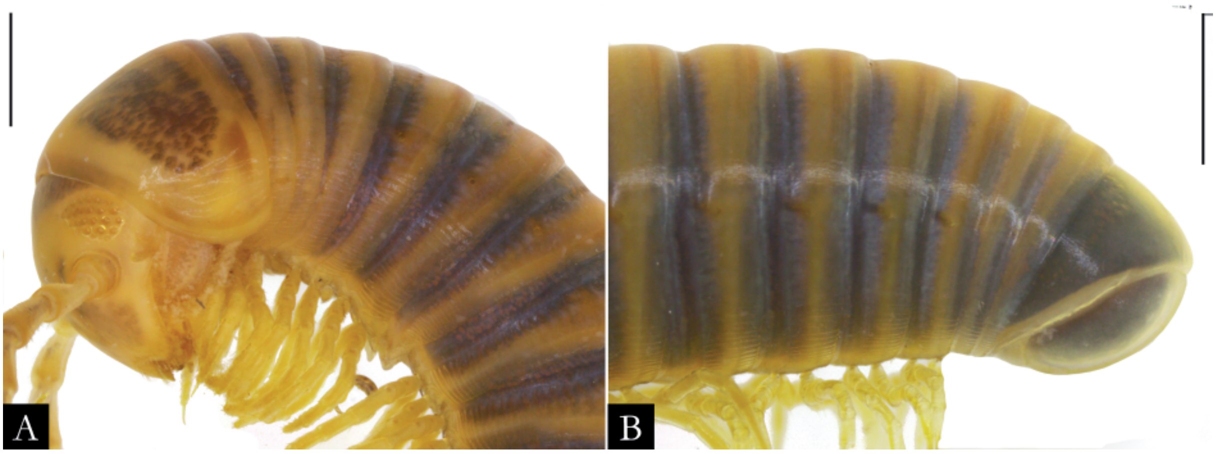

Fig. 123. *Pseudonannolene segmentata* Silvestri, 1895, ♂ (IBSP 1931), in lateral view. **A**. Anterior region. **B**. Posterior region. Scale bars = 1 mm.

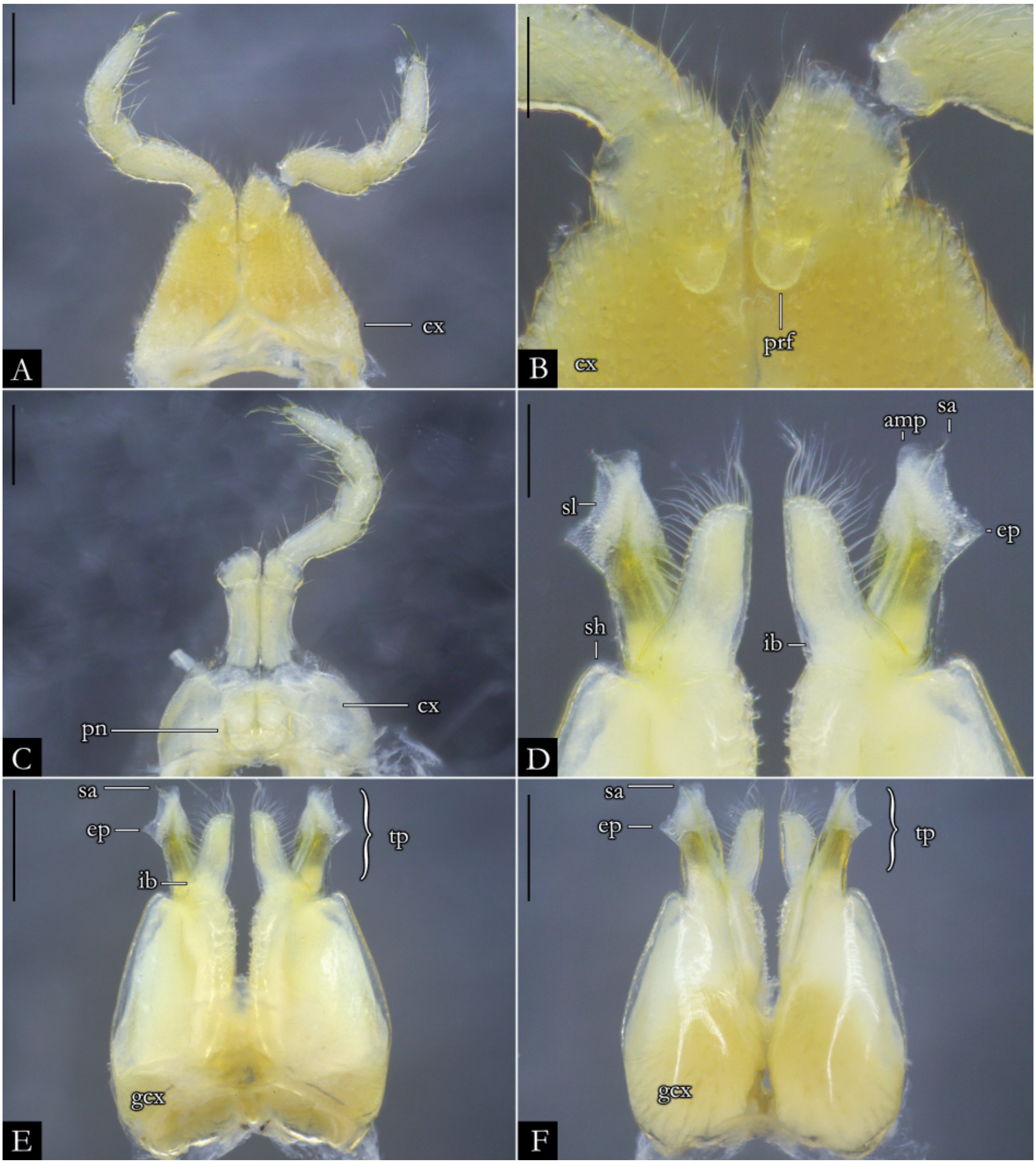

Fig. 124. *Pseudonannolene segmentata* Silvestri, 1895, ♂ (IBSP 1931). **A**. First leg-pair. **B**. Detail of prefemur. **C**. Second leg-pair. **D**. Detail of telopodites, in anal view. **E**. Gonopods, in anal view. **F**. Gonopods, in oral view. Abbreviations: see Material and methods. Scale bars = 0.5 mm.

Fig. 125. *Pseudonannolene silvestris* Schubart, 1944, ♂ (IBSP 2272), in lateral view. **A**. Anterior region. **B**. Posterior region. Scale bars = 1 mm.

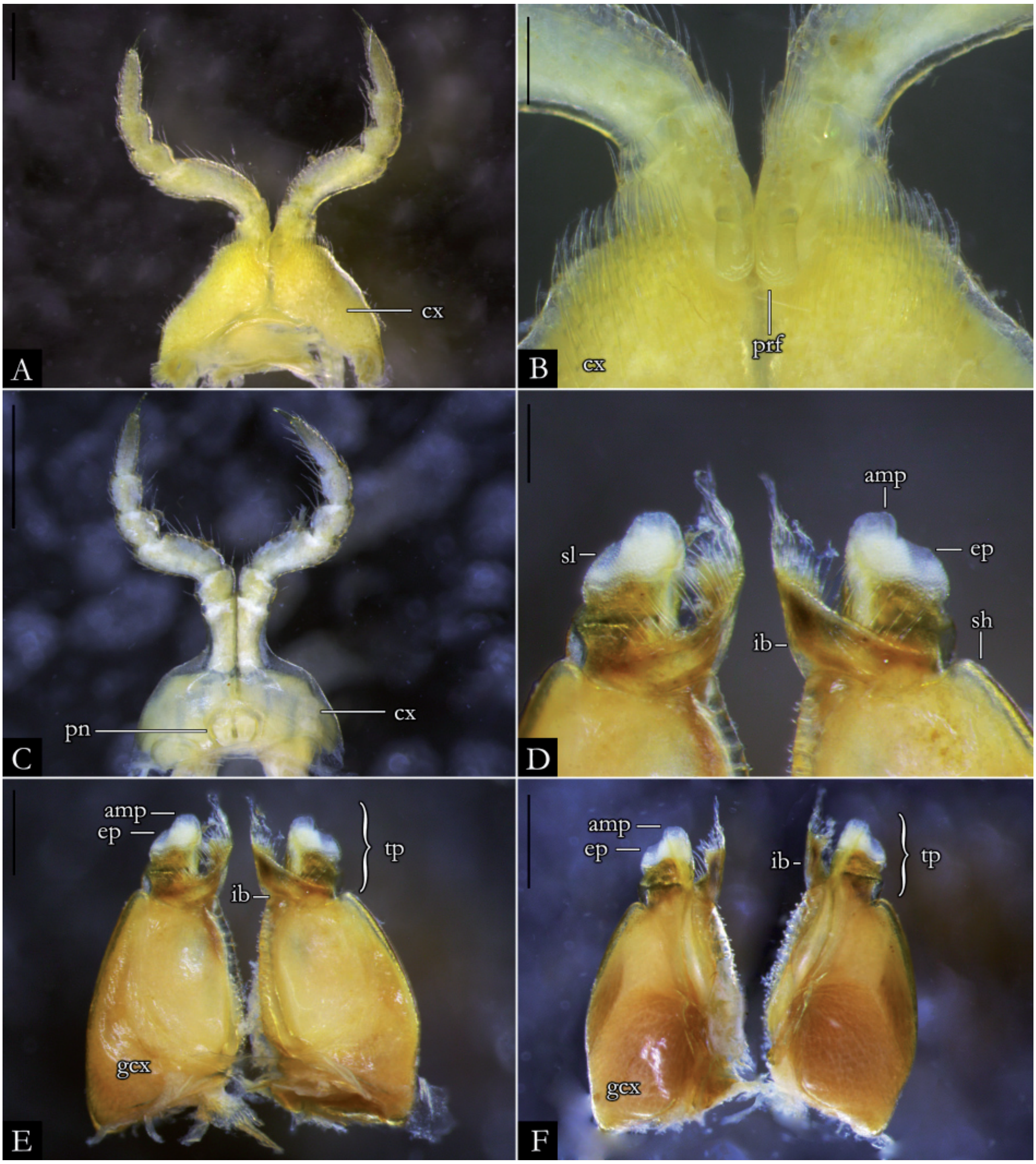

Fig. 126. *Pseudonannolene silvestris* Schubart, 1944, ♂ (IBSP 2271). **A**. First leg-pair. **B**. Detail of prefemur. **C**. Second leg-pair. **D**. Detail of telopodites, in anal view. **E**. Gonopods, in anal view. **F**. Gonopods, in oral view. Abbreviations: see Material and methods. Scale bars: A, C, E–F = 0.5 mm; B, D = 0.2 mm.

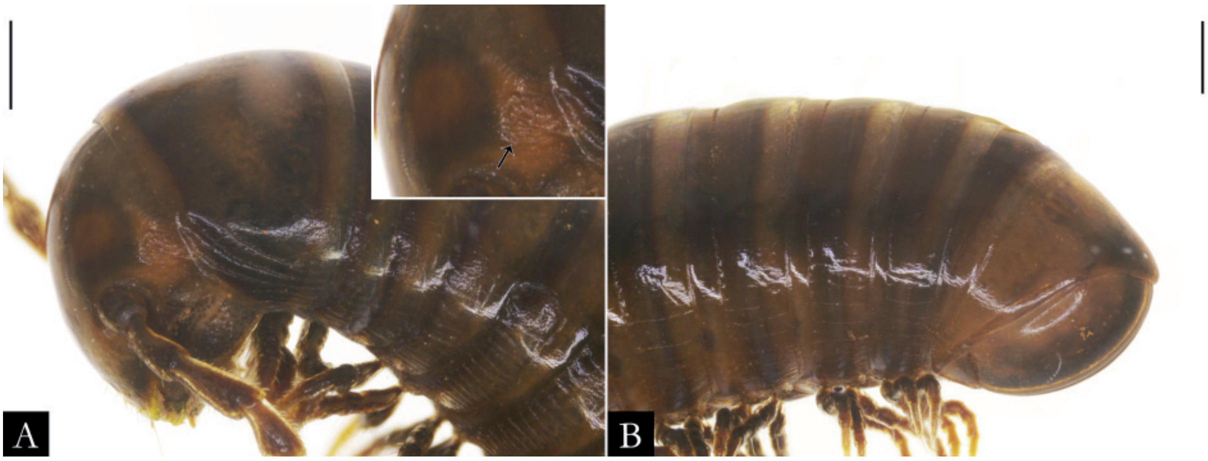

Fig. 127. *Pseudonannolene spelaea* Iniesta & Ferreira, 2013, ♂ (IBSP 5923), in lateral view. **A**. Anterior region (arrows indicating the ommatidial cluster). **B**. Posterior region. Scale bars = 0.5 mm.

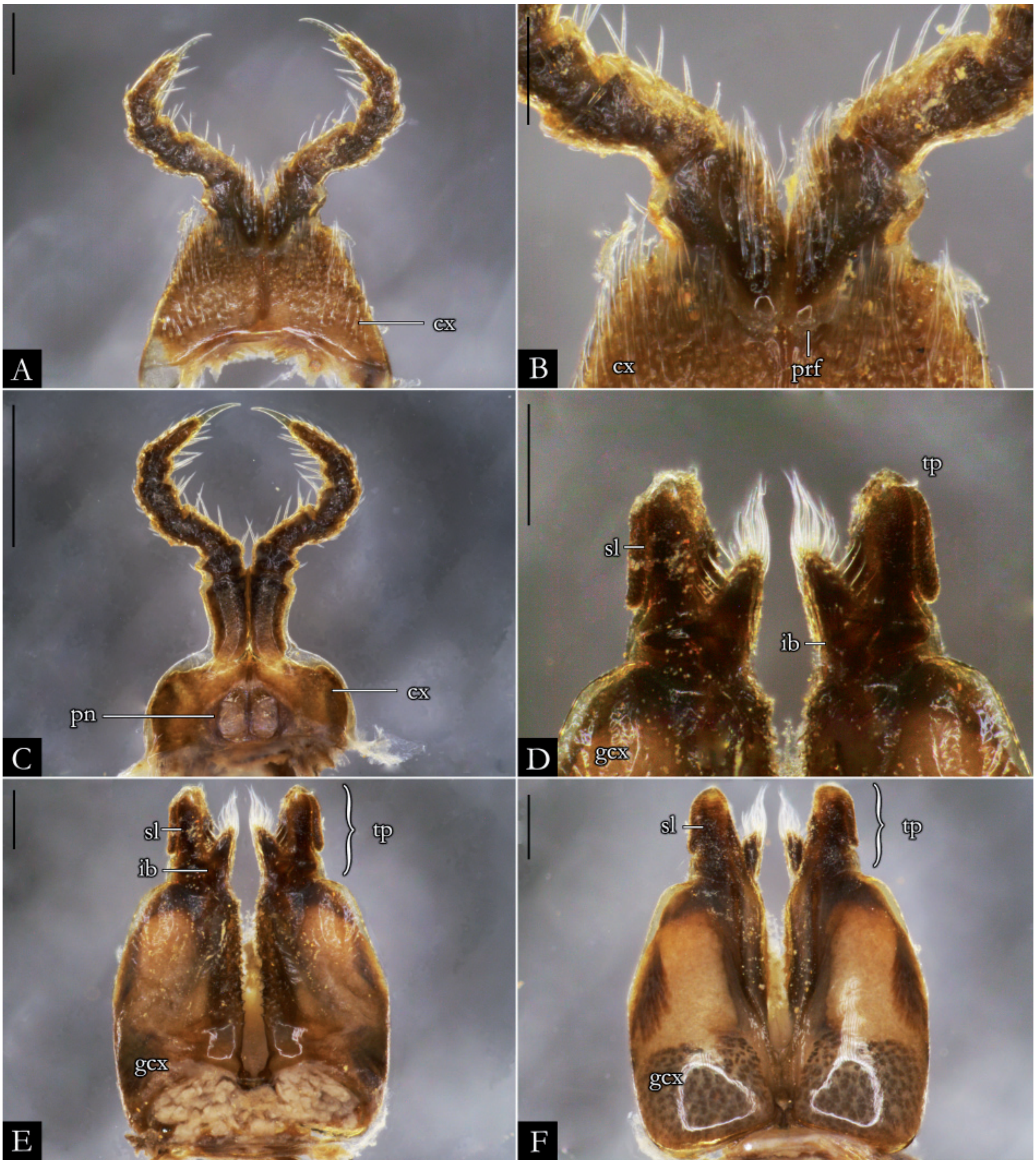

Fig. 128. *Pseudonannolene spelaea* Iniesta & Ferreira, 2013, ♂ (IBSP 5923). **A**. First leg-pair. **B**. Detail of prefemur. **C**. Second leg-pair. **D**. Detail of telopodites, in anal view. **E**. Gonopods, in anal view. **F**. Gonopods, in oral view. Abbreviations: see Material and methods. Scale bars = 0.2 mm.

Fig. 129. *Pseudonannolene strinatii* Mauriès, 1974, ♀ (IBSP 7635), in lateral view. **A**. Anterior region. **B**. Posterior region. Scale bars = 1 mm.

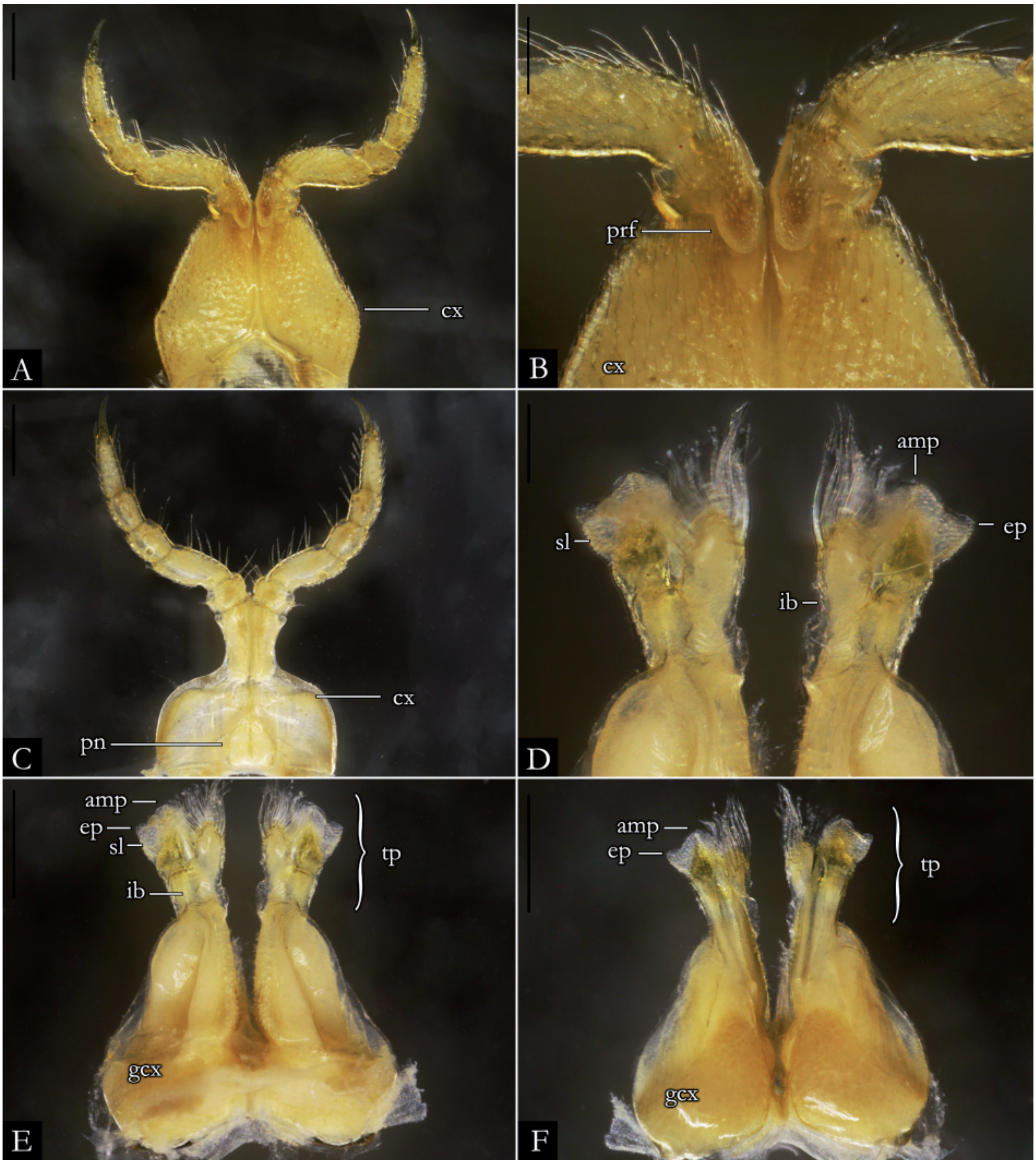

Fig. 130. *Pseudonannolene strinatii* Mauriès, 1974, ♂ (IBSP 7633). **A**. First leg-pair. **B**. Detail of prefemur. **C**. Second leg-pair. **D**. Detail of telopodites, in anal view. **E**. Gonopods, in anal view. **F**. Gonopods, in oral view. Abbreviations: see Material and methods. Scale bars: A, C, E–F = 0.5 mm; B, D = 0.2 mm.

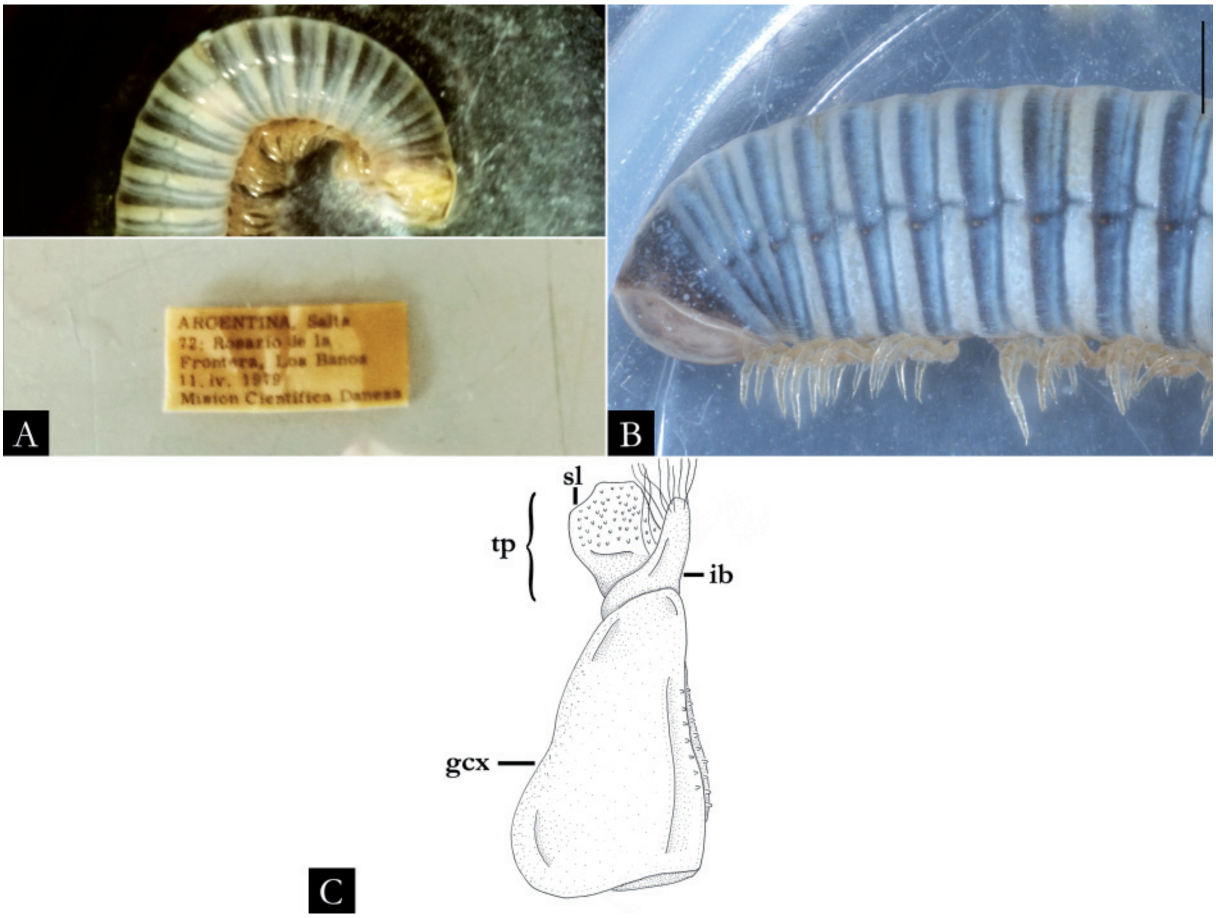

Fig. 131. *Pseudonannolene sulcatula* Silvestri, 1895, ♀ (NHMD). **A**. Body rings, in lateral view, and original label. **B**. Posterior region in lateral view. **C**. Schematic drawing of right gonopod in anal view (modified from Silvestri 1895b: fig. 14). Abbreviations: see Material and methods. Images not to scale.

Fig. 132. *Pseudonannolene tocaiensis* Fontanetti, 1996, paratype, ♂ (MZSP 942), in lateral view. **A**. Anterior region. **B**. Posterior region. Scale bars = 1 mm.

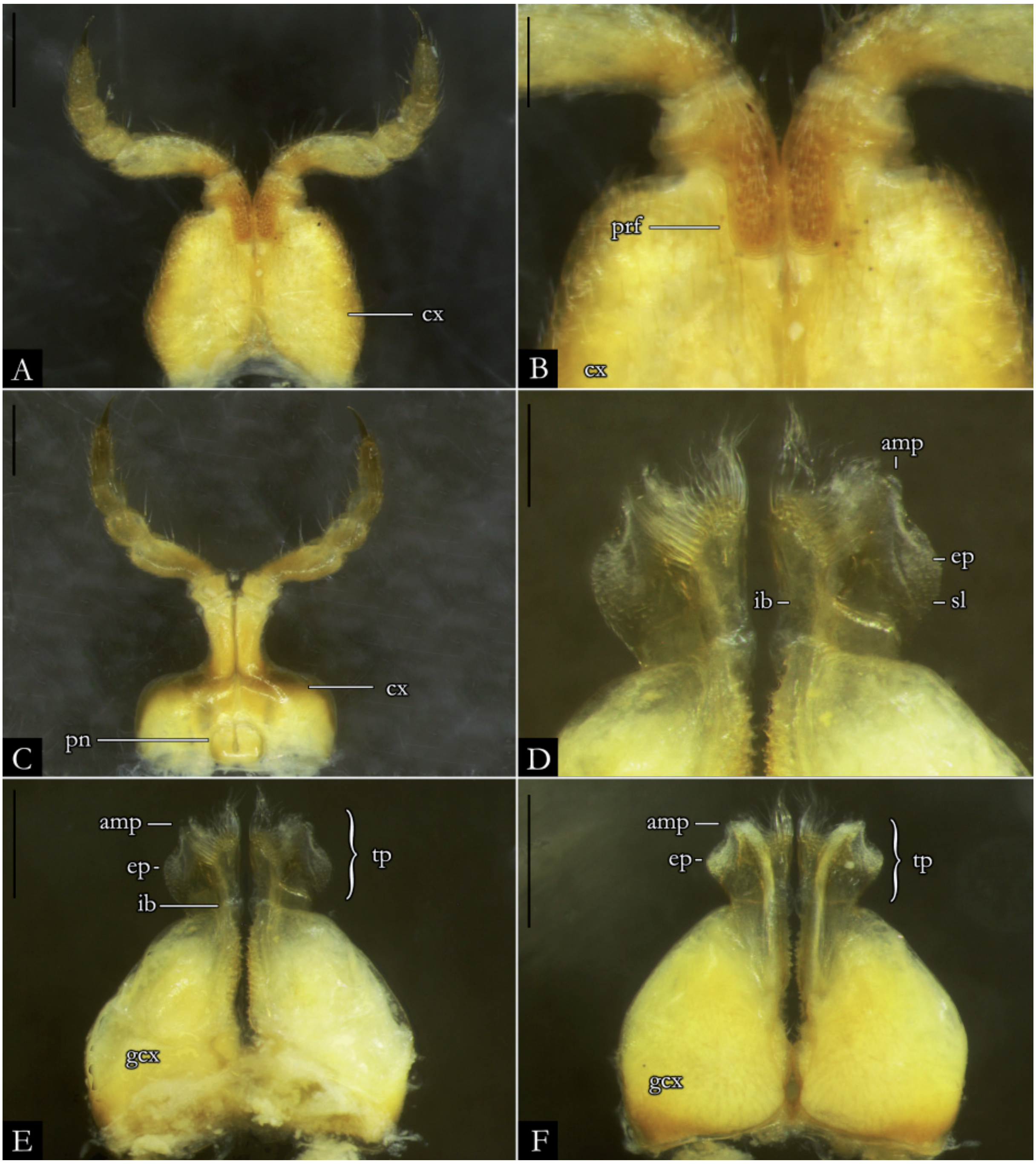

Fig. 133. *Pseudonannolene tocaiensis* Fontanetti, 1996, paratype, ♂ (MZSP 942). **A**. First leg-pair. **B**. Detail of prefemur. **C**. Second leg-pair. **D**. Detail of telopodites, in anal view. **E**. Gonopods, in anal view. **F**. Gonopods, in oral view. Abbreviations: see Material and methods. Scale bars: A, C, E–F = 0.5 mm; B, D = 0.2 mm.

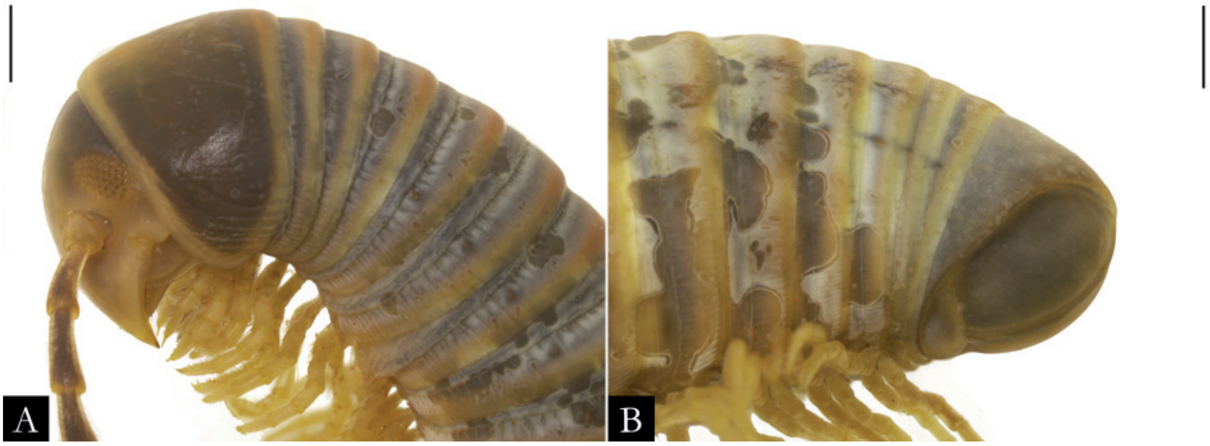

Fig. 134. *Pseudonannolene tricolor* Brölemann, 1902, ♂ (IBSP 964), in lateral view. **A**. Anterior region. **B**. Posterior region. Scale bars = 1 mm.

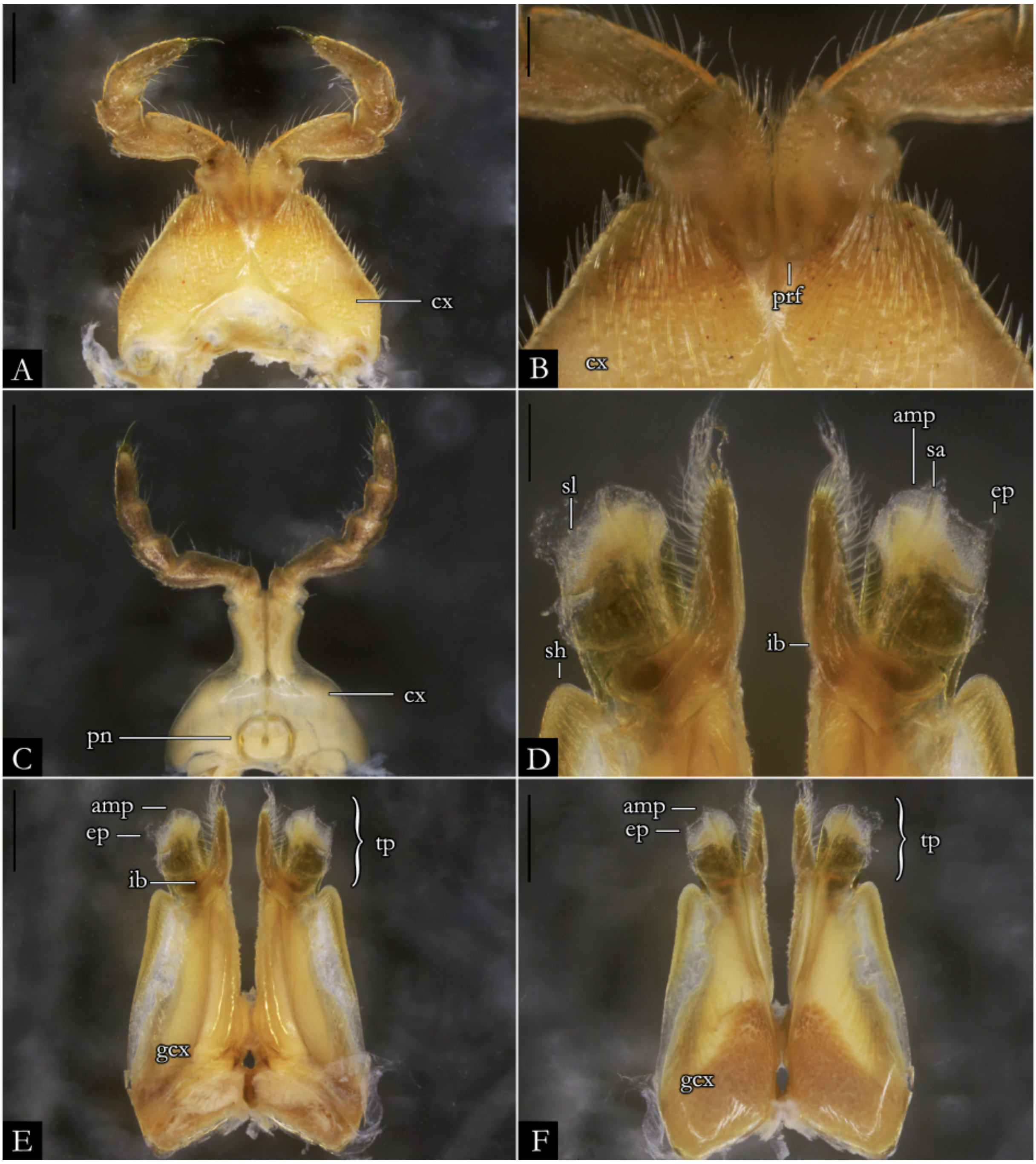

Fig. 135. *Pseudonannolene tricolor* Brölemann, 1902, ♂ (IBSP 964). **A**. First leg-pair. **B**. Detail of prefemur. **C**. Second leg-pair. **D**. Detail of telopodites, in anal view. **E**. Gonopods, in anal view. **F**. Gonopods, in oral view. Abbreviations: see Material and methods. Scale bars: A, C, E–F = 0.5 mm; B, D = 0.2 mm.

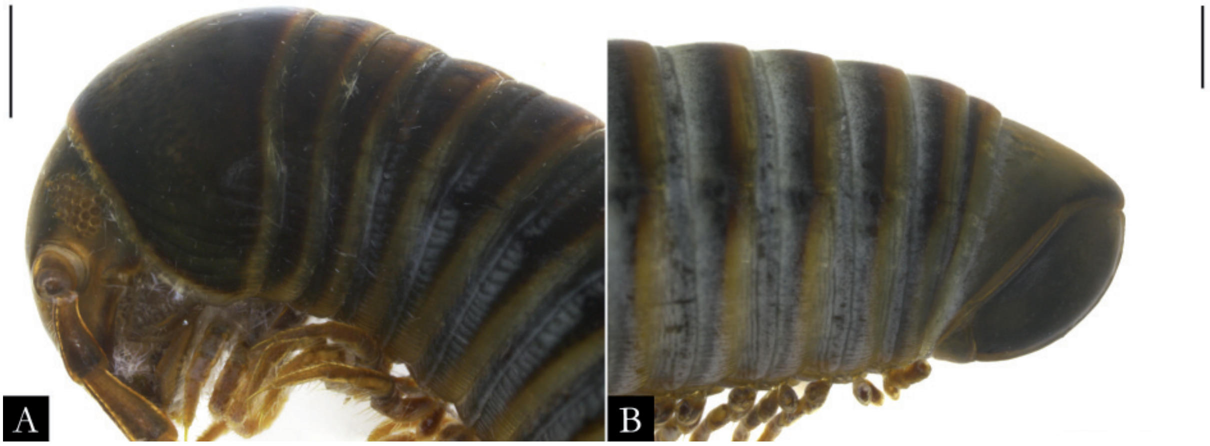

Fig. 136. *Pseudonannolene typica* Silvestri, 1895, holotype, ♂ (MCSN), in lateral view. **A**. Anterior region. **B**. Posterior region. Scale bars = 1 mm.

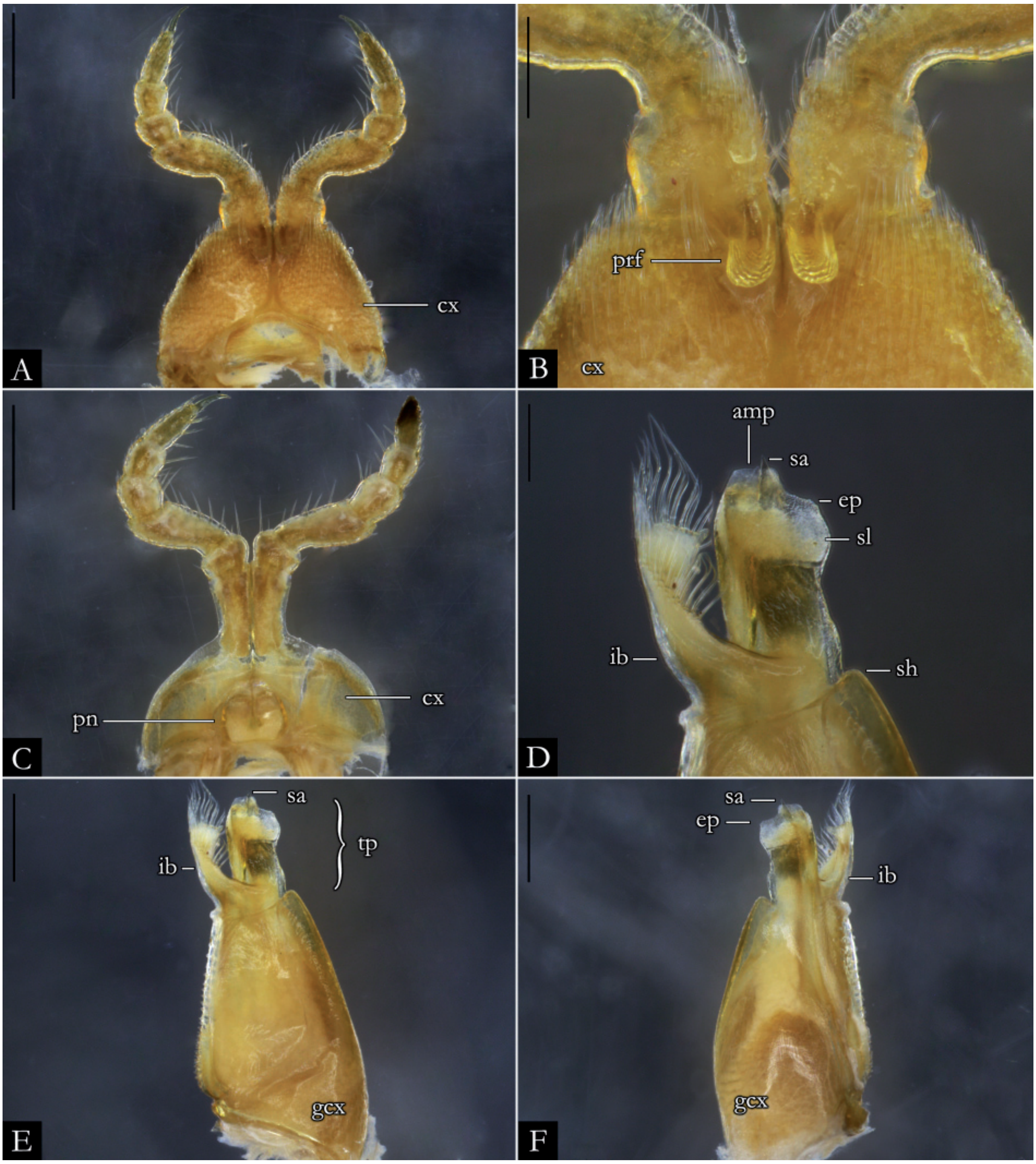

Fig. 137. *Pseudonannolene typica* Silvestri, 1895, holotype, ♂ (MCSN). **A**. First leg-pair. **B**. Detail of prefemur. **C**. Second leg-pair. **D**. Detail of telopodite, in anal view. **E**. Left gonopod, in anal view. **F**. Left gonopod, in oral view. Abbreviations: see Material and methods. Scale bars = 0.5 mm.

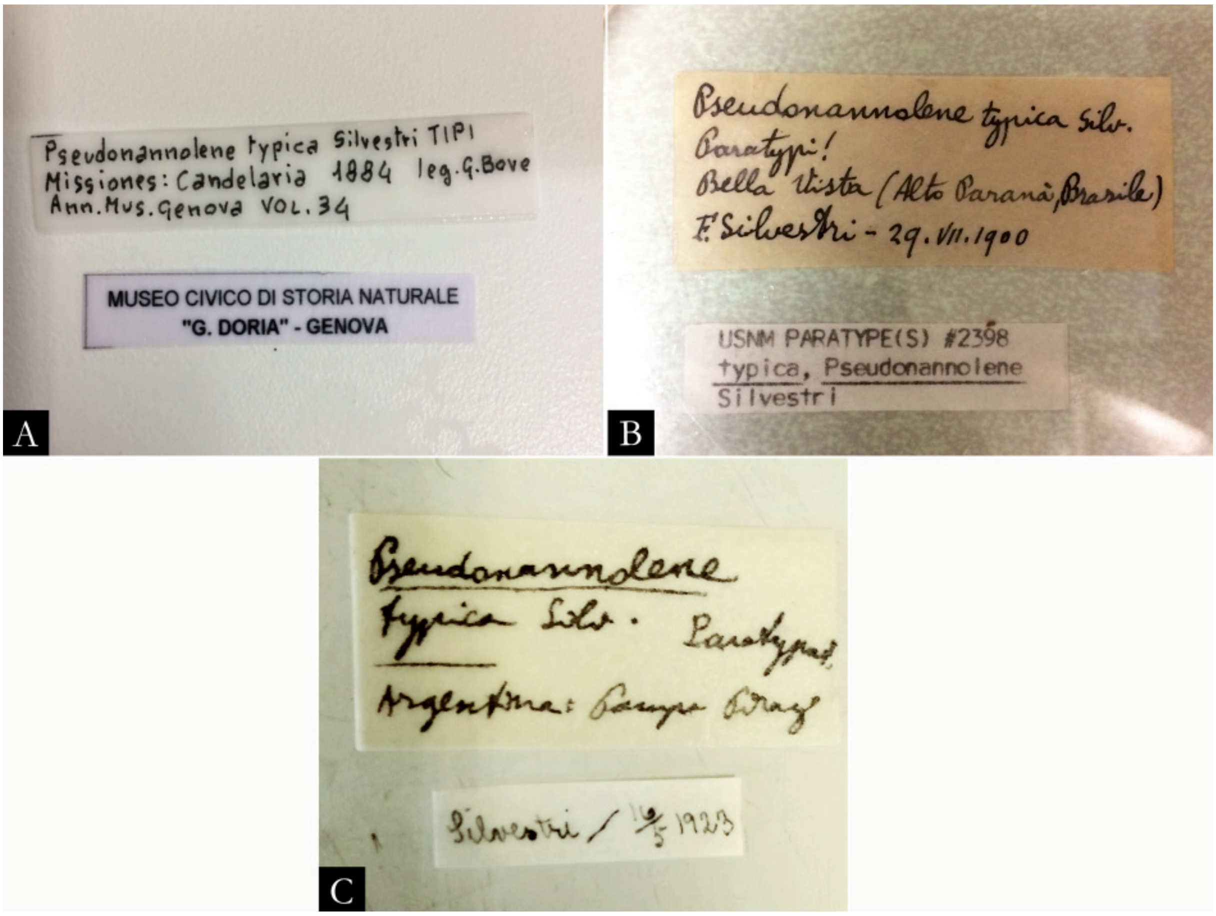

Fig. 138. *Pseudonannolene typica* Silvestri, 1895, holotype, ♂ (MCSN) and paratypes (USNM). **A–C**. Original labels of type material. Images not to scale.

Fig. 139. Type material of the junior subjective synonym *Pseudonannolene abbreviata* Silvestri, 1902 (= *P. typica* Silvestri, 1895). **A**. Anterior region. **B**. Posterior region. **C**. Original label of female syntype (USNM 2031). **D**. Original label of female syntype (ZMB 2887). Images not to scale.

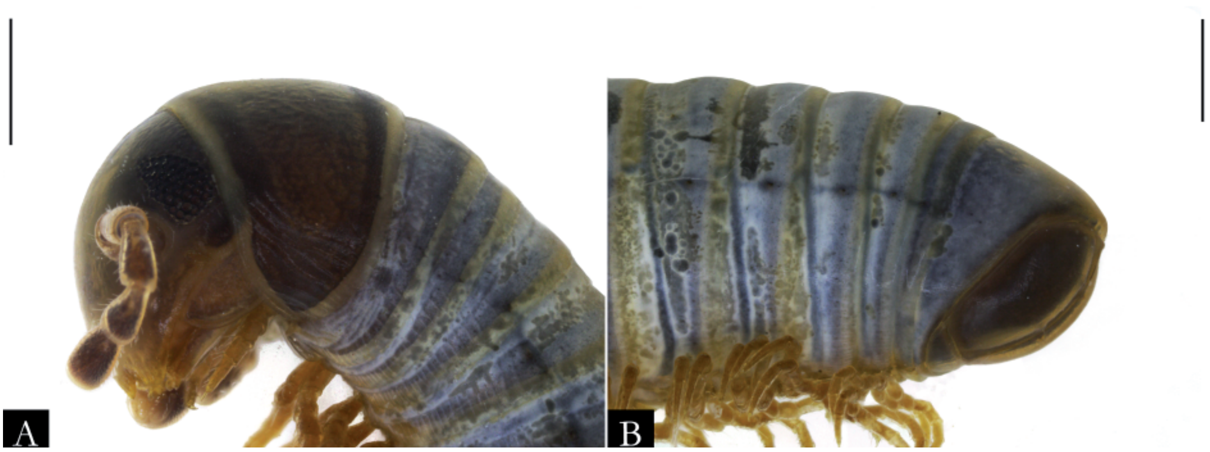

Fig. 140. *Pseudonannolene urbica* Schubart, 1945, ♀ (IBSP 7887), in lateral view. **A**. Anterior region. **B**. Posterior region. Scale bars = 0.5 mm.

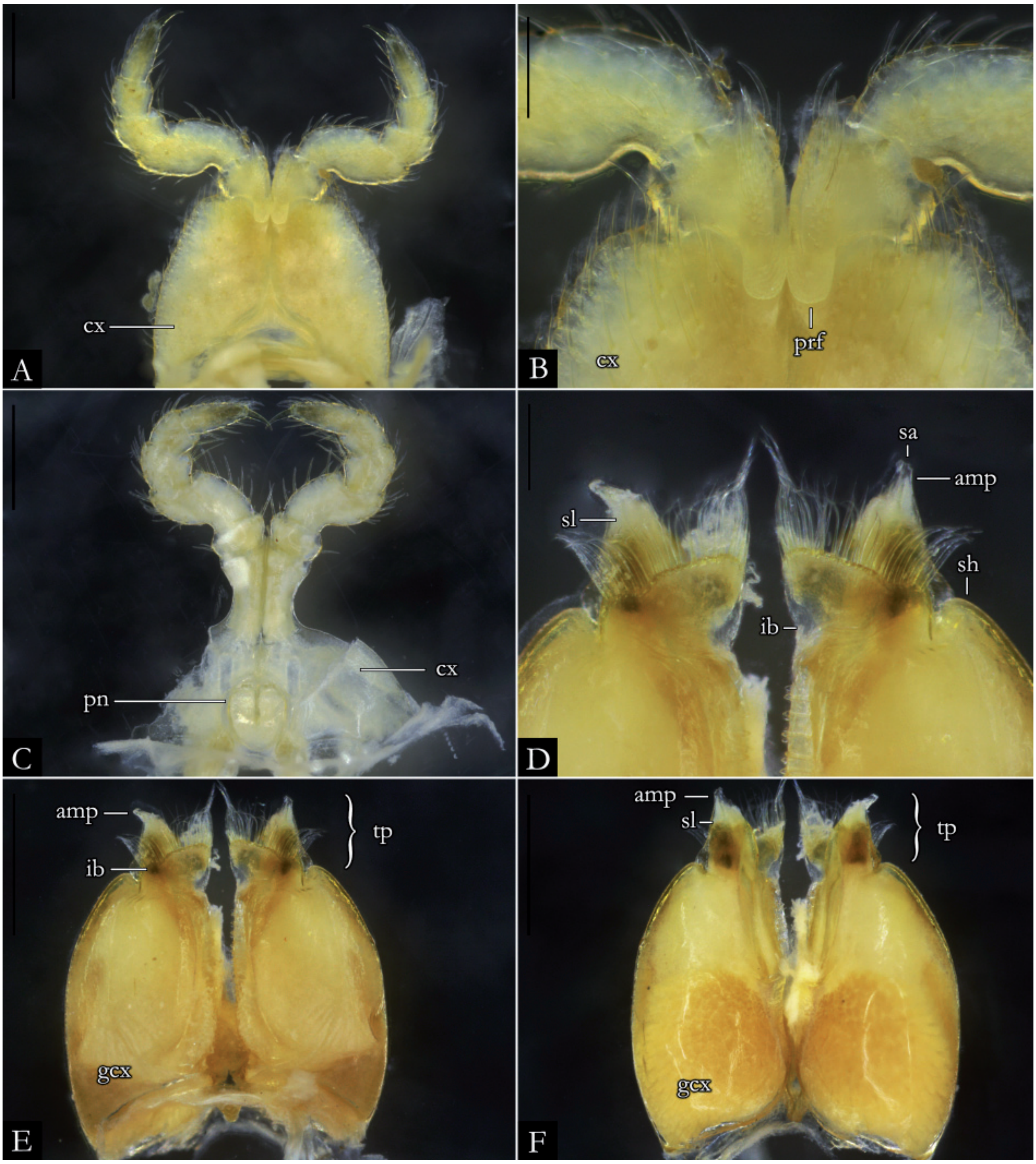

Fig. 141. *Pseudonannolene urbica* Schubart, 1945, ♂ (IBSP 2007). **A**. First leg-pair. **B**. Detail of prefemur. **C**. Second leg-pair. **D**. Detail of telopodites, in anal view. **E**. Gonopods, in anal view. **F**. Gonopods, in oral view. Abbreviations: see Material and methods. Scale bars: A, C, E–F = 0.5 mm; B, D = 0.2 mm.

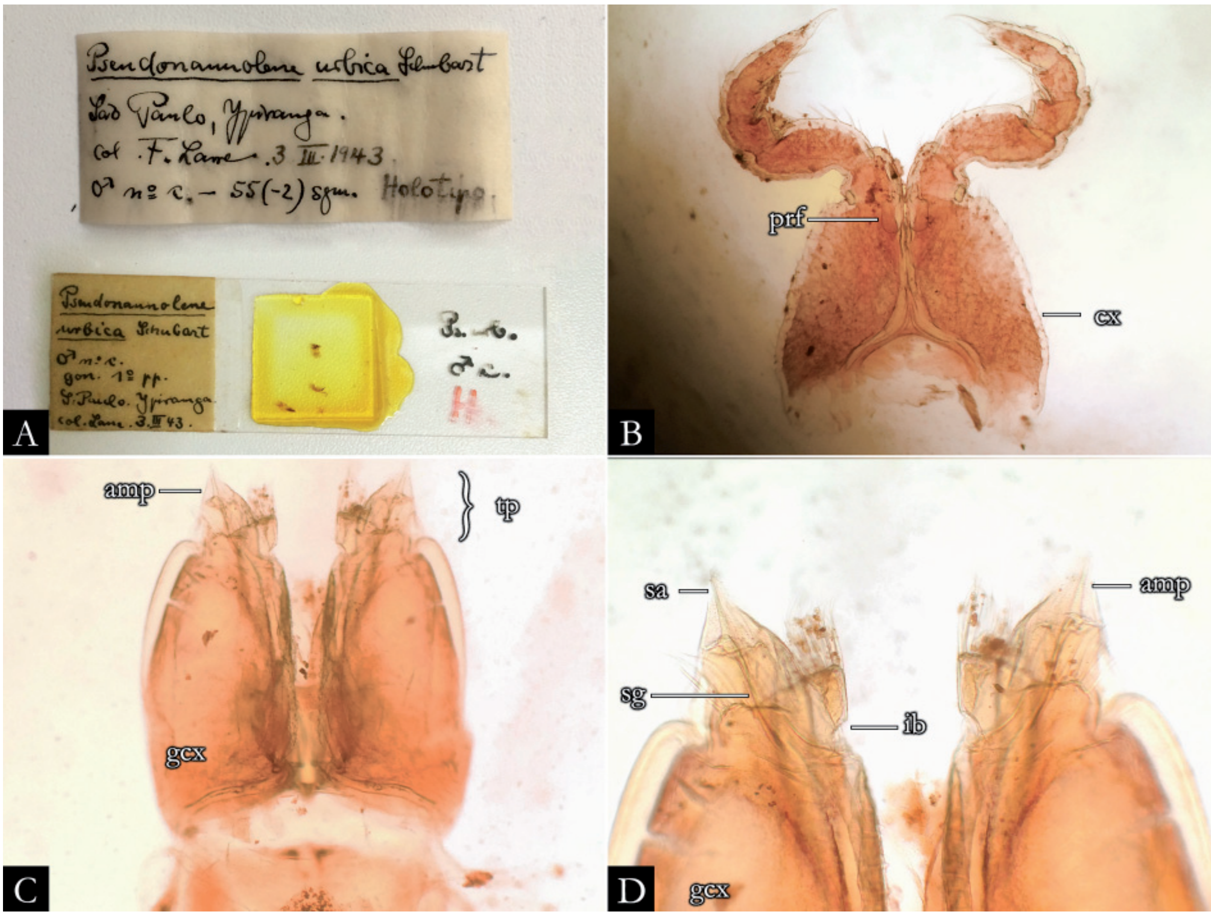

Fig. 142. *Pseudonannolene urbica* Schubart, 1945, holotype, ♂ (MZSP). **A**. Sexual structures of type material mounted on microscope slide. **B**. First leg-pair. **C**. Gonopods, in oral view. **D**. Detail of telopodites, in oral view. Abbreviations: see Material and methods. Images not to scale.

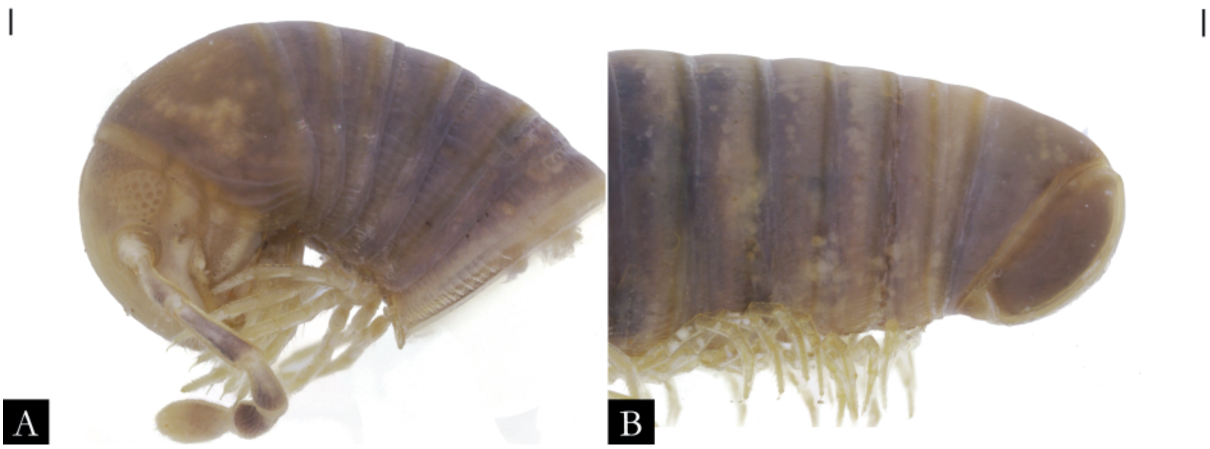

Fig. 143. *Pseudonannolene xavieri* Iniesta & Ferreira, 2014, ♂ (MNRJ 30148), in lateral view. **A**. Anterior region. **B**. Posterior region. Scale bars = 0.2 mm.

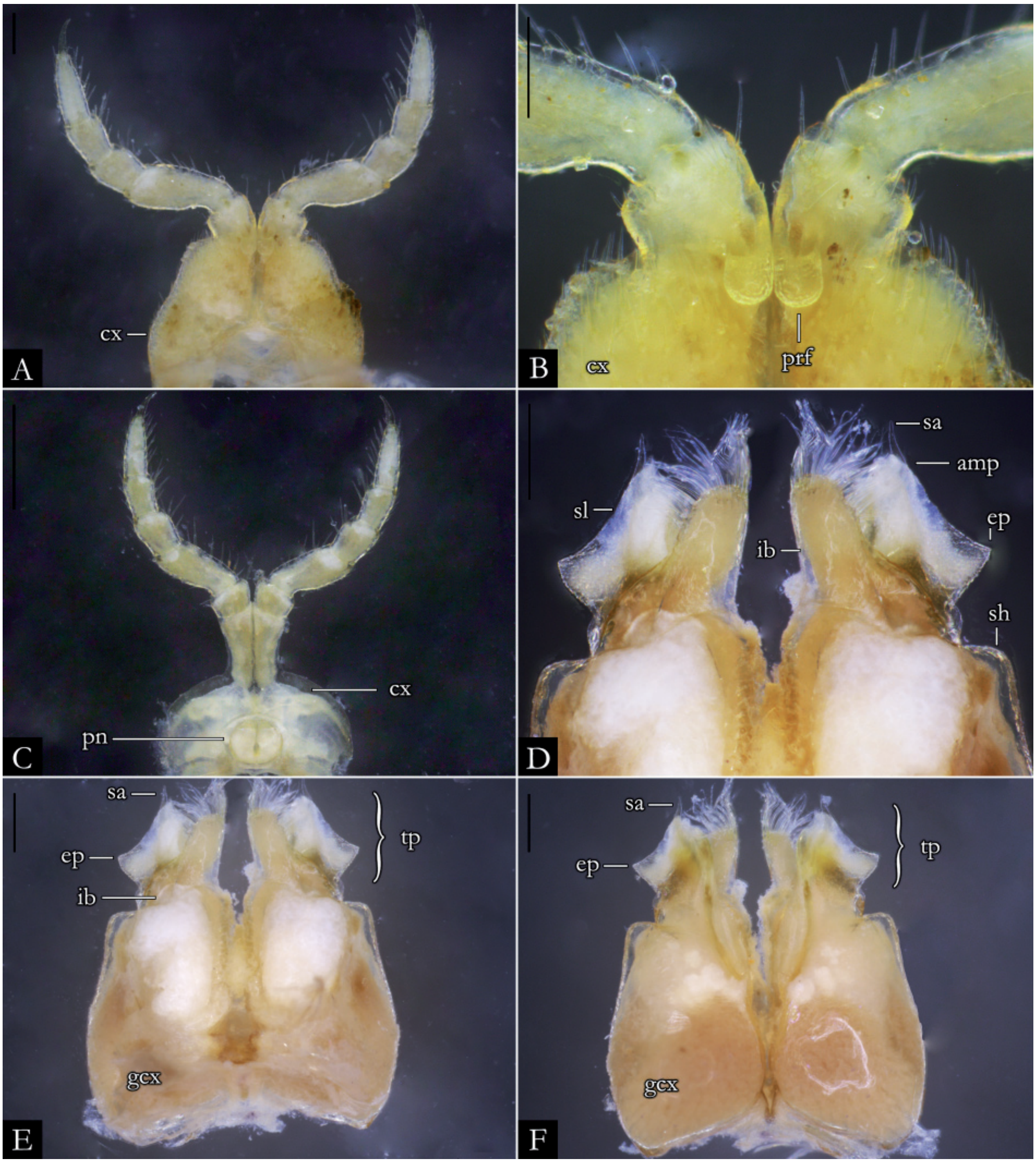

Fig. 144. *Pseudonannolene xavieri* Iniesta & Ferreira, 2014, ♂ (MNRJ 30148). **A**. First leg-pair. **B**. Detail of prefemur. **C**. Second leg-pair. **D**. Detail of telopodites, in anal view. **E**. Gonopods, in anal view. **F**. Gonopods, in oral view. Abbreviations: see Material and methods. Scale bars = 0.2 mm.

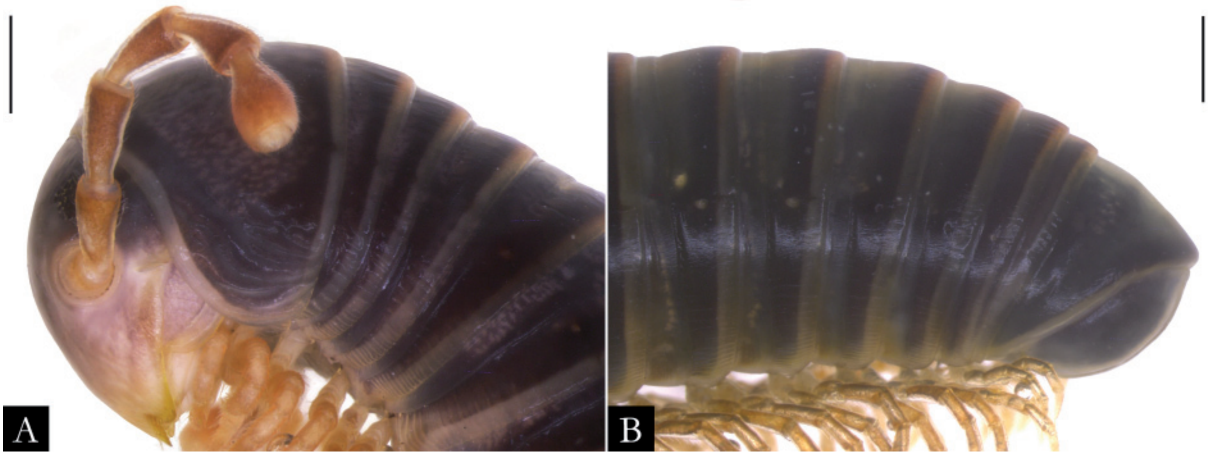

Fig. 145. *Pseudonannolene alata* sp. nov., holotype, ♂ (IBSP 7874), in lateral view. **A**. Anterior region. **B**. Posterior region. Scale bars = 1 mm.

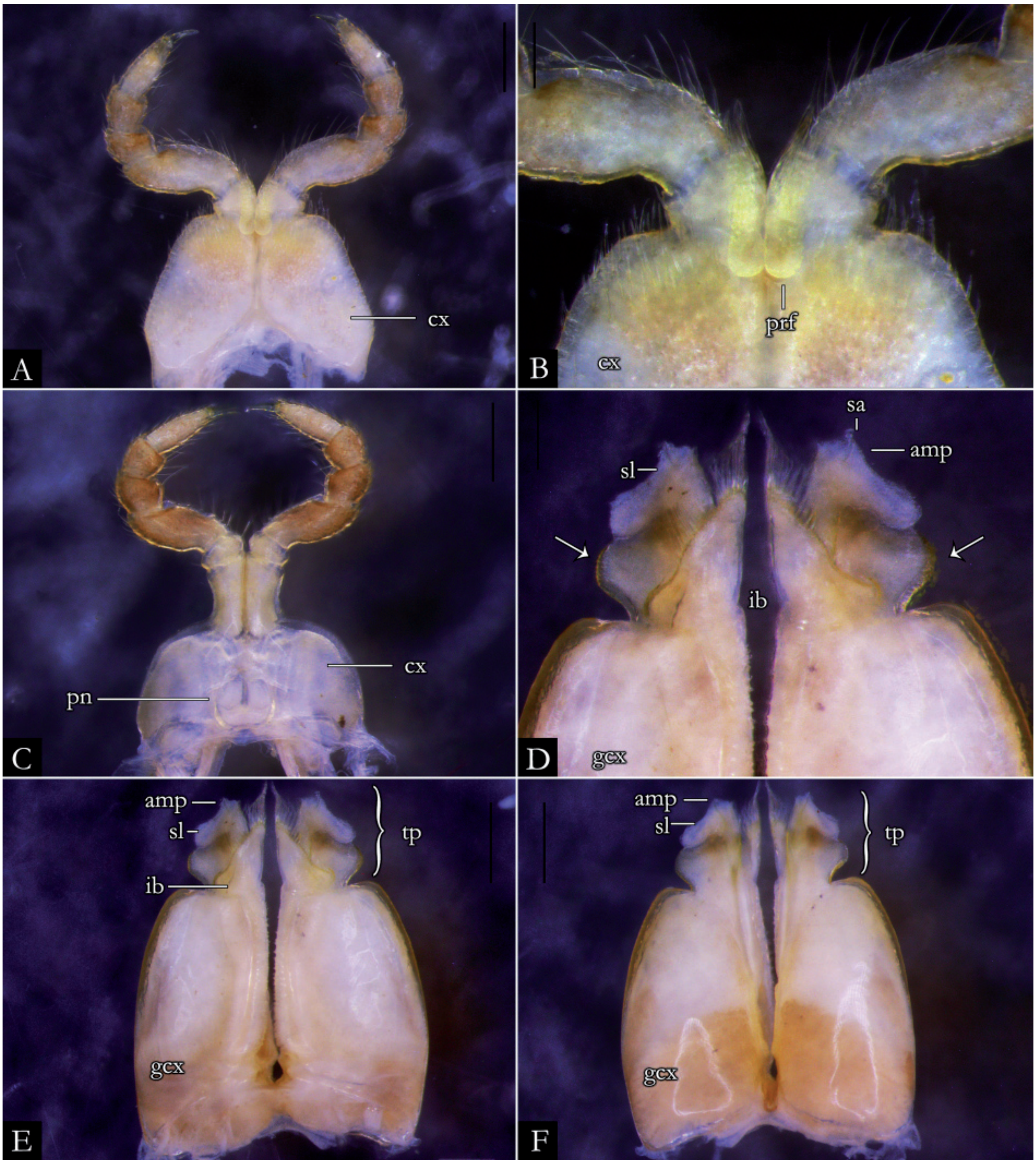

Fig. 146. *Pseudonannolene alata* sp. nov., holotype, ♂ (IBSP 7874). **A**. First leg-pair. **B**. Detail of prefemur. **C**. Second leg-pair. **D**. Detail of telopodites, in anal view. **E**. Gonopods, in anal view. **F**. Gonopods, in oral view. Abbreviations: see Material and methods. Scale bars: A, C, E–F = 0.5 mm; B, D = 0.2 mm.

Fig. 147. *Pseudonannolene aurea* sp. nov., paratype, ♂ (IBSP 5854), in lateral view. **A**. Anterior region. **B**. Posterior region. Scale bars = 1 mm.

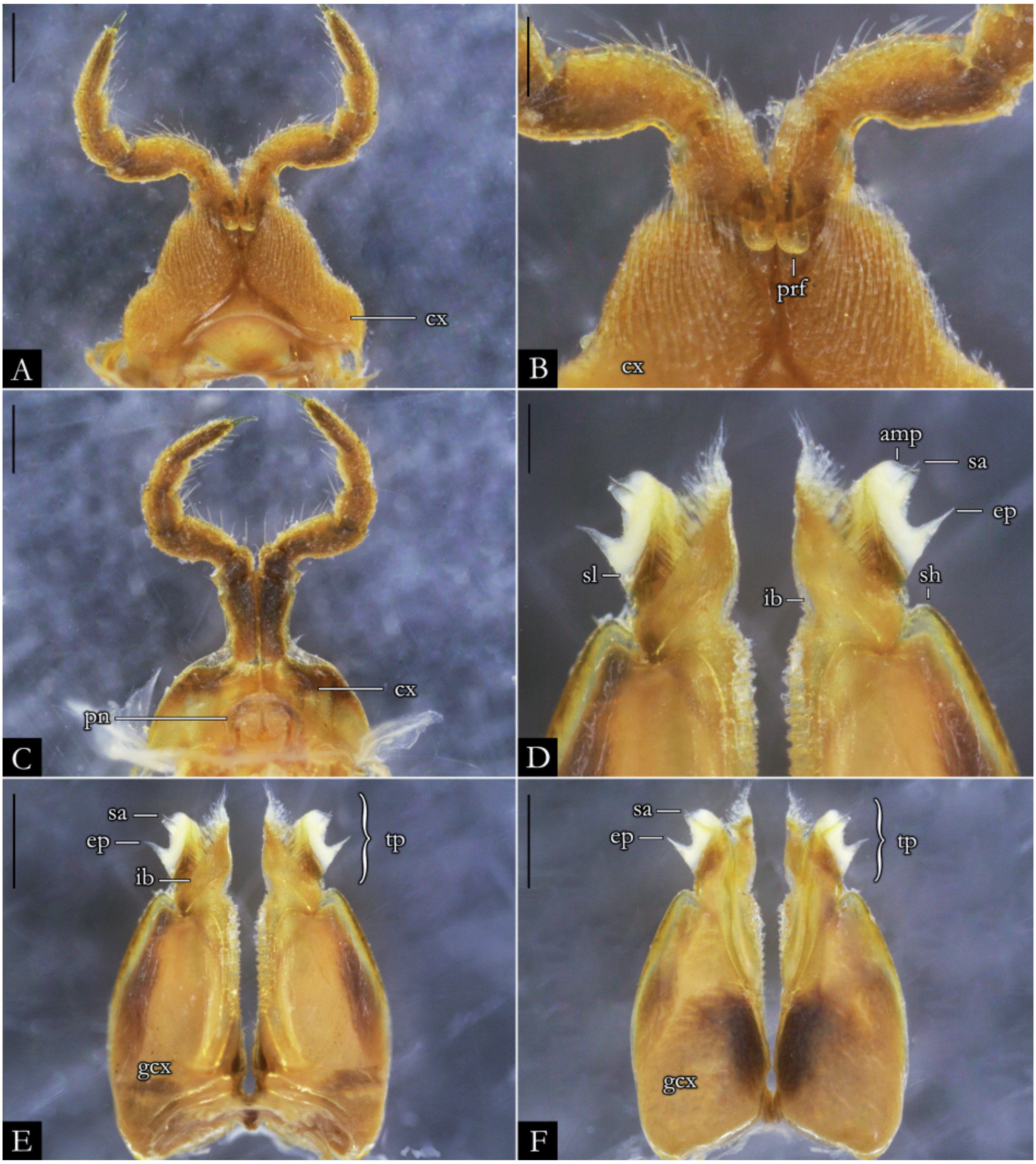

Fig. 148. *Pseudonannolene aurea* sp. nov., paratype, ♂ (IBSP 5854). **A**. First leg-pair. **B**. Detail of prefemur. **C**. Second leg-pair. **D**. Detail of telopodites, in anal view. **E**. Gonopods, in anal view. **F**. Gonopods, in oral view. Abbreviations: see Material and methods. Scale bars: A, C, E–F = 0.5 mm; B, D = 0.2 mm.

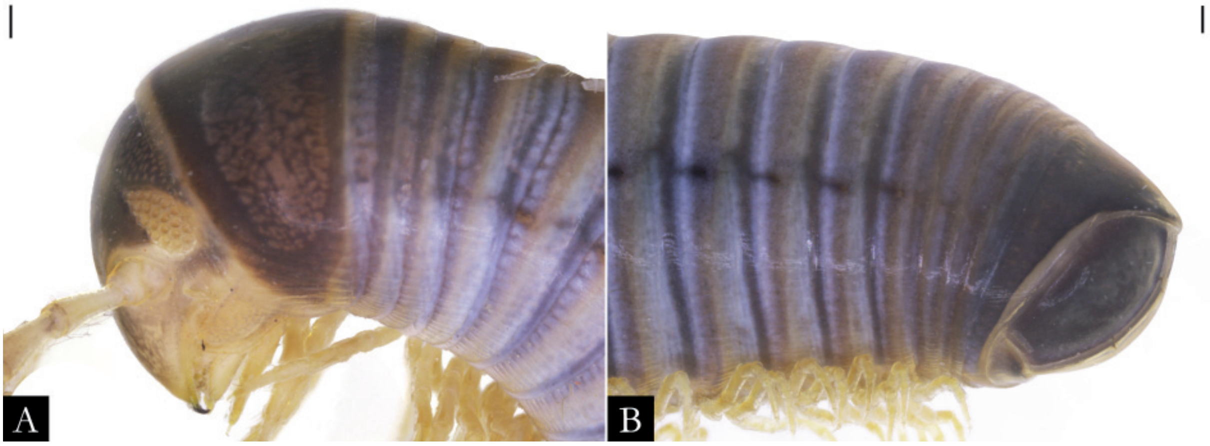

Fig. 149. *Pseudonannolene bucculenta* sp. nov., ♀ (IBSP 3350), in lateral view. **A**. Anterior region. **B**. Posterior region. Scale bars = 0.2 mm.

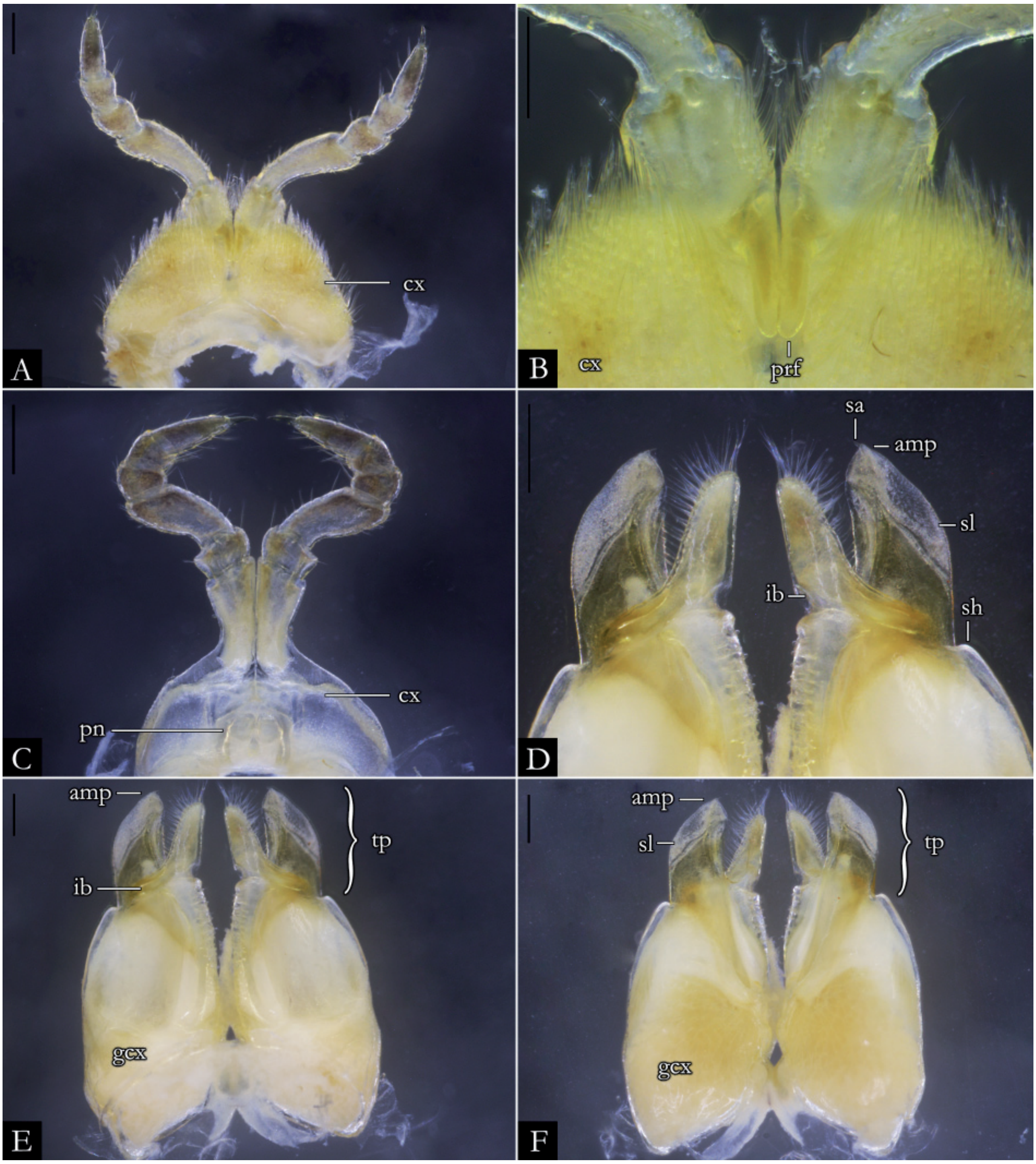

Fig. 150. *Pseudonannolene bucculenta* sp. nov., ♂ (IBSP 3350). **A**. First leg-pair. **B**. Detail of prefemur. **C**. Second leg-pair. **D**. Detail of telopodites, in anal view. **E**. Gonopods, in anal view. **F**. Gonopods, in oral view. Abbreviations: see Material and methods. Scale bars = 0.2 mm.

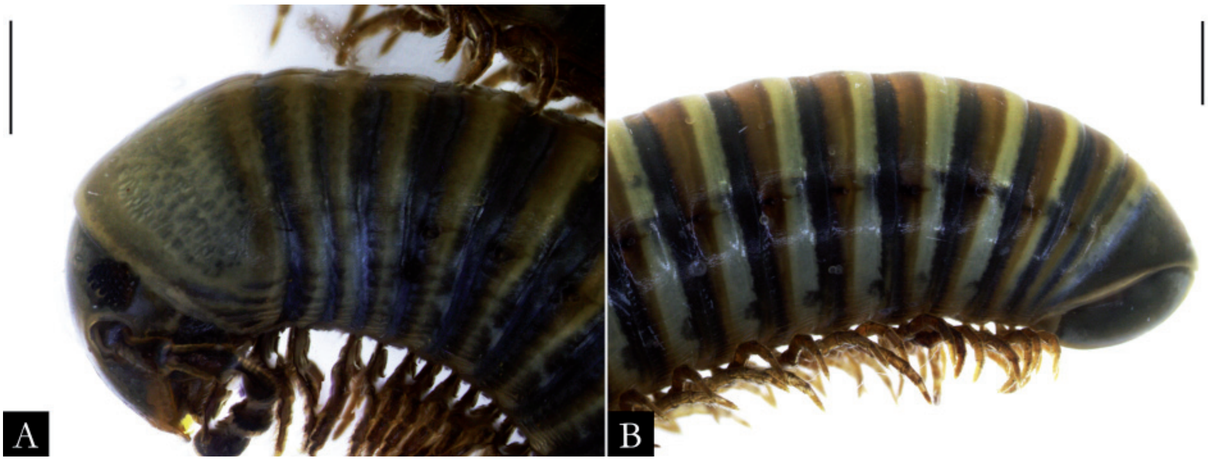

Fig. 151. *Pseudonannolene curvata* sp. nov., holotype, ♂ (MCN), in lateral view. **A**. Anterior region. **B**. Posterior region. Scale bars = 1 mm.

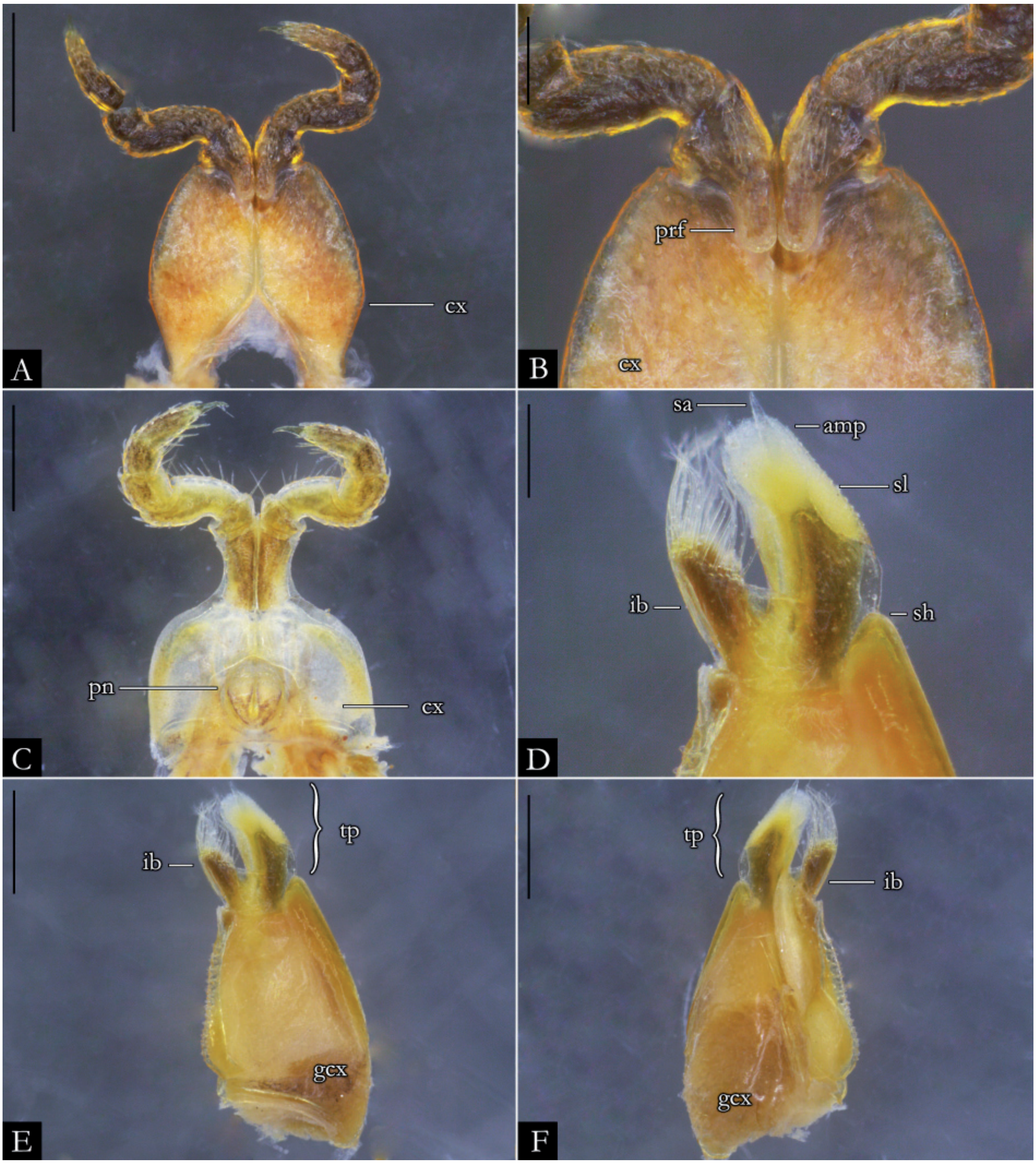

Fig. 152. *Pseudonannolene curvata* sp. nov., holotype, ♂ (MCN). **A**. First leg-pair. **B**. Detail of prefemur. **C**. Second leg-pair. **D**. Detail of telopodite, in anal view. **E**. Left gonopod, in anal view. **F**. Left gonopod, in oral view. Abbreviations: see Material and methods. Scale bars: A, C, E–F = 0.5 mm; B, D = 0.2 mm.

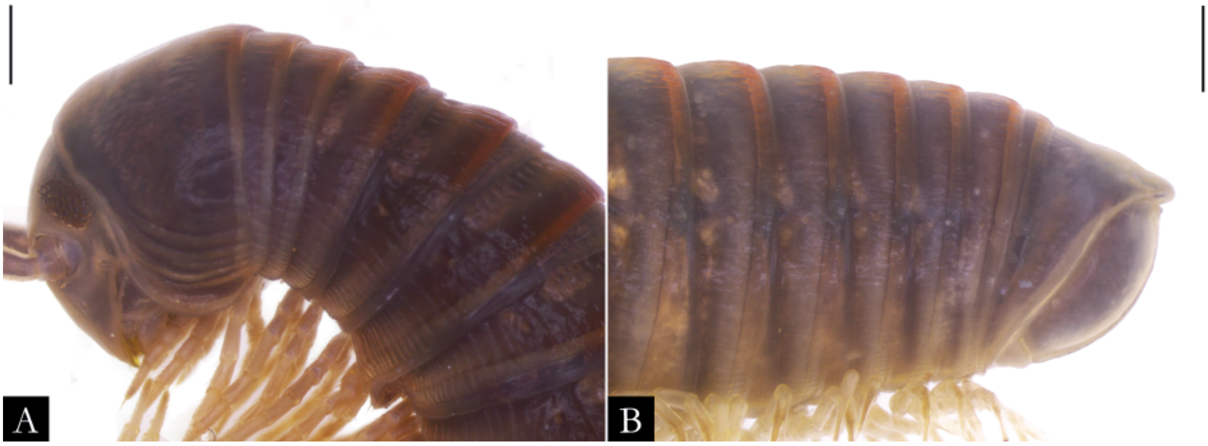

Fig. 153. *Pseudonannolene granulata* sp. nov., holotype, ♂ (MNRJ), in lateral view. **A**. Anterior region. **B**. Posterior region. Scale bars = 1 mm.

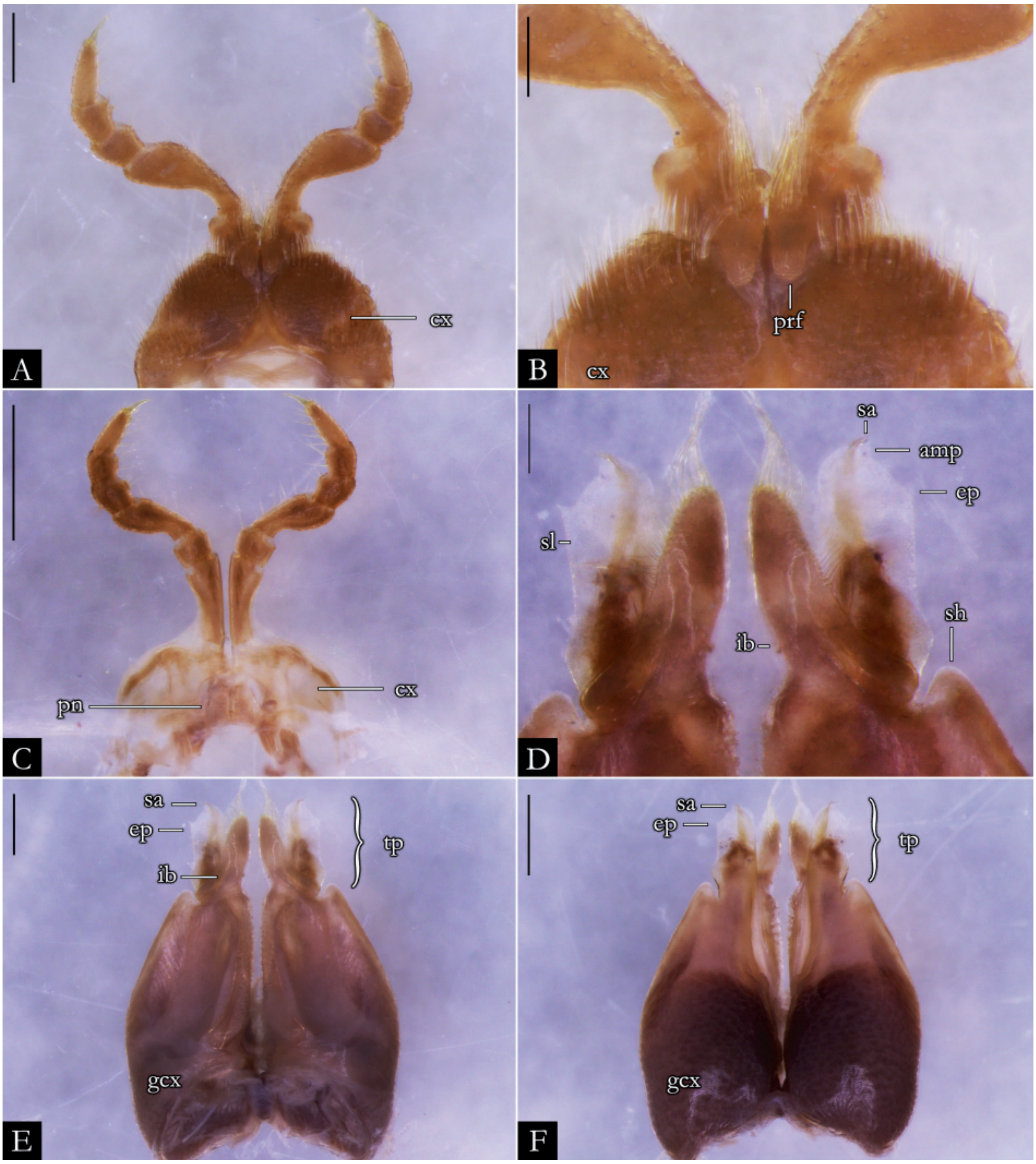

Fig. 154. *Pseudonannolene granulata* sp. nov., paratype, ♂ (MNRJ). **A**. First leg-pair. **B**. Detail of prefemur. **C**. Second leg-pair. **D**. Detail of telopodites, in anal view. **E**. Gonopods, in anal view. **F**. Gonopods, in oral view. Abbreviations: see Material and methods. Scale bars: A, C, E–F = 0.5 mm; B, D = 0.2 mm.

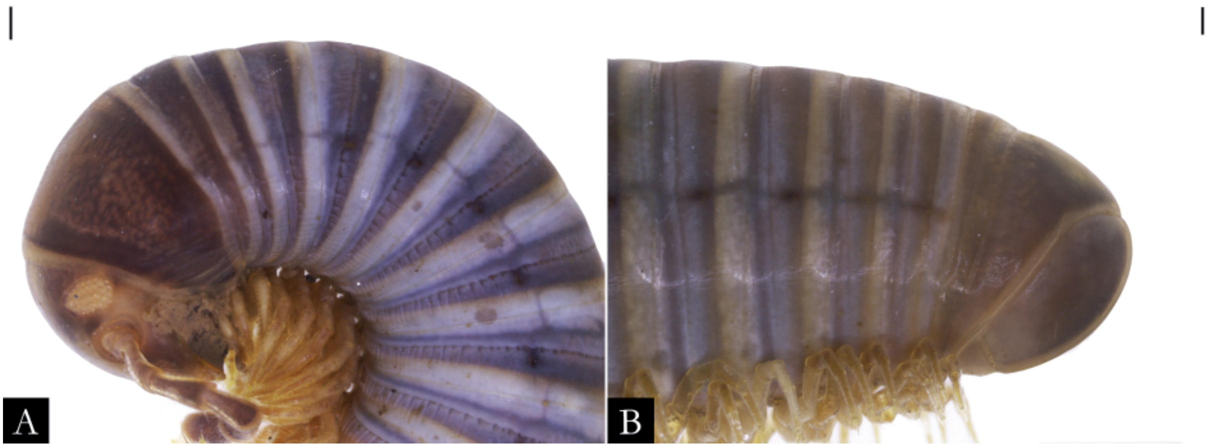

Fig. 155. *Pseudonannolene insularis* sp. nov., paratype, ♀ (IBSP 1231), in lateral view. **A**. Anterior region. **B**. Posterior region. Scale bars = 0.2 mm.

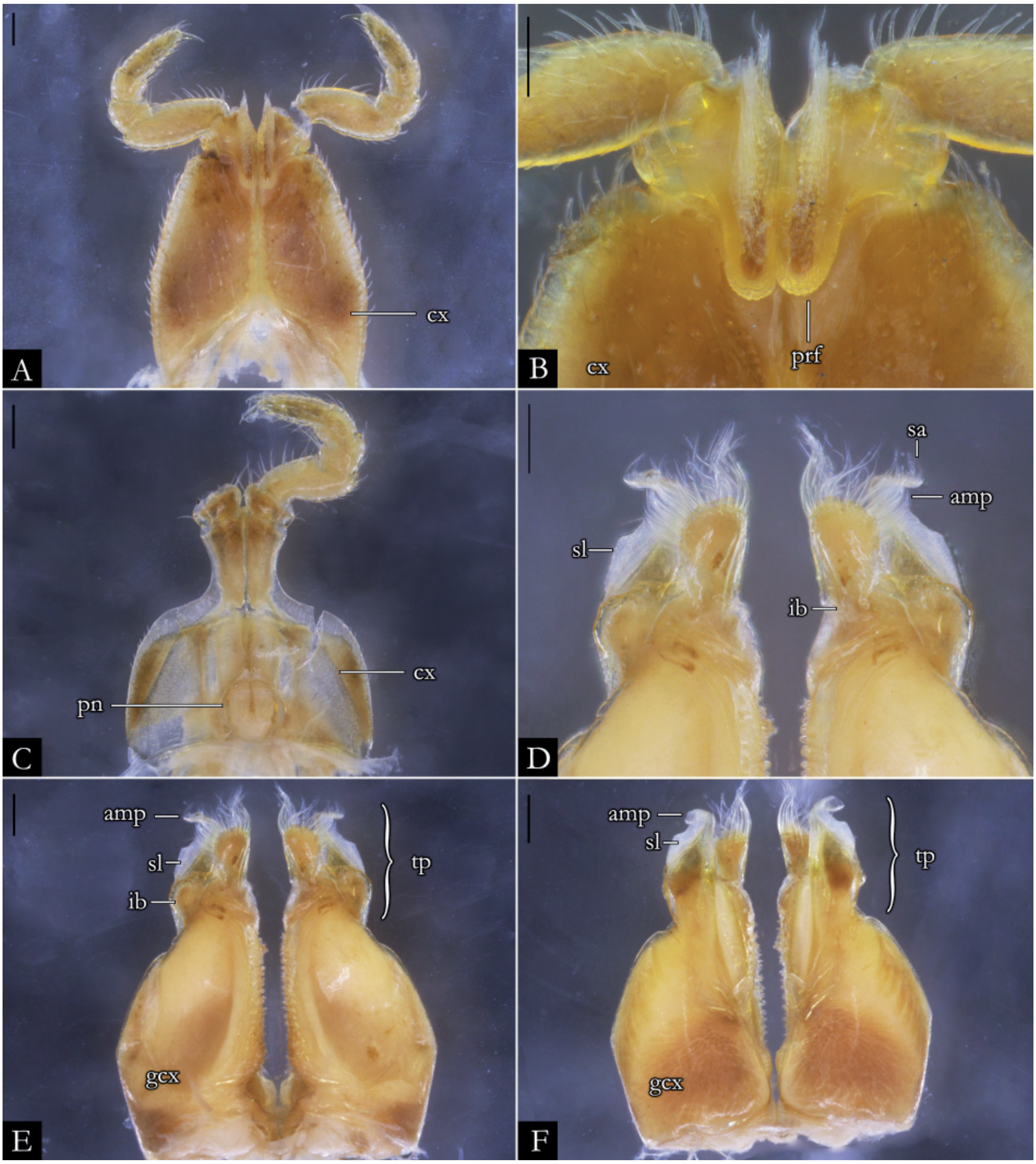

Fig. 156. *Pseudonannolene insularis* sp. nov., ♂ (IBSP 1233). **A**. First leg-pair. **B**. Detail of prefemur. **C**. Second leg-pair. **D**. Detail of telopodites, in anal view. **E**. Gonopods, in anal view. **F**. Gonopods, in oral view. Abbreviations: see Material and methods. Scale bars = 0.2 mm.

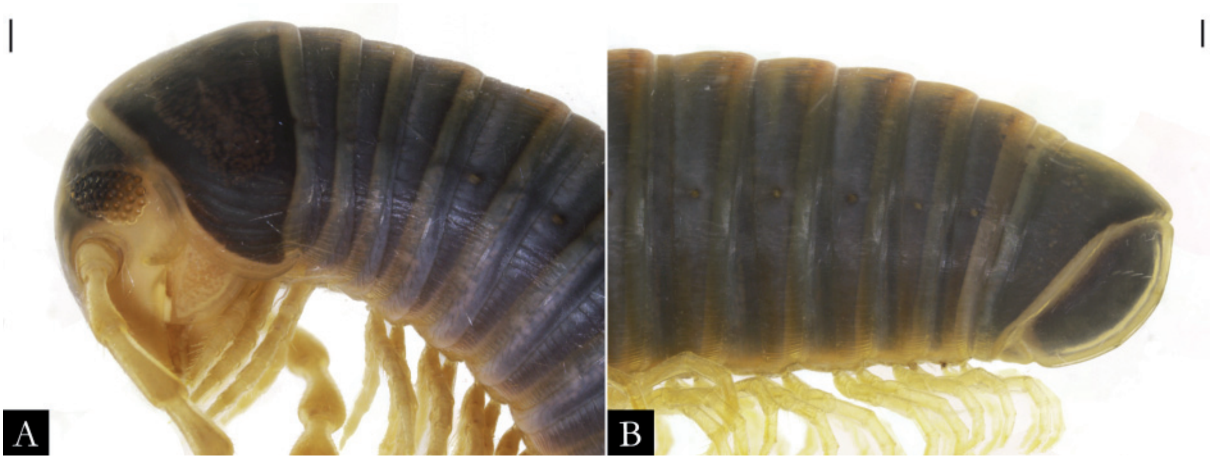

Fig. 157. *Pseudonannolene morettii* sp. nov., ♀ (IBSP 2471), in lateral view. **A**. Anterior region. **B**. Posterior region. Scale bars = 0.2 mm.

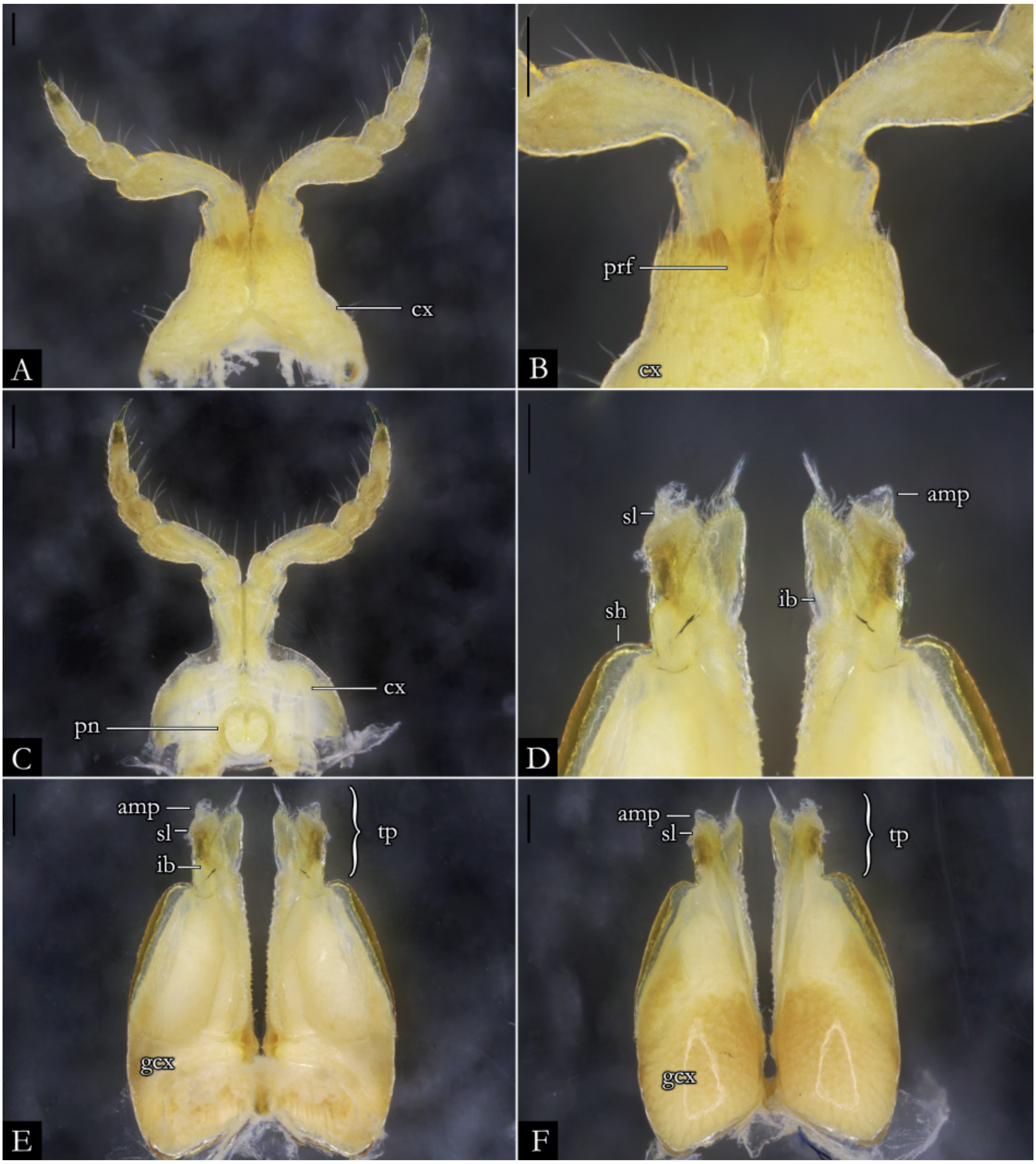

Fig. 158. *Pseudonannolene morettii* sp. nov., ♂ (IBSP 2476). **A**. First leg-pair. **B**. Detail of prefemur. **C**. Second leg-pair. **D**. Detail of telopodites, in anal view. **E**. Gonopods, in anal view. **F**. Gonopods, in oral view. Abbreviations: see Material and methods. Scale bars = 0.2 mm.

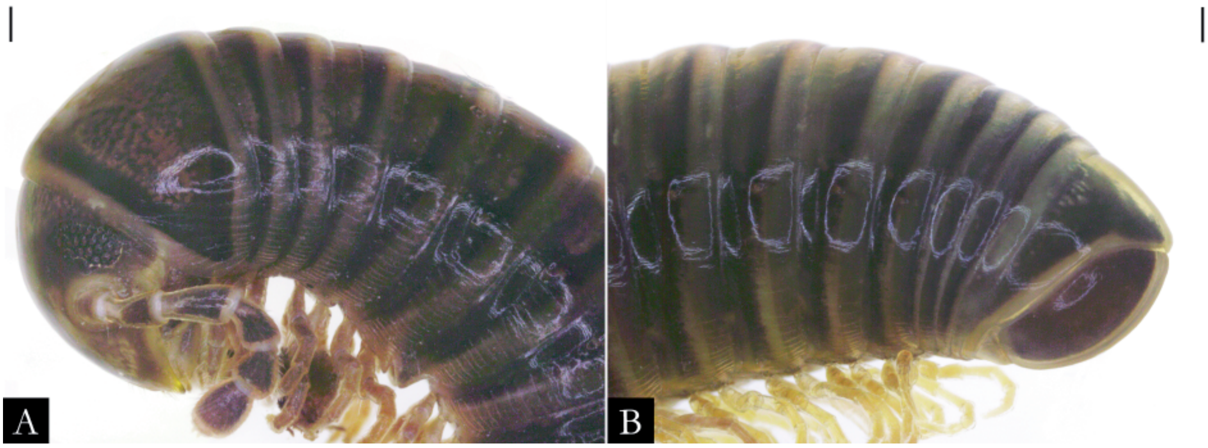

Fig. 159. *Pseudonannolene nicolau* sp. nov., paratype, ♂ (ABAM), in lateral view. **A**. Anterior region. **B**. Posterior region. Scale bars = 0.2 mm.

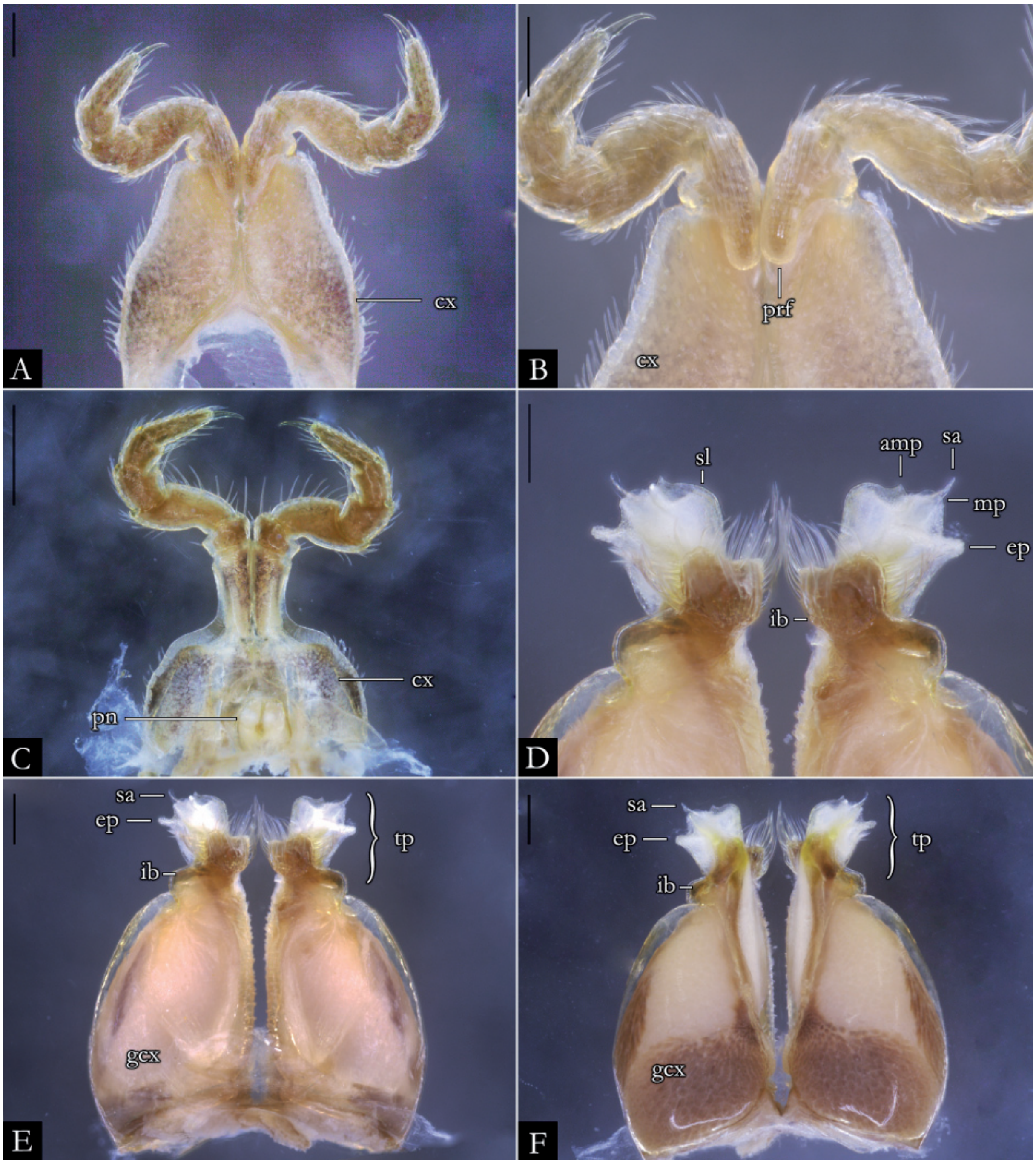

Fig. 160. *Pseudonannolene nicolau* sp. nov., paratype, ♂ (ABAM). **A**. First leg-pair. **B**. Detail of prefemur. **C**. Second leg-pair. **D**. Detail of telopodites, in anal view. **E**. Gonopods, in anal view. **F**. Gonopods, in oral view. Abbreviations: see Material and methods. Scale bars = 0.2 mm.

Fig. 161. *Pseudonannolene brevis* Silvestri, 1902, ♀ syntype (USNM 2021). **A**. Anterior region, in lateral view. **B**. Posterior region, in lateral view. **C**. Original label of type material. Images not to scale.

Fig. 162. *Pseudonannolene rugosetta* Silvestri, 1897, ♀ holotype (ISNB). **A**. Anterior region, in lateral view. **B**. Posterior region, in lateral view. **C–D**. Original labels of type material. Images not to scale.

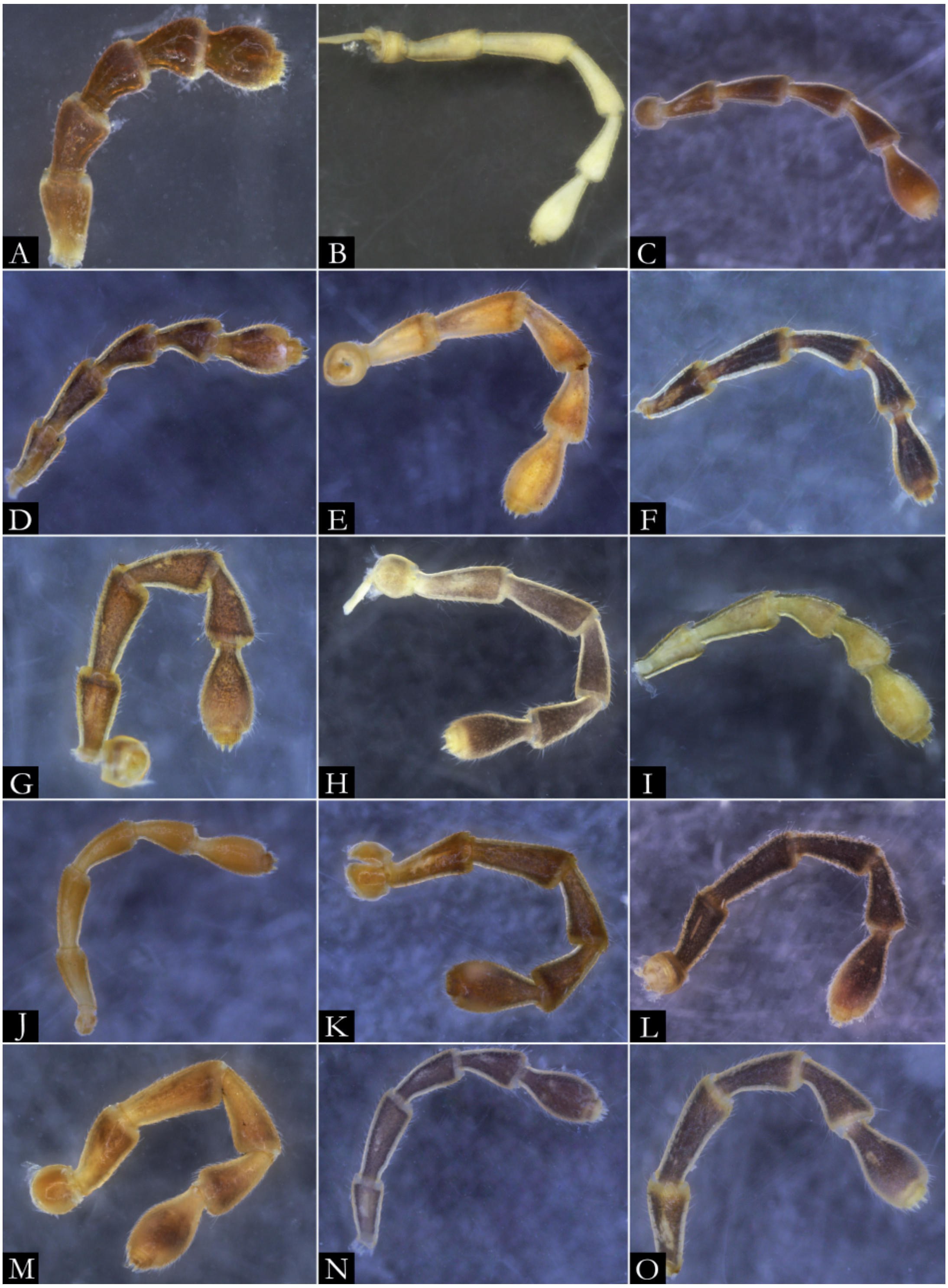

Fig. 163. Stereoscopic images of antennae of species of *Pseudonannolene* Silvestri, 1895. **A**. *P. albiventris* Schubart, 1952. **B**. *P. anapophysis* Fontanetti, 1996. **C**. *P. alata* sp. nov. **D**. *P. buhrnheimi* Schubart, 1960. **E**. *P. caatinga* Iniesta & Ferreira, 2014. **F**. *P. erikae* Iniesta & Ferreira, 2014. **G**. *P. fontanettiae* Iniesta & Ferreira, 2014. **H**. *P. halophila* Schubart, 1949. **I**. *P. inops* Brölemann, 1929. **J**. *P. leopoldoi* Iniesta & Ferreira, 2014. **K**. *P. longicornis* (Porat, 1888). **L**. *P. magna* Udulutsch & Pietrobon, 2003. **M**. *P. maritima* Schubart, 1949. **N**. *P. mesai* Fontanetti, 2000. **O**. *P. microzoporus* Mauriès, 1987. Images not to scale.

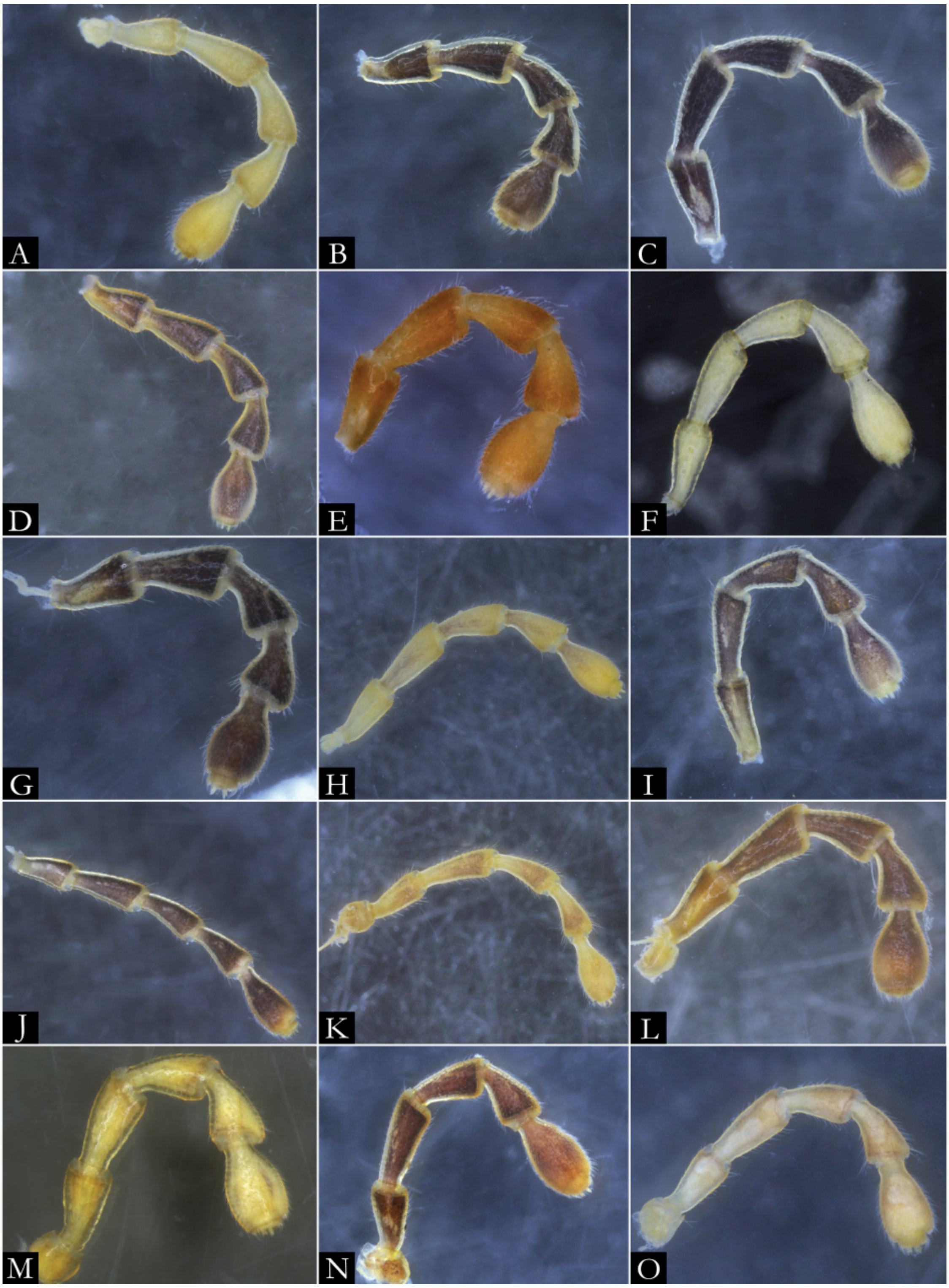

Fig. 164. Stereoscopic images of antennae of species of *Pseudonannolene* Silvestri, 1895. **A**. *P. morettii* sp. nov. **B**. *P. nicolau* sp. nov. **C**. *P. bucculenta* sp. nov. **D**. *P. occidentalis* Schubart, 1958. **E**. *P. parvula* Silvestri, 1902. **F**. *P. patagonica* Brölemann, 1902. **G**. *P. paulista* Brölemann, 1902. **H**. *P. robsoni* Iniesta & Ferreira, 2014. **I**. *P. rolamossa* Iniesta & Ferreira, 2013. **J**. *P. silvestris* Schubart, 1944. **K**. *P. strinatii* Mauriès, 1974. **L**. *P. tricolor* Brölemann, 1902. **M**. *P. typica* Silvestri, 1895. **N**. *P. insularis* sp. nov. **O**. *P. urbica* Schubart, 1945. Images not to scale.

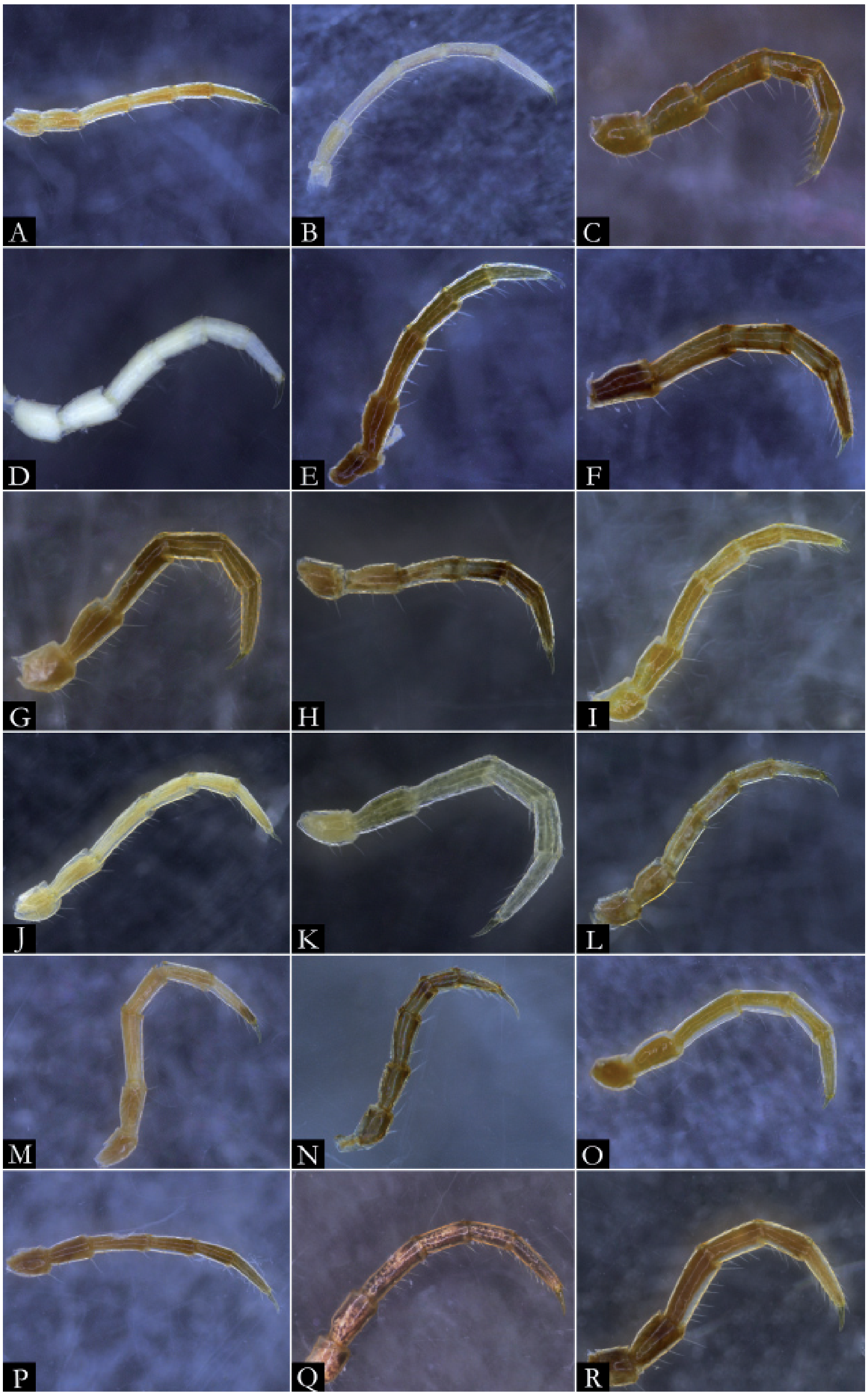

Fig. 165. Stereoscopic images of midbody legs of species of *Pseudonannolene* Silvestri, 1895. **A**. *P. ambuatinga* Iniesta & Ferreira, 2013. **B**. *P. anapophysis* Fontanetti, 1996. **C**. *P. alata* sp. nov. **D**. *P. bovei* Silvestri, 1895. **E**. *P. buhrnheimi* Schubart, 1960. **F**. *P. caatinga* Iniesta & Ferreira, 2014. **G**. *P. callipyge* Brölemann, 1902. **H**. *P. curtipes* Schubart, 1960. **I**. *P. fontanettiae* Iniesta & Ferreira, 2014. **J**. *P. halophila* Schubart, 1949. **K**. *P. imbirensis* Fontanetti, 1996. **L**. *P. inops* Brölemann, 1929. **M**, *P. leopoldoi* Iniesta & Ferreira, 2014. **N**. *P. leucomelas* Schubart, 1947. **O**. *P. longicornis* (Porat, 1888). **P**. *P. lundi* Iniesta & Ferreira, 2015. **Q**. *P. magna* Udulutsch & Pietrobon, 2003. **R**. *P. maritima* Schubart, 1949. Images not to scale.

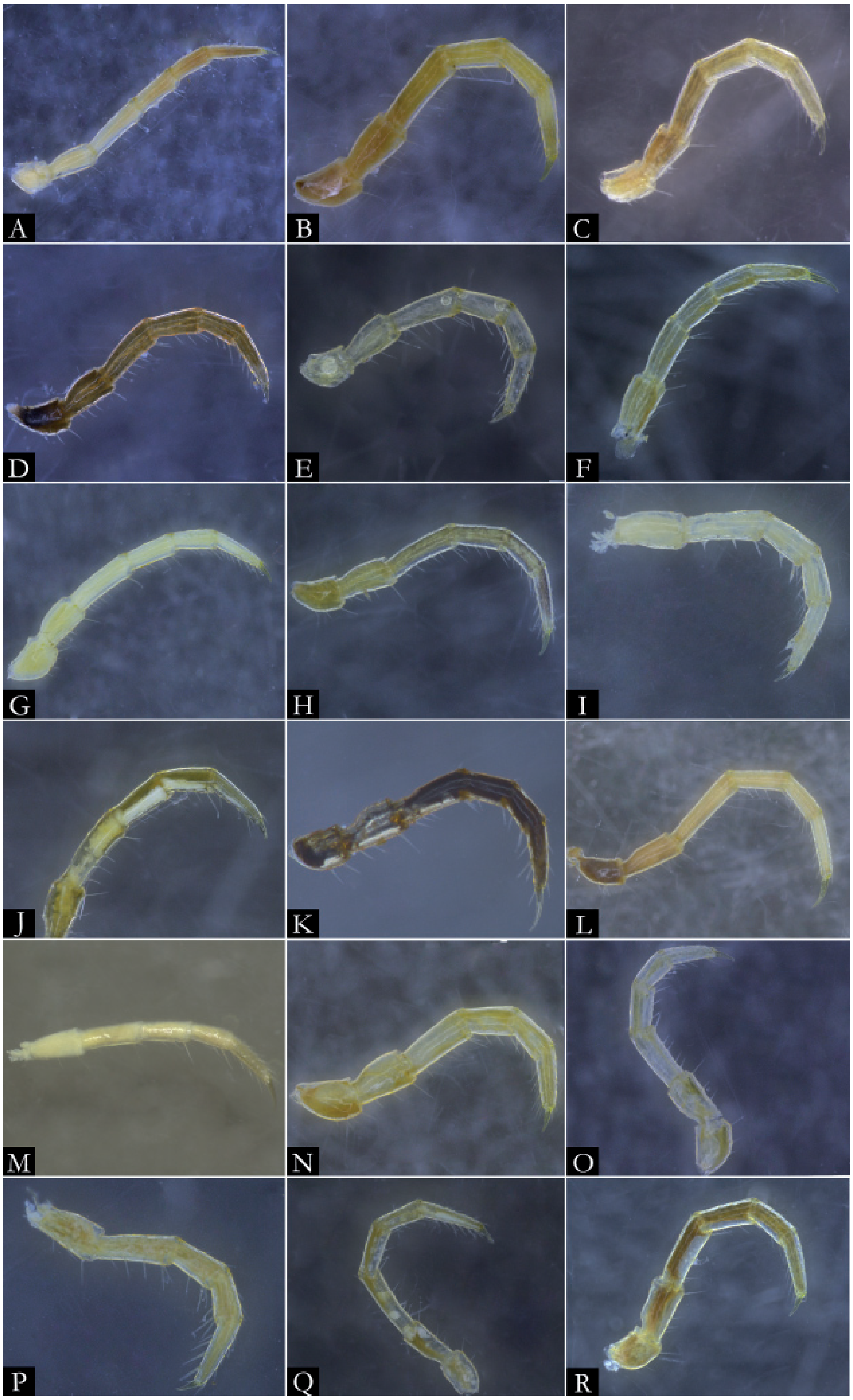

Fig. 166. Stereoscopic images of midbody legs of species of *Pseudonannolene* Silvestri, 1895. **A**. *P. mesai* Fontanetti, 2000. **B**. *P. microzoporus* Mauriès, 1987. **C**. *P. ophiiulus*. **D**. *P. parvula* Silvestri, 1902. **E**. *P. patagonica* Brölemann, 1902. **F**. *P. paulista* Brölemann, 1902. **G**. *P. robsoni* Iniesta & Ferreira, 2014. **H**. *P. rolamossa* Iniesta & Ferreira, 2013. **I**. *P. rugosetta* Silvestri, 1897. **J**. *P. silvestris* Schubart, 1944. **K**. *P. spelaea* Iniesta & Ferreira, 2013. **L**. *P. strinatii* Mauriès, 1974. **M**. *P. tocaiensis* Fontanetti, 1996. **N**. *P. tricolor* Brölemann, 1902. **O**, *P. typica* Silvestri, 1895. **P**. *P. urbica* Schubart, 1945. **Q**. *P. xavieri* Iniesta & Ferreira, 2014. **R**. *P. insularis* sp. nov. Images not to scale.

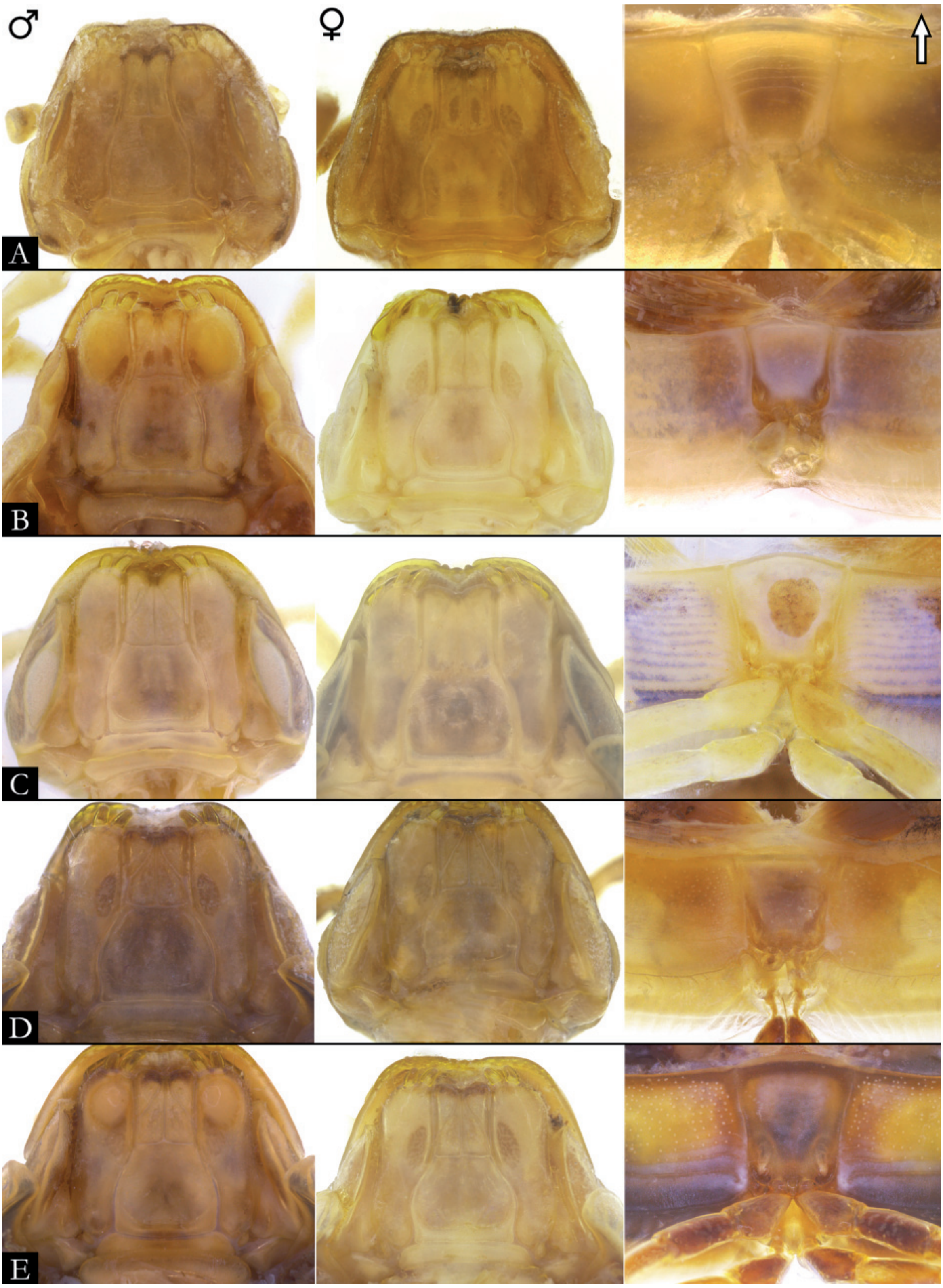

Fig. 167. Stereoscopic images of gnathochilarium and anterior sternum of species of *Pseudonannolene* Silvestri, 1895. **A**. *P. albiventris* Schubart, 1952. **B**. *P. ambuatinga* Iniesta & Ferreira, 2013. **C**. *P. anapophysis* Fontanetti, 1996. **D**. *P. buhrnheimi* Schubart, 1960. **E**. *P. caatinga* Iniesta & Ferreira, 2014. Images not to scale.

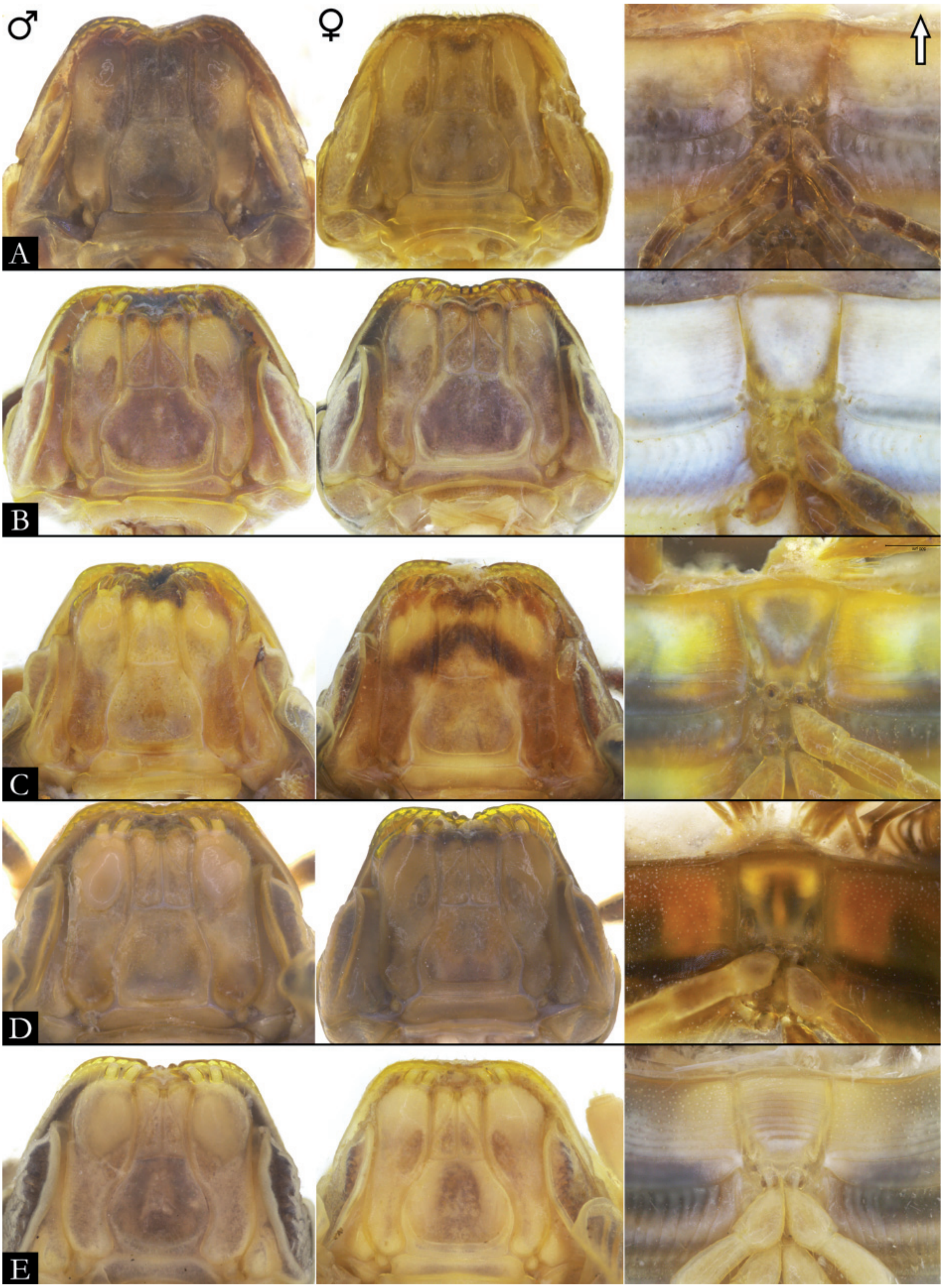

Fig. 168. Stereoscopic images of gnathochilarium and anterior sternum of species of *Pseudonannolene* Silvestri, 1895. **A**. *P. curtipes* Schubart, 1960. **B**. *P. erikae* Iniesta & Ferreira, 2014. **C**. *P. fontanettiae* Iniesta & Ferreira, 2014. **D**. *P. callipyge* Brölemann, 1902. **E**. *P. halophila* Schubart, 1949. Images not to scale.

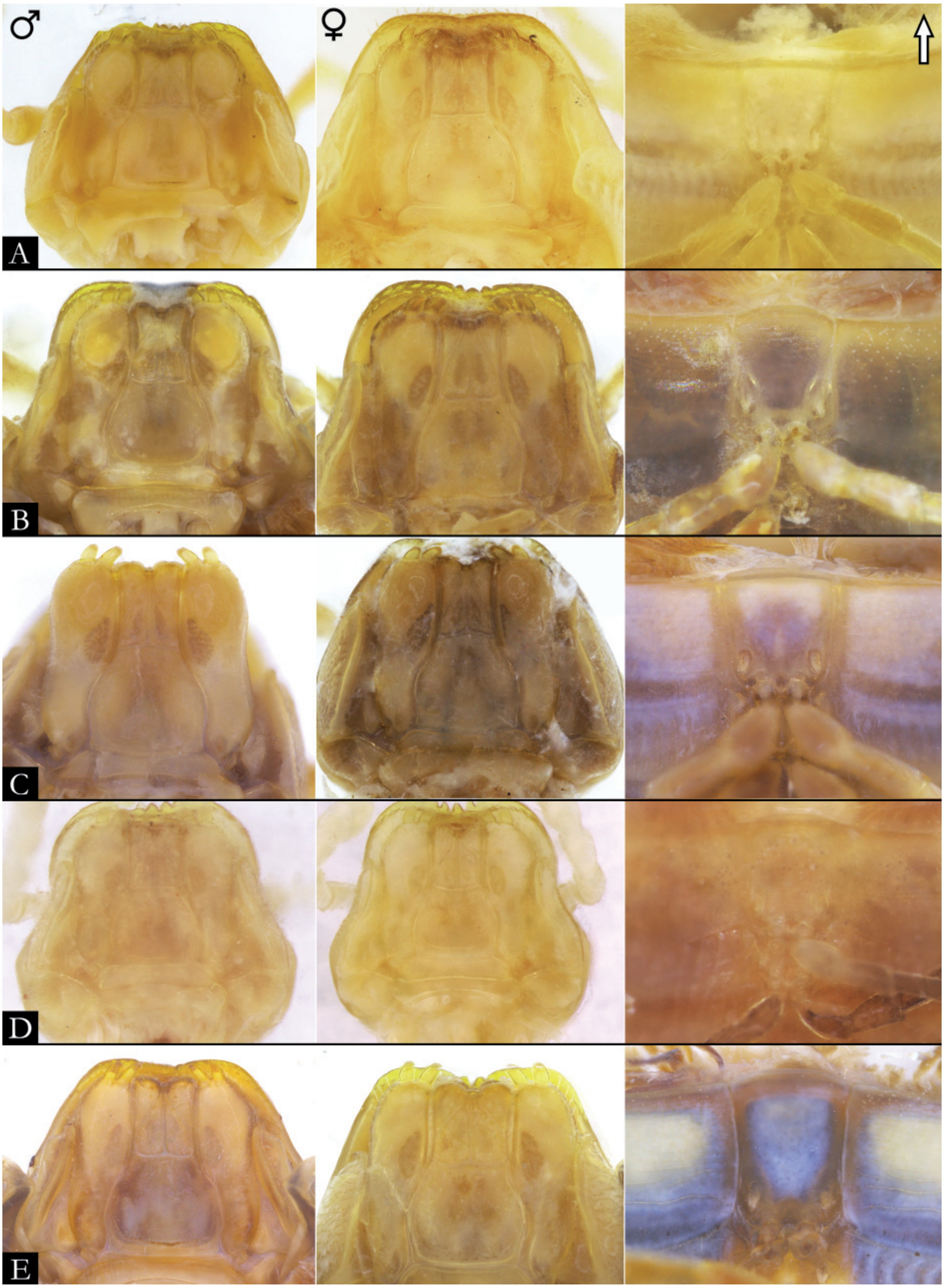

Fig. 169. Stereoscopic images of gnathochilarium and anterior sternum of species of *Pseudonannolene* Silvestri, 1895. **A**. *P. imbirensis* Fontanetti, 1996. **B**. *P. inops* Brölemann, 1929. **C**. *P. leopoldoi* Iniesta & Ferreira, 2014. **D**. *P. leucocephalus* Schubart, 1944. E. *P. longicornis* (Porat, 1888). Images not to scale.

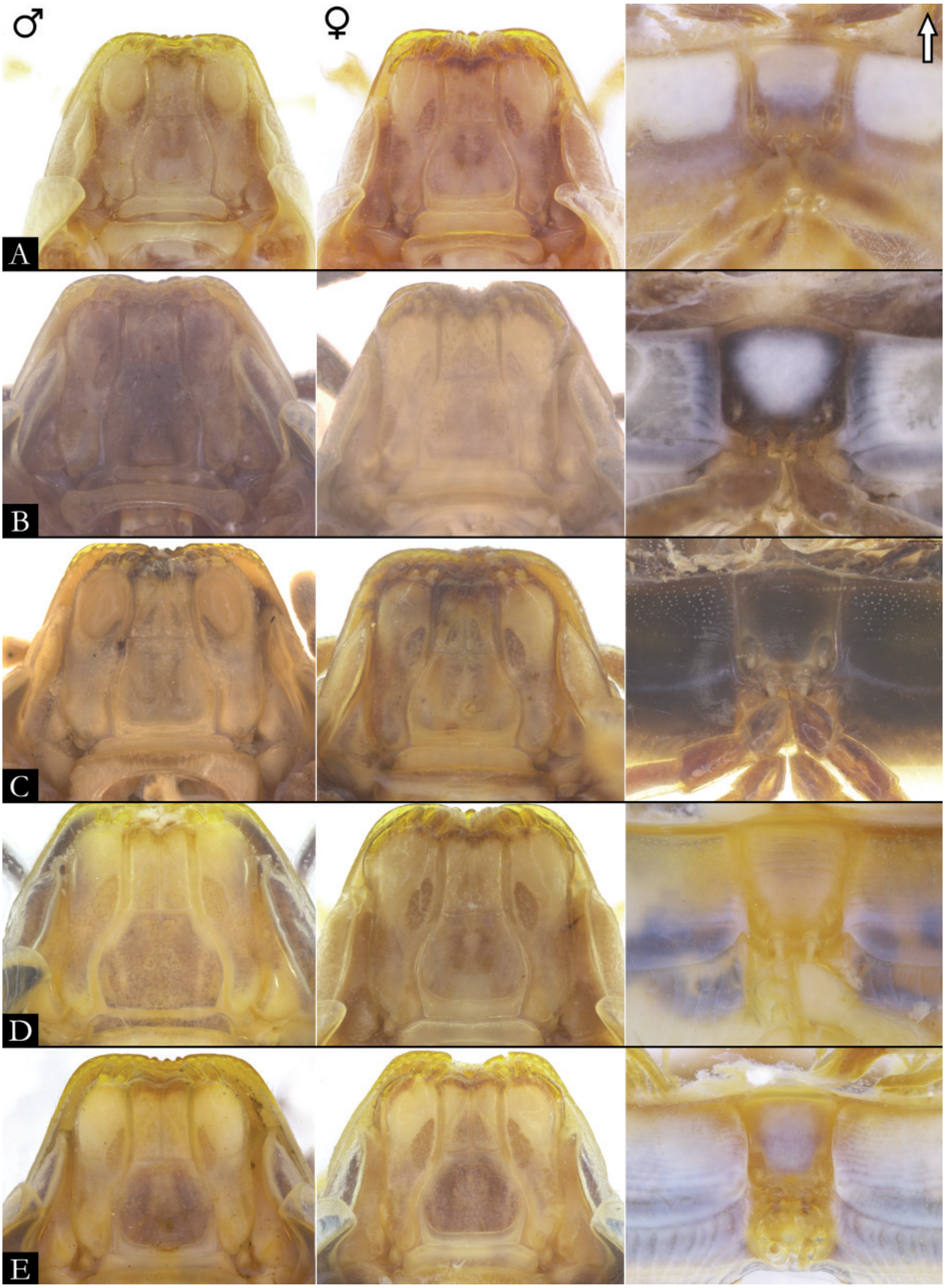

Fig. 170. Stereoscopic images of gnathochilarium and anterior sternum of species of *Pseudonannolene* Silvestri, 1895. **A**. *P. lundi* Iniesta & Ferreira, 2015. **B**. *P. magna* Udulutsch & Pietrobon, 2003. **C**. *P. maritima* Schubart, 1949. **D**. *P. mesai* Fontanetti, 2000. **E**. *P. microzoporus* Mauriès, 1987. Images not to scale.

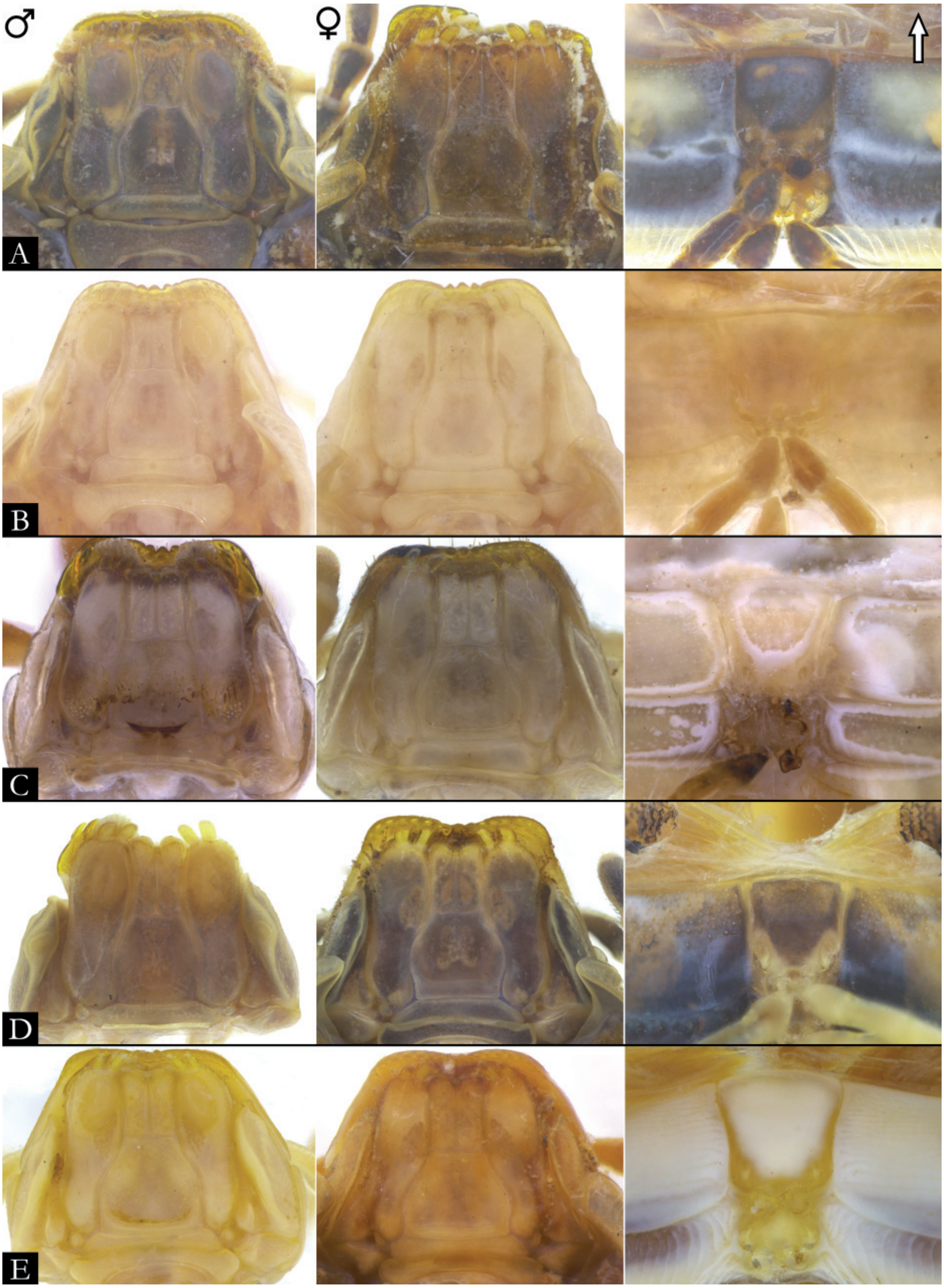

Fig. 171. Stereoscopic images of gnathochilarium and anterior sternum of species of *Pseudonannolene* Silvestri, 1895. **A**. *P. occidentalis* Schubart, 1958. **B**. *P. ophiiulus* Schubart, 1944. **C**. *P. parvula* Silvestri, 1902. **D**. *P. paulista* Brölemann, 1902. **E**. *P. robsoni* Iniesta & Ferreira, 2014. Images not to scale.

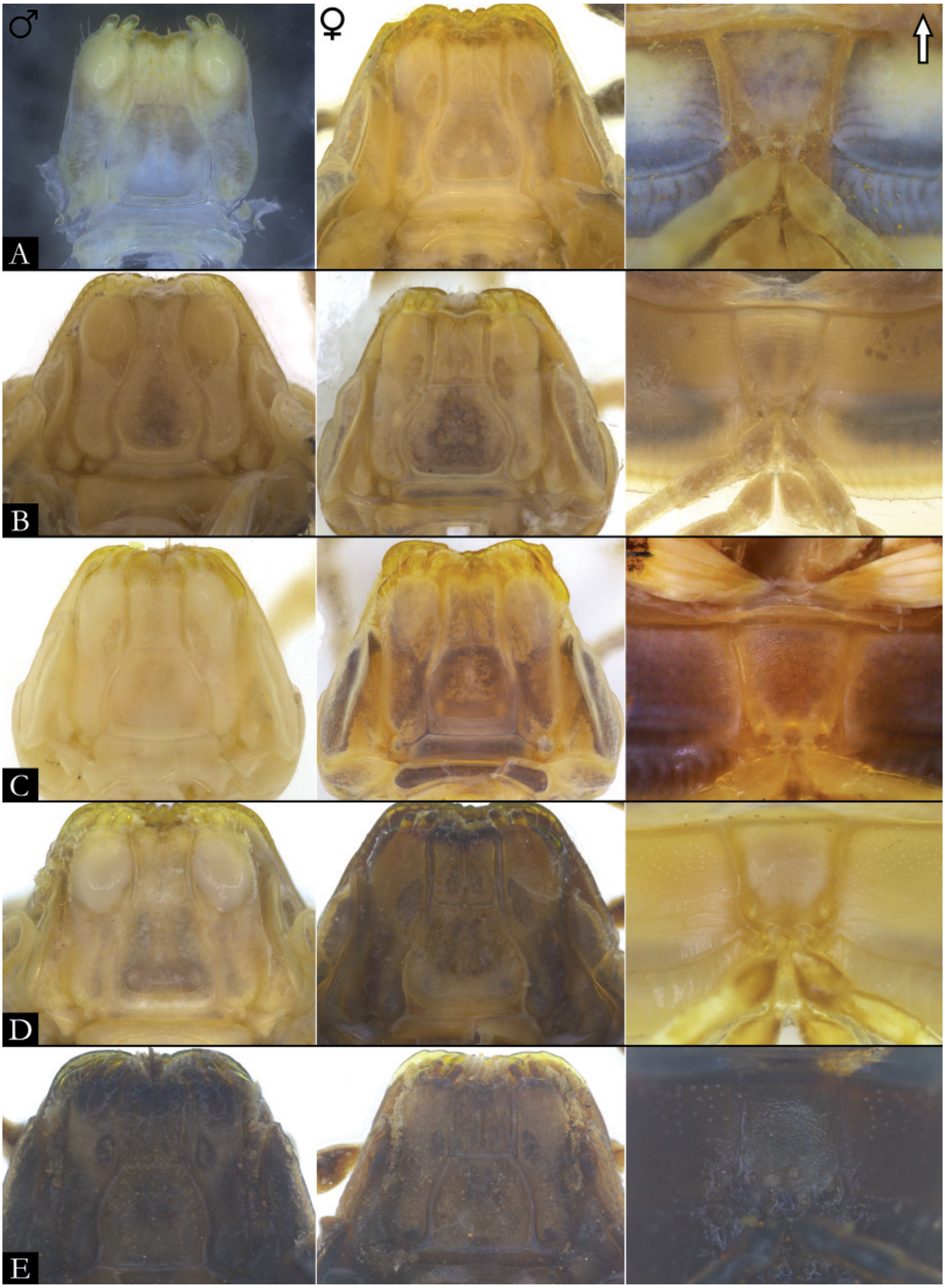

Fig. 172. Stereoscopic images of gnathochilarium and anterior sternum of species of *Pseudonannolene* Silvestri, 1895. **A**. *P. rolamossa* Iniesta & Ferreira, 2013. **B**. *P. sebastianus* Brölemann, 1902. **C**. *P. segmentata* Silvestri, 1895. **D**. *P. silvestris* Schubart, 1944. **E**. *P. spelaea* Iniesta & Ferreira, 2013. Images not to scale.

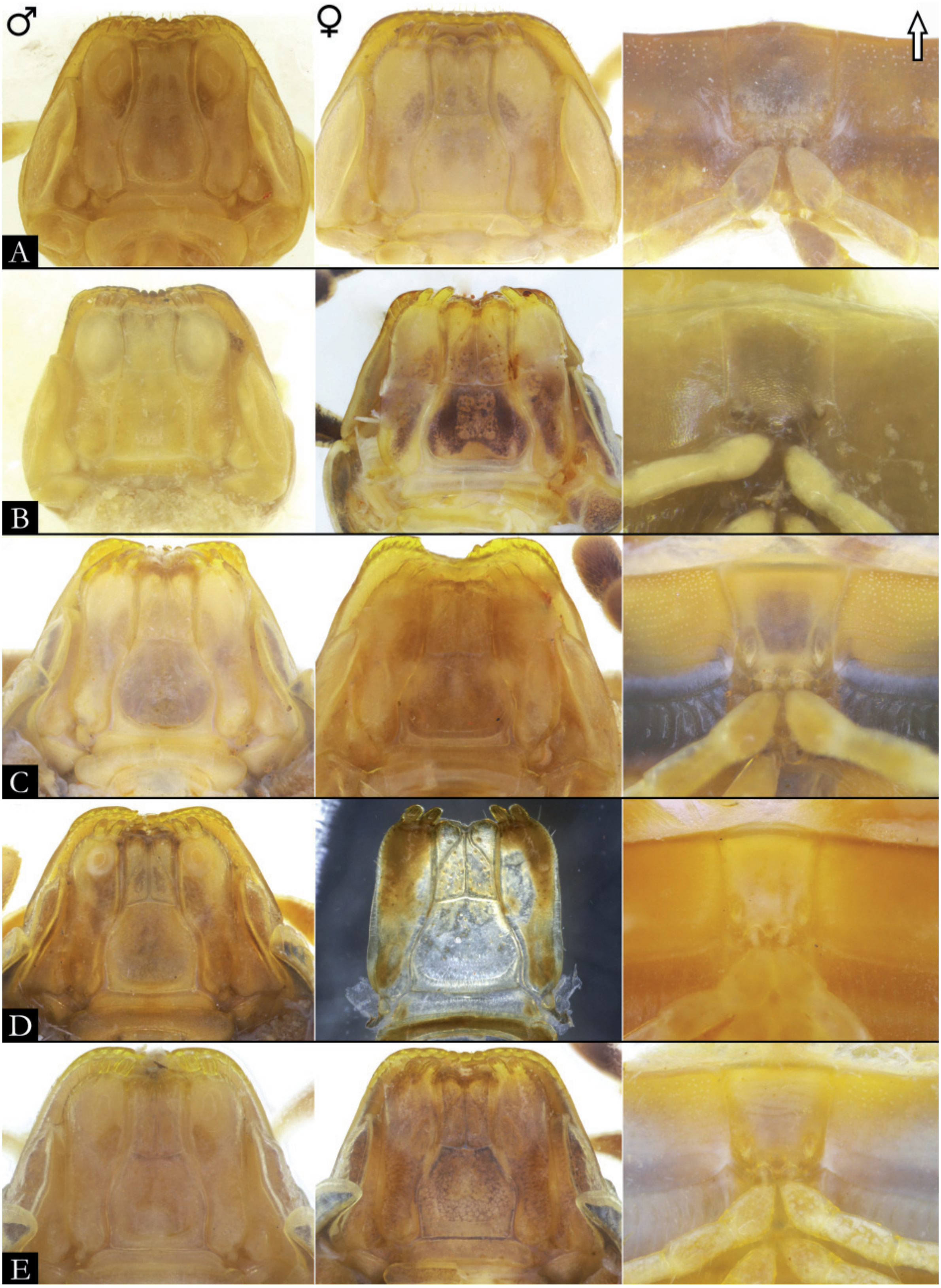

Fig. 173. Stereoscopic images of gnathochilarium and anterior sternum of species of *Pseudonannolene* Silvestri, 1895. **A**. *P. strinatii* Mauriès, 1974. **B**. *P. tocaiensis* Fontanetti, 1996. **C**. *P. tricolor* Brölemann, 1902. **D**. *P. typica* Silvestri, 1895. **E**. *P. urbica* Schubart, 1945. Images not to scale.

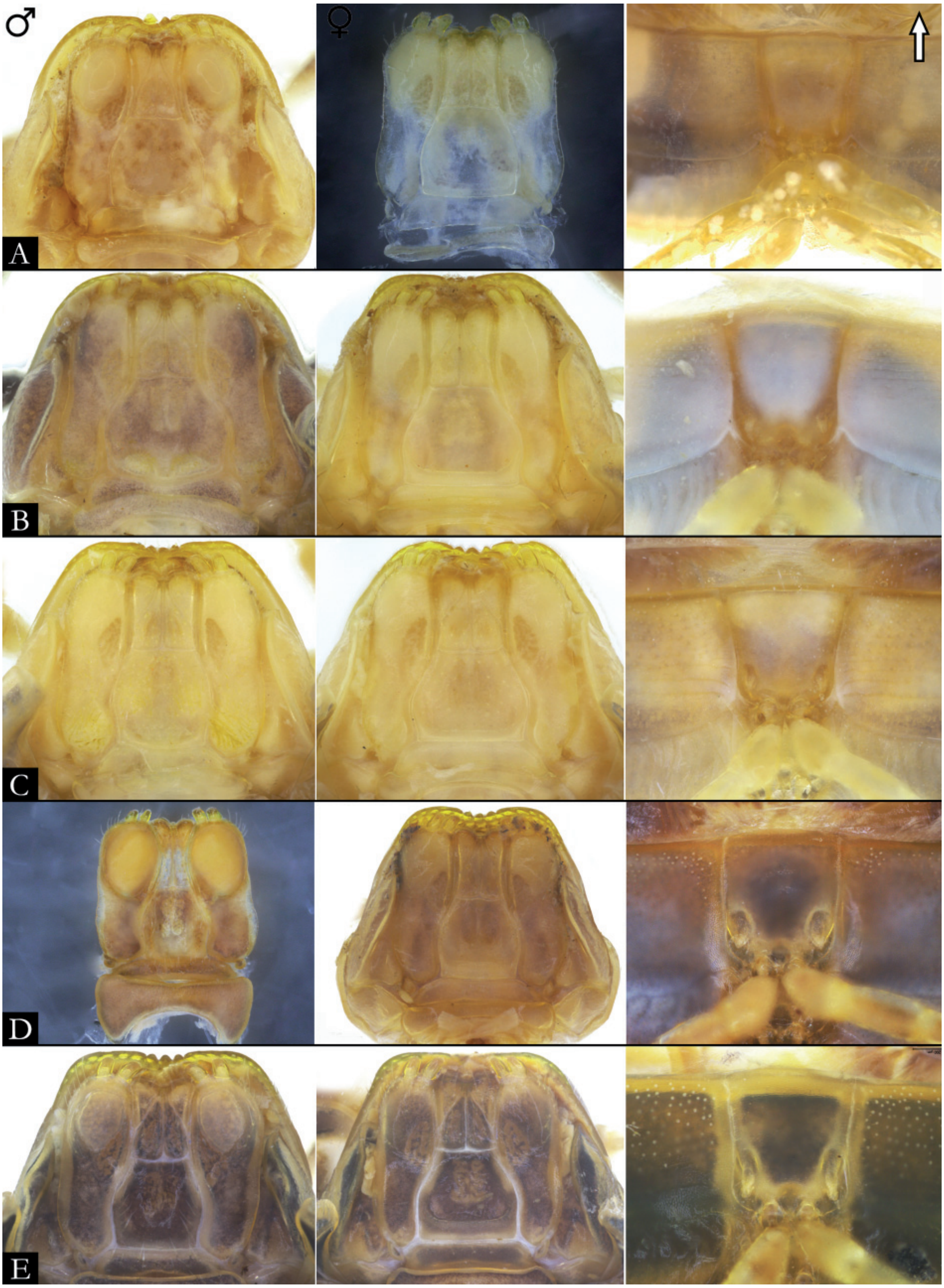

Fig. 174. Stereoscopic images of gnathochilarium and anterior sternum of species of *Pseudonannolene* Silvestri, 1895. **A**. *P. xavieri* Iniesta & Ferreira, 2014. **B**. *P. bucculenta* sp. nov. **C**. *P. morettii* sp. nov. **D**. *P. insularis* sp. nov. **E**. *P. nicolau* sp. nov. Images not to scale.

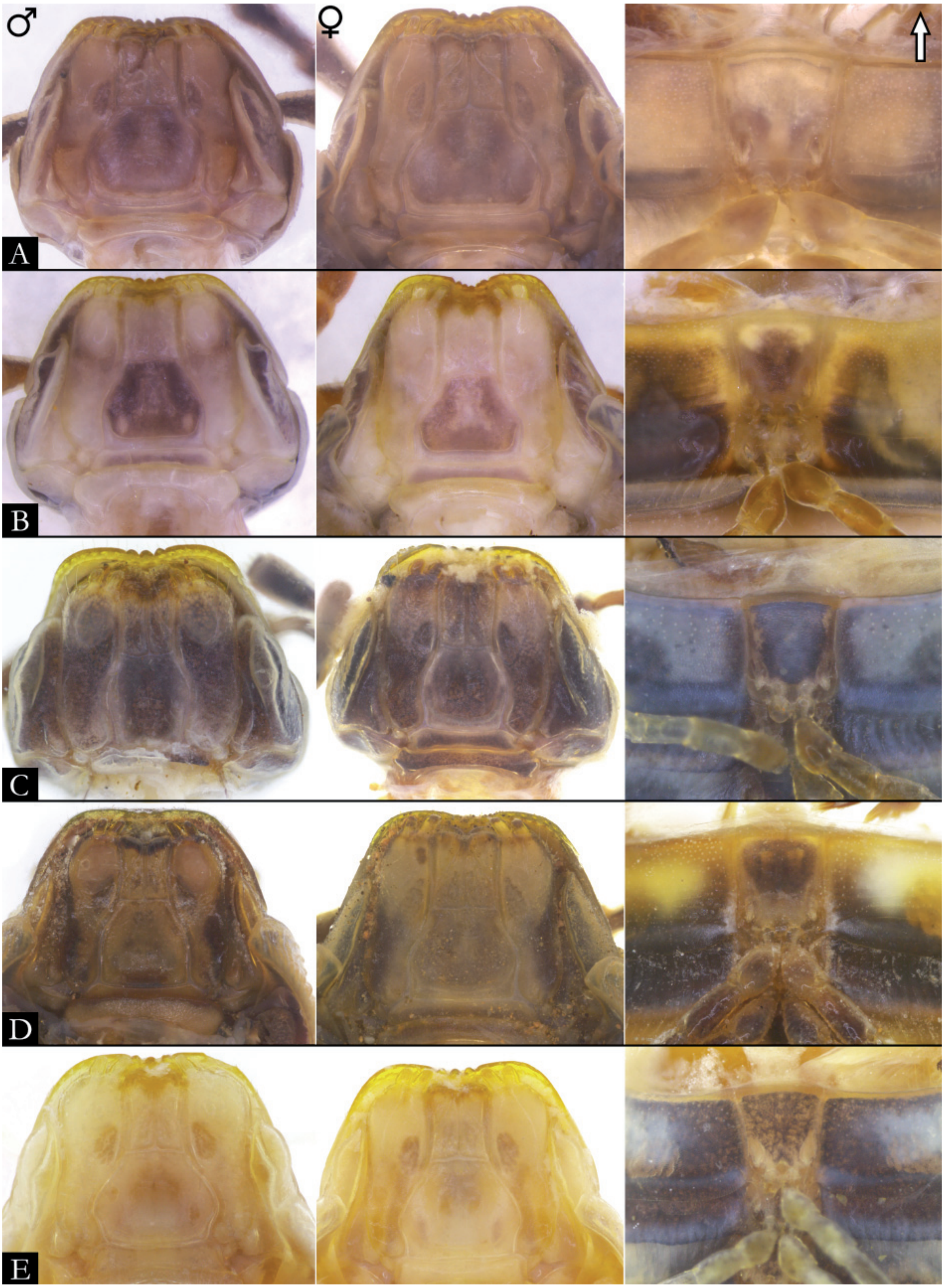

Fig. 175. Stereoscopic images of gnathochilarium and anterior sternum of species of *Pseudonannolene* Silvestri, 1895. **A**. *P. granulata* sp. nov. **B**. *P. alata* sp. nov. **C**. *P. curvata* sp. nov. **D**. *P. aurea* sp. nov. **E**. *P. alegrensis*. Images not to scale.

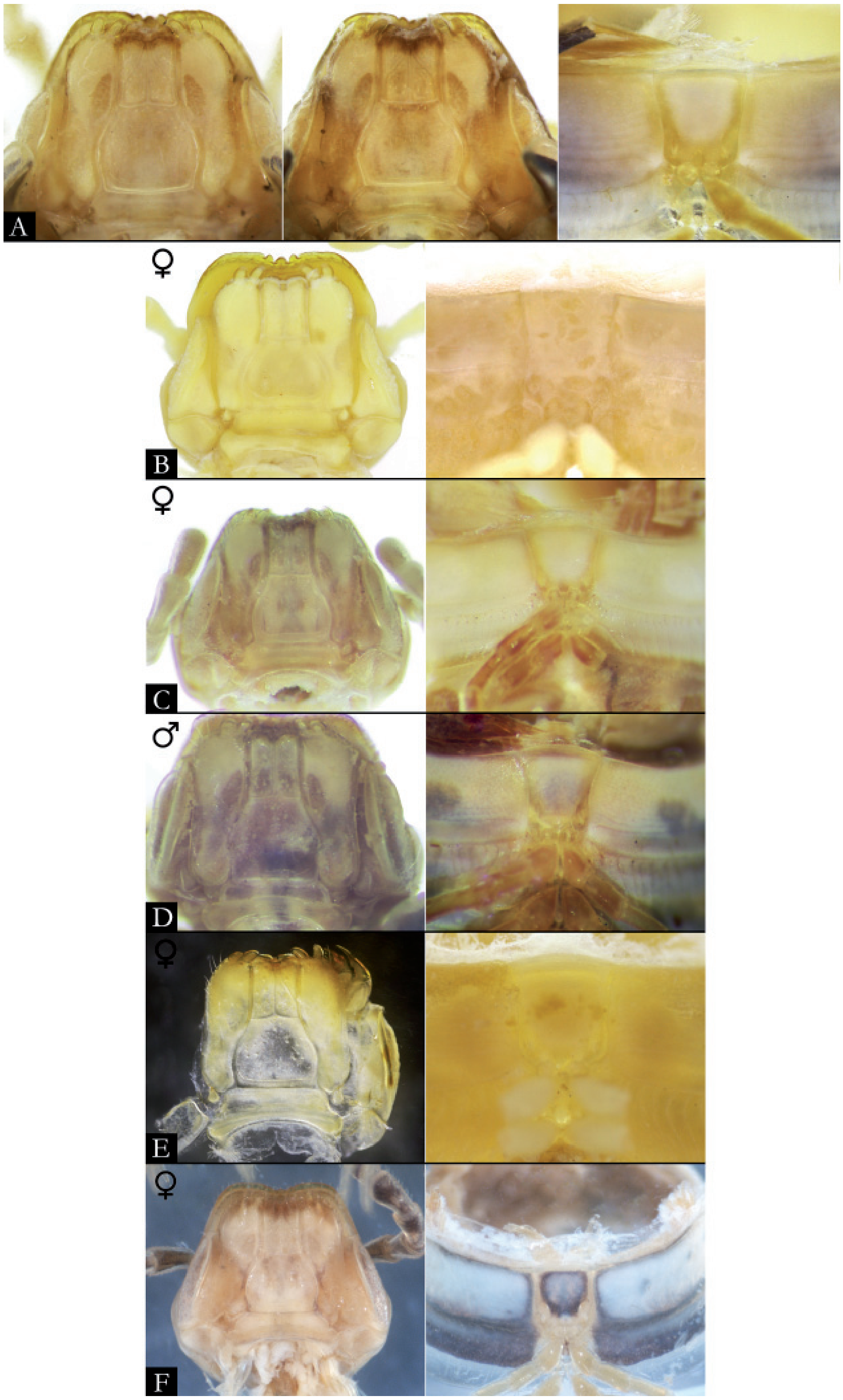

Fig. 176. Stereoscopic images of gnathochilarium and anterior sternum of species of *Pseudonannolene* Silvestri, 1895. **A**. *P. pusilla* Silvestri, 1895. **B**. *P. bovei* Silvestri, 1895. **C**. *P. brevis* Silvestri, 1902. **D**. *P. centralis* Silvestri, 1902. **E**. *P. rugosetta* Silvestri, 1897. **F**. *P. sulcatula* Silvestri, 1895. Images not to scale.

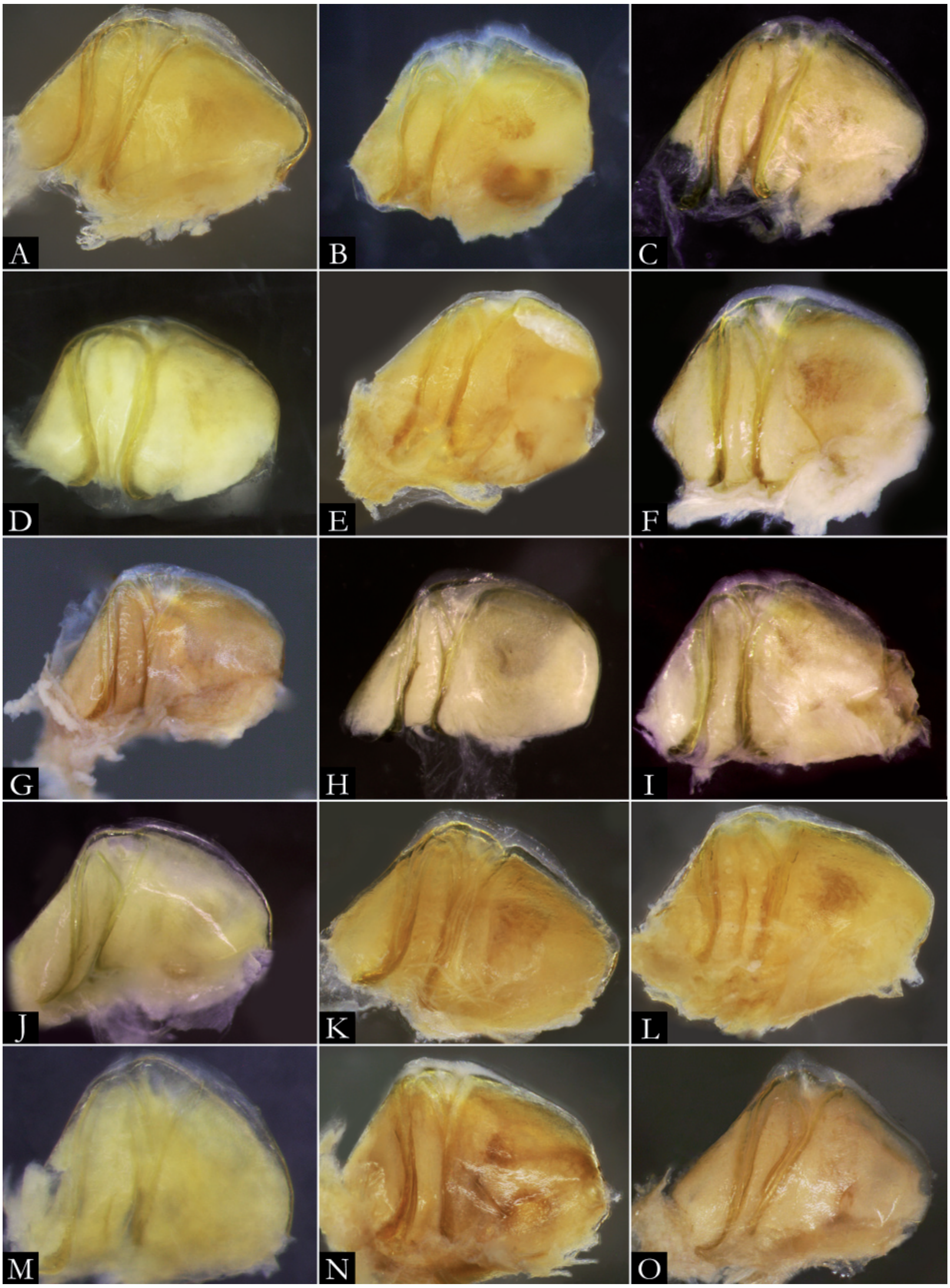

Fig. 177. Stereoscopic images of left vulva of species of *Pseudonannolene* Silvestri, 1895, in oral view. **A**. *P. albiventris* Schubart, 1952. **B**. *P. alegrensis* Silvestri, 1897. **C**. *P. ambuatinga* Iniesta & Ferreira, 2013. **D**. *P. anapophysis* Fontanetti, 1996. **E**. *P. buhrnheimi* Schubart, 1960. **F**. *P. caatinga* Iniesta & Ferreira, 2014. **G**. *P. callipyge* Brölemann, 1902. **H**. *P. erikae* Iniesta & Ferreira, 2014. **I**. *P. fontanettiae* Iniesta & Ferreira, 2014. **J**. *P. halophila* Schubart, 1949. **K**. *P. imbirensis* Fontanetti, 1996. **L**. *P. inops* Brölemann, 1929. **M**. *P. leucocephalus* Schubart, 1944. **N**. *P. longicornis* (Porat, 1888). **O**. *P. lundi* Iniesta & Ferreira, 2015. Images not to scale.

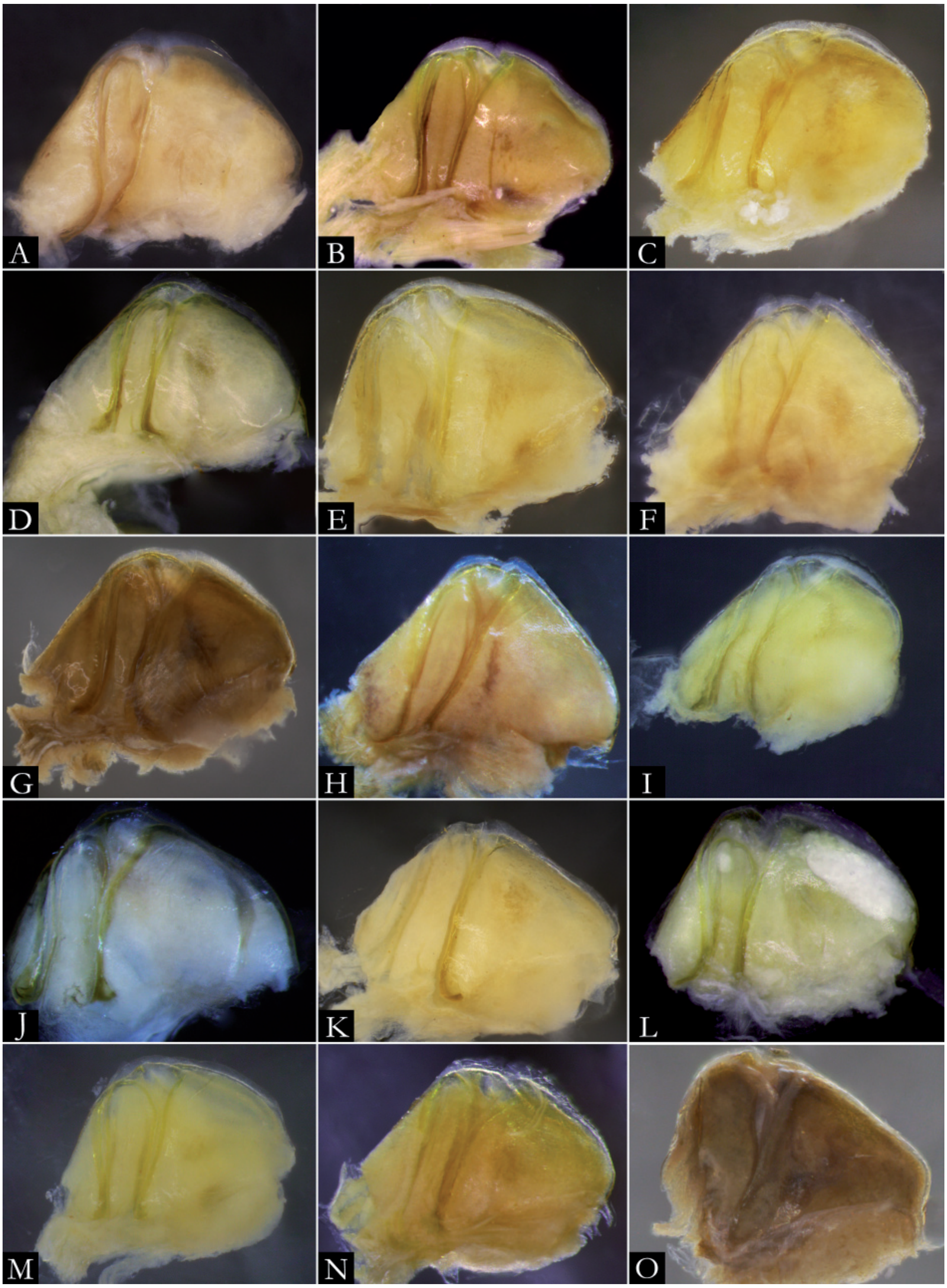

Fig. 178. Stereoscopic images of left vulva of species of *Pseudonannolene* Silvestri, 1895, in oral view. **A**. *P. magna* Udulutsch & Pietrobon, 2003. **B**. *P. maritima* Schubart, 1949. **C**. *P. mesai* Fontanetti, 2000. **D**. *P. microzoporus* Mauriès, 1987. **E**. *P. occidentalis* Schubart, 1958. **F**. *P. ophiiulus* Schubart, 1944. **G**. *P. parvula* Silvestri, 1902. **H**. *P. pusilla* Silvestri, 1895. **I**. *P. paulista* Brölemann, 1902. **J**. *P. robsoni* Iniesta & Ferreira, 2014. **K**. *P. rolamossa* Iniesta & Ferreira, 2013. **L**. *P. sebastianus* Brölemann, 1902. **M**. *P. segmentata* Silvestri, 1895. **N**. *P. silvestris* Schubart, 1944. **O**. *P. spelaea* Iniesta & Ferreira, 2013. Images not to scale.

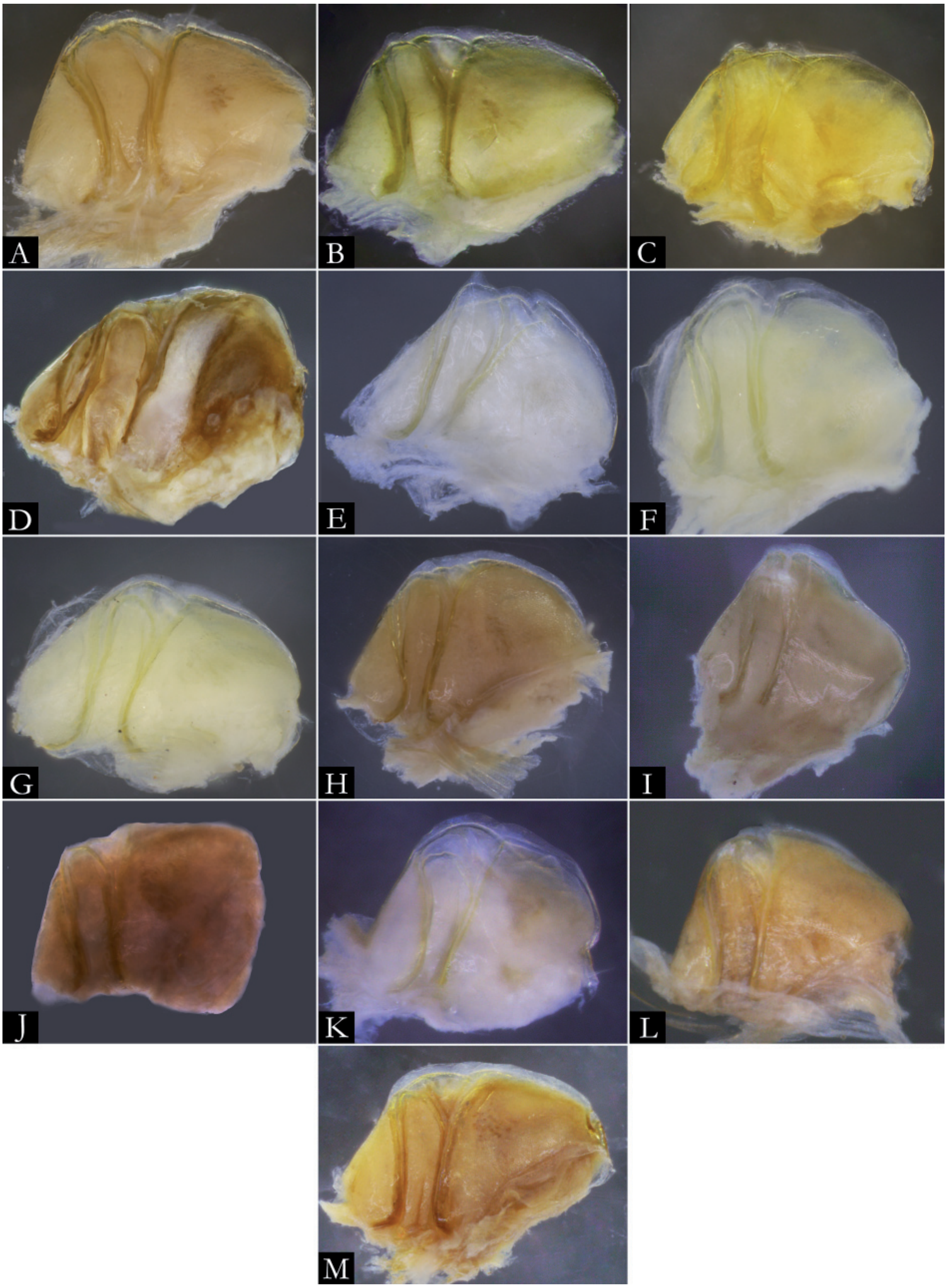

Fig. 179. Stereoscopic images of left vulva of species of *Pseudonannolene* Silvestri, 1895, in oral view. **A**. *P. strinatii* Mauriès, 1974. **B**. *P. tocaiensis* Fontanetti, 1996. **C**. *P. tricolor* Brölemann, 1902. **D**. *P. typica* Silvestri, 1895. **E**. *P. xavieri* Iniesta & Ferreira, 2014. **F**. *P. bucculenta* sp. nov. **G**. *P. morettii* sp. nov. **H**. *P. insularis* sp. nov. **I**. *P. nicolau* sp. nov. **J**. *P. granulata* sp. nov. **K**. *P. alata* sp. nov. **L**. *P. curvata* sp. nov. **M**. *P. aurea* sp. nov. Images not to scale.

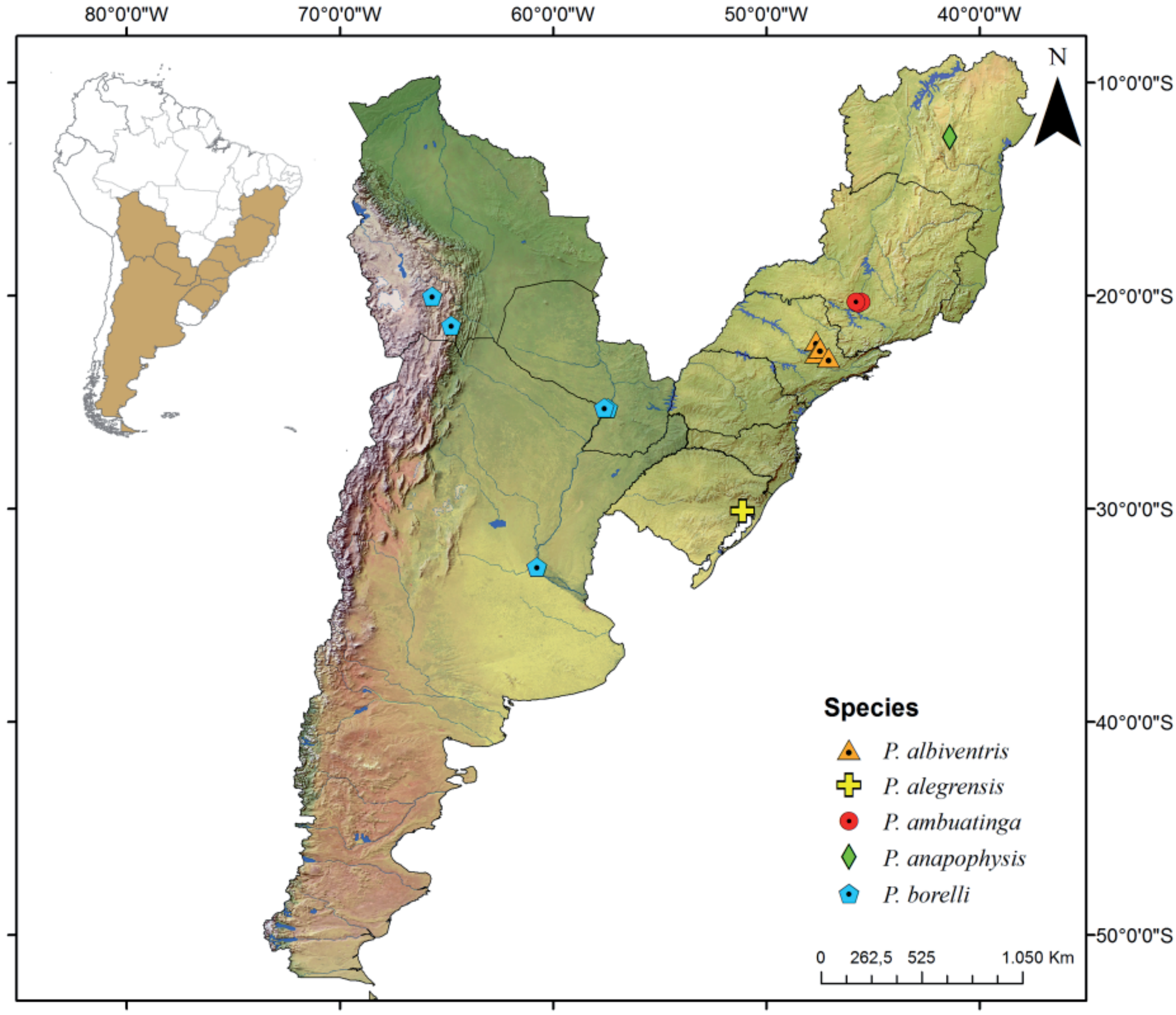

Fig. 180. Distribution map of the species *Pseudonannolene albiventris* Schubart, 1952, *P. alegrensis* Silvestri, 1897, *P. ambuatinga* Iniesta & Ferreira, 2013, *P. anapophysis* Fontanetti, 1996, and *P. borelli* Silvestri, 1895.

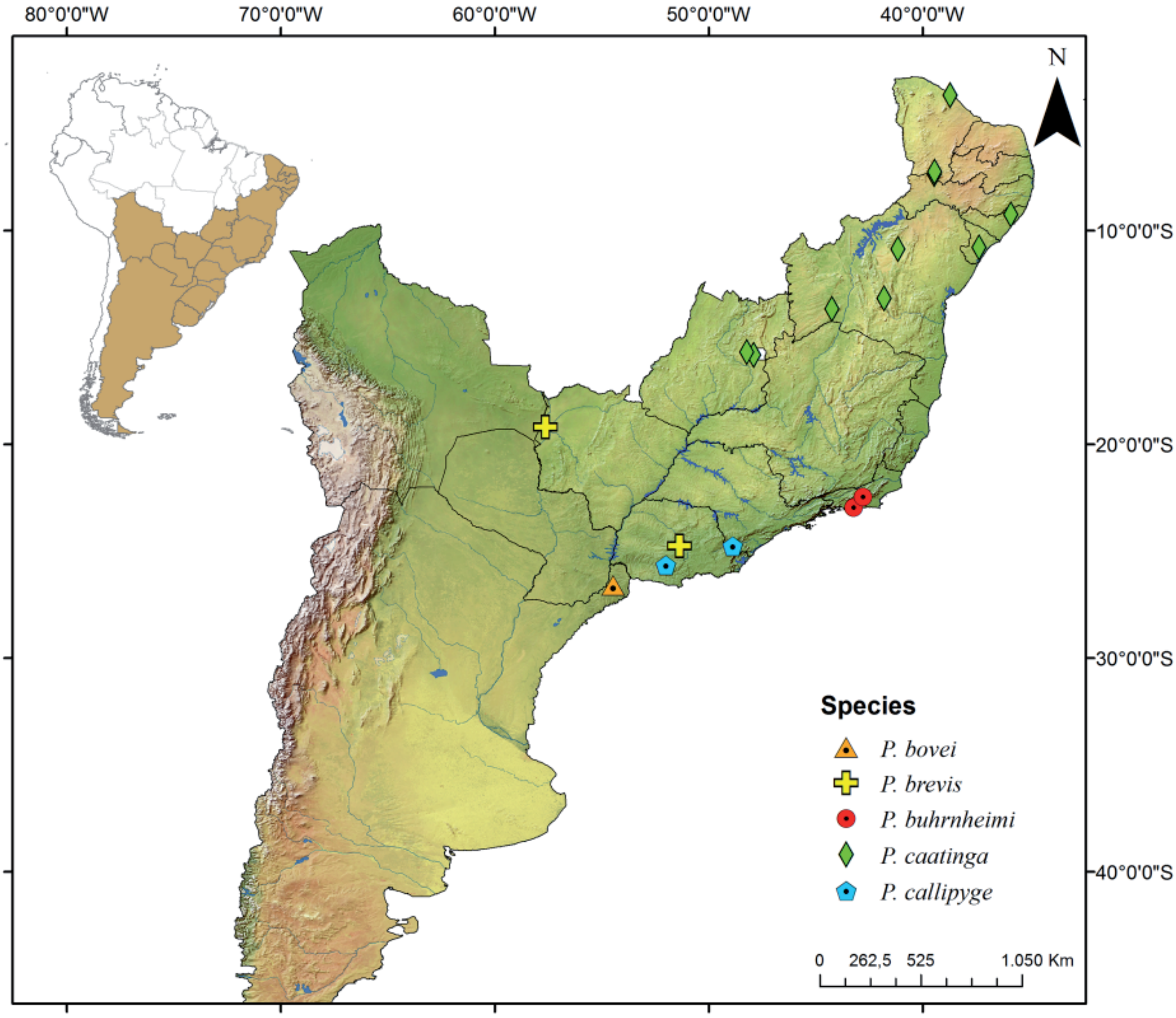

Fig. 181. Distribution map of the species *Pseudonannolene bovei* Silvestri, 1895, *P. brevis* Silvestri, 1902, *P. buhrnheimi* Schubart, 1960, *P. caatinga* Iniesta & Ferreira, 2014, and *P. callipyge* Brölemann, 1902.

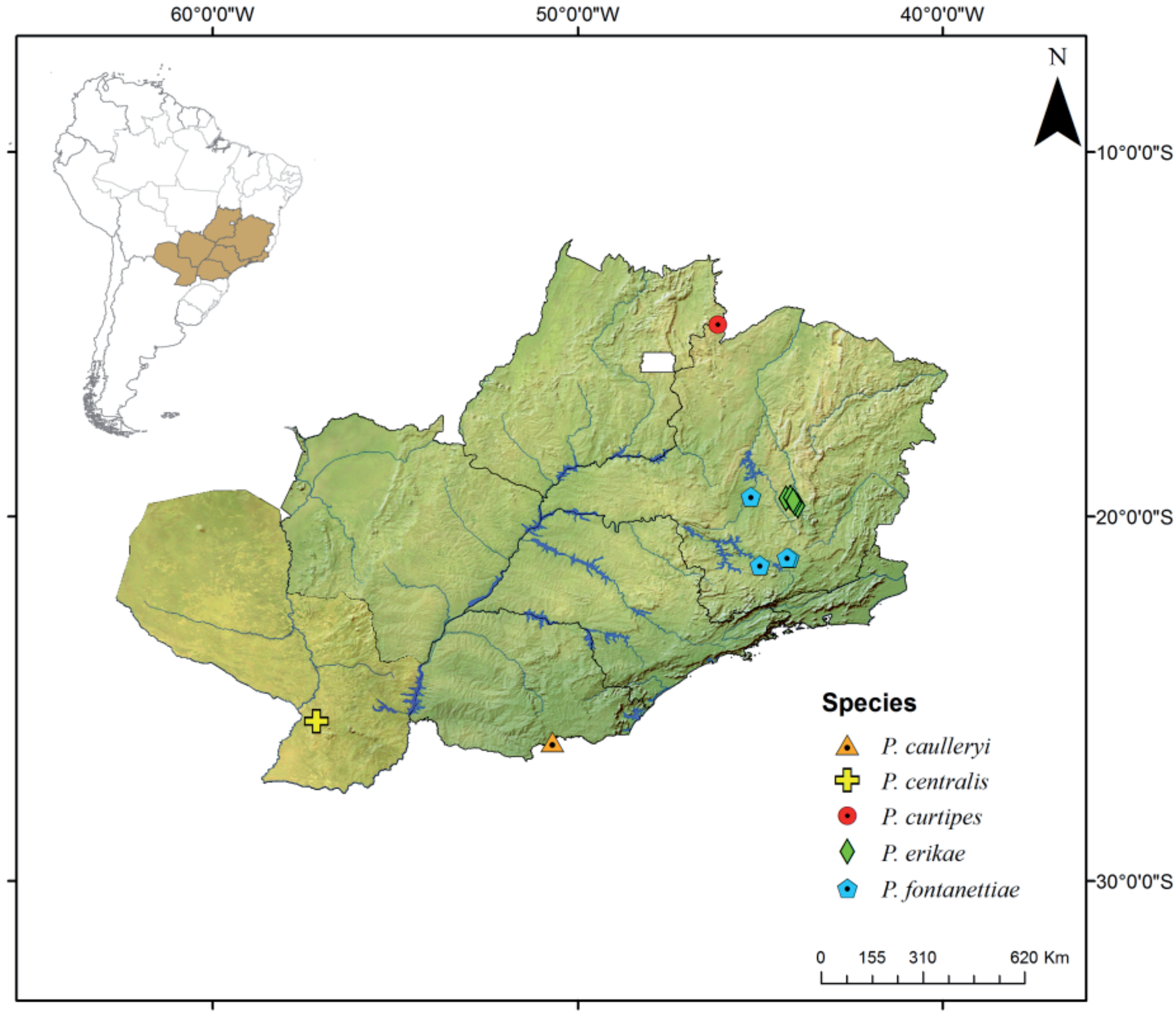

Fig. 182. Distribution map of the species *Pseudonannolene caulleryi* Brölemann, 1929, *P. centralis* Silvestri, 1902, *P. curtipes* Schubart, 1960, *P. erikae* Iniesta & Ferreira, 2014 and *P. fontanettiae* Iniesta & Ferreira, 2014.

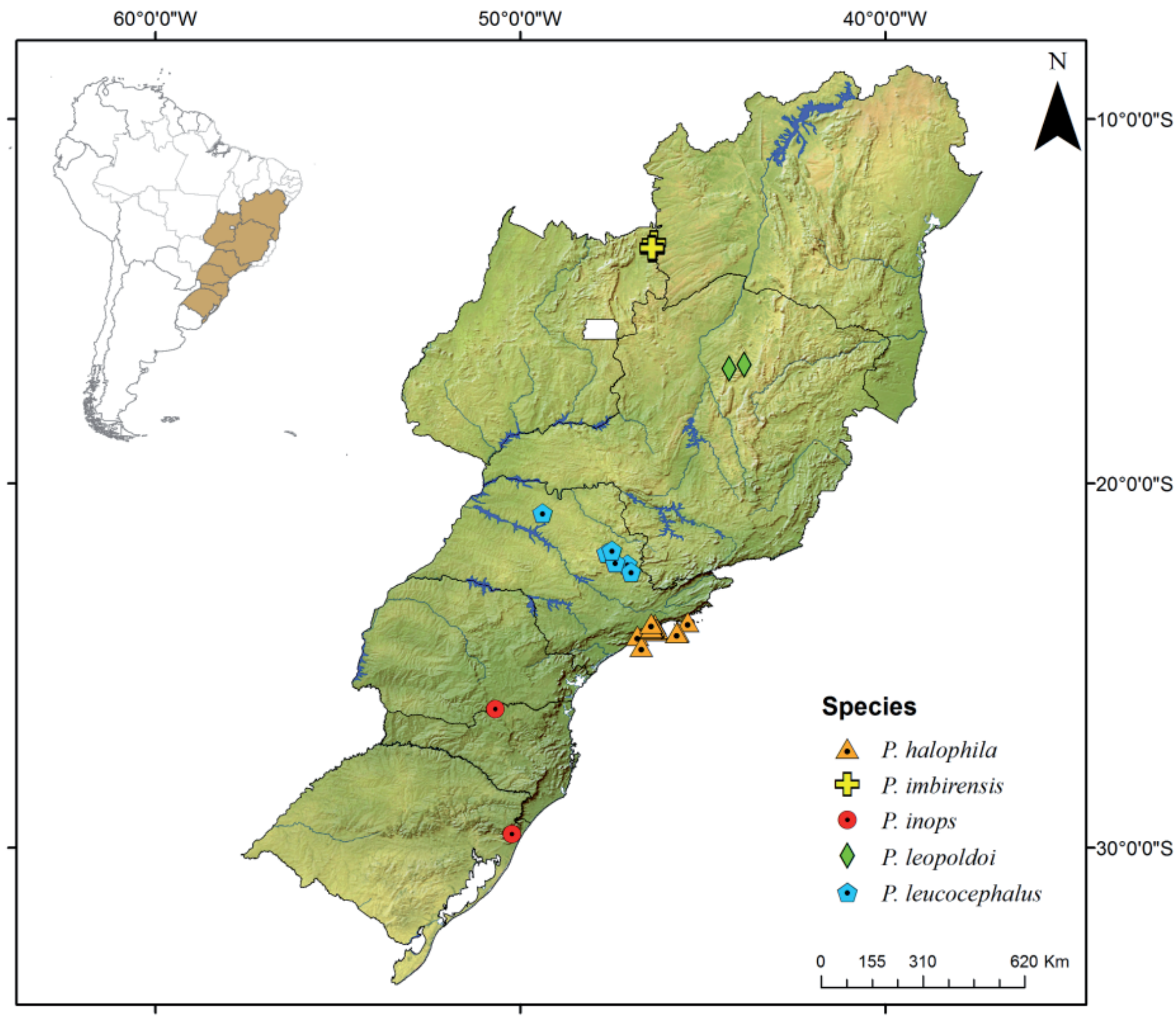

Fig. 183. Distribution map of the species *Pseudonannolene halophila* Schubart, 1949, *P. imbirensis* Fontanetti, 1996, *P. inops* Brölemann, 1929, *P. leopoldoi* Iniesta & Ferreira, 2014, and *P. leucocephalus* Schubart, 1944.

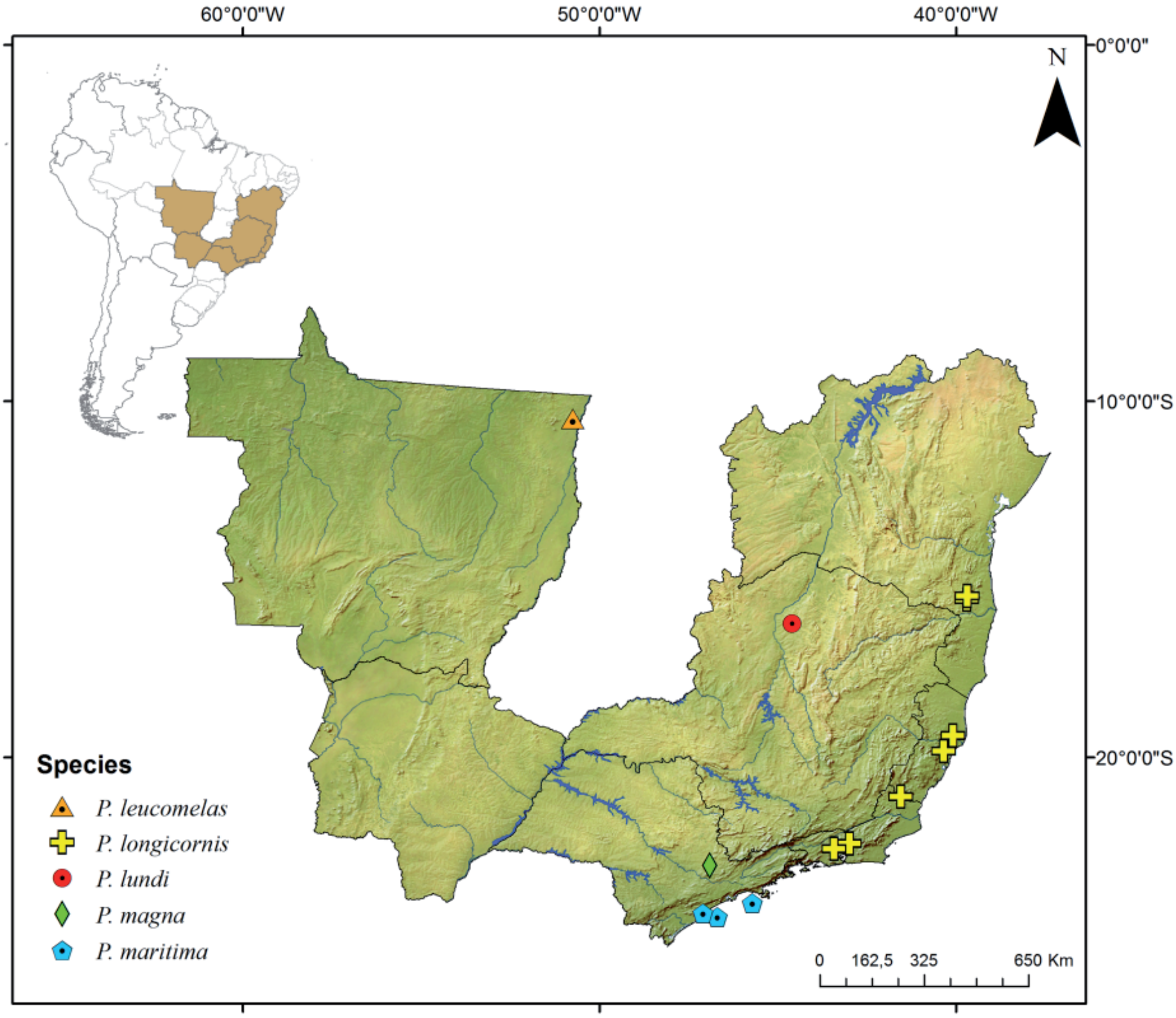

Fig. 184. Distribution map of the species *Pseudonannolene leucomelas* Schubart, 1947, *P. longicornis* (Porat, 1888), *P. lundi* Iniesta & Ferreira, 2015, *P. magna* Udulutsch & Pietrobon, 2003, and *P. maritima* Schubart, 1949.

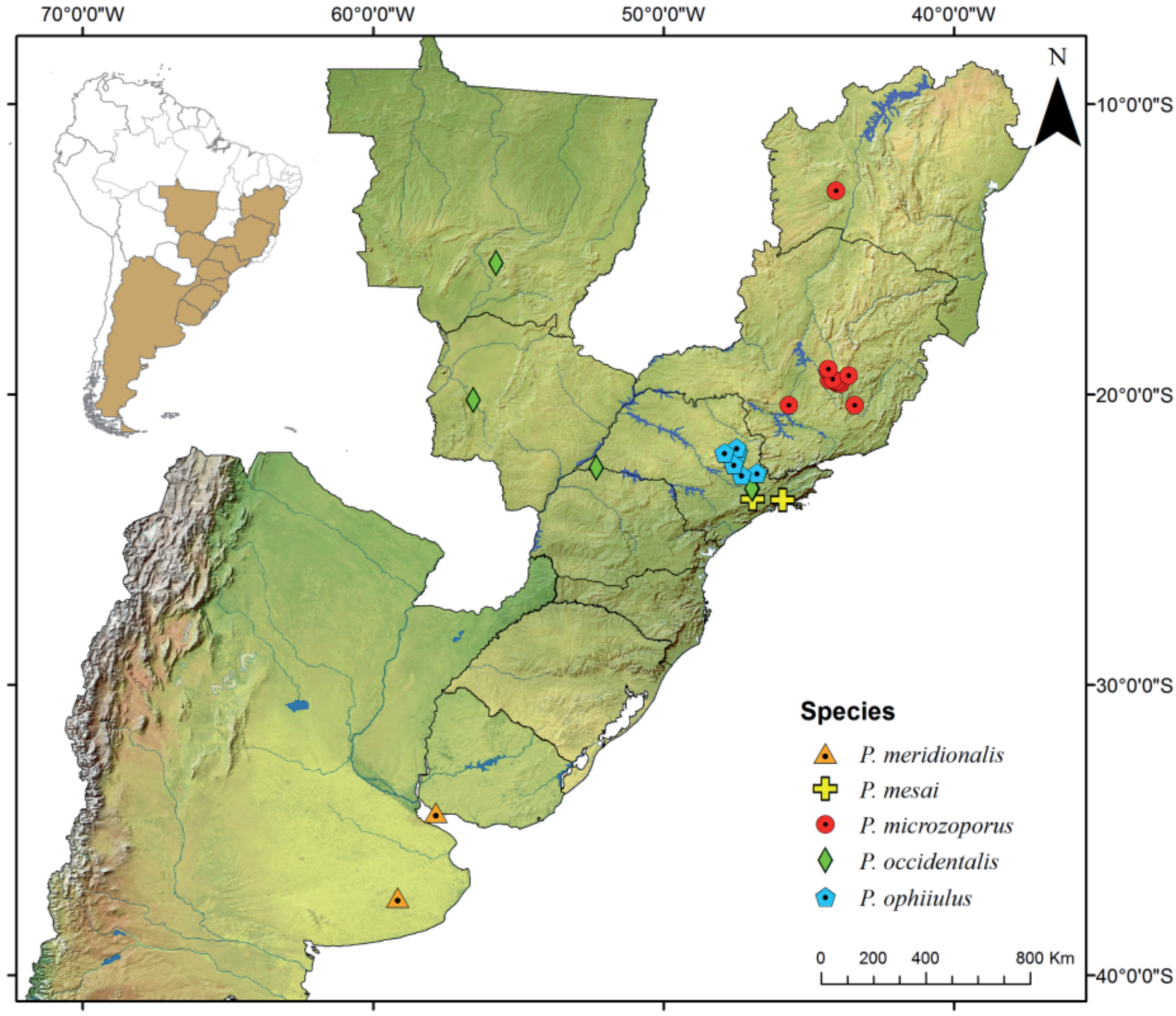

Fig. 185. Distribution map of the species *Pseudonannolene meridionalis* Silvestri, 1902, *P. mesai* Fontanetti, 2000, *P. microzoporus* Mauriès, 1987, *P. occidentalis* Schubart, 1958, and *P. ophiiulus* Schubart, 1944.

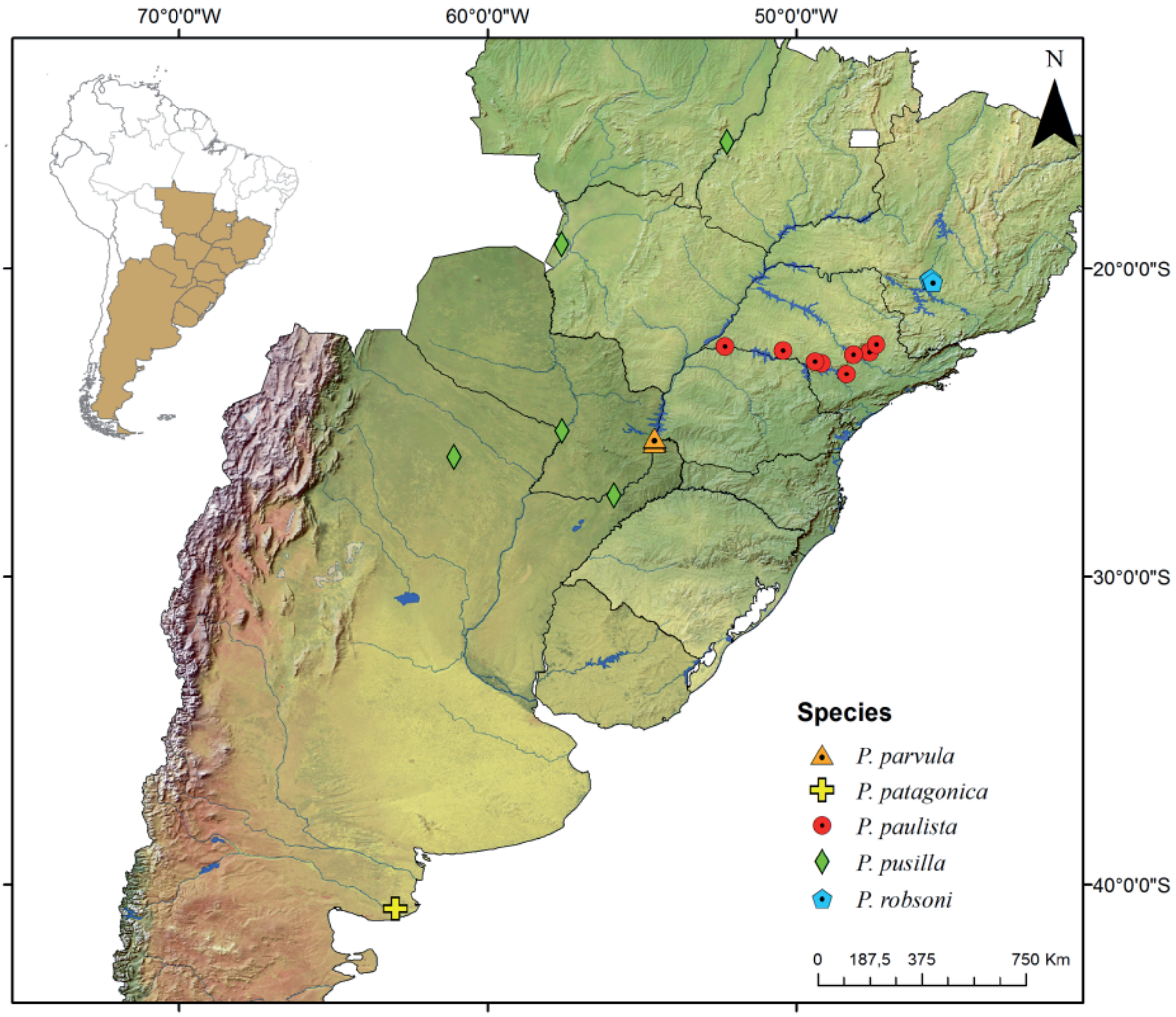

Fig. 186. Distribution map of the species *Pseudonannolene parvula* Silvestri, 1902, *P. patagonica* Brölemann, 1902, *P. paulista* Brölemann, 1902, *P. pusilla* Silvestri, 1895, and *P. robsoni* Iniesta & Ferreira, 2014.

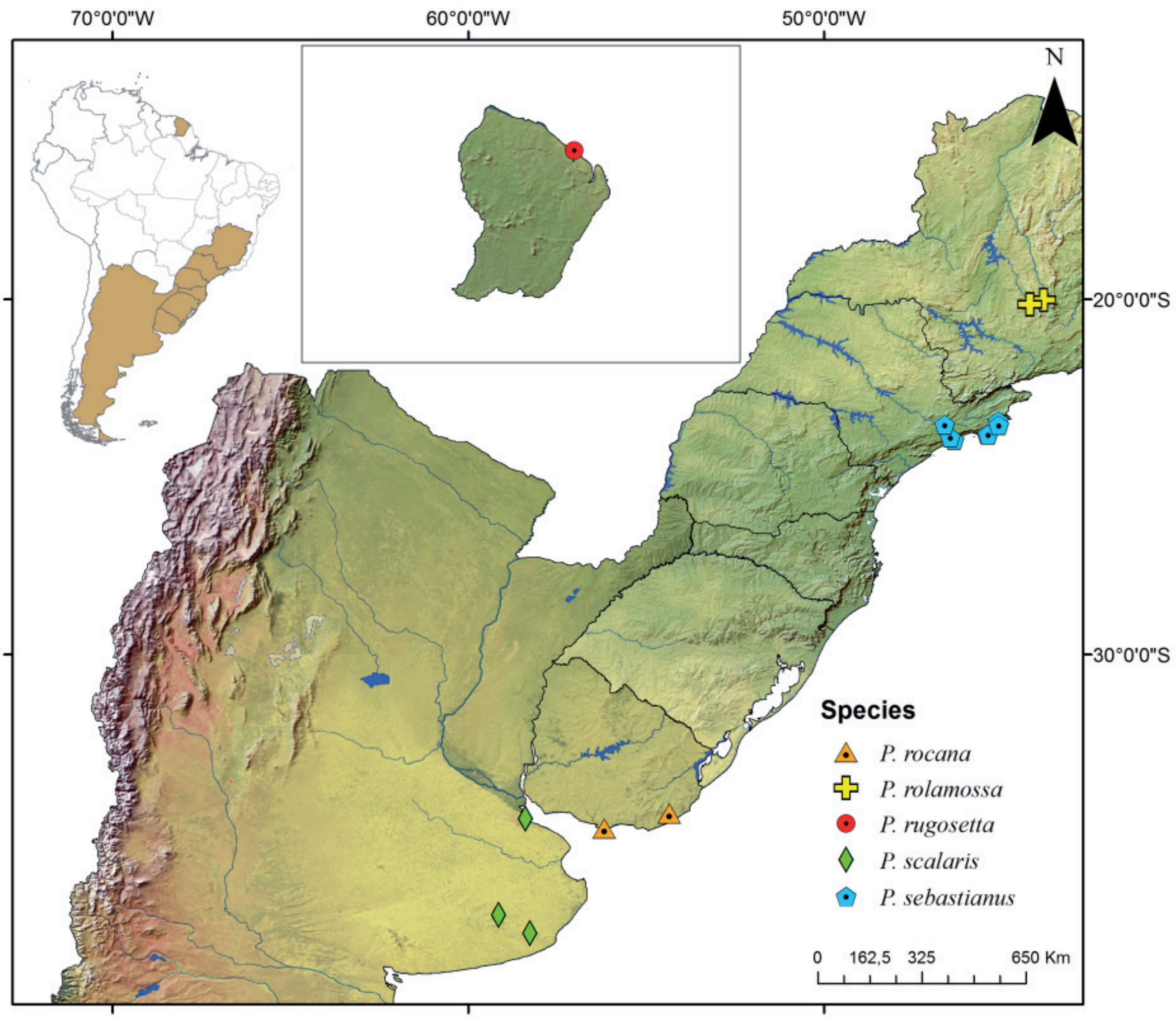

Fig. 187. Distribution map of the species *Pseudonannolene rocana* Silvestri, 1902, *P. rolamossa* Iniesta & Ferreira, 2013, *P. rugosetta* Silvestri, 1897, *P. scalaris* Brölemann, 1902, and *P. sebastianus* Brölemann, 1902.

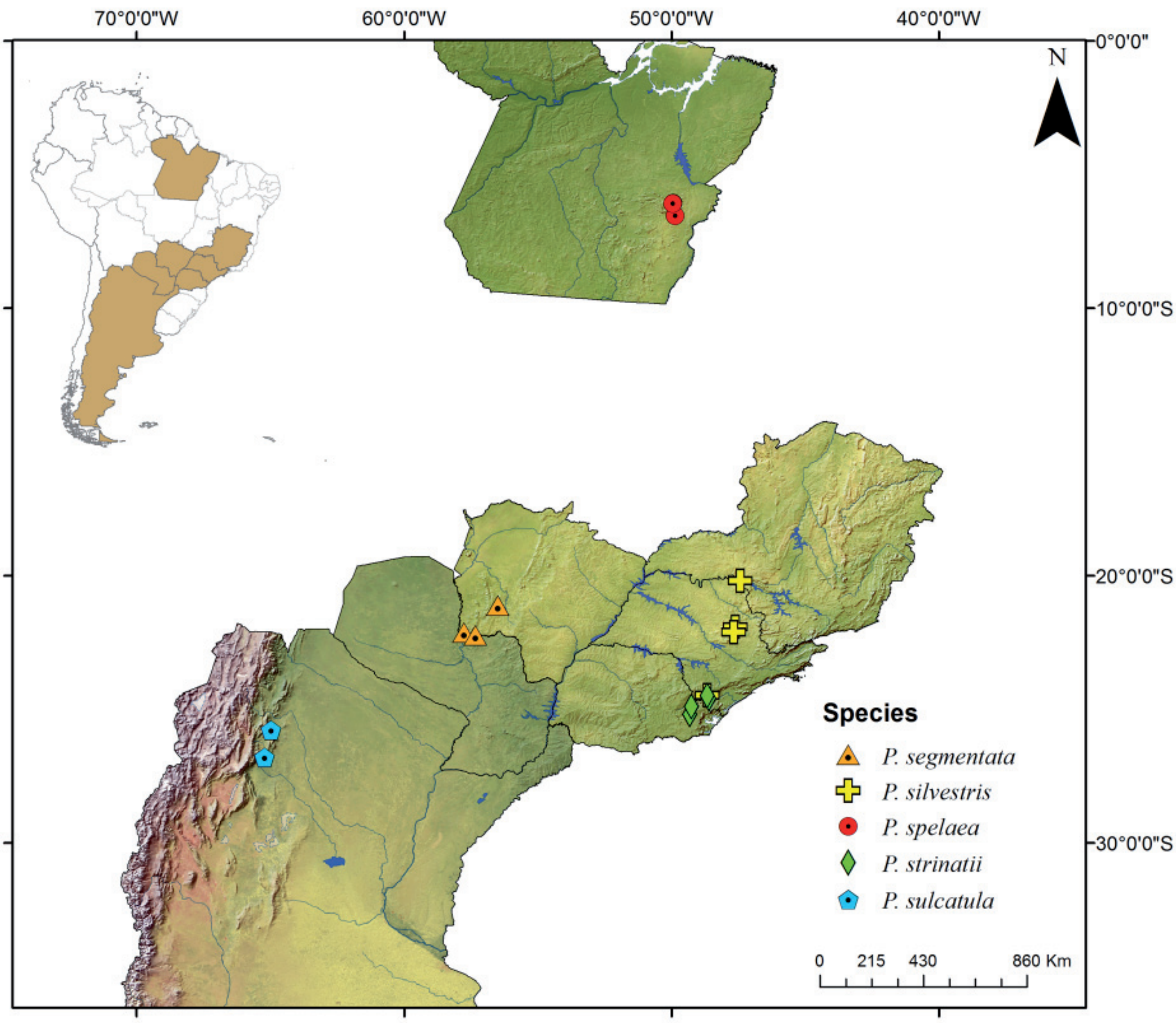

Fig. 188. Distribution map of the species *Pseudonannolene segmentata* Silvestri, 1895, *P. silvestris* Schubart, 1944, *P. spelaea* Iniesta & Ferreira, 2013, *P. strinatii* Mauriès, 1974, and *P. sulcatula* Silvestri, 1895.

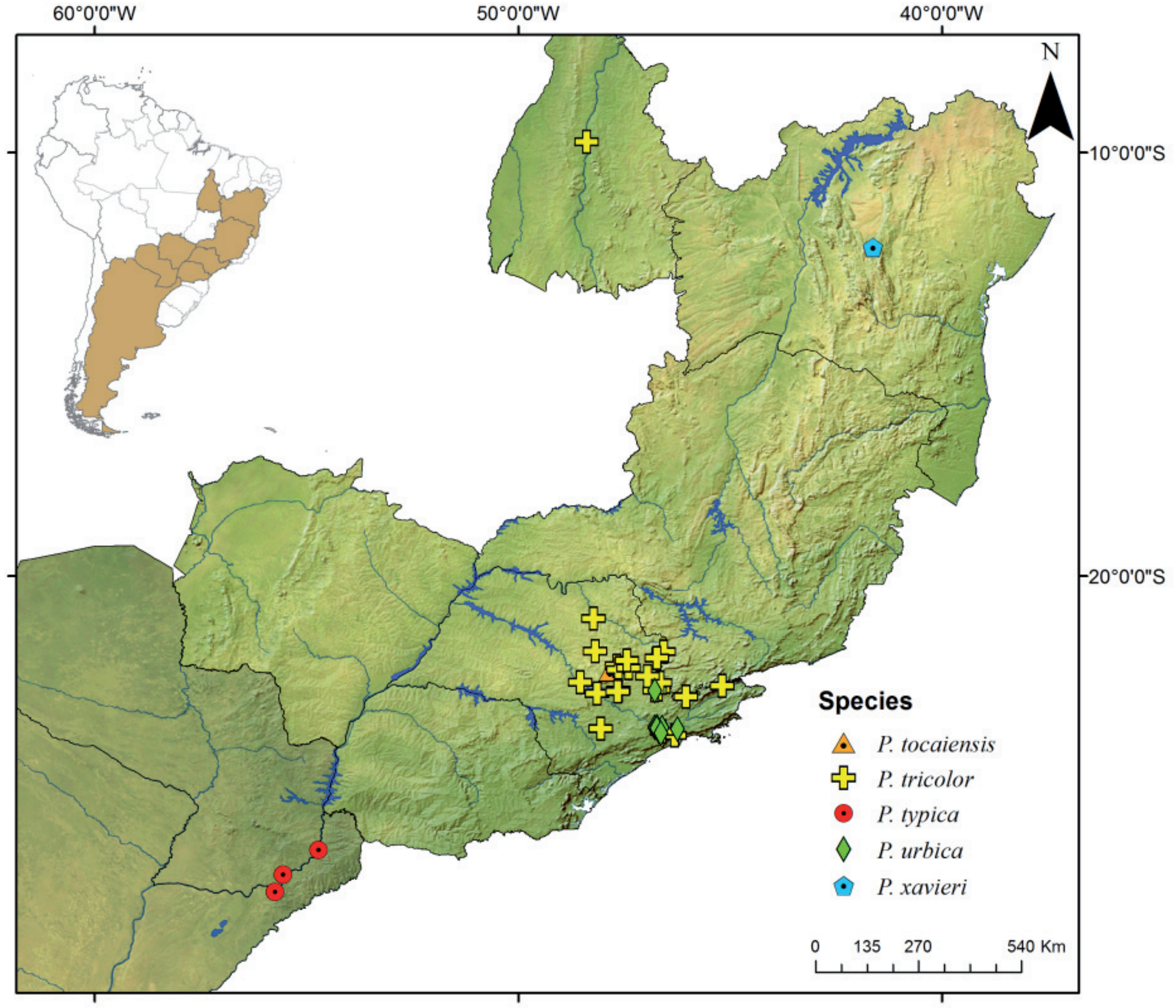

Fig. 189. Distribution map of the species *Pseudonannolene tocaiensis* Fontanetti, 1996, *P. tricolor* Brölemann, 1902, *P. typica* Silvestri, 1895, *P. urbica* Schubart, 1945, and *P. xavieri* Iniesta & Ferreira, 2014.

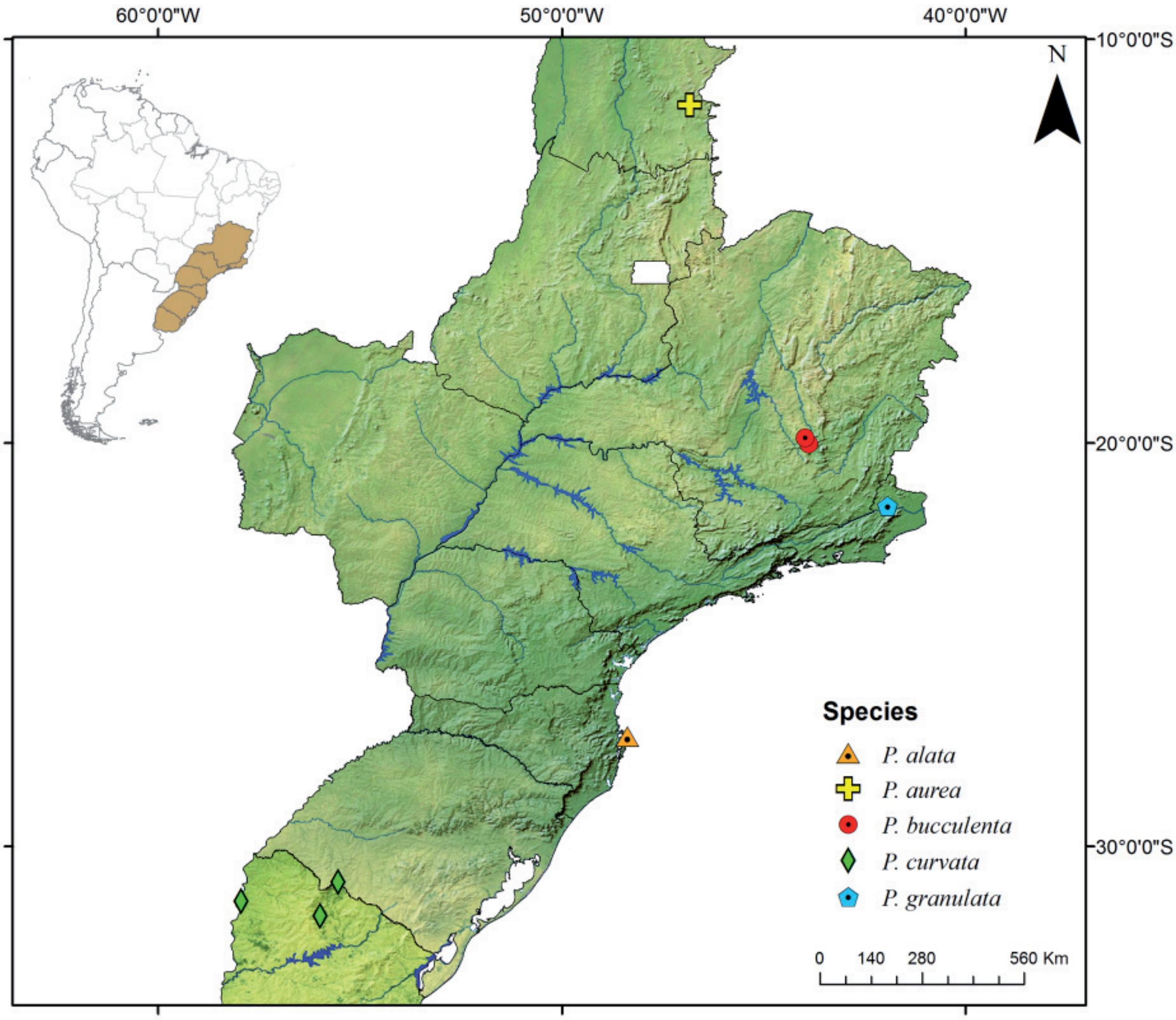

Fig. 190. Distribution map of the species *Pseudonannolene alata* sp. nov., *P. aurea* sp. nov., *P. bucculenta* sp. nov., *P. curvata* sp. nov., and *P. granulata* sp. nov.

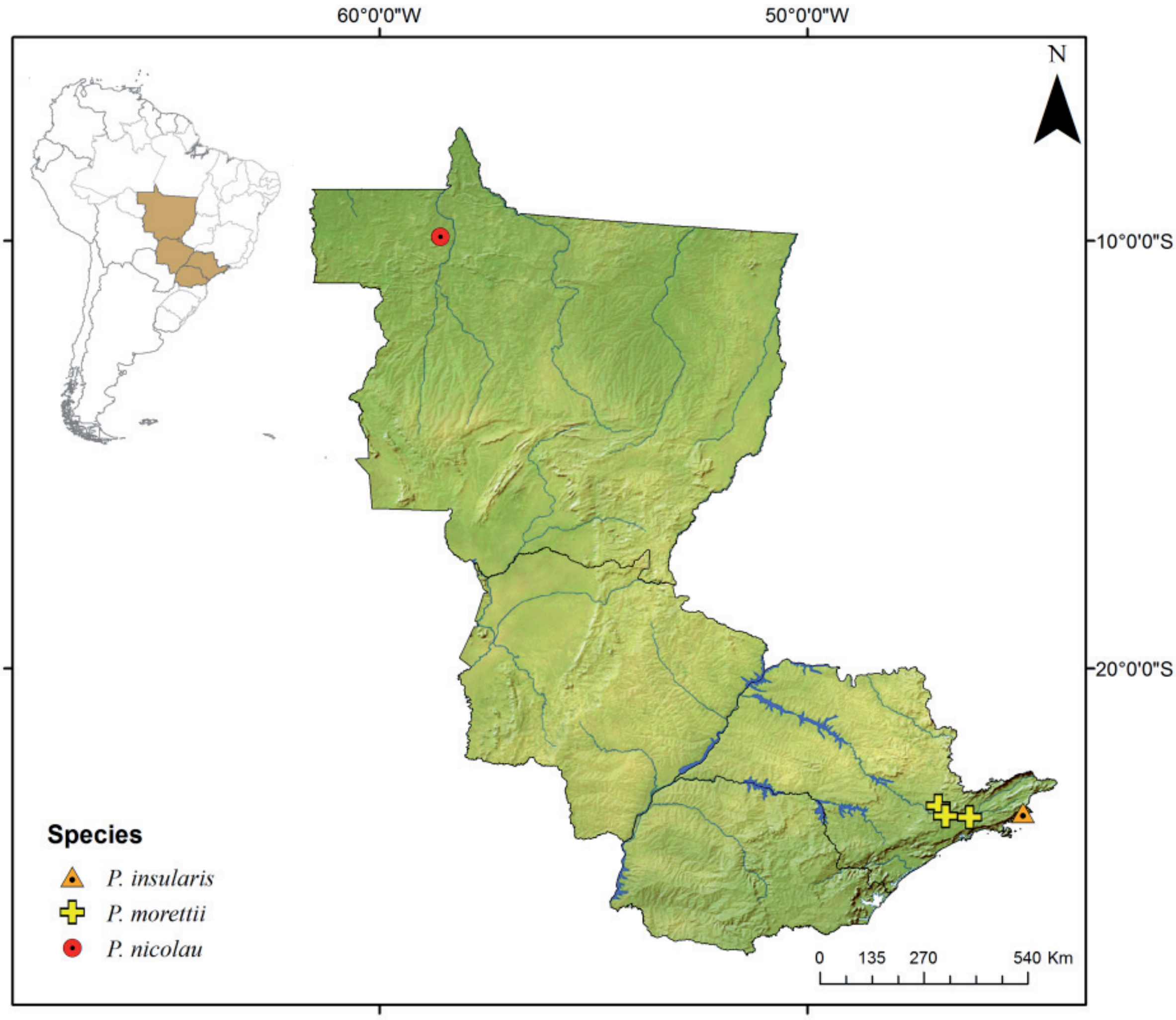

Fig. 191. Distribution map of the species *Pseudonannolene insularis* sp. nov., *P. morettii* sp. nov., and *P. nicolau* sp. nov.

References

Akkari N. & Enghoff H. 2012. Review of the genus *Ommatoiulus* in Andalusia, Spain (Diplopoda: Julida) with description of ten new species and notes on a remarkable gonopod structure, the fovea. *Zootaxa* 3538: 1–53. https://doi.org/10.1111/j.1096-0031.2008.00229.x

Akkari N., Gilgado J.D., Ortuño V.M. & Enghoff H. 2018. Out of the dark void: *Ommatoiulus longicornis* n. sp., a new julid from Spain (Diplopoda, Julida) with notes on some troglobiomorphic traits in millipedes. *Zootaxa* 4420: 415–429. https://doi.org/10.11646/zootaxa.4420.3.7

Álvares E.S.S. & Ferreira R.L. 2002. *Coarazuphium pains*, a new species of troglobitic beetle from Brazil (Coleoptera: Carabidae: Zuphiini). *Lundiana* 3(1): 41–43.

Arias J.S. 2017. An event model for phylogenetic biogeography using explicitly geographical ranges. *Journal of Biogeography* 44: 2225–2235. https://doi.org/10.1111/jbi.13024

Arias J.S., Szumik C.A. & Goloboff P.A. 2011. Spatial analysis of vicariance: a method for using direct geographical information in historical biogeography. *Cladistics* 27: 617–628. https://doi.org/10.1111/j.1096-0031.2011.00353.x

Attems C. 1926. Myriopoda. *In*: Kükenthal W. (ed.) *Handbuch der Zoologie* 4 (1): 1–402.

Ázara L.N. & Ferreira R.L. 2014. Two new troglobitic *Newportia* (*Newportia*) from Brazil (Chilopoda: Scolopendromorpha). *Zootaxa* 3881 (3): 267–278. https://doi.org/10.11646/zootaxa.3881.3.5

Barbo F.E., Nogueira C.C. & Sawaya R.J. 2021. Vicariance and regionalization patterns in snakes of the South American Atlantic Forest megadiverse hotspot. *Journal of Biogeography* 48 (4): 823–833. https://doi.org/10.1111/jbi.14040

Barcia D.L., DaSilva M.B., Conti L.A. & Carbayo F. 2020. Areas of endemism of land planarians (Platyhelminthes: Tricladida) in the Southern Atlantic Forest. *PLoS ONE* 15 (7): e0235949. https://doi.org/10.1371/journal.pone.0235949

Batista C.B., Lima I.P. & Lima M.R. 2021. Beta diversity patterns of bats in the Atlantic Forest: how does the scale of analysis affect the importance of spatial and environmental factors? *Journal of Biogeography* 48 (1): 1–10. https://doi.org/10.1111/jbi.13928

Bichuette M.E., Simões L.B., Zepon T., von Schimonsky D.M. & Gallão J.E. 2019. Richness and taxonomic distinctness of cave invertebrates from the northeastern state of Goiás, central Brazil: a vulnerable and singular area. *Subterranean Biology* 29: 1–33. https://doi.org/10.3897/subtbiol.29.30418

Boock O.J. & Lordello L.G.E. 1952. Diplópoda depredador de tubérculos de batatinha. *Bragantia* 12 (10–12): 343–348. https://doi.org/10.1590/S0006-87051952000400006

Bouzan R.S., Iniesta L.F.M., de Souza C.A.R., Zampaulo R.A. & Brescovit A.D. 2019a. Taxonomic review of the Amazonian millipede genus *Parastenonia* Hoffman, 1977 and description of a new species from iron-ore caves (Polydesmida: Chelodesmidae). *Journal of Natural History* 53 (45–46): 2781–2799. https://doi.org/10.1080/00222933.2020.1749956

Bouzan R.S., Iniesta L.F.M. & Brescovit A.D. 2019b. Cladistic analysis and description of a new species of the Brazilian genus *Atlantodesmus* Hoffman, 2000 (Diplopoda: Polydesmida: Chelodesmidae). *European Journal of Taxonomy* 538: 1–17. https://doi.org/10.5852/ejt.2019.538

Bouzan R.S., Iniesta L.F.M. & Brescovit A.D. 2021. Cladistic analysis and taxonomic review of the millipede tribe Arthrosolaenomeridini Hoffman, 1976 (Polydesmida: Chelodesmidae). *Zootaxa* 4970 (2): 201–256. https://doi.org/10.11646/zootaxa.4970.2.1

Bornschein M.R., Firkowski C.R., Belmonte-Lopes R., Corrêa L., Ribeiro L.F., Morato S.A.A., Antoniazzi-Jr R.L., Reinert B.L., Meyer A.L.S., Cini F.A. & Pie M.R. 2016. Geographical and altitudinal distribution of *Brachycephalus* (Anura: Brachycephalidae) endemic to the Brazilian Atlantic Rainforest. *PeerJ* 4: e2490. https://doi.org/10.7717/peerj.2490

Brazeau M.D. 2011. Problematic character coding methods in morphology and their effects. *Biological Journal of the Linnean Society* 104 (3): 489–498. https://doi.org/10.1111/j.1095-8312.2011.01755.x

Bremer K. 1988. The limits of amino acid sequence data in angiosperm phylogenetic reconstruction. *Evolution* 42 (4): 795–803. https://doi.org/10.1111/j.1558-5646.1988.tb02497.x

Bremer K. 1994. Branch support and tree stability. *Cladistics* 10 (3): 295–304. https://doi.org/10.1111/j.1096-0031.1994.tb00179.x

Brölemann H.W. 1902a. Myriapodes du Musée de Sao Paulo. *Revista do Museu Paulista* 5: 35–237. https://doi.org/10.5962/bhl.part.9824

Brölemann H.W. 1902b. Myriapodes recueillis par M.E. Gounolle au Brésil. *Annales de la Société entomologique de France* 71: 649–694. Available from https://www.biodiversitylibrary.org/page/8252053 [accessed 10 Feb. 2023].

Brölemann H.W. 1903. Myriapodes recueillis au Pará par Monsieur le Prof. E.A. Goeldi, Directeur du Musée. *Zoologischer Anzeiger* 26 (691): 177–196.

Brölemann H.W. 1904. Myriapodes du Museu Paulista, II[e] mémorie: Manaos. *Revista do Museu Paulista* 6: 63–96. https://doi.org/10.5962/bhl.part.26467

Brölemann H.W. 1909. *Os Myriapodos do Brazil. Catalogos da Fauna Brazileira*. Museu Paulista, São Paulo, Brasil.

Brölemann H.W. 1919. Myriapodes. *Mission du Service géographique de l'armée pour la mesure d'un Arc de méridien équatorial en Amérique du Sud sous le contrôle scientifique de l'Académie des Sciences, 1899-1906* 10: 235–275. https://doi.org/10.5962/bhl.title.980

Brölemann H.W. 1920. Diplopoda. *In*: Voyage de Ch. Alluaud et R. Jeannel en Afrique Orientale (1911–1912). *Résultats scientifiques. Myriapoda, III.* L. Lhomme, Paris. https://doi.org/10.5962/bhl.title.152165

Brölemann H.W. 1929. Myriapodes recueillis aus Brésil par M. le professeur Caullery, membre de l'institut. *Mémoires de la Société zoologique de France* 29 (1): 1–37.

Bueno-Villegas J., Sierwald P. & Monteros A.E. 2008. Phylogeny of the millipede genus *Sphaeriodesmus* Peters, 1864 (Polydesmida: Sphaeriodesmidae) based on morphological characters. *Organisms, Diversity & Evolution* 8: 99–120. https://doi.org/10.1016/j.ode.2007.03.001

Calvanese V.C., Brescovit A.D. & Bonato L. 2019. Revision of the Neotropical species of Aphilodontinae (Geophilomorpha, Geophilidae), with eight new species and a first phylogenetic analysis of the subfamily. *Zootaxa* 4698 (1): 1–72. https://doi.org/10.11646/zootaxa.4698.1.1

Campos K.A. & Fontanetti C.S. 2004. Chromosomal characterization of *Pseudonannolene strinatii* (Spirostreptida, Pseudonannolenidae). *Iheringia* 94 (1): 53–56. https://doi.org/10.1590/S0073-47212004000100009

Carl J. 1913a. Diplopodenstudien I. Die Gonopoden von *Epinannolene* und *Pseudonannolene*. *Zoologischer Anzeiger* 42: 174–177.

Carl J. 1913b. Diplopodenstudien II. Eine neue Physiostreptiden-Gattung. *Zoologischer Anzeiger* 42 (5): 212–216.

Carl J. 1914. Die Diplopoden von Columbien nebst Beiträgen zur Morphologic der Stemmatoiuliden. *Memoires de la Société neuchâteloise des Sciences naturelles* 5: 821–993.

Chagas-Jr A. & Bichuette M.E. 2018. A synopsis of centipedes in Brazilian caves: hidden species diversity that needs conservation (Myriapoda, Chilopoda). *ZooKeys* 737: 13–56. https://doi.org/10.3897/zookeys.737.20307

Chamberlin R.V. 1918. Myriapods from Nashville, Tennessee. *Psyche* 25: 23–30. https://doi.org/10.1155/1918/65230

Chamberlin R.V. 1922. Notes on West Indian millipeds. *Proceedings of the United States National Museum* 61 (10): 1–19. https://doi.org/10.5479/si.00963801.61-2431.1

Cook O.F. 1895. Introductory note on the families of Diplopoda. *In*: Cook O.F. & Collins G.N. (eds) *The Craspedosomatidae of North America*. Annals of the New York Academy of Sciences 9. New York Academy of Sciences, New York.

Culver D.C. & Shear W.A. 2012. Myriapods. *In*: White W.B.& Culver D.C. (eds) *Encyclopodia of Caves*: 538–541. Academic Press, Chennai. https://doi.org/10.1016/B978-0-12-383832-2.00078-5

Dauby G., Stévart T., Droissart V., Cosiaux A., Deblauwe V., Simo-Droissart M., Sosef M.S.M., Lowry II P.P., Schatz G.E., Gereau R.E. & Couvreur T.L.P. 2017. ConR: an R package to assist large-scale multispecies preliminary conservation assessments using distribution data. *Ecology and Evolution* 7 (24): 11292–11303. https://doi.org/10.1002/ece3.3704

de Pinna M.C.C. 1991. Concepts and tests of homology in the cladistic paradigm. *Cladistics* 7 (4): 367–394. https://doi.org/10.1111/j.1096-0031.1991.tb00045.x

Deharveng L. & Bedos A. 2018. Diversity of terrestrial invertebrates in subterranean habitats. *In*: Moldovan O.T., Kovác L. & Halse S. (eds) *Cave Ecology. Ecological Studies*. Springer Nature Switzerland AG. https://doi.org/10.1007/978-3-319-98852-8_7

Demange J.-M. 1964. Les appendices postériqueurs (9^{e} paire) du diplopsegment gonopodial (VII^{e}) des Spirostreptoidea (Myriapodes Diplopodes). *Bulletin du Muséum national d'histoire naturelle, 2^{e} série* 36: 191–210.

Desutter-Grandcolas L., D'Haese C. & Robillarda T. 2003. The problem of characters susceptible to parallel evolution in phylogenetic analysis: a reply to Marquès and Gnaspini (2001) with emphasis on cave life phenotypic evolution. *Cladistics* 19: 131–137. https://doi.org/10.1111/j.1096-0031.2003.tb00301.x

Enghoff H. 1981. A cladistic analysis and classification of the millipede order Julida. *Zeitschrift für zoologische Systematik und Evolutionsforschung* 19: 285–319.

Enghoff H. 1991. A revised cladistic analysis and classification of the millipede order Julida with establishment of four new families and description of a new nemasomatoid genus from Japan. *Zeitschrift für zoologische Systematik und Evolutionsforschung* 29: 241–263. https://doi.org/10.1111/j.1439-0469.1991.tb00671.x

Enghoff H. 1992. The size of a millipede. *In*: Meyer E., Thaler K. & Schedl W. (ed.) *Advances in Myriapodology*. *Berichte des naturwissenschaftlich-medizinischen Vereins in Innsbruck* Suppl. 10: 47–56.

Enghoff H. 1995. A revision of the Paectophyllini and Calyptophyllini: millipedes of the Middle East (Diplopoda, Julida, Julidae). *Journal of Natural History* 29: 685–786. https://doi.org/10.1080/00222939500770241

Enghoff H. 1996. The penis as a phylogenetic character in the millipede family Julida. *Mémoires du Muséum national d'histoire naturelle N.S.* 169: 313–326.

Enghoff H. & Reboleira A.S.P.S. 2017. Diversity of non-Laboulbenialean fungi on millipedes. *Studies in Fungi* 2 (1): 130–137. https://doi.org/10.5943/sif/2/1/15

Enghoff H. & Reboleira A.S.P.S. 2020. The first blind spirostreptid millipede, found in a cave in Morocco; with notes on the genus *Odontostreptus* Attems, 1914 (Diplopoda, Spirostreptida, Spirostreptidae). *European Journal of Taxonomy* 668: 1–11. https://doi.org/10.5852/ejt.2020.668

Enghoff H., Golovatch S.I., Short M., Stoev P. & Wesener T. 2015. Diplopoda – Taxonomic overview. *In*: Minelli A. (ed.) *Treatise on Zoology – Anatomy, Taxonomy, Biology. The Myriapoda Vol. 2*: 363–453. Brill, Leiden and Boston. https://doi.org/10.1163/9789004188273_017

Escapa I.H. & Catalano S.A. 2013. Phylogenetic analysis of Araucariaceae: integrating molecules, morphology, and fossils. *International Journal of Plant Sciences* 174 (8): 1153–1170. https://doi.org/10.1086/672369

Ferrer J., Wingert J.M. & Malabarba L.R. 2014. Description of a new species and phylogenetic analysis of the subtribe Cynopoecilina, including continuous characters without discretization (Cyprinodontiformes: Rivulidae). *Zoological Journal of the Linnean Society* 172: 846–866. https://doi.org/10.1111/zoj.12190

Fitch W.M. 1971. Toward defining course of evolution minimum change for a specific tree topology. *Systematic Zoology* 20: 406–416. https://doi.org/10.1093/sysbio/20.4.406

Fleming K., Johnston P., Zwartz D., Yokoyama Y., Lambeck K. & Chappell J. 1998. Refining the eustatic sea-level curve since the Last Glacial Maximum using farand intermediate-field sites. *Earth and Planetary Science Letters* 163: 327–342. https://doi.org/10.1016/S0012-821X(98)00198-8

Fontanetti C.S. 1990. Meiotic prophase in Diplopoda. *Revista Brasileira de Genética* 13 (4): 697–703.

Fontanetti C.S. 1996. Description of three cave diplopods of *Pseudonannolene* Silvestri (Diplopoda, Pseudonannolenida, Pseudonannolenidae). *Revista Brasileira de Zoologia* 13 (2): 427–433. https://doi.org/10.1590/S0101-81751996000200013

Fontanetti C.S. 2000. Description and chromosome number of a species of *Pseudonannolene* Silvestri (Arthropoda, Diplopoda, Pseudonannolenidae). *Revista Brasileira de Zoologia* 17 (1): 187–191. https://doi.org/10.1590/S0101-81752000000100014

Fontanetti C.S. 2002. Taxonomic importance of the prefemoral process of the first pair of legs in males of the genus *Pseudonannolene* (Diplopoda, Spirostreptida). *Folia Biologica (Cracow)* 50 (3–4): 199–202.

Fontanetti C.S., Udulutsch R.G. & Pietrobon T.A.O. 2003. A new species of cave milipede of genus *Pseudonannolene* (Diplopoda): description and karyotype. *Periódico de Biociências: secção Zoologia, Rio Grande do Sul* 11 (1): 65–68.

Freitas V.C., David J.A. & Fontanetti C.S. 2004. Caverna da Toca: comportamento e biologia do diplopodo *Pseudonannolene tocaiensis* Fontanetti, 1996 (Spirotreptida). *O Carste (Belo Horizonte)* 16 (2): 38–42.

Gallão J.E. & Bichuette M.E. 2018. Brazilian obligatory subterranean fauna and threats to the hypogean environment. *ZooKeys* 746: 1–23. https://doi.org/10.3897/zookeys.746.15140

Gallo J.S. & Bichuette M.E. 2017. Is there correlation between photophobia and troglomorphism in Neotropical cave millipedes (Spirostreptida, Pseudonannolenidae)? *Zoomorphology* 137 (2): 273–289. https://doi.org/10.1007/s00435-017-0389-0

Gallo J.S. & Bichuette M.E. 2019. O que mudou na distribuição dos diplópodes *Pseudonannolene* Silvestri, 1895 nas cavernas do Brasil 18 anos após a sinopse de Trajano e colaboradores (2000)?. *Espeleo-Tema* 29 (1): 41–55. https://doi.org/10.3897/aca.1.e30225

Gallo J.S. & Bichuette M.E. 2020. *Pseudonannolene canastra* sp. nov. (Diplopoda, Spirostreptida) – A new troglobitic millipede from the southwestern state of Minas Gerais, Brazil. *Subterranean Biology* 35: 33–47. https://doi.org/10.3897/subtbiol.35.51183

Gatesy J., Matthee C., Desalle R. & Hayashi C. 2002. Resolution of a supertree/supermatrix paradox. *Systematic Biology* 51: 652–664. https://doi.org/10.1080/10635150290102311

Giribet G. 2003. Stability in phylogenetic formulations and its relationship to nodal support. *Systematic Biology* 52 (4): 554–564. https://doi.org/10.1080/10635150390223730

Goloboff P.A. 1993. Estimating character weights during tree search. *Cladistics* 9: 83–91. https://doi.org/10.1111/j.1096-0031.1993.tb00209.x

Goloboff P.A. 2008. Calculating SPR distances between trees. *Cladistics* 24: 591–597. https://doi.org/10.1111/j.1096-0031.2007.00189.x

Goloboff P.A. & Catalano S.A. 2010. Phylogenetic morphometrics (II): algorithms for landmark optimization. *Cladistics* 26: 1–10. https://doi.org/10.1111/j.1096-0031.2010.00302.x

Goloboff P.A. & Catalano S.A. 2016. TNT version 1.5, including a full implementation of phylogenetic morphometrics. *Cladistics* 32: 221–237. https://doi.org/10.1111/cla.12160

Goloboff P.A. & Farris J.S. 2001. Methods for quick consensus estimation. *Cladistics* 17: 26–34. https://doi.org/10.1111/j.1096-0031.2001.tb00102.x

Goloboff P.A., Mattoni C.I. & Quinteros A.S. 2006. Continuous characters analyzed as such. *Cladistics* 22: 589–601. https://doi.org/10.1111/j.1096-0031.2006.00122.x

Goloboff P.A., Farris J. & Nixon K. 2008. TNT: a free program for phylogenetic analysis. *Cladistics* 24: 774–786. https://doi.org/10.1111/j.1096-0031.2007.00189.x

Goloboff P.A., Galvis A.T. & Arias J.S. 2018. Parsimony and model-based phylogenetic methods for morphological data: comments on O'Reilly et al. *Paleontology* 61: 625–630. https://doi.org/10.1111/pala.12353

Golovatch S.I., Hoffman R.L., Adis J., Marques A.D., Raizer J., Silva F.H.O., Ribeiro R.A.K., Silva J.L. & Pinheiro T.G. 2005. Millipedes (Diplopoda) of the Brazilian Pantanal. *Amazoniana* 18 (3/4): 273–288.

Goodman M., Olson C.B., Beeber J.E. & Czelusniak J. 1982. New perspectives in the molecular biological analysis of mammalian phylogeny. *Acta Zoologica Fennica* 169: 19–35.

Grant T. & Kluge A.G. 2008a. Clade support measures and their adequacy. *Cladistics* 24: 1051–1064. https://doi.org/10.1111/j.1096-0031.2008.00231.x

Grant T. & Kluge A.G. 2008b. Credit where credit is due: the Goodman-Bremer support metric. *Molecular Phylogenetics and Evolution* 49: 405–406. https://doi.org/10.1016/j.ympev.2008.04.023

Hijmans R.J., Cruz M., Rojas E. & Guarino L. 2001. *DIVA–GIS, Version 1.4. A Geographic Information System for the Management and Analysis of Genetic Resources Data*. Manual. International Potato Center, Lima, Peru.

Hinchliff C.E. & Roalson E.H. 2013. Using supermatrices for phylogenetic inquiry: an example using the sedges. *Systematic Biology* 62: 205–219. https://doi.org/10.1093/sysbio/sys088

Hoffman R.L. 1965. A second species in the diplopod genus *Choctella* (Spirostreptidfa: Choctellidae). *Proceedings of the Biological Society of Washington* 78: 55–58. Available from https://www.biodiversitylibrary.org/page/34562389 [accessed 21 Feb. 2023].

Hoffman R.L. 1980. *Classification of the Diplopoda*. Múseum d'histoire naturelle, Genève.

Hoffman R.L. 1981. Chelodesmid studies. XVII. Synopsis of the tribe Platinodesmini, with the proposal of two new genera. *Acta Zoologica Lilloana* 36 (2): 85–95.

Hoffman R.L. 1982. Chelodesmid studies. XVIII. A synopsis of the genus *Sandalodesmus* Silvestri, 1902, and proposal of the new tribe Sandalodesmini. *Spixiana* 5 (3): 247–259.

Hoffman R.L. 1984. A new species of *Epinannolene* from the Amazon Basin, Brazil (Spirostreptida: Pseudonannolenidae). *Myriapodologica* 1 (13): 91–94.

Hoffman R.L. 1990. Myriapoda IV. Polydesmida: Oxydesmidae. *Das Tierreich* 107: 1–115. https://doi.org/10.1515/9783110744989

Hoffman R.L. 1999. Checklist of the Millipedes of North and Middle America. *Virginia Museum of Natural History Special Publication* 8: 1–584

Hoffman R.L. & Florez E. 1995. The milliped genus *Phallorthus* revalidated: another facet of a taxonomic enigma (Spirostreptida: Pseudonannolenidae). *Myriapodologica* 3 (13): 115–126.

Hoffman R.L., Golovatch, S.I., Adis J. & de Morais J.W. 1996. Practical keys to the orders and families of millipedes of the Neotropical region (Myriapoda: Diplopoda). *Amazoniana* 14 (1–2): 1–35.

Hoffman R.L., Golovatch S.I., Adis J. & de Morais J.W. 2002. Diplopoda. *In*: Adis J. (ed.) *Amazonian Arachnida and Myriapoda*: 505–533. Pensoft Publishers, Sofia-Moscow.

Hollier J., Schiller E. & Akkari N. 2017. An annotated list of the Diplopoda described by Aloïs Humbert alone and with Henri de Saussure, and the Diplopoda from Saussure's Mexico expedition. *Revue suisse de Zoologie* 124 (2): 203–224. https://doi.org/10.5281/zenodo.893503

Hovenkamp P. 1997. Vicariance events, not areas, should be used in biogeographical analysis. *Cladistics* 13: 67–79. https://doi.org/10.1111/j.1096-0031.1997.tb00241.x

Hovenkamp P. 2001. A direct method for the analysis of vicariance patterns. *Cladistics* 17: 260–265. https://doi.org/10.1006/clad.2001.0176

Humphries C.J. 2004. Homology, characters and continuous variables. *In*: MacLeod N. & Forey P.L. (eds) *Morphology, Shape and Phylogeny*: 8–26. Taylor & Francis e-Library. https://doi.org/10.1201/9780203165171.ch2

Iniesta L.F.M & Ferreira R.L. 2013a. The first troglobitic *Pseudonannolene* from Brazilian iron ore caves (Spirostreptida: Pseudonannolenidae). *Zootaxa* 3669 (1): 85–95. https://doi.org/10.11646/zootaxa.3669.1.9

Iniesta L.F.M & Ferreira R.L. 2013b. Two new species of *Pseudonannolene* Silvestri, 1895 from Brazilian limestone caves (Spirostreptida: Pseudonannolenidae): synotopy of a troglophilic and a troglobiotic species. *Zootaxa* 3702 (4): 357–369. https://doi.org/10.11646/zootaxa.3702.4.3

Iniesta L.F.M & Ferreira R.L. 2013c. Two new species of *Pseudonannolene* Silvestri, 1895 from Brazilian iron ore caves (Spirostreptida: Pseudonannolenidae). *Zootaxa* 3716 (1): 75–80. https://doi.org/10.11646/zootaxa.3716.1.6

Iniesta L.F.M & Ferreira R.L. 2014. New species of *Pseudonannolene* Silvestri, 1895 from Brazilian limestone caves with comments on the potential distribution of the genus in South America (Spirostreptida: Pseudonannolenidae). *Zootaxa* 3846 (3): 361–397. https://doi.org/10.11646/zootaxa.3846.3.3

Iniesta L.F.M & Ferreira R.L. 2015. *Pseudonannolene lundi* n. sp., a new troglobitic millipede from a Brazilian limestone cave (Spirostreptida: Pseudonannolenidae). *Zootaxa* 3949 (1): 123–128. https://doi.org/10.11646/zootaxa.3949.1.6

Iniesta L.F.M., Bouzan R.S. & Brescovit A.D. 2019. On the millipede genus *Heteropyge*: description of the adults of *H. araguayensis* and revalidation of *H. bidens* (Diplopoda: Spirostreptida: Spirostreptidae). *Iheringia, Série Zoologia* 109: 1–13. https://doi.org/10.1590/1678-4766e2019032

Iniesta L.F.M., Enghoff H., Brescovit A.D. & Bouzan R.S. 2020. Phylogenetic placement of the monotypic genus *Holopodostreptus* Carl, 1913 and notes on the systematics of Pseudonannolenidae (Spirostreptida: Cambalidea). *Invertebrate Systematics* 34: 661–677. https://doi.org/10.1071/IS20012

Jeekel C.A.W. 1963. Diplopoda of Guiana (1–5). *In*: Gijskes D.C.& Hummelinck P.W. (eds) *Studies on the Fauna of Suriname and Other Guyanas* No. 11: 1–157. Martinus Nijhoff, The Hague.

Jeekel C.A.W. 1965. A revision of the South American Paradoxosomatidae in the Museo Civico di Storia Naturale di Genova (Diplopoda, Polydesmida). *Annali del Museo civico di storia naturale Giacomo Doria* 75: 99–125. Available from https://www.biodiversitylibrary.org/page/35589326 [accessed 21 Feb. 2023].

Jeekel C.A.W. 1970 [1971]. Nomenclator generum et familiarum Diplopodorum: a list of the genus and family-group names in the Class Diplopoda from the 10th edition of Linnaeus, 1758, to the end of 1957. *Monografieën van de Nederlandse Entomologische Vereniging* 5 (1–12): 1–412.

Jeekel C.A.W. 1985. The distribution of the Diplochaeta and the "lost" continente Pacifica (Diplopoda). *Bijdragen tot de Dierkunde* 55 (1): 100–112.

Jeekel C.A.W. 2004. A bibliographic catalogue of the "Cambaloidea" (Diplopoda, Spirostreptida). *Myriapod Memoranda* 7: 43–109.

Junta V.G.P., Castro-Souza R.A. & Ferreira R.L. 2020. Five new species of *Phalangopsis* Serville, 1831 (Orthoptera: Phalangopsidae) from Brazilian caves in the Amazon Forest. *Zootaxa* 4859 (2): 151–194. https://doi.org/10.11646/zootaxa.4859.2.1

Karam-Gemael M., Izzo T.J. & Chagas-Jr A. 2018. Why be red listed? Threatened Myriapoda species in Brazil with implications for their conservation. *ZooKeys* 741: 255–269. https://doi.org/10.3897/zookeys.741.21971

Karanovic T., Lee S. & Lee W. 2018. Instant taxonomy: choosing adequate characters for species delimitation and description through congruence between molecular data and quantitative shape analysis. *Invertebrate Systematics* 32: 551–580. https://doi.org/10.1071/IS17002

Kitching I.J., Forey P.L., Humphries C.J. & Williams D.M. 1998. *Cladistics. Second Edition. The theory and Practice of Parsimony Analysis*. The Systematics Association Publication no. 11. Oxford University Press, Inc., New York.

Koch M. 2015. General morphology. *In*: Minelli A. (ed.) *Treatise on Zoology – Anatomy, Taxonomy, Biology. The Myriapoda Vol. 2*: 7–67. Leiden and Boston, Brill.

Koch N.M., Soto I.M. & Ramírez M.J. 2014. First phylogenetic analysis of the family Neriidae (Diptera), with a study on the issue of scaling continuous characters. *Cladistics* 3: 142–165. https://doi.org/10.1071/IS17002

Koch N.M., Soto I.M & Ramírez M.J. 2015. Overcoming problems with the use of ratios as continuous characters for phylogenetic analyses. *Zoologica Scripta* 44 (5): 463–474. https://doi.org/10.1111/zsc.12120

Korsós Z. & Johns P.M. 2009. Introduction to the taxonomy of Iulomorphidae of New Zealand, with descriptions of two new species of *Eumastigonus* Chamberlin, 1920 (Diplopoda: Spirostreptida: Epinannolenidea). *Zootaxa* 2065: 1–24. https://doi.org/10.11646/zootaxa.2065.1.1

Korsós Z. & Read H.J. 2012. Redescription of *Zinagon chilensis* (Silvestri, 1903) from Chile, with a species list of Iulomorphidae from the Southern Hemisphere (Diplopoda: Spirostreptida: Epinannolenidea). *Zootaxa* 3493: 39–48. https://doi.org/10.11646/zootaxa.3493.1.4

Krabbe E. 1982. Systematik der Spirostreptidae (Diplopoda, Spirostreptomorpha). *Abhandlungen und Verhandlungen des Naturwissenschaftlichen Vereins in Hamburg* 24: 1–476.

Liu W. & Wynne J.J. 2019. Cave millipede diversity with the description of six new species from Guangxi, China. *Subterranean Biology* 30: 57–94. https://doi.org/10.3897/subtbiol.30.35559

Liu W., Golovatch S.I., Wesener T. & Tian M. 2017. Convergent evolution of unique morphological adaptations to a subterranean environment in cave millipedes (Diplopoda). *PLoS ONE* 12 (2): e0170717. https://doi.org/10.1371/journal.pone.0170717

Loomis H.F. 1941. New genera and species of Millipeds from the Southern peninsula of Haiti. *Journal of the Washington Academy of Sciences* 31: 188–195.

Loomis H.F. 1962. Two unusual Central American spirostreptid millipede species. *Proceedings of the Biological Society of Washington* 75: 47–52.

Lordello L.G.E. 1954. Observação sobre alguns Diplópodos de interesse agrícola. *Anais da Escola Superior de Agricultura "Luiz de Queiroz"* 11: 69–76. https://doi.org/10.1590/S0071-12761954000100004

Löwenberg-Neto P. 2014. Neotropical region: a shapefile of Morrone's (2014) biogeographical regionalisation. *Zootaxa* 3802 (2): 300. https://doi.org/10.11646/zootaxa.3802.2.12

Maddison W.P. 1993. Missing data versus missing sharacters in phylogenetic analysis. *Systematic Biology* 42 (4): 576–581. https://doi.org/10.1093/sysbio/42.4.576

Magalhães I.L.F & Ramírez M.J. 2017. Relationships and phylogenetic revision of *Filistatinella* spiders (Araneae: Filistatidae). *Cladistics* 3: 142–165. https://doi.org/10.1071/IS16083

Marques A.C. & Gnaspini P. 2001. The problem of characters susceptible to parallel evolution in phylogenetic reconstructions: suggestion of a practical method and its application to cave animals. *Cladistics* 17: 371–381. https://doi.org/10.1111/j.1096-0031.2001.tb00131.x

Martin L., Morner N.A., Flexor J.M. & Suguio K. 1986. Fundamentos e reconstrução de antigos níveis marinhos do Quaternário. *Boletim do Instituto de Geociências, Publicacão Especial* 4: 1–161. https://doi.org/10.11606/issn.2317-8078.v0i4p01-161

Mauriès J-P. 1974. Un cambalide cavernicole du Brésil, *Pseudonannolene strinatii* n. sp. (Myriapoda–Diplopoda). *Revue suisse de Zoologie* 81 (2): 545–550. https://doi.org/10.5962/bhl.part.146025

Mauriès J-P. 1977. Le genre *Glyphiulus* Gervais, 1847, et sa place dans la classification des Cambalides, à propos de la description d'une nouvelle espèce du Viêt-Nam (Diplopoda, lulida, Cambalidea). *Bulletin du Muséum national d'histoire naturelle* (3) 431: 243–250.

Mauriès J-P. 1980. Diplopdes Chilognathes de la Guadeloupe et ses dépendances. *Bulletin du Muséum national d'histoire naturelle, 4e série, Section A, Zoologie* 2: 1059–1111.

Mauriès J-P. 1983. Cambalides nouveaux ou peu connus d'Asie, d'Amérique et d'Oceanie. I. Cambalidae et Cambalopsidae (Myriapoda, Diplopoda). *Bulletin du Muséum national d'histoire naturelle, 4e série, Section A, Zoologie* 5 (A, 1): 247–276.

Mauriès J-P. 1987. Cambalides nouveaux et peu connus d'Asie, d'Amérique et d'Océanie. II. Pseudonannolenidae, Choctellidae (Myriapoda, Diplopoda). *Bulletin du Muséum national d'histoire naturelle, 4e série, Section A, Zoologie* 9 (1): 169–199.

Mauriès J-P. & Enghoff, H. 1990. A new genus of cambaloid millipedes from Vietnam (Diplopoda: Spirostreptida: Cambalopsidae). *Entomologica Scandinavica* 21: 91–96. https://doi.org/10.1163/187631290X00076

Mauriès J-P. & Geoffroy J.-J. 2000. Nouvelle description, classification, répartition et variations morphologiques interpopulations d'un diplopode troglobie du sud-est du Brésil (Diplopoda, Polydesmida, Chelodesmidae). *Zoosystema* 22 (1): 153–168.

Mesibov R. 2017a. Iulomorphid millipedes (Diplopoda, Spirostreptida, Iulomorphidae) of Tasmania, Australia. *ZooKeys* 652: 1–36. https://doi.org/10.3897/zookeys.652.12035

Mesibov R. 2017b. A new and unusual species of *Amastigogonus* Brölemann, 1913 from Tasmania, Australia (Diplopoda, Spirostreptida, Iulomorphidae). *ZooKeys* 687: 45–51. https://doi.org/10.3897/zookeys.687.14872

Mesibov R. 2019. Cambaloid millipedes of Tasmania, Australia, with remarks on family-level classification and descriptions of two new genera and four new species (Diplopoda, Spirostreptida). *ZooKeys* 827: 1–17. https://doi.org/10.3897/zookeys.827.32969

Miyoshi A.R., Gabriel V.A., Fantazzini E.R. & Fontanetti C.S. 2005. Microspines in the pylorus of *Pseudonannolene tricolor* and *Rhinocricus padbergi* (Arthropoda, Diplopoda). *Iheringia, Série Zoologia* 95 (2): 183–187. https://doi.org/10.1590/S0073-47212005000200008

Morrone J.J. 2014. Biogeographical regionalisation of the Neotropical region. *Zootaxa* 3782 (1): 1–110. https://doi.org/10.11646/zootaxa.3782.1.1

Mwabvu T., Hamer M.L. & Slotow R.H. 2007. A taxonomic review of the southern African millipede genus, *Bicoxidens* Attems, 1928 (Diplopoda: Spirostreptida: Spirostreptidae), with the description of three new species and a tentative phylogeny. *Zootaxa* 1452: 1–23. https://doi.org/10.11646/zootaxa.1452.1.1

Mwabvu T., Hamer M.L., Slotow R.H. & Barraclough D. 2010. A revision of the taxonomy and distribution of *Archispirostreptus* Silvestri 1895 (Diplopoda, Spirostreptida, Spirostreptidae), and description of a new spirostreptid genus with three new species. *Zootaxa* 2567: 1–49. https://doi.org/10.11646/zootaxa.2567.1.1

Nasserzadeh, H., Alipanah H. & Gilasian E. 2017. Phylogenetic study of the genus *Sternolophus* Solier (Coleoptera, Hydrophilidae) based on adult morphology. *ZooKeys* 712: 69–85. https://doi.org/10.3897/zookeys.712.14085

Nixon K.C. 1999–2004. Winclada (BETA) ver. ASADO 1.89. Published by the author, Ithaca, New York, NY.

Oliveira R.R.M., Vasconcelos S., Pires E.S., Pietrobon T., Prous X. & Oliveira G. 2019. Complete mitochondrial genomes of three troglophile cave spiders (*Mesabolivar*, Pholcidae). *Mitochondrial DNA Part B: Resources* 4 (1): 251–252. https://doi.org/10.1080/23802359.2018.1547139

Parizotto D.R., Pires A.C., Mise K.M., Ferreira R.L. & Sessegolo G.C. 2017. Troglobitic invertebrates: Improving the knowledge on the Brazilian subterranean biodiversity through an interactive multi-entry key. *Zootaxa* 4365 (4): 401–409. https://doi.org/10.11646/zootaxa.4365.4.1

Pellegrini T.G., Ferreira R.L., Zampaulo R.A. & Vieira L. 2020. *Coarazuphium lundi* (Carabidae: Zuphiini), a new Brazilian troglobitic beetle, with the designation of a neotype for *C. pains* Álvares & Ferreira, 2002. *Zootaxa* 4878 (2): 287–304. https://doi.org/10.11646/zootaxa.4878.2.4

Pena-Barbosa J.P.P., Sierwald P. & Brescovit A.D. 2013. On the largest chelodesmid millipedes: taxonomic review and cladistic analysis of the genus *Odontopeltis* Pocock, 1894 (Diplopoda; Polydesmida; Chelodesmidae). *Zoological Journal of the Linnean Society* 169 (4): 737–764. https://doi.org/10.1111/zoj.12086

Penteado C.H.S. & Hebling-Beraldo M.J.A. 1991. Respiratore response is a Brazilian millipede, *Pseudonannolene tricolor*, to declining oxygen pressures. *Physiological Zoology* 64 (1): 232–241. https://doi.org/10.1086/physzool.64.1.30158521

Pimvichai P., Enghoff H. & Panha S. 2009a. A revision of the *Thyropygus allevatus* group. Part 1: the *T. opinatus* subgroup (Diplopoda: Spirostreptida: Harpagophoridae). *Zootaxa* 2016: 17–50. https://doi.org/10.11646/zootaxa.2016.1.2

Pimvichai P., Enghoff H. & Panha S. 2009b. A revision of the *Thyropygus allevatus* group. Part 2: the *T. bifurcus* subgroup (Diplopoda: Spirostreptida: Harpagophoridae). *Zootaxa* 2165: 1–15. https://doi.org/10.11646/zootaxa.2165.1.1

Pimvichai P., Enghoff H. & Panha S. 2010. The Rhynchoproctinae, a south-east Asiatic subfamily of giant millipedes: cladistic analysis, classification, four new genera and a deviating new species from north-west Thailand (Diplopoda: Spirostreptida: Harpagophoridae). *Invertebrate Systematics* 24: 51–80. https://doi.org/10.1071/IS09052

Pimvichai P., Enghoff H. & Panha S. 2011a. A revision of the *Thyropygus allevatus* group. Part 3: the *T. induratus* subgroup (Diplopoda: Spirostreptida: Harpagophoridae). *Zootaxa* 2941: 47–68. https://doi.org/10.11646/zootaxa.2941.1.3

Pimvichai P., Enghoff H. & Panha S. 2011b. A revision of the *Thyropygus allevatus* group. Part 4: the *T. cuisinieri* subgroup (Diplopoda: Spirostreptida: Harpagophoridae). *Zootaxa* 2980: 37–48. https://doi.org/10.11646/zootaxa.2980.1.3

Pinto-da-Rocha R. 1995. Sinopse da fauna cavernícola do Brasil (1907–1994). *Papéis Avulsos de Zoologia* 39 (6): 61–172.

Pinto-da-Rocha R., Dasilva M.B. & Bragagnolo C. 2005. Faunistic similarity and historical biogeography of the harvestmen of southern and southeastern Atlantic Rain Forest of Brazil. *Journal of Arachnology* 33: 290–299. https://doi.org/10.1636/04-114.1

Porat C.O. Von. 1888. Über einige exotische Iuliden des Brüsseler-Museums. *Annales de la Société entomologique de Belgique* 32: 205–256.

R Core Team. 2017. *R: A Language and Environment for Statistical Computing*. R Foundation for Statistical Computing, Vienna, Austria. Available from http://www.Rproject.org/.270 [accessed 21 Feb. 2023].

Rae T.C. 2004. Scaling, polymorphism and cladistic analysis. *In*: MacLeod N. & Forey P.L. (eds) *Morphology, Shape and Phylogeny*: 45–52. Taylor & Francis e-Library. https://doi.org/10.1201/9780203165171.ch4

Reboleira A.S.P.S., Malek-Hosseini M.J., Sadeghi S. & Enghoff E. 2015. Highly disjunct and highly infected millipedes – A new cave-dwelling species of *Chiraziulus* (Diplopoda: Spirostreptida: Cambalidae) from Iran and notes on Laboulbeniales ectoparasites. *European Journal of Taxonomy* 146: 1–18. https://doi.org/10.5852/ejt.2015.146

Rieppel, O. & Kearney, M. 2002. Similarity. *Biological Journal of the Linnean Society* 75 (1): 59–82. https://doi.org/10.1046/j.1095-8312.2002.00006.x

Rodrigues B.V.B., Cizauskas I. & Rheims C.A. 2018. Description of *Paracymbiomma* gen. nov., a new genus of prodidomid spiders from the Neotropical region (Araneae: Prodidomidae) including a new troglobite species. *Zootaxa* 4514 (3): 301–331. https://doi.org/10.11646/zootaxa.4514.3.1

Rodrigues D.J., Izzo T.J. & Battirola L.D. 2011. *Descobrindo a Amazônia Meridional: biodiversidade da Fazenda São Nicolau*. Pau e Prosa Comunicação Ltda., Cuiabá-MT.

Rodrigues D.J., Vaz-De-Mello F.Z. & Silveira R.M. 2019. Biodiversity studies through public-private partnership (PPP): the case of Fazenda São Nicolau in the northwest of Mato Grosso. *Anais da Academia Brasileira de Ciências* 91: 1–4. https://doi.org/10.1590/0001-3765201920190097

Rodrigues P.E.S., Campos L.A., Ott R. & Rodrigues E.N.L. 2019. Phylogeny of three species groups of *Rhinocricus* Karsch, 1881 based on morphological characters (Diplopoda, Spirobolida, Rhinocricidae). *Organisms Diversity & Evolution* 20: 1–13. https://doi.org/10.1007/s13127-019-00421-3

Schubart O. 1942. Os Myriápodes e suas relações com a agricultura – Com uma bibliografia completa sôbre o assunto. *Papéis avulsos do Departamento de Zoologia* 2 (16): 205–234.

Schubart O. 1944. Os Diplopodos de Pirassununga. *Acta Zoologica Lilloana* 2: 321–440.

Schubart O. 1945a. Diplópodos de Monte Alegre. *Papéis avulsos do Departamento de Zoologia* 6 (23): 283–320.

Schubart O. 1945b. Sobre os representantes Brasileiros da familia Spirostreptidae. *Anais da Academia Brasileira de Ciências* 17: 51–87.

Schubart O. 1947. Os diplopodos da viagem do naturalista Antenor Leitao de Carvalho aos rios Araguaia e Amazonas em 1939 e 1940. *Boletim do Museu Nacional do Rio de Janeiro / Zoologia* 82: 1–74.

Schubart O. 1949. Os diplopoda de algumas ilhas do litoral paulista. *Memórias do Instituto Butantan* 21: 203–254.

Schubart O. 1952. Diplopoda de Pirassununga IV. Adenda à fauna regional. *Dusenia* 3 (6): 403–420.

Schubart O. 1958. Sôbre alguns Diplopoda de Mato Grosso e Goiás, Brasil e a família Spirostreptidae. *Arquivos do Museu Nacional* 46: 203–252.

Schubart O. 1960. Novas especies brasileiras das familias Spirostreptidae e Pseudonannolenidae (Diplopoda, Opistospermophora). *Actas da Sociedade de Biologia do Rio de Janeiro* 4 (6): 74–79.

Sereno P.C. 2007. Logical basis for morphological characters in phylogenetics. *Cladistics* 23: 565–587. https://doi.org/10.1111/j.1096-0031.2007.00161.x

Shear W.A. 1969. A synopsis of the cave millipeds of the United States, with an illustrated key to genera. *Psyche* 76 (2): 126–143. https://doi.org/10.1155/1969/70437

Shear W.A. 1973a. *Jarmilka alba*, n. gen., n. sp. (Diplopoda: Spirostreptida: Cambalidae), a new millipede from a cave in Belize. *Association for Mexican Cave Studies Bulletin* 5: 43–45.

Shear W.A. 1973b. Millipeds (Diplopoda) from Mexican and Guatemalan caves. *Accademia, Nazionale dei Lincei, Problemi Attuali di Scienza e di Cultura* 171 (2): 239–305.

Shelley R.M. 2002. A revised, annotated, family-level classification of the Diplopoda. *Arthropoda Selecta* 11 (3): 187–207.

Shelley R.M. & Golovatch S.I. 2015. Nomenclator generum et familiarum diplopodorum III. A lista of the genus-, family-, and ordinal-group names proposed in the Class Diplopoda from 1 January 2000–31 December 2014. *Arthropoda Selecta* 24 (1): 1–27. https://doi.org/10.15298/arthsel.24.1.01

Sierwald P. & Reft A.J. 2004. The millipede collections of the world. *Fieldiana, N.S.*103 (1532): 1–100.

Silva J.M.C., Sousa M.C. & Castelletti C.H.M. 2004. Areas of endemism for passerine birds in the Atlantic forest, South America. *Global Ecology and Biogeography* 13: 85–92. https://doi.org/10.1111/j.1466-882X.2004.00077.x

Silvestri F. 1895a. Chilopodi e diplopodi raccolti dal capitano G. Bove e dal Prof. L. Balzan nell'America meridionale. *Annali del Museo civico di storia naturale di Genova, serie 2* (14): 764–783. Available from http://biodiversitylibrary.org/page/7940804 [accessed 13 Feb. 2023].

Silvestri F. 1895b. Viaggio del dottor Alfredo Borelli nella Repubblica Argentina e nel Paraguay. XIV. Chilopodi e Diplopodi. *Bollettino del musei di zoologia e di anatomia comparata della Reale Università di Torino* 10 (203): 1–12. https://doi.org/10.5962/bhl.part.8048

Silvestri F. 1896. I Diplopodi. Parte I. – Sistematica. *Annali del Museo civico di storia naturale di Genova, serie 2* (16): 121–254. Available from https://biodiversitylibrary.org/page/7697911 [accessed 13 Feb. 2023].

Silvestri F. 1897a. Systema Diplopodum. *Annali del Museo civico di storia naturale di Genova, serie 2* (18): 644–651. Available from https://biodiversitylibrary.org/page/7785907 [accessed 13 Feb. 2023].

Silvestri F. 1897b. Viaggio del Dott. Alfredo Borelli nel Chaco boliviano e nella Repubblica Argentina. IV. Chilopodi e Diplopod. *Bollettino del musei di zoologia e di anatomia comparata della Reale Università di Torino* 12 (283): 1–11. https://doi.org/10.5962/bhl.part.4564

Silvestri F. 1897c. Neue Diplopoden. *Abhandlungen und Berichte des Königlichen Zoologischen und Anthropologisch-Ethnographischen Museums zu Dresden* 6 (9): 1–23.

Silvestri F. 1897d. Description des especes nouvelles de Myriapodes du Musee royal d'Histoire naturelle de Bruxelles. *Annales de la Société entomologique de Belgique* 41: 345–362.

Silvestri F. 1902. Viaggio del Dr. A. Borelli nel Matto Grosso. VII. Diplopodi. *Bollettino del musei di zoologia e di anatomia comparata della Reale Università di Torino* 17 (432): 1–25. https://doi.org/10.5962/bhl.part.26628

Silvestri F. 1903. Classis Diplopoda, Vol. I – Anatome, Pars la – Segmenta, Tegumentum, Musculi. *In*: Berlese A. (ed.) *Acari Myriopoda et Scorpiones hucusque in Italia reperta* 346: 1–272.

Sket B. 2008. Can we agree on an ecological classification of subterranean animals? *Journal of Natural History* 42: 1549–1563. https:// doi.org/10.1080/00222930801995762

Somer K.M. 1986. Multivariate allometry and removal of size with principal components analysis. *Systematic Biology* 35 (3): 359–368. https://doi.org/10.1093/sysbio/35.3.359

Souza T.S., Prado R.A. & Fontanetti C.S. 2012. High content of constitutive heterochromatin in two species of *Pseudonannolene* (Diplopoda). *Caryologia* 58 (1): 47–51. https://doi.org/10.1080/00087114.2005.10589431

Strong E.E. & Lipscomb D. 1999. Character coding and inapplicable data. *Cladistics* 15: 363–371. https://doi.org/10.1111/j.1096-0031.1999.tb00272.x

Su Y.N. 2016. A simple and quick method of displaying liquid-preserved morphological structures for microphotography. *Zootaxa* 4208 (6): 592–593. https://doi.org/10.11646/zootaxa.4208.6.6

Thiele K. 1993. The Holy Grail of the perfect character: the cladistic treatment of morphometric data. *Cladistics* 9: 275–304. https://doi.org/10.1111/j.1096-0031.1993.tb00226.x

Trajano E. 1987. Fauna cavernícola brasileira: composição e caracterização preliminar. *Revista Brasileira de Zoologia* 3 (8): 533–561. https://doi.org/10.1590/S0101-81751986000400004

Trajano E. & Gnaspini-Netto P. 1991. Composição da fauna cavernícola brasileira, com uma análise preliminar da distribuição dos táxons. *Revista Brasileira de Zoologia* 7 (3): 383–407. https://doi.org/10.1590/S0101-81751990000300017

Trajano E., Golovatch S.I., Geoffroy J.-J. Pinto-da-Rocha R. & Fontanetti C.S. 2000. Synopsis of brazilian cave-dwelling millipedes (Diplopoda). *Papéis Avulsos de Zoologia* 41 (18): 259–287.

Verhoeff K.W. 1894. Beiträge zur Anatomie und Systematik der Juliden. *Verhandlungen der Zoologisch-botanischen Gesellschaft in Wien* 44: 137–162.

Verhoeff K.W. 1943. Ueber einige Diplopoden aus Minas Gerais (Brasilien). *Arquivos do Museu Nacional* 37: 249–288.

Viggiani V. 1973. Le specie descritte da Filippo Silvestri (1873–1949). *Bollettino del Laboratorio di entomologia agraria "Filippo Silvestri"* 30: 351–417.

Wesener T. & VandenSpiegel D. 2009. A first phylogenetic analysis of giant pill-millipedes (Diplopoda: Sphaerotheriida), a new model Gondwanan taxon, with special emphasis on island gigantism. *Cladistics* 25: 545–573. https://doi.org/10.1111/j.1096-0031.2009.00267.x

Wesener T., Enghoff H. & Wägele J.W. 2008. Pachybolini – A tribe of giant Afrotropical millipedes: arguments for monophyly and the description of a new genus from Madagascar (Diplopoda: Spirobolida: Pachybolidae). *Invertebrate Systematics* 22 (1): 37–53. https://doi.org/10.1071/IS07008

Yamaguti H.Y. & Pinto-da-Rocha R. 2009. Taxonomic review of Bourguyiinae, cladistic analysis, and a new hypothesis of biogeographic relationships of the Brazilian Atlantic Rainforest (Arachnida: Opiliones, Gonyleptidae). *Zoological Journal of the Linnean Society* 166: 319–362. https://doi.org/10.1111/j.1096-3642.2008.00484.x

Manuscript received: 18 February 2022
Manuscript accepted: 25 November 2022
Published on: 27 April 2023
Topic editor: Tony Robillard
Section editor: Nesrine Akkari
Desk editor: Pepe Fernández

Printed versions of all papers are also deposited in the libraries of the institutes that are members of the *EJT* consortium: Muséum national d'histoire naturelle, Paris, France; Meise Botanic Garden, Belgium; Royal Museum for Central Africa, Tervuren, Belgium; Royal Belgian Institute of Natural Sciences, Brussels, Belgium; Natural History Museum of Denmark, Copenhagen, Denmark; Naturalis Biodiversity Center, Leiden, the Netherlands; Museo Nacional de Ciencias Naturales-CSIC, Madrid, Spain; Leibniz Institute for the Analysis of Biodiversity Change, Bonn – Hamburg, Germany; National Museum of the Czech Republic, Prague, Czech Republic.

Supplementary files

Supp. file 1. Character descriptions. https://doi.org/10.5852/ejt.2023.867.2109.8869

Supp. file 2. List of terminal taxa scored for the cladistic analysis.
https://doi.org/10.5852/ejt.2023.867.2109.8871

Supp. file 3. Data matrix of continuous characters. https://doi.org/10.5852/ejt.2023.867.2109.8873

Supp. file 4. Figures for the cladistic analysis (Figs 192–223).
https://doi.org/10.5852/ejt.2023.867.2109.8875

Fig. 192. Continuous characters coded for the cladistic analysis of *Pseudonannolene* Silvestri, 1895. **A**. Antenna of *P. strinatii* Mauriès, 1974 (ISLA 20622). **B**. Midbody leg of *P. strinatii* (ISLA 20622). **C**. Gnathochilarium of *P. erikae* Iniesta & Ferreira, 2014 (IBSP 3331). Abbreviations:

ant^3 = antennomere 3; fm = femur; GnW = gnathochilarium width; GnL = gnathochilarium length. Scale bars = 0.5 mm.

Fig. 193. Violin and Box plots of measured values for the continuous characters (chars. 1–3) in the cladistic analysis of *Pseudonannolene* Silvestri, 1895. The raw data were transformed into log10 for better visualization. Horizontal lines and the points out of plots refer to the median and outliers, respectively.

Fig. 194. Characters 4–6 and their character states. Head in frontal view. **A**. *P. robsoni* Iniesta & Ferreira, 2014 (IBSP 3526). **B**. *P. occidentalis* Schubart, 1958 (IBSP 1998). **C**. *Holopodostreptus braueri* Carl, 1918 (MNRJ). **D**. *P. microzoporus* Mauriès, 1987 (IBSP 5735). Labral setae highlighted in yellow and supralabral setae in red. Roman numerals refer to the supralabral setae. Scale bars: A–B, D = 0.5 mm; C = 0.2 mm.

Fig. 195. Characters 7–8 and their character states. Anterior region. **A**. Antenna of *Epinannolene exilio* (Brölemann, 1904) (INPA), baciliform setae on antennomere V in detail. **B**. Antenna of *P. robsoni* Iniesta & Ferreira, 2014 (IBSP 3526), baciliform setae on antennomere V in detail. **C**. Head of *P. halophila* Schubart, 1949 (IBSP 1101), in lateral view. **D**. Head of *P. spelaea* Iniesta & Ferreira, 2013 (IBSP 5923), in lateral view. Ommatidial cluster in detail. Scale bars: A = 0.15 mm; B = 0.25 mm; C = 1 mm; D = 0.5 mm.

Fig. 196. Characters 9–10, 15–16 and their character states. Gnathochilarium, ventral view. **A**. *Holopodostreptus braueri* Carl, 1918 (MNRJ). **B**. *Choctella cumminsi* Chamberlin, 1918 (MCZ). **C**. *Epinannolene* sp. (ICN). **D**. *Pseudonannolene robsoni* Iniesta & Ferreira, 2014 (IBSP 3325). SEM image of promentum of *P. robsoni* (IBSP 3506), in detail. Scale bars: A, C = 0.2 mm; B, D = 0.5 mm.

Fig. 197. Characters 11–14 and their character states. Gnathochilarium, ventral view. **A**. *P. erikae* Iniesta & Ferreira, 2014 (IBSP 3331). **B**. *Holopodostreptus braueri* Carl, 1918 (MNRJ). **C**. *Epinannolene* sp. (ICN). **D**. *Pseudonannolene robsoni* Iniesta & Ferreira, 2014 (IBSP 3325). **E**. *P. bucculenta* sp. nov. (IBSP 3402), paired projections highlighted in purple. **F**. *P. morettii* sp. nov. (IBSP 2459), long setae scattered on the stipes and mentum highlighted in yellow. Scale bars: A–D = 0.2 mm; E–F = 0.5 mm.

Fig. 198. Characters 17–18 and their character states. Gnathochilarium, ventral view. **A**. *Amastigogonus fossuliger* (Verhoeff, 1944) (NHMD). **B**. *Pseudonannolene granulata* sp. nov. (MNRJ), proximal projections bearing setae on the stipes. Scale bars = 0.5 mm.

Fig. 199. Character 19 and its character states. Gnathochilarium, ventral view. **A**. *Pseudonannolene robsoni* Iniesta & Ferreira, 2014 (IBSP 3440). **B**. *P. paulista* Brölemann, 1902 (IBSP 3402). **C**. *P. morettii* sp. nov. (IBSP 2459). **D**. *P. occidentalis* Schubart, 1958 (IBSP 1998). Scale bars: A–B, D = 0.5 mm; C = 0.2 mm.

Fig. 200. Characters 20–22 and their character states. **A**. Anterior region of *Epinannolene* sp. (ICN). **B**. Anterior region of *Pseudonannolene robsoni* Iniesta & Ferreira, 2014 (IBSP 3441), collum of *P. robsoni* (IBSP 3506), in detail. **C**. Midbody ring of *P. robsoni* (IBSP 3506). **D**. Midbody ring of *P. granulata* sp. nov. (MNRJ). **E**. Anterior region of *P. buhrnheimi* Schubart, 1960 (IBSP 2397). Scale bars: A–B = 0.5 mm; C–D = 0.2 mm; E = 1 mm.

Fig. 201. Character 23 and its character states. Anterior sternum. **A**. *Pseudonannolene fontanettiae* Iniesta & Ferreira, 2014 (IBSP 3759). **B**. *P. paulista* Brölemann, 1902 (IBSP 1908). **C**. *P. sebastianus*

Brölemann, 1902 (IBSP 1390). **D**. *P. caatinga* Iniesta & Ferreira, 2014 (IBSP 2180). Scale bars: A, C = 0.5 mm; B, D = 0.25 mm.

Fig. 202. Characters 24–27 and their character states. **A**. Midbody leg of *Pseudonannolene halophila* Schubart, 1949 (IBSP 1101). **B**. Tarsus of midbody leg of *P. halophila* (IBSP 1101). **C**. Posterior region of *P. alegrensis* Silvestri, 1897 (MCN626). **D**. Posterior region of *Epinannolene* sp. (ICN). **E**. Posterior region of *P. granulata* sp. nov. (MNRJ). **F**. Posterior region of *P. buhrnheimi* Schubart, 1960 (IBSP 2397). Scale bars: A = 0.25 mm; B = 0.1 mm; C–F = 0.5 mm.

Fig. 203. Character 28 and its character states. Coxae of first leg-pair of males. **A**. *Epinannolene* sp. (ICN). **B**. *Pseudonannolene caatinga* Iniesta & Ferreira, 2014 (IBSP 2180). **C**. *P. halophila* Schubart, 1949 (IBSP 1091). Scale bars: A–B = 0.25 mm; C = 0.5 mm.

Fig. 204. Characters 29–31 and their character states. Coxae of first leg-pair of males. **A**. *Pseudonannolene caatinga* Iniesta & Ferreira, 2014 (IBSP 1389). **B**. *P. leucocephalus* Schubart, 1944 (MZSP 1060). **C**. *Epinannolene* sp. (ICN). **D**. *P. halophila* Schubart, 1949 (IBSP 3297). **E**. *P. anapophysis* Fontanetti, 1996 (IBSP 5209). Scale bars: A, D–E = 0.5 mm; B–C = 0.2 mm.

Fig. 205. Characters 32–34 and their character states. Tarsus of first leg-pair of males. **A**. *Choctella hubrichti* Hoffman, 1965 (USNM). **B**. *Pseudonannolene caatinga* Iniesta & Ferreira, 2014 (IBSP 2166). Image A not to scale. Scale bar = 0.25 mm.

Fig. 206. Characters 35–37 and their character states. Prefemur of first leg-pair of males. **A**. *Pseudonannolene anapophysis* Fontanetti, 1996 (IBSP 5209). **B**. *Holopodostreptus braueri* Carl, 1918 (MNRJ). **C**. *Choctella hubrichti* Hoffman, 1965 (USNM). **D**. *P. magna* Udulutsch & Pietrobon, 2003 (MZSP 941). Scale bars: A = 0.5 mm; B = 0.1 mm; D = 0.2 mm. Image C not to scale.

Fig. 207. Characters 38–41 and their character states. Prefemur and prefemoral process of first leg-pair of males. **A**. *Epinannolene* sp. (ICN). **B**. *Pseudonannolene caatinga* Iniesta & Ferreira, 2014 (IBSP 2180). **C**. *P. maritima* Schubart, 1949 (IBSP 979). **D**. *Holopodostreptus braueri* Carl, 1918 (MNRJ). Scale bars: A, C = 0.2 mm; B, D = 0.1 mm.

Fig. 208. Characters 42–46 and their character states. Second leg-pair of males. **A**. *Choctella hubrichti* Hoffman, 1965 (USNM). **B**. *Phallorthus colombianus* Chamberlin, 1952 (FMNH). **C**. *Pseudonannolene occidentalis* Schubart, 1958 (IBSP 1998). **D**. *Holopodostreptus braueri* Carl, 1918 (MNRJ). Scale bars: B, D = 0.1 mm; C = 0.2 mm. Image A not to scale.

Fig. 209. Characters 47–49 and their character states. Second leg-pair of males. **A**. *Phallorthus colombianus* Chamberlin, 1952 (FMNH). Penis of *Epinannolene* sp. (ICN), in detail. **B**. *Pseudonannolene imbirensis* Fontanetti, 1996 (MZSP 1035). **C**. *P. halophila* Schubart, 1949 (IBSP 3671). Scale bars = 0.25 mm.

Fig. 210. Characters 50–52 and their character states. Vulva. **A**. *Holopodostreptus braueri* Carl, 1918 (MNRJ), in anal view. **B**. Vulvae adhered on second leg-pair of *Pseudonannolene microzoporus* Mauriès, 1987 (IBSP), in anal view. **C**. Right vulva of *Holopodostreptus braueri* Carl, 1918 (MNRJ), in oral view. **D**. Right vulva of *P. ophiiulus* Schubart, 1944 (MZSP), in anal view. Scale bars: A, C–D = 0.2 mm; B = 0.5 mm.

Fig. 211. Characters 54–58 and their character states. Gonopods. **A**. Left gonopod of *Holopodostreptus braueri* Carl, 1918 (MNRJ), in mesal view. **B**. Left gonopod of *Pseudonannolene maritima*

Schubart, 1949 (IBSP 979), in mesal view. **C**. *P. microzoporus* Mauriès, 1987 (IBSP 3427), in anal view. **D**. *P. strinatii* Mauriès, 1974 (ISLA 20622), in oral view. **E**. *P. tricolor* Brölemann, 1902 (IBSP 964), in oral view. **F**. *Phallortus colombianus* Chamberlin, 1952 (FMNH), in oral view. Detail of right gonopod of *Holopodostreptus braueri* Carl, 1918 (MNRJ), in oral view. Scale bars: A = 0.2 mm; B = 0.25 mm; C–F = 0.5 mm.

Fig. 212. Characters 58–63 and their character states. Gonopods. **A**. *Pseudonannolene occidentalis* Schubart, 1958 (IBSP 1998), in oral view. **B**. Gonocoxae of *P. lundi* Iniesta & Ferreira, 2015 (ISLA 8685), in oral view. **C**. Mesal cavity of *Holopodostreptus braueri* Carl, 1918 (MNRJ), in mesal view. **D**. *P. paulista* Brölemann, 1902 (IBSP 1908), in mesal view. Globular projection bearing setae on mesal cavity, in detail. **E**. *Choctella cumminsi* Chamberlin, 1918 (USNM). **F**. *P. caatinga* Iniesta & Ferreira, 2014 (IBSP 2166). Scale bars: A = 0.5 mm; B–C = 0.2 mm; D, F = 0.5 mm. Image E not to scale.

Fig. 213. Character 64 and its character states. Gonopods in oral view. **A**. *Pseudonannolene caatinga* Iniesta & Ferreira, 2014 (IBSP 2166). **B**. *P. paulista* Brölemann, 1902 (IBSP 1908). Scale bars: A = 0.5 mm; B = 0.25 mm.

Fig. 214. Characters 65–68 and their character states. Gonopods. **A**. Distal region of gonopods of *Phallorthus colombianus* Chamberlin, 1952 (FMNH), in anal view. **B**. Distal region of gonopods of *Pseudonannolene buhrnheimi* Schubart, 1960 (IBSP 2397), in anal view. **C**. Left gonopod of *P. alegrensis* Silvestri, 1897 (MCN 626), in anal view. **D**. Left gonopod of *P. typica* Silvestri, 1895 (MCSN), in anal view. **E**. Distal region of gonopods of *P. erikae* Iniesta & Ferreira, 2014 (IBSP 3331), in anal view. **F**. Right gonopod of *Holopodostreptus braueri* Carl, 1918 (MNRJ), in oral view. Scale bars: A, F = 0.1 mm; B–C = 0.2 mm; D–E = 0.5 mm.

Fig. 215. Character 69 and its character states. Telopodites. **A**. *Pseudonannolene ambuatinga* Iniesta & Ferreira, 2013 (IBSP 3442). **B**. *P. alata* sp. nov. (IBSP 7879). Scale bars = 0.2 mm.

Fig. 216. Characters 70–73 and their character states. Gonopods. **A**. *Phallorthus colombianus* Chamberlin, 1952 (FMNH). **B**. *Holopodostreptus braueri* Carl, 1918 (MNRJ). Left telopodite, in anal view. **C**. *Pseudonannolene imbirensis* Fontanetti, 1996 (MZSP 1035). **D**. *P. nicolau* sp. nov. (ABAM). **E**. *P. occidentalis* Schubart, 1958 (IBSP 1998). Scale bars: A–C = 0.1 mm; D–E = 0.1 mm.

Fig. 217. Characters 74–76 and their character states. Solenomere of left gonopod, in anal view. **A**. *Pseudonannolene buhrnheimi* Schubart, 1960 (IBSP 2397). **B**. *P. nicolau* sp. nov. (ABAM). **C**. *P. rolamossa* Iniesta & Ferreira, 2013 (ISLA 1504). Scale bars: A = 0.2 mm; B–C = 0.1 mm.

Fig. 218. Characters 77–78 and their character states. Solenomere of left gonopod, in anal view. **A**. *Pseudonannolene caatinga* Iniesta & Ferreira, 2014 (IBSP 2166). **B**. *P. inops* Brölemann, 1929 (IBSP 2559). **C**. *P. robsoni* Iniesta & Ferreira, 2014 (IBSP 3588). **D**. *P. albiventris* Schubart, 1952 (MZSP 1007). **E**. *P. paulista* Brölemann, 1902 (IBSP 1908). Scale bars: A, C = 0.1 mm; B, D–E = 0.1 mm.

Fig. 219. Characters 79–82 and their character states. Gonopods. A. *Pseudonannolene albiventris* (MZSP 1007). **B**. *P. rolamossa* Iniesta & Ferreira, 2013 (IBSP). **C**. *P. caatinga* Iniesta & Ferreira, 2014 (IBSP 2166). **D**. *P. buhrnheimi* Schubart, 1960 (IBSP 2397). **E**. *P. spelaea* Iniesta & Ferreira, 2013 (IBSP 6071). **F**. *Holopodostreptus braueri* Carl, 1918 (MNRJ). Scale bars: A–C = 0.2 mm; D = 0.5 mm; E–F = 0.1 mm.

Fig. 220. Characters 83–84 and their character states. Gonopods. **A**. *Epinannolene* sp. (ICN). **B**. *Pseudonannolene typica* Silvestri, 1895 (MCSN). **C**. *Phallorthus colombianus* Chamberlin, 1952 (FMNH). **D**. *P. ambuatinga* Iniesta & Ferreira, 2013 (IBSP 3442). Scale bars: A = 0.5 mm; B = 0.1 mm; C–D = 0.2 mm.

Fig. 221. Character 85 and its character states. Internal branch. **A**. *Epinannolene exilio* (Brölemann, 1904) (INPA). **B**. *Pseudonannolene tricolor* Brölemann, 1902 (IBSP 964). **C**. *P. nicolau* sp. nov. (ABAM). Scale bars: A–B = 0.2 mm; C = 0.1 mm.

Fig. 222. Characters 86–90 and their character states. Internal branch. **A**. *Phallorthus colombianus* Chamberlin, 1952 (FMNH). **B**. *Pseudonannolene ambuatinga* Iniesta & Ferreira, 2013 (IBSP 3442). **C**. *Epinannolene exilio* (Brölemann, 1904) (INPA). **D**. *P. robsoni* Iniesta & Ferreira, 2014 (IBSP 3441). **E**. *P. occidentalis* Schubart, 1958 (IBSP 1998). **F**. *P. typica* Silvestri, 1895 (MCSN). SEM image of distal region of the internal branch, *P. fontanettiae* Iniesta & Ferreira, 2014 (IBSP), in detail (distal projection highlighted in red). Scale bars = 0.2 mm.

Fig. 223. Character 91 and its character states. Internal branch. **A**. *Pseudonannolene scalaris* Brölemann, 1902 (MZSP). **B**. *P. urbica* Schubart, 1945 (IBSP 2007). Scale bars = 0.2 mm.